Design, synthesis and biological evaluation of antidiabetic agents.

A thesis submitted to the National University of Ireland in fulfillment of the requirements for the degree of

Doctor of Philosophy

by

Robert Devine, B.Sc.

Department of Chemistry,

National University of Ireland Maynooth,

Maynooth, Co. Kildare, Ireland

October 2013

Research Supervisor: Dr. John Stephens

Head of Department: Dr. John Stephens

Table of Contents

Declaration

I declare that the work presented in this thesis was carried out in accordance with the regulations of NUI Maynooth. The work is original, except where indicated by reference, and has not been submitted before, in whole or in part, to this or any other university for any other degree.

Signed:_____Date: _____

Acknowledgements

To my second group, the Findaly lab (Jose, Connor, Darren, Kate and Pam), thank you for all the help and advice during my efforts at trying to become a biologist. I would like to thank Gemma especially for always having time and the patience to reply to my bombardment of emails. I really appreciate it and I wouldn't have been able to finish this thesis without your help and advice.

Thank you to everybody else in the department; Fino and John Kealy, for the countless and much appreciated abuse, Haixin for all the papers and jellies, Orla, Wayne, Niall Maher, Keely, Andy, Chiggy, Barry, the Mc Manus lab and to anybody who I've forgotten. Thank you for the kindness, friendship and memories over the past few years.

To all my "home" friends, Aaron, Carlo, Richie, Marty, Tom, Burkey, Jess, Laura, Jen, Jen Dunne and Niamh, thank you all for allowing me to forget about chemistry. I would like to particularly thank my oldest friends Colm and Murray. Thank you for your friendship, support and loyalty over the years. I wouldn't have gotten through this without the regular night outs and the cups of tea.

To Kelly, I don't know where to begin or how to adequately describe how much I love, respect and appreciate you. I would not have made it through this last year without you. I am so lucky to have you in my life and I am so grateful for you being there during the stressful times, particularly in the past number of months. You are an amazing person and I feel privileged to be your boyfriend.

Lastly, I would like to thank my family. To Mam and Dad, I don't have enough room left to describe how much I appreciate everything you have done for me. Your support and encouragement, not just during my PhD, but throughout my life has gotten me to where I am today. You have allowed me to finish my PhD without having to worry about anything. I couldn't have asked for better parents and I love you. To Có, thank you for always being there, even when I am a man of few words. You are a great sister and even better friend and I love and appreciate you. To Nana, thank you again for all the support, especially for slipping me a few pound, "quietly", when I needed it. You're mad as a brush but I still love you. To Jack, I always think about you and I will never forget you. I know how proud you would be.

Dedication

To my parents, Liam and Carmel, with all my love.

Thank you for everything.

Abstract

Diabetes Mellitus is a metabolic disease characterised by hyperglycaemia, resulting from an inability to secrete insulin, a resistance to insulin or both. The number of individuals suffering from Type-2 diabetes (T2D) is currently 336 million and this number is expected to surpass 552 million by the year 2030. Consequently, there exists a need for novel antidiabetic agents for the treatment of T2D.

The retinol transporter, RBP4, is a possible target for the treatment of T2D as elevated levels of this protein are found in T2D sufferers. Compounds that reduce the levels of RBP4 *in vivo* have been found to improve the diabetic condition. Disruption of the RBP4-TTR complex is a known method for decreasing the levels of RBP4. Therefore, reducing the levels of RBP4 provides a mechanism to treat/manage T2D and allows for the identification and synthesis of novel antidiabetic agents.

Computational studies were used to identify compounds (**1**, **2** and **3**) that bind within RBP4 and have the potential to prevent the formation of the RBP4-TTR complex. Biological assays (SPR, fluorometric binding assay) were performed on these compounds to verify their ability to bind within the protein cavity of RBP4 and inhibit the formation of the RBP4-TTR complex.

A SAR study of compound **1** uncovered compound **4** which was more active than its parent compound in the SPR assay. A subsequent SAR study performed on the new lead compound **4** to identify the functional groups necessary for its biological activity. The derivatives required for this study were synthesised using a variety of chemical processes and were tested in an assay to assess their ability to stimulate muscle cells to take up glucose. This study uncovered a number of compounds with increased activity (**64**, **79** and **82**).

While the glucose uptake assay allowed for the identification of a number of active compound **4** derivatives, it also indicated that a secondary protein target was involved as the glucose uptake assay was RBP4 independent. A method for identifying this unknown target was therefore needed. The method chosen involved immobilising active compounds on an affinity column, which is composed of sepharose beads. A solution of cellular proteins is then passed through the column and the subsequent bound proteins are lysed and analysed by mass spectrometry. Immobilisation of compounds onto this column first required the attachment of a PEG linker to each molecule. Compounds **4**

and **79** were successfully immobilised on the affinity column; at the time of writing, the results from their biological evulation remain outstanding.

A SAR study was also performed on compounds **2** and **3**. This uncovered compound **115**, which proved to be highly active in the glucose uptake assay. A number of derivatives of compound **2** and **3** have been designed, synthesised and characterised and are currently awaiting biological evaluation.

Animal studies were carried out on compounds **1**, **4** and **2**. Compounds **1** and **4** proved to be more effective than compound **2** at improving the insulin and glucose tolerance of diabetic mice, while also causing a reduced weight gain. Compound **4** was administered to animals after 17 weeks, once insulin resistance had been established. Compound **4** was found to restore both glucose and insulin sensitivity to normal levels.

A number of additional animal studies were considered involving compound **4**; however these required aqueous solutions of the compound. As compound **4** had proven to be insoluble in aqueous solutions, a method for preparing these solutions was needed. Cyclodextrins (CD) were chosen and the use of 20 eq of hydroxylpropyl-β-CD (HPBCD) gave a 0.02 M 5% DMSO/H_2O solution of compound **4**. The dissolution of compound **4** may have occurred due to the formation of an inclusion complex. A phase solubility diagram, SEM, DSC and NMR were used in the characterisation of the inclusion complex.

List of Abbreviations

ADME = Absorption, Distribution, Metabolism, Excretion

ADP = Adenosine triphosphate

AMP = Adenosine monophosphate

AMPK = 5' adenosine monophosphate-activated protein kinase

Ar = Aryl

ATP = Adenosine-5'-triphosphate

Boc = *t*-Butyloxycarbonyl

BINAP = (2,2'-Bis(diphenylphosphino)-1,1'-binaphthyl)

BOP = (Benzotriazol-1-yloxy)tris(dimethylamino)phosphonium hexafluorophosphate

Bu = Butyl

BuLi = Butyl lithium

°C = Degrees Celsius

CD = Cyclodextrin

$CDCl_3$ = Deuterated chloroform

CDI = 1,1'-Carbonyldiimidazole

CD_3OD = Deuterated methanol

cm^{-1} = Wavenumbers

CPM/ mg protein = Counts per minute per milligram of protein

CuTC = Copper(I)-thiophene-2-carboxylate

DCM = Dichloromethane

DCC = *N,N*-Dicyclohexylcarbodiimide

dd = doublet of doublets

DEPT = Distortionless enhancement by polarization transfer

DIPEA = *N,N*-Diisopropylethylamine

DMAP = Dimethylaminopyridine

DMF = Dimethylforamide

DMSO = Dimethylsulfoxide

DSC = Differential scanning calorimetry

D_2O = Deuterium oxide

d_6-DMSO = deuterated dimethylsulfoxide

Et = Ethyl

Et_2O= Diethyl ether

EtOAc = Ethyl acetate

EtOH = Ethanol

Fen = Fenretinide

HBA = Hydrogen Bond Acceptor

HBD = Hydrogen Bond Donor

HFD = High Fat Diet

HOAc = Acetic acid

hrs = Hours

HOBt = Hydroxybenzotriazole

HPBCD = Hydroxylpropyl-β-cyclodextrin

HR-MS = High resolution mass spectrometry

HSQC = Heteronuclear single quantum coherence

Hz = Hertz

iPr = iso-Propyl

J = coupling constant

m = $meta$

M = Molar

m = multiplet

Me = Methyl

MeOH = Methanol

mins = Minutes

mmol = millimole

m.p. = Melting point

MW = Microwave

NADH = The reduced form of nicotinamide adenine dinucleotide

NaO^{t}Bu = Sodium *tert*-butoxide

NBS = *N*-Bromosuccinimide

NEt$_3$ = Triethylamine

NMP = *N*-Methyl-2-pyrrolidone

NMR = Nuclear magnetic resonance

o = ortho

p = para

PEG = Polyethylene glycol

Pet. Ether = Petroleum ether

ppm = Parts per million

Pr = Propyl

p-TSA = *para* toluene sulfonic acid

q = Quartet

RBP4 = Retinol binding protein 4

ROESY = Rotating-frame nuclear Overhauser effect correlation spectroscopy

ROH = Retinol

rt = Room temperature

s = Singlet

SAR = Structure activity relationship

SEM = Scanning electron microscopy

S_NAr = Nucleophilic aromatic substitution

SPR = Surface plasmon resonance

SUR = Sulfonylurea receptors

*t*Bu = *tert*-Butyl

TBTU = (*O*-Benzotriazol-1-yl)-1,13,3-tetramethyluronium tetrafluoroborate

TFA = Trifluoroacetic acid

THF = Tetrahydrofuran

TLC = Thin layer chromatography

TMS = Trimethylsilyl

TOF = Time of flight

TTR = Transthyretin

T1D = Type-1 diabetes

T2D = Type-2 diabetes

λ = Wavelength (nm)

1. Introduction.

1.1   Introduction

Diabetes Mellitus (diabetes) is a metabolic disease that is characterised by an increased level of plasma glucose (hyperglycaemia) resulting from an inability to secret insulin, a resistance to insulin or both.[1,2] Over the past number of years the shift towards calorific diets and sedentary lifestyles has resulted in the prevalence of diabetes and its complications, with roughly 366 million people worldwide currently affected.[3] If this trend is to continue the number of individuals affected is predicted to rise to a staggering 552 million by the year 2030, with a large number of sufferers remaining undiagnosed.[3,4] The increase in obesity and reduction in physical activity has meant that in 2007 diabetes was the seventh leading cause of death in the U.S with the cost of treating this disease exceeding $110 billion annually.[5] The rapid increase in the incidence of diabetes has meant that it is the only non-infectious disease classified as an epidemic by the World Health Organization (WHO).[6] Of the 285 million current sufferers, it has been reported that 90% suffer from Type-2 Diabetes (T2D) with the remaining percentage of individuals suffering from Type-1 Diabetes (T1D).[6] T1D can be described as a complete insulin deficiency due to the autoimmune destruction of the insulin producing β-cells of the pancreas.[7] The more common T2D can be characterised by a reduction/lack of insulin secretion from pancreatic cells and/or the observed resistance of target tissues to insulin.[8]

Hyperglycaemia associated with T1D and T2D causes microvascular and macrovascular issues leading to complications such as retinopathy, nephropathy, neuropathy, accelerated atherosclerosis, stroke and coronary heart disease.[9,5]

1.2   Microvascular complications

Diabetic microvascular complications arise due to the damage caused to the small blood vessels such as the capillaries, arterioles and venules. This occurs as a result of hyperglycaemia with the development of these complications being directly related to the duration and severity of the hyperglycaemic condition.[10] The severity of these complications is obvious as diabetic nephropathy is the leading cause of kidney failure in the western world with 43% of patients requiring dialysis or transplantation, while

diabetic retinopathy is the most prevalent cause of acquired blindness in the developed world.[2,7]

1.2.1   Diabetic Nephropathy

The condition that occurs as a result of damage to the kidney cells is known as diabetic nephropathy or Kimmelstiel-Wilson syndrome.[10] Diabetic nephropathy progresses through a series of characteristic stages. The first recognizable stage of nephropathy is microalbuminuria, which is the presence of the protein albumin in urine. Normally, albumin is too large to pass through the glomerulus but damage caused to these cells due to hyperglycaemia allows for this protein to pass from the blood stream into the urine.[2] Microalbuminuria is followed by macroalbuminuria and is similar to the first stage only for the increased concentration of albumin found in the urine. The increase in concentration of albumin in urine is due to the increased damage caused to the renal glomerulus.[2] The final stage of diabetic nephropathy is known as end-stage renal disease and results in the patient requiring either dialysis or a kidney transplant.[2,10]

1.2.2   Diabetic Retinopathy

Diabetic retinopathy is the most common microvascular complication associated with hyperglycaemia causing injury to the retina leading to blindness.[10] This condition manifests in T1D sufferers twenty years after initial diagnosis while it is found in T2D patients as early as seven years after diagnosis.[10]

The presence of glucose can cause damage to the retinal cells in a number of ways. Aldose reductase is an enzyme involved in the polyol pathway which is responsible for the conversion of glucose into sorbitol. When a hyperglycaemic state is in effect, this causes high levels of sorbitol to accumulate within cells. The osmotic stress that cells are exposed to due to the accumulation of sorbitol has been suggested as a possible mechanism for the development of microvascular conditions such as retinopathy.[10,11] The osmotic stress can cause damage in the form of microaneurysms and thickening of membranes.[10] Other mechanisms have also been suggested to contribute to the injury of microvessels. These include the non-enzymatic formation of glycoproteins and oxidative stress.[10]

1.2.3   Diabetic Neuropathy

Diabetic neuropathy describes the damage caused to nerves as a result of excess glucose in the blood stream. Over time, excess glucose damages the walls of the blood vessels that supply the nerves with oxygen and nutrients resulting in injury.[10] The mechanism responsible for this injury is similar to that of retinopathy.[10] Peripheral neuropathy describes the injury caused to the nerves outside of the brain or spinal cord. The combination of peripheral neuropathies with vascular disease can lead to ulcer formation, gangrene and poor healing of the lower limbs and ultimately amputation.[2] Peripheral neuropathy can manifest in several forms with focal and generalized neuropathies most commonly encountered.[2,10]

Focal neuropathy best describes the damage that occurs to one or a few nerves. One such example is carpal tunnel syndrome which results in a tingling sensation in limbs and periods of "nighttime" numbness. [12]   Other types of conditions most frequently associated with focal neuropathies include; peroneal nerve and third cranial nerve palsies and diabetic amyotrophy to name but a few.[2]

Generalized neuropathies are often termed polyneuropathies. The most common form of diabetic neuropathy is the generalized condition known as sensorimotor polyneuropathy.[10] This is a systematic condition that affects, amongst other nerves, the autonomic nervous system (nerves associated with the internal organs and gut).[2] Individuals experience tingling, electric sensations or numbness.[10]

1.3   Macrovascular complications

The effects of persistent hyperglycaemia are not limited to complications associated with the microvascular system. Many conditions which cause damage to the macrovascular vessels resulting in cardiovascular disease (CVD) have been well documented. The prevalence of CVD is far greater in individuals with T2D than T1D, with CVD accounting for 70% of all deaths in T2D sufferers.[2] Although the occurrence of CVD may be due in part to obesity, which is synonymous with diabetes and in particular T2D, other mechanisms such as atherosclerosis are suggested to play a pivotal role in diabetes associated CVD. [9,6,7,10, 13] Atherosclerosis is defined as the narrowing of the inner walls of the arteries due to the accumulation of lipids, macrophages and

fibrous elements.[14,15] Diabetes is known to increase the incidence of conditions such as dyslipidaemia and hypertension which aid in the development of atherosclerosis.[16]

1.3.1   Dyslipidaemia

Dyslipidaemia is a condition in which the blood contains an abnormal amount of lipids. While many classes of dyslipidaemia exist, the phenotype that best characterises diabetic dyslipidaemia is high plasma triglyceride concentration and increased levels of low density lipoprotein (LDL) cholesterol, which can be converted to the more atherogenic small density LDL. Decreased levels of high density lipoprotein (HDL) cholesterol is also associated with diabetic dyslipidaemia.[17,18,19] High levels of LDL cholesterol have been associated with cardiovascular complications while high levels of HDL cholesterol tends to be associated with individuals with fewer cardiovascular issues.

Hyperinsulinaemia has been implicated in the mechanism of this altered lipid state.[17,18] The increased levels of insulin in circulation causes an increase in free fatty acid release from insulin resistant adipose tissue which in turn promotes the secretion of apolipoprotein B (apoB).[18] ApoB is a major component of very low density lipoprotein (VLDL) cholesterol which can be metabolised to atherogenic remnant lipoproteins thus promoting atherosclerosis.[13, 17,18] Hyperinsulinaemia has also been shown to decrease the activity of lipoprotein lipase which is the main enzyme involved in the clearance of VLDL cholesterol.[13]

The presence of VLDL also decreases the level of serum HDL cholesterol.[17,18] Cholersteryl ester transfer protein (CETP) stimulates the transfer of triglycerides from VLDL to HDL, which produces a HDL-triglyceride particle that can be more easily cleared from circulation than normal HDL. Other studies suggest that key enzymes involved in the metabolism and synthesis of HDL cholesterol are altered in individuals with insulin resistance while tumour necrosis factor (TNF)-α has also been suggested to lower plasma levels of HDL cholesterol.[17] The combination of the above events leads to the development of dyslipidaemia and ultimately CVD.[13]

1.4   Type-1 Diabetes

T1D is characterized by absolute insulin deficiency resulting in increased levels of plasma glucose (hyperglycaemia). The insulin deficiency is due to the autoimmune destruction of the insulin producing β-cells resulting in a life-long need for exogenous insulin.[20,21,1] Reports suggesting that at the time of diagnosis only 10-20% of the β–cell function remains and that the first sign of the cell mediated destruction of islet cells is the emergence of the four autoantibodies; insulin autoantibodies, islet cell antibodies, glutamate decarboxylase autoantibodies and autoantibodies to the tyrosine phosphatase-related IA-2 molecule.[1] As the disease was predominantly diagnosed in children under 4 years of age, T1D was given the title of juvenile diabetes. Recent data suggests however that 50-60% of T1D sufferers are 16-18 years of age and that the disease is also present at low levels in adults.[2]

One hypothesis for the cell mediated autoimmune attack suggests that each person is susceptible to the development of T1D with some more susceptible than others.[2] Those with a greater susceptibility to autoimmune attack inherit this trait from their parents but the activation of these high susceptibility genes requires exposure to one or more external environmental triggers.[2]

The genes encoding for high susceptibility are mainly found in the Human Leukocyte Anitgen (HLA) locus and this genotype is known as the HLA DR or HLA DQ genotypes. The HLA system is the name given to the human Major Histocompatability Complex (MHC) and is an essential component of the immune system functioning to present antigens from inside or outside the cell to immune cells, such as T cells or helper T cells, for example.[14] It is thought that these genes are responsible for 50% of the occurrence of this high susceptibility with the environmental triggers such as viruses (e.g. enterovirus), environmental toxins or early exposure to foods such as milk proteins, gluten or cereals needed to "stimulate" β-cell destruction.[1,2]

This hypothesis is supported by the fact that these individuals are also highly susceptible to other autoimmune diseases such as Hashimoto's thyroiditis, Grave's disease, Addison's disease, coeliac disease and myasthenia gravis.[2] Other hypotheses have been suggested that try to explain how these susceptibility genes are triggered. One such theory is the hygiene hypothesis. This hypothesis has been implicated as the

cause of other allergic diseases and is now gaining attention as a possible contributor to the occurrence of T1D. A lack of exposure to microbes at an early age can impact the development and programming of the immune system resulting in the prevalence of allergic diseases such as asthma.[1,2]

1.4.1   Treatment and management

The management and treatment of T1D involves the appropriate administration of insulin, the monitoring of blood glucose levels and nutritional planning. As T1D is an autoimmune disease, patients are regularly screened for other autoimmune conditions such as thyroid dysfunction and coeliac disease.[2] Medications are also required to treat the micro- and macrovascular conditions described previously.[2]

1.5   Type-2 Diabetes

T2D is a complex metabolic disorder that is characterised by a loss of β-cell function and mass, impaired insulin secretion, an increase in hepatic glucose production and varying levels of insulin resistance in target tissues including the liver and muscle. It is a multifaceted metabolic disease that results from a combination of genetic and environmental factors such as diet, age and level of physical activity.[22] Those that are destined to develop diabetes inherit genes from their parents that encode for traits such as loss of β-cell function and obesity.[23]

Genetics and an inappropriate lifestyle lead to obesity which is responsible for a number of life-threatening diseases such as T2D, hypertension, dyslipidaemia and CVD. An important link between the above conditions and obesity is insulin resistance.[7,16] An increase in adipose tissue, in particular visceral fat, stimulates the production and release of a series of mediators that affect insulin sensitivity.[16] Free fatty acids (FFAs) and TNF-α, as well as interleukin (IL)-6 and leptin have all been implicated in the mechanism of obesity induced insulin resistance.[16] The presence of obesity and insulin resistance may be present for many years before the development of conditions such as T2D.[16]

Once a basal level of insulin resistance has been established, β-cell function and mass begins to be impaired.[22] Insulin resistance causes the pancreatic β-cells to over-produce insulin to accommodate the reduction in insulin sensitivity.[22] Hyperglycaemia ensues as the pancreatic cells are unable to produce enough insulin to compensate for the lack of

glucose uptake due to insulin resistance.[16,22] Overtime the hypersecretion of insulin in response to hyperglycaemia causes β-cells to become exhausted and thus "wear out" halting the secretion of insulin *via* normal mechanisms.[22,23] Although some reports suggest that the exact mechanism involved in β-cell dysfunction is not known, others postulate that the involvement of conditions such as dyslipidaemia and hyperglycaemia, contribute to this impaired function.[24] Mechanisms such as oxidative stress and endoplasmic reticulum (ER) stress caused by hyperglycaemia and obesity, have been implicated in β-cell dysfunction by inducing β-cell dedifferentiation and apoptosis.[24] The progression to full-blown T2D occurs when the over production of insulin by β-cells cannot compensate for insulin resistance with the rate of β-cell failure determining the rate at which T2D progresses.[22,23]

1.5.1 Treatment

The management and treatment of T2D involves increasing insulin secretion and improving insulin sensitivity and hyperglycaemia. A number of combined methods exist that focus around improving the metabolic syndrome. This generally occurs in the order of nutrition therapy and increased physical activity, oral antidiabetic pharmaceuticals and ultimately exogenous insulin therapy.[25]

Improving ones diet, moving away from sedentary behaviour and increasing physical activity are key components when combatting T2D, particularly amongst overweight and obese patients. This involves strict control of food intake and requires regular monitoring of blood glucose levels. Occasionally this is satisfactory for controlling the diabetic condition; however in most cases when inadequate glycaemic control prevails, pharmaceutical intervention in the form of an antidiabetic agent is needed.[26] When this does not rectify the problem, a second, complementary pharmaceutical may be needed with the addition of exogenous insulin.[26,27]

1.5.1.1 Antidiabetic agents

Numerous antidiabetic agents have emerged in the past number of years aimed at improving T2D, exerting their influence through a plethora of biological targets and allowing for a complementary cocktail of pharmaceutical agents to be used.[7] This is in stark contrast to previous pharmaceutical strategies where sulfonylureas were the only antidiabetic agents available for treating T2D in the U.S before 1995.[7]

1.5.1.1.1 Sulfonylureas

Although sulfonylureas are not used in the treatment of early stage diabetes they are still widely used later on in the progression of the disease.[28] They bind to sulfonylurea receptors (SUR) where they work by stimulating the release of insulin from the pancreas by inhibiting ATP-activated K^+ channels found in the plasma membrane.[29,30] Inhibition leads to the depolarization of the membrane and activation of voltage gated Ca^{2+} channels due to the changes in the electrical potential difference. This causes an intracellular influx of Ca^{2+} which increases the concentration of cytoplasmic Ca^{2+} causing the activation of the proteins involved in insulin secretion. These hypoglycaemic agents further increase serum levels of insulin by preventing the hepatic induced clearance of insulin.[26]

Sulfonylureas are also known to act directly on the insulin secreting granules found in β-cells.[29,30] A free-diffusion mechanism allows the sulfonylurea compound to move across the lipid membrane layer and enter the β-cell. Here the drug acts directly on the insulin secretory components inducing the release of insulin from the pancreas.[29,30] This exocytosis is more common to second and third generation sulfonylureas due to their increased lipid-solubility.[26] Glimepiride is an example of a third generation sulfonylurea (**Figure 1.1**).[31]
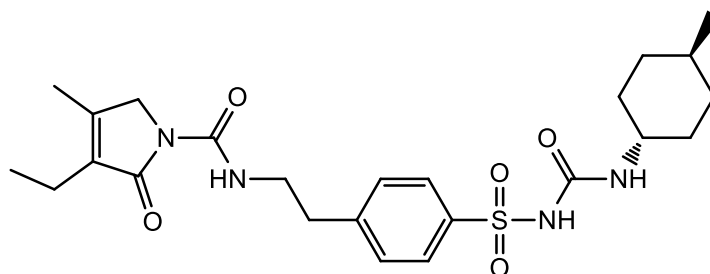
Figure 1.1. Structure of glimepiride.[32]

As with most pharmacologically active substances, the family of sulfonylurea compounds have a number of adverse side effects to their use. Headaches, dizziness, and gastrointestinal issues are the less severe side effects while hypoglycaemia and hyponatraemia, a decrease in serum sodium levels, represent the more serious issues associated with their use.[26,28,33] Ironically, sulfonylureas have also been implicated in causing weight gain amongst its users.[26]

1.5.1.1.2 Meglitinides

Meglitinides are a class of non-sulfonylurea insulin secretagogues that work in a similar fashion to sulfonylureas by stimulating the release of insulin from the pancreas by inhibiting ATP-activated K^+ channels.[34] The principal meglitinide used is repaglinide (**Figure 1.2**). The K^+ channels in question contain not only SUR but also consist of pore forming Kir6.x subunits that associate with the various SUR. Repaglinide is known to bind to both Kir6.2 and SUR1 where it stimulates the closure of the K^+ channels.[35] It has a better effect on post prandial glucose levels than on fasting glucose levels due to its relatively short elimination half-life of one hour. Elimination occurs *via* biliary excretion, a characteristic which allows its use in individuals with renal insufficiencies.[28] As with the sulfonylurea family of antidiabetic drugs, repaglinide also induces hypoglycaemia, however it is slightly less effective in comparison to common sulfonylureas.[28]
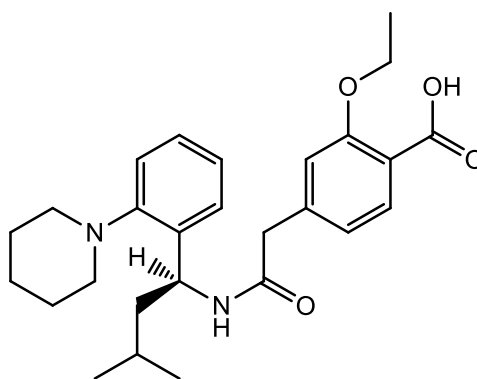
Figure 1.2. Structure of repaglinide.[35]

1.5.1.1.3 Biguanides

Biguanides are a class of anti-hyperglycaemic drugs that have been used in the control and treatment of T2D for many years. Originally three biguanides, metformin, phenformin and buformin were all used; however metformin is the only drug of this class still administered to patients today. This is due to the fact that phenformin and buformin were found to cause lactic acidosis, while only 3 in 100,000 patients presented with lactic acidosis following the use of metformin.[26]

1.5.1.1.3.1 Metformin

Metformin is a first-line antidiabetic drug used in the treatment of T2D (**Figure 1.3**).[28] Although there is a slight risk of associated lactic acidosis, it is still the first drug of choice for many clinicians. This is due to the fact that metformin does not induce hypoglycaemia or weight gain like many other antidiabetic agents. It can also be used in combination with other antidiabetic agents, as well as insulin.[36] Metformin works by decreasing the production of hepatic glucose, notably hepatic glucogenesis which is the synthesis of glucose from non-carbohydrate sources, as well as decreasing intestinal glucose absorption.[26,36] It has also been suggested to slightly improve insulin sensitivity and stimulate fatty acid oxidation.[26,36] Although the exact mechanism by which metformin exerts its antidiabetic effect in the body is not known, it has been found to activate Adenosine monophosphate-activated protein kinase (AMPK).[36,37]

AMPK is a heterotrimeric protein complex that is involved in cellular energy homeostasis where it regulates energy levels by monitoring the amounts of ATP and AMP.[38] AMPK regulates lipid and glucose metabolism and activation of AMPK by small molecules such as metformin has shown to stimulate the uptake of glucose by skeletal muscles and reduce hepatic gluconeogenesis.[38,39] A commonly proposed mechanism for the metformin induced activation of AMPK is inhibition of mitochondrial respiration by acting at Complex I.
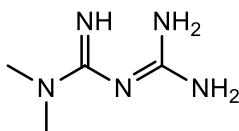
Figure 1.3. Structure of metformin.[40]

1.5.1.1.3.1.1 Mitochondrial respiration and the electron transport chain

Cellular respiration is a cumulative process that consists of three metabolic stages; glycolysis, the citric acid cycle and oxidative phosphorylation (electron transport and chemiosmosis).[14] Glycolysis and the citric acid cycle catabolically break down glucose and other organic substances. Glycolysis is the process by which glucose is metabolised to produce two molecules of pyruvate. This occurs in the cytosol of the cell and is followed by the citric acid cycle, which takes place in the mitochondrial matrix, and oxidizes a pyruvate derivative to carbon dioxide.[14]

Redox reactions are key processes of both the citric acid cycle and glycolysis. Dehydrogenase enzymes transfer electrons from substrates to NAD^+ (nicotinamide adenine dinucleotide) thus forming the reducing agent NADH.[14] The third step of cellular respiration involves the transport of electrons across a series of membrane bound proteins located in the inner membrane of the mitochondria. These proteins accept electrons from the redox processes that occur in the first two respiratory steps and pass electrons from one protein to another. This is known as the electron transport chain and culminates in the production of energy. The energy released at each step of the transport chain is used to make ATP (Adenosine-5'-triphosphate). This mechanism of ATP synthesis is called oxidative phosphorylation.[14]

The electron transport chain is composed of a series of molecules that are located in the inner mitochondrial membrane. The formation of cristae, due to the folding of the inner membrane, increases the surface area of the mitochondria membrane which allows for thousands of copies of the transport chain to be present in each mitochondrion. The chain is mostly composed of proteins which are found in multiprotein complexes labelled complex I to IV (**Figure 1.4**).[14]

Complex I, also known as NADH dehydrogenase (ubiquinone), is the first protein involved in the electron transport chain and catalyses the transfer of two electrons from NADH to ubiquinone (Q, **Figure 1.4**). It is composed of 45 different subunits and is one of the largest known membrane bound protein complexes with a size of ~ 980 kDa.[41,42] The binding site of NADH is located in the hydrophilic domain of Complex I where the primary electron acceptor, flavin mononucletide (FMN), is also located. Electrons are passed from NADH to FMN which then returns to its oxidized state as it passes electrons to the iron-sulphur group, Fe-S. The next redox reaction involves the oxidation of the Fe-S group and the reduction of the small hydrophobic ubiquinone molecule, Q. Ubiquinone is the only non-protein unit within the electron transport chain and is found within the membrane as opposed to being a component of a particular complex.[14]

NADH is not the only source of electrons for the electron transport chain. Another product of glycolysis and the citric acid cycle, flavin adenine dinucleotide ($FADH_2$), also contributes electrons. Unlike NADH however, $FADH_2$ adds electrons at Complex II rather than Complex I (**Figure 1.4**).

Cytochromes (cyt) are responsible for the remaining transport of electrons. Several different cytochrome proteins are found in the mitochondrial membrane, each containing a heme group for transporting electrons.[14] Water is formed when the last cytochrome, cyt a3, transfers its electrons to molecular oxygen which acquires two H^+ ions from the surrounding aqueous solution (**Figure 1.4**).

The electron transport chain does not directly produce ATP. It serves to accommodate the flow of electrons from metabolites of food (i.e. NADH) to molecular oxygen where it breaks the free-energy drop into smaller steps that release energy in more reasonable and manageable amounts.[14] The process of chemiosmosis is responsible for the production of ATP. This is the process by which energy stored in a ionic gradient is used to fuel cellular work.[14]
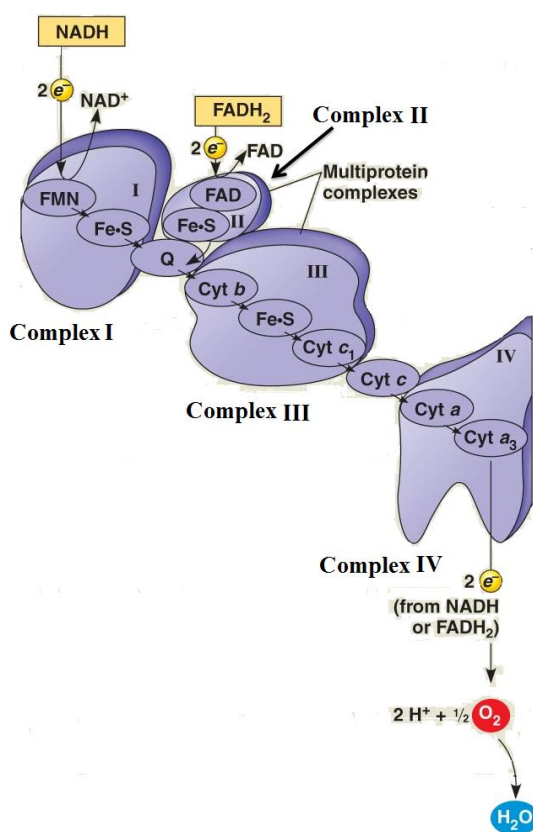
Figure 1.4. The components of the electron transport chain.[14]

The exergonic flow of electrons from Complex I to Complex IV pumps H^+ ions from the mitochondrial matrix to the intermembrane space. Complex I pumps four H^+ ions from the matrix into the intermembrane space while the other complexes pump two H^+

ions each (**Figure 1.5**). This creates an H^+ gradient with the ions trying to move back across the membrane. This type of gradient is known as a proton-motive force.

The protein complex ATP synthase is located in the inner membrane of mitochondria. This complex is an ion pump that uses the energy of an ion gradient to power the synthesis of ATP. The H^+ gradient created from the electron transport chain powers the synthesis of ATP. ATP synthases are the only sites on the membrane through which H^+ ions can permeate back into the mitochondrial matrix. The exergonic flow of H^+ ions causes the synthesis of ATP from the phosphorylation of ADP (**Figure 1.5**).
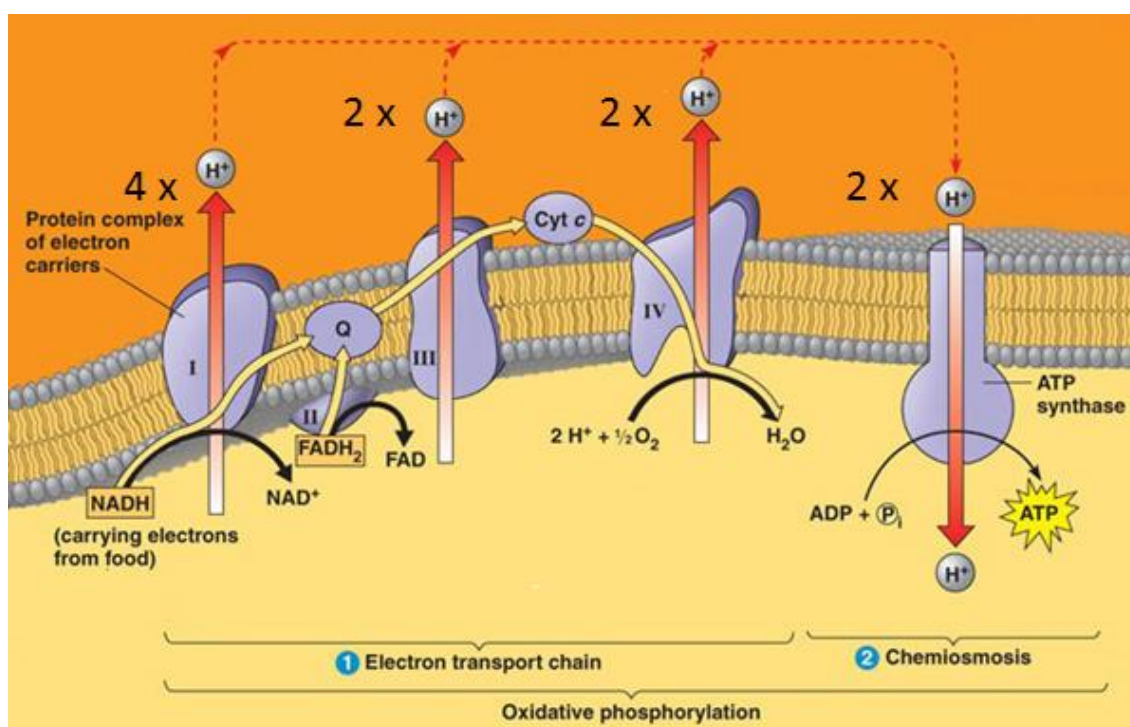
Figure 1.5. The electron transport chain.[14] Yellow arrows represent the flow of electrons.

Ouyang *et al*. suggested that the activation of AMPK by metformin involves an increase in the production of AMP.[37] The mechanism by which this increase in AMP occurs has been postulated to involve the inhibition of mitochondrial respiration by acting at Complex I. Disrupting the action of Complex I would affect the production of ATP which would lead to elevated levels of free ADP.[37] This would subsequently cause increased levels of AMP through the action of adenylate kinase. Inhibition of mitochondrial respiration is strongly linked to an increase in glucose transport into cells.[37]

1.5.1.1.4 Thiazolidinediones

Thiazolidinediones (TZDs) are a class of insulin-sensitizer antidiabetic agents that improve insulin resistance and maintain β-cell function.[43] They do not increase the risk of hypoglycaemia when administered as a monotherapy or in combination with other insulin sensitizers like metformin.[28] TZDs are agonists of the peroxisome proliferator activated receptor (PPAR) subtype PPAR-γ, with the TZD derivative, rosiglitazone, the most potent and selective PPAR-γ agonist (**Figure 1.6**).[28,44,45]
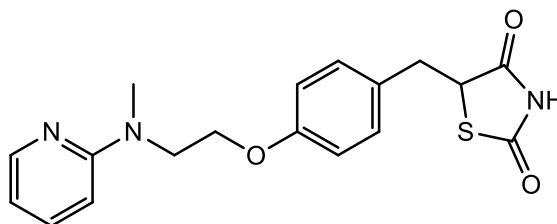
Figure1.6 Structure of rosiglitazone.[45]

1.5.1.1.4.1 Peroxisome proliferator activated receptors (PPARs)

PPARs are members of the nuclear hormone receptor superfamily of transcription factors that are activated by the binding of small ligands. These receptors are responsible for inducing or repressing the transcription of a number of genes that have a marked effect on cellular function including the regulation of glucose, cholesterol and lipid metabolism.[43] They can be categorized into three subtypes: PPAR-α, -γ and -β/δ with PPAR-γ the most widely investigated subtype in T2D.[44]

1.5.1.1.4.1.1 PPAR-γ

The expression of PPAR-γ mainly occurs in adipose tissue with lower concentrations of the receptor found in heart, colon, kidney, intestine, skeletal muscles and macrophages.[44] This PPAR subtype is crucial in adipogenesis which is the differentiation of preadipocytes into adipocytes. It plays a vital role in insulin sensitivity, cell cycle regulation and cell differentiation and has been implicated in the regulation of genes involved in the metabolism of glucose and lipids.

Insulin resistance in muscle cells has been associated with increased levels of circulating FFAs and triglycerides resulting in impaired lipid storage. The role of TZDs

in treating T2D is thought to be through adipogenesis which improves this lipid storage.[45]

1.5.1.1.4.2 Side effects

The first reported antidiabetic TZD, troglitazone, was removed from the market as it caused rare life threatening hepatitis (**Figure 1.7**). The main side effects associated with the use of other TZD analogues include significant weight gain, fluid retention and CVD.[44] Fluid retention can itself lead to heart failure in the cases of pre-existing CVD and in some cases has led to anaemia.[28] Unlike the sulfonylurea antidiabetic agents, rosiglitazone does not cause hypoglycaemia when administered as a monotherapy or when used in conjunction with other diabetic pharmaceuticals such as metformin.[28]
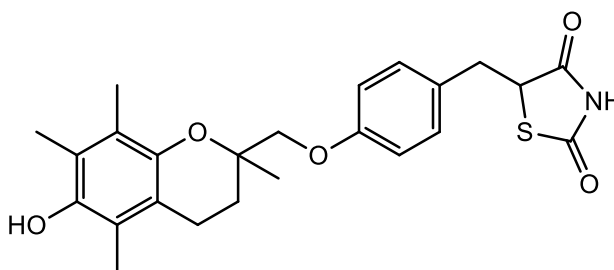
Figure 1.7. Structure of troglitazone.[46]

1.5.1.1.5 Alpha-glucosidase inhibitors

The polysaccharide starch is composed of numerous monosaccharides bound together by α- or β- glycosidic linkages.[47] The process by which starch is metabolised to glucose within the human body is carried out by four hydrolytic enzymes. Salivary and pancreatic amylases hydrolyse starch into shorter linear and branched dextrin molecules by cleaving the starch α-1,4 bonds. Dextrins are then hydrolysed by maltase-glucoamylase and sucrose-isomaltase producing the monosaccharide glucose which can be used for cellular respiration.[47]

Inhibition of one of these enzymes presents itself as a possible target in the treatment of T2D as its inhibition would result in the lowering of glucose levels. The pseudotetrasaccharide acarbose does this by inhibiting the pancreatic α-amylase enzyme α-glucosidase, located in the small intestine (**Figure 1.8**).[47,48] Inhibition of this enzyme delays the absorption of carbohydrates by the small intestine which results in decreasing the post prandial rise in plasma glucose. This molecule has been found to improve

insulin sensitivity and has not been associated with weight gain.[48] Other molecules that also act on the glucosidase enzymes are miglitol and voglibose. The main side effects associated with their use are gastrointestinal problems such as flatulence, diarrhoea and digestive discomfort.[28]
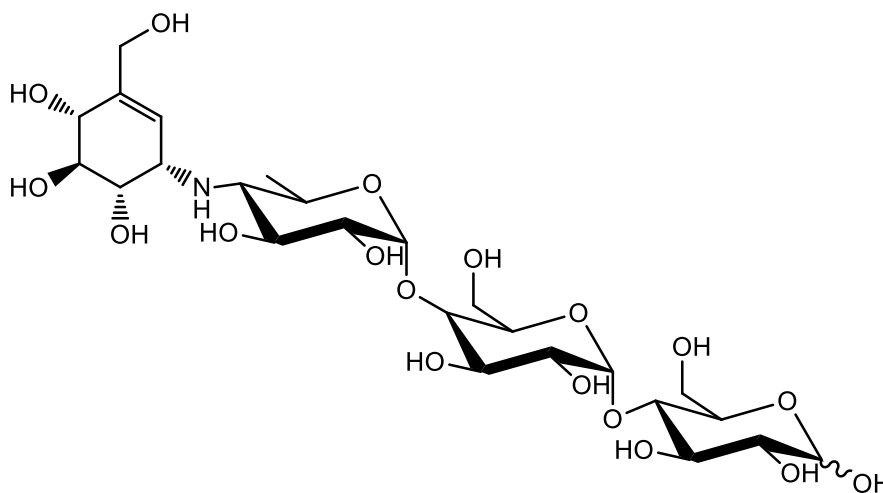
Figure 1.8. Structure of acarbose.[47]

1.5.1.2 Alternative protein targets

As the incidence of diabetes grows so too does the need for new antidiabetic therapeutics. Therapies are needed that can improve hyperglycaemia while preventing associate weight gain. The most recent antidiabetic pharmaceuticals involve targeting a number of proteins that differ to the previously mentioned protein targets. These include for example, the direct and indirect activation of incretin hormones and the inhibition of a sodium-glucose transporter.

1.5.1.2.1 Dipeptidylpeptidase IV (DPPIV) inhibitors

DPPIV is a membrane bound serine protease found on the surface of epithelial cells where it has been identified as an inhibitor of the incretin hormone glucagon-like peptide (GLP-1). This hormone is secreted by L-cells of the intestinal tract after food intake and promotes the secretion of insulin, improves insulin sensitivity, increases β-cell mass and reduces appetite.[25,49] Decreased levels of GLP-1 are found in T2D sufferers with inhibition of DPPIV shown to increase the levels of GLP-1 and therefore improve insulin secretion.[50]

There are currently five DPPIV inhibitors approved for use: sitagliptin, saxagliptin, vildagliptin, linagliptin and alogliptin, with sitagliptin the first DPPIV inhibitor approved in 2005 (**Figure 1.9**).[50] These compounds have shown to reduce or not affect the incidence of CVD while hypoglycaemia does not occur as their effect on β-cells ends when glucose levels return to normal.[28,51]
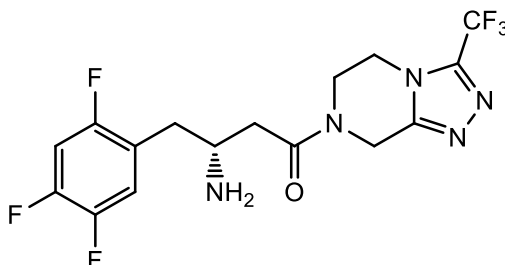
Figure 1.9. Structure of sitagliptin.[52]

1.5.1.2.2 Na⁺-coupled glucose co-transporters (SGLT)

The kidneys play a substantial role in glucose homeostasis. They are involved in the consumption of glucose for metabolism, gluconeogenesis and the filtration and reabsorption of filtered glucose. Glucose circulates unbound throughout the body *via* the blood stream and is filtered at the glomerulus. It is reabsorbed by the kidneys to prevent large amounts of the monosaccharide being lost by filtration. The mechanism by which glucose enters cells and is reabsorbed involves the glucose transport (GLUT) proteins but a Na⁺-coupled glucose co-transporter (SGLT) is primarily responsible for the renal reabsorption of glucose. The SGLT proteins use the energy generated by a Na⁺ gradient to pump glucose across the apical membrane and back into the circulatory system.[27] There are two known SGLT isoforms; SGLT1 and SGLT2.

SGLT1 is mainly found in the intestinal tract but is also located in the heart and kidney. This is a low capacity glucose transporter that is responsible for only small amounts of glucose reabsorption in the kidneys.[53] SGLT2 however, is a high capacity glucose transporter that is found predominantly in the renal convoluted tubule. SGLT2 is responsible for roughly ninety per cent of renal reabsorption of filtered glucose while SGLT1 accounts for the remaining ten per cent.[27,54]

Mascitti *et al*. reported that inhibition of SGLT2 results in the loss of glucose in urine (glucosuria).[55] This was supported by Jurczak *et al*. who stated that SGLT2 knockout

mice demonstrated reductions in plasma glucose and insulin levels while preventing the loss of β-cell mass.[54] As the expression of SGLT1 is not restricted to the kidneys and its inhibition has been suggested to cause dehydration, drug candidates are required to demonstrate selectivity for SGLT2 over SGLT1.[53] A number of pharmaceutical agents, such as tofogliflozin, are selective for SGLT2 and have the potential to be used as antidiabetic agents (**Figure 1.10**).[53]
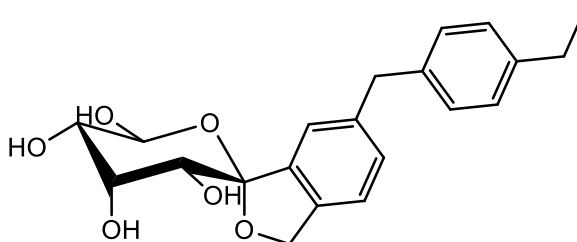
Figure 1.10. Structure of tofogliflozin.[53]

1.5.1.2.3   Retinol binding Protein 4

The retinol transporter, retinol binding protein 4 (RBP4), has been implicated in the process of T2D. Elevated levels of serum RBP4 have been reported in insulin resistant humans with RBP4 having a possible involvement in preventing cellular responses to insulin, generating insulin resistance and the development of T2D.[56,57] This protein therefore has the potential to be used as a target for the control and treatment of T2D.[57]

The expression of the glucose transporter, GLUT4, responsible for the transport of glucose intracellularly, is downregulated in adipose tissue in conjunction with insulin resistance. Although adipose tissue contributes very little to glucose consumption and homeostasis, it does act as an endocrine organ by secreting molecules that can enhance (e.g. leptin) or impair (e.g. TNF- α) the action of insulin.[58] Yang *et al*. reported that there is a decrease in the expression of GLUT4 from adipose tissues in the majority of insulin resistant states. Although the mechanism by which this occurs is not known, it was found that RBP4 was upregulated in the adipose tissue of insulin resistant humans and that this elevated level of RBP4 may be a link between the decreased expression of GLUT4 in adipocytes and insulin resistance.[58] This may also be another explanation for the link between obesity and insulin resistance.[57] The elevated levels of RBP4 may also

be acting on muscle cells, causing insulin resistance, however the mechanism by which this occurs has yet to be clarified.[57]

RBP4 is a member of the lipocalin family of proteins which are extracellular proteins that bind small, typically hydrophobic molecules, such as retinoids and steroids.[59] The 21 kDa monomeric RBP4 is synthesised primarily in the liver but also in adipose tissue and functions to transport vitamin A (retinol, ROH) to extrahepatic tissues.[57] It is composed of an N-terminal coil, eight anti-parallel β-strands, which form a β-barrel, and a short α-helix near the C-terminus (**Figure 1.11**). There are four highly variable loops that connect the β-strands A and B, C and D, E and F and G and H.[60] When transporting ROH, the vitamin molecule is accommodated within the β-barrel. The ring structure is innermost, buried within the protein cavity, the polyene chain is fully extended and the terminal hydroxyl functionality is almost solvent exposed in the region of the loops AB, CD, EF and GH.[57,60] The protein cavity is lined with hydrophobic residues that make specific interactions with ROH, thus stabilising the vitamin within the β-barrel.[61]
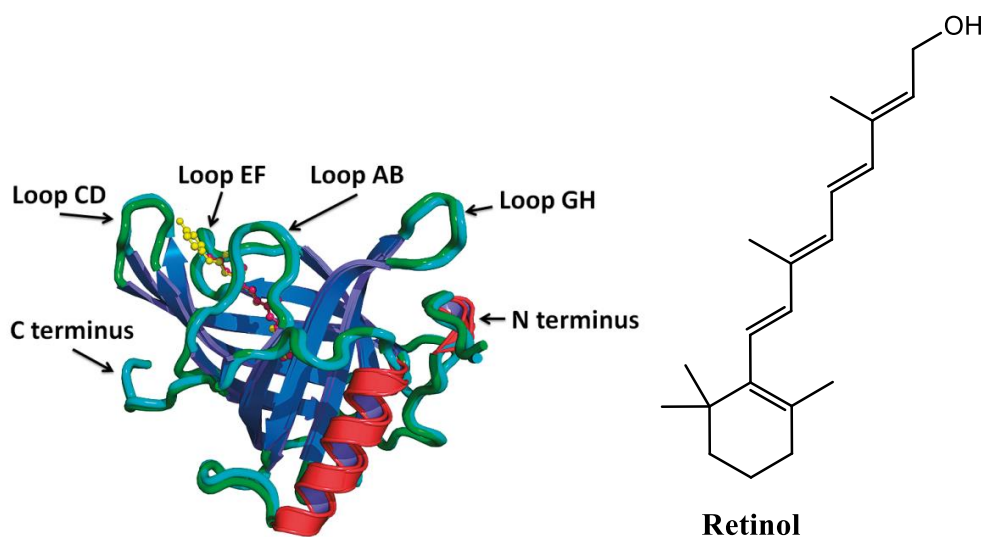
Figure 1.11. Structure of *holo*-RBP4 with ROH (yellow) bound and the structure of ROH.[57]

Holo-RBP4 (i.e. RBP4 with ROH bound inside the β-barrel) is released from the liver complexed to a second, homotetrameric protein transthyretin (TTR). TTR is a thyroid binding hormone, synthesised in hepatic tissues, whose purpose is to distribute thyroids.[60] It is a 55 kDa protein that binds to *holo*-RBP4 and stabilises the RBP4-ROH complex.[60] The absence of ROH from the RBP4 β-barrel results in a weaker interaction

between RBP4 and TTR. As *holo*-RBP4 is small enough to be removed from circulation by renal filtration the formation of the 76 kDa RBP4-TTR prevents this renal filtration due to its increased size.

There are multiple contacts between the entrance loops of RBP4 and TTR, with loop EF making the strongest interaction. The presence of ROH stabilises the RBP4-TTR complex in the form of a hydrogen bond between the hydroxyl group of ROH and the carbonyl of a TTR glycine amino acid residue.[61,62] As *apo*-RBP4 (i.e. RBP4 without ROH bound inside the β-barrel) has a reduced affinity for TTR, once the RBP4-TTR complex has delivered ROH to its target tissues, the proteins disassociate resulting in the renal filtration of *apo*-RBP4.[62] This highlights the importance of ROH in the formation of the RBP4-TTR complex and demonstrates that replacing ROH with an alternative ligand may disrupt the formation of the RBP4-TTR complex, which will result in the renal filtration of RBP4. Thus, the serum levels of RBP4 will be reduced and may improve the diabetic condition.

Kahn *et al*. discovered that the synthetic retinoid, Fenretinide (Fen) possessed the ability to compete with ROH for binding within RBP4, causing the disruption of the RBP4-TTR complex resulting in the renal filtration of RBP4 (**Figure 1.12**). This ultimately led to a reduction in the levels of serum RBP4 which prevented high-fat diet-induced obesity, insulin resistance and hepatic steatosis.[56] Like ROH, Fen is accommodated within the RBP4 β-barrel with the cyclohexene ring innermost and the polyene chain extended out towards the opening of the protein cavity. Fen however, possesses a hydroxyphenyl amide group, replacing the hydroxyl group found in ROH. The presence of the aromatic ring not only prevents the formation of the stabilising hydrogen bond between ROH and a TTR glycine residue, it may also interfere with the position of the loops at the entrance of the cavity, through steric hindrance. These interactions are essential for the formation of a stabile interaction between RBP4 and TTR their absence prevents the formation of the RBP4-TTR complex. The ability of Fen to improve insulin resistance indicates that the RBP4 protein is a viable target in the battle against T2D.
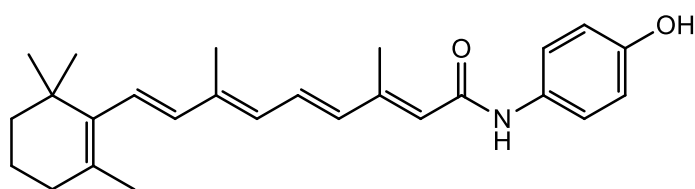
Fenretinide

Figure 1.12. Structure of Fen.[57]

1.5.1.3 Pharmacokinetics and Pharmacodynamics

The above antidiabetic drugs manage to overcome the long and arduous journey involved in reaching their target protein. To do this they must possess the necessary pharmacokinetic properties and appropriate ADME profile.[63,64] Pharmacokinetics is the study of how a drug behaves in the human body.[63] The four main topics in this branch of pharmacology are the absorption, distribution, metabolism and excretion of a drug within the body, which is often referred to as the ADME scheme. Once a drug has overcome the many hurdles encountered on its journey to its protein target, the drug must possess the necessary binding properties. Pharmacodynamics is the study of how a drug binds to its target and the effect it has on the body.[63]

1.5.1.3.1 Pharmacokinetics

A compound with the best binding affinity does not always make the best drug candidate. The drug has to be able to traverse the many obstacles present *in vivo* such as stomach acid, digestive enzymes, hepatic enzymes etc. and when necessary pass through the appropriate membranes to reach its target. Orally administered drugs have to survive the challenges present during absorption, distribution, metabolism and excretion to reach the target protein. To survive these obstacles the drug has to possess the appropriate ADME characteristics.[63]

1.5.1.3.1.1 Absorption

Drug absorption describes how a drug reaches the blood supply which is the deciding factor in how the drug is administered. Oral administration is generally the method of choice and is the most common form of administration.[63]

Orally administered drugs enter the gastrointestinal (GI) tract where they are met by digestive enzymes, gastric juices and hydrochloric acid. For a compound to be a

successful orally administered drug it must be stable to these inhospitable conditions. For example, insulin is acid labile and is degraded by the HCl in the stomach. For this reason it is administered intravenously. A drug that is stable to these conditions then passes through the fatty cell membrane of the GI tract and into the blood stream. Once in the blood stream the drug is transported to the liver where it must withstand the degradative hepatic enzymes.[63]

For a drug to be able to pass through the lipid membrane of the GI tract, it must have the appropriate hydrophilic and hydrophobic character. If the drug is too hydrophilic it will not be able to pass through the lipid membrane however, if it is too hydrophobic it will not be solubilized in the gut and may be dissolved by globules of fat. The presence of amines in a drug can be used to combat this hydrophobic-hydrophilic issue. As amines are weak bases, they can be ionized in the blood and equilibrate between the ionized and unionized form. Ionized drugs have better hydrophilic properties and can give the drug adequate water solubility. The unionized form can improve the hydrophobic character and allow for the drug to pass through lipid membranes. From this it is clear that the pK_a of a drug molecule is an important pharmacological property.

Orally absorbed drugs usually adhere to Lipinski's rule of five. These rules are a set of general guidelines for a drug to be successfully administered orally, but do not determine if a compound will be a successful drug candidate.[65] They state that:

- the drug has a molecular weight less than 500 g/mol
- contains no more than five hydrogen bond donor groups
- contains no more than ten hydrogen bond acceptor groups
- has a calculated logP (a measure of a drug's hydrophobicity) value less than +5.

Most orally administered drugs follow these rules but another criterion involves the number of rotatable bonds. The number of rotatable bonds can be used to describe the flexibility of the molecule. It was found that the more flexible a molecule is, the less likely it is to be orally active.[65] A polar surface area (PSA) of less than or equal to 140 Å^2 has also been suggested as recommended feature for a compound to be a successful drug.[65]

1.5.1.3.1.2 Distribution

Once in the blood stream, a drug is distributed throughout the body to various tissues and organs. Hydrophobicity is again an important factor and can determine if a drug is able to pass from the blood stream and into its target cell. If a drug is too hydrophobic it can be absorbed by fatty tissue and removed from the circulatory system however, if it is not hydrophobic enough it will not be able to pass through the lipid membrane. Ionized drugs also face distributary issues. They can bind to various macromolecules and be expelled from the blood stream or interact with plasma proteins such as albumin. Interactions involving plasma proteins results in an inadequate concentration of free drug reaching the target protein. Other barriers that some drug molecules have to overcome include the blood brain barrier. Here the capillaries are lined with tightly compacted cells which do not contain pores and contain a lipid rich coating. This makes it difficult for polar drugs such as penicillin to reach the brain.[63]

1.5.1.3.1.3 Metabolism

Drugs can be metabolised by a number of enzymes which cause a number of structural modifications, rendering the molecule biologically inactive or can increase the chance of renal clearance. This can occur in a number of tissues but generally most of these enzymatic transformations occur in the liver. Orally administered drugs experience what is known as the "first pass effect" which describes how drugs, taken orally, are directed to the liver once they enter the circulatory system. Here a certain percentage of the drug is metabolised by the hepatic enzymes before it can reach its target protein.[63]

The metabolism of drugs typically involves Phase I and Phase II metabolic reactions. Phase I one reactions generally involve the action of cytochrome P450 which is responsible for the majority of the metabolic transformations that occur. These reactions involve the addition of polar groups to the drug molecules by oxidase, reductase and hydrolase enzymes. *N*-Methyl groups and aromatic rings are examples of groups that are vulnerable to oxidation by oxidase enzymes while nitro and azo groups are susceptible to reductase enzymes. Cytochrome P450 can add such polar groups to foreign drug molecules to increase their water suability so they are more likely to be cleared *via* renal filtration. One example is the reduction of a keto group to an alcohol by the reductase enzyme NADH dehydrogenase.[64]

Highly polar functional groups can be added to drug molecules in Phase II metabolic reactions. The enzyme uridine-5'-diphospho (UDP) glucuronosyl transferase is responsible for attaching the highly polar glucuronic acid group to drug molecules. This results in the formation of *O*-glucuronides which are extremely polar and readily excreted.

1.5.1.3.1.4 Excretion

Drugs can be excreted in sweat, bile or exhaled but the kidneys are responsible for the majority of drug excretion. The kidneys remove chemicals, which are deemed as waste by the body, from the blood stream. Thus drugs and their metabolites are eventually removed in urine. Drugs and their metabolites enter the nephron of the kidneys through filtration; however each compound that enters is not directly removed. Non-polar drugs are reabsorbed into the blood supply while polar drugs, which can include the products of metabolism in the liver, remain in the nephron where they can be excreted in urine due to their increased aqueous solubility.[63]

1.5.1.3.1.5 Drug delivery

The ways in which the body can metabolise and destroy a drug molecule are vast. To combat this, there exist a number of drug delivery methods that protect the drug molecule from degradation allowing it to reach its target. Methods also exist that improve properties such as water solubility, which further increase the likelihood of a drug interacting with its target protein. These methods include the use of prodrugs or macromolecules such as cyclodextrins.[66,67] These methods will be explained in further detail in Chapter 5.

1.5.1.3.2 Pharmacodynamics

Pharmacodynamics is the study of how a drug binds to its target protein and evokes a biological response. It focuses on the key interactions such as hydrogen bonding, van der Waals forces and ionic interactions, to name a few, that are necessary for a drug to interact and sufficiently bind to a target protein. Structure activity relationship (SAR) studies can be used to identify the functional groups necessary for biological activity. This can involve preparing analogues where a particular functional group is altered or removed in order to determine if it will cause a change to activity. Certain functional

groups can also be important to activity as they can play a key role in the pharmacokinetics of a molecule. They can affect certain properties such as logP and pK_a for example. A pharmacophore model summarizes all the functional groups that are essential for activity, whether they are required for binding to a protein or improving the pharmacokinetic properties of the molecule.[63]

1.6   Aims

The aims of this project include:

- The identification of a lead molecule with the ability to disrupt the RBP4-TTR complex, with the goal of treating/managing T2D.

- Confirm its ability to disrupt the RBP4-TTR complex by means of biological assays including a fluorometric binding assay and a surface plasmon resonance assay.

- Assess its ability to treat/manage T2D in an animal model.

- The synthesis and characterisation of this lead molecule.

- A SAR study of the active lead compound to identify the key functional groups necessary for biological activity using the high throughput glucose uptake assay.

- Use the information gathered from the SAR study to possibly identify compounds that are more active than the initial lead compound. This will include the subsequent synthesis and characterization of these molecules.

- The design of a method for the identification of the secondary protein target. This will involve the derivitization of active compounds.

- The identification and synthesis of structurally distinct families of compounds which are also capable of inhibiting the RBP4-TTR complex with the aim to treat/manage T2D.

- Improve the ADME properties of an active compound to allow its use in aqueous solutions.

2. Identification of hit compounds 1, 2 and 3.

2.1   Computational studies leading to compound 1, 2 and 3.

The computational studies carried out by our collaborator Prof. Colin Fishwick (University of Leeds), involved the use of the eHiTS (electronic High Throughput Screening) software package (SimBioSys Inc.). The software docked flexible ligands within the RBP4 receptor (PDB: 1FEL) and rapidly and systematically counted mappings of interacting atoms between the RBP4 receptor and the ligand database using an exhaustive search algorithm. The binding pocket was first determined from the X-ray crystal structure of RBP4.

The software used a flexible docking method which allowed both the receptor and ligand to adopt numerous conformations and poses, thus avoiding severe steric clashes between the receptor and ligand. The binding mode for each conformation was determined and a binding score was assigned based on binding affinity for RBP4.

From a database of 57,576 compounds, compound **3**, **2** and **3** were uncovered (**Figure 2.1**). These compounds passed Lipinski's guidelines (< 5 hydrogen bond donors; < 10 hydrogen bond acceptors; molecular weight < 500; logP < 5), which indicated that the compound had potential to be used as a bioavailable and orally administered drug. The compounds were purchased from Maybridge (www.Maybridge.com) and tested in an assay to elucidate if it was capable of disrupting the RBP4-TTR complex formation. The assay used was surface plasmon resonance (SPR).
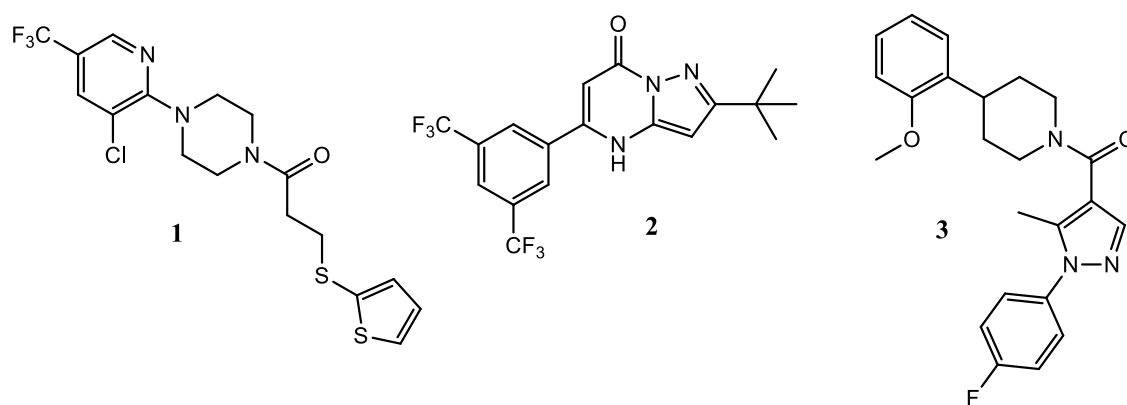
Figure 2.1. Structure of compounds **1**, **2** and **3**.

2.2   Surface Plasmon Resonance (SPR) analysis of 1, 2 and 3

Surface Plasmon Resonance (SPR) is an optical method used for measuring molecular interactions.[68] SPR involves immobilizing a binding molecule (e.g. *holo*, His-RBP4) onto the surface of a sensor chip. A certain concentration of compound (e.g. **1**, **2** or **3**) is then injected over the chip surface in a solution of SPR running buffer. This is followed by an injection of another binding molecule (e.g. untagged TTR).[69] Binding of molecules (i.e. formation of a complex) causes a change in mass on the sensor chip resulting in changes in the refractive index of the SPR running buffer. Changes to the refractive index indicate if binding has occurred and appears as an increase in resonance units (RU).[70]

The SPR experiments involving compounds **1**, **2** and **3**, carried out by our collaborator and it required *holo*, His-tagged RBP4 to be immobilized on the surface of a sensor chip.[69] Both TTR and the natural ligand ROH were then injected over the surface. This was followed by compound **1**, **2** and **3** which were tested at a range of varying concentrations (0-10 µM). At 0 µM of each compound formation of the RBP4-TTR complex occurred. This resulted in an increase in mass at the surface of the chip, causing changes to its refractive index which caused changes in the RU (**Figure 2.2**). As the concentration of each compound increased from 0-10 µM, a decrease in RU occurred. This was due to the fact that compounds **1**, **2** and **3** are capable of docking within the β-barrel of RBP4 and disrupting/preventing the formation of the RBP4-TTR complex.

(a)
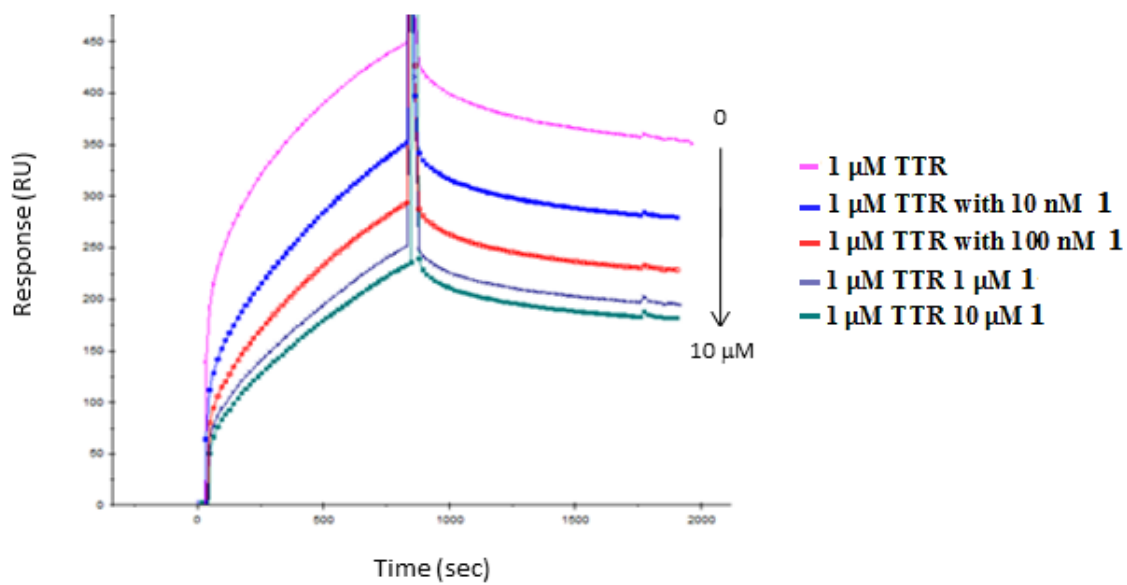
(b)
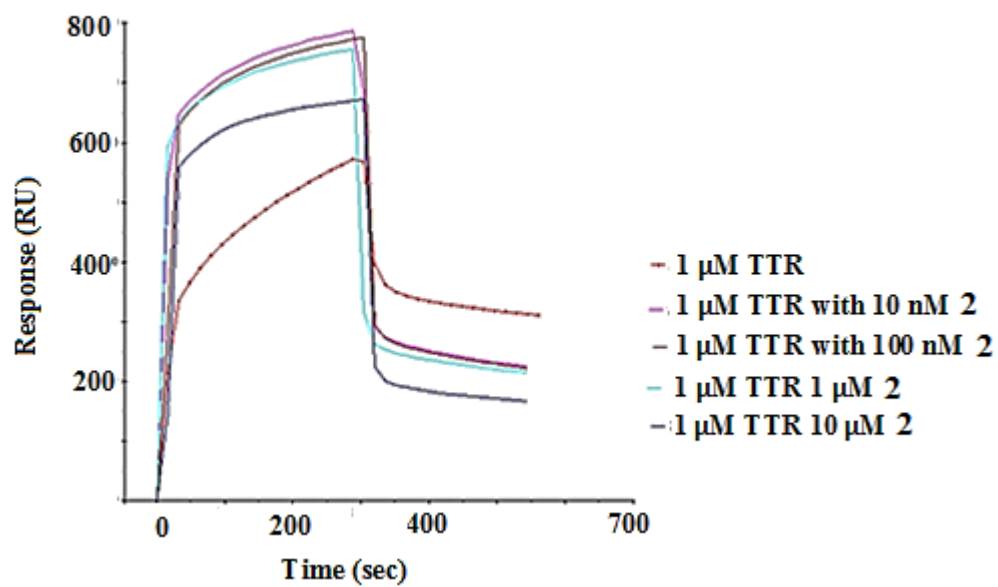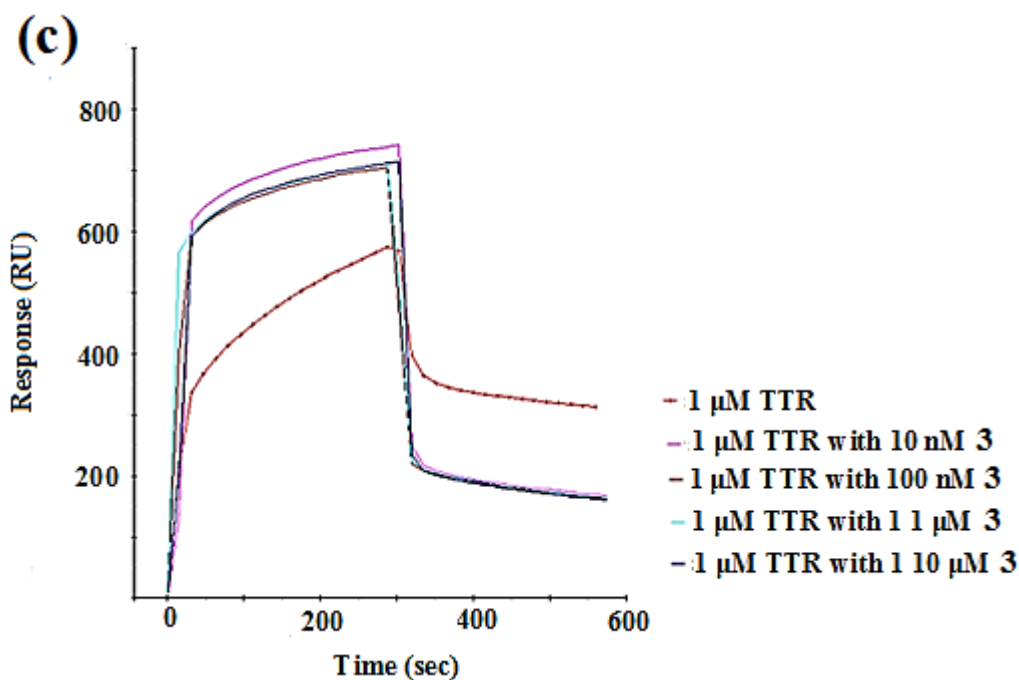
Figure 2.2: SPR analysis of (**a**) compound **1**, (**b**) compound **2** and (**c**) compound **3** Increasing concentrations of **1**, **2** and **3** result in a decrease in RU which corresponds to the inhibition of the interaction between 200 nM His-tag, bound RBP4 and 1 μM TTR.[69]

Figure 2.3 (a) is a 2D representation of the binding of **1** within RBP4. Compound **1** is predicted to bind with its pyridine ring buried in the protein cavity and its thiophene ring exposed at the loops of RBP4. Compound **1** exhibited key interactions with the residues Tyr90 and Arg121 in the RBP4 cavity. These interactions were also observed with the binding of the compound A1120 (**Figure 2.3 (b)**). This compound is a known inhibitor of the RBP4-TTR complex. It is believed that its binding within the RBP4 protein causes a conformational change at the entrance to the protein pocket by interfering with the position of the loops.[71,72] This prevents RBP4 from forming a stable interaction with TTR thus causing renal clearance of RBP4.[71] Compound **1** may act similarly to A1120 when disrupting the formation of the RBP4-TTR complex. The thiophene ring may serve to affect the position of the loops at the entrance of the protein cavity through steric hindrance. As previously mentioned, the hydroxyl group, found in ROH, is important for stabilizing the RBP4-TTR interaction. Therefore the removal of this group and its replacement with a thiophene ring, as found in compound **1**, may further destabilize the RBP4-TTR interaction.

(a)

(b)
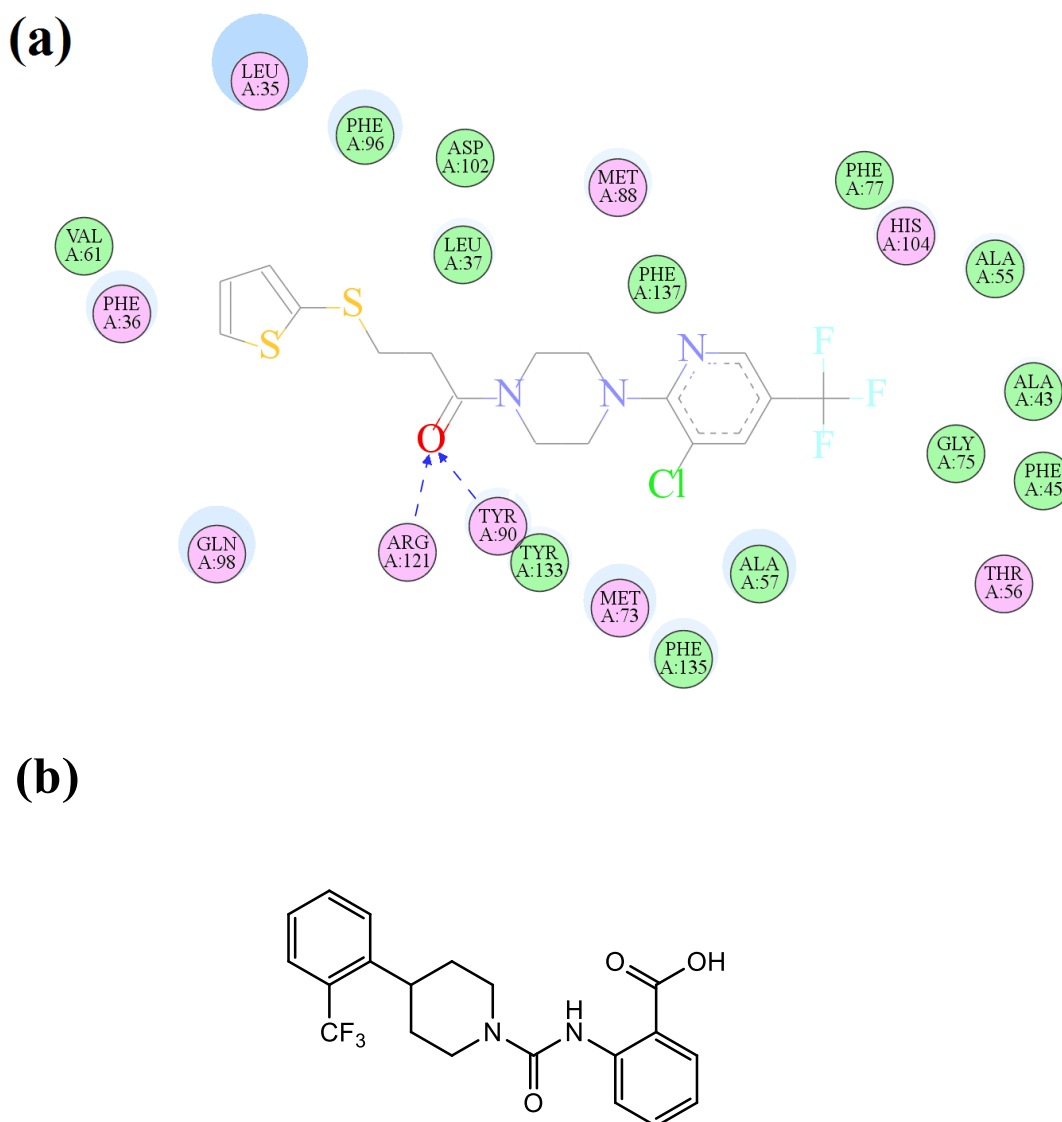
A1120

Figure 2.3. (a) Two dimensional (2D) depiction of the binding pose of **1** within RBP4, as depicted using the computer program MOE. Blue arrow indicates hydrogen bond interactions with the group at the base of the arrow the HBD and the group at the head of the arrow the HBA, blue shadow indicates solvent exposed residues, hydrophobic residues are all coloured with a green interior, polar residues are coloured with a purple interior **(b)** Structure of **A1120**.

2.3   Animal studies using compound 1, 2 and 3.

From the SPR assay, compounds **1**, **2** and **3** proved to be effective disruptors of the RBP4-TTR complex. As described in Chapter 1, the ability to disrupt the RBP4-TTR complex, thus lowering serum RPB4, is linked to improvements in insulin resistance. The use of the retinoid like compound Fen has shown this to be true as its use prevented high-fat diet (HFD) induced obesity, and the development of insulin resistance in mice, through the lowering of serum RBP4 levels.[56] Following this logic, the ability of compounds **1**, **2** and **3** to control/treat/reduce insulin resistance in mice, was investigated. A study examining the effects of these compound on a group of mice exposed to a HFD was thus performed by our collaborator.[69]

Two groups consisting of eight mice were exposed to a HFD so as to induce insulin resistance. Group A was exposed to a HFD which included either compound **1**, **2** and **3** at 0.04% w/w, relative to the quantity of food given.[69] This involved 400 mg of each compound be dissolved in 10 mL of DMSO which was then mixed in a 1 kg batch of HFD food.[69] Group B (control) only received a HFD with 10 mL of DMSO.[69]

2.3.1   Glucose tolerance testing (GTT) and insulin tolerance testing (ITT) of compound 1.

After 8 weeks, Group A and Group B (control) were both subjected to a glucose tolerance test (GTT), which examined how quickly glucose is cleared from the blood after a bolus of glucose is administered. An insulin tolerance test (ITT) was also performed which examined insulin sensitivity. Mice underwent a period of fasting (12 hours for GTT and 4 hours for ITT) before whole blood sampling was performed. An intra-peritoneal injection of either glucose or insulin was administered and whole blood sampling was subsequently performed on conscious mice at 30 minute intervals (**Figure 2.4**).[69]

Improved glucose handling and the ability to clear glucose more rapidly was observed in mice treated with **1**, compared to control.[69] Also, results from the ITT showed that mice treated with **1** also experienced improved insulin sensitivity.[69] Lower glucose levels at the varying time point indicates a more sensitized response to insulin (**Figure 2.4** (ITT)).
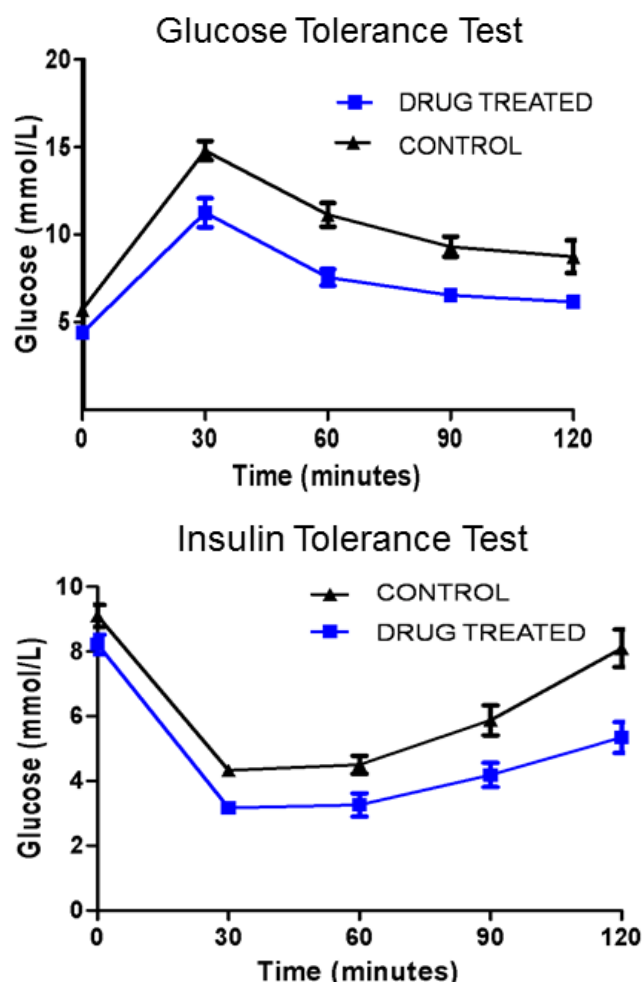
Figure 2.4: GTT and ITT results for Group A (drug treated; **1** (blue)) and Group B (Control (black)) insulin resistant mice. The decrease in glucose concentrations for both GTT and ITT indicate improved glucose handling with the use of compound **1**.

2.3.2   Glucose tolerance and insulin tolerance testing of compound 2 and 3.

Improved glucose handling and the ability to clear glucose more rapidly was observed in mice treated with compound **2**, compared to control (**Figure 2.5 (a)**). Compound **1** proved to be more effective than compound **2**. Insulin sensitivity was not greatly improved in mice treated with compound **3**, as seen from the results of the ITT (**Figure2.5 (b)**).

(a)

(b)
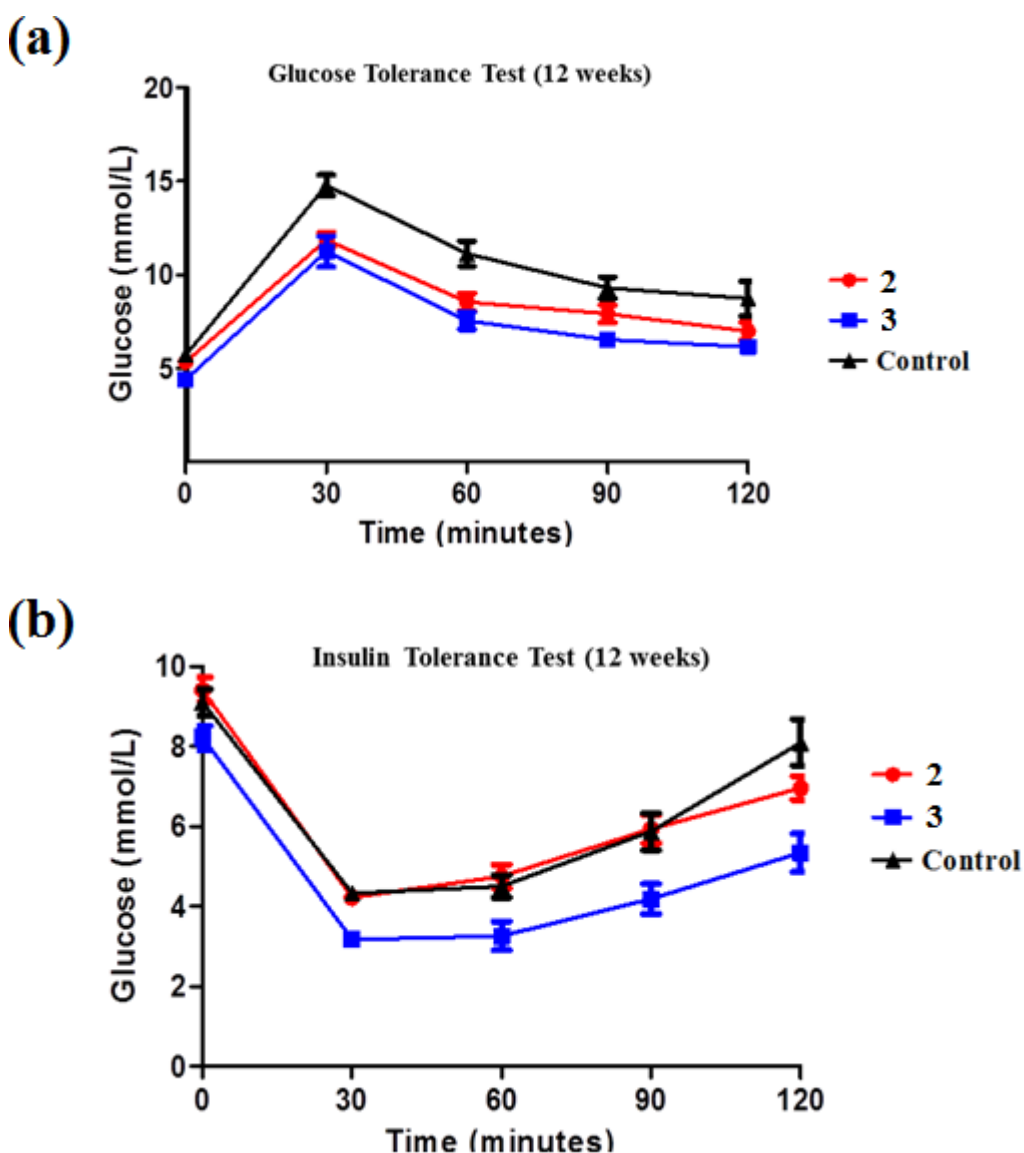
Figure 2.5: (a) GTT for drug treated (compound **2** and **3**) and insulin resistant (control) mice and **(b)** ITT results for drug treated (compound **2** and **2**) and insulin resistant (control) mice.

2.3.3   Weight loss studies with compounds 1 and 2.

Obese individuals are at a greater risk of T2D as increased fat mass leads to reduced insulin sensitivity. The link between obesity and insulin resistance described in Chapter 1. Ford *et al.* have reported that the risk of diabetes increases by 4.5% to 9% for every 1 kg increase in weight.[73] Obesity can also lead to other life threatening conditions such as dyslipidemia and cardio vascular disease. A number of current pharmaceuticals cause weight gain, which results in a worsening glycaemic control over time. Therefore

weight loss is a corner stone in the treatment and management of T2D.[56,74,16,7] New pharmaceuticals are therefore needed that improve insulin resistance without causing weight gain.

As well as showing improved the insulin and glucose profiles in mice, mice treated with **1** also exhibited a reduced weight gain over the 8 week period when compared to a control (**Figure 2.6 (a)**). Trials performed by our collaborators proved that this reduced weight gain was not due to a preference in food nor was it due to a reduced food intake.[69] This reduced weight gain was most likely a secondary effect as a result of the improved insulin resistant profile caused be the use of **1**. Although compound **2** was not as effective at reducing weight gain as compound **1**, a reduction in weight was still observed (**Figure 2.6 (b)**). This ability to cause a reduced weight gain is a remarkable characteristic of an antidiabetic drug.

(a)
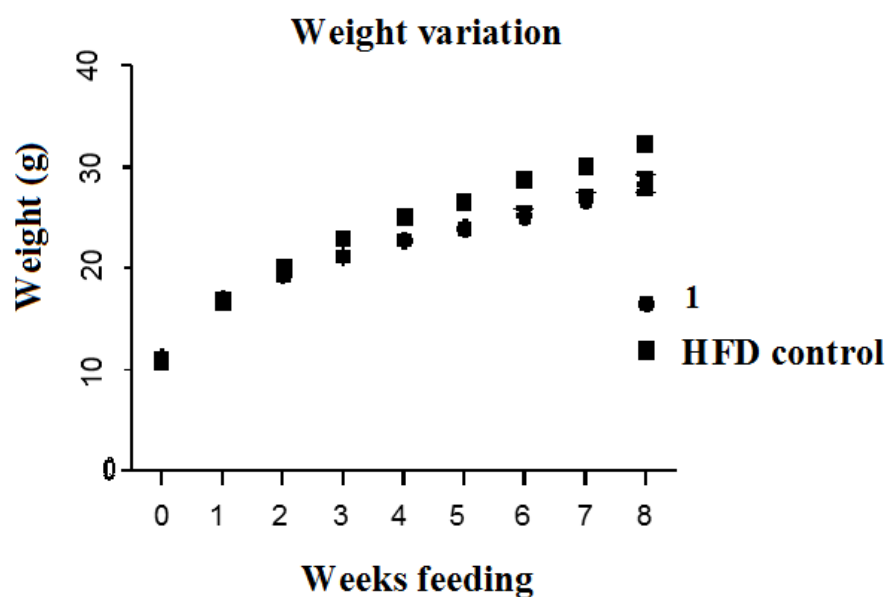
(b)
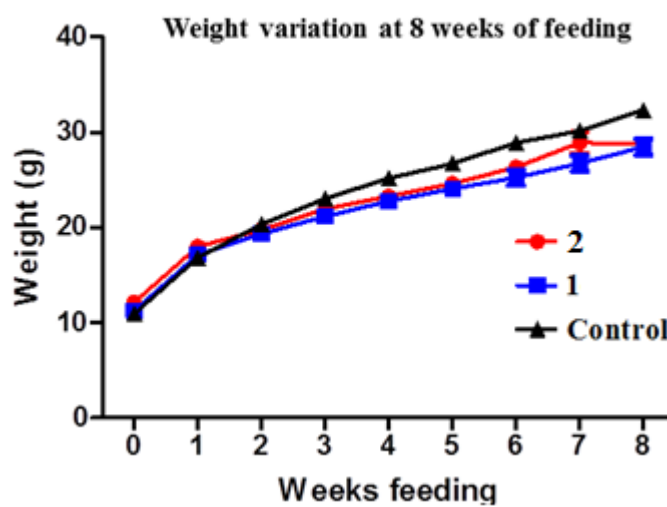
Figure 2.6: Weight variation in diabetic mice over an 8 week period (**a**)
Compound **1** (**b**) Compound **2**.

2.4 Initial structure activity relationship (SAR) study of compounds related to compound 1.

The excellent results obtained from both the SPR assay and the animal studies led to a desire to optimize compound **1** in terms of its antidiabetic properties. Eight compounds, **4**-**11**, were initially identified by systematically removing functional groups from the amide **1** (**Table 2.1**). For example, the aromatic nitrogen and the sulphur atom in the alkyl chain were removed to investigate their possible roles as HBA, while a carbonyl group was introduced into the alkyl as an alternative HBA. The chlorine atom was removed to examine its effect on the electronic properties of the aromatic ring. These compounds were subsequently synthesised and underwent a series of assays, namely fluorometric binding assay, SPR and glucose uptake assay.
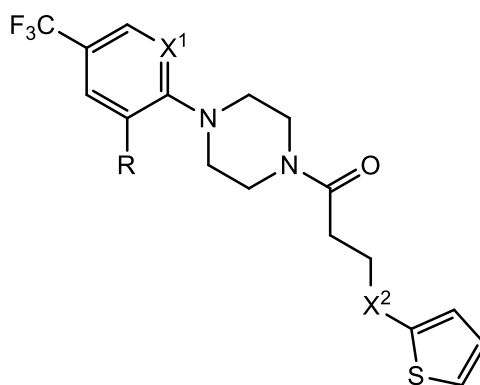
Compound	R	X^1	X^2
1	Cl	N	S
4	H	CH	CH_2
5	H	CH	C=O
6	H	N	C=O
7	Cl	N	C=O
8	H	N	CH_2
9	Cl	N	CH_2
10	H	CH	S
11	Cl	CH	CH_2

Table 2.1: Structures of compounds **1-11**.

39

2.4.1   Fluorimetric Binding Assay

The Fluorimetric Binding Assay quantitatively measures a compounds ability to dock within *apo*-RBP, by measuring the level of tryptophan fluorescence quenching that occurs.[57] A compounds ability to quench tryptophan fluorescence was evaluated at 280 and 350 nm. ROH and Fen, both known ligands of RBP4, showed the expected quenching of the tryptophan residue. However, the amide **4** and its analogue **5** both showed an unexpected increase in fluorescence **Figure 2.7 (a)**. Although this increase was not expected, conformational changes at or around the tryptophan residue may be responsible and this increase may still indicate some level of interaction between **4/5**and RBP4.[75]

Other analogues however showed no increase in fluorescence but showed a slight quenching affect indicating binding had occurred. Compound **9** was shown to quench the tryptophan residue better than the non-retinoid A1120 (**Figure 2.7 (b)**).[71,72]
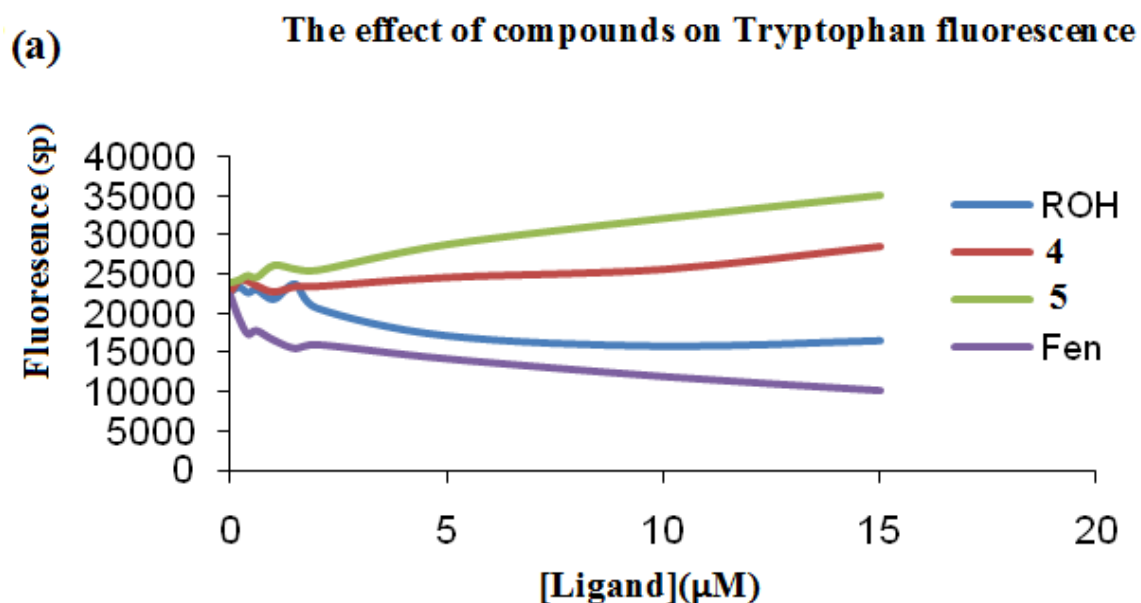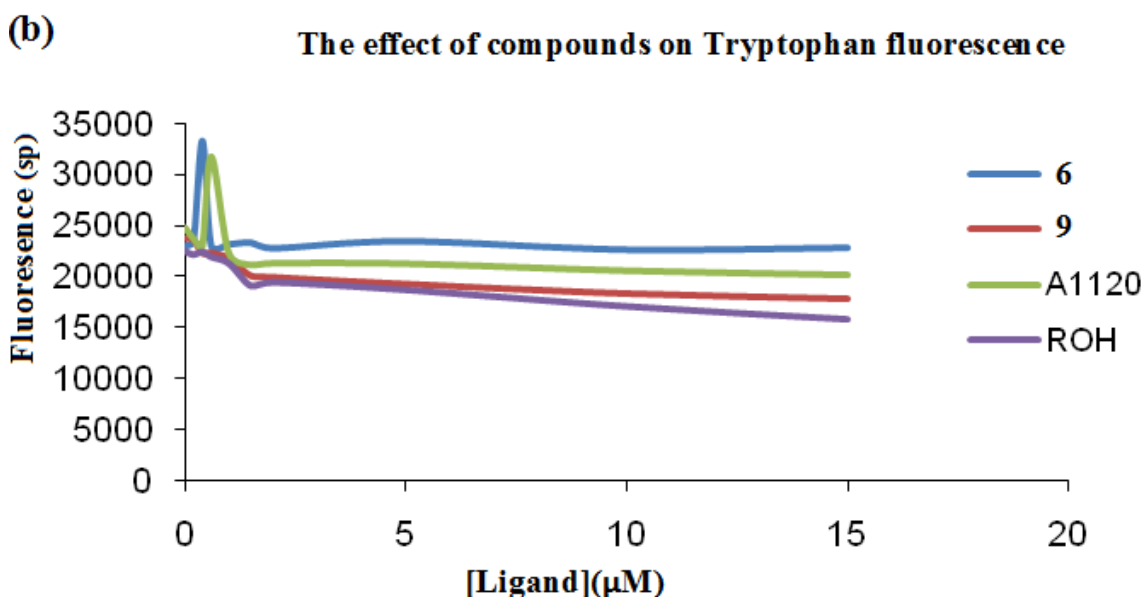
Figure 2.7. Fluorometric binding assay of **(a)** ROH, **4**, **5** and Fen **(b)** ROH, **6**, **9** and A1120. The binding of compounds to His tagged, *apo*-RBP4 was monitored by titration of the intrinsic fluorescence emission of the protein in the presence of increasing concentrations of compounds (0, 0.2, 0.4, 0.6, 1.0, 1.5, 2.0, 5.0, 10.0, 15.0 µM). The quenching of protein fluorescence due to the transfer of energy to the ligand was evaluated using excitation and emission wavelengths of 280 and 350 nm, respectively.

2.4.2 Surface Plasmon Resonance analysis of the derivative of the compound 1, compound 4.

SPR analysis was carried out by our collaborators in the same manner as previously mentioned in **section 2.2**.[69] His-RBP4 was immobilized on the surface of the chip, while TTR, ROH and **4** were consecutively injected over the surface. Results of the SPR assay show compound **4** to be a highly effective disruptor of the RBP4-TTR complex with results indicting that it was more potent than **4**.[69] The potency of **4** as a disruptor of the RBP4-TTR complex is more evident when the SPR results are compared to that of Fen.[56] From the SPR assay it is clear that the activity of **1** as a disruptor of the RBP4-TTR complex was further optimized in the form of **4** (**Figure 2.8**).

Compounds **5-11** were not tested in the SPR assay. However, their activity was examined in a glucose uptake assay.

41
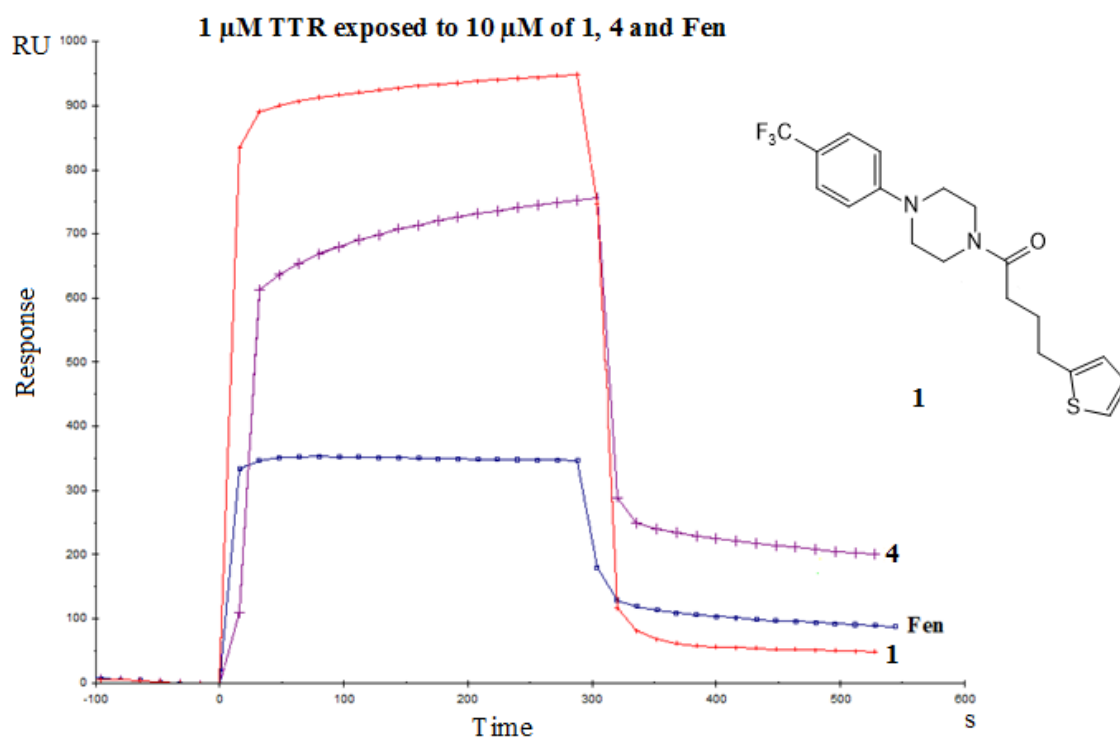
Figure 2.8: SPR assay results of 1 µM TTR exposed to 10 µM of **1**, **4** and Fen. SPR assay performed in SPR running buffer at a flow rate of 10 µL/min at 25 ºC.

2.4.3   Glucose Uptake Assay and the derivatives of compound 1 and compound 4.

Muscle cells are the main consumers of glucose within the body and extract glucose from the blood *via* an insulin dependent mechanism. Glucose is metabolised intracellularly by a process known as glycolysis.[14] This is a multi-step, catabolic process consisting of the breakdown of glucose into pyruvate, a pivotal point of aerobic respiration.[14] An example of a key step in glucose metabolism, glycolysis, is the phosphorylation of glucose by the enzyme hexokinase into glucose-6-phosphate.[14]

A distinct characteristic of T2D is the decreased sensitivity of muscle cells to insulin.[76] When insulin is used as a treatment, it stimulates the uptake of glucose by muscle cells. Therefore, a compound that is capable of stimulating this uptake of glucose within muscle cells would be useful as a diabetic treatment. Compounds were subsequently tested for their ability to induce the uptake of radiolabelled glucose within muscle cells.

The glucose uptake assay measures the amount of ^{3}H deoxy-2-glucose, a tritiated analogue of deoxy-2-glucose, taken up by muscle cells. ^{3}H deoxy-2-glucose is used as its biochemical properties allow for it to be easily traced and measured within a cell.[77]

As with glucose, the glucose transporter GLUT4 also transports ^{3}H deoxy-2-glucose into muscle cells. Here it is phosphorylated by hexokinase to give ^{3}H deoxy-2-glucose-6-phosphate which is then susceptible to hydrolysis by the enzyme glucose-6-phosphatase.[77] As muscle cells have extremely low levels of this enzyme, the tritiated substance remains in the cell where it can be quantitatively measured.[77]

2.4.3.1 Compound 4 induced glucose uptake

The glucose uptake assay was carried out by our collaborator Dr. Darren Martin.[69] Incubation of C2C12 muscle cells with 10 µM of compound **4** followed by exposure to 1µCi/ml ^{3}H deoxy-2-glucose, stimulated the uptake of ^{3}H deoxy-2-glucose within the cells. This stimulation was significant compared to basal (i.e. a control), which are cells exposed to ^{3}H deoxy-2-glucose in the absence of a drug. This stimulation was time dependent with **4** only causing the uptake of glucose after cells were incubated with compound **4** overnight (**Figure 2.9**).
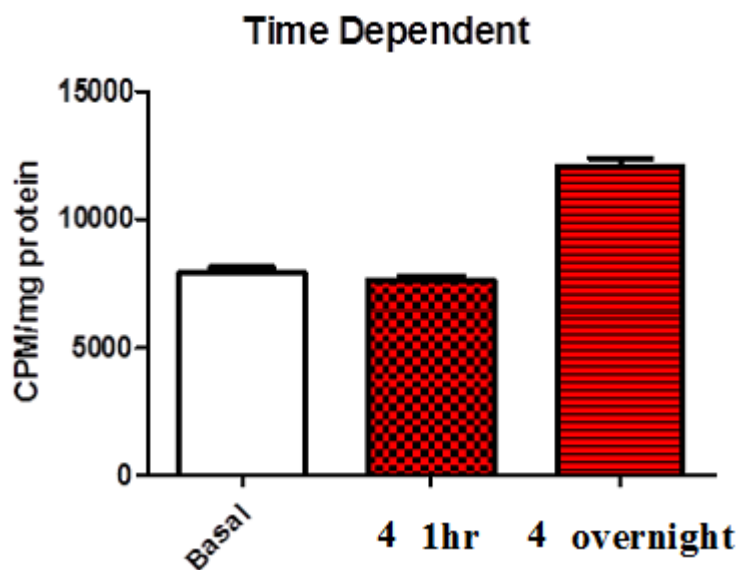
Figure 2.9: Time dependent compound **4** induced glucose uptake. C2C12 muscles cells incubated for 1 hr or overnight in the presence of compound **4**. Cells then exposed to ^{3}H deoxy-2-glucose for 10 mins and a scintillation count of the C2C12 muscle cells performed.

Surprisingly, when other compounds such as **1** and Fen, which were both highly active in the SPR assay, were tested for their ability to stimulate glucose uptake, they were found to be inactive (**Figure 2.10**).
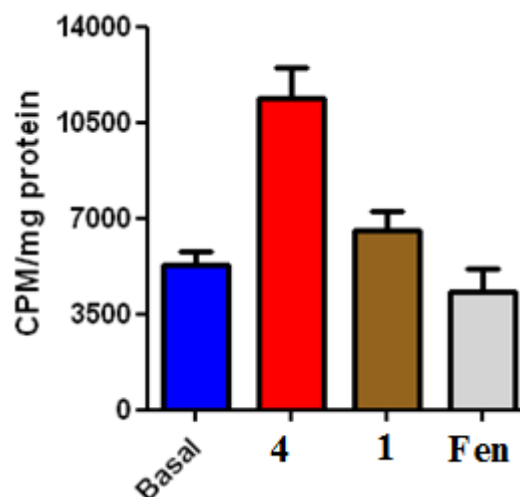
Figure 2.10: Glucose uptake assay results for **1**, **4** and Fen. C2C12 muscle cells incubated overnight at 37 ºC in the presence 10 µM of each compound. Cells then exposed to ^{3}H deoxy-2-glucose for 10 mins and a scintillation count of the C2C12 muscle cells performed.

The success of **4** in the glucose uptake assay, and its increased potency compared to **1**, rendered it necessary to identify the functional groups responsible for evoking the biological response. A structure activity relationship (SAR) study was carried out to ascertain the functional groups responsible and their possible role in stimulating glucose uptake.

2.5   Conclusion.

The aims of this section of the project were achieved with the identification of three RBP4-TTR inhibitors. Compounds **1**, **2** and **3** proved to be active in the SPR assay confirming their ability to inhibit the formation of the RBP4-TTR complex. Animal studies were also encouraging as these compounds were successful in controlling glucose levels but also improving insulin sensitivity in mice.

An additional important result was the reduced weight gain observed with the use of compound **1**. As many current antidiabetic drugs have the unwanted side effect of weight gain, a compound that can act as an insulin substitute while reducing weight gain would be highly beneficial to the diabetic patient.

A SAR study was performed on the amide **1** which led to the design and synthesis of eight compounds, **4-11**, which were tested in a number of assays such as the fluorometric binding assay and the glucose uptake assay. Compound **4** proved to be more active than compound **1** in the SPR assay and the glucose uptake assay.

3. Synthesis of compound 1 and its derivatives, 4-81.

3.1   Introduction

The piperazine heterocycle is found in a wide range of biologically active molecules. For example, it is present in drugs responsible for the treatment of HIV and osteoarthritis while the piperazine containing *N*-substituted-6-acylbenzothiazolones are active analgesics.[78,79] The piperazine molecule itself is of biological interest as it has been reported to function as a potent anthelmintic, removing either *Enterobius* or *Ascaris* from humans.[80]

The biogenic amine, 5-hydroxtryptamine (5-HT), commonly known as serotonin, is a neurotransmitter that controls a number of important biological processes by interacting with a family of receptors known as 5-HT receptors.[14,81] The serotonin receptors are subdivided into the seven classes 5-HT$_{1-7}$, with 5-HT$_6$ the most recently discovered.[81] A number of antipsychotic and antidepressant drugs are known to bind to this receptor. The below piperazine containing antagonists, **12** and **13**, have been shown to have a high affinity for the 5-HT$_6$ receptor (**Figure 3.1**).
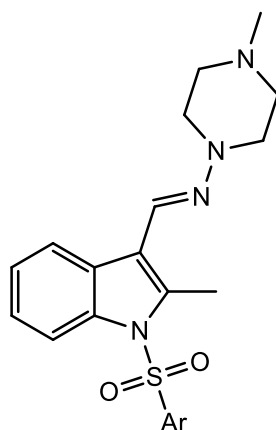
Figure 3.1. 5-HT$_6$ antagonists, **12**: Ar = 5-chloro-2-methoxy-4-methylphenyl, **13:** Ar = 5-(dimethylamino)napthyl.[81]

Interestingly, it has been shown that antagonists of this receptor cause a reduction in appetite and an increase in weight loss. As a result, this receptor is being investigated for its role in the treatment of obesity.[81]

3.1.1   Arylpiperazines and their synthesis

Numerous antifungal, antibacterial, antidepressant, antipsychotic, antihypertensive and even recreational drugs, contain arylpiperazines. As previously described, they are

particularly common in the field of neuroscience where they are often found in ligands for dopamine and serotonin receptors.[82] As the arylpiperazine moiety is present in a broad and diverse range of pharmaceuticals and biologically active compounds, various synthetic approaches are needed to allow access to the necessary arylpiperazine derivatives. The formation of the C-N arylpiperazine bond can be performed using a variety of synthetic approaches, including metal catalysed reactions, nucleophilic aromatic substitutions (S_NAr) and cyclocondensations involving anilines.[83,84,85]

3.1.2   Metal catalysed arylpiperazine synthesis

3.1.2.1 Ullmann reaction

First reported in 1901, the traditional Ullmann reaction involves the homocoupling of aryl halides in the presence of copper powder, with reaction temperatures generally in excess of 200 °C.[86,87,88,89] Attempts have been made throughout the years to improve these harsh conditions with the use of activated and alternative metals, such as nickel and palladium. Work by Nadri *et al*. has allowed for the homocoupling of bromobenzene using palladium diacetate and a phosphine ligand at 100 °C with the biaryl product isolated in a quantitative yield.[90]

Ullmann type reactions involve the coupling of nucleophiles such as phenols or amines with aryl halides. This generally involves the use of copper salts such as CuI with reaction temperatures typically ranging from 100-150 °C.[88,91] For example, Ma *et al*. reported the CuI catalysed coupling of an aryl halide with an amino acid, while Hoffmann-la Roche *et al*. utilised the Ullmann type aryl-amine bond formation in the synthesis of the below arylpiperazine **14** (**Scheme 3.1**).[88,92] The proposed mechanism for the copper catalysed Ullmann reaction is shown in **Scheme 3.2** where the mechanism is thought to proceed through two possible pathways; (**A**) oxidative addition of the aryl halide occurs primarily or (**B**) transmetallation is the first step in the pathway. Both pathways culminate in the formation of a Cu(II) species followed by an elimination step to give the coupled product and the regeneration of the Cu(I) halide.[93]
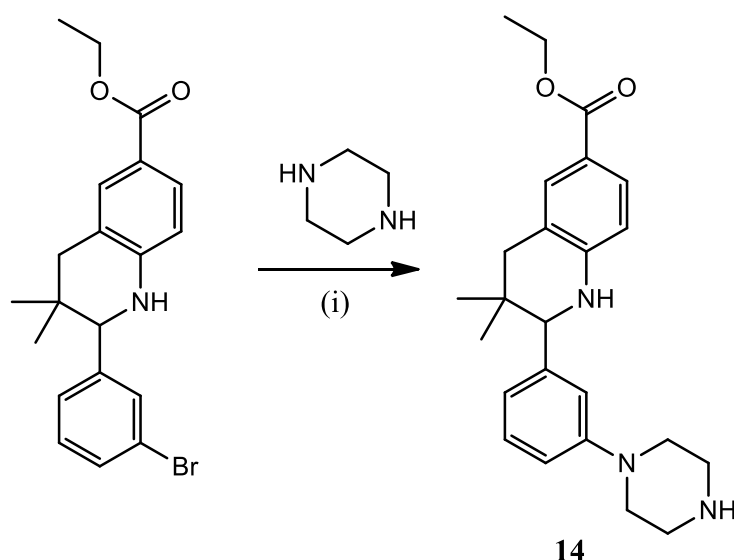
Scheme 3.1: The Ullmann type C-N bond formation, (i) CuI, *N*, *N*-dimethylglycine hydrochloride, K_2CO_3, DMSO, 16 hrs, 120 °C, 80%.[92]
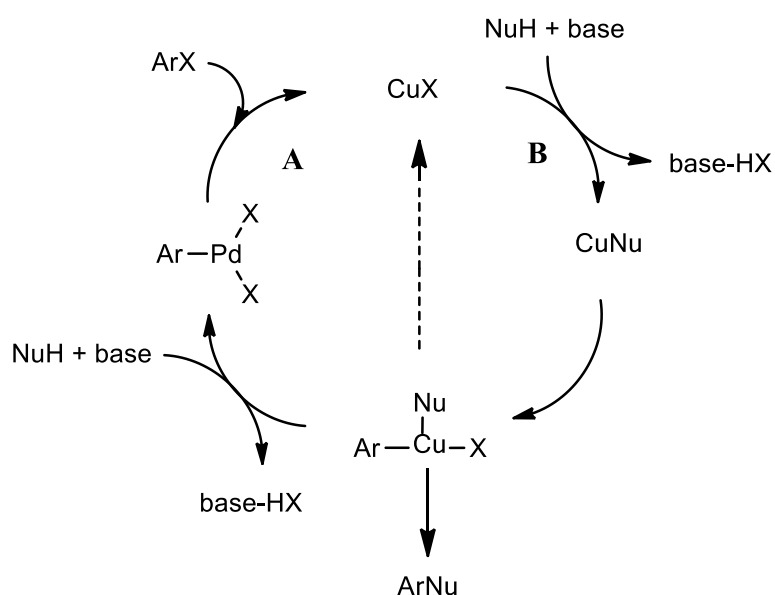
Scheme 3.2: The proposed mechanism for cooper catalysed Ullmann coupling.[93]

3.1.2.2 Buchwald-Hartwig amination

Discovered by Stephen L. Buchwald and John F. Hartwig, this amination involves aryl-amine couplings mediated by a palladium catalyst and typically a suitable phosphine ligand.[94] In 1994, both Buchwald and Hartwig independently reported aryl-amine couplings employing a combination of palladium and tin.[95,96] However, due to the

toxicity associated with the use of stannanes, this was quickly followed by a tin-free synthesis (**Scheme 3.3**).[97,98]
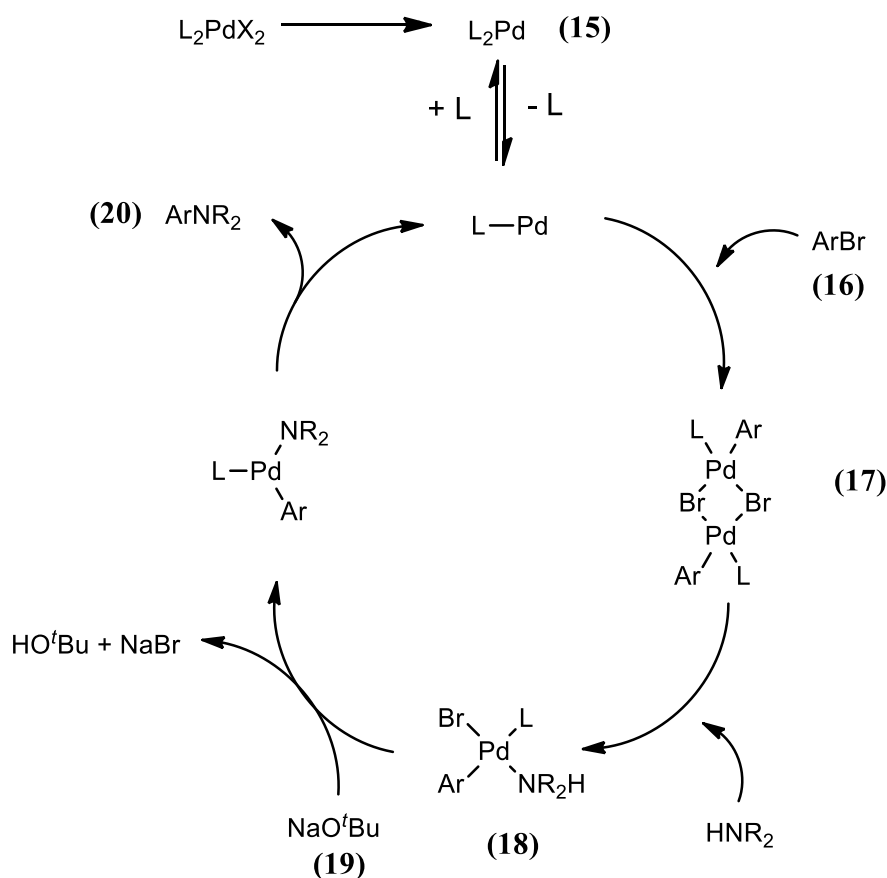
Scheme 3.3: Tin-free, palladium catalyzed aryl-amine coupling.[98]

The mechanism of the Buchwald-Hartwig amination proceeds through steps similar to that of a palladium catalyzed C-C bond formation. Reduction of Pd(II) to Pd(0) (**15**) is followed by oxidative addition of the aryl halide (**16**) to the Pd(0) species. This affords a dimeric aryl halide complex (**17**). The dimer is then cleaved by the amine to give a monometallic aryl halide intermediate which contains a single phosphine and a single amine ligand (**18**). The acidity of the amino proton is increased due to coordination of the amine to the palladium. This allows for the deprotonation of the acidic proton by a suitable base such as LHMDS or NaO^{t}Bu (**8**). Reductive elimination of the amine containing complex produces the arylamine (**20**) and regenerates the Pd(0) complex.

This palladium catalyzed reaction was used for the synthesis of the below arylpiperazine (**21**), which was a precursor for the adenosine receptor subtype, A$_{2A}$, antagonist **22** (**Scheme 3.4**). The A$_{2A}$ receptor is expressed in the striatum of the brain and stimulates

adenylate cyclase activity which controls AMP levels and thus plays a vital role in motor function. It is known that A_{2A} antagonists prevent motor function disturbances and have the potential to act as a new class of anti-symptomatic drug for conditions such as Parkinson's disease.[99]
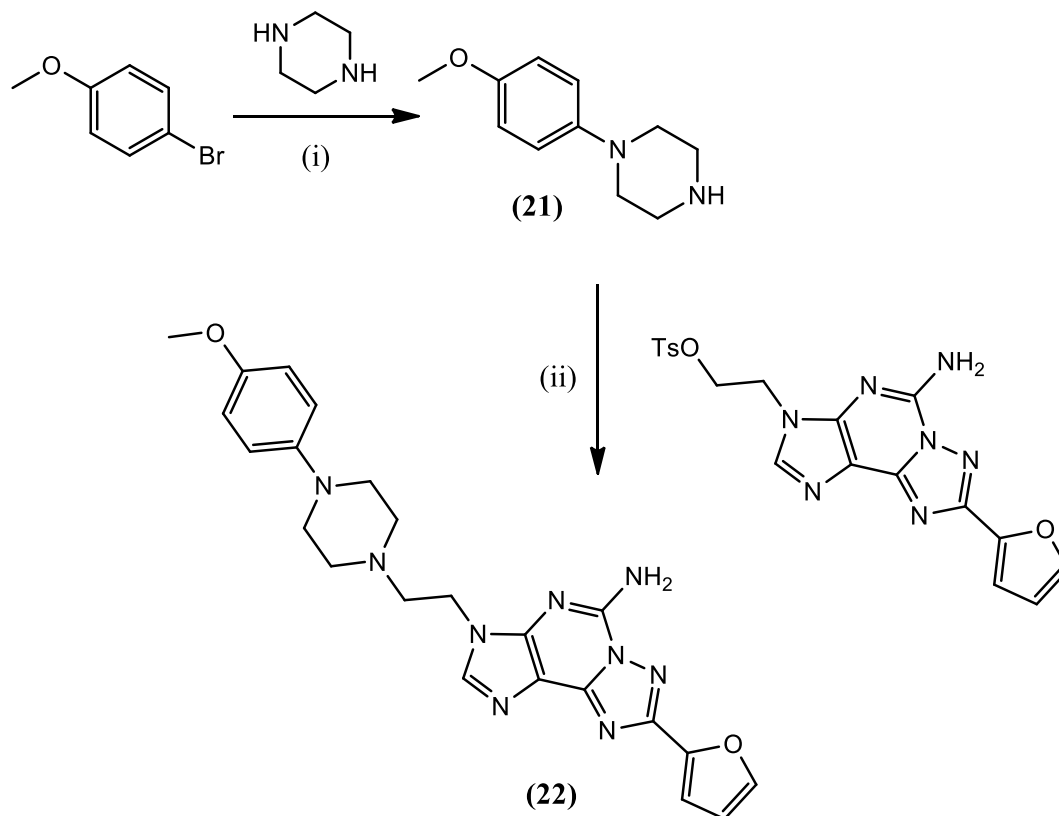
Scheme 3.4: Buchwald-Hartwig amination for the synthesis of arylpiperazines, (i) $Pd_2(dba)_3$, NaO^tBu, BINAP, toluene, 80 °C, overnight, 70% (ii) DMF, 90 °C, 5 hrs, 60%.[99]

3.1.3 Nucleophilic aromatic substitution (S_NAr)

Nucleophilic aromatic substitution is an addition-elimination reaction where a nucleophile is added to an aromatic ring resulting in the loss of a suitable leaving group. Common nucleophiles include groups containing nitrogen or oxygen such as cyanides, while halides generally act as the leaving group. The presence of an electron withdrawing group, such as a nitro or CF_3 group, *ortho* and/or *para* to the leaving group, is required in order to create an electron poor, hence electrophilic aromatic ring.[100]

The addition of the nucleophile to the aromatic ring is the slow rate determining step as it disrupts aromaticity, while the elimination of the leaving group is the faster step as it involves the restoration of aromaticity (**Scheme 3.5**).[100]
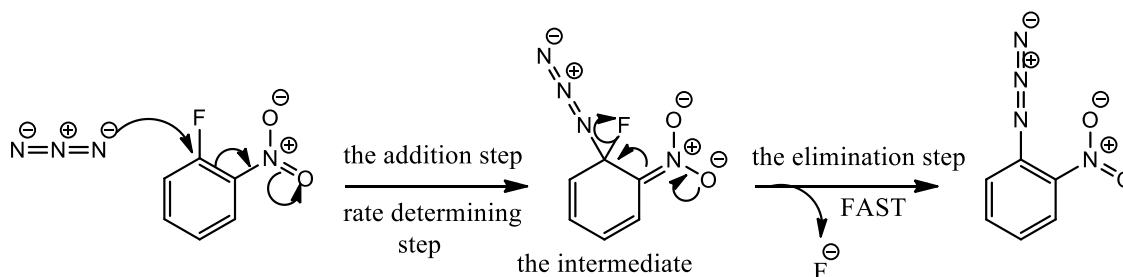
Scheme 3.5: Nucleophilic aromatic substitution: The addition-elimination mechanism.[100]

As can be seen from the above scheme, fluoride is a useful leaving group in S_NAr reactions. F$^-$ is regarded as poor leaving group in other transformations, due to the strength of the C-F bond. However its enormous inductive effect, which stabilises the anionic intermediate, aids in the aromatic ring's acceptance of the nucleophiles electrons.[100]

3.1.3.1 S_NAr reactions and microwave (MW) irradiation

S_NAr reactions generally employ conventional heating methods in the synthesis of arylpiperazines, and typically involve heating at reflux in a suitable solvent. However, reaction times can be long. In general, the use of MW irradiation can shorten the reaction time and in some cases, improve yields. MW irradiation has been successfully employed in the synthesis of arylpiperazines.[101]

3.1.3.2 Microwave Synthesis

Since Gedye and Majetich first reported the use of MW for the acceleration of organic reactions, the use of MW heating has become a valuable tool to synthetic chemists.[102] MW synthesis is capable of decreasing reaction times and improving yields due to its efficient method of energy transfer.[102]

A MW is a form of electromagnetic energy that consists of an electric field and a magnetic field.[102] Microwaves are found at the lower end of the electromagnetic spectrum, between radio and infrared frequencies, and are characterized in the 0.3 to

300 GHz frequency range.[103] The energy of a MW photon at this range only affects molecular rotation and does not possess sufficient energy to cleave molecular bonds, therefore molecular structure is unaffected.[103] MW assisted heating can involve the direct coupling of microwaves with the reactant molecules. The ability of microwaves to heat a substance depends on a materials capacity for absorbing energy and converting it into heat.[103] Unlike conventional heating methods which rely on conduction or convection for the transfer of energy, MW energy is primarily transferred by dielectric loss. The electric field is responsible for the transfer of energy from MW to material *via* dipole rotation or ionic conduction.

MW irradiation can cause an increase in the rate of reaction. The rapid increase in temperature provides the reaction system with a large amount of energy relative to the energy needed to overcome the activation barrier. This fact is responsible, not only for the increase in reaction rates, but also for the improved yields. From the Arrhenius equation (**Equation 3.1**), it is clear that an increase in temperature results in an increase in the rate of reaction.[104]

$$k = Ae^{-Ea/RT}$$

Equation 3.1: The Arrhenius equation.

3.1.3.3 Arylpiperazine synthesis

Although the scope of metal catalysed arylpiperazine synthesis is broad, one disadvantage associated with this synthetic approach is the cost of the metal catalysts and if required, the ligand.[105] MW irradiation offers a facile and versatile approach to arylpiperazine synthesis without the use of costly metal catalysts or ligands. This was evident in the synthesis of a series of substituted arylpiperazines carried out by Meng *et al.*.[105] Here piperazine, *N*-methylpiperazine or morpholine were reacted with a variety of substituted fluorobenzene derivatives using *N*-methyl-2-pyrrolidone (NMP) as a solvent. In one such example, 1,2,4,5-tetrafluorobenzene was reacted with all three amines to give the arylpiperazines in excellent yields and short reaction times (**Scheme 3.6**).[105]
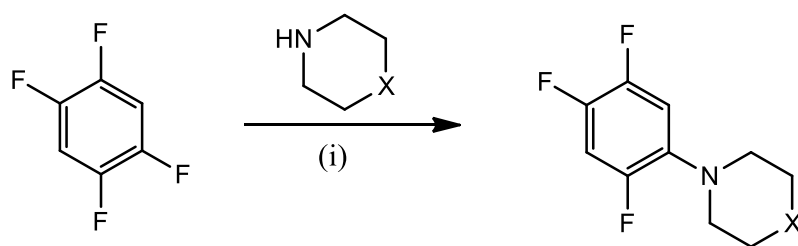
Entry	X	Time (hrs)	Yield (%)
1	NH	1.5	87
2	N(CH$_3$)	1	90
3	O	1	86

Scheme 3.6: Synthesis of fluorinated arylpiperazines using MW irradiation (i) K$_2$CO$_3$, NMP, MW.[105]

Aromatase is a member of the cytochrome P450 family that is involved in the catalytic conversion of C19 steroids to oestrogens.[106,107] Exposure to oestrogens has been linked to the promotion of hormone related diseases such as breast cancer with expression of aromatase more significantly induced in cancerous breast tissue compared to healthy tissue.[106, 108] For this reason aromatase inhibitors provide a viable option for the decrease in oestrogen production and thus the treatment of breast cancer.[106,107,108]

The compound letrozole (**Scheme 3.7**) is an active aromatase inhibitor used in the clinical treatment of breast cancer.[109] Compound **23** is a letrozole analogue synthesised in the search for a new lead compound where MW assisted arylpiperazine synthesis was used to generate the arylpiperazine from the fluorobenzene precursor.[109] The compound was synthesised in an extremely short reaction time and in an excellent yield, demonstrating the efficiency of MW assisted arylpiperazine synthesis.
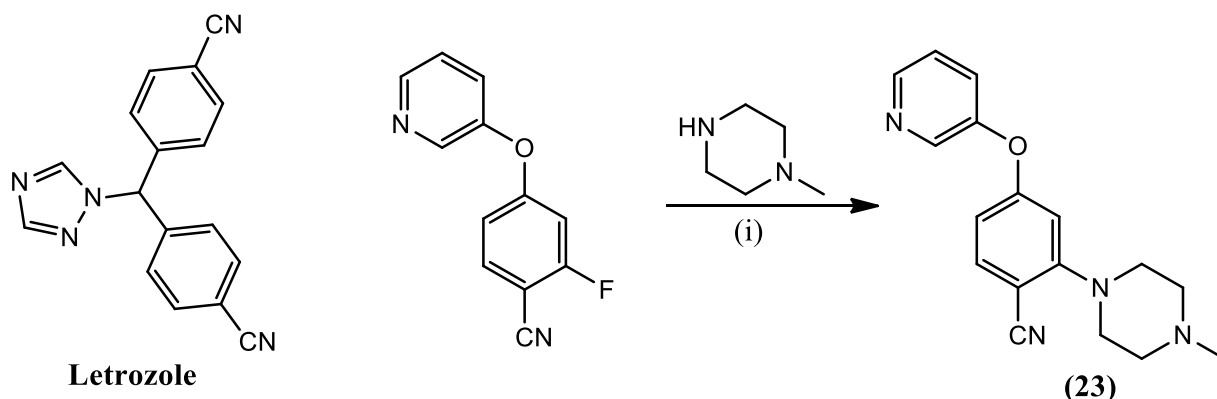
Scheme 3.7: Structure of letrozole and the synthesis of compound **23** with similar biological activity to Letrozole, (i) NMP, MW, 15 mins, 95%.[109]

The efficiency of arylpiperazine synthesis using MW conditions was apparent in the synthesis of the piperazine 1-(pyridin-2-yl)piperazine (**Scheme 3.8, 24**). Bromopyridine was reacted with piperazine in the absence of a solvent to give the arylpiperazine in a 54% yield after twenty minutes.[110] When Milkiewicz *et al*. attempted the synthesis of **24** using metal catalysis, a substantial reduction in yield was observed. 2-Bromopyridine and piperazine were reacted in the presence of the palladium catalyst tris-(dibenzylideneacetone)dipalladium[(0)] and 2,2'-bis-(diphenylphosphino)-1,1'- binaphthyl. The reaction was heated at reflux in toluene for eighteen hours, however an almost twenty per cent reduction in yield compared to the MW assisted approach, was observed.[111]
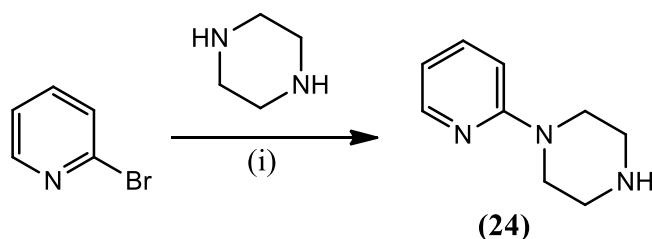
Scheme 3.8: Synthesis of the arylpiperazine **24**, (i) 150 °C, 20 mins, 54%.[111]

3.1.4   Cyclocondensations

Previous examples saw the arylpiperazine moiety synthesised from aryl halides and piperazine *via* a nucleophilic aromatic substitution. An alternative approach to this involves a cyclocondensation reaction between anilines and *N*, *N*-bis(2-haloethyl)amines (**Scheme 3.9**).
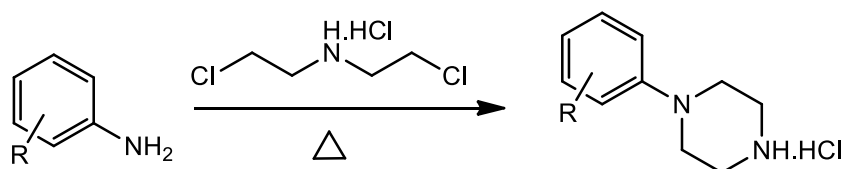
Scheme 3.9: Synthesis of arylpiperazines *via* cyclocondensation of anilines and *N*, *N*-bis(2-haloethyl)amines.

A broad range of anilines can be used in this cyclocondensation approach, resulting in the synthesis of a vast array of arylpiperazine derivatives. This was demonstrated by Liu *et al.* who heated the appropriate aniline and *N,N*-bis(2-chloroethyl)amine in diethylene glycol monomethyl ether at 150 °C resulting in the formation of the HCl salt of the arylpiperazine.[82] The nature of the aniline substituent did not greatly affect the cyclocondensation with arylpiperazines generated in yields ranging from 66-95% (**Scheme 3.10**).
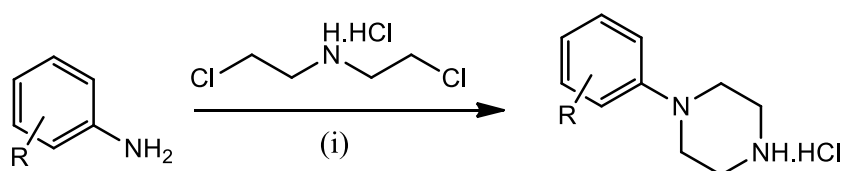
Entry	R	Yield(%)*
1	H	79
2	4-nitro	90
3	3-CO$_2$Et	90
4	3-OMe	95

Scheme 3.10: Synthesis of arylpiperazines *via* cyclocondensation (i) diethylene glycol monomethyl ether, 150 °C, *Isolated yields based on free amine.[82]

This approach was also employed by Juvale *et al.* to produce a series of arylpiperazine derivatives which were subsequently used to synthesise a number of quinazoline piperazole analogues (**Scheme 3.11, 25**).[112]

(25)
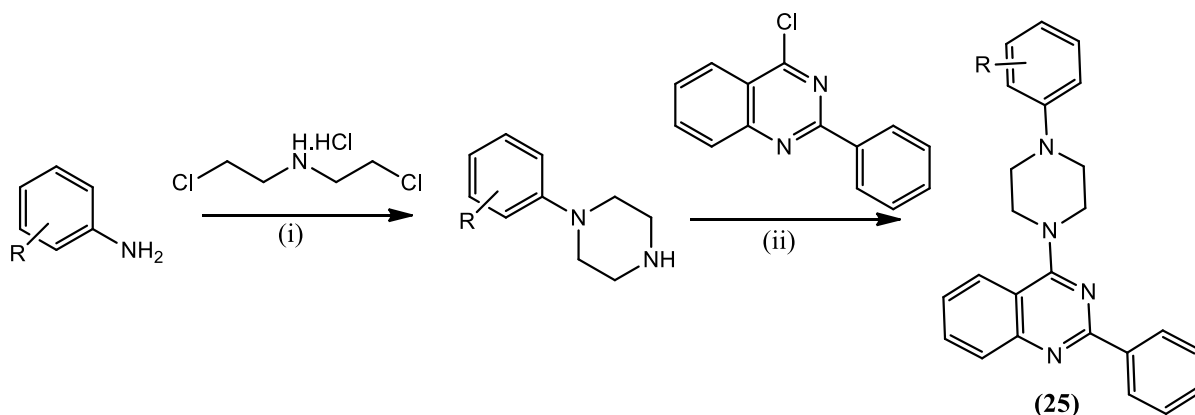
Scheme 3.11: Preparation of arylpiperazines *via* a cyclocondensation approach and subsequent synthesis of quinazoline piperazoles, (i) diethyleneglycol monomethyl ether, reflux, 6–12 hrs, 55-65% (ii) K_2CO_3, *iso*propanol, reflux, 10–12 hrs, 45–64%.[112]

3.1.5   Synthesis of amide bonds

Amide bonds can be synthesised in a variety of ways, with the most common method involving the use of coupling reagents to activate the carboxylic acid *in situ*. In the absence of coupling reagents, the merger of these two groups, with the required loss of water, can only happen at high temperatures and such conditions can be damaging to the overall integrity of the reactants. Therefore coupling reagents are often used to increase the reactivity of one of the reagents. The simplest way of doing this is by activating the carboxylic acid with the use of coupling reagents; thus forming an activated species (**Scheme 3.12**).[113] Coupling reagents are used to generated more reactive intermediates such as acid chlorides, anhydrides, carbonic anhydrides or activated esters.[113]
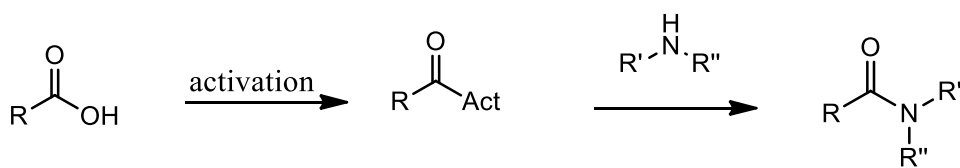
Scheme 3.12: Activation of carboxylic acid leading to amide bond formation.[113]

3.1.5.1 Types of coupling reagents

A wide variety of coupling reagents exist ranging from carbodiimides, the very first coupling reagents synthesised, to the potentially explosive benzotriazoles.[113] Such a variety of reagents exist as the coupling reagent needs to be able to deal with a broad range of substrates and their differing reactivities.[113] Two of the more common reagents are described in more detail below.

3.1.5.1.1 Carbodiimides

Carbodiimides were the first coupling reagents employed in amide bond formation and are still widely used to this day. One of the most commonly used carbodiimides is dicyclohexylcarbodiimide (DCC), which has been used as a coupling reagent since 1955.[114] Its use produces the white, and generally insoluble, by-product dicyclohexyl urea (DCU), which can be easily removed by filtration.[113]

The mechanism of action first involves the formation of the activated ester intermediate, the *O*-acylurea (**26**), which is then attacked by the nucleophilic amine to yield the amide product and the DCU (**27**) by-product (**Scheme 3.13**). Formation of an amide *via* an anhydride species (**28**) can also occur if enough carboxylic acid is present in the reaction mixture. In this case, the carboxylate anion attacks the activated ester forming the anhydride. This is subsequently attacked by the amine giving the desired amide product. The *O*-acylurea species can also give rise to an *N*-acyl urea by product (**29**) (**Scheme 3.13**).
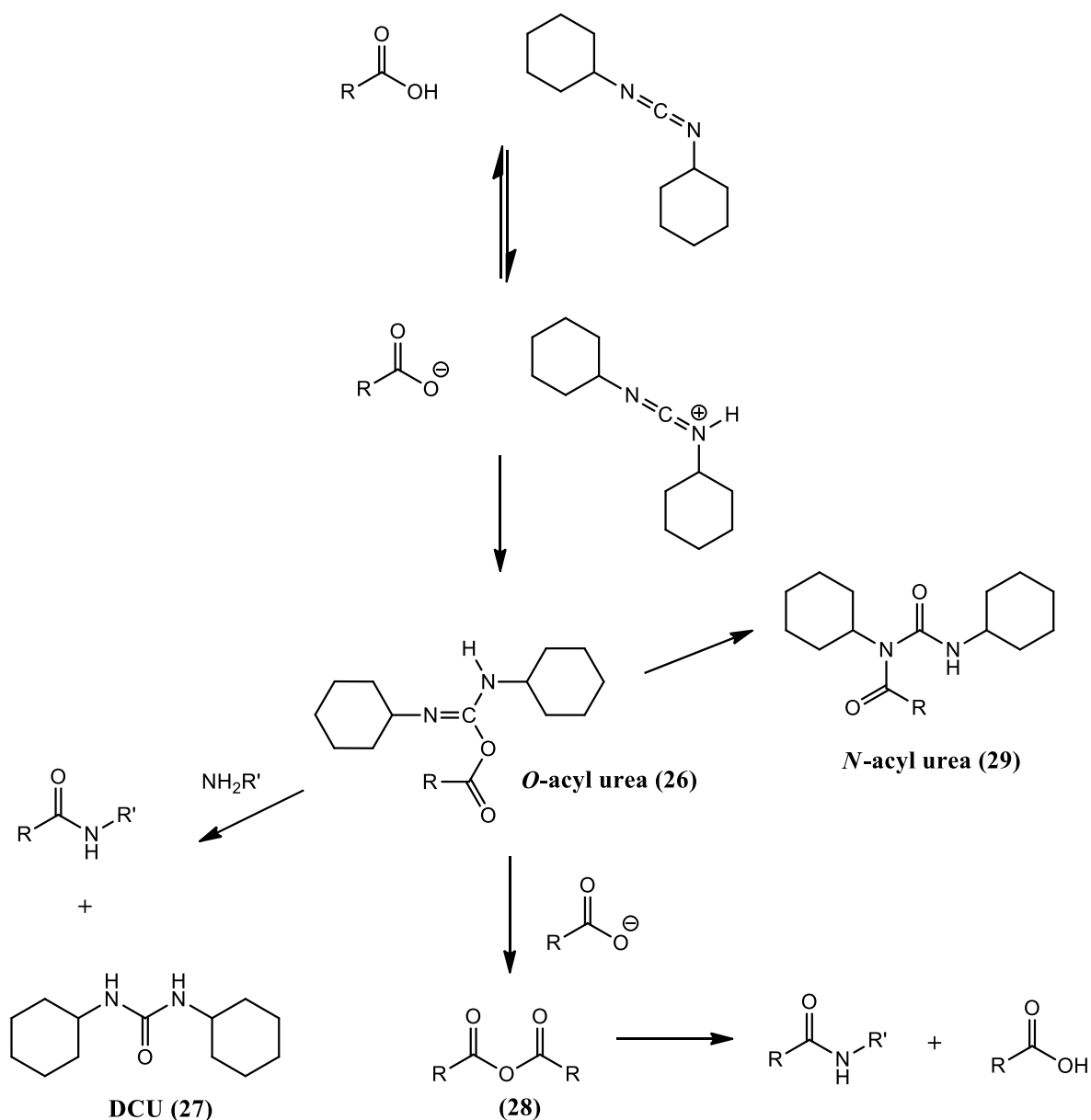
Scheme 3.13: Amide bond formation using DCC coupling reagent.[113]

3.1.5.1.2 Hydroxy benzotriazoles

Benzotriazoles react with carboxylic acids in the same manner as carbodiimides to form the OAt/OBt activated esters.[114] Although benzotriazoles are often used as the uronium or aminium salts, the presence of the counter ion was not found to affect its ability to assist in the formation of amide bonds.[114]

3.2   Synthesis of compound 1 and the derivatives of compound 1.

The final step in the synthesis of compound **1** and many of its derivatives, involved the generation of an amide (**Scheme 3.14**). The below scheme shows the retrosynthetic pathway for the synthesis of the amide **1** from a substituted arylpiperazine and the carboxylic acid **30**.
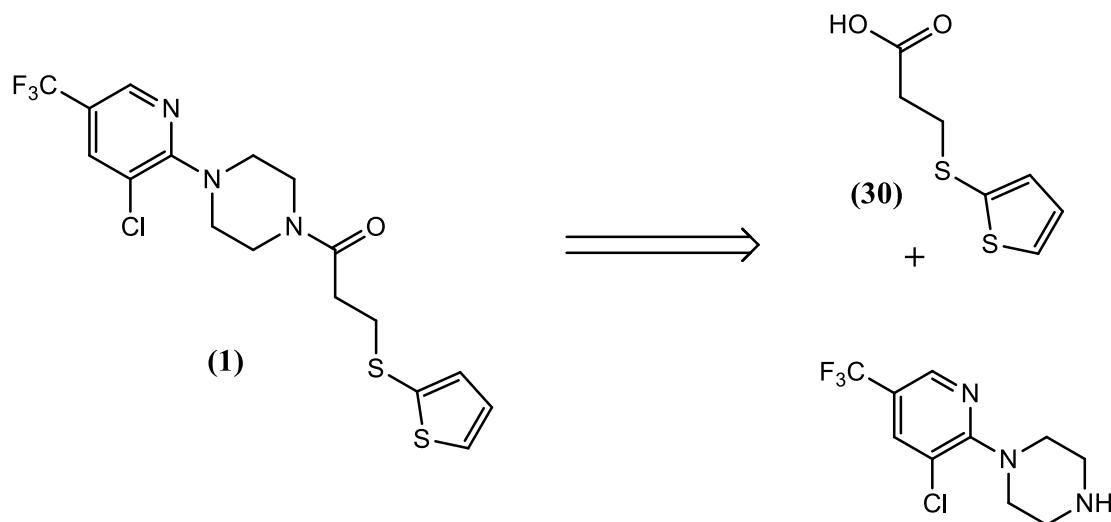
Scheme 3.14: The formation of an amide bond from an amine and a carboxylic acid.

3.2.1   Synthesis of compound 1

Synthesis of the amide **1** involved a two-step process. Firstly, the carboxylic acid, 3-(thiophen-2-ylthio)propanoic acid (**30**), was synthesized from 3-bromopropanoic acid and thiophene-2-thiol. We first employed a literature procedure where nucleophilic attack by the thiol on the electron deficient carbon-halide bond, in the presence of base at rt, produced the desired carboxylic acid in a 50% yield.[115] We then used an improved synthesis, reported by Hammam *et al.*, which saw the reagents heated at reflux in EtOH for 5 hours.[116] This gave the carboxylic acid **30** in an 85% yield (**Scheme 3.15**).
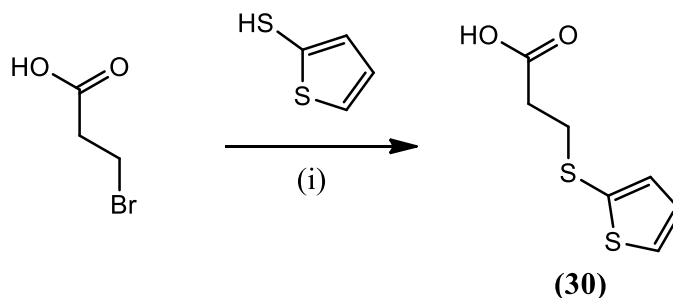
Scheme 3.15: Synthesis of compound **30**, (i) K_2CO_3, EtOH, reflux, 5 hrs, 85%.

Formation of the amide bond was conducted using the hydroxyl benzotriazoles HOBt and TBTU. The activated OBt ester underwent nucleophilic attack by the electron rich substituted piperazine, 3-chloro-5-(trifluoromethyl)pyridin-2-yl)piperazine, resulting in the formation of the desired amide **1** in a 71% yield (**Scheme 3.16**).
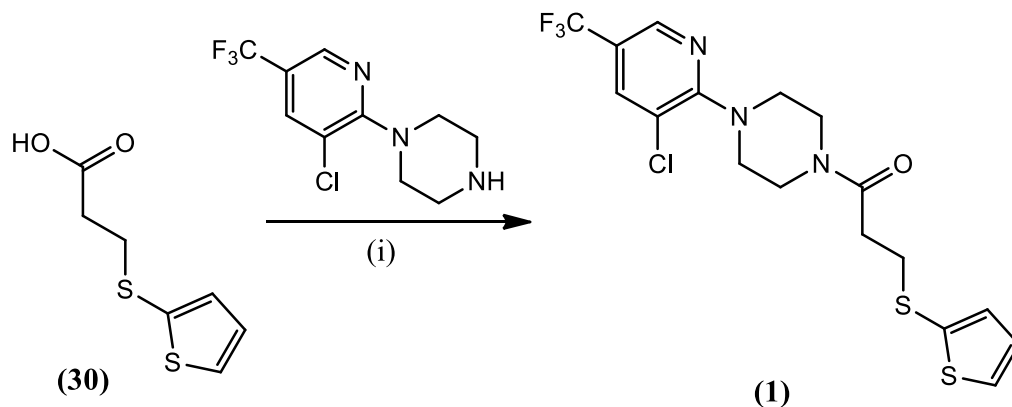
Scheme 3.16: Synthesis of **1**, (i) HOBt, TBTU, NEt$_3$, DMF, N$_2$, rt, overnight, 71%.

NMR spectroscopy verified the formation of **1** with two triplets present at 3.11 and 2.68 ppm, both with coupling constant values of 7.1 Hz. These peaks resonating at this chemical shift are characteristic of the two methylene groups found in the alkyl chain of **1**. The presence of the CF$_3$ group in compound **1**, and other compound **1** derivatives containing the trifluoromethyl phenyl group, is evident from the ^{13}C NMR spectra shown below. The 100% natural abundance and the spin of $I = $ ½ of ^{19}F, allows heteronuclear coupling between ^{13}C and ^{19}F to occur. The observed quartet, resonating at 123.8 ppm with a coupling costant of 270.0 Hz, is indicative of the CF$_3$ carbon atom while the quartet resonating at 121.2 ppm with a coupling constant of 33.0 Hz is characteristic of the *ipso C*-CF$_3$ carbon (**Figure 3.2**). The formation of the amide bond was confirmed by IR spectroscopy due to the presence of the band at 1636 cm^{-1}.
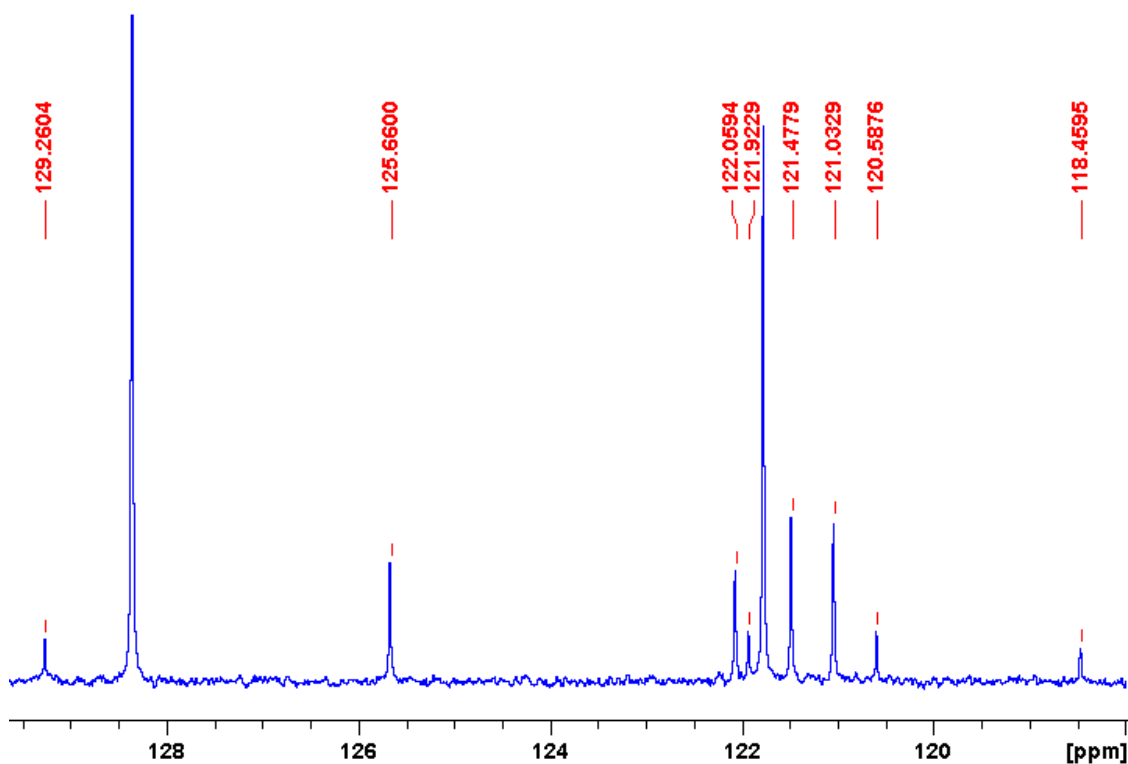
Figure 3.2. Expanded view of a region of the ^{13}C NMR spectrum of **1** in CDCl$_3$.

The *J* values diminish as the carbons become more distant from the fluorine atoms. Thus the quartet with coupling constants of 4.1 and 3.3 Hz at 143.6 and 136.7 ppm respectively represent the carbon atoms *meta* to the piperazine ring (**Figure 3.3**).
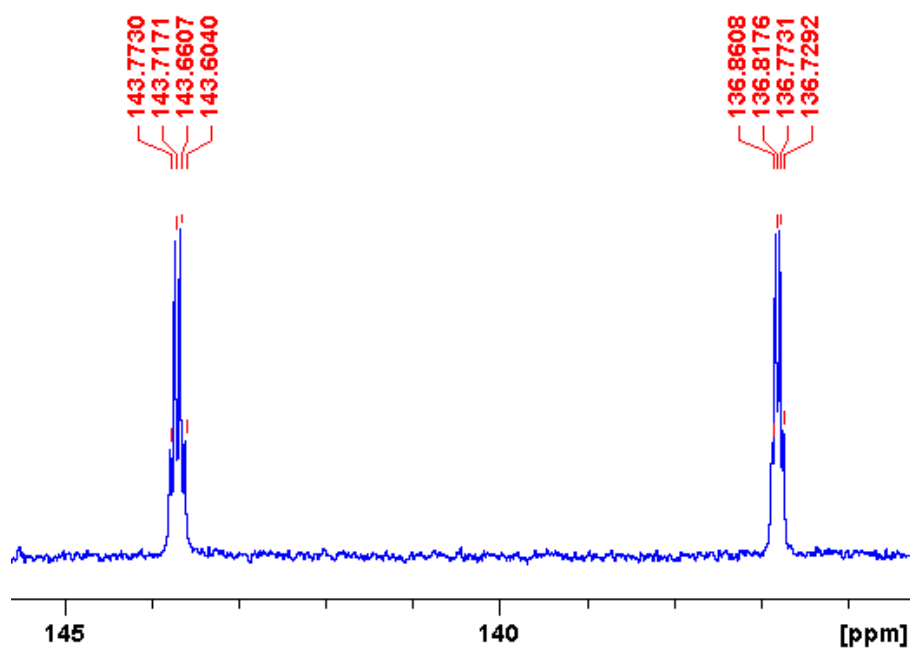
Figure 3.3. Expanded view of a region of the ^{13}C NMR spectrum of **1** in CDCl$_3$.

62

3.2.2   Synthesis of derivatives of compound 1.

The synthetic strategy for the synthesis of the derivatives of the amide **1** centered on a final coupling reaction. In many cases either the piperazine unit or the carboxylic acid unit had to be synthesised prior to the coupling (**Scheme 3.19**).
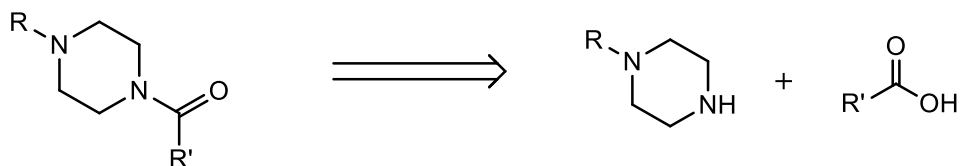
Scheme 3.19: Synthetic strategy for the synthesis of derivatives of compound **1**.

3.2.2.1 Synthesis of derivatives of compound 1 with changes to the arylpiperazine

The synthesis of derivatives of compound **1** with changes to the arylpiperazine group involved the coupling of a variety of different arylpiperazines with 4-(2-thienyl)butyric acid (**Scheme 3.20**). For example, derivatives were synthesised where R was equal to groups such as CF_3 or NO_2, X^1 and X^2 were nitrogen atoms or a -CH and Z was a sigma bond or a methylene group. A number of the necessary arylpiperazines were commercially available while other piperazines were synthesised using nucleophilic aromatic substitutions (S_NAr) and the palladium catalyzed Buchwald-Hartwig amination. The construction of the piperazine moiety from anilines was also utilized in the synthesis of a selection of piperazines.[83,84,85]
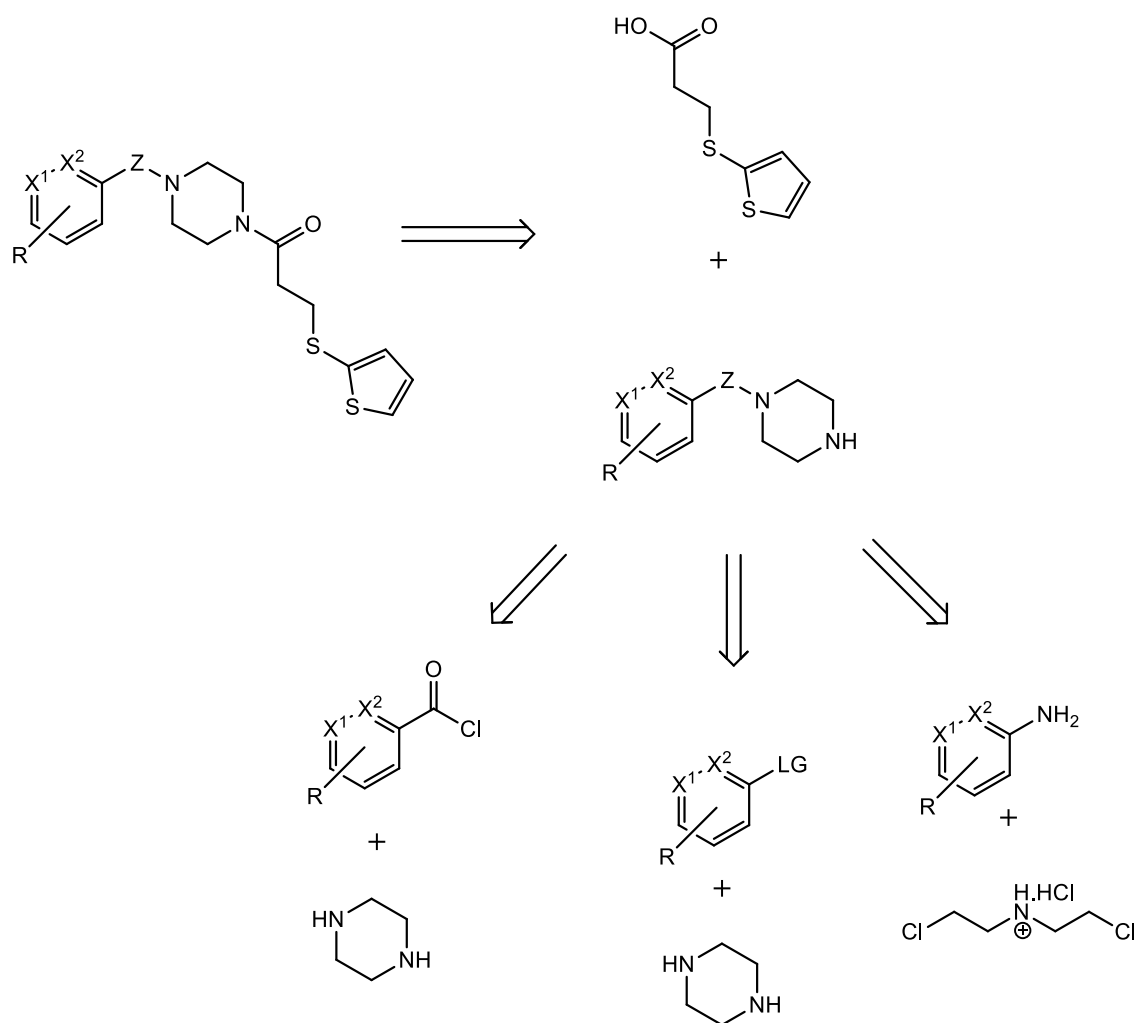
Scheme 3.20: Retrosynthesis of derivatives of compound **1** with changes to the arylpiperazine.

3.2.2.1.1 Synthesis of piperazines *via* S_NAr

The preparation of compound **11** involved the synthesis of the substituted piperazine, 1-(2-chloro-4-(trifluoromethyl)phenyl)piperazine (**31**, **Scheme 3.21**), from 2-chloro-1-fluoro-4-(trifluoromethyl) benzene and piperazine *via* a nucleophilic aromatic substitution. The aryl halide and piperazine were heated at reflux in DMF overnight in the presence of base. However, this afforded a complex mixture which included the mono- (**31**) and di- substituted (**32**) products (**Scheme 3.22**). An alternative approach was then chosen in which the piperazine was Boc protected. The protected piperazine was subsequently heated at reflux in DMF in the presence of the aryl halide. This gave rise to the Boc protected product, albeit in a 10% yield.
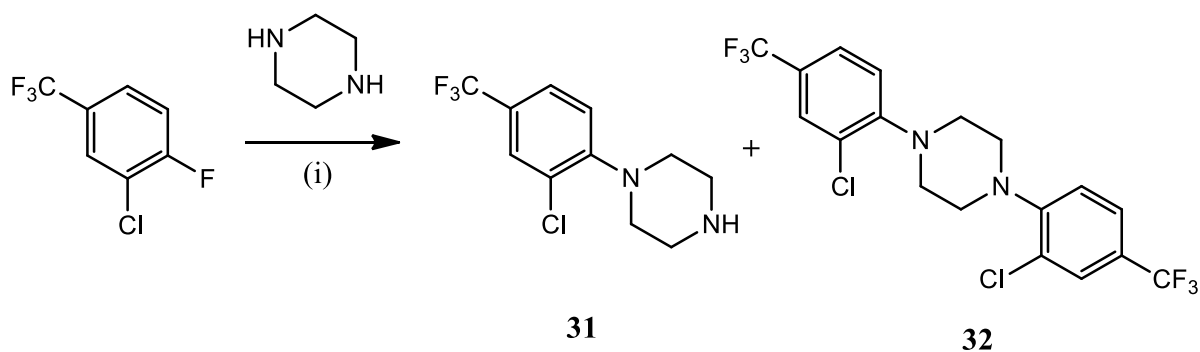
Scheme 3.22: Synthesis of **31** *via* S$_N$Ar, (i) K$_2$CO$_3$, DMF, reflux, overnight.

3.2.2.1.2 Buchwald-Hartwig amination in the synthesis of arylpiperazines

The arylpiperazine **33**, which was previously commercially available, became restricted during the course this project. As this piperazine was a key intermediate in the synthesis of our lead compound, **4**, its synthesis was necessary. The literature focused our attention on a palladium catalysed Buchwald-Hartwig amination. This involved the use of 2-(2',6'-dimethoxybiphenyl)dicyclohexylphosphine (SPhos) and bis(dibenzylideneacetone)-palladium (0) (Pd(dba)$_2$) (**Scheme 3.23**). The product, compound **33**, was isolated in a 40% yield.[83]
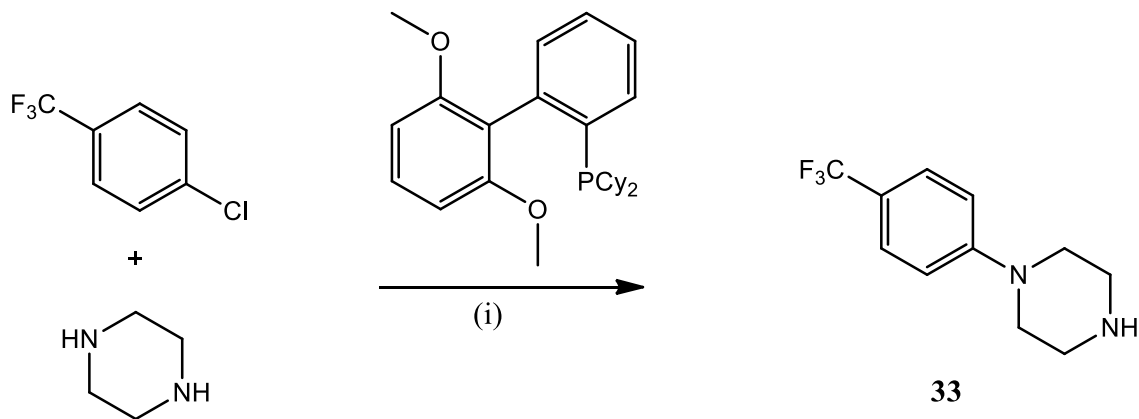
Scheme 3.23: Synthesis of piperazine **33**, (i) Pd(dba)$_2$, THF, Toluene, NaO^{t}Bu, 90 °C, 8 hrs, 40%.

3.2.2.1.3 MW assisted, S$_N$Ar synthesis of arylpiperazines

As the commercial availability of the piperazine **33** became restricted and a low yield of 10% was obtained in the synthesis of the piperazine **31** using conventional heating methods, an improved and more economical synthetic approach to arylpiperazines was sought. Our aim was to synthesise the arylpiperazines in shorter reaction times and in greater yields. We were attracted to a palladium free synthesis described in the literature where only the aryl halide, piperazine and 1-methyl-pyrrolidin-2-one (NMP) were employed. It involved a nucleophilic aromatic substitution (S$_N$Ar), facilitated by microwave irradiation.[101] Our efforts using this methodology are described below.

The microwave assisted synthesis of the arylpiperazines consisted of heating the appropriate benzotrifluoride at 200 °C, in a microwave reactor, and in the presence of piperazine, for 30 minutes. Piperazine **31** was successfully synthesised in a 61% yield (**Scheme 3.24**). The increase in yield, compared to the previously discussed conventional heating method, highlights the effectiveness of MW irradiation in organic synthesis (**Table 3.1**).
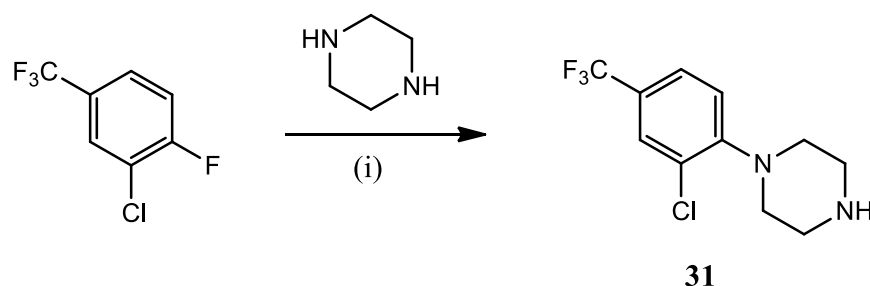
Scheme 3.24: Synthesis of **31**, (ii) NMP, MW (300 W), 200 °C, 20 mins, 61%.

These conditions were also employed in the synthesis of piperazine **33**. Although an increase in yield was observed compared to the palladium synthesis of **33**, the yield was lower than that for **31**. This lower yield can be explained due to the presence of a chlorine atom, instead of a fluorine atom, *para* to the CF$_3$ group as seen in the synthesis of **31**. As previously described, the presence of fluorine increases the rate of reaction due to its enormous inductive effect.[100]

Compound	Reaction type	Yield (%)
31	Conventional heating	10
31	MW assisted heating	61
33	Palladium catalysed reaction	40
33	MW assisted heating	50

Table 3.1: MW assisted synthesis of arylpiperazines **31** and **33**.

The MW conditions were also applied to the synthesis of piperazine **34** (**Scheme 3.25**). The product was carried forward and used in the coupling with 4-(2-thienyl)butyric acid without any further purification.
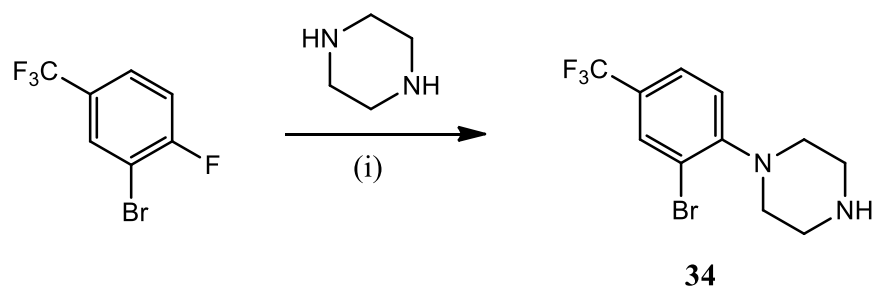
Scheme 3.25: Synthesis of **34**, (i) NMP, MW (300 W), 200 °C, 20 mins.

The importance of the electron withdrawing CF_3 group was evident during the attempted synthesis of **35** (**Scheme 3.26**). Even with the aid of MW irradiation the desired substituted piperazine could not be formed, instead starting materials were recovered. We believe that the lack of reactivity was due to the presence of a *para* CH_3 group instead of a CF_3. CH_3 groups are slightly electron donating whereas CF_3 groups are strongly electron withdrawing. As such a CF_3 activates an aromatic ring towards nucleophilic substitution whereas a CH_3 group would have the opposite effect.
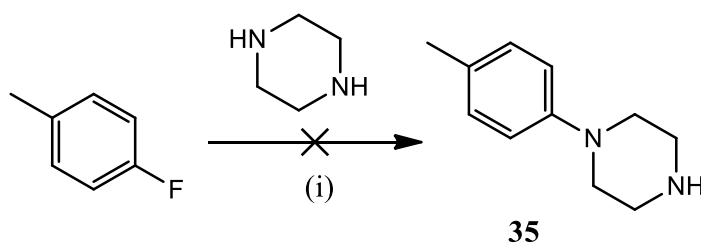
Scheme 3.26: Attempted synthesis of **35** using MW irradiation, (i) NMP, MW (300 W), 200 °C, 20 mins, product not isolated.

The CF_3 group stabilises the anionic charge formed after nucleophilic attack on the aromatic ring. Unlike other electron withdrawing groups, such as a nitro group, which stabilizes an anionic charge by conjugation, the CF_3 group stabilises a charge through an inductive effect.[100] The electron withdrawing properties of fluorine polarize C-F bonds allowing it to stabilise an anionic charge.[100] An alternative approach was therefore necessary for the synthesis of **35**.

3.2.2.1.4 Cyclocondensations

An alternative method for the preparation of substituted piperazines consisted of the use of anilines and bis(2-chloroethyl)amine.HCl. This S_N2 reaction constructs the piperazine ring from a disubstituted amine salt to give the HCl salt of the arylpiperazine. This method relies on the nucleophilic nature of the aniline and does not require an electron withdrawing group, as with S_NAr reactions. In fact, the presence of an electron withdrawing group would be detrimental as it would reduce the nucleophilicty of the primary amine.

Piperazine **35** was therefore synthesised from *p*-toluidine and bis(2-chloroethyl)amine.HCl by heating at reflux in bis(2-methoxyethyl) ether for 16 hours.[85] This gave the HCl salt of the arylpiperazine, which was then stirred in a 5% NaOH solution to afford the free amine (**Scheme 3.27**). A high boiling solvent was used for this coupling as high temperatures were required due to the reduced nucleophilicty of aromatic amines. This reduced nucleophilicty is characteristic of anilines due to the delocalisation of electrons into the aromatic ring.[100]
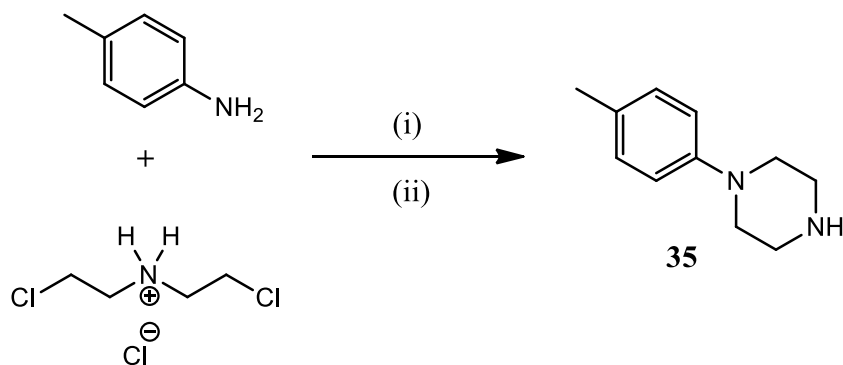
Scheme 3.27: Synthesis of **35**, (i) bis(2-methoxyethyl) ether, reflux, 16 hrs (ii) 5% NaOH, rt, 4 hrs, 13%.

This method was also used to synthesise the piperazine **36**. As with **35**, an aniline derivative, 4-(*tert*-butyl)aniline, was reacted with bis(2-chloroethyl)amine.HCl in the dissolved in bis(2-methoxyethyl) ether. The HCl salt of the substituted piperazine was isolated in a 63% yield. The free amine was then isolated using 5% NaOH (**Scheme 3.28**).
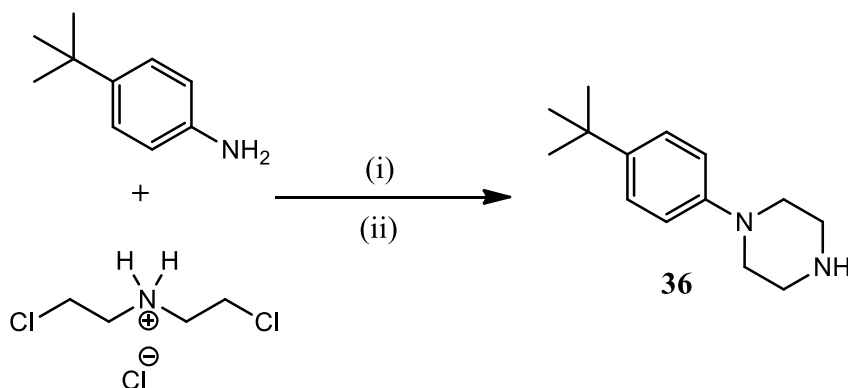
Scheme 3.28: Synthesis of **36**, (i) bis(2-methoxyethyl) ether, reflux, 16 hrs, 63% (ii) 5% NaOH, rt, 4 hrs, 87%.

3.2.2.1.5 Synthesis of alkyl/acyl piperazines

Introduction of a carbonyl group or methylene group between the piperazine and trifluoromethyl phenyl group first required the synthesis of the arylpiperazines **37** and **38**. Nucleophilic substitution of the appropriate benzotrifluoride derivative, using piperazine, gave access to the required amines.

Compound **37** was synthesised using an excess (2 eq) of piperazine. Piperazine was added to a solution of 4-(trifluoromethyl)benzoyl chloride in DCM at 0 °C. Although an excess of piperazine was used, the major product isolated was the disubstituted product (**39**). However, a sufficient amount of the monosubstituted product was isolated for use in the subsequent coupling reaction (**Scheme 3.29**).

37   **39**
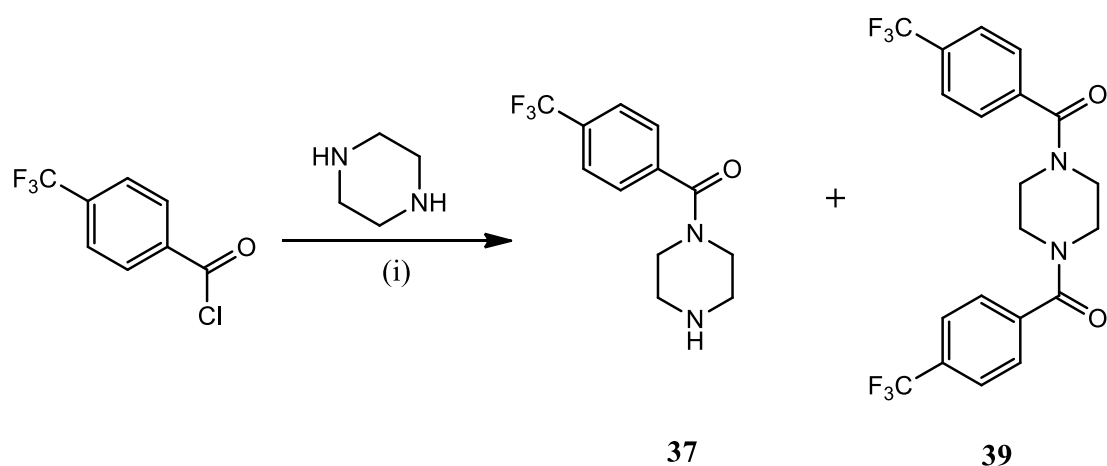
Scheme 3.29: Synthesis of **37**, (i) DCM, DIPEA, 0 °C-rt, 2 hrs, 3% for compound **37** and 82% for **39**.

A fourfold excess of piperazine was also used in the synthesis of **38**, which involved heating the reaction mixture containing piperazine and 1-(bromomethyl)-4-(trifluoromethyl)benzene at 85 °C in toluene (**Scheme 3.30**).[117] An excess was used to prevent the disubstitution of the piperazine. The monosubstituted product was isolated in a 57% yield.

38
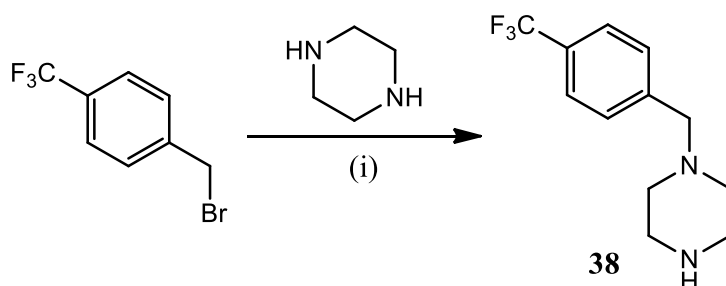
Scheme 3.30: Synthesis of **38**, (i) Toluene, 85 °C, 2 hrs, 57%.

3.2.2.2 Condensations

The final derivatives of compound **1** were prepared in a similar fashion to compound **1** with the use of the coupling agents HOBt and TBTU in the last step (**Table 3.2**). Some of the required piperazines were synthesised as described previously and then coupled with 4-(2-thienyl)butyric acid to give the final derivatives. As a number of the piperazines and functionalised carboxylic acids, needed to synthesise the necessary derivatives, were commercially available these derivatives could be synthesised in one step by reacting the appropriate piperazine and carboxylic acid. The following tables provide the yields and structures of the derivatives of compound **1**.
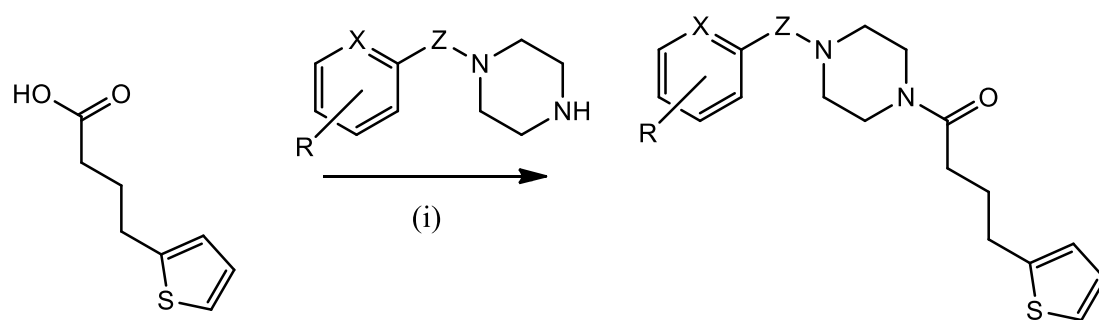
Compound	R	X	Z	Yield (%)
4	*p*-CF$_3$	CH	-	80
8	*p*-CF$_3$	N	-	80
9	*o*-Cl, *p*-CF$_3$	N	-	64
11	*o*-Cl	CH	-	80
40	*p*-F	CH	-	71
41	*o*-CF$_3$	CH	-	63
42	*p*-NO$_2$	CH	-	75
43	bis(*m*-CF$_3$)	CH	-	39
45	3-Cl, 4-CF$_3$	N	-	68
46	*o*-Br, *p*-CF$_3$	CH	-	50
47	H	CH	-	59
48	*p*-CH$_3$	CH	-	24
49	*p*-*t*Bu	CH	-	86
50	*p*-CF$_3$	CH	C=O	50
51	*p*-CF$_3$	CH	CH$_2$	73

44	10
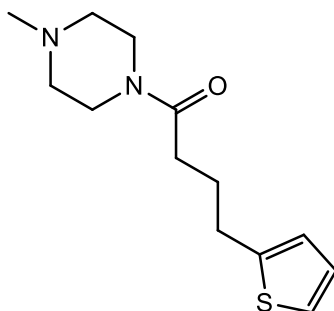
Table 3.2: Yields (%) of amide products, (i) HOBt, TBTU, NEt₃, DMF, N₂, rt, overnight, - = sigma bond.

The amide **4** was synthesised in an 80% yield with NMR spectroscopy used to support its synthesis. The presence of the peak at 171.0 ppm in the ^{13}C NMR spectrum supports the presence of the amide carbon atom. The presence of this group is further supported by IR spectroscopy due to the band at 1653 cm^{-1}. The presence of the CF$_3$ group is evident due to the quartets resonating at 126.5 ppm (J = 3.6 Hz), 24.6 (J = 270.0 Hz) and 121.2 (J = 33.0 Hz). The synthesis of compound **4** was also supported by HR-MS.

The mono fluorinated derivative of compound **4**, the amide **40**, was characterized using the splitting pattern resulting from the presence of the fluorine atom. The *ipso* carbon atom was identified as a doublet with the characteristic *J* value of 238.1 Hz, while the *ortho* (*J* = 22.0 Hz), *meta* (*J* = 7.3 Hz), and *para* (*J* = 2.2 Hz), carbon atoms were identified based on the size of their *J* values. Again, the size of the *J* value decreased as the fluorine atom became more distant (**Figure 3.4**).

(a)
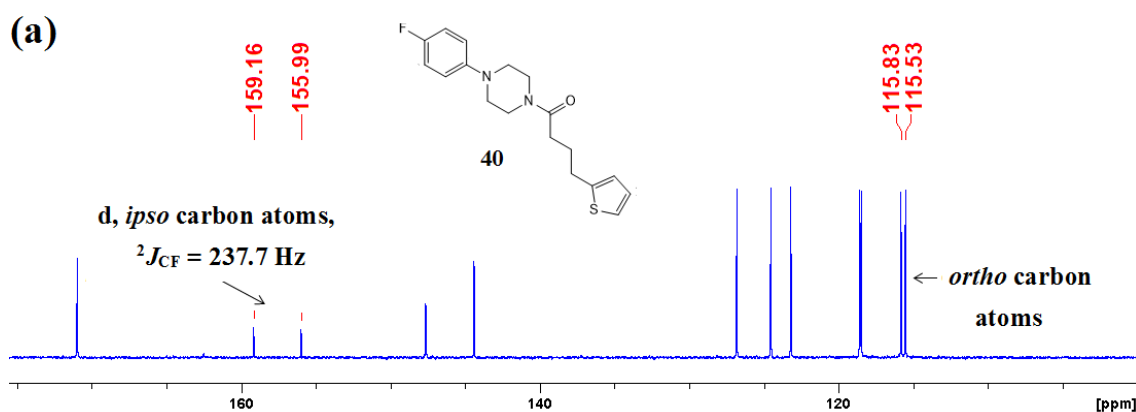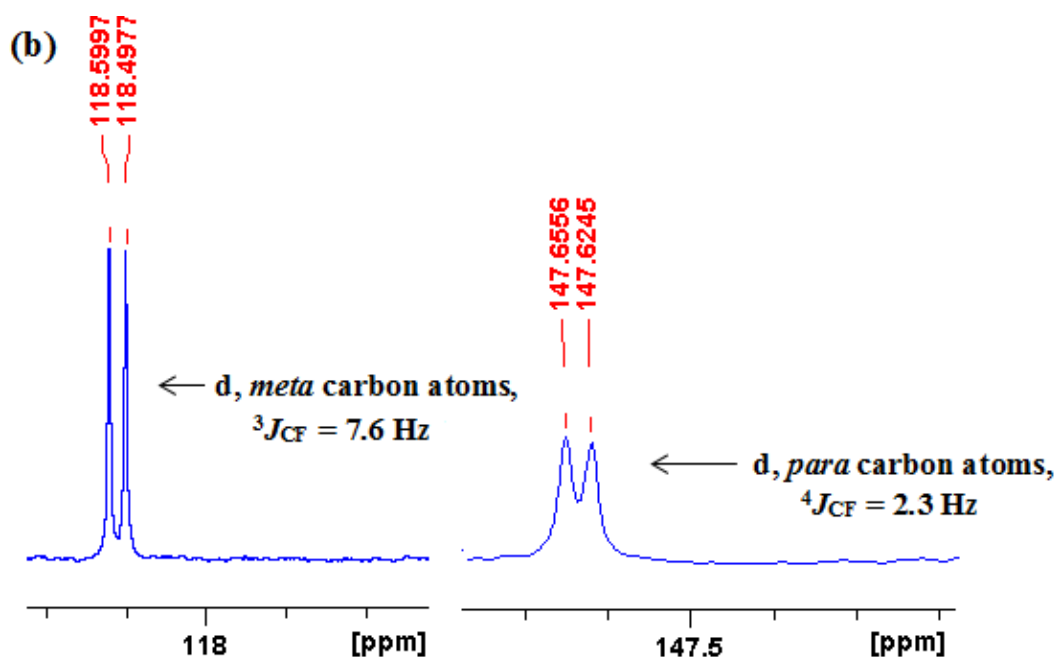
Figure 3.4 (a) and **(b)** Expanded view of portions of the ^{13}C NMR spectrum of amide **40** in CDCl$_3$.

Compounds **52**, **53** and **54**, **Table 3.3**, were also synthesised to investigate the biological importance of the phenyl ring and the piperazine ring. All three were synthesised in one coupling step from the same carboxylic acid and corresponding amine; (1-cyclohexylpiperazine for **52**, (4-(trifluoromethyl)phenyl)hydrazine for **53** and 4-(4-(trifluoromethyl)phenyl)piperidine for **54**. Their structures and yields are shown in **Table 3.3.**

Compound	Structure	Yield (%)
52		70
53		69
54		48
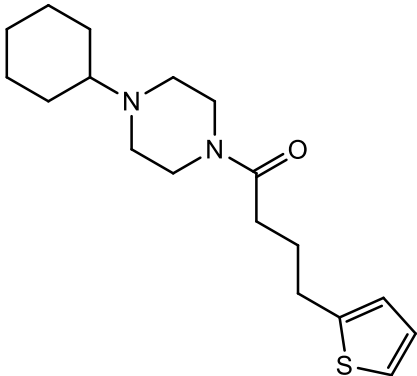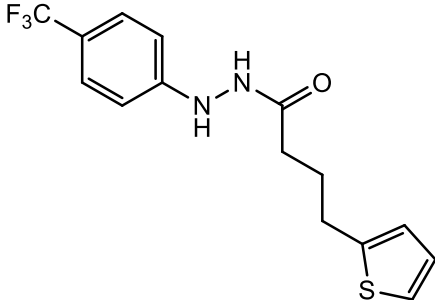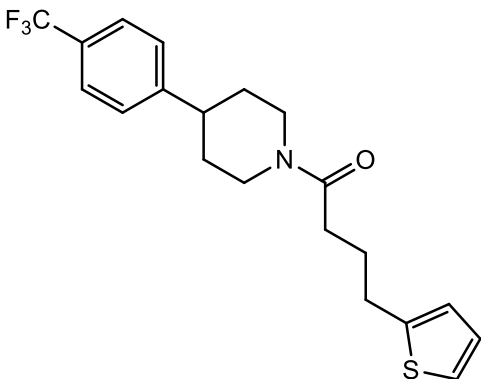
Table 3.3: Structures and yields (%) of compounds **52**, **53** and **54**.

The successful synthesis of **53** was supported by the ^{1}H NMR spectrum where the peak resonating at 6.38 ppm, integrating for one proton, indicated the presence of the amide proton. The presence of the amide proton is also clear from the IR spectrum where an N-H stretch at 3309 cm^{-1} and an N-H bend at 1614 cm^{-1} are present. The synthesis of **53** was also supported by HR-MS.

A number of the carboxylic acids, needed to synthesize the necessary derivatives of compound **1** with changes to the alkyl chain or thiophene ring, were commercially available. These acids were reacted with the arylpiperazine **33** to afford the desired

derivatives (**Table 3.4**). The derivatives synthesised contained variations in X or Z. For example, X was varied by increasing or decreasing the length of the carbon chain or by introducing heteroatoms such as sulphur. The Z group was varied by introducing groups such as a furanyl heterocycle or a carboxylic acid.
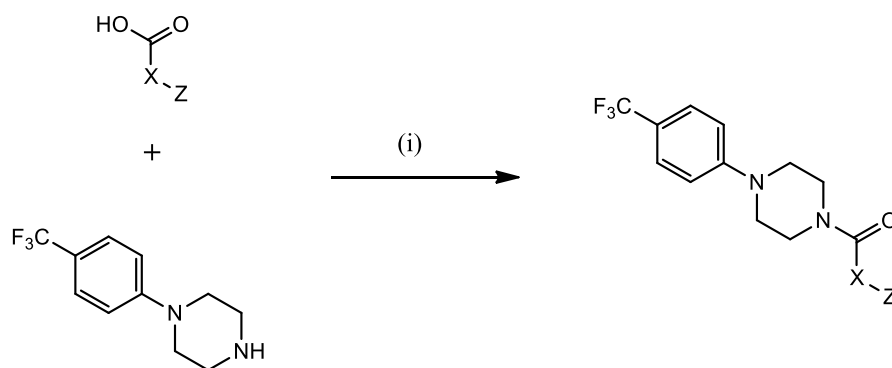
Compound	X	Z	Yield (%)
5	$(CH_2)_2C=O$	2-thienyl	81
10	$(CH_2)_2S$	2-thienyl	63
55	$(CH_2)_4$	2-thienyl	25
56	$(CH_2)_5$	2-thienyl	75
57	$(CH_2)_6$	CH_3	63
58	CH_3	-	57
59	$(CH_2)_2$	2-thienyl	44
60	$(CH_2)_3$	CH_3	57
61	CH_2	2-thienyl	20
62	$(CH_2)_2$	2-furanyl	31
63	$(CH_2)_3$	4-pyrazolo	10
64	$(CH_2)_4$	Ph	44
65	-	2-thienyl	73

Table 3.4: Yields (%) of amide products, (i) HOBt, TBTU, NEt_3, DMF, N_2, rt, overnight, - = sigma bond.

Good to moderate yields were generally encountered, with the exception of **55**, **61** and **63**. A lower isolated yield was obtained for **55** and **61** as multiple purification steps were required to provide a pure compound. A 10% yield was observed for **63** due to the presence of a secondary amine in the pyrazole ring. The secondary pyrazole amino group would have been expected to be less nucleophilic than the piperazinyl amino group due to the delocalization of its lone pair of electrons into the aromatic ring.[100] However, its reactivity may still have been sufficient to also attack the OBt activated ester, resulting in the possible production of undesired side products. Presence of unwanted side products and the difficulty in isolating a free amine made purification *via* column chromatography difficult resulting in a reduced yield.

Amides **6** and **7** are derivatives of compound **1** which were synthesised with changes to both the arylpiperazine and the alkyl chain. Both **6** and **7** were synthesised in one coupling step from the corresponding commercially available piperazine and carboxylic acid. The structures and yields for these products are shown in **Table 3.5.**
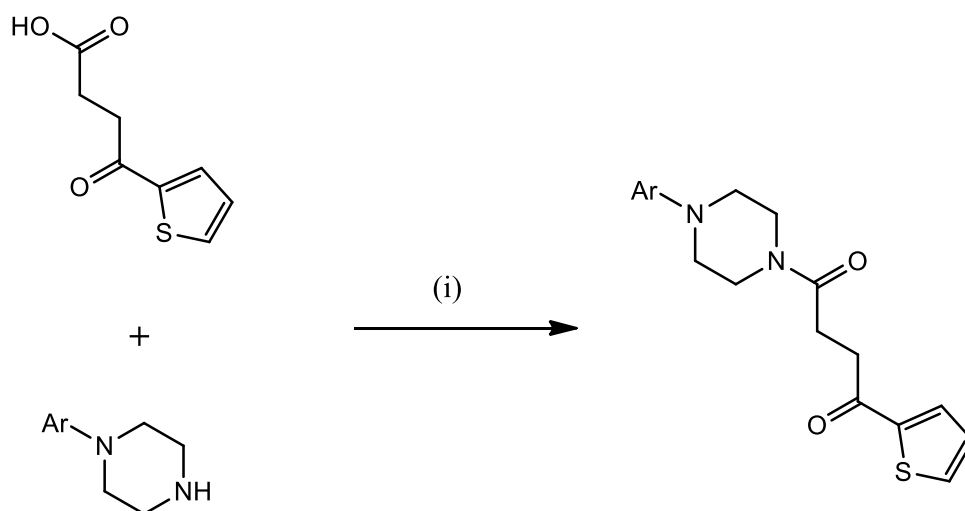
Compound	Structure	Yield (%)
6		63
7		70

Table 3.5: Structures and yields (%) of compounds **6** and **7**, (i) HOBt, TBTU,

NEt$_3$, DMF, N$_2$, rt, overnight.

3.2.2.3 Synthesis of compound 66

An alcohol group was introduced into the alkyl chain by reduction of the keto group in **5** (**Scheme 3.31**). NaBH$_4$ was used as the reducing agent[118] and **66** was produced in an 81% yield.
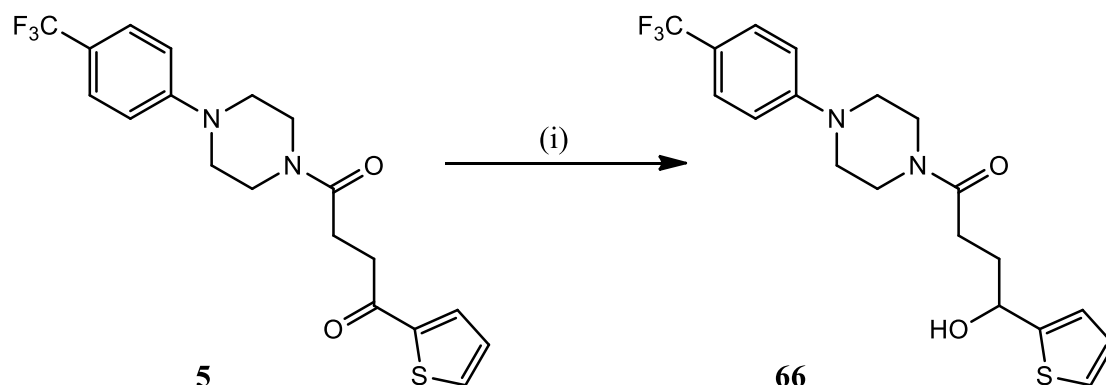
Scheme 3.31: Synthesis of **66**, (i) NaBH$_4$, MeOH, 50 °C, overnight, 81%.

The introduction of an alcohol group into the alkyl chain was evident from the IR spectrum with a peak at 3383 cm^{-1}, characteristic of a secondary alcohol. ^{1}H NMR spectroscopy confirmed the reduction was successful, due to the presence of the C-H signal as a multiplet ranging from 5.08–5.04 ppm and integrating for one proton. The chemical shift of this proton is indicative of a proton adjacent to an electronic withdrawing group such as an oxygen atom. The chemical shift of the carbon atom resonating at 68.6 ppm was suggestive of a carbon next to an electron withdrawing oxygen atom. HSQC experiments confirmed the correlation between the aforementioned proton and carbon.

3.2.2.4 Synthesis of compound 67

In the first attempt to synthesise **67**, methyl piperazine and 1-chloro-4-(trifluoromethyl)benzene were heated at reflux in toluene for 24 hours (**Scheme 3.32**, (i)) Only starting materials were recovered and hence different conditions were subsequently employed (**Scheme 3.32**). The reagents were heated at reflux in DMF but the use of a higher boiling solvent did not have any effect and again starting materials were recovered (**Scheme 3.32**, (ii)). MW irradiation was employed and the two reagents were heated at 200 °C (300W). The S$_N$Ar was successful although the yield was low

and purity poor (**Scheme 3.32,** (iii)). Finally, an alternative approach was employed which did not involve the synthesis of **67** *via* a S_NAr.

The arylpiperazine **33** was methylated using an excess of formic acid and formaldehyde. This reductive amination, known as an Eschweiler-Clarke reaction, involves the reduction of the formed imine by a formate anion (**Scheme 3.32**, (iv)). The methylated piperazine **67** was isolated in 72% yield and its presence was supported by ^{1}H NMR spectroscopy. A singlet resonating at 2.32 ppm and integrating for three protons is indicative of a methyl group adjacent to an electron withdrawing nitrogen. HR-MS also supported the formation of **67**.
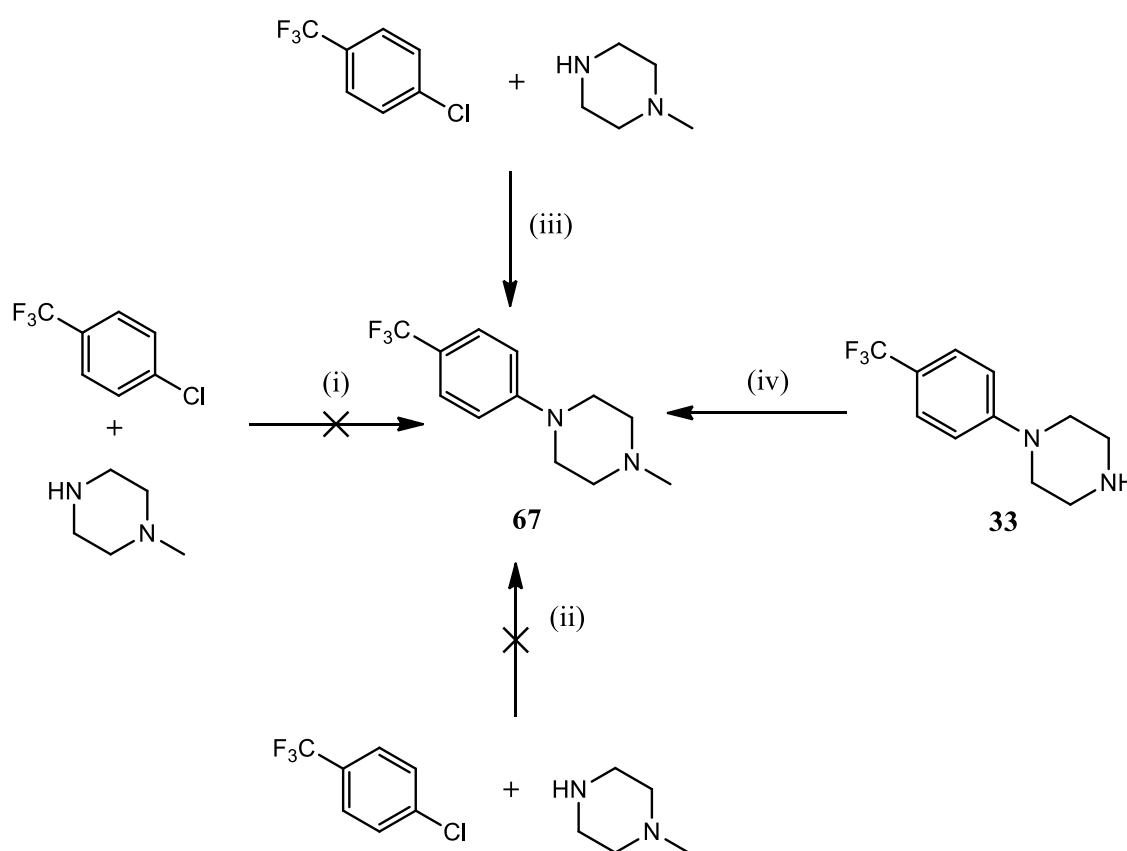
Scheme 3.32: Retrosynthetic route and attempted synthesis of **67**, (i) Toluene, reflux, 24 hrs (ii) DMF, reflux, 24 hrs (iii) NMP, MW (300 W), 200 °C, 20 mins, 9% (iv) formaldehyde, formic acid, EtOH, reflux, 3 hrs, 72%.

3.2.2.5 Synthesis of compound 70

Given the role of amide bonds in biological systems, it was necessary to investigate the importance of the amide bond of compound **4** for glucose uptake assay. As such **70** was

designed and synthesised as it differed from **4** only in the absence of the amide carbonyl. The synthetic route, outlined in **Scheme 3.33**, involved the reduction of 4-(2-thienyl)butyric acid to 4-(thiophen-2-yl)butan-1-ol (**77**), using lithium aluminium hydride.[119] The desired substitution of the alcohol **68**, with compound **33**, first required the conversion of the alcohol into a better leaving group. In this case, the alcohol was converted into the methanesulfonate derivative (**69**) using methanesulfonyl chloride.
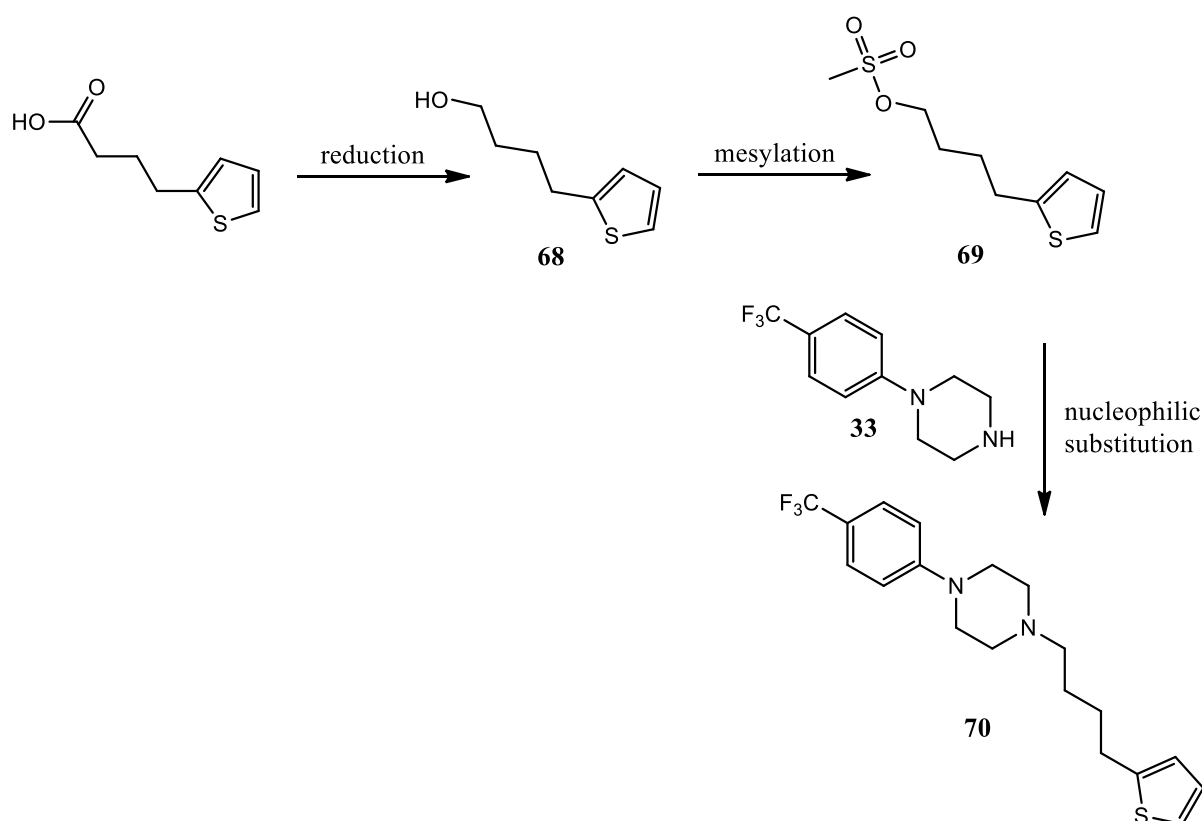
Scheme 3.33: Synthetic route for the synthesis of compound **70**.

The mesylation mechanism involves the elimination of HCl from the sulfonyl chloride (**71**) to give the sulfene (**72**) (**Scheme 3.34**). This is followed by attack of **68** on the electrophilic sulphur by to give **69**.[120]
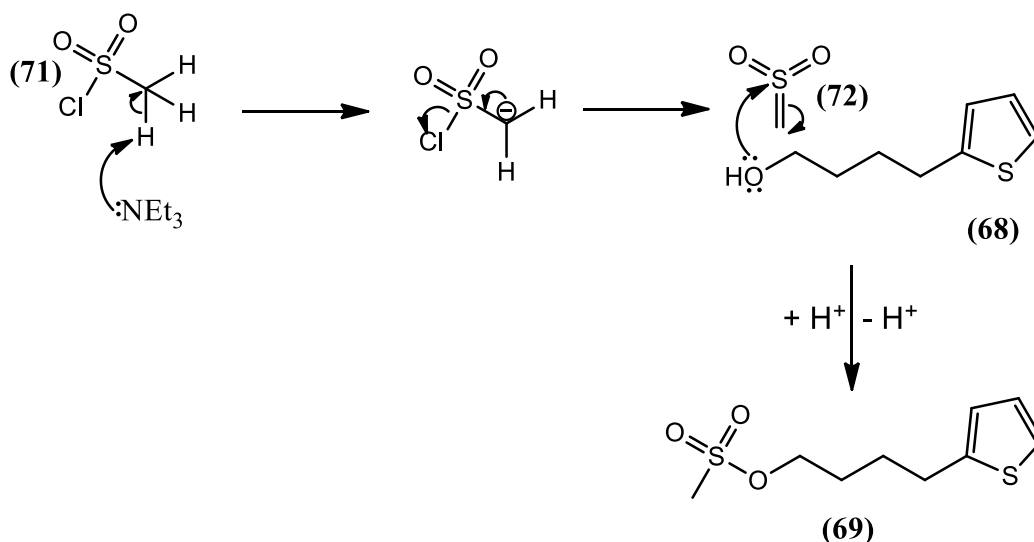
Scheme 3.34: Formation of **69** and the mechanism for the mesylation of an alcohol.[120]

The heating of compounds **33** and **69** in refluxing acetonitrile, in the presence of Na_2CO_3, gave derivative **70** in a 91% yield (**Scheme 3.35**). The absence of the carbonyl group was supported by the ^1H NMR spectrum with the presence of the additional CH_2 peak resonating at 2.86 ppm, with a coupling constant value of 7.2 Hz and integrating for two protons. The chemical shift, the size of the coupling constant and the multiplicity are all suggestive of the presence of a methylene group adjacent to both an electron withdrawing substituent, such as a nitrogen a methylene group. The absence of the carbonyl group in the IR and the ^{13}C NMR spectrum was clear, while the presence of the peak at 29.7 ppm in the ^{13}C NMR spectrum supported the presence of the methylene group. The peak at 29.7 ppm was also observed out of phase in the DEPT135 experiment confirming it was due to a CH_2.
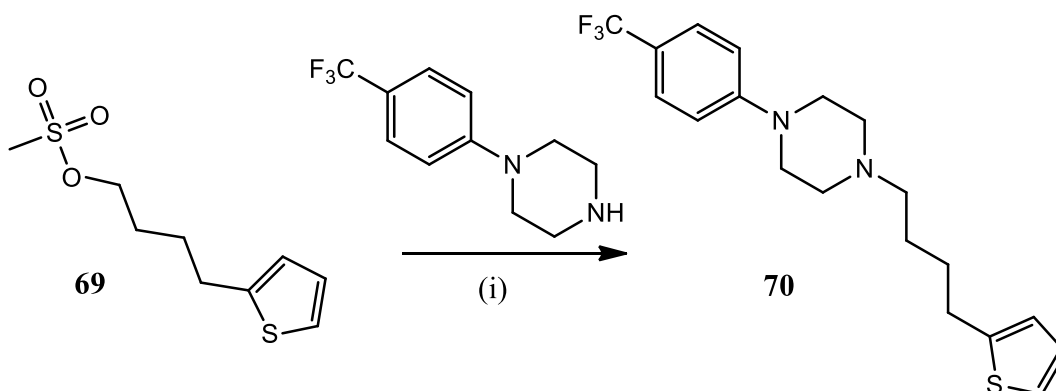
Scheme 3.35: Synthesis of **70**, (i) Na_2CO_3, CH_3CN, reflux, 24 hrs, 91%.

3.2.2.6 Synthesis of compound 73

Compound **73** was synthesised in order replace the electron withdrawing CF_3 group with an electron donating amino group. The first attempt at the synthesis of this derivative involved the use of the coupling reagents HOBt an TBTU to couple the arylpiperazine 4-(piperazin-1-yl)aniline with 4-(2-thienyl)butyric acid. Due to the presence of the aniline functional group, a complex mixture was obtained and **73** was isolated in only 10% yield. An alternative approach was taken which employed the reduction of **42** using the platinum oxide catalyst, known as Adams catalyst, in a hydrogen atmosphere. This gave rise to the formation of **73** in an isolated of 57% yield (**Scheme 3.36**).
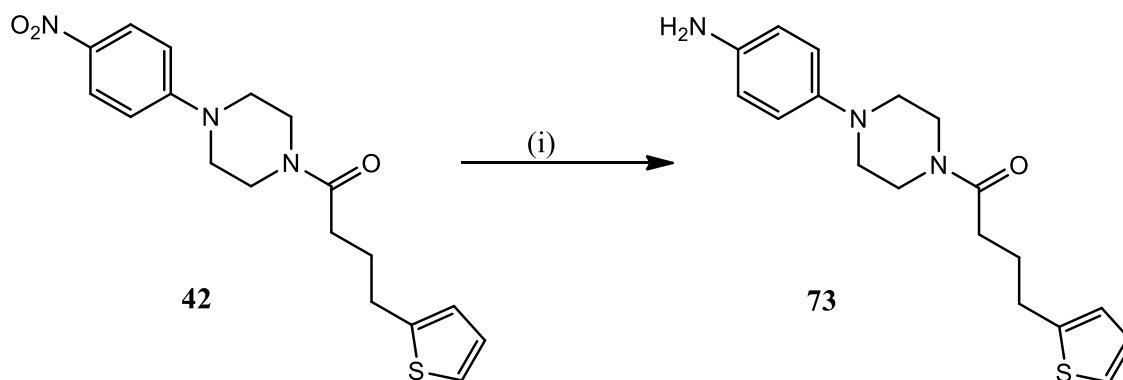
Scheme 3.36: Synthesis of **73**, (i) PtO_2, H_2, MeOH, rt, overnight, 57%.

3.2.2.7 Synthesis of functionalized thiophene derivatives

Due to the ability of thiophene heterocycles to undergo electrophilic aromatic substitutions, it was maybe considered possible to substitute the C2 position of the thiophene ring found in the amide **4**. *N*-Bromosucinimide was used to brominate **4**, however a complex mixture was obtained, possibly due to unwanted bromination of the trifluoromethylphenyl group. An alternative strategy was needed. The methyl ester **74** was treated with the brominating reagent, resulting in the selective bromination at the C2 position of the thiophene ring. The radical mechanism for this bromination is shown in **Scheme 3.37**. This gave the brominated derivative **75** which was hydrolysed to the carboxylic acid derivative **76** using base catalysed ester hydrolysis (**Scheme 3.38**). The carboxylic acid **76** was then coupled to the piperazine **33** using HOBt and TBTU (**Scheme 3.38**). Compound **77** was isolated in a 55% yield. [^1]H NMR spectroscopy

supported the synthesis of the amide **77** with two doublets, both integrating for one proton, resonating at 6.84 and 6.56 ppm. The chemical shift and the multiplicity indicate that these peaks are due to the presence of the aromatic thiophene protons. The size of the coupling constant, J = 3.3 Hz, may be explained due to the presence of the electron withdrawing bromine at C5. The presence of this electron withdrawing group can remove electron density from the thiophene ring, which may weaken the communication between the two aromatic protons therefore resulting in the observed small coupling constant of 3.3 Hz. The peak at 652 cm^{-1} in the IR spectrum is also indicative of a C-Br bond.
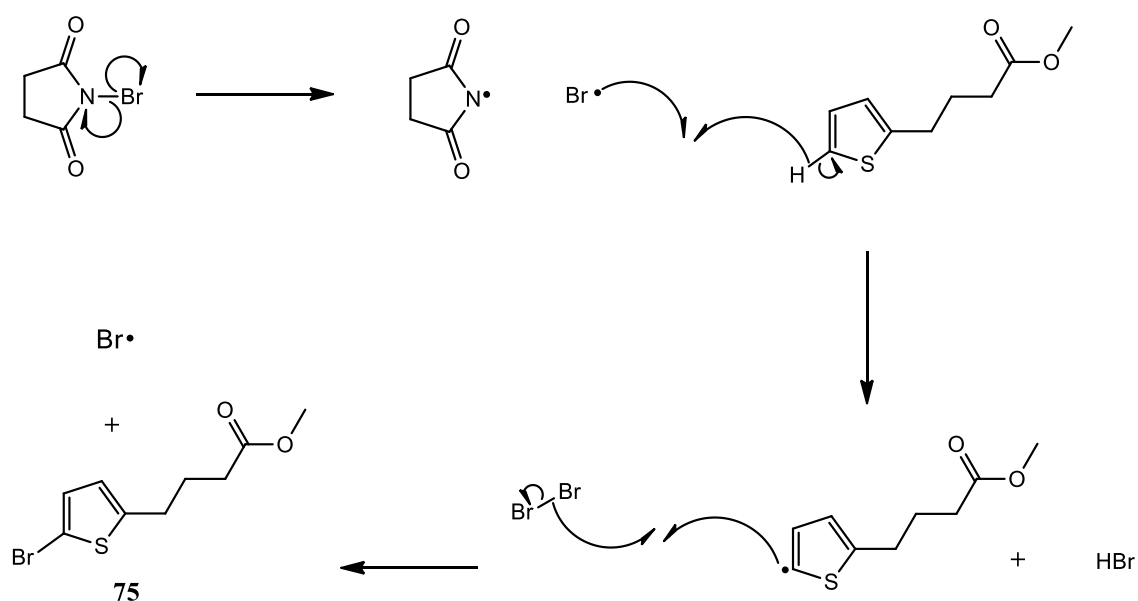
Scheme 3.37: Mechanism for the bromination of compound **75**.
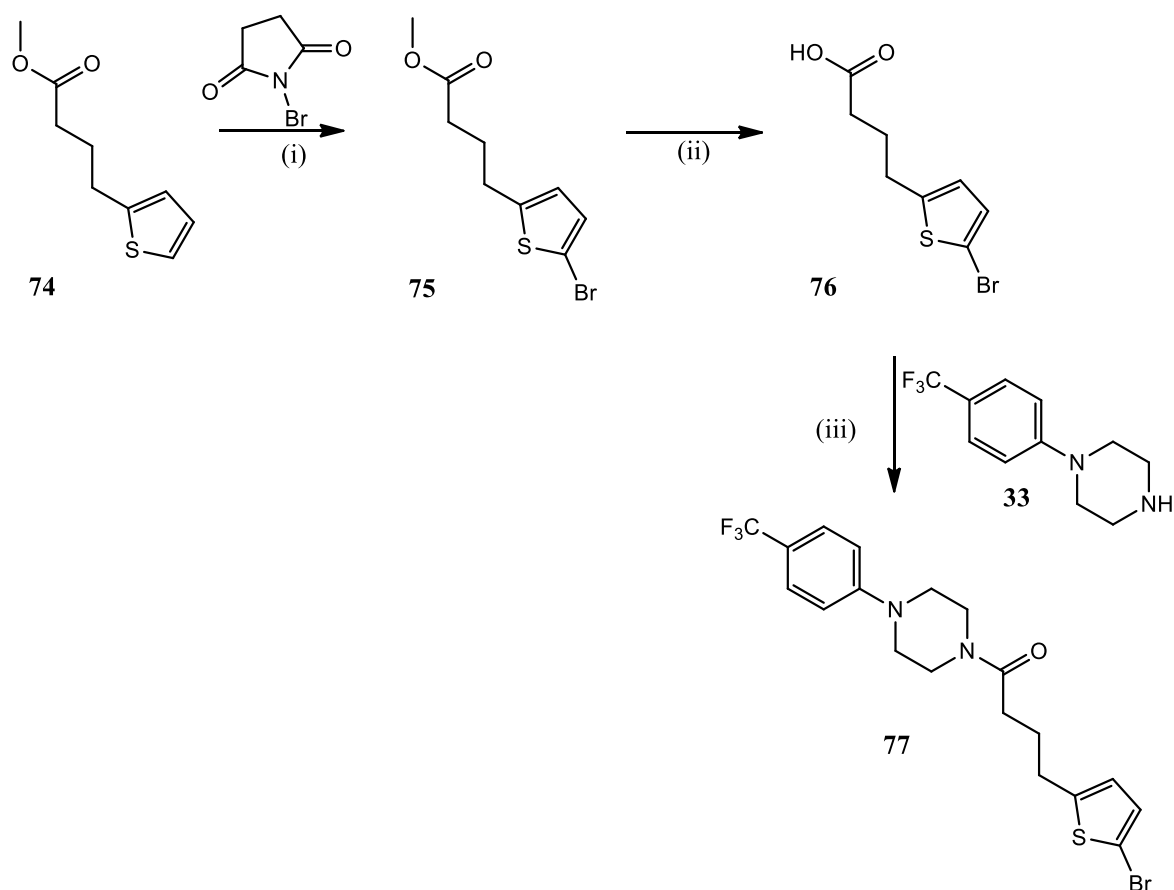
Scheme 3.38: Synthesis of **77**, (i) THF, 0 °C-rt, 4 hrs, 80% (ii) KOH, EtOH, 3 hrs, 35% (iii) HOBt, TBTU, NEt$_3$, DMF, N$_2$, overnight, 55%.

The amide **77** was then used to further functionalise the thiophene ring. The palladium catalysed Suzuki reaction generated compound **78** from **77** and trifluoromethylphenyl boronic acid in an 82% yield (**Scheme 3.39**).
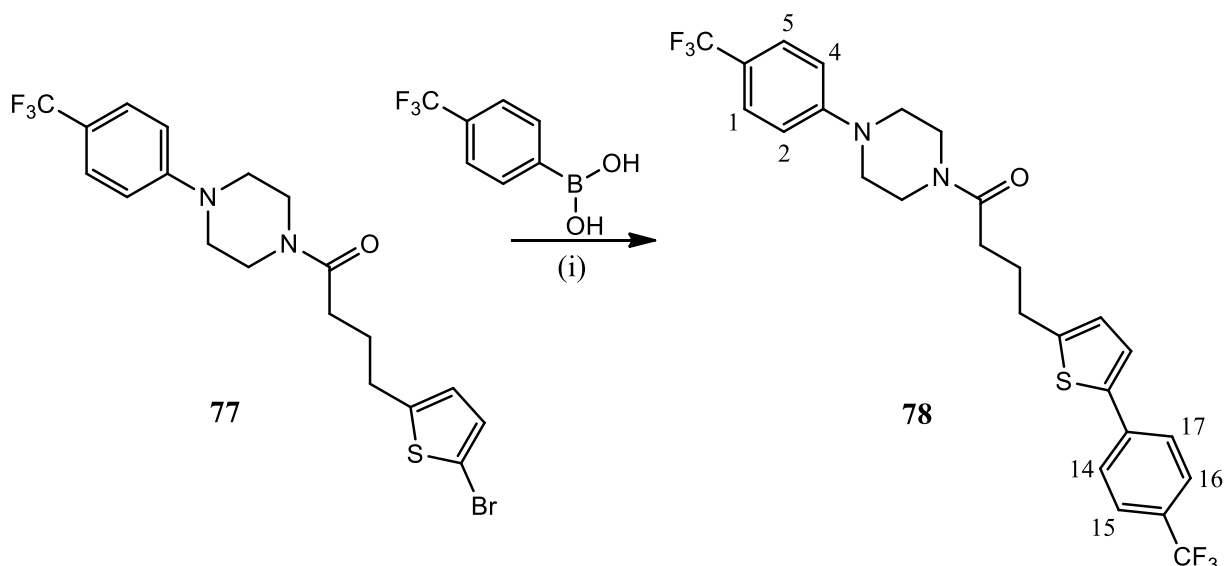
Scheme 3.39: Palladium catalysed synthesis of **78**, (i) Pd(PPh$_3$)$_4$, Na$_2$CO$_3$, THF, N$_2$, reflux, 6 hrs, 82%.

As H14, H17 and H15, H16 have similar chemical shifts, the observed splitting followed a second order splitting pattern (**Figure 3.5**). This occurred as the difference between the chemical shifts of the two protons (Δδ) was similar to the *J* value, with Δδ equal to 15 Hz and *J* equal to 8.6 Hz. This phenomenon allowed for the differentiation between the aromatic protons of the two different trifluoromethyl phenyl groups as the splitting observed for H1, H5 and H2, H4 followed a first order splitting pattern, with a Δδ equal to 177.8 Hz and a *J* value of 8.7 Hz. It was then possible to differentiate between the protons in the *ortho* and *meta* positions of both trifluoromethyl phenyl groups due to the splitting pattern observed in the ^{13}C NMR spectrum resulting from the CF$_3$ group and combining this with a HSQC spectrum.
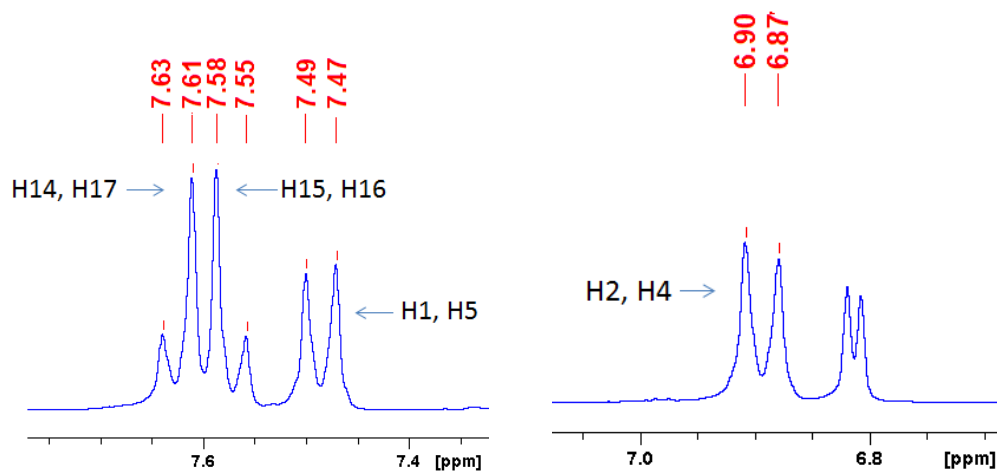
Figure 3.5. Expansion of two distinct regions of the ^{1}H NMR spectrum of **78** in CDCl$_3$.

3.2.2.8 Synthesis of compound 79 and 81.

The arylpiperazine **33** and azelaic acid were used in the synthesis of the biologically active compound **79** (**Scheme 3.40**). HOBt and TBTU were used to form the amide bond, with **79** produced in a 30% yield. The observed low yield was due to the formation of the disubstituted product, **80**, which was isolated by flash chromatography.
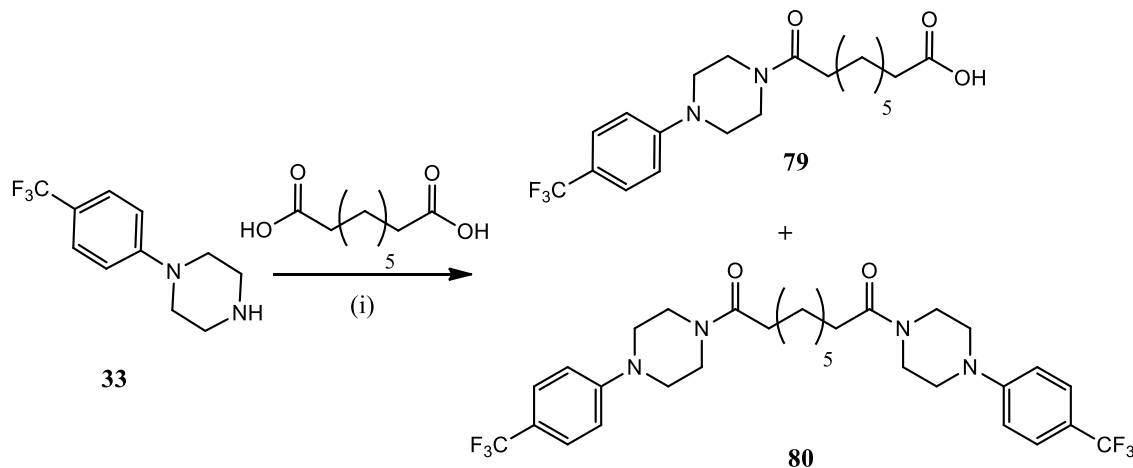
Scheme 3.40: Formation of **79** and **80**, (i) 2 eq of carboxylic acid, 1 eq of **33**, HOBt, TBTU, NEt$_3$, DMF, N$_2$, rt, 5 hrs, **79** (30%), **80** (63%).

Due to the high biological activity of **79** large amounts were required for subsequent biological testing. As a result, it was necessary to optimise its synthesis. To avoid the disubstitution, the methyl ester, monomethyl azelate, was coupled to **33** using an alternative benzotriazole, benzotriazol-1-yloxytris(dimethylamino)-phosphonium hexafluorophosphate (BOP) (**Scheme 3.41**). The methyl ester product, **52**, which was also highly active in the glucose uptake assay, was isolated in a 98% yield. The presence of **81** was supported by HR-MS, ^{1}H NMR and ^{13}C NMR spectroscopy. The presence of the singlet, integrating for three protons, at 3.66 ppm in the ^{1}H NMR spectrum indicated the methyl ester peak. 2D HSQC experiments suggested the presence of the methyl ester carbon at 54.4 ppm in the ^{13}C NMR. The ^{13}C NMR further supported the synthesis of the product with the quartets resonating at 126.4 ppm ($J = 3.3$ Hz), 124.5 ppm ($J = 269.7$ Hz) and 121.2 ppm ($J = 32.8$ Hz) indicating the presence of the trifluoromethyl phenyl group. The ester was converted to the carboxylic acid *via* base catalysed ester hydrolysis to give **79** in an 80% yield (**Scheme 3.41**). The hydrolysis of the ester was evident from the ^{1}H NMR and the ^{13}C NMR spectrum, where the peaks at 3.66 ppm and 54.4 ppm were no longer observed. The broad singlet

resonating at 10.30 ppm in the ^{1}H NMR spectrum is also characteristic of the carboxylic acid -OH peak. HR-MS also supported the presence of **79**.
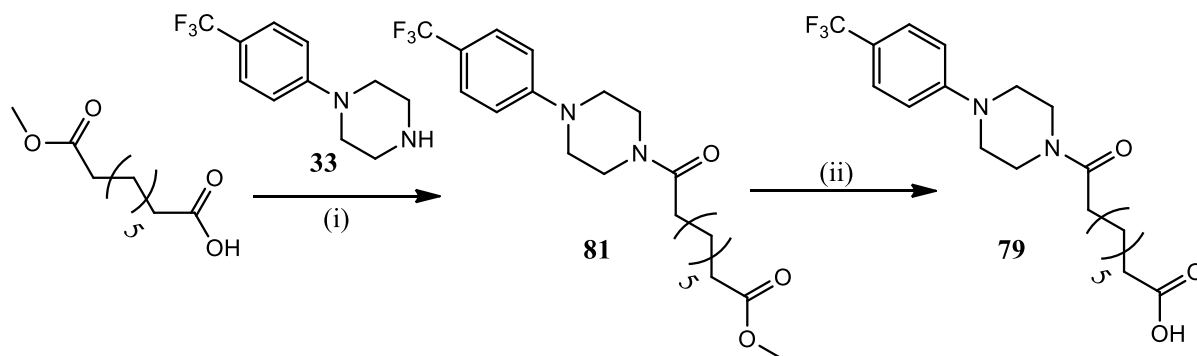
Scheme 3.41: Synthesis of **79** and **81**, (i) BOP, NEt$_3$, DCM, N$_2$, rt, overnight, 98% (ii) KOH, EtOH, reflux, 4 hrs, 80%.

3.3   Conclusion

Amide bond formation was the key final step in the synthesis of the compound **1**, **4** and the derivatives of these compounds. The coupling reagents HOBt and TBTU were used in most cases with the amide product generally isolated in acceptable yields. A large number of target compounds were synthesised and made available for biological evaluations.

The synthesis of a number of arylpiperazines, required to investigate the importance of this functional group, involved the use of a number of different synthetic methods. Metal catalysed reactions were used in some cases, but MW assisted S_NAr gave access to the same arylpiperazines in an improved yield and reduced reaction time. From the synthesis of arylpiperazines, it was clear that:

- MW synthesis was useful to access arylpiperazines containing electron withdrawing groups,

- The cyclocondensation approach was useful to access arylpiperazines that did not contain an electro withdrawing group,

- MW conditions improved yields and reduced reaction times.

4. Synthesis of compound 2 and its derivatives 92 and 104-122 and compound 3 and its derivatives, 138-144.

4.1   Introduction

The pyrazole motif is found in a diverse array of biologically active molecules ranging from antimicrobials and anti-inflammatories to compounds with analgesic activities.[121] The agrochemical industry also avails of the activity of this heterocycle with the pesticides cyanopyrafen and tebufenpyrad both bearing pyrazole functionalities.[122,123] Whether it is present as the core scaffold or simply as a pendant functionality, the pyrazole heterocycle is an extensively used functional group in medicinal chemistry. For example, a number of blockbuster drugs, such as celebrex and viagra, boast the use of this aromatic moiety (**Figure 4.1**).[124,125]
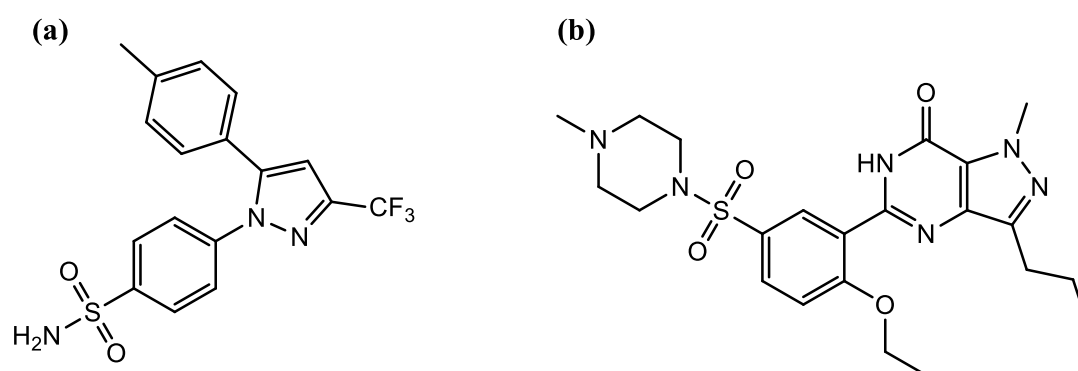
Figure 4.1. Structures of the pyrazole containing (**a**) celebrex and (**b**) viagra. [124,125]

4.1.1   Synthesis of pyrazoles from 1,3-diketones

Owing to the medicinal importance of this heterocycle, much attention has been given to the development of methods that give access to a variety of substituted derivatives. The most common and efficient route exploits the use of 1,3-diketones and hydrazines.[126] This cyclocondensation reaction allows for the synthesis of a variety of substituted pyrazoles as the nature of the pyrazole substituent can be simply changed through altering the 1,3-diketone or hydrazine employed.

The general procedure for the synthesis of pyrazoles from these two reactants involves heating the 1,3-diketone in a suitable organic solvent, at reflux, in the presence of the hydrazine. Synthesis of the 1,3-diketone from either acid chlorides or ketones, in the presence of a strong base, is often required making the pyrazole synthesis a two-step process. However, Heller *et al*. reported a one-pot synthesis of a number of 3,4,5- and *N*-substituted pyrazoles.[126] The initial preparation of 1,3-diketones *in situ* from acid

chlorides and a lithium enolate, before the substituted hydrazine was added to give the desired pyrazole product, with yields in the range of 43% to 89% (**Scheme 4.1**).

Yields: 43-89%
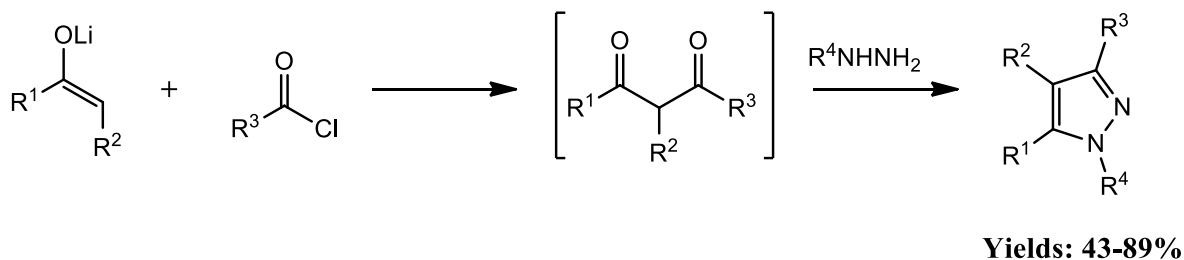
Scheme 4.1: The synthesis of substituted pyrazoles.[126]

4.1.1.1 Synthesis of pyrazoles using 1,3-diketones: Solvent-free approach

Recently this method of synthesising substituted pyrazoles has evolved beyond the use of organic solvents. A "greener" approach involves the grinding of the familiar 1,3-diketones with solid hydrazinium carboxylate, where the grinding of the reactants accelerates the chemical process.[127] The use of the solid zwitterionic hydrazinium carboxylate avoids the use of solvents and the toxic liquid hydrazine, allowing the formation of pyrazoles at relatively moderate temperatures (70 °C).[128]

Hydrazinium carboxylate is synthesised as a solid crystalline material from hydrazine and supercritical carbon dioxide.[127] The solid hydrazinium carboxylate and the 1,3-diketone are ground in air, causing the decomposition of the hydrazinium carboxylate to reveal an anhydrous source of hydrazine. The mixture is then placed in a vial for a suitable period of time and at an appropriate temperature. This results in the formation of the pyrazole compound in high yields (> 96%) and excellent selectivity.[128] Lee *et al.* synthesised a number of substituted pyrazoles, such as 3,4,5-trimethyl-1*H*-pyrazole using this method (**Scheme 4.2**).[128]

Hydrazinium carboxylate
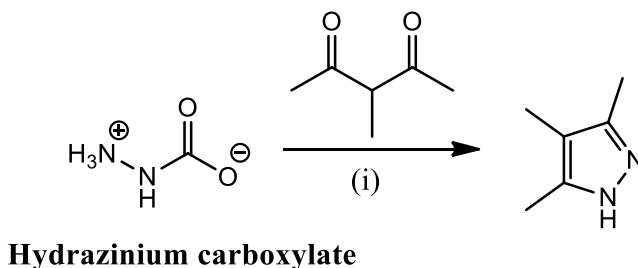
Scheme 4.2: Synthesis of 3,4,5-trimethyl-1*H*-pyrazole, (i) 70 °C, 2 hrs, 96%.[128]

3,4,5-Trimethyl-1*H*-pyrazole was synthesised by heating either a neat solution of hydrazine hydrate and 3-methylpentane-2,4-dione at 70 °C for two hours or in THF at reflux for two hours. Both of these methods culminated in a reduced yield, with the pyrazole isolated in a 77% yield for the neat solution and a 90% yield when heated at reflux in THF. Unknown side products were also observed resulting in a need for a purification step, which was not necessary when hydrazinium carboxylate was used. The efficiency of the solid state approach was claimed to be due to the anhydrous hydrazine that was produced when the hydrazinium carboxylate sublimes.[128] The lack of water present in the hydrazine produced from the hydrazinium carboxylate was said to prevent the formation of side products, as seen with the other two approaches.

4.1.1.2 Substituted 1,3-diketones

Substituting 1,3-diketones at the α-carbon can give access to a variety of carbonyl containing pyrazole derivatives. This approach involves synthesising highly active enaminone intermediates from dicarbonyls and formamide acetals. This is then followed by a reaction with substituted hydrazines giving the carbonyl containing pyrazole (**Scheme 4.3**). This approach can also be extended to the use of β-ketoesters and malonates, showing the diversity of dicarbonyls that can be exploited.[129] Carboxylic acid containing derivatives can then be obtained from the ester derivatives through hydrolysis.

R = Alkyl or O-Alkyl   **Enaminone**
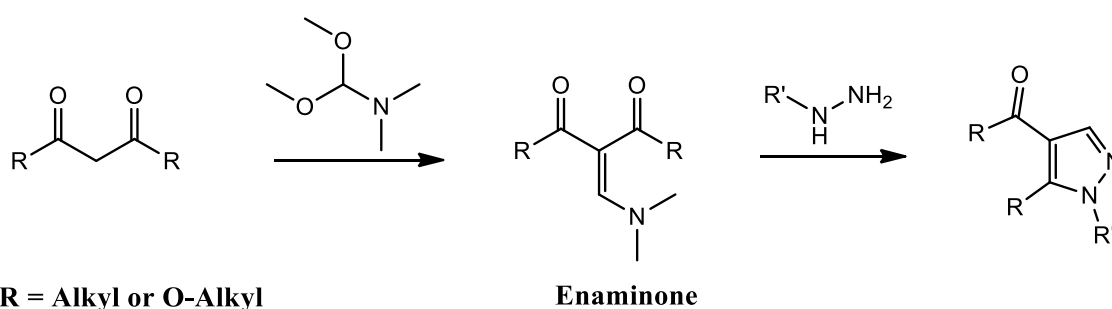
Scheme 4.3: Synthesis of enaminones from dicarbonyl compounds and reaction to give pyrazoles.[129]

4.1.1.3 Use of β-substituted ketones

While 1,3-diketones and substituted 1,3-diketones allow for the synthesis of a variety of substituted pyrazoles the use of β-ketonitriles and hydrazines allows for the preparation of a number of 5-aminopyrazole derivatives.[130] The nature of the β-ketonitrile can be

modified with relative ease *via* variation of the ketoester from which it is derived. This allows access to an array of substituted 5-aminopyrazoles.[130] In addition, Bagely *et al.* reported the synthesis of these aminopyrazoles in methanol at 120 °C using MW irradiation, giving substituted 5-aminopyrazoles in excellent yields (> 80%) after forty minutes.[130]

4.1.2   Synthesis of pyrazoles using a 1,3-dipolar cycloaddition

Copper mediated Huisgen 1,3-cycloaddition has been extensively reported for the formation of 1,2,3-triazoles and this approach can also be applied to the formation of alternative nitrogen containing five membered heterocycles.[131] Hanamoto described a copper free synthesis of substituted pyrazoles using 1,3-cycloadditions where the addition of the 1,3-dipole, azidomethane, to the dipolarophile, tributyl(3,3,3-trifluoroprop-1-yn-1-yl)stannane, resulted in the substituted pyrazole, **82** (**Scheme 4.4**).[131] Furthermore, the metal catalysed cross coupling reaction of **82** with a variety of halogenated reactants gave access to a number of substituted pyrazoles. For example, the substituted pyrazole, **83**, was isolated in an impressive 81% yield.
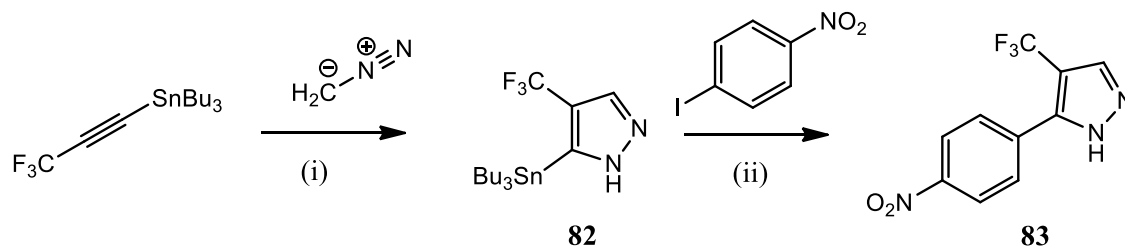
Scheme 4.4: Pyrazole synthesis *via* 1,3-cycloaddition followed by metal catalysed substitution, (i) Et_2O, 0 °C, 1.5 hrs, 70% (ii) $Pd(PPh_3)_4$, LiCl, CuTC, DMSO, 81%.[131]

While the Hanamoto approach, described above, required a metal catalysed step to introduce functional diversity, Aggarwal *et al.* reported a metal free approach where by the functional diversity was introduced by first derivitizing the 1,3-dipole and/or the dipolarophile.[131,132] Functional diazo 1,3-dipoles were generated *in situ*, avoiding the handling of the toxic and potentially explosive material.[132] The condensation of tosylhydrazine with aldehydes followed by treatment with aqueous sodium hydroxide gave a solution of a tosylhydrazone sodium salt. Heating of the tosylhydrazone at 50 °C generated the diazo compound *in situ.* Addition of the alkyne followed by heating at 50

°C allowed for the generation of a number of derivatized pyrazoles in good yields (24-67%) and with good selectivity (**Scheme 4.5**).[132]
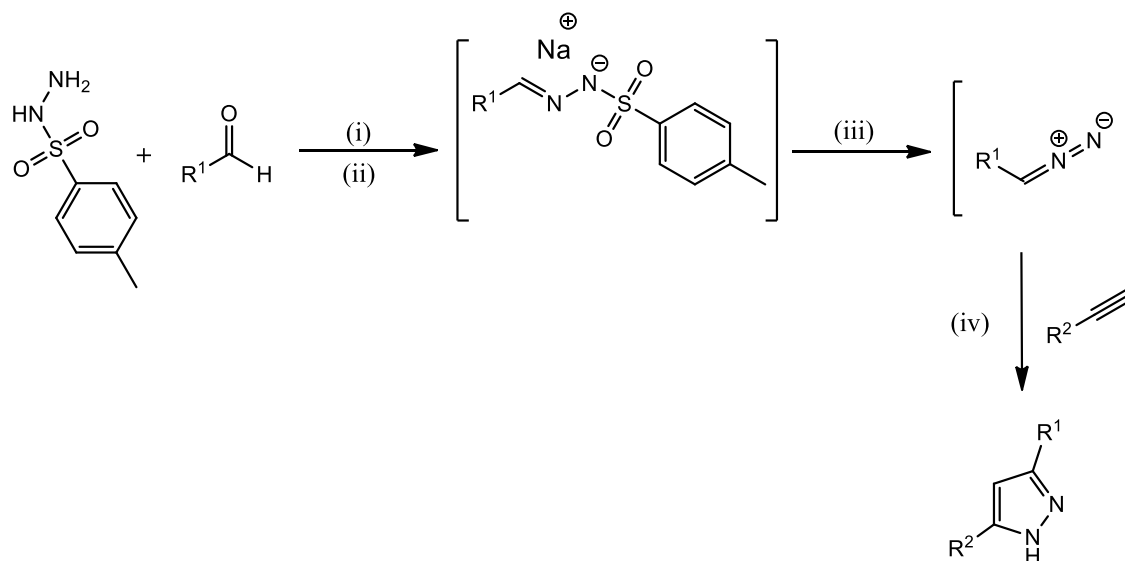
Scheme 4.5: Synthesis of 3,5-disubstituted pyrazoles, (i) CH$_3$CN, rt, 3 hrs (ii) 5 M aqueous NaOH, rt, 20 mins (iii) 50 °C (iv) 50 °C, 48 hrs 24-67%.[132]

4.1.3   Metal catalysed pyrazole synthesis

Work published by Martin *et al*. provided an insight into the formation of pyrazoles *via* copper mediated processes.[133] This consisted of an initial copper catalysed amidation of a haloenyne, by a Boc protected hydrazine, followed by an intramolecular hydroamidation. A subsequent deprotection step, involving the use of trifluoroacetic acid provided the free pyrazoles product in excellent yields. By varying the nature of the hydrazine as well as the substitution pattern on the haloenyne, a high level of derivitization was achieved (**Scheme 4.6**).
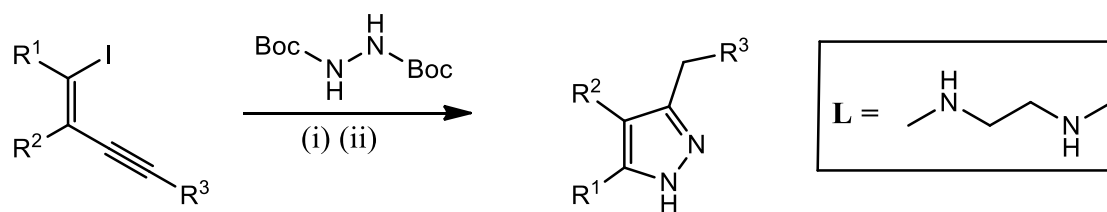
Scheme 4.6: Copper catalysed pyrazole formation, (i) CuI (5 mol%), L (20 mol%), Cs$_2$CO$_3$, THF, 80 °C, 6-16 hrs (ii) TFA, DCM, rt.[133]

Transition metals can also be used to generate *N*-arylated pyrazoles with the previously described palladium catalysed Buchwald-Hartwig amination or variations of the copper mediated Ullmann reaction commonly used.[134,135,136]

4.1.4 Regioselectivity

The synthesis of pyrazoles can be somewhat challenging due to the difficulties in controlling the regioselectivity. If the two electrophilic sites have similar electronic properties or if the hydrazine nitrogen atoms have similar nucleophilicities, a mixture of regioisomers can occur.[137] One such example is the synthesis of *N*-methylpyrazoles. When Olivera *et al.* attempted the synthesis 4,5-bis(2-bromo-4,5-dimethoxyphenyl)-1-methyl-1*H*-pyrazole from the enaminoketone **84**, an almost 50:50 mixture of regioisomers **85** and **86** was obtained.[137] This was due to the similar reactivities of the hydrazine nitrogen atoms.[138,139,140] The influence that the hydrazine molecule has on regioselectivity is further exemplified in the use of *N*-phenylhydrazine, which was used to synthesise the pyrazole **87**. This resulted in the isolation of only a single *N*-substituted isomer (**Scheme 4.7**). This was due to the differences in the reactivities of the hydrazine nitrogen atoms, with the nitrogen atom bound to the aromatic ring less nucleophilic due to the delocalisation of its lone pair of electrons into the aromatic ring. Other factors that can affect regioselectivity include the steric interactions of the substituents on the reactants and the pyrazole tautomerism.[132, 137] When Olivera reacted the enaminoketone **84** with hydrazine, this afforded a mixture of the pyrazole tautomers **88** and **89**.[137] The similar reactivities observed for the two nitrogen atoms allowed either nitrogen atom to attack either of the electrophilic sites.[137]
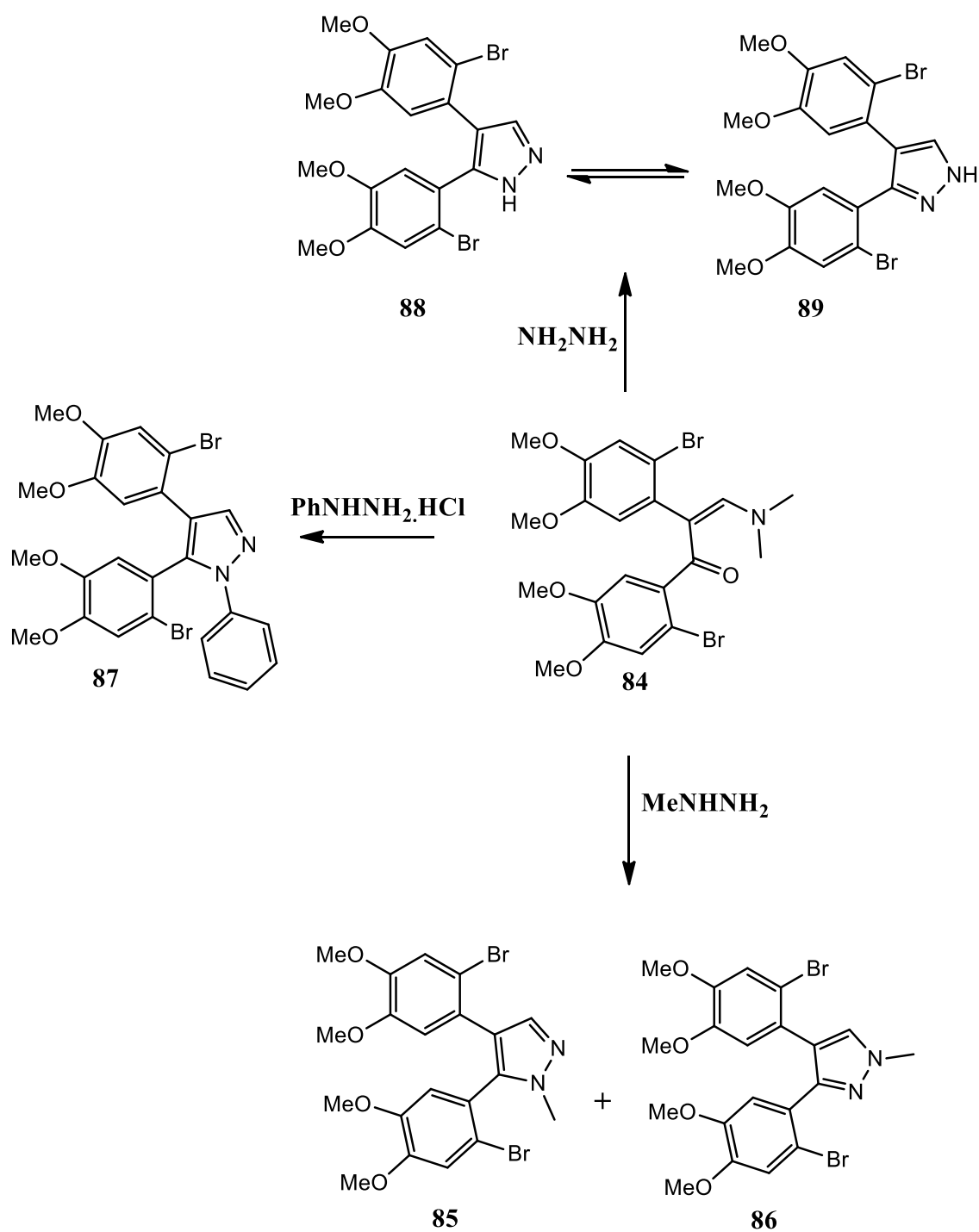
Scheme 4.7: Regioselectivity during pyrazole synthesis.[137]

4.2   Synthesis of derivatives of compound 2

Synthesis of derivatives of compound **2** involved the construction of the pyrimidone scaffold from substituted β-ketoesters and amino pyrazoles. This methodology required heating the two starting materials at reflux in acetic acid for the appropriate amount of time. Introduction of various substituents at the C2 position involved the use of an amino pyrazole with the desired substituent in the 3-position of the heterocycle. Similarly, introduction of various substituents at the C7 position involved the use of an appropriate β-ketoester, as shown in **Scheme 4.8**. The mechanism for the formation of the pyrimidinone product is shown in **Scheme 4.9.**
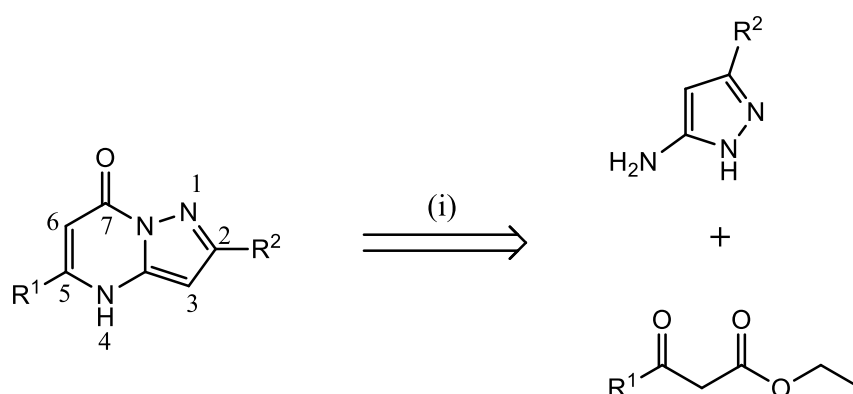
Scheme 4.8: Retrosynthesis of derivatives of compound **2** (i) HOAc, reflux, 4 hrs.
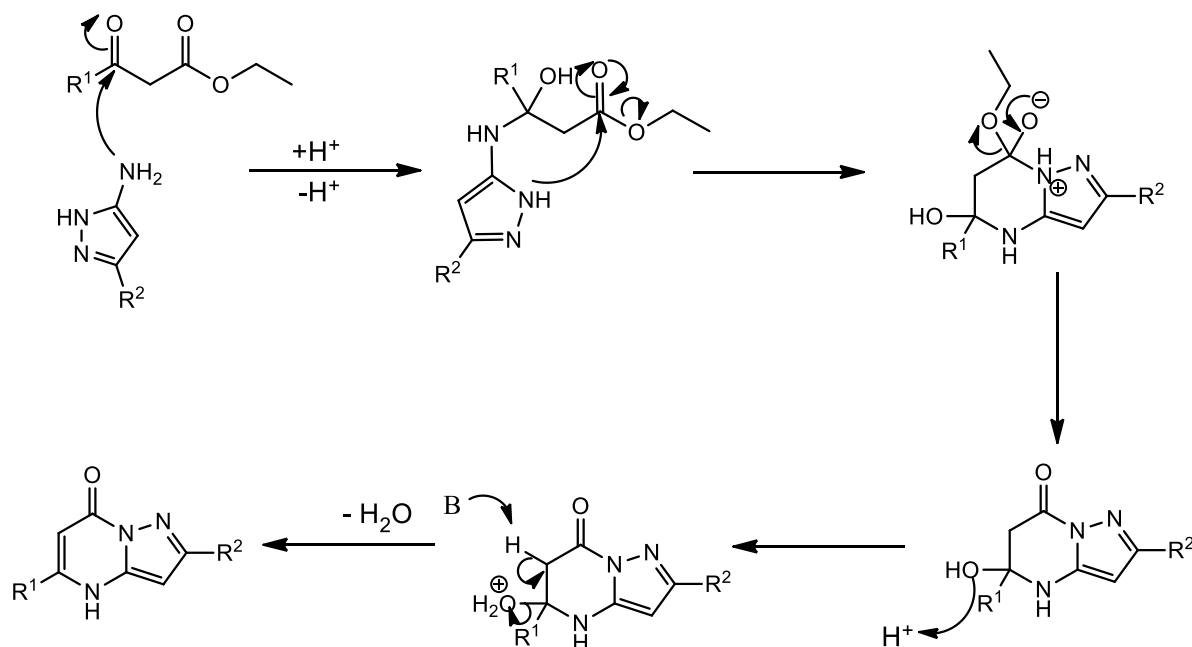
Scheme 4.9: Mehanism for the formation of the pyrimidinone scaffold.

A number of derivatives of compound **2** were synthesised to investigate the effect that altering the substituents at various positions would have on biological activity. In order to produce these analogues, we first had to synthesise the appropriate substituted amino pyrazole and/or β-ketoester in several cases. Once synthesised, the pyrimidone structure was constructed as before by refluxing the two reagents in acetic acid for the appropriate amount of time. The following section discusses the synthesis of these building blocks.

4.2.1   Synthesis of amino pyrazole building blocks for derivatizing compound 2 at the C2 position

4.2.1.1 Synthesis of compound 91

The first derivative of interest required replacement of the *tert*-butyl group at the C2 position with a hydrogen, thus, 1*H*-pyrazol-5-amine was required. The proposed retrosynthetic route for the preparation of this derivative (**92**) is outlined in **Scheme 4.10**. This involved the synthesis of the substituted nitrile, **90**, which would be used to prepare 1*H*-pyrazol-5-amine (**91**). The previously mentioned condensation reaction conditions would then be used to synthesise the functionalised pyrimidone **92**.
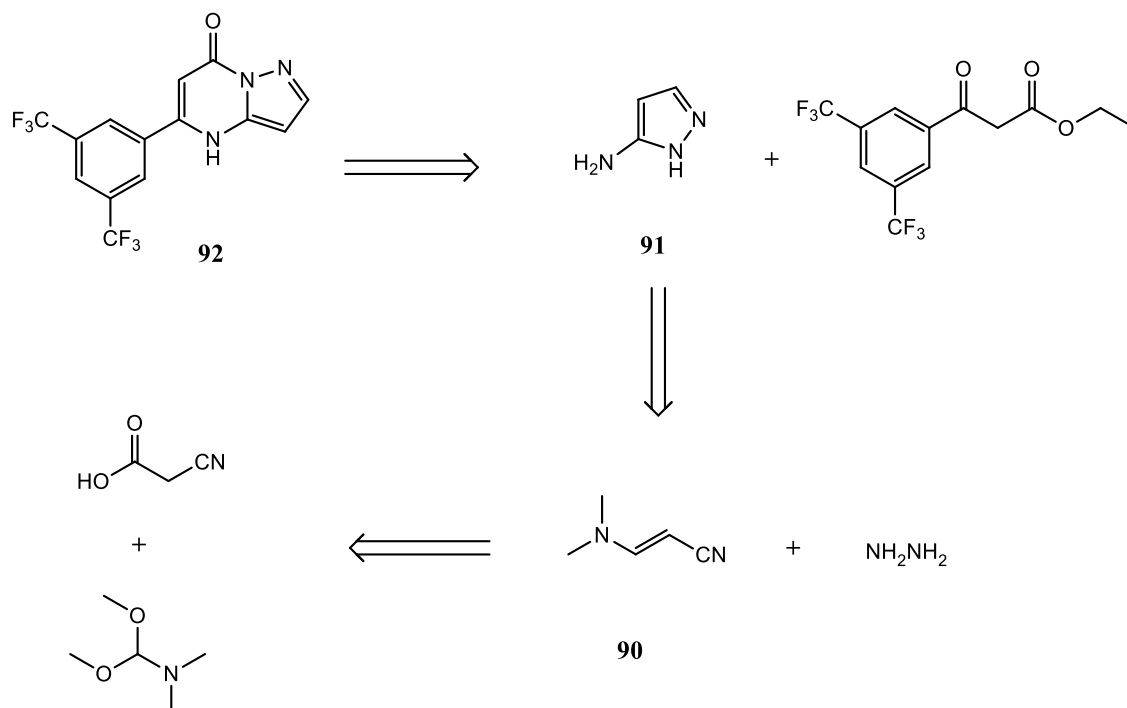
Scheme 4.10: Retrosynthesis of compound **92**.

The synthesis of the aminopyrazole **91** first required the synthesis of the precursor (*E*)-3-(dimethylamino)acrylonitrile (**90**) (**Scheme 4.11**). The condensation of dimethylformamide dimethyl acetal and cyanoacetic acid gave **90** in 87% yield. The presence of the product was supported by the ^{1}H NMR spectrum with the two doublets resonating 6.88 ppm and 3.61 ppm indicative of the two alkene protons. The coupling constant (J = 13.5 Hz) between the two protons indicated the predominance of the *E* isomer. This large coupling constant is characteristic of a *trans* product as the C-H bonds are 180° to each other.[100] This value would have been larger only for the presence of the electronic withdrawing nitrile which withdraws electrons from the C-H bond weakening through bond communications.[100] Compound **90** was also verified by HR-MS, where the [M + H]$^+$ ion of mass 97.0763 m/z was found.

Once synthesised, the substituted nitrile was reacted with hydrazine monohydrate, using the method reported by Cuny *et al*.[141] This method involved heating **90** and hydrazine monohydrate at 110 °C, for 2 days, in an EtOH/H$_2$O solution. The desired amino pyrazole, **91**, was obtained, albeit in a 25% yield (**Scheme 4.11**).
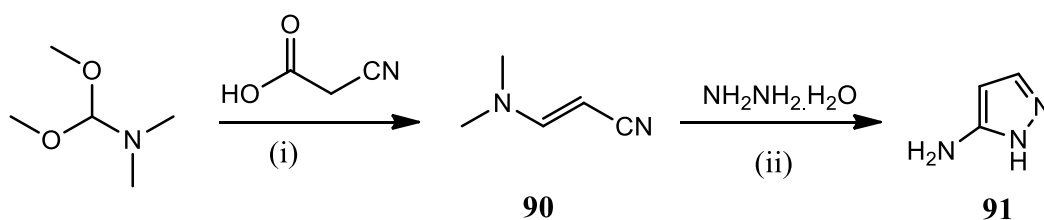
Scheme 4.11: Synthesis of **90** and **91**, (i) 1,4 dioxane, reflux, 2 hrs, 87% (ii) EtOH, H$_2$O, 110 °C, 2 days, 25%.

We were keen to improve the yield, and reduce the reaction time, and a search of the literature found a report by Bagley *et al*. using MW irradiation. This synthetic route involved the use of β-ketonitriles and substituted hydrazines for the synthesis of substituted amino pyrazoles (**Scheme 4.12**).[130]
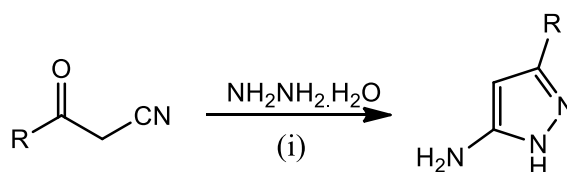
Scheme 4.12: MW assisted synthesis of 3-substituted amino pyrazoles.[130]

For this reason, 3-oxopropanenitrile was prepared *in situ* from 3,3-diethoxypropionitrile using standard acetal deprotection conditions, as was reported by Yin *et al*. and El-Araby *et al*. (**Scheme 4.13**).[142,143] The substituted nitrile was reacted with hydrazine monohydrate using the MW conditions described by Bagley *et al*.[130] Unfortunately, a complex mixture was observed and 1*H*-pyrazol-5-amine was not isolated.
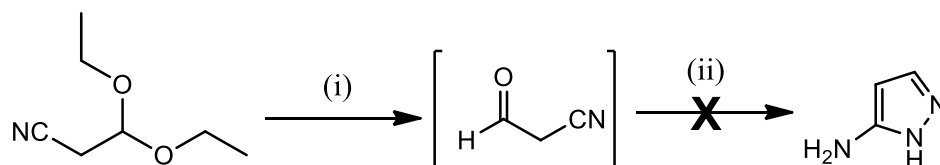
Scheme 4.13: Synthesis of 3-oxopropanenitrile, (i) TFA, H_2O, 6 hrs, 5 °C (ii) $NH_2.NH_2.H_2O$ MeOH, MW, 100 W, 40 mins, 120 °C.

The previous attempt to synthesis 1*H*-pyrazol-5-amine involved the use of **90** and conventional heating conditions. We wondered if the conditions reported by Bagley *et al*. could be used in the preparation of 1*H*-pyrazol-5-amine.[130] The nitrile **90** and hydrazine monohydrate were again reacted, however, this time they were heated in MeOH at 120 °C for forty minutes at 300 W. This method allowed for the isolation of 1*H*-pyrazol-5-amine (**91**) in an 80% yield and provided a facile, efficient and novel synthetic route to 1*H*-pyrazol-5-amine from (*E*)-3-(dimethylamino)acrylonitrile (**Scheme 4.14**).
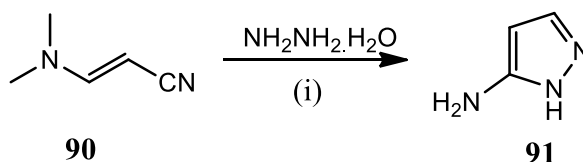
Scheme 4.14: Synthesis of **91** (i) MeOH, MW, 120 °C, 300 W, 40 mins, 80%.

4.2.1.2 Synthesis of compounds 93 and 96

The introduction of aromatic substituent at the C2 position required the synthesis of amino pyrazoles containing the appropriate aromatic substitution at the 3-position of the pyrazole heterocycle. The microwave assisted synthesis of substituted amino pyrazoles reported by Bagley *et al*. proved to be a highly effective method for synthesising the pyrazole **91**.[130] As such, the same methodology was applied to the synthesis of pyrazoles **93** (**Scheme 4.15**) and **96** (**Scheme 4.16**).

A simple phenyl group was introduced at the C3 position of **93**. The substituted pyrazole **93** was synthesised from 3-oxo-3-phenylpropanenitrile and hydrazine monohydrate (**Scheme 4.15**).

93

Scheme 4.15: Synthesis of pyrazole **93**, (i) MeOH, MW, 300 W, 40 mins, 120 °C, 75%.

Heterocycles can have positive effects on the biological efficacy of a compound. The heteroatom can become involved in hydrogen bonding and the presence of p orbitals can stabilise the drug:protein interaction through pi stacking.[63] To synthesise the necessary amino pyrazole, 3-(thiophen-2-yl)-1H-pyrazol-5-amine (**96**), *via* the method by Bagley *et al.*, we first needed to synthesise the β-ketonitrile **95** (**Scheme 4.16**).[130]

94   **95**

96

Scheme 4.16: Synthesis of pyrazole **96**, (i) DMAP, DCC, EtOAc, 0 °C-rt, overnight, 99% (ii) n-BuLi, THF, -78 °C, 3 hrs, 70% (iii) MeOH, MW, 300 W, 40 mins, 120 °C, 55%

Chapter 3 saw the use of coupling reagents to increase the activity of a carboxylic acid by generating an activated ester *in situ*. These activated esters are generally not isolated as they are highly reactive. The synthesis of **95** required the activation of thiophene-2-carboxylic acid and this was achieved through its reaction with benzotriazole in the presence of DMAP and DCC. In this case the reactivity of the carbonyl carbon was increased by the formation of the benzotriazole derivative **94**. Unlike previously mentioned activated species, it was possible to isolate this benzotriazole in an excellent yield of 99%. Compound **94** was not susceptible to hydrolysis by atmospheric water and therefore was isolated and used without the need for anhydrous conditions.

To produce the β-ketonitrile **95**, the method reported by Katritzky *et al*., involving the use of *n*-BuLi and acetonitrile at -78 °C, was employed.[144] This involved the *n*-BuLi mediated depotonation of acetonitrile followed by its reaction with compound **94**. Compound **95** was formed in a 70% yield and was subsequently reacted with hydrazine monohydrate using the conditions inspired by Bagley *et al*.[130]

Nenaidenko *et al*. previously reported the synthesis of **96** from trichloroacetonitrile and hydrazine monohydrate using conventional heating, with the amino pyrazole reported to be isolated in a 53% yield after four hours.[145] The use of MW irradiation to synthesise **96** from **95** and hydrazine monohydrate represents a novel and efficient method for synthesising the amino pyrazole in a shorter reaction time without any reduction in yield.

4.2.2   Synthesis of β-ketoester building blocks for derivatizing compound 2 at the C5 position.

To investigate the importance of the substituent at the C5 position, a number of β-ketoester building blocks were required. A number of methodologies were used to synthesize these building blocks and this will be discussed in the following sections.

4.2.2.1 Synthesis of compound 98

4.2.2.1.1   Acetal deprotection

Substitution of the bis(trifluoromethylphenyl) at the C5 position, group first required the synthesis of the appropriate precursors. For example, to replace the aryl motif with a hydrogen atom, it was first necessary to synthesise compound **97**. The synthetic

approach involved the deprotection of the acetal, ethyl 3,3-diethoxypropanoate, using standard acetal deprotection conditions, as described by Lu *et al*.[146] The characteristic aldehydic peak, which resonated at 9.81 ppm, was present in the crude ^{1}H NMR spectrum, however **97** was not isolated. Edvinsson *et al*. suggested that formyl acetic esters can be thermally unstable leading to decomposition.[147] In addition, Sato reported the polymerization of **97** at room temperature.[148] For these reasons, compound **97** was generated *in situ* and reacted directly with 3-*iso*-propyl-1*H*-pyrazol-5-amine (**Scheme 4.17**). However, this method did not yield the desired derivative of compound **2** with a complex mixture being obtained. Therefore an alternative synthetic approach was taken.
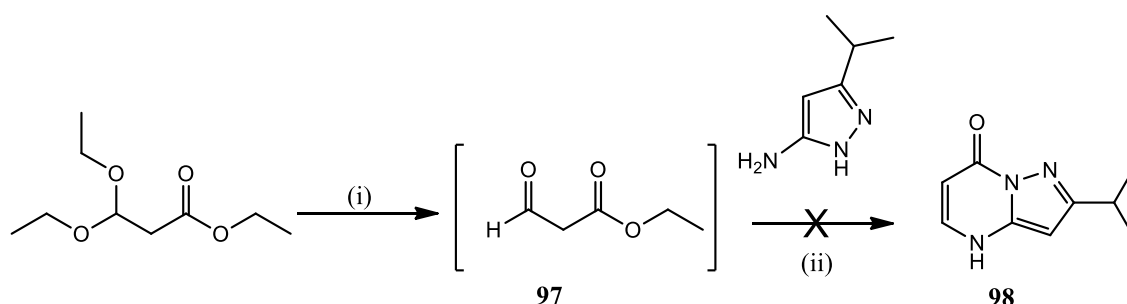
Scheme 4.17: Preparation of **98** from **97**, (i) TFA, DCM, H_2O, rt, 5 hrs (ii) HOAc, reflux, no product isolated.

4.2.2.1.2 Synthesis of compound 97 from 2,2-dimethyl-1,3-dioxane-4,6-dione (Meldrum's acid)

The use of Meldrum's acid is a well-known method for the preparation of β-ketoesters (**Scheme 4.18**). This method relies on the acidity of the α-protons, allowing for simple alkylation at this position. Once alkylated, the desired ketoester can be obtained through a ring opening step by heating the substituted Meldrum's acid in an appropriate alcohol. The nature of the ester substituent is determined by the type of alcohol used, while the substituent at the α-carbon determines the nature of the ketone functionality (**Scheme 4.18**). According to Sato *et al*., once heated the formation of the desired β-ketoester from the substituted Meldrum's acid can proceed *via* two different mechanisms; either by *in situ* formation of a ketene or through alcoholysis.[148]
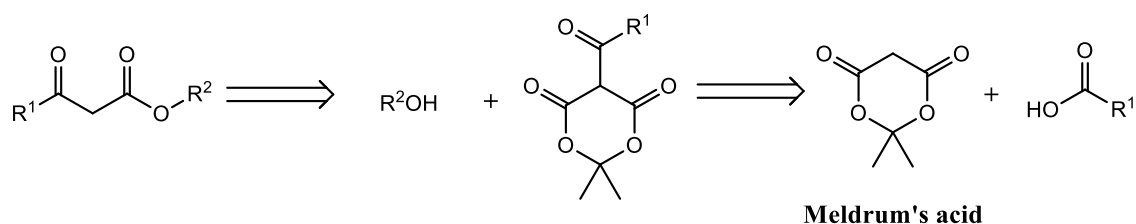
Scheme 4.18: Retrosynthesis of ketoesters from Meldrum's acid.

The use of Meldrum's acid can also be adapted to allow the formation of formyl acetic esters.[147] To synthesize **97** using this method, it was first necessary to synthesis formyl Meldrum's acid (**99**, **Scheme 4.19**). To introduce a formyl group at the α-carbon, 1,1'-carbonyldiimidazole (CDI) was used to activate formic acid in the presence of DMAP and pyridine. This approach was developed from the method proposed by Dolle *et al.* which saw the introduction of an acetyl group at the α-carbon of Meldrum's acid.[149] Various reports detailed the isolation of this acetyl Meldrum's acid in good to moderate yields.[150,151,152] However, this approach did not prove effective for the synthesis of **97**. It was not possible to isolate formyl Meldrum's acid (**99**) due to the complexity of the reaction mixture. Also, when the reaction was mixture carried forward, without any further purification and heated at reflux in the presence of EtOH, a complex mixture was still observed with the ^{1}H NMR void of any characteristic peaks for **97**. The absence of **97** may have been due to its instability, as described by Sato and Edvinsson, or due to the volatility of formic acid. [148,147]
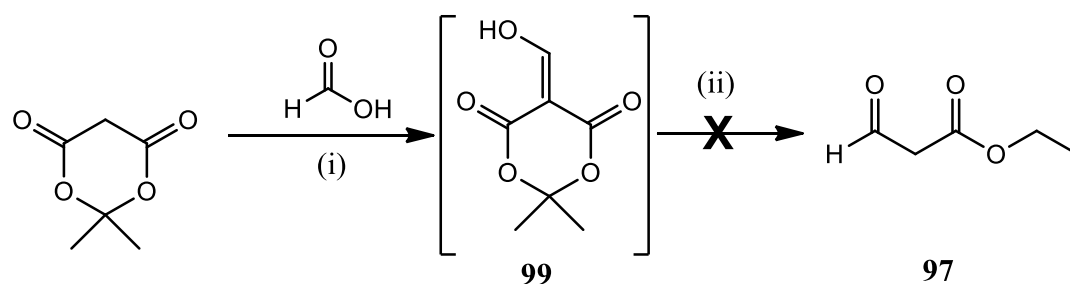
Scheme 4.19: Synthesis of compound **99**, (i) CDI, DMAP, DCC, DCM, N_2, rt, overnight, product not isolated (ii) EtOH, reflux, 5 hrs, product not isolated.

An alternative approach for the synthesis of formyl Meldrum's acid was therefore needed. Again, the literature directed our search towards an appropriate method involving the use of triethyl orthoformate. Here the condensation of triethyl orthoformate with Meldrum's acid provided compound **100** quantitatively. ^{1}H NMR

spectroscopy supported the formation of the product with the presence of the alkenyl proton at 8.23 ppm. The quartet and triplet resonating at 4.42 ppm and 10.36 ppm, integrating for two and three protons respectively, with a coupling constant value of 7.0 Hz, is indicative to the presence of an ethylene group. Acid catalyzed hydrolysis of **100** then afforded the necessary formyl Meldrum's acid, **99**, in an acceptable yield (**Scheme 4.20**). This was confirmed by ^{1}H NMR spectroscopy, where the ethyl group, observed in the ^{1}H NMR spectrum for **100**, was no longer present. The alkene proton was still present at 8.64 ppm and a broad singlet, corresponding to the presence of the hydroxyl group, resonated at 8.20 ppm. This product was not subsequently used in the synthesis of compound **98** due to the success of an alternative method for the synthesis of compound **98**.
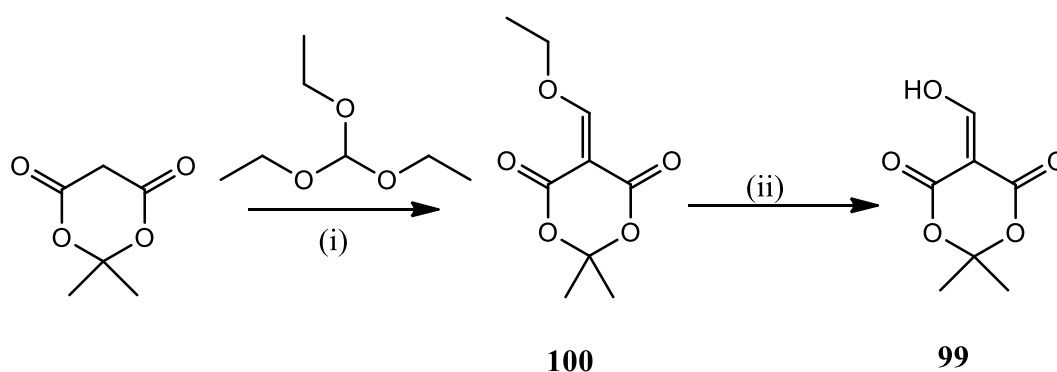
Scheme 4.20: Synthesis of **99** and **100**, (i) 85 °C, quantitative (ii) 2 M aqueous HCl, 2 hrs, 50%.

4.2.2.1.3 Use of the sodium salt of compound 97 in the synthesis of 98

During the course of the Meldrum's acid work, we were simultaneously trying to synthesize **98** using a different method (**Scheme 4.21**). This alternative approach, described by Senga *et al.*, involved the synthesis of the enol tautomer of **97**, as the sodium salt.[153] The method consisted of heating a suspension of EtOAc, ethyl formate and elemental sodium at 27 °C under an inert atmosphere. From this, the sodium salt of **97** was generated *in situ* and reacted immediately with 3-*iso*-propyl-1*H*-pyrazol-5-amine. The preparation of **97** as the sodium salt possibly prevented the polymerization of the product, a problem suggested by Sato.[148] This allowed for the subsequent synthesis and isolation of **98** in an adequate yield (**Scheme 4.21**). The two doublets, resonating at 7.80 ppm and 5.63 ppm in the ^{1}H NMR spectrum, both with an integral

value of one and both with a coupling constant of 7.50 Hz, is highly indicative to the presence of the alkene protons of the product **98**. The doublet resonating at 1.24 ppm, integrating for six protons verifies the presence of the *iso*-propyl. IR spectroscopy confirmed the formation of the amide bond, with the presence of the carbonyl signal at 1675 cm^{-1}. Elemental analysis also supported the presence of this derivative of compound **2**.

sodium salt of **97**

98
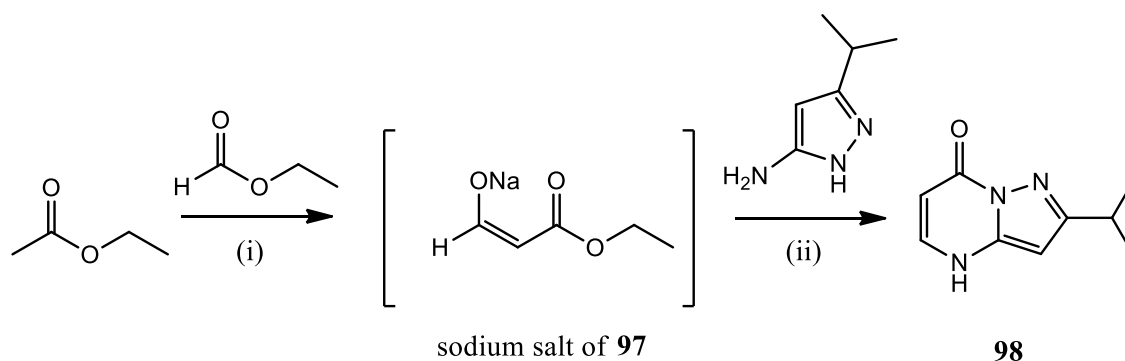
Scheme 4.21: Synthesis of **98** from the sodium salt of **97** (i) Na, 27 °C, 12 hrs (ii) EtOH, reflux, 5 hrs, 15%.

A viable method for the synthesis of **98** has been identified and this process was then used for the synthesis of **101** (**Scheme 4.22**). The same conditions were used, with exception to the amino pyrazole, with 3-(*tert*-butyl)-1*H*-pyrazol-5-amine added to the sodium salt of **97**. A similar yield was observed, with compound **101** isolated in a 13% yield. The low yield of **98** and **101** may be due to the decomposition of the sodium enolate of compound **97**. ^{13}C NMR spectroscopy supported the formation of the product with the signal resonating at 161.2 ppm arising due to the presence of the amide carbonyl. The formation of the carbonyl was further supported by IR spectroscopy with the presence of the carbonyl signal at 1673 cm^{-1}. The two alkenyl carbons were confirmed by the 2D HSQC experiment and were found to resonate at 138.8 ppm and 95.2 ppm.
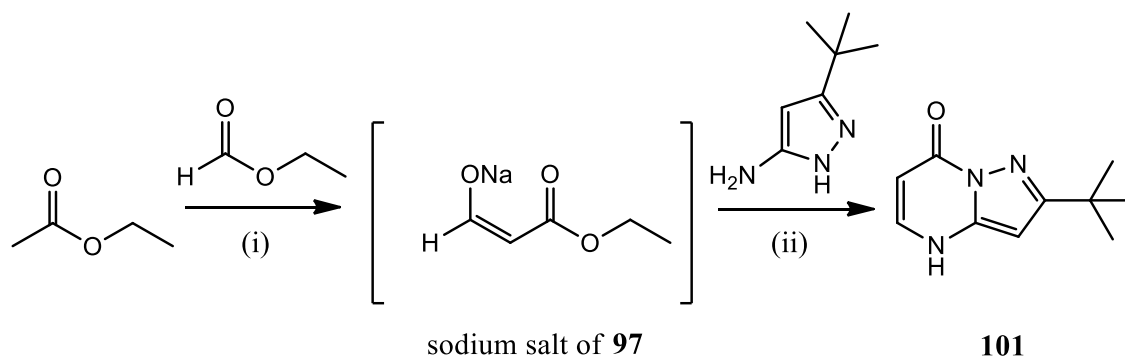
Scheme 4.22: Synthesis of **101** from the sodium salt of **97** (i) Na, 27 °C, 12 hrs (ii) EtOH, reflux, 5 hrs, 13%.

4.2.2.2 Synthesis of compound 102

The position of the CF_3 group within the bis(trifluoromethylphenyl) at the C5 position was also investigated. Construction of this derivative first required the synthesis of the β-ketoester, **102**. An alternative approach, deviating from the use of Meldrum's acid was employed and saw **102** being synthesized from 1-(4-(trifluoromethyl) phenyl)ethanone, sodium hydride and a large excess of diethyl carbonate (**Scheme 4.23**). The formation of the product was supported by ^{1}H NMR spectroscopy with the two doublets, both integrating for two protons and both with a coupling constant value of 8.0 Hz, resonating at 8.06 and 7.75 ppm, indicative of the aromatic protons *ortho* and *meta* to the trifluoromethyl phenyl group. This data corresponded to the ^{1}H NMR data published by Pidathala *et al.*[154] Compound **102** was not isolated but was used as the crude product.
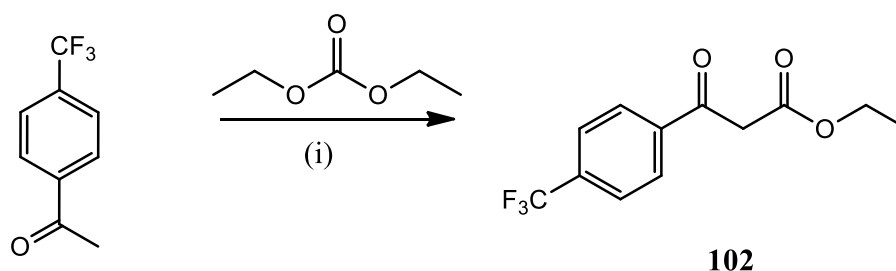
Scheme 4.23: Synthesis of compound **102**, (i) NaH, 80 °C, 1.5 hrs, 71% (crude yield).

4.2.2.3 Synthesis of compound 103

The synthetic procedure involving the use of Meldrum's acid was revisited to synthesise the β-ketoester **103** (**Scheme 4.24**). Here **103** was synthesised from thiophene-2-

carboxylic acid and Meldrum's acid by way of an intermediate which in turn underwent a ring opening, in the presence of EtOH and *para* toluene sulfonic acid, to allow the formation of **103** in 39% yield. The synthesis of the β-ketoester **103** was confirmed by ^{1}H NMR spectroscopy by the presence of the singlet, resonating at 3.83 ppm, integrating for two protons, which was indicative of the presence of the alpha hydrogen's. The thiophene ring was characterised by the presence of three multiplets, all integrating for one proton and all resonating in the aromatic region of the ^{1}H NMR spectrum. They were found in the ranges of 7.66-7.65 ppm, 7.62-7.60 ppm and 7.07-7.04 ppm respectively. The ^{1}H NMR data for compound **103** was in agreement with the reported literature data.[155]
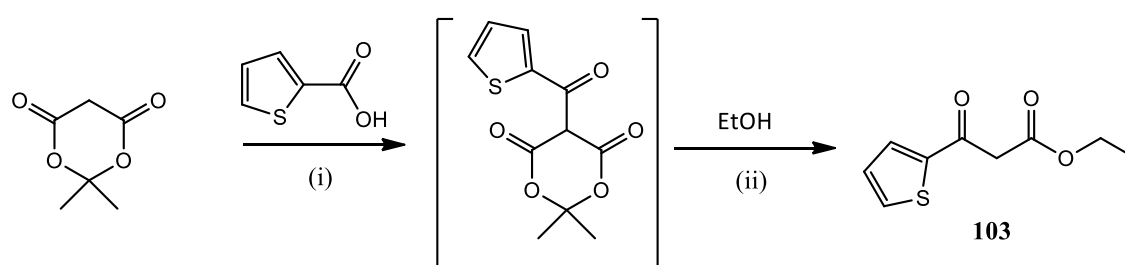
Scheme 4.24: Synthesis of **103** (i) DMAP, DCC, DCM, N_2, 0 °C-rt, 2 hrs (ii) EtOH, *p*-TSA, N_2, reflux, 1 hr, 39%.

4.2.3   Condensation

The derivatives of compound **2** were synthesised using the condensation conditions described above. **Table 4.1** shows the yields for each derivative.
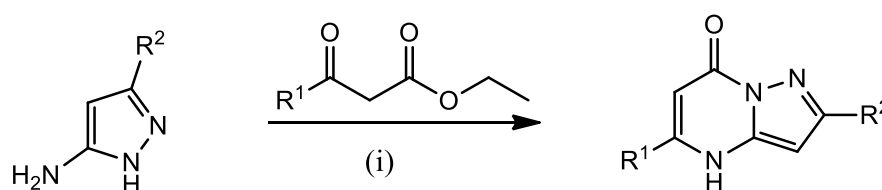
Compound	R^1	R^2	% Yield	Charton value for R^1.[156]
2	bis(*m*-CF$_3$)	*t*Bu	18	*
92	bis(*m*-CF$_3$)	H	-^{b}	-
104	Me	*t*Bu	78	0.52

105	Et	*t*Bu	33[a]	0.56
106	*i*Pr	*t*Bu	65	0.76
107	*t*Bu	*t*Bu	23	1.24
108	Ph	*t*Bu	40	1.66
109	Me	*i*Pr	69	0.52
110	Et	*i*Pr	63	0.56
111	*n*Pr	*i*Pr	72	0.68
112	*i*Pr	*i*Pr	66	0.76
113	*t*Bu	*i*Pr	13	1.24
114	Ph	*i*Pr	30	1.66
115	bis(*m*-CF$_3$)	*i*Pr	27	*
116	2-thienyl	*i*Pr	-[b]	-
117	bis(*m*-CF$_3$)	Me	49	*
118	bis(*m*-CF$_3$)	*Et*	42	*
119	bis(*m*-CF$_3$)	Ph	21	*
120	bis(*m*-CF$_3$)	2-thienyl	30	*
121	*p*-CF$_3$	*i*Pr	30[c]	*
122	mono(*m*-CF$_3$)	*i*Pr	30	*

Table 4.1: Structures and yields (%) of derivatives of **2** (i) HOAc, reflux, 4 hrs. *Charton value for bis(*m*-CF$_3$) not available. Charton value for phenyl = 1.66 and CF$_3$ = 0.91. [a] low yield may be due to issues associated with the purification of the compound and is not indicative of a decrease in yield due to the presence of the Et substituent. [b] product not isolated. [c] crude starting material used.

From **Table 4.1**, it could be suggested that when the ketone R^1 substituent is a bulky, sterically hindered group, low yields are obtained. The increasing Charton values for these substituents correspond somewhat to a decrease in yield, i.e. an increase in steric effects causes a decrease in yield. The presence of the methyl substituent (Charton value = 0.52) for example, resulted in the isolation of compound **104** in a 78% yield. When a

tert-butyl substituent (Charton value = 1.24) was introduced, a significant reduction in yield was observed with compound **107** isolated in a 23% yield. The presence of a bulky group may hinder the primary nucleophilic amine of the pyrazole group from attacking the ketone carbonyl, resulting in a low yield. This hypothesis may also explain the low yields observed for **113**, **114**, **116**, **121** and **122** compared to those obtained for **109**, **110**, **111** and **112**. The low yield obtained for compound **105** may be due to a work up issue. Several purification steps were required to purify this derivative.

To produce compound **92** (**Scheme 4.25**), the previously synthesised pyrazole **91** and the commercially available ethyl 3-(3, 5-bis(trifluoromethyl)phenyl)-3-oxopropanoate were heated at reflux, in acetic acid, for four hours. The reaction yielded a complex crude mixture and the presence of the product was uncertain from the ^{1}H NMR spectrum. Flash chromatography was used to reduce the complexity of the mixture however the product could not be isolated.
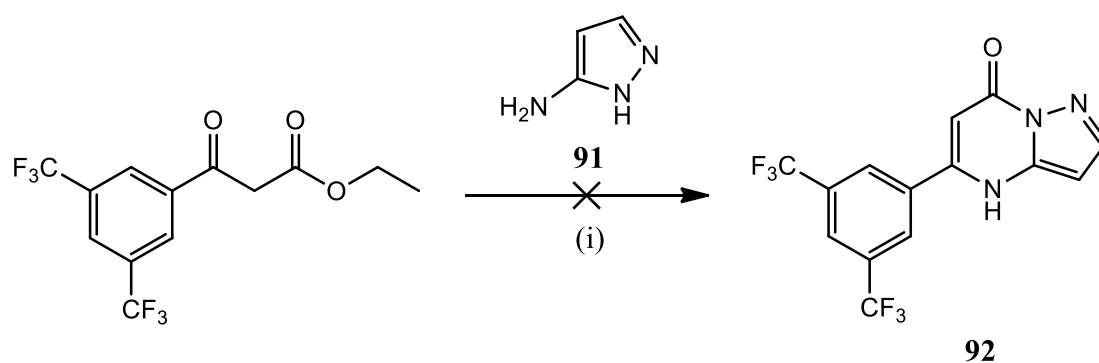
Scheme 4.25: Attempted synthesis of compound **92** (i) HOAc, reflux, 4 hrs.

The importance of the position of the CF$_3$ functionality within the bis(trifluoromethylphenyl) at the C5 position was also investigated. To produce compound **121**, the previously described crude mixture containing the ketoester **102** and 3-*iso*-propyl-1*H*-pyrazol-5-amine were heated at reflux, in acetic acid, for four hours (**Scheme 4.26**). The desired pyrimidinone was isolated in a 30% yield.
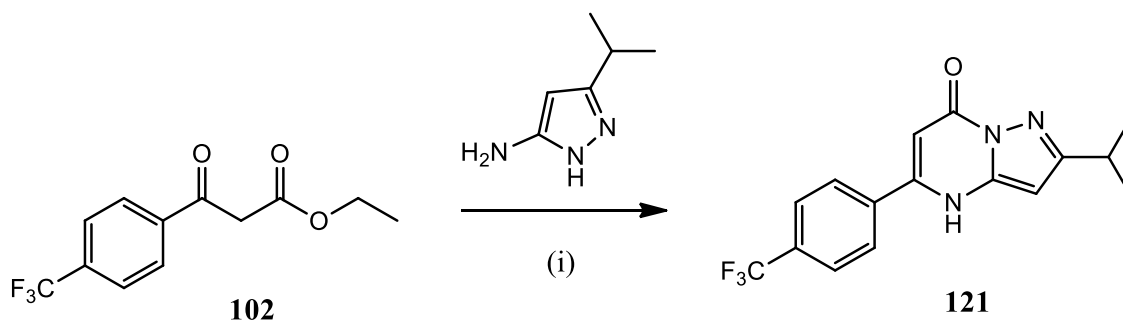
Scheme 4.26: Synthesis of compound **121** (i) HOAc, reflux, 4 hrs, 30%.

To access the derivative of compound **2**, **116**, in which a thiophene heterocycle would be introduced at the C5 position to replace the bis(trifluoromethylphenyl) moiety, the previously synthesised β-ketoester **103** and 3-*iso*-propyl-1*H*-pyrazol-5-amine were heated at reflux for 4 hrs. Although the trusted method used to synthesise the pyrimidone derivatives was employed, the pyrimidone **116** could not be isolated. Various purification attempts were made, however **116** was not isolated in an acceptable level of purity (**Scheme 4.27**). The synthesis of **116** was not reattempted.
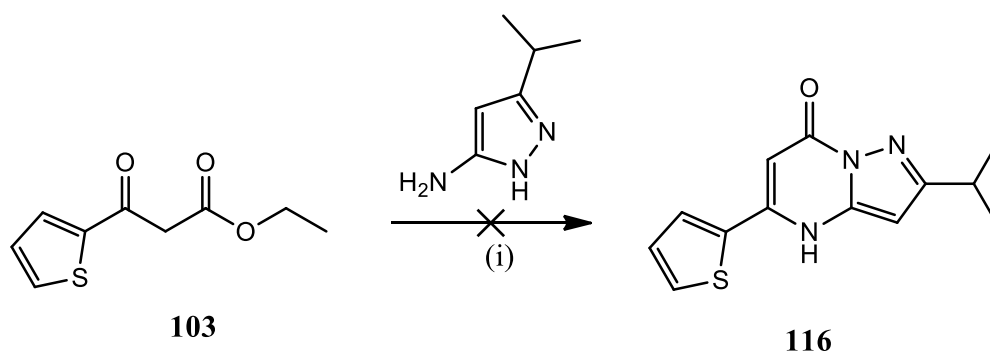
Scheme 4.27: Attempted synthesis of compound **116** (i) HOAc, reflux, 4 hrs.

4.2.4   Synthesis of compound 123

A derivative of compound **4** was also synthesised in which changes were made to the pyrimidone scaffold. This involved the alkylation of the secondary amine, in the 4-position of the ring, to give the derivative, **123**. The synthesis was carried out by heating a suspension of compound **115**, potassium carbonate and DMF at reflux for eight hours in the presence of iodoethane (**Scheme 4.28**). Although compound **123** was isolated in a less than desirable yield, it was obtained in high purity.

112
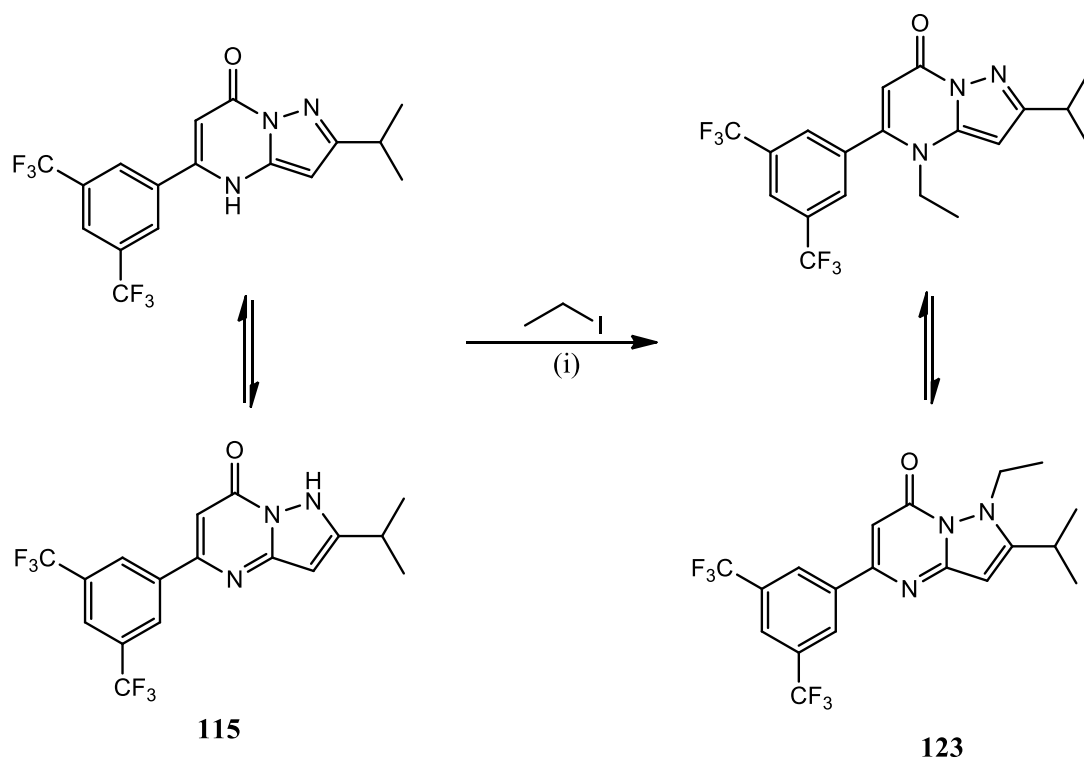
Scheme 4.28: Synthesis of compound **123** (i) K_2CO_3, DMF, 8 hrs, reflux, 18%.

4.3   Synthesis of derivatives of compound 3

The synthesis of compound **2** and its family of derivatives saw the use of β-ketoesters and pyrazoles to produce the pyrimidone scaffold, with MW irradiation used to synthesise the 5-amino-1*H*-pyrazoles precursors. The construction of the derivatives of compound **3** also employed the use of β-ketoesters, hydrazines and pyrazoles; however, here substituted hydrazines and substituted β-ketoesters were manipulated to produce the *N*-substituted pyrazoles from which the **3** analogues were derived (**Scheme 4.29**).

Compound 3: $R^1 = o\text{-OMe}$
$\quad\quad\quad\quad\quad R^2 = Me$
$\quad\quad\quad\quad\quad R^3 = F$
$\quad\quad\quad\quad\quad X = CH$
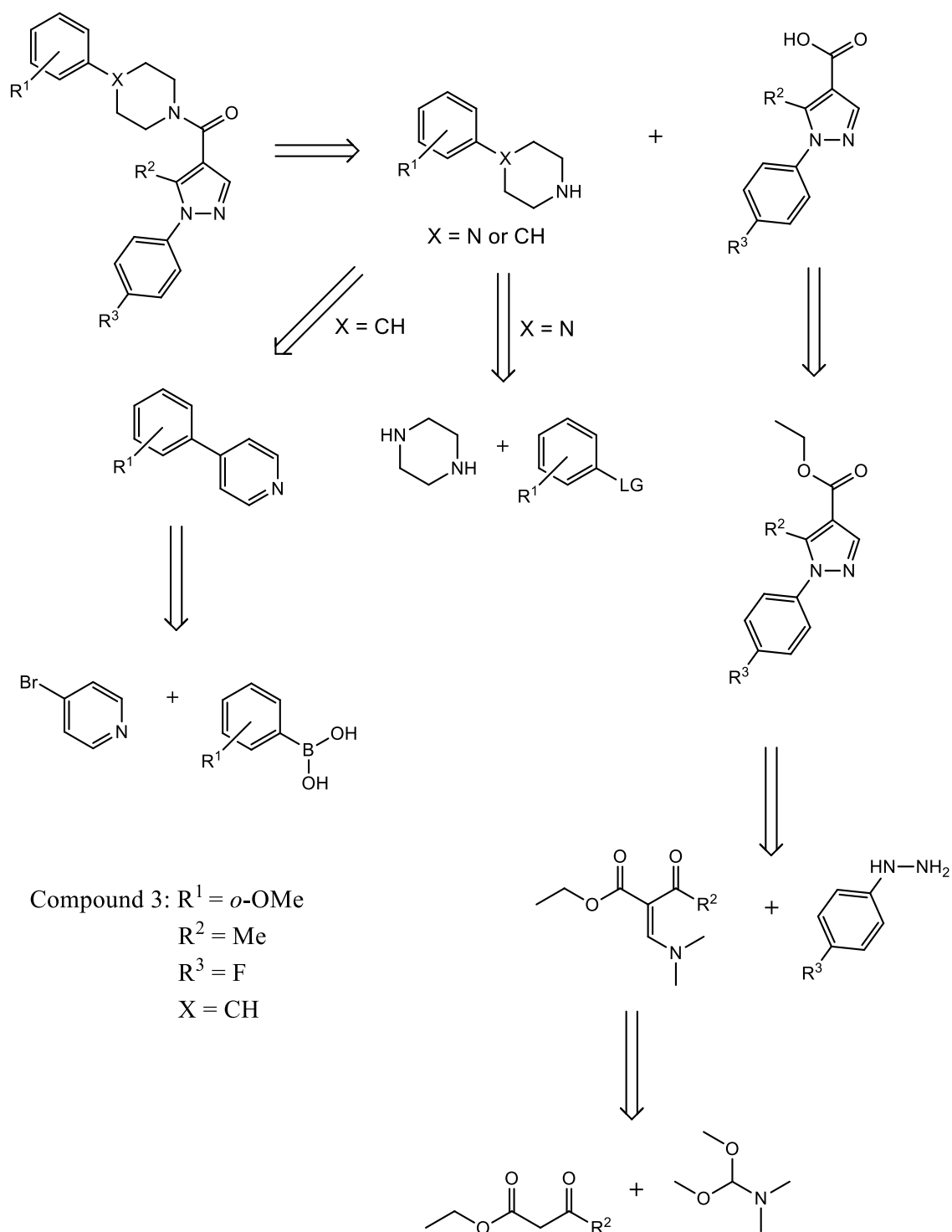
Scheme 4.29: Retrosynthetic route for the synthesis of derivatives of compound **3**.

The synthesis of two fragments, an *N*-substituted pyrazole building block and an arylpiperidine building block were required. The *N*-substituted pyrazoles were synthesised by reacting a substituted phenylhydrazine derivative with the activated β-enamino ketoester. The arylpiperazines were synthesised using the methods described in

Chapter 3 while the palladium catalysed Suzuki coupling was used in the formation of the arylpiperidine. Selective reduction using Adams catalyst gave access to the desired arylpiperidine. Once the necessary fragments were synthesised, compound **3** was obtained using the HOBt/TBTU coupling conditions described in Chapter 3. This synthetic approach was used to generate a number of derivatives of compound **3** (**Scheme 4.29**).

4.3.1 Synthesis of *N*-substituted pyrazole building blocks

Synthesis of the *N*-substituted pyrazoles first required the synthesis of the necessary substituted β-enamino ketoester, using the mild conditions reported by Bach *et al.*.[157] This method was used to allow access to compounds **124** and **125** (**Scheme 4.30**), from which the *N*-substitute pyrazole was synthesised.
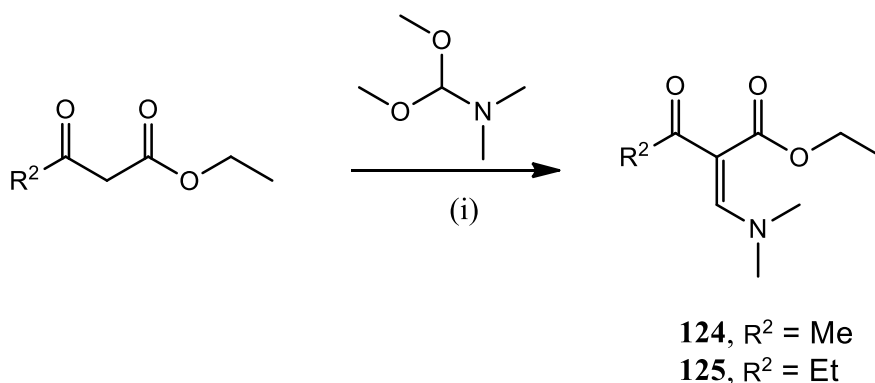
Scheme 4.30: Synthesis of β-enamino ketoesters **124** and **125** (i) rt, overnight, **124** (83%), **125** (96%, crude yield)

The synthesis of *N*-substituted pyrazoles from β-enamino ketoesters involved the use of *N*-substituted hydrazines. This process can be described as involving the use of [3+2]-atom fragments where the β-enamino ketoester is used as a 3-atom building block while the substituted hydrazine contributes a 2-atom fragment.[158]

The nature of the substituted *N*-hydrazine can affect regioselectivity with a mixture of regioisomers observed in some cases.[137] For example, Olivera *et al.*[137] reported that the use of *N*-methylhydrazine can produce a mixture of isomers, however this phenomenon is not observed with the use of *N*-phenylhydrazines.[137] In this case only the single isomer of the pyrazole is produced and can be explained due to the differences in the nucleophilicities of the nitrogen atoms found in *N*-phenylhydrazines.[137]

With compounds **124** and **125** synthesised, the *N*-substituted pyrazoles were then generated. As substituted phenylhydrazines were used, regioselectivity was not an issue with the single isomer of each pyrazole isolated. **Table 4.2** shows the synthesis of these pyrazoles.
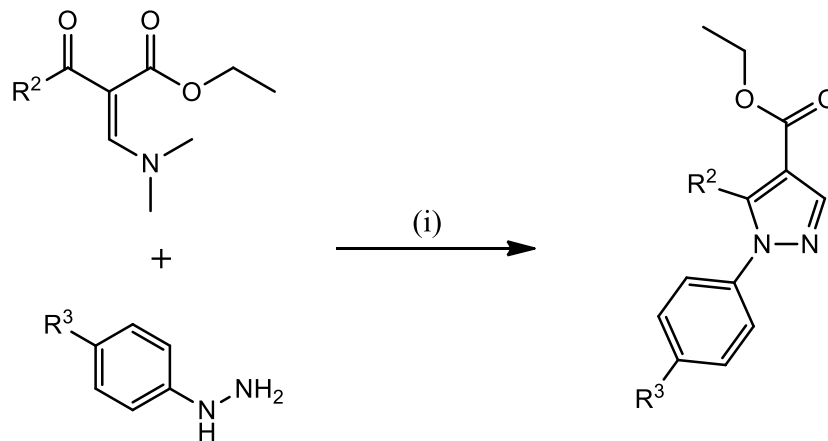
Compound	R^2	R^3	Yield (%)
126	Me	F	90
127	Me	H	97
128	Me	Cl	94*
129	Me	OMe	94*
130	Et	F	90

Table 4.2: Synthesis of *N*-substituted pyrazole (i) KOH, EtOH, reflux, 5 hrs. *Crude yield.

Base catalysed ester hydrolysis was then used to generate the 4-carboxylic acid derivatives (**Table 4.3**).
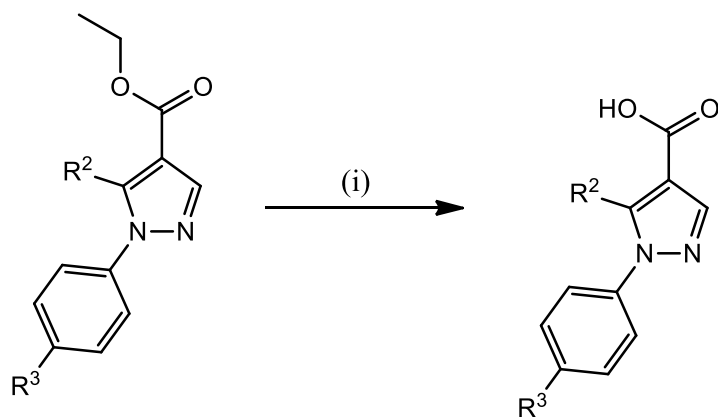
Compound	R^2	R^3	Yield (%)
131	Me	F	80
132	Me	H	93
133	Me	Cl	58
134	Me	OMe	33
135	Et	F	96

Table 4.3: Synthesis of *N*-substituted pyrazole (i) EtOH, reflux, 2 hrs.

4.3.2   Synthesis of compound 137

With the pyrazole fragment synthesised, the next task involved the synthesis of 4-(2-methoxyphenyl)piperidine **137**. The synthesis was performed using the approach reported by Zhang *et al*., in which palladium catalysed Suzuki conditions were exploited to yield the first building block of the arylpiperidine.[159] This involved the palladium catalysed coupling of (2-methoxyphenyl)boronic acid and 4-bromopyridine hydrochloride to afford **136**, which was then selectively reduced using Adam's catalyst to give the substituted arylpiperidine in a 18% yield (**Scheme 4.31**).
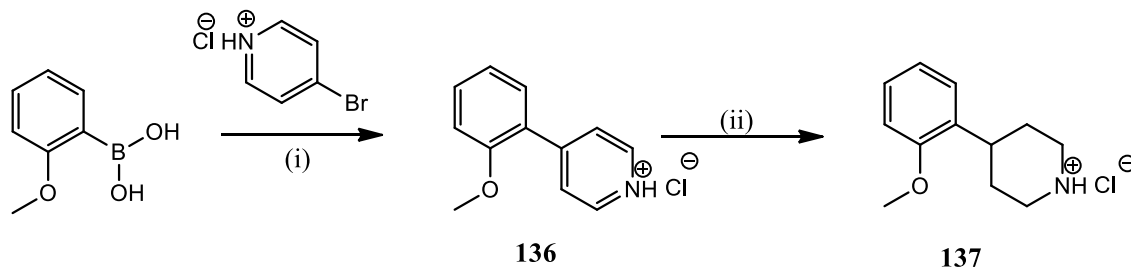
Scheme 4.31: Synthesis of compound **137** (i) Pd(PPh$_3$)$_4$, Cs$_2$CO$_3$, toluene, reflux, 24 hrs (ii) PtO, MeOH, H$_2$, overnight, 18%.

117

4.3.3   Condensation

Once the two building blocks were isolated, compound **3** and the derivatives of compound **3** were synthesised using the HOBt/TBTU coupling conditions. **Table 4.4** shows the structures and yields of the final amide containing derivatives.
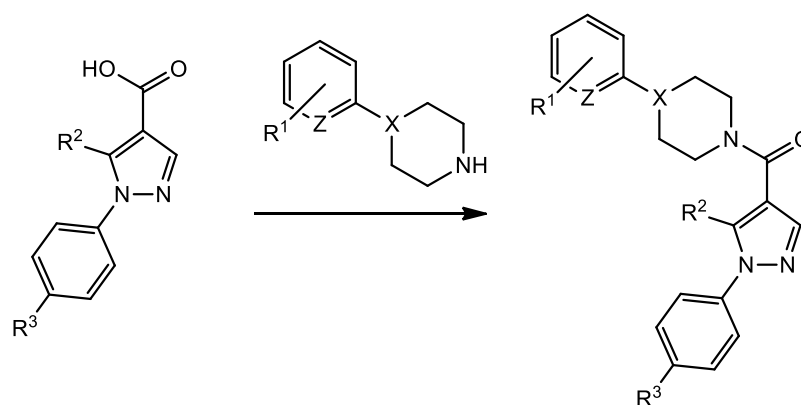
Compound	R^1	R^2	R^3	X	Z	Yield (%)
3	*o*-OMe	Me	F	CH	CH	77
138	*p*-CF$_3$	Me	H	N	CH	36
139	*o*-Cl, *p*-CF$_3$	Me	Cl	N	N	46
140	*o*-OMe	Me	OMe	CH	CH	62
141	*o*-OMe	Et	F	CH	CH	67
142	*o*-OMe	Me	F	N	CH	71
143	H	Me	F	N	CH	81
144	H	Me	F	CH	CH	60

Table 4.4: Synthesis of compound **3** and the derivatives of compound **3** (i) HOBt, TBTU, NEt$_3$, DMF, rt, overnight.

The synthesis of compound **3** was supported by ^{13}C NMR spectroscopy where the presence of the NMR active fluorine atom, *para* to the pyrazole ring, caused the splitting of the *ipso*, *ortho*, *meta* and *para* carbons. This was evident by the presence of the doublets at 115.8 ppm ($J = 23.1$ Hz), 127.3 ppm ($J = 8.0$ Hz), 135.8 ppm ($J = 3.4$ Hz) and 162.0 ppm ($J = 244.2$ Hz), where the size of the coupling constant decreased

with an increase in distance from the fluorine atom. The presence of the methoxy group was also supported by ^{1}H NMR spectroscopy with the sharp singlet, integrating for three protons, resonating at 3.86 ppm. HR-MS further supported the formation of the product with the peak of mass 394.1944 m/z corresponding to the M+H ion of compound **3**.

^{1}H NMR data of compound **3** recorded at room temperature showed two broad signals at 4.43 ppm and 3.06 ppm, both integrating for two protons. These peaks arose from the piperidine methylene protons, adjacent to the amide bond, experiencing restricted rotation about the N-CO bond. The amide group is likely to exhibit partial double-bond character as the lone pair of electrons on the amide nitrogen delocalise into the carbonyl group. This restricted rotation would have resulted in the two methylene groups being non-equivalent (at low temperatures) and would have also caused the emergence of rotational isomers in the NMR spectrum. At temperatures below room temperature, these rotational isomers would likely have been visible in the ^{1}H NMR spectrum, as the rotation about the amide bond would have been expected to be sufficiently slow. As the temperature increased however, the signals coalesce and an average of the signals is observed, thus causing the broad signals seen in the ^{1}H NMR spectrum at 30 °C (**Figure 4.2**). As the temperature was further increased, the rate of rotation about the amide bond increases and thus the peaks further coalesce resulting in the formation of the well-defined peaks, (**Figure 4.2**, T = 60 °C).
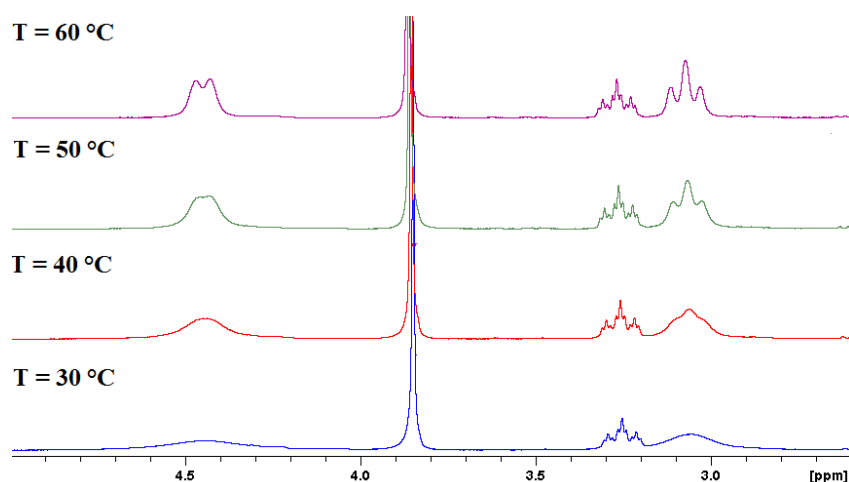
Figure 4.2. Expanded view of the variable temperature ^{1}H NMR study of **3** in CD$_3$CN.

4.4   Conclusion.

A number of derivatives of compound **2** were synthesised that contained changes to the groups at the C2 and C5 positions. It was found that the presence of a sterically bulky group at the C5 position results in a reduced yield. Generally, an increase in Charton value corresponded with a decrease in yield, as seen for compounds **113** and **114**. These compounds are awaiting biological testing.

A number of derivatives of compound **3** was also synthesised, with a number of compounds which probed the importance of the fluorophenyl and methoxy groups for example, synthesised. These compounds are also awaiting biological testing.

5. Biological evaluation of compound 1 and its derivatives, 4-81.

5.1   Structure activity relationship (SAR) study of compounds related to 4 using the glucose uptake assay.

Molecular modelling led to the selection of compound **1** from a library of compounds and its ability to disrupt the RBP4-TTR complex was verified by means of SPR. The initial hit-to-lead efforts produced eight derivatives of **1** and uncovered compound **4** (**Figure 5.1**) as our lead compound as it exhibited greater potency than its parent compound in both the SPR and glucose uptake assays. Therefore, our aim was to develop a SAR study around **4** with the possibility of further optimization. Fifty compounds, including compounds **5**-**11**, were designed and synthesised and their activity within the glucose uptake assay was assessed.
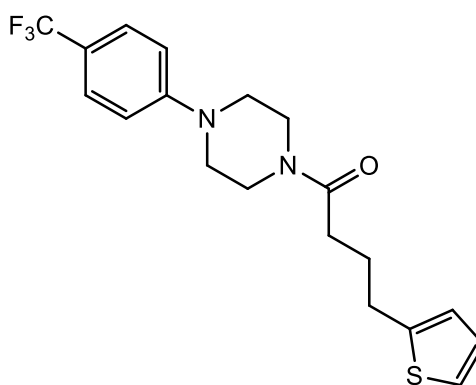
Figure 5.1: Structure of compound **4**.

5.1.1.1 Effect of altering trifluoromethyl phenyl group

Several pharmaceuticals, such as fluoxetine (prozac), the active ingredient of many anti-depressants, contain a trifluoromethyl (CF_3) group (**Figure 5.2**).[160] The presence of a fluorine atom, in the form of single fluorine or a trifluoromethylated group, can alter numerous properties of a drug. For example, a SAR study of fluoxetine showed that removal of the *para* CF_3 from the phenolic ring greatly reduced its biological efficacy.[161] The absence of the sterically bulky CF_3 group caused the molecule to adopt a less favourable conformation which inhibited its ability to bind to its target protein.[161]
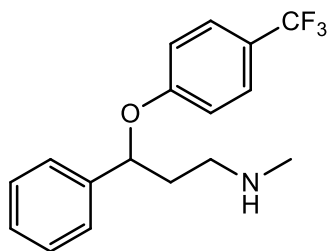
Figure 5.2: Structure of fluoxetine.[160]

As a trifluoromethyl phenyl group was present in both **1** and **4**, the importance of this group was investigated. Several compounds were designed, synthesised and tested in which alterations to the trifluormethylphenyl group were made (**Table 5.1**). Compound **1** was also synthesised at this stage. Although the glucose uptake assay produced a consistent result for each compound relative to basal and compound **4**, the absolute level of ^{3}H deoxy-2-glucose taken up by the cells varied from assay to assay. As a result a qualitative measurement of activity is reported. This produced a trend for each compound with compounds labelled as active or inactive compared to basal levels or active but less active than **4**.
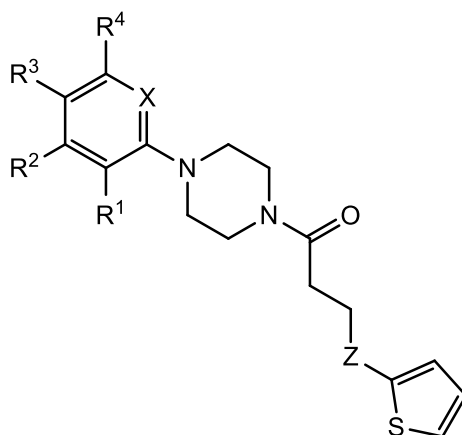
Compound	R^1	R^2	R^3	R^4	X	Z	Glucose uptake assay activity*
1	Cl	H	CF_3	H	N	S	Inactive
4	H	H	CF_3	H	H	CH_2	Active
6	H	H	CF_3	H	N	C=O	Inactive
7	Cl	H	CF_3	H	N	C=O	Inactive
8	H	H	CF_3	H	N	CH_2	Inactive
9	Cl	H	CF_3	H	N	CH_2	Inactive
11	Cl	H	CF_3	H	H	CH_2	Inactive
40	H	H	F	H	H	CH_2	Inactive
41	CF_3	H	H	H	H	CH_2	Inactive
42	H	H	NO_2	H	H	CH_2	Active **
43	H	CF_3	H	CF_3	H	CH_2	Active**
45	H	H	CF_3	Cl	N	CH_2	Inactive
46	Br	H	CF_3	H	H	CH_2	Inactive
47	H	H	H	H	H	CH_2	Inactive
73	H	H	NH_2	H	H	CH_2	Inactive

44   Inactive

53   Inactive
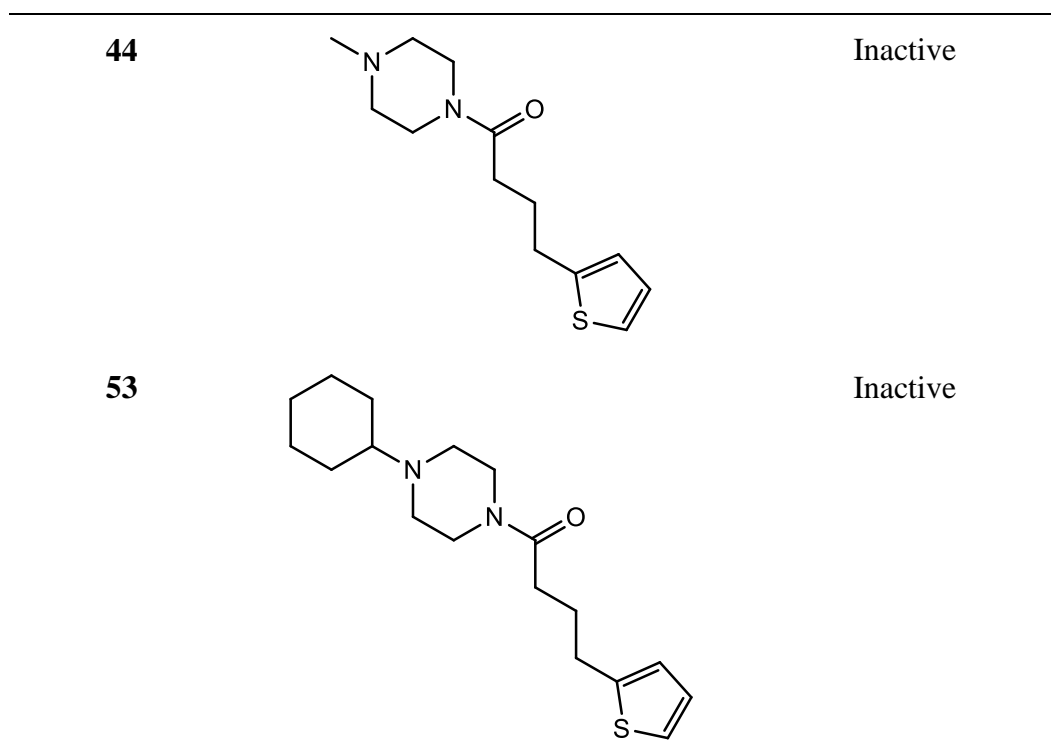
Table 5.1: Structure and activity of derivatives of compound **4**, *Activity of compounds in glucose uptake assay compared to basal level **Active, but less active than **4**.

The removal of the *para* CF$_3$ group resulted in a loss of or reduced activity in the glucose uptake assay, as seen in the below histograms (**Figure 5.3**). Derivatives **40**, **41**, **47**, **52** and **73** were all inactive while, **42** and **43** were only marginally active when compared to **4**. The absence of the *para* CF$_3$ group may have resulted in a loss of activity for a number of reasons, which will be discussed in the following pages.
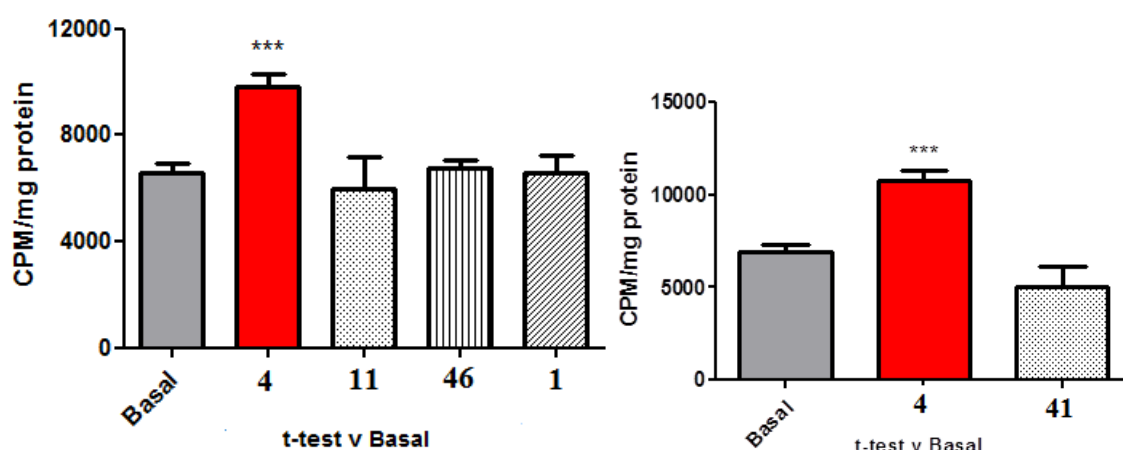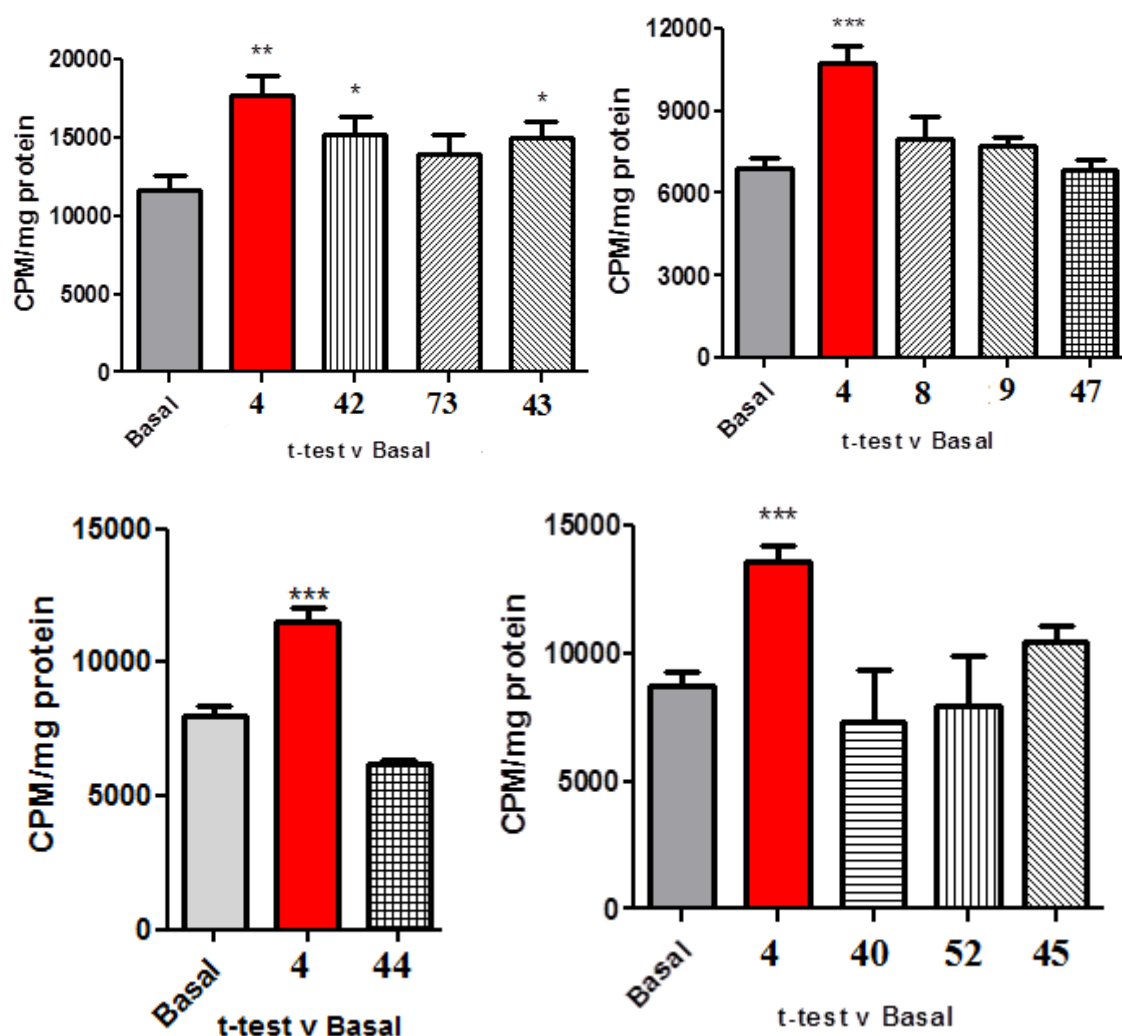
Figure 5.3. Glucose uptake assay results of derivatives of compound **4**. C2C12 muscle cells incubated overnight at 37 °C in the presence 10 µM of each compound. Cells then exposed to ^{3}H deoxy-2-glucose for 10 mins and a scintillation count of the C2C12 muscle cells performed.

5.1.1.1.1   Role of CF$_3$ substituent

5.1.1.1.1.1   Steric Bulk

Firstly, like fluoxetine, the steric bulk of the *para* CF$_3$ group may have caused the compound to adopt a suitable conformation for binding to its target protein.[161] Loss of this steric bulk could cause the molecule to adopt a less favourable conformation resulting in a loss of/decreased activity. This could be the case for compounds **40**, **42**, **47**, **52** and **73**.

The position of the bulky CF$_3$ group was also important. When the derivatives containing an *ortho* or *meta* CF$_3$ substituent were tested, it was found that the compounds were less active than **4** (e.g. **43**) or completely inactive (e.g. **41**).

5.1.1.1.1.2 Lipophilicity

CF$_3$ substituents also contribute to the overall lipophilicity of a molecule.[161] Lipophilicity governs a drugs ability to permeate lipid membranes and dock within a hydrophobic protein cavity.[162] It affects aqueous solubility and can play a role in drug metabolism, pharmacokinetics, pharmacodynamics and toxicology.[162] Lipophilicity is measured in terms of the logP where P, the partition coefficient, describes the tendency of an uncharged substance to dissolve in an immiscible biphasic system at equilibrium.[161] This is generally calculated experimentally using octanol and water as the biphasic system and measures the concentration of the neutral substance found in the octanol or water layers.[161]

The greater the logP value, the greater the lipophilicity, while the lower the logP value, the greater the hydrophilicity (i.e. the greater the aqueous solubility).[161] Waring *et al.* reported that compounds with large logP values tend to exhibit increased toxicity, decreased solubility, poor metabolic clearance and reduced specificity for binding to protein receptors.[162] Purser *et al.* eluded to the fact that an inadequate lipophilicity can have deleterious effects with regards to crossing lipid membranes.[161] Drugs require an adequate lipophilicity to be able to pass through the lipid membrane but not become trapped within it.[161] As passive transport is the most common mode of cell permeation for drugs, an adequate lipophilicity is essential.

Drug molecules are exposed to a variety of different environments in the body, depending on the method of administration. The pH for example, can vary significantly from 2.0 in the stomach to 7.4 in the blood stream.[163] As many drugs contain functional groups that are susceptible to ionization, and as logP refers to the unionized neutral state of a molecule, a method for quantifying the aqueous solubility of ionized molecules is needed.[163] LogD is the pH dependent distribution factor that is related to logP by the acid dissociation constant pK$_a$.[163] This coefficient more accurately describes the aqueous solubility of a drug *in vivo*.

Table 5.2 shows the logP values, calculated by Chemdraw software, for **4**, **40**, **47**, **52**, and **73**. The loss of the CF_3 decreased the logP value thus decreasing the lipophilicity, this may have rendered the compounds incapable of crossing the lipid membrane and evoking a biological response.[162] Alternatively, if the derivatives were capable of crossing the lipid membrane, the reduced lipophilicity may have prevented the compounds from binding to their target protein.[162]

Compound	logP*	logD**
4	4.79	4.67
40	4.02	3.93
47	3.87	3.79
52	3.34	2.79
73	3.06	2.95

Table 5.3: LogP and logD values of compound **4** and its derivatives, *calculated using Chemdraw software, ** calculated using MarvinSketch software.

5.1.1.1.2 Effect of substituting the phenyl ring

Altering the phenyl ring, replacing the CF_3 group or completely substituting the trifluoromethyl phenyl group, led to a decrease in activity (**Table 5.1, Figure 5.3**).

Replacing the *para* CF_3 group, with a nitro or amino group, altered the electronic properties of the aromatic ring. In both cases, a reduction in glucose uptake was observed. As a *para* nitro substituent is more electron withdrawing than a *para* CF_3 group, this would have reduced the electron density of the aromatic ring.[100] The electron withdrawing chlorine and bromine atoms will also have affected the electronic properties of the aromatic ring and may have contributed to loss of activity in compounds **1**, **7**, **9**, **11**, **45** and **46**.

The presence of a primary amine in the *para* position would have increased electron density, as the lone pair of electrons can delocalise into the aromatic ring. This may also be the case for compounds **6** and **8**, and may also contribute to the loss of activity seen in **1**, **7**, **9** and **45**. Changes to the electron density of the aromatic ring may have had a

negative influence on the binding mode of the aromatic ring to the protein target.[63] The substituent itself could directly affect binding as an F, NH_2 or NO_2 group will have markedly different binding characteristics e.g. H-bonding (donor or acceptor), hydrophobicity and electrostatic interactions.

5.1.1.1.3 Loss of six membered aromatic ring

Although the loss of activity observed from **52** may be attributed to the loss of the *para* CF_3 group, the absence of the planar aromatic ring may also have influenced this change in activity. As aromatic rings are hydrophobic planar structures, they can interact with flat hydrophobic regions of a protein binding site *via* van der Waals forces or hydrophobic interactions.[63] Also, aromatic rings present the opportunity for a molecule to be involved in π-π stacking, which would further stabilise a ligand-protein interaction.[164]

Cyclohexane rings adopt non planar conformations such as the boat and chair.[100] Although axial protons can interact, albeit weakly, with the protein, it keeps the rest of the cyclohexane ring at a distance (**Figure 5.4**).[63] This prevents further stabilising interactions.
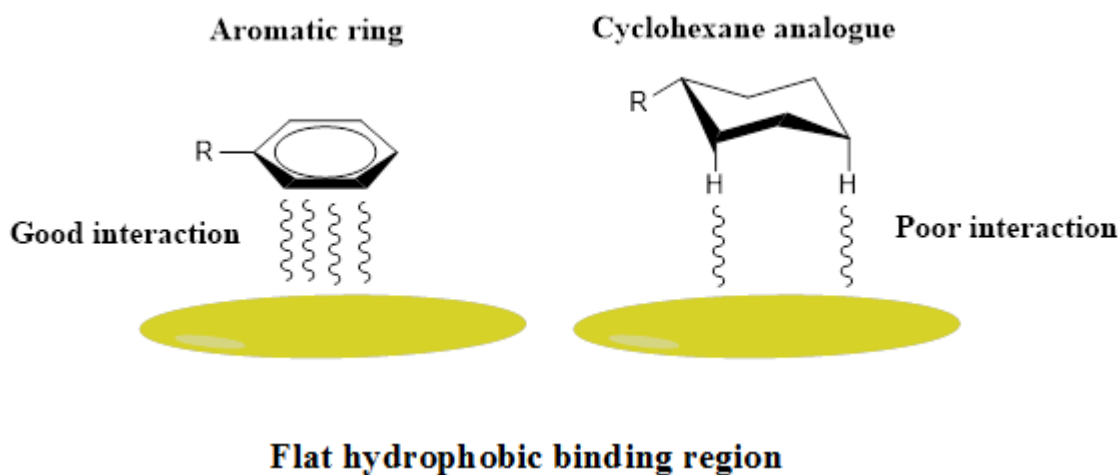
Figure 5.4. A comparison of binding between a planar aromatic ring or a non-planar cyclohexyl ring.

This could explain the loss of activity observed for compound **2**. Also, as the unknown binding site may be a flat, narrow hydrophobic pocket, which would accommodate the planar aromatic ring in **4**, the non-planar cyclohexyl ring in **52** may not be able to fit

within the protein binding site, resulting in a loss of activity.[63] Also, the absence of stabilising π- π stacking could also play a role in the loss of activity.

The importance of the aromatic group can also be seen from the glucose uptake assay results for **44**. Removal of the trifluoromethyl phenyl group resulted in a loss of activity. This can be attributed to the reasons described above.

Overall, alterations to the trifluoromethyl phenyl group resulted in a decrease or a loss of activity for all compounds. Therefore, the presence of a trifluoromethyl phenyl group at this position is considered necessary for biological activity.

5.1.1.2 Effect of altering the substituted piperazine ring

Piperazine rings are commonly found in biologically active compounds and their importance has been reported extensively in the literature. The derivatives of compound **4**, **53**, **54** and **74** were designed and synthesised with a view to determine the importance of the piperazine ring (**Table 5.4**).

Compound	Structure	Glucose uptake assay activity*
4		Active
53		Inactive
54		Active**
74		Inactive
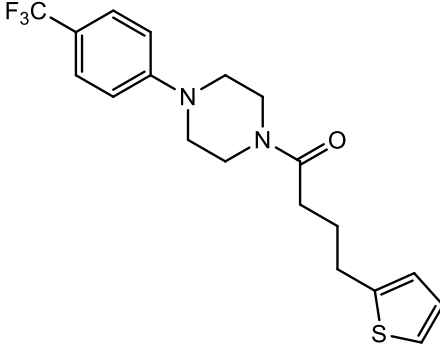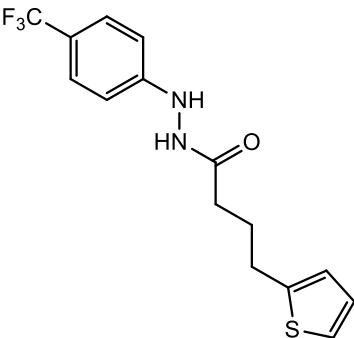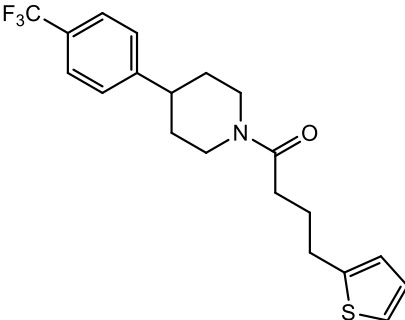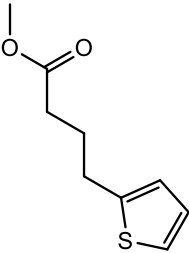
Table 5.4: Structure and activity of derivatives of compound **4**, * Activity of compounds in glucose uptake assay compared to basal level **Active compared to basal, but less active than **4**.

Changes to the piperazine ring resulted in a loss/ decrease of activity in the glucose uptake assay (**Figure 5.5**). Compound **74**, in which the arylpiperazine was replaced by a

methyl ester, proved to be inactive, highlighting the importance of the substituted piperazine with respect to induced glucose uptake.

Figure 5.5. Glucose uptake assay results of compound **4** derivatives. C2C12 muscle cells incubated overnight at 37 ºC in the presence 10 μM of each compound. Cells then exposed to ^{3}H deoxy-2-glucose for 10 mins and a scintillation count of the C2C12 muscle cells performed.

The importance of the piperazine ring itself was investigated through a study of compound **53**. Here the ring was removed and replaced with a hydrazine functionality. The removal of the piperazine proved to be deleterious and the compound was unable to stimulate glucose uptake. The piperazine ring in compound **4** may allow the molecule to adopt an appropriate conformation for binding to the protein. It may orientate the molecule so as to form more stable interactions with its target.

The role of the nitrogen atom adjacent to the aromatic ring was also probed, with **54** exhibiting a reduced activity compared to **4**. Removal of this nitrogen can affect the pK_a of the molecule which may cause changes to the pharmacokinetics of the molecule and how the drug molecule interacts with the protein target.[165] This nitrogen atom cannot act as a hydrogen bond donor as it is a tertiary amine, nor can it act as a hydrogen bond acceptor due to the delocalization of its lone pair of electrons into the aromatic ring.[63] This amine however, may participate in ionic bond formation. Thus, removal of the Ar-N nitrogen may have removed the possibility of forming an ionic bond with the target protein, therefore reducing its biological effect.

There was an overall reduction in activity when changes were made to the piperazine ring, demonstrating the importance of this group in **4**.

5.1.1.3 Effect of removing the amide carbonyl

Amide bonds are found in a wide variety of biologically active compounds ranging from met-enkephalin, the body's natural pain killer, to atorvastatin and penicillin.[63] Amide bonds can interact with protein targets through hydrogen bonding.[63] The carbonyl oxygen can form two hydrogen bonds as it possesses two lone pairs of electrons (**Figure 5.6**). The amide N-H can only serve as a hydrogen bond donor as its single lone pair of electrons delocalise into the adjacent carbonyl group.[63] The amide group is therefore an important functional group for protein-ligand interactions.
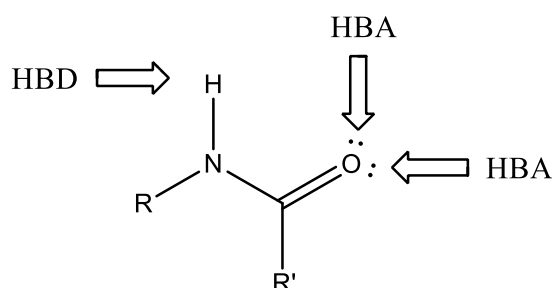
Figure 5.6. Hydrogen bond interactions of amides.[63]

The amide group in **4** could have functioned in a similar fashion to that described above, however without the amide nitrogen acting as a hydrogen bond donor due to the fact it is a tertiary amide. It was hypothesised that the removal of the amide carbonyl would diminish the biological activity of the compound. This was the case, as seen in **Figure 5.7**, where **70** did not induce glucose uptake within C2C12 muscle cells. Removal of the carbonyl may have prevented the formation of a hydrogen bond interaction between the protein target and **70**.
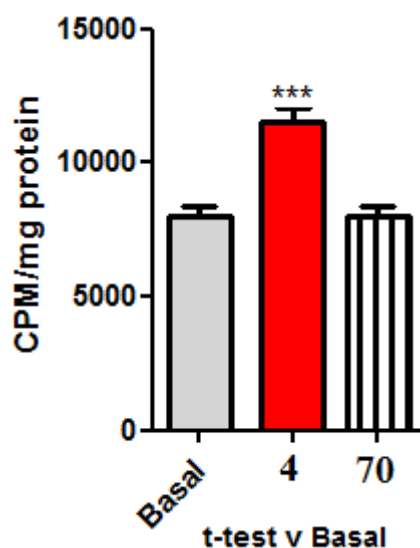
Figure 5.7. Glucose uptake assay results of **70**. C2C12 muscle cells incubated overnight at 37 ºC in the presence 10 μM of each compound. Cells then exposed to ^{3}H deoxy-2-glucose for 10 mins and a scintillation count of the C2C12 muscle cells performed.

As **4** contained an amide bond, it would have experienced some restricted rotation.[100] This would have reduced the number of conformations that compound **4** could adopt. Introducing free rotation about the nitrogen atom, by removing the carbonyl group, may have allowed the compound to adopt numerous conformations. Therefore, the difficulty in adopting the suitable conformation for interacting with the protein target may have increased.

The loss of activity observed when the amide carbonyl was removed highlights the important role that this group plays in the biological activity of compound **4**.

5.1.1.4 Effect of altering the alkyl chain

Introducing a carbonyl group into the alkyl chain diminished biological activity, as was seen with **5**. Although the loss of activity observed for **6** and **7** may be due to the presence of the aromatic nitrogen atom, they also contain a carbonyl group on the alkyl chain.

The presence of the π-bond would have affected the polarity of the molecule.[100] This may have affected its ability to bind to the target protein, thus reducing activity (**Figure 5.8**, **Table 5.5**).

When a primary alcohol (**66**), or a sulphur atom (**10**), was introduced into the alkyl chain, a complete loss of activity was not observed. Both compounds **66** and **10** remained active compared to the control, but were not as active as **4**. Compound **66** may have acted as a hydrogen bond acceptor and donor due to the presence of the primary alcohol.[63] The sulphur atom may have functioned by acting as a hydrogen bond acceptor.[166] These interactions may have assisted in the ligand-protein binding interaction.

Both **1** and **10** contain a sulphur atom in the alkyl chain. However, a loss in activity was observed for **1** and not for **10**. Therefore, the loss of activity can be attributed to the substitution of the arylpiperazine.
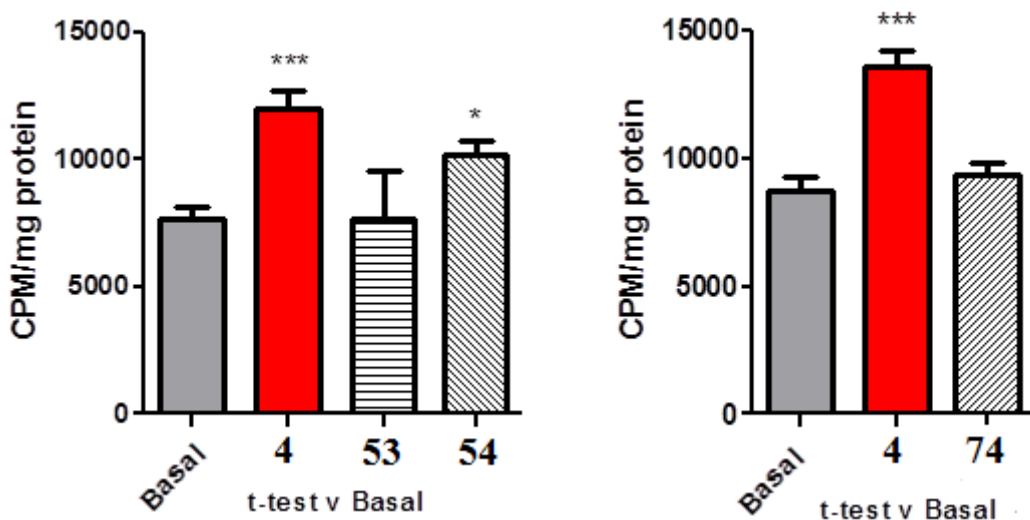

Figure 5.8. Glucose uptake assay results of compound **4** derivatives. C2C12 muscle cells incubated overnight at 37 ºC in the presence 10 µM of each compound. Cells then exposed to ^{3}H deoxy-2-glucose for 10 mins and a scintillation count of the C2C12 muscle cells performed.
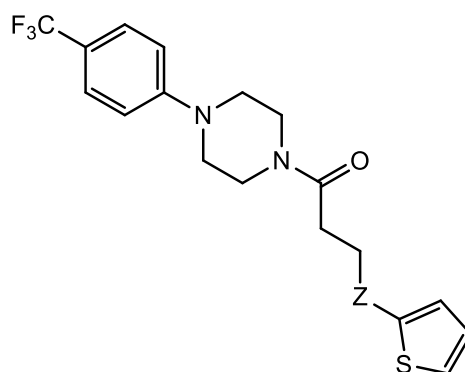
Compound	Z	Glucose uptake assay Activity*
4	CH$_2$	Active
5	C=O	Inactive
10	S	Active**
66	CHOH	Active**

Table 5.5: Structure and activity of derivatives with varying alkyl chain lengths, *Glucose uptake assay activity compared to basal **Active compared to basal, but less active than **4**.

When the section of the molecule, from the amide carbonyl to C5 of the thiophene ring was altered, a significant change in the biological activity of these derivatives was observed. Increasing the length of this section of the molecule generated the active compounds **55** and **56**, with **55** proving to be as active as **4** (**Figure 5.9**, **Table 5.6**). Increasing the length of this section of the molecule may not affect the relative position of the arylpiperazine moiety within the protein target and therefore does not affect activity. Alternatively, it may be that the position of the arylpiperazine is in fact affected but that the new position allows for interactions to occur, which are as stable as the interactions observed between compound **4** and the protein target.

Replacing the thiophene ring with a butyl group (**57**) also resulted in a compound that was as active as **4** in the glucose uptake assay (**Figure 5.9**, and **Table 5.6**). As both compound **4** and **57** were similar in length, it could be concluded that it is the length of the molecule that is important for activity, and not the presence of a heterocycle.

A significant reduction in the length of the molecule greatly impacted the ability of certain compounds to stimulate glucose uptake, with compounds **58** and **67** both proving to be inactive (**Figure 5.9**, **Table 5.6**). This was also the case for **59**, where the length of the molecule from the amide carbonyl to the carbon in the C5 position of the thiophene ring was only 7.71 Å, compared to 10.233 Å observed for compound **4**. Only a slight loss of activity was observed when compound **60** was tested in the glucose uptake assay. Here the length of this section of the molecule, from the amide carbon to terminal methyl group, was shortened 6.078 Å. Similar resulted were observed for the amide **61** where the length of the molecule from the amide carbonyl to the carbon in the C5 position of the thiophene was 7.187 Å (**61**) (**Figure 5.9**, **Table 5.6**).

Reducing the length of the molecule, as was seen in compounds **58**, **59** and **67** could have several affects, for example it may change the relative position of the substituted phenyl ring within the protein which in turn may have affected binding of the molecule within the target.[63] The alkyl chain may conceivably take part in a hydrophobic binding interaction with the target, which could be reduced with the reduction in the length of this part of the molecule.
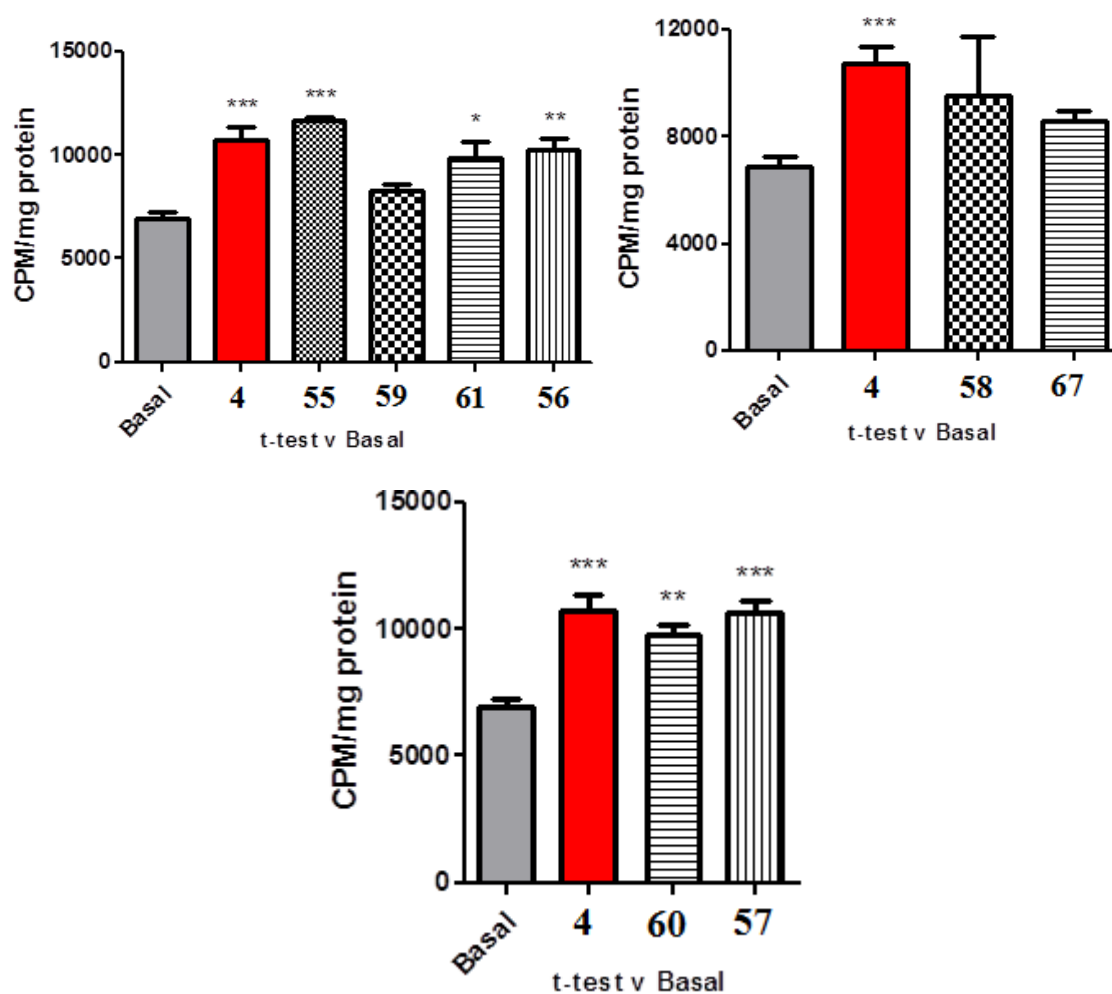
Figure 5.9. Glucose uptake assay results of compound **4** derivatives. C2C12 muscle cells incubated overnight at 37 ℃ in the presence 10 µM of each compound. Cells then exposed to ^{3}H deoxy-2-glucose for 10 mins and a scintillation count of the C2C12 muscle cells performed.
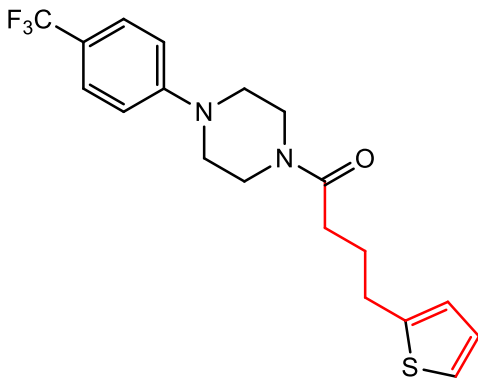
Compound	Structure	Length (Å)[†]	Glucose uptake assay activity*
4		10.233	Active
55		11.756	Active***
56		13.279	Active**
57		10.647	Active***
58		1.509	Inactive
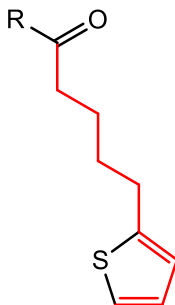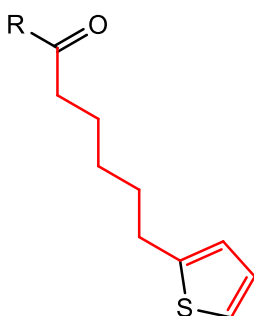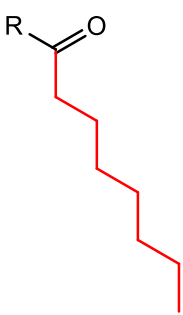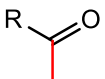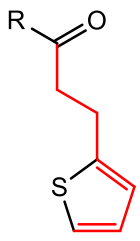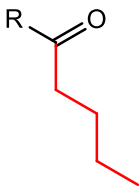
59		7.710	Inactive
60		6.078	Active**
61		7.187	Active**
67		1.438	Inactive
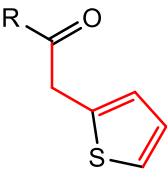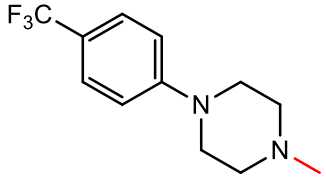
R =
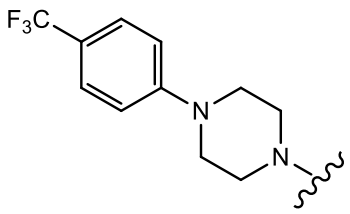
Table 5.6: Structures and activities of derivatives of compound **4**, *Glucose uptake assay activity compared to basal **Active but not as active as **4**, ***As active as **4**,[†] bond length measured from amide carbonyl to C5 position of thiophene or to the terminal alkyl carbon.

5.1.1.5 Effect of replacing the thiophene heterocycle

A heterocycle is an aromatic or saturated cyclic moiety that contains one or more heteroatoms such as N, O, S, Si, B, Se or P.[167] Heterocycles are extremely important functionalities in drug discovery. Numerous pharmaceuticals exist that contain one, if not more, heterocycles. They can be found in therapeutics responsible for the treatment of cancer, cardiovascular disease and diabetes.[167,168]

A heterocycle can interact with a protein binding site through various bonding interactions.[63] For example, the heteroatom can interact through hydrogen bonding or ionic bonding, while the heterocycle as a whole can interact *via* hydrophobic interactions, van der Waals forces or π-stacking.[63,164]

3-(Furan-2-yl)propanoic acid was the only relevant commercially available starting material that could have been used in the synthesis of a furan containing derivative of compound **4**. This resulted in compound **62**, a compound of reduced length, compared to compound **4,** which also contained a furanyl heterocycle.

Like the sulphur atom in the thiophene ring, the oxygen atom in the furan ring has two lone pairs of electrons. Both heterocycles find one of their lone pairs delocalised into the aromatic ring, while the other lone pair is found in the sp^2 hybrid orbital in the same plane as the heterocyclic ring.[167] The lone pair of electrons in the sp^2 hybridised orbital allows these heteroatoms to serve as a hydrogen bond acceptor.

The thiophene ring was also replaced with a pyrazole heterocycle to give derivative **63** (**Table 5.7**). The presence of a secondary amine allows this heterocycle to act as a hydrogen bond donor.

Compound **63** remained active in the glucose uptake assay, while **62** proved to be inactive (**Figure 5.10**). When the glucose uptake assay results for compound **59** and **62**, which are both similar in length (7.71 Å and 8.696 Å) and only differ in the heterocycle (thiophene or furan respectively), were compared, it was found that the results were similar. This indicated that replacing the thiophene ring with a furanyl derivative did not affect biological activity. The equivalent comparison for the pyrazole containing derivative is between **4** and **63**, where a slight reduction in activity was observed for **63**.

These results again suggest that the nature of the heterocycle is not of critical importance and that it is the overall length of the molecule that may be crucial for activity.
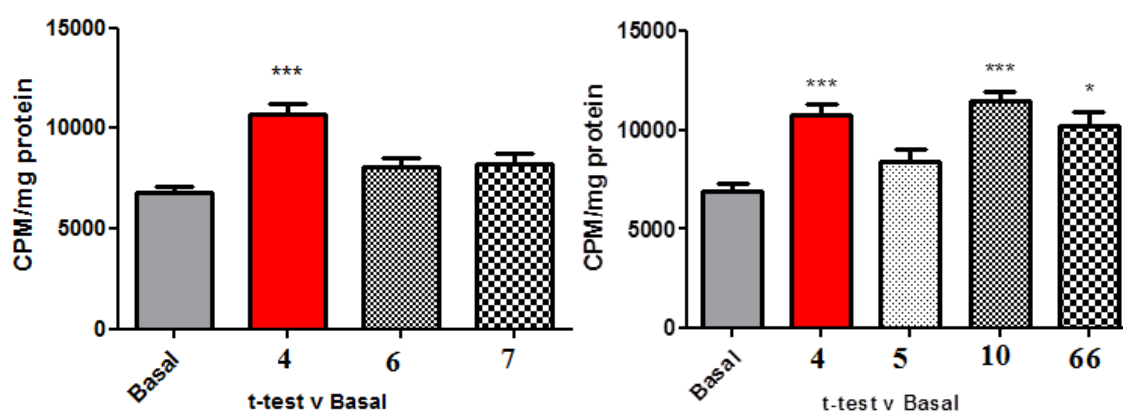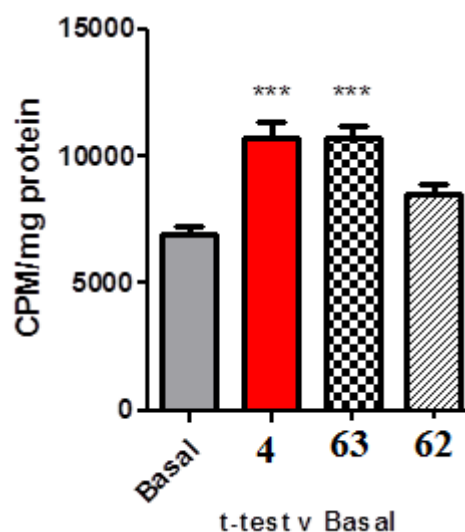
Figure 5.10. Glucose uptake assay results of compound **62** and **63**. C2C12 muscle cells incubated overnight at 37 ℃ in the presence 10 μM of each compound. Cells then exposed to ^{3}H deoxy-2-glucose for 10 mins and a scintillation count of the C2C12 muscle cells performed.

Compound	Structure	Length (Å)†	Glucose uptake assay Activity*
4[a]		10.233	Active
62[a]		8.696	Inactive
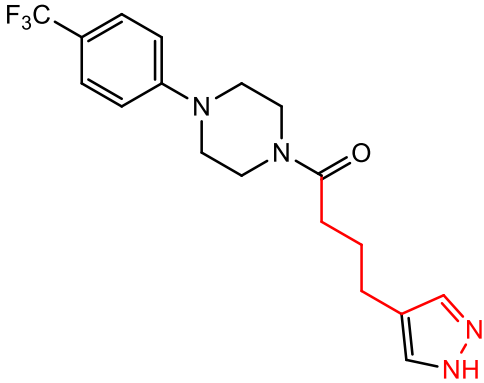
63[b]   F$_3$C   10.108   Active**

Table 5.7: Structure and activity of derivatives of **4** with alternative heterocycles, *Glucose uptake assay activity compared to basal **Active compared to basal, but less active than **4**, [a] heterocycle substituted at the C2, [b] heterocycle substituted at C4. [†] bond length measured from amide carbonyl to C5 position of thiophene or furanyl ring or to the N1 nitrogen of the pyrazole.

The thiophene ring was also replaced by a benzyl group. This gave rise to the derivative **64**, which proved to be more active than **4** at stimulating glucose uptake (**Figure 5.11**).

As described previously, aromatic rings are hydrophobic moieties that can interact with hydrophobic regions of a protein.[63] They can also form binding interactions *via* van der Waals forces and become involved in π-stacking with other aromatic groups.[164] Such interactions may have resulted in the improved activity

Steric factors may also have influenced the molecules binding mode due to the presence of a different aromatic ring.[63] This may have altered the orientation of the ligand resulting in a superior binding and thus increased activity.[63] Similarly, the presence of an alternative aromatic ring may have allowed for a better fit of this part of the molecule in the protein binding site.
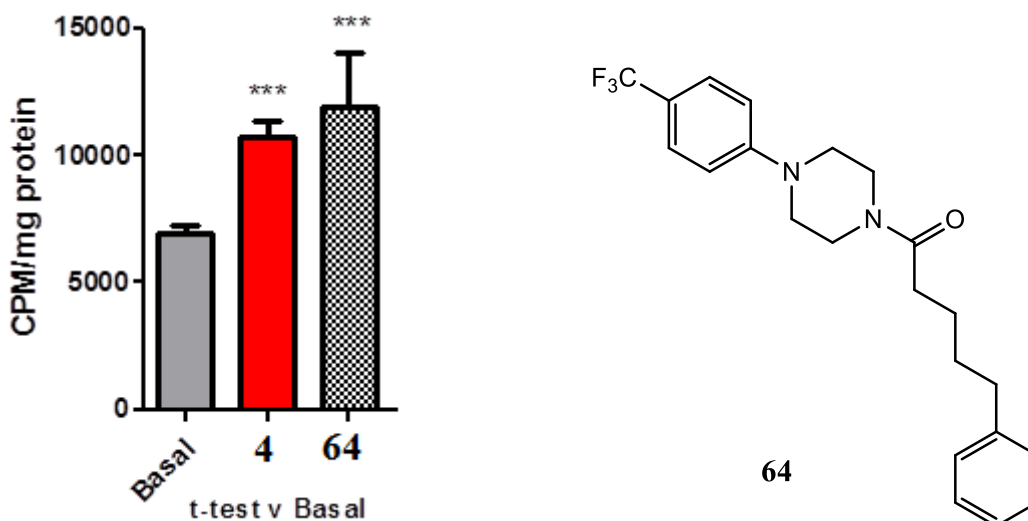
Figure 5.11: Glucose uptake assay results and structure of **64**. C2C12 muscle cells incubated overnight at 37 ºC in the presence 10 µM of each compound. Cells then exposed to ^{3}H deoxy-2-glucose for 10 mins and a scintillation count of the C2C12 muscle cells performed.

Previous results suggested that the presence of a heterocycle at the terminus of the alkyl chain was not required for activity. Consequently, we investigated the effect of introducing an alternative functional group at this position would have on glucose uptake. We chose to introduce a carboxylic acid functionality at the alkyl chain terminus as these groups are found in a variety of biologically active compounds. They serve as hydrogen bond donors or acceptors or, alternatively, they can exist as the carboxylate ion and form ionic interactions.[63] Introduction of this group would also allow for the compound to be easily derivatized due to the reactivity of the carboxylic acid. This activity would prove to be important when we came to immobilising the compound on a solid support, see Chapter 7.

As a result, compound **79** was synthesised and tested in the glucose uptake assay. The presence of the carboxylic acid resulted in a compound that was more active than **4** and **57** (**Figure 5.12**). The ability of the carboxylic acid group to form hydrogen bonds or ionic bonds may be responsible for this increase in activity.
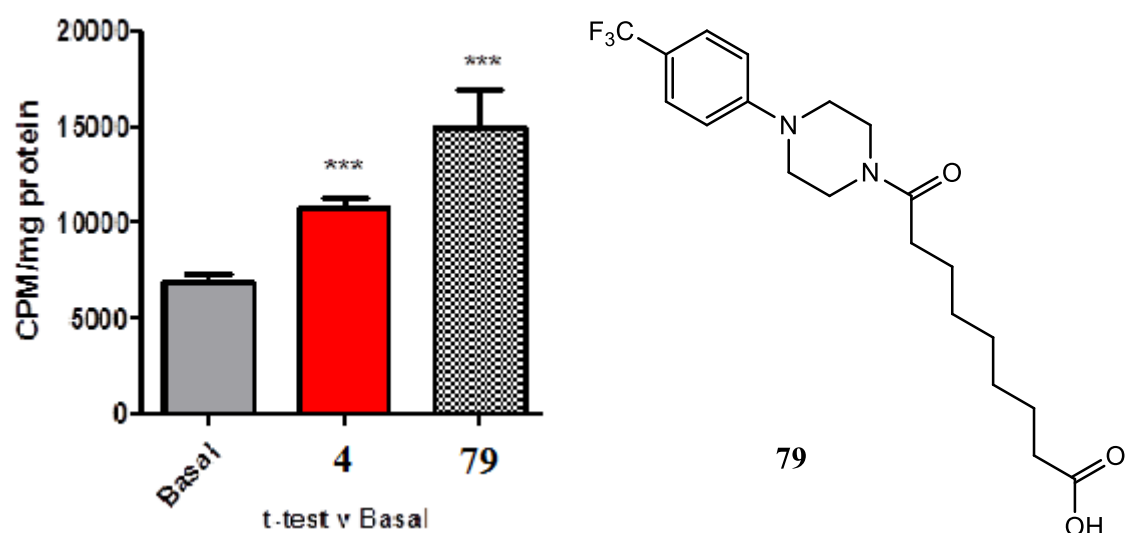
Figure 5.12: Glucose uptake assay results and structure of compound **79**. C2C12 muscle cells incubated overnight at 37 °C in the presence 10 µM of each compound. Cells then exposed to ^{3}H deoxy-2-glucose for 10 mins and a scintillation count of the C2C12 muscle cells performed.

A methyl ester was also introduced at the alkyl chain terminus; compound **81**. This compound proved to be more active than **4** and **57** and as active as **79** at stimulating glucose uptake (**Figure 5.13**). Again, the presence of a hydrogen bond acceptor in the form of a carbonyl group may be responsible for the increase in activity compared to **4** and **57**.
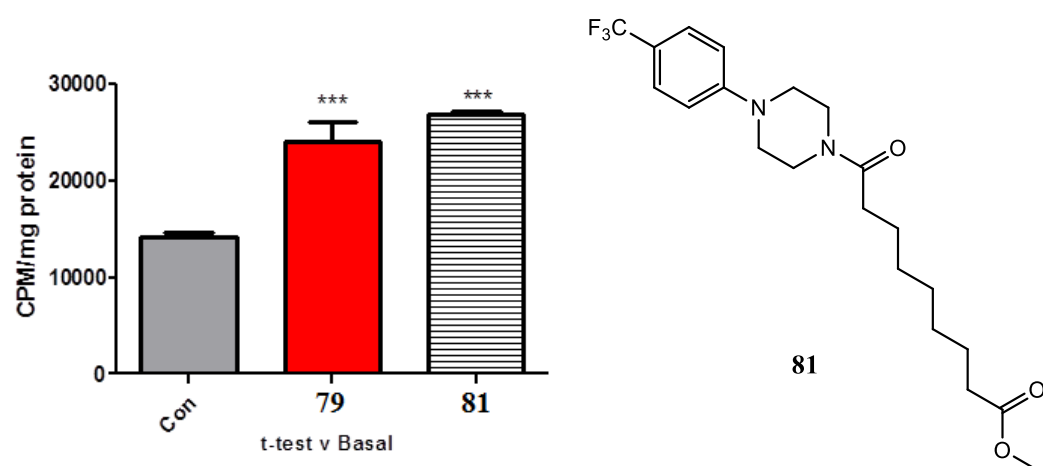
Figure 5.13: Glucose uptake assay results and structure of compound **81**. C2C12 muscle cells incubated overnight at 37 °C in the presence 10 µM of each compound. Cells then exposed to ^{3}H deoxy-2-glucose for 10 mins and a scintillation count of the C2C12 muscle cells performed.

5.2   Animal studies on compound 4.

A 16 week animal study was carried out in a similar fashion to that mentioned in **section 2.3**. The study was comprised of three groups: Group A contained 12 mice on a HFD that were exposed to **4** dissolved in DMSO; Group B contained 12 mice on a HFD that contained only DMSO; and Group C contained 8 mice that were fed a normal CHOW diet. All animals were exposed to the given diet 1 week prior to the introduction of **4** or DMSO. This was to allow the animals to acclimatise to the change in diet.[69]

5.2.1   Glucose tolerance and insulin tolerance testing.

After 16 weeks, GTT and ITT were performed as before. **Figure 5.14** shows that **4** dramatically improved the animal's ability to clear glucose, when compared to animals on a HFD only. Also, improved insulin sensitivity can be observed as lower glucose levels at the varying time point indicates a more sensitized response to insulin.

An intervention study was also performed. Compound **4** was administered to animals after 17 weeks, once insulin resistance had been established. Compound **4** was found to restore both glucose and insulin sensitivity to normal levels (**Figure 5.14**).

These exceptional results confirm that **4** can actively improve the hyperglycaemic profile of a diabetic animal model. The results from the intervention study also show that **4** has the potential to be used as an antidiabetic agent in the treatment of T2D. The use of a small molecule as an insulin substitute would have many positive effects for those requiring insulin therapies. It could prevent the need for daily injections and would therefore greatly improve the quality of life.
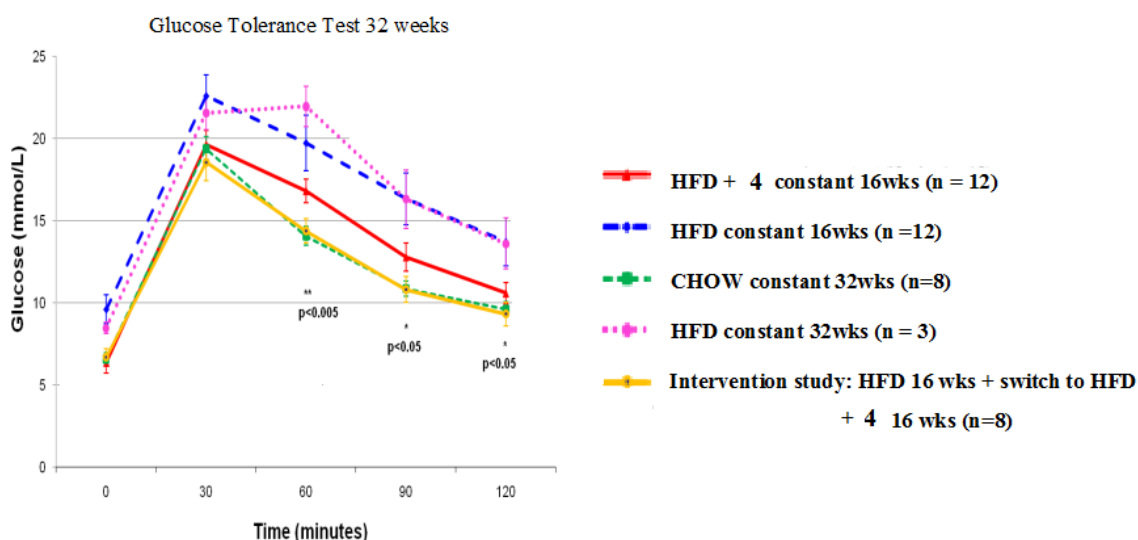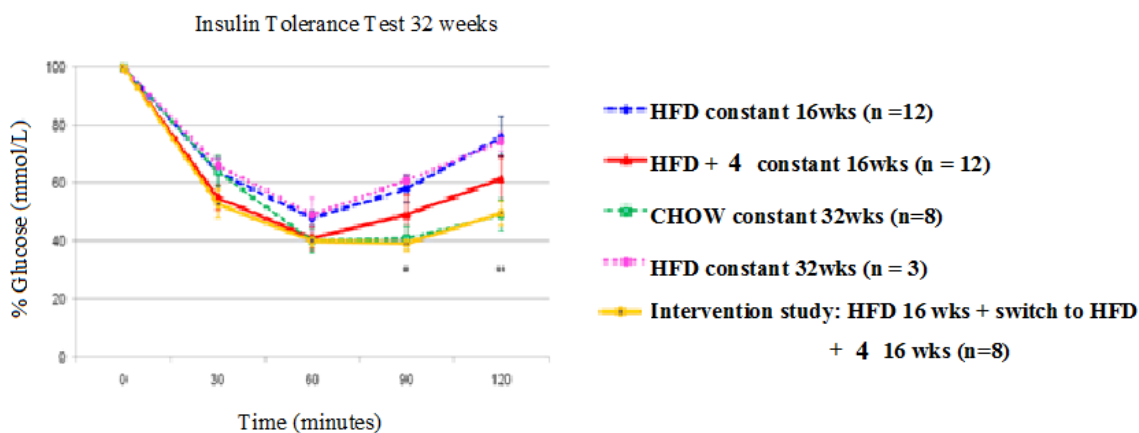
Figure 5.14. Results for compound **4**, Glucose and Insulin Tolerance Test and Intervention Study.

5.3   A pharmacophore model for compound 4.

5.3.1   Pharmacophores

The results of the glucose uptake assay identified functional groups in the compound **4** required for activity. Changes to the trifluoromethyl phenyl group, the piperazine ring and/or the carbonyl group all resulted in a loss of activity. However, changes to the alkyl chain and/or thiophene ring were tolerated. Once the active groups were established, this information was used to identify a suitable pharmacophore.

A pharmacophore can be defined as the spacial orientation of necessary features (functional groups) required for activity while disregarding the molecular framework that holds them together.[64,169] Applications can include mining of virtual libraries (virtual screening) for hit discovery and hit to lead optimization.[170]

The CATALYST software, as implemented in Accelrys Discovery Studio 3.5, can be used to generate 3D pharmacophore models from a collection of molecules that are diverse in both structure and activity by employing programs such as HipHop and Hypogen.

HipHop provides feature-based alignment of a collection of compounds and matches the chemical features of a new molecule, against drug candidate molecules. The resulting models can be used to search chemical databases to find new lead candidates. Inactive molecules can also provide vital information which can be used to place excluding

volume features. Hypogen generates predictive 3D models based on values which can be used to quantitatively predict the activity of new compounds.

To develop a pharmacophore model, the bioactive conformation of a ligand can be obtained from the co-crystallised structure of the target protein, if available.[64] Alternatively, if the bioactive conformation is not known, the conformations of a range of active compounds can be aligned and a common feature pharmacophore can be generated.[64]

5.3.2   Development of Training set

Each active and inactive compound was assigned a principal number, with 2 being most active, 1 being active and 0 being inactive based on the results from the glucose uptake assay (**Table 5.8**).

Compound	Principal No	Compound	Principal No.
4	2	**5**	0
64	2	**6**	0
79	2	**7**	0
81	2	**8**	0
146	2	**9**	0
10	1	**11**	0
42	1	**38**	0
43	1	**40**	0
55	1	**41**	0
56	1	**45**	0
57	1	**47**	0
59	1	**52**	0
60	1	**53**	0
61	1	**54**	0
62	1	**58**	0
63	1	**67**	0
66	1	**73**	0
1	0	**74**	0

Table 5.8: Active and inactive compounds based on results from glucose uptake assay.

All the active compounds with a principal number of 2 were included within the training set. Five inactive compounds, selected by means of clustering, were also included so as to incorporate excluded volumes.

5.3.2.1 Clustering

Clustering involves assigning a set of molecules into subsets, or clusters, so that each molecule in that cluster has similar characteristics. The aim is to create a number of subsets so that molecules in the same subset are similar while molecules in different subsets are as dissimilar as possible.[171] For example, the compounds in cluster 2 all lack a *para* CF$_3$ group while the compounds in cluster 3 all contain a pyridine ring in the place of a phenyl ring. This method was applied to all inactive compounds with a principal number of 0 (**Table 5.9**).

Compound	Cluster	Compound	Cluster
58	1	45	3
67	1	6	3
70	1	8	3
40	2	9	3
52	2	1	3
47	2	53	4
74	2	54	4
41	2	5	5
73	2	46	5
7	3	11	5

Table 5.9: Clustered inactive compounds, with cluster centres shown in red.

Five clusters were created that included varying numbers of compounds. A member of each cluster, the cluster centre (shown in red in **Table 5.9**), was chosen to be included within the training set. From this we had established a training set that included **4**, **9**, **46**, **47**, **54**, **64**, **67**, **79**, **81** and **146**.

5.3.2.2 Excluded Volumes

While the features of the pharmacophore were derived from the active compounds, the information about the inactive compounds was used to allow the algorithm to place excluded volumes.

Excluded volumes are volume locations that active compounds cannot occupy; they represent a single steric constraint.[172] They are acquired by using inactive ligands and are represented by grey spheres.

5.3.3   Methods

The HipHop module in Discovery Studio elucidated 10 common feature pharmacophores from a set of active ligands. The algorithms used information from inactive ligands to place excluded volumes. Compounds were defined as most active, active or inactive based on their performance in the glucose uptake assay. The conformation generation method was set to "BEST". MaxOmitFeature was set at 0 or 1 with 1 indicating that the compound must map to all but one of the features in the generated pharmacophore model. The validation fitting method was set to flexible or rigid, with the flexible setting allowing for each conformation of the ligand to be slightly modified to better fit the pharmacophore. The number of excluded volumes, developed from the inactive compounds, was set at 0, 5 or 10.

A set of features, from which the pharmacophore could be composed of, were selected from a catalogue of available features. From analysis of the active compounds, the features were selected based on the features most likely to make up the pharmacophore. The set included: Hydrogen bond acceptor (HBA), Hydrogen bond donor (HBD), Hydrophobic (H), Hydrophobic aromatic (HAr), Hydrophobic aliphatic (HA), Positive charge (PC), Ring Aromatic (RAr).

Ten models were then developed from the previously prepared training set which included both active and inactive compounds.

5.3.3.1 Generation of Conformations

As the bioactive conformation of our compounds was not experimentally available, a common feature method was used to generate the pharmacophore. The "BEST" method was used to generate 255 conformations for each compound within the training set.

Unlike the alternative "FAST" method which generates conformations systematically, the "BEST" method generates conformations stochastically.[173] The "BEST" mode is able to replicate the ligand-bound conformation of molecules. However, computation times are significantly longer compared to the "FAST" method.[173]

5.3.3.2 Validation of Pharmacophore Models (Receiver Operating Characteristic curves)

As the pharmacophore analysis produced 10 models for each set of conditions used, subsequent refinement was required so as to identify the model with the most relevance. A validation protocol was used to test the models ability to identify active compounds from a larger set of decoys (validation/ test set). The test set included all other experimentally tested compounds, active (12) and inactive (20), which were not included in the training set. Receiver Operating Characteristic (ROC) curves were used to quantify this ability.

ROC curves (**Figure 5.15**) can be used to test the ability of a pharmacophore model to determine between active and inactive compounds within a test set.[174] These curves plot the true positive rate (sensitivity, y-axis) against the false positive rate (1 minus specificity, x-axis).[175] The closer the ROC score value is to 1, the more relevant the pharmacophore model.[174]
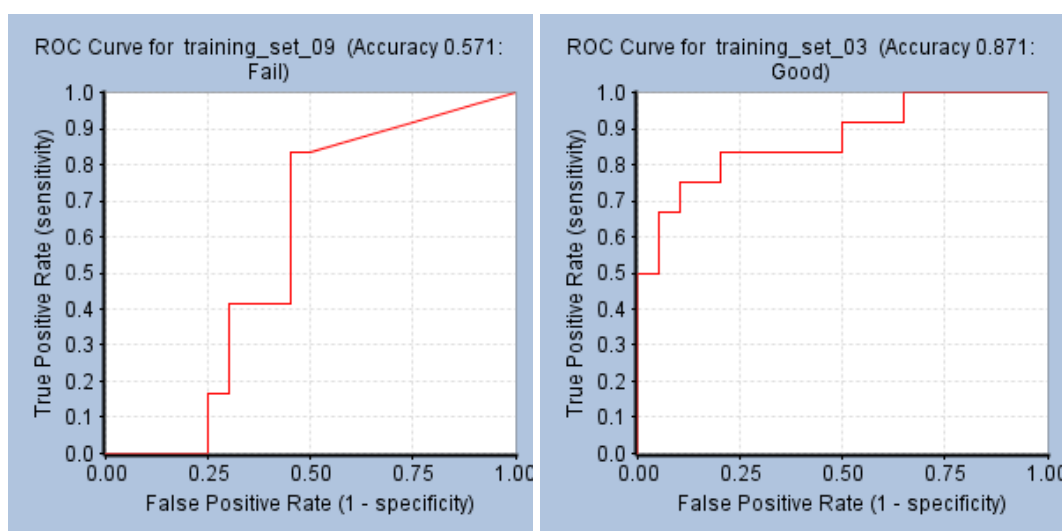
Figure 5.15. ROC curves of varying accuracy.

5.3.4 Pharmacophore Development and Validation

From the initial 10 pharmacophore models generated using the conditions described in Entry A, (**Table 5.9**, **section 5.3.4**) the pharmacophore with a ROC score of 0.642, proved to be the best model). Features included hydrogen bond acceptor, hydrophobic, hydrophobic aromatic and ring aromatic. To identify the necessary features and to improve the quality of the pharmacophore, the model was refined by altering various settings such as number of excluded volumes, maximum omitted features (max. omit features), types of features and alternating the validation fitting method between rigid and flexible. Altering the maximum number of omitted features, from 0 to 1, meant that compounds must include all but one feature in the generated pharmacophore. Alternating between rigid and flexible within the validation fitting method, allowed for each conformation of the ligand to be slightly altered to better fit the pharmacophore model.

Entry	Max. Omit Feature	Flexible/ Rigid fit	Max. Excluded Volume	Best ROC score	Features
A	0	Flexible	0	0.642	HBA, H, HAr, RAr.
B	1	Rigid	0	0.808	HBA, H, HAr, RAr
C	1	Flexible	0	0.825	HBA, H, HAr, RAr
D	1	Flexible	10	0.842	HBA, H, HAr, RAr
E	0	Flexible	5	0.713	HBA, H, HAr, RAr
F	1	Flexible	5	0.871	HBA, H, HAr, RAr
G	0	Flexible	5	0.877	HBA, H x 2, RAr.*

Table 5.9: Results from Pharmacophore development. HBA = Hydrogen bond donor, HBD = Hydrogen bond donor, H = Hydrophobic, HA = Hydrophobic Aliphatic, HAr = Hydrophobic Aromatic, RAr = Ring Aromatic.* HAr feature at alkyl chain terminus removed.

Pharmacophore A underwent additional refinement to improve the pharmacophore. Encouraging results were observed when the max. omit. feature was set at 1 and the fitting method set to rigid. From the 10 pharmacophore models generated using the conditions described for pharmacophore B (**Table 5.9**, Entry B), the pharmacophore model B, with a ROC score of 0.808, proved to be the best. However, when the validation fitting method was set at flexible, a pharmacophore with an improved ROC score of 0.825 was obtained (**Table 5.9**, Entry C, **Figure 5.16**)
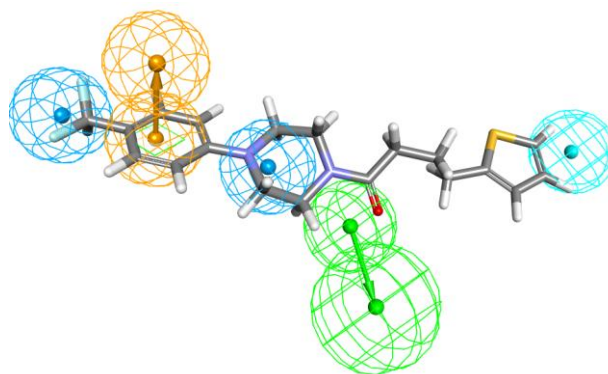
Figure 5.16. Pharmacophore Entry C, ROC score 0.825, with **4** mapped. Blue = H, orange = RAr, green = HBA, cyan = HAr

The model was further refined by introducing excluded volumes. This uncovered Entry D, with a ROC score of 0.842 (**Figure 5.17**). The inactive derivative **67** is also mapped to the pharmacophore, Entry D, in the below diagram. As can be seen from the illustration, **67** does not contain the HBA or the HAr features present in **4**.
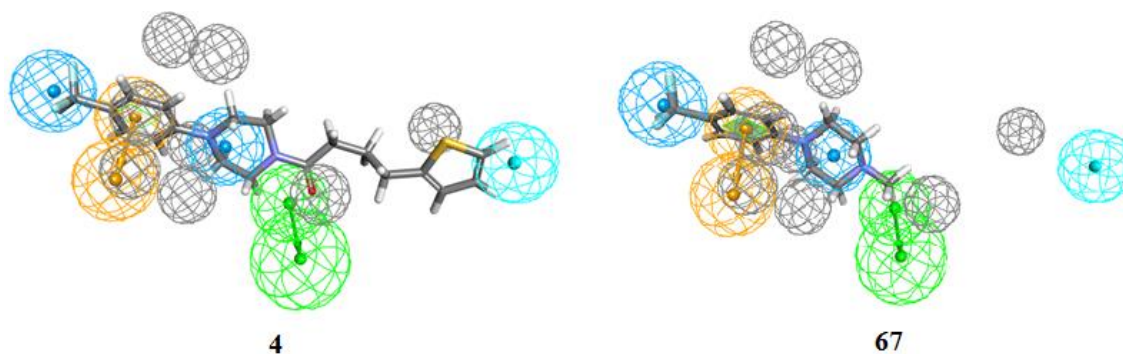
Figure 5.17. Pharmacophore Entry D (ROC score = 0.842) with **4** (active) and **67** (inactive) mapped. Grey = Excluded volumes, blue = H, orange = RAr, green = HBA, cyan = HAr

Reducing the number of excluded volumes, from 10 to 5, and allowing for no features to be omitted, gave pharmacophore Entry E with a ROC score of 0.713. However, it was found that allowing one feature to be omitted resulted in a pharmacophore with an improved ROC score of 0.871 (**Table 5.9**, Entry F).

From results of the glucose uptake assay, the thiophene heterocycle, represented by the hydrophobic aromatic (HAr) feature, proved to be non-essential for activity. Therefore, the presence of a feature at the alkyl chain terminus was removed. As a feature was removed, it was necessary to set the max. omit feature equal to 0. This was to ensure the

pharmacophore had an acceptable number of 4 features. The excluded volumes were also set at 5 (**Table 5.9**, Entry G). The pharmacophore, Entry G, with a ROC score of 0.877 (**Figure 5.18**) best represents the functional groups within the family of compound **4** derivatives that are responsible for evoking a biological response. **Figure 5.19** shows both **4** and **79** mapped.
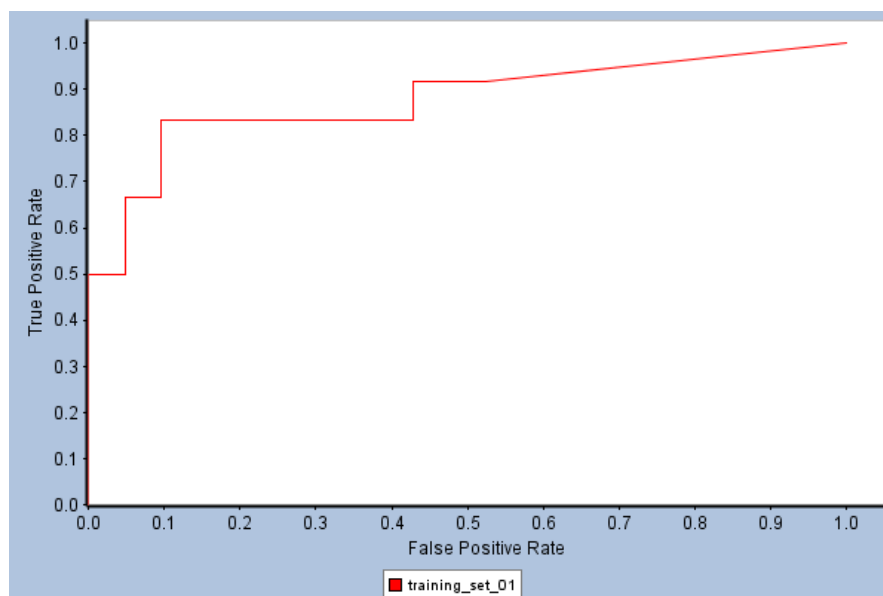
Figure 5.18. ROC curve for Entry G.
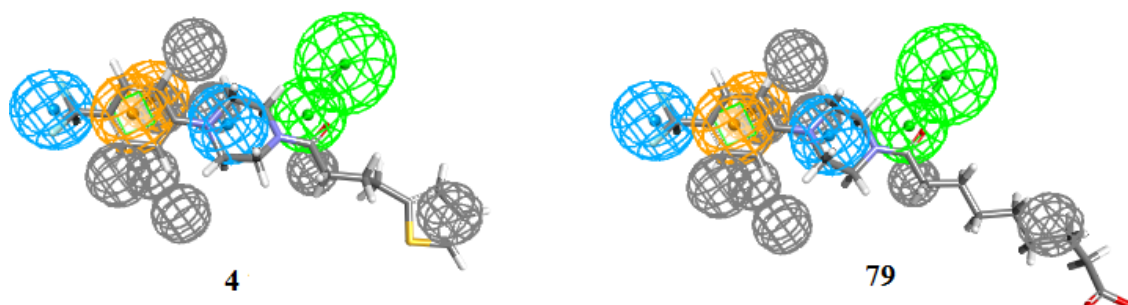
Figure 5.19. 4 and **79** mapped to pharmacophore G. Blue = H, orange = RAr, green = HBA.

Both active compounds have groups that match all the features of the pharmacophore. They include the trifluoromethyl group and piperazine ring (H, Blue), the aromatic ring (HAr, Cyan) and the amide carbonyl functionality (HBA, Green). No inactive compounds were able to be mapped to the pharmacophore as the max. omit feature was set at zero.

Results of the glucose uptake assay have identified the pharmacophore features necessary for activity. As a result the pharmacophore, Entry G with a ROC score of 0.877, has been constructed and can be used to predict the ability of future compounds to act on the protein target.

5.4   Conclusion

A SAR study was subsequently performed on compound **4** to determine the key functional groups responsible for evoking such a biological response. A number of conclusions were drawn from this study:

- changes to the trifluoromethyl phenyl group are not tolerated

- a piperazine ring is essential

- an amide carbonyl is required

- the thiophene ring is not necessary for activity

- the length of the molecule may play a vital role in ligand/protein interactions.

It was possible to optimise **4** and generate compounds with greater potency with the knowledge that it was the length of the molecule and not the presence of a terminal heterocycle that was critical for biological activity. The heterocycle was therefore replaced with different functional groups which led to the discovery of a number of compounds, such as compounds **64** (terminal phenyl), **79** (terminal carboxylic acid) and **82** (terminal ester), which proved to be more active than compound **4**.

Compound **4** was as active as its predecessor, compound **1**, in an animal model. More importantly however were the results obtained with the use of compound **4** in an intervention study. Here we saw that the use of compound **4** restored both glucose and insulin sensitivity to normal levels

The information obtained from the SAR study allowed for the development of a pharmacophore model. The developed model best represents the key functional groups required for a molecule to act on the protein target and stimulate glucose uptake. The final pharmacophore model had a ROC score of 0.877.Future work

A number of compounds have been subsequently synthesised, which will allow us to further investigate what functional groups in compound **4** are required to evoke a biological response. For example, the derivatives of compound **4**, **48** and **49**, contain *para* CH$_3$ and *tert*-butyl groups respectively, as opposed to the CF$_3$ group found in **4** (**Figure 5.20**). Results for these compounds from the glucose uptake assay may indicate whether it is the steric bulk of the CF$_3$ alone that is important for biological activity. The synthesis of these compounds and subsequent derivatives of compound **4** were discussed in Chapter 3. The structures of the compounds from this section, and subsequent sections, awaiting testing are highlighted (†) in the experimental section.
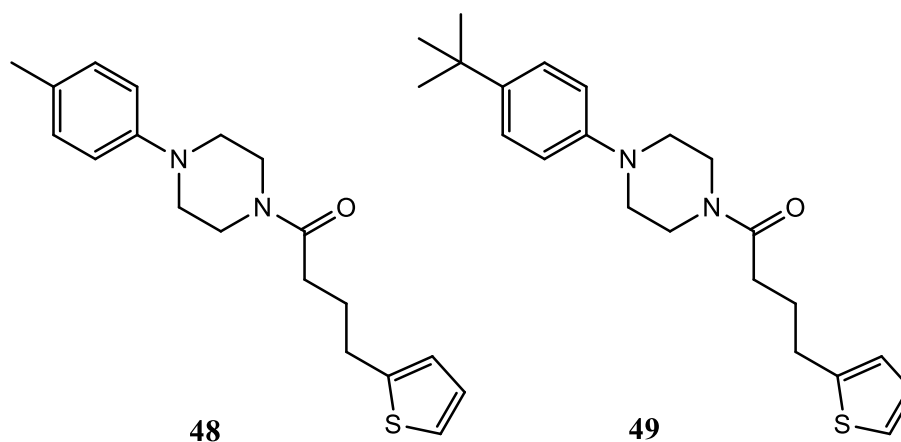
Figure 5.20. Structures of **48** and **49**.

6. Biological evaluation of compound 2 and its derivatives, 92 and 104-122.

6.1   Biological testing of pyrimidinone 2 and the derivatives of 2

The pyrimidone containing **2** displayed similarities to **1** in that it was also inactive in the glucose uptake assay, suggesting a single mechanism of action (**Figure 6.1**). Compound **2** may have evoked its biological response by disrupting the RBP4-TTR interaction. It was unlike compound **4** in that it was not able to stimulate glucose uptake by acting through the unknown protein target.
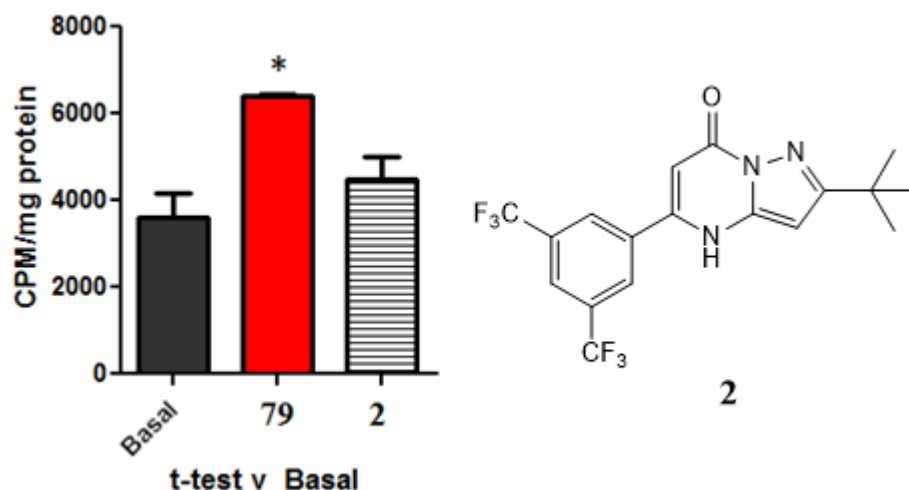
Figure 6.1. Glucose uptake assay results and structure for compound **2**. C2C12 muscle cells incubated overnight at 37 ºC in the presence 10 μM of each compound. Cells then exposed to ^{3}H deoxy-2-glucose for 10 mins and a scintillation count of the C2C12 muscle cells performed.

Although initial results from the glucose uptake assay were discouraging, a SAR study of **2** was still performed. The SAR study of compound **1**, which was also inactive in the glucose uptake assay, led to the highly active **4** and **79**. It was therefore hoped that a SAR study of compound **2** would lead to useful compounds.

A number of compounds were initially synthesised that probed the significance of the *tert*-butyl and phenyl functionalities (**Figure 6.2**), with **105** and **115** the first compounds tested in the glucose uptake assay.

The results from the assay showed that by replacing the *tert*-butyl group with an *iso*-propyl substituent, a compound (**115**) with similar activity to **79** was generated (**Figure 6.2**). This suggested that the sterically bulky *tert*-butyl group may have been responsible for the observed inactivity of **2** in the glucose uptake assay. This is in agreement with the Charton values, which are used to describe the steric effects of substituent.[176] A *tert*-

butyl group has a Charton value of 1.24 which is greater than the Charton value of an *iso*-propyl group (Charton value = 0.76).[156] This indicates that a *tert*-butyl is more sterically demanding than an *iso*-propyl group and can impose a greater steric effect on a protein target.[176]

The size of the alkyl substituent may have prevented the compound from interacting with the protein target that is responsible for the glucose uptake effect. The presence of this less bulky *iso*-propyl substituent may have allowed the substituent to fit into a hydrophobic pocket that is too small for a *tert*-butyl group. Such a hydrophobic interaction could have stabilised the drug-protein interaction.[63]

Like compound **2**, compound **105** also proved to be inactive. This may be due to the presence of the *tert*-butyl group as opposed to changing the bis(trifluoromethylphenyl) group. Therefore, the importance of the bis(trifluoromethylphenyl) group required further investigation.
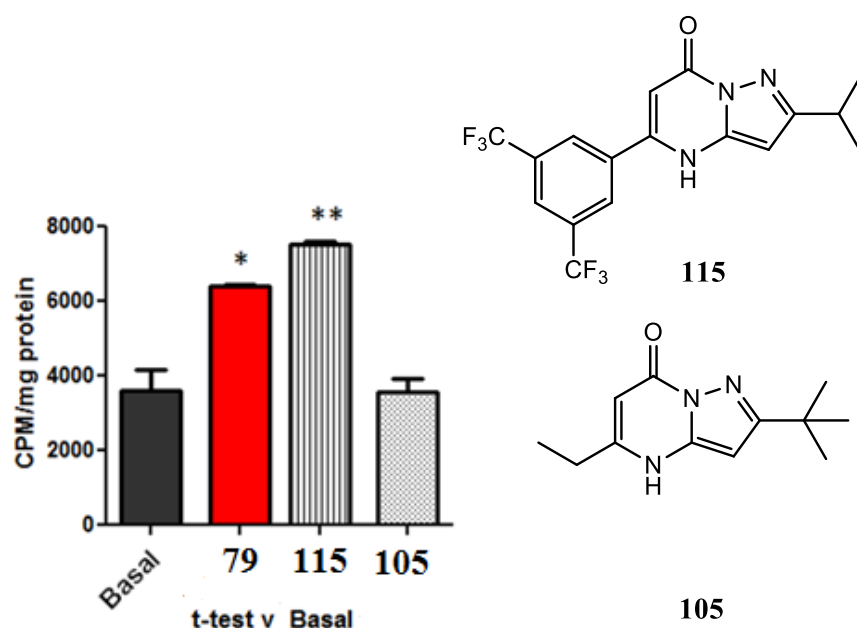
Figure 6.2. Glucose uptake assay results for **105** and **115**. Compound **115** shows similar activity to compound **79** while compound **105** is inactive in the glucose uptake assay. C2C12 muscle cells incubated overnight at 37 °C in the presence 10 μM of each compound. Cells then exposed to ^{3}H deoxy-2-glucose for 10 mins and a scintillation count of the C2C12 muscle cells performed.

To do this, a number of derivatives of **2** were synthesised, where structural alterations were made at the bis(trifluoromethylphenyl) substituted, C5 position **Table 6.1**. This family of compounds are awaiting biological testing.
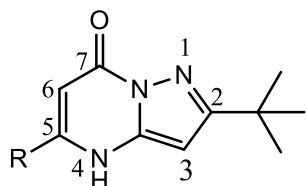
Compound	R
101	H
104	Me
105	Et
106	*i*Pr
107	*t*Bu
108	Ph

Table 6.1: Structures of derivatives of compound **2**.

6.2   Derivatives of compound 115.

As compound **115** had a biological activity similar to **79** and **4**, a family of derivatives of **115** were prepared which could be used to identify the functional groups responsible for inducing the biological response. This family focused on investigating the importance and type of substituent present at the C2 and the C5 position (**Figure 6.3**).
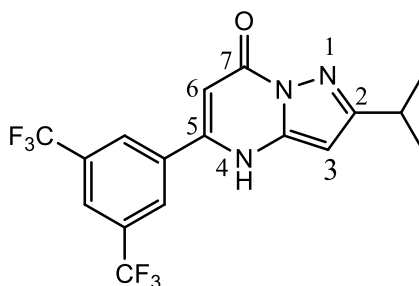
Figure 6.3. Structure of compound **115**.

6.2.1   Effect of the substituent at C2 for the derivatives of compound 115.

The significance of the substituent at the C2 position was evident when the activities of **2** and **115** were compared. For this reason, a number of derivatives were synthesised that further explored the effect of the substituent at this position. A number of **115**

derivatives were synthesised with the aim of assessing their ability to stimulate glucose uptake. **Table 6.2** shows the series of compound **115** derivatives synthesised. This family of compounds are awaiting biological testing
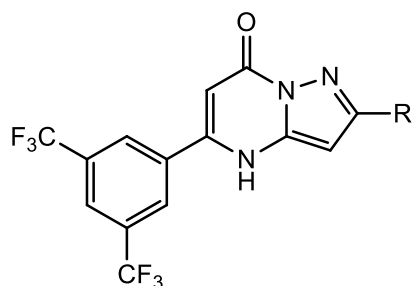
Compound	R
117	Me
118	Et
119	Ph
120	2-thienyl

Table 6.2: Structures of derivatives of compound **115**.

6.2.2   Effect of the substituent at C5 for the derivatives of compound 115.

The glucose uptake assay results for the derivative **105** could not provide a conclusion on the biological significance of the bis(trifluoromethylphenyl) functional group. This was due to the presence of the *tert*-butyl group which was previously identified as inhibiting a compound's ability to stimulate glucose uptake. For this reason, a series of **115** derivatives that probed the relevance of the substituent at C5 were synthesised, with the aim of testing their activity in the glucose uptake assay (**Table 6.3**). This family of compounds are awaiting testing.

Compound	R
98	H
109	Me
110	Et
111	*n*Pr
112	*i*Pr
113	*t*Bu
114	Ph
121	4-trifluoromethylphenyl
122	3-trifluoromethylphenyl
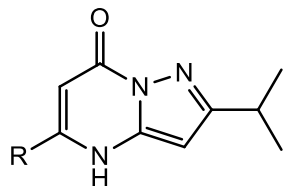
Table 6.3: Structures of derivatives of compound **115**.

6.3 Conclusion.

Biological evaluation of compound **2** and the derivatives of this compound led to the identification of compound **115** which proved to be highly active in the glucose uptake assay. The presence of the *iso*-propyl group in the C2 position in compound **115** as opposed to the *tert*-butyl group in the C2 position in compound **2** may have allowed the substituent to fit into a hydrophobic pocket that is too small for a *tert*-butyl group. As a result of this improved activity, a number of derivatives of compound **115** were designed and synthesised and are currently awaiting biological evaluation.

Chapter 4 saw the synthesis of a number of derivatives of compound **3**. These compounds are also awaiting biological evaluation.

7. Identification of secondary protein target.

The initial aim of this project was to treat T2D by reducing serum levels of RBP4. Compound **1** and its derivatives were designed and synthesised to dock within the protein cavity of RBP4, causing disruption to the RBP4-TTR complex. It was expected that this would result in renal excretion of RBP4 and lower the serum levels of this protein. A compounds ability to induce RBP4-TTR disruption was assessed using the SPR assay, with **1** and **4** proving to be highly effective. The high throughput glucose uptake assay was then employed to test the ability of subsequent derivatives to induce glucose uptake in muscle cells. Compound **4**, and several other compounds, were capable of inducing this uptake and this led to the identification of the highly active, **79**. The glucose uptake assay however was an RBP4 independent assay. RBP4 was not necessary for compound **4** and the other active derivatives to stimulate the uptake of glucose. When cells were stimulated with and without RBP4, no difference in activity was observed (**Figure 7.1**). This indicated that the biological activity of the **1** derivatives was not derived from their inhibition of the RBP4-TTR interaction alone and that they were also working through a secondary protein target.
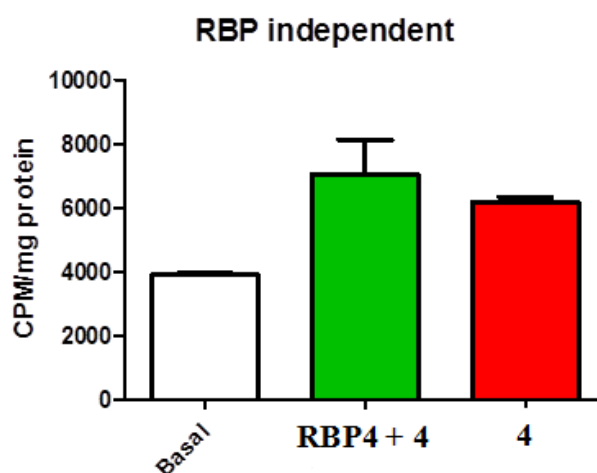
Figure 7.1. RBP4 independent glucose uptake. Compound **4** stimulated glucose uptake by C2C12 muscle cells is independent of an RBP4 supported mechanism. C2C12 muscle cells incubated overnight at 37 ℃ in the presence 10 μM of each compound. Cells then exposed to ^{3}H deoxy-2-glucose for 10 mins and a scintillation count of the C2C12 muscle cells performed.

7.1   Immobilisation of active compounds on an affinity column

Kosaka *et al*. described a method for the identification of an unknown small molecule protein target a using affinity purification and mass spectrometry.[177] This molecule, **Figure 7.2**, was found to increase glucose uptake in myocytes through the activation of AMPK.

The identification of the protein target involved immobilising the active molecule **145** on an affinity column, *via* an organic linker, where the affinity column was made up of agarose beads. Compound **145** was immobilised on to the agarose bead *via* the carboxylic acid group. Kosaka *et al*. had previously performed a SAR study of this compound and found that the pharmacological activity was not affected when the furancarboxylic acid moiety was substituted. As a result the molecule was covalently bound to the agarose bead *via* the carboxylic acid group. Binding proteins, which were isolated from target cell lysate, were then passed through the affinity column. Trypsin was used to remove the bound proteins which were then analysed using mass spectrometry.[177]
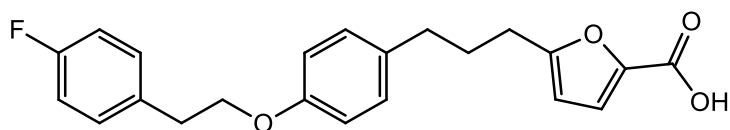
Figure 7.2. Structure of compound **145**.[177]

Using the Kosaka method, both **4** and **79** were immobilized onto an agarose bead, commercially known as sepharose. As the affinity purification step was to be performed in an aqueous environment, we chose to use a linker that had adequate hydrophilic properties. For this reason, we chose to attach compounds **4** and **79** to the sepharose bead *via* a polyethylene glycol (PEG) linker. A PEG6 linker, which would create enough space between the active derivatives and the bead, was chosen so as not to hinder the active molecule's ability to bind to the target protein.

7.1.1   Immobilisation of 4 and 79 onto the affinity column

The alcohol group present in the alkyl chain of **66** presented a viable option for attaching the chain to **4**. Attaching at this position would leave both the arylpiperazine end and the thiophene ring free to interact with the protein target (**Figure 7.3**). This

approach was attempted but was not successful. An alternative approach was also explored for attaching linker/bead to compound **4**.

66-PEG construct
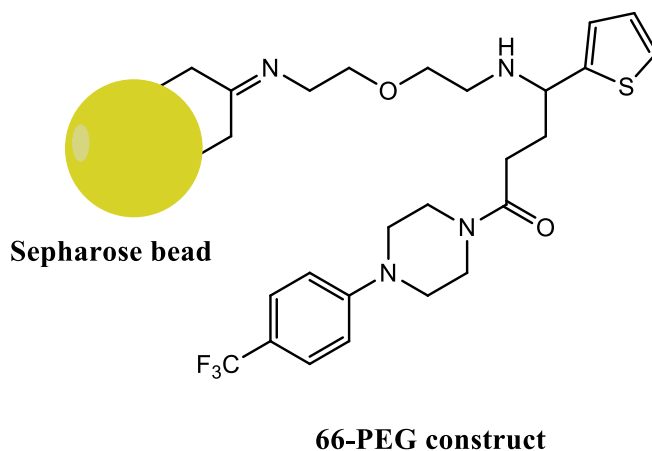
Figure 7.3. Proposed structure for the immobilization of compound **4** derivative onto a sepharose bead.

The SAR study revealed that changes to the thiophene ring were tolerated, but changes to the arylpiperazine and/or carbonyl functionality resulted in a loss of activity. Therefore, **4** was functionalised at the thiophene end so as to allow the attachment of the PEG linker at the heteroaroamtic ring. Once the amino PEG linker was attached, the **4**-PEG construct was immobilised onto the sepharose bead (**Figure 7.4**).

4-PEG construct
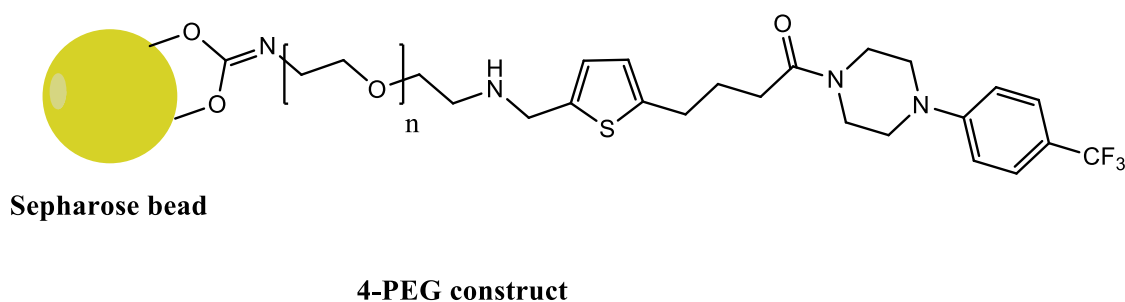
Figure 7.4. Immobilisation of **4** onto a sepharose bead.

The SAR study also revealed that the biological activity of **79** remained if the carboxylic acid moiety was substituted with a methyl ester (**81**). We also chose to assess the effect attaching a PEG linker would have on the biological activity of **79**. For this reason **79** was coupled to 2-methoxyethanamine to give compound **146 (Figure 7.5)**. The activity of this derivative was then investigated in the glucose uptake assay, with excellent results being obtained.
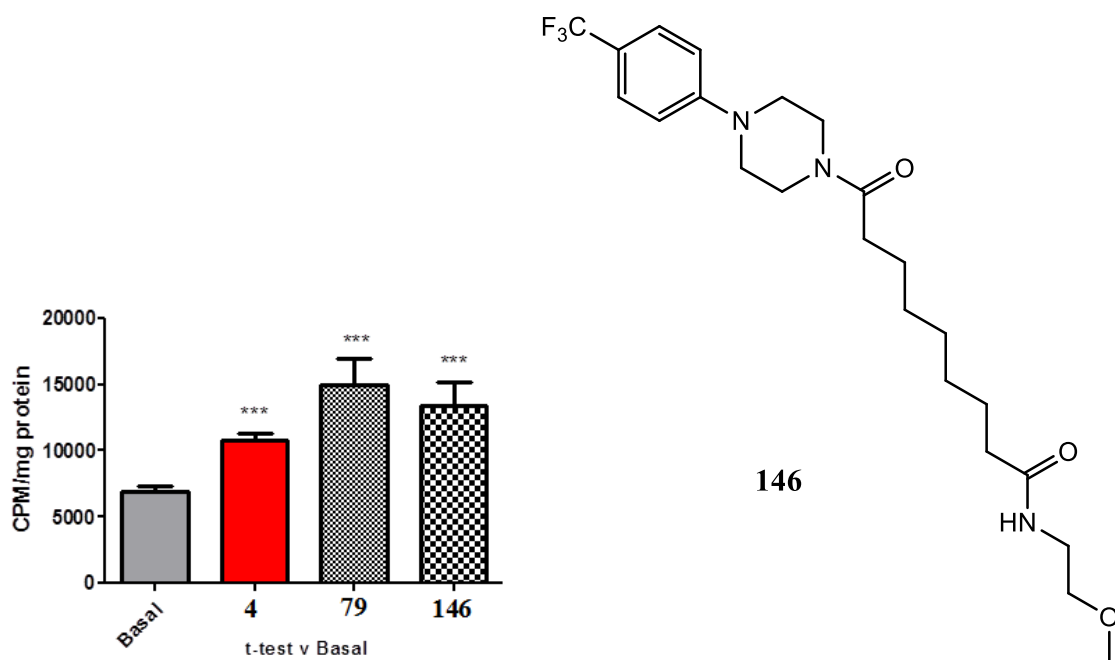
Figure 7.5. Structure and glucose uptake assay results and structure of **146**. Compound **55** increases the uptake of ^{3}H deoxy-2-glucose by C2C12 muscle cells, compared to compound **4** and is as active as compound **79**. C2C12 incubated overnight at 37 ºC in the presence 10 µM of each compound. Cells then exposed to ^{3}H deoxy-2-glucose for 10 mins and a scintillation count of the C2C12 muscle cells performed.

From **Figure 7.5**, it is clear that **146** is more active than **4** and as active as **79**. Therefore, as substituting **79** with a small PEG linker did not affect the biological activity of the molecule, we decided to proceed with attaching a longer PEG linker *via* the carboxylic acid. As **79** contained a carboxylic acid functionality, the PEG linker could be attached using amide bond formation. The **79**-PEG construct could then be attached to the sepharose bead (**Figure 7.6**).

Separose bead
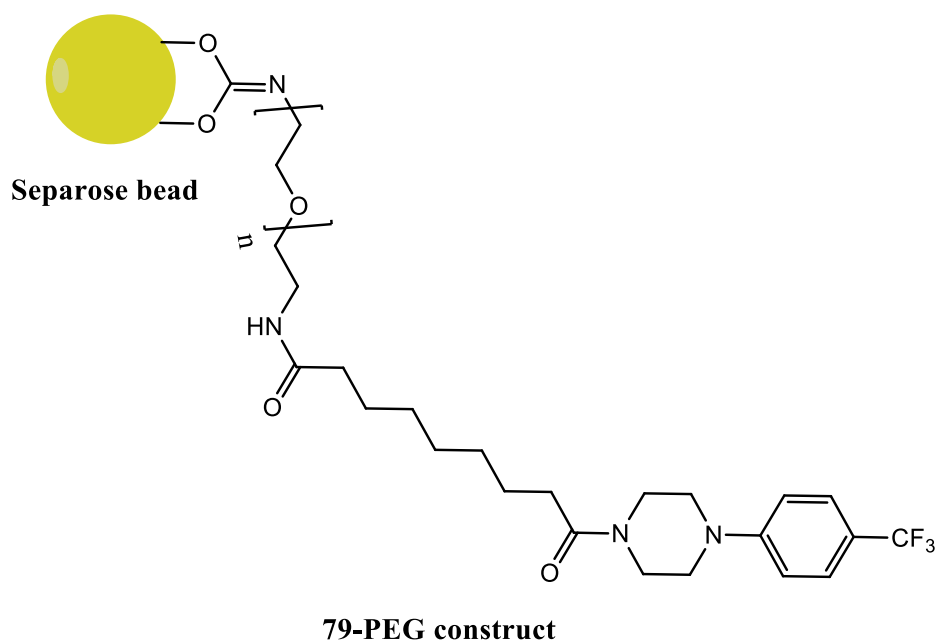
79-PEG construct

Figure 7.6. Immobilisation of **79** onto a sepharose bead.

7.1.2   Synthesis of PEG constructs of 4 and 79.

The alcohol group found in the alkyl chain of **66** allowed for the possible attachment of the PEG linker at this position. Functionalising **66** with a PEG linker first required the activation of the alcohol. The secondary alcohol was reacted with tosyl chloride with the aim of introducing a leaving group at this position (**Scheme 7.1**). However, only starting materials were recovered.
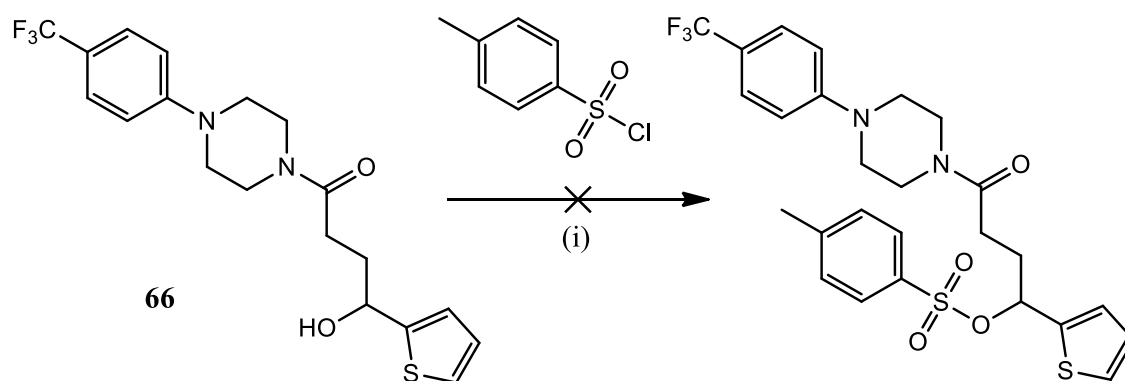
Scheme 7.1: Synthetic route for the attempted tosylation of **66**, (i) NEt$_3$, DMAP, DCM, 0 °C-rt, overnight.

Mesylation of the alcohol was also attempted but again only starting materials were recovered. The lack of reactivity of the alcohol at this position maybe due to it being a

sterically hindered secondary alcohol. As a result an alternative strategy for attaching the PEG linker to compound **4** was employed.

As previously mentioned, the glucose uptake assay revealed a tolerance for changes to the thiophene ring, As such; it was decided to attach the PEG linker to the thiophene ring. Thiophene rings readily undergo electrophilic aromatic substitutions, as observed previously and hence it is possible to substitute a thiophene at the C2 position.[100] The synthetic approach that was chosen was to formylate the thiophene ring, using tin(IV)chloride and dichloromethyl methyl ether, as the methylating agent. This Rieche type formylation gave compound **147**. This would then allow the amino PEG linker be attached to **147** *via* a reductive amination (**Scheme 7.2**).
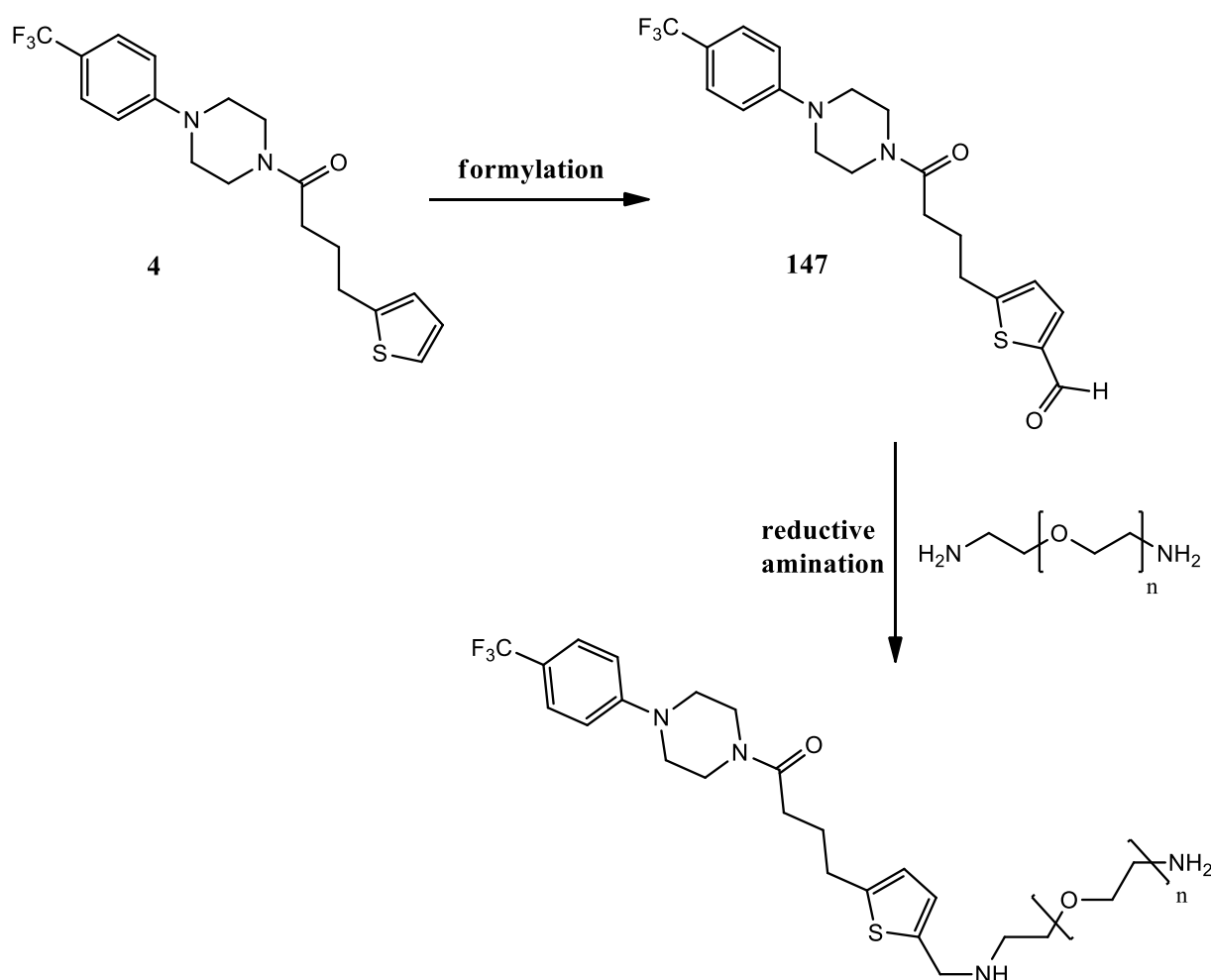
Scheme 7.2: Synthetic route to the **4**-PEG construct.

The formylated derivative of **4**, **147**, was isolated in a 62% yield. The presence of the product was clear from the characteristic aldehydic peak at 9.82 ppm in the ^{1}H NMR

spectrum while the quartet resonating at 123.5 ppm in the ^{13}C NMR spectrum, with a coupling constant of 270.0 MHz, indicated the presence of the trifluoromethyl phenyl group. Also, the aldehydic carbonyl stretch at 1661 cm^{-1} is indicative of the presence of an aldehyde moiety.

Reductive aminations involve the formation of an imine, followed by its reduction, to give the aminated product. In this instance, NaBH$_4$ was used as the reducing agent. To facilitate the attachment of the PEG linker to **147** and its subsequent attachment to the sepharose bead, a diamino PEG linker was required (**Scheme 7.3**).
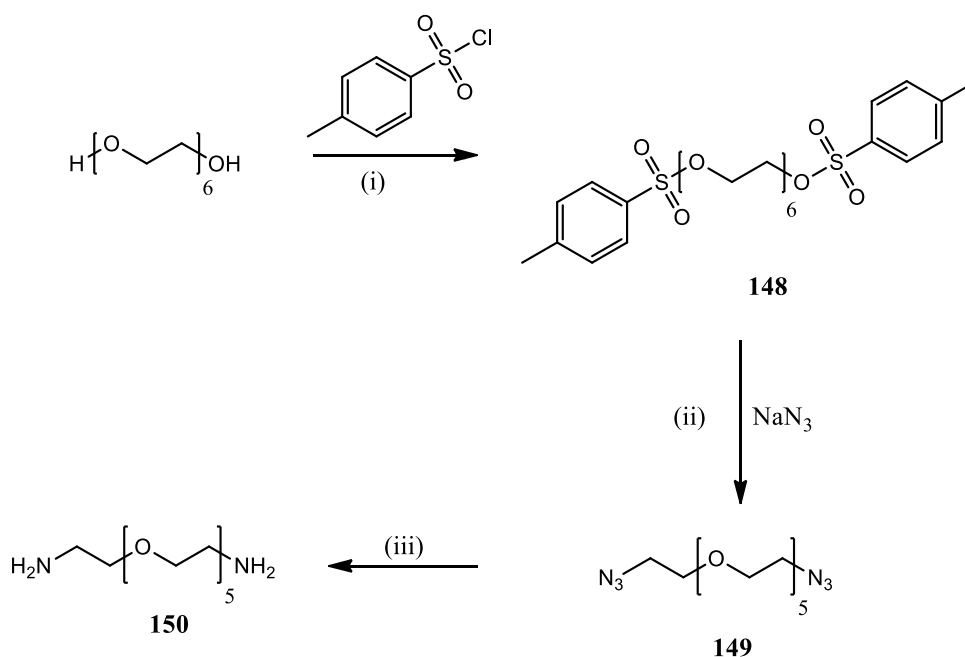
Scheme 7.3: Synthesis of diamino PEG6 linker **90**, (i) NEt$_3$, DMAP, DCM, 0 °C-rt, overnight, 94% (ii) CH$_3$CN, reflux, 48 hrs, 54% (iii) PtO$_2$, H$_2$, MeOH, 48 hrs, 82%.

Tosylation of hexaethylene glycol (**148**) followed by nucleophilic substitution of the resulting product allowed for the formation of the diazido PEG6 linker (**149**). The presence of compound **149** was determined from the IR spectrum with the presence of the characteristic azide peak at 2106 cm^{-1}. The azide was then reduced to the primary amine, using Adams catalyst, affording the diamino PEG6 linker (**150**) in an 82% yield. With the linker now prepared, it was possible to attempt the reductive amination with **147**.

Dou *et al*. reported the substitution of an aldehyde, by means of reductive amination, using a diamino PEG linker.[178] This method was attempted but a complex mixture was

obtained. As a result, the diamino PEG6 linker was then reacted with di-*tert*-butyl dicarbonate (Boc), to give the mono protected PEG6 linker. The reductive amination with **147** was subsequently attempted. Again, the desired aminated product was not formed. Instead, what was observed was the reduction of the aldehyde to the primary alcohol **151** (**Figure 7.7**).
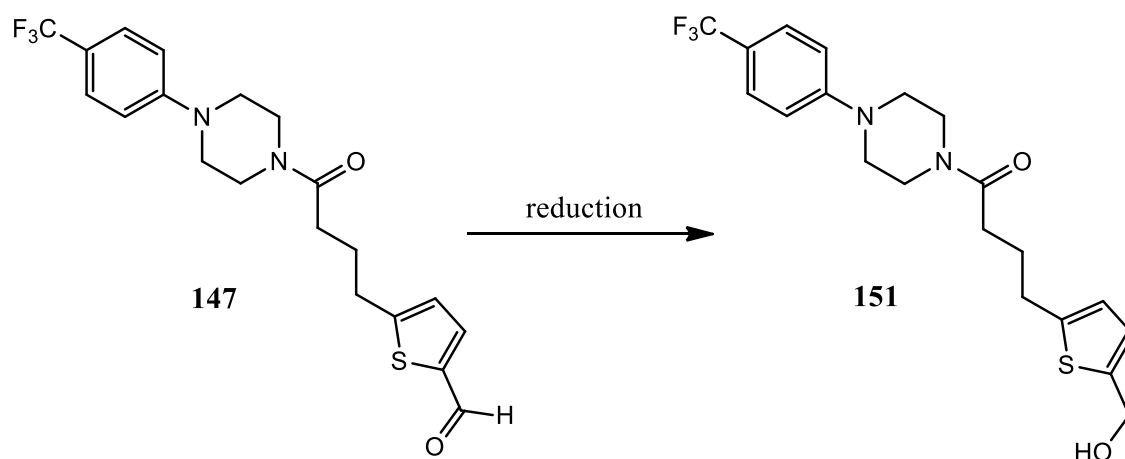
Figure 7.7. Reduction of **147** to **151**.

Figure 7.8 shows the ^{1}H NMR spectra for **147** and **151**. The absence of the aldehyde peak at 9.82 ppm and the presence of a methylene peak at 4.66 ppm are indicative of a reduction having occurred. The presence of the alcohol was also determined by mass spectrometry. An ionized product of mass 413.1505 m/z was detected which is indicative of the protonated alcohol product. From the ^{13}C NMR spectrum it was clear that the aldehyde functional group was no longer present with the absence of the peak at 181.1 ppm which is characteristic for the aldehyde carbon. Also HSQC experiments showed a correlation between the methylene ^{1}H signal at 4.66 ppm and the ^{13}C signal at 58.7 ppm. The chemical shift of this peak indicates the presence of a methylene group beside an electron withdrawing oxygen atom.
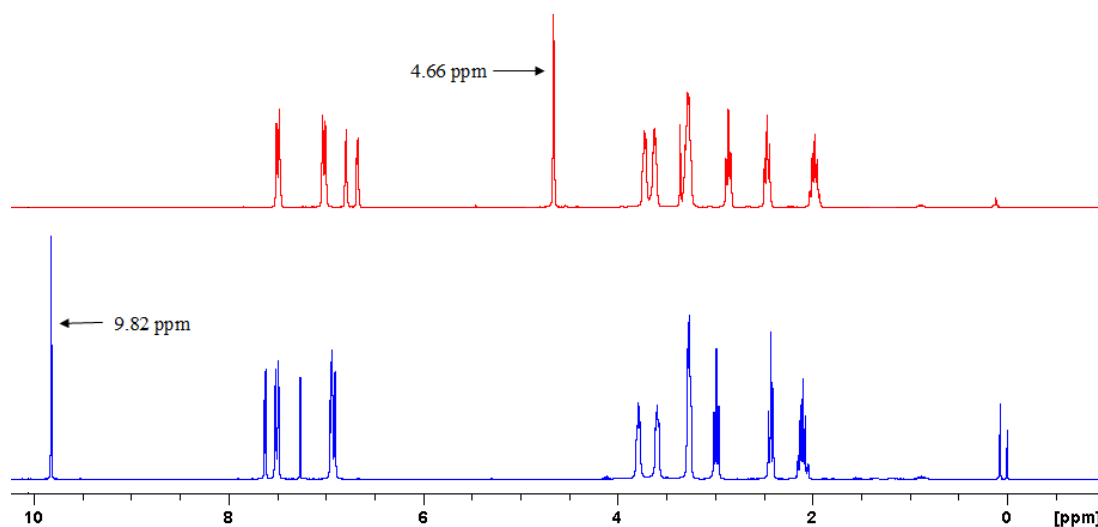
Figure 7.8. The ^{1}H NMR spectra of **147** (blue) and **151** (red).

In order to determine whether the problem lay with the aldehyde (**147**) or the diamino PEG6 linker (**150**) a reductive amination was attempted using **147** and a simpler amine, propan-1-amine. This reaction successfully led to the aminated product **152**, in a 56% yield (**Scheme 7.4**), and suggested that the problem lay with compound **150**.
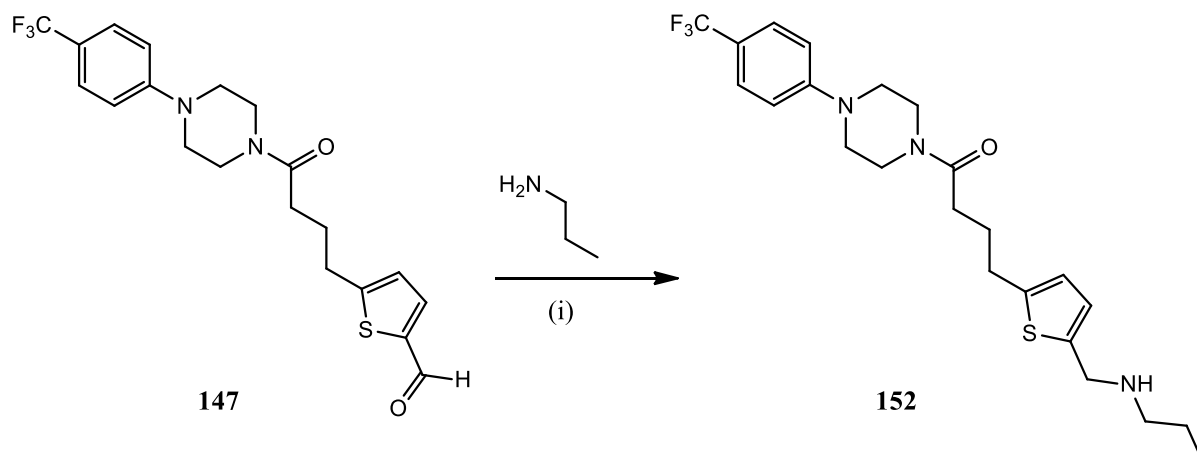
Scheme 7.4: Synthesis of compound **152**, (i) NaBH$_4$, MeOH, 3 hrs, 56%.

An alternative synthetic approach was taken involving the use of a shorter PEG linker, PEG3. In addition, a different protection strategy was employed. Hence, only one of the azide moieties of the diazido PEG3 linker, which was synthesised as for compound **149**, was selectively transformed into an amine (**154**) using a Staudinger reduction (**Scheme 7.5**).[179] The reaction mechanism for this transformation is shown below (**Scheme 7.6**)
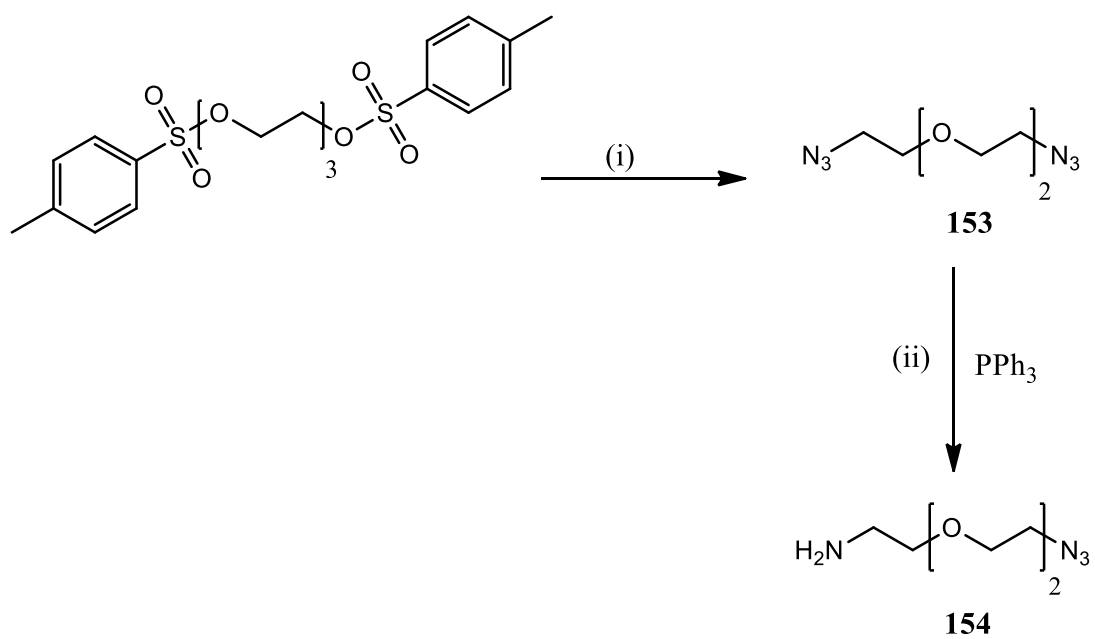
Scheme 7.5: Staudinger reduction, (i) NaN_3, CH_3CN, reflux, 48 hrs, 80% (ii) 1 M HCl,

Et_2O, EtOAc, 99%.
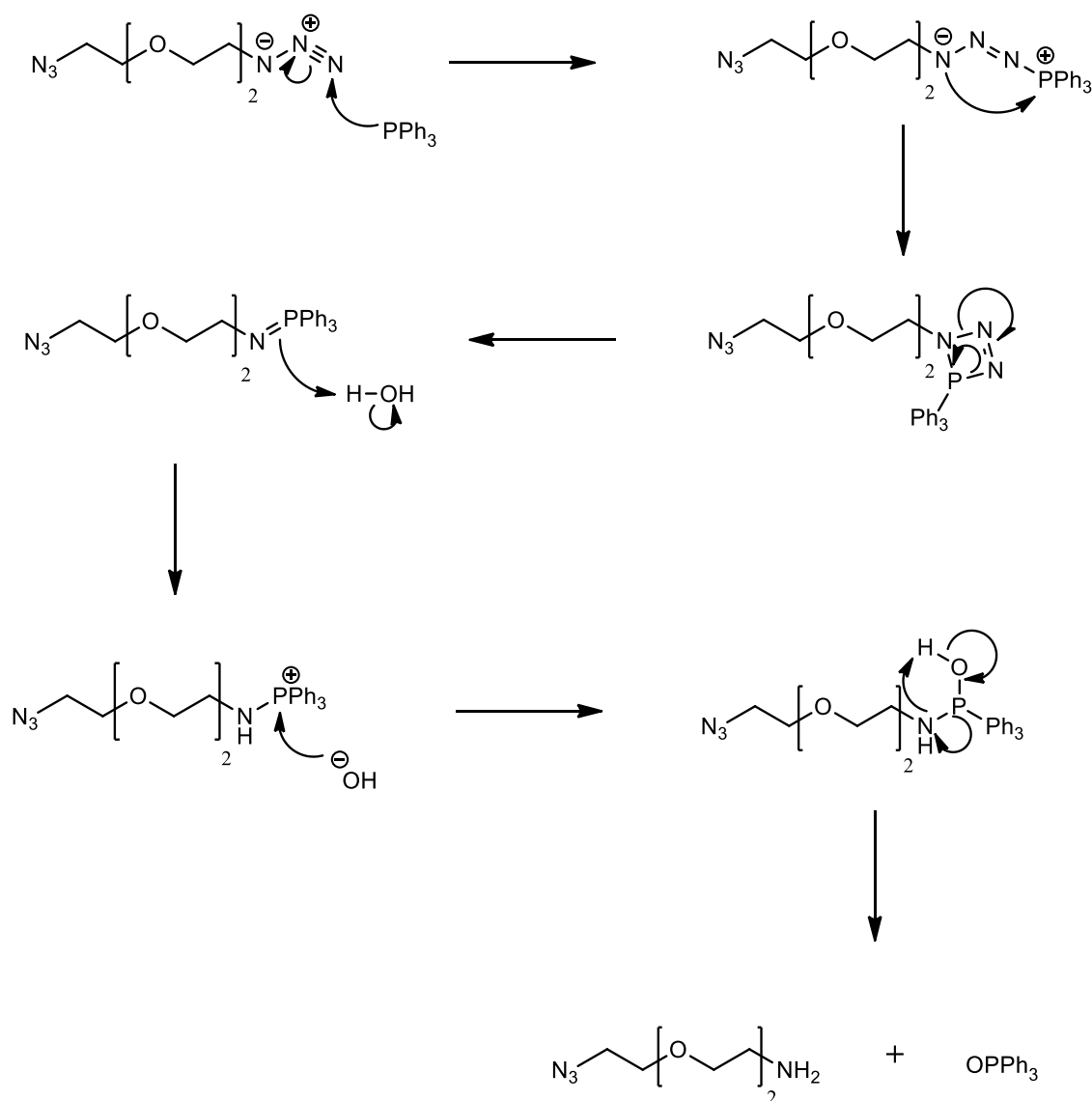
Scheme 7.6: The reaction mechanism for the Staudinger reduction of compound **153** to give compound **154**.

The presence of the mono amino PEG3 was confirmed by both HR-MS and IR, where the characteristic azide peak was observed at 2109 cm^{-1} in the IR spectrum.

With **154** successfully synthesised, linking this compound to **147** was then performed *via* a reductive amination using the same conditions as before. This resulted in the successful isolation and characterisation of the desired aminated product, **155**, in a 76% yield (**Scheme 7.7**). The IR spectrum indicated the presence of **155** with peaks at 2111 and 1607 cm^{-1}, characteristic for an azide and an amide respectively. Also, ^{13}C NMR spectroscopy highlighted the presence of the CF$_3$ group with a quartet having a coupling constant value of 268 Hz found at 124.6 ppm. From the ^{1}H NMR it was clear that the

formation of **155** had occurred with the presence of the singlet at 3.94 ppm indicating the presence of the methylene group adjacent to the electron withdrawing secondary amine.
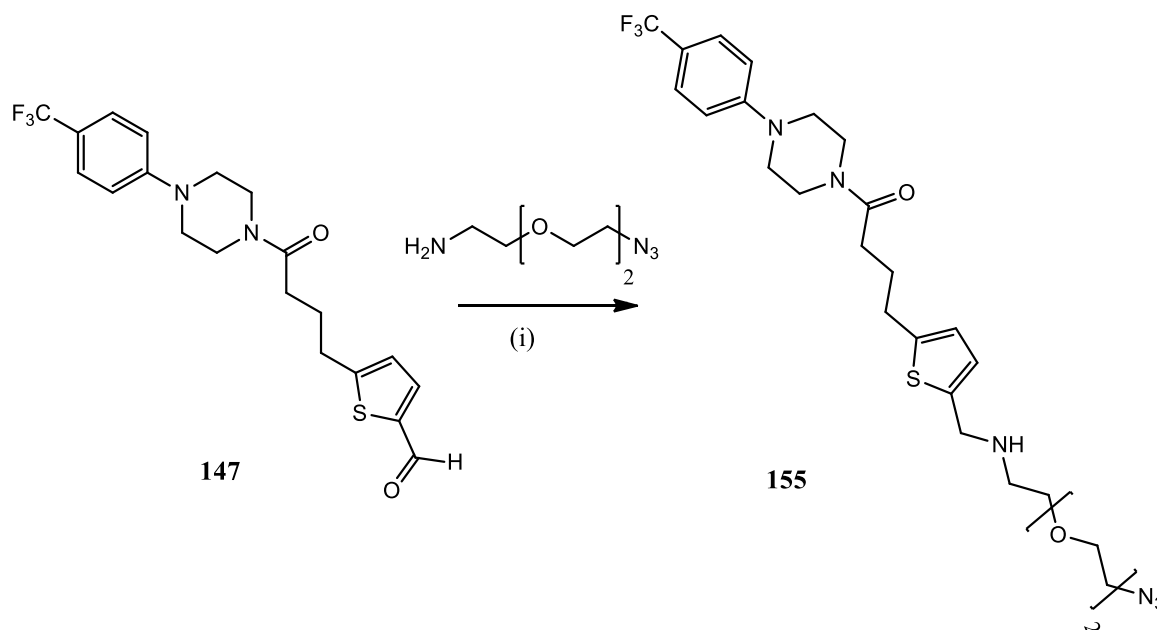
Scheme 7.7: Synthesis of **155**, (i) NaBH$_4$, MeOH, 3 hrs, 76%.

The presence of the azide moiety not only allowed for the effective linkage of **154** to **147**, it also upon reduction, gave access to the free amine required to attach **155** to the sepharose bead. A Staudinger reduction was again utilised to convert the terminal azide into the primary amine (**Scheme 7.8**). This gave **156** in a 43% yield. The absence of the azide peak in the IR spectrum, as well as the presence of the N-H stretch at 3420 cm^{-1} and the N-H bend at 1640 cm^{-1} verified the reduction of the azide to the amine was successful. ^{13}C NMR spectroscopy indicated the presence of the trifluoromethyl phenyl group with the quartets at 125.4 ($J = 3.0$ Hz), 123.5 ($J = 268.7$ Hz) and 120.1 ($J = 32.3$ Hz).
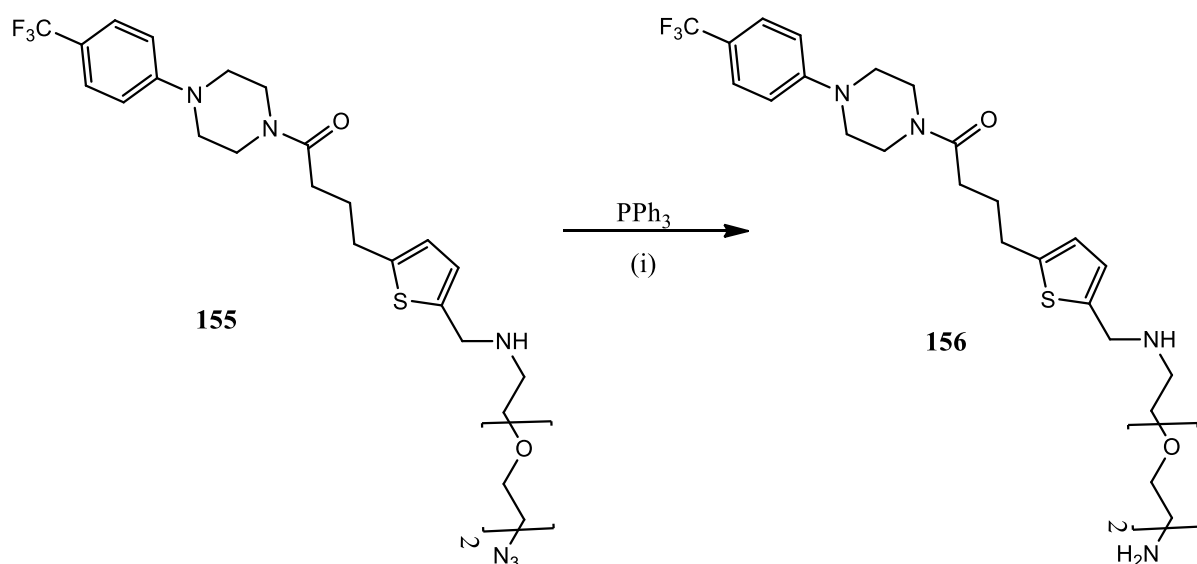
Scheme 7.8: Synthesis of **156**, (i) 1 M HCl, Et$_2$O, EtOAc, 1h 0 ºC then rt, overnight 43%.

Due to the presence of the terminal carboxylic acid, **79** did not require additional functionalization, prior to the attachment of the PEG3 linker. Compound **154** was attached to **79** using HOBt and TBTU. This gave **157** in a 96% yield. The azide was then converted to the free amine, using the Staudinger reduction as before, to yield compound **158** (**Scheme 7.9**).
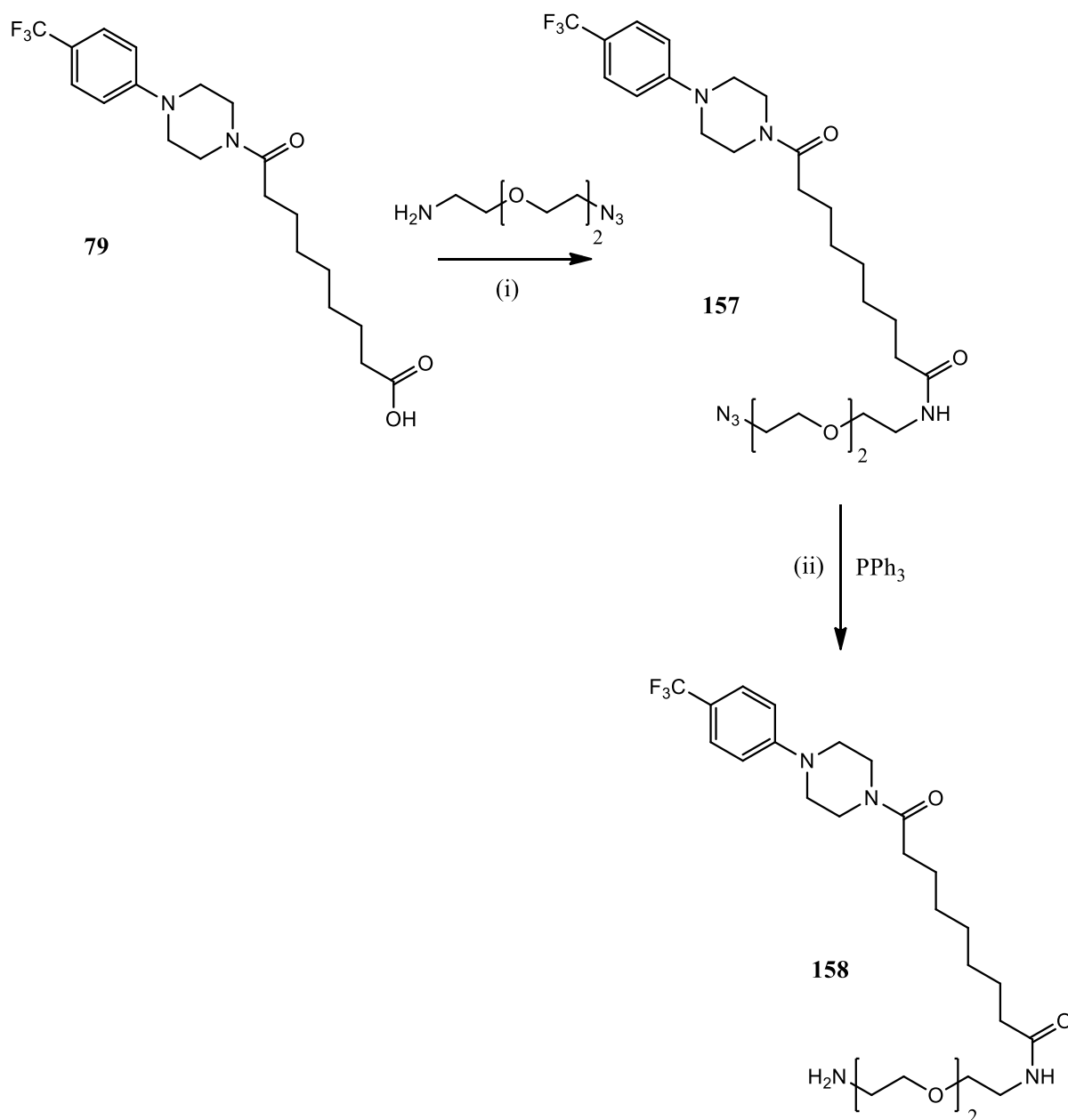
Scheme 7.9: Synthesis of **157** and **158**, (i) HOBt, TBTU, NEt$_3$, DMF, rt, overnight, 96% (ii) 1 M HCl, Et$_2$O, EtOAc, 0 °C then rt, overnight, 25%.

Again the absence of the azide peak in the IR spectrum and the presence of the N-H stretch at 3373 cm^{-1} and the N-H bend at 1643 cm^{-1} indicated the reduction of the azide to the amide was successful. The presence of the trifluoromethyl phenyl group was supported by the presence of the quartets at 126.4 ppm (J = 3.3 Hz), 124.6 ppm (J = 270.0 Hz) and 11.0 ppm (J = 32.5 Hz) in the ^{13}C NMR spectrum.

7.1.3   Immobilization of 156 and 158 onto the sepharose beads

With the PEG3 linker attached to the active compounds, they were next immobilized onto the sepharose bead. The bead in question was a cyanogen activated sepharose and was commercially available as the activated derivative from Sigma Aldrich. Compounds **156** and **158** were then attached to the sepharose bead as shown in (**Scheme 7.10**).

NH₂R = 156, 158
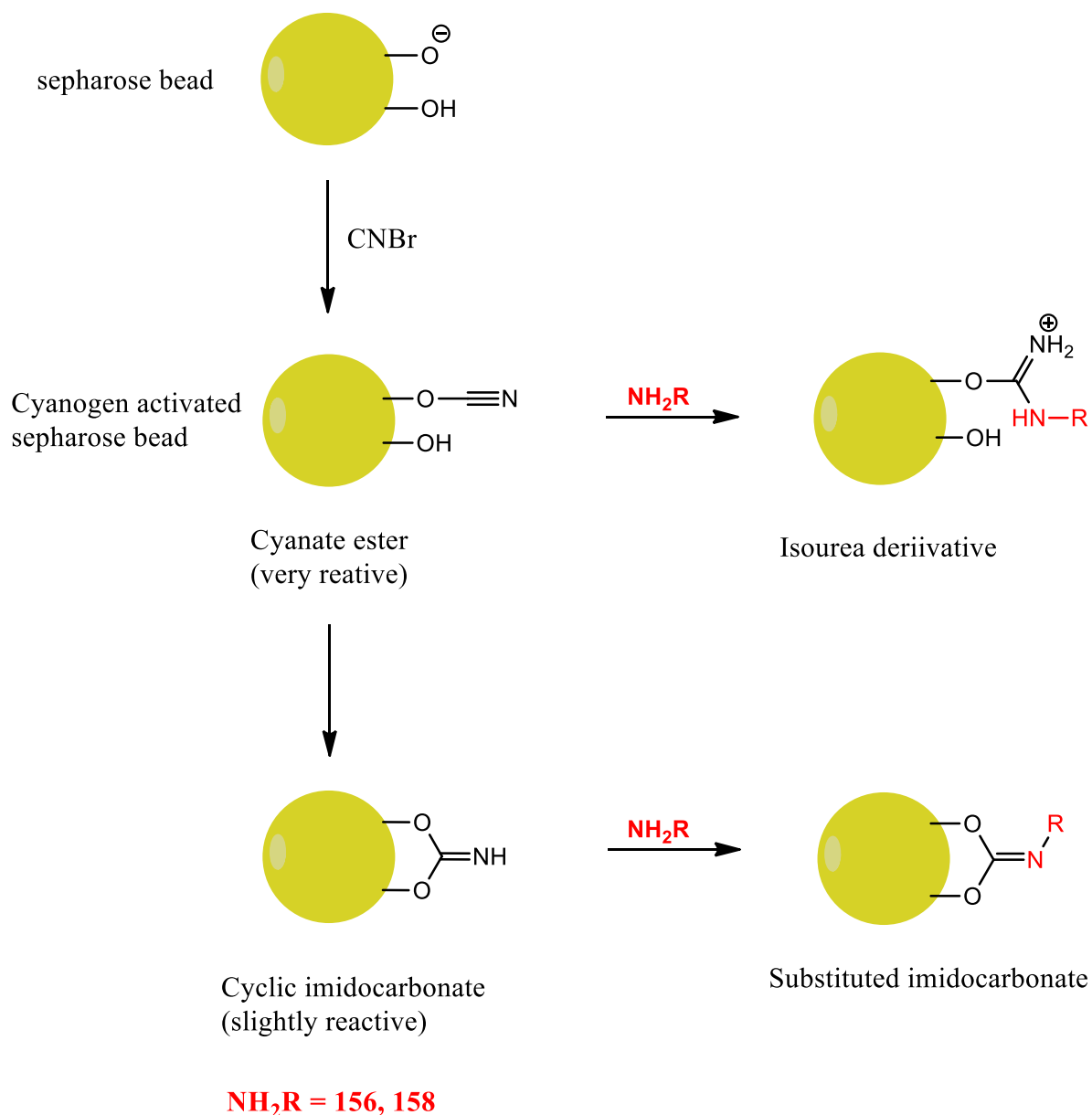
Scheme 7.10: Immobilisation of **156** and **158** onto the sepharose bead.

The aqueous washes, obtained by flushing the affinity column with three column volumes of distilled water, were extracted with DCM. This was to determine the amounts of unbound **156** and **158** and thus the amount of **156** and **158** immobilised on

the bead. The organic DCM layer was dried, concentrated and analysed by NMR spectroscopy for the presence of **156** or **158**. The affinity column was also washed with MeOH to ensure the removal of any excess unbound **156** and **158**. The MeOH wash was also concentrated and analysed by NMR spectroscopy. The resultant residues, from the extracted aqueous washes and the MeOH washes, contained both **156** and **158** respectively, albeit in small amounts. **Table 7.1** highlights the amount of recovered unbound compound found in the aqueous and organic washes and the percentage of compound immobilized on the bead.

Compound	Starting amount (mg)	aqueous washes (mg)	MeOH wash (mg)	amount immobilized (mg)	% compound immobilized
156	23	4	1	18	78
158	20	1	3	16	80

Table 7.1: Percentage of compounds **156** and **158** immobilized on Sepharose bead.

Analysis of the various washes indicated that immobilization had occurred. Although a number of publications do not report a method for verifying immobilization, other reports alluded to the use of certain tests for verification.[180,181] In any case, we wanted to further test the immobilization process.

Sepharose beads are commonly used for the immobilization of peptides.[182] The process of attaching peptides to the bead is similar to the one described above. However, to verify that the peptides have been immobilized, amino acid analysis is performed.[183] This involves cleaving the bound molecule by means of hydrolysis and analysing the remaining residue. As this would be destructive to the ligand a different strategy was chosen.

McMahon *et al*. reported that the immobilization of a substance onto the sepharose bead was verified by means of an observed colour change.[184] As **156** and **158** were both colourless oils, no such colour change was expected and the beads remained white.

To counteract this problem, a coloured derivative was synthesised to test the efficiency of the immobilization process. The glucose uptake assay uncovered a derivative, **42**, which was active, but less active than **4**. Compound **42**, which contains a *para* nitro

group instead of the *para* CF$_3$ found in **4**, was an orange solid and it was hypothesised that its attachment to the sepharose bead would result in a colour change. Immobilization of **42** would leave the beads orange allowing verification of the immobilization protocol.[184]

7.1.4   Synthesis of a coloured derivative of 158.

The previous synthetic approaches used to attach **154** to the active derivatives, **4** and **79**, could not be used for the functionalization of **42**. As nitro groups are readily reduced to the corresponding amines, formylation of **42** followed by a reductive amination could result in the reduction of the nitro group. Therefore, an alternative route was needed.

The attempted synthesis of the **42**-bead conjugate is shown in **Scheme 7.11**. This involved the formylation of **74** using the conditions previously described. The PEG linker was then attached to the formylated ester derivative (**159**) *via* a reductive amination to give compound **160**. This was then deprotected using base catalysed ester hydrolysis revealing the carboxylic acid (**161**), which was verified by ^{1}H NMR spectroscopy due to the absence of the methyl ester peak and by IR spectroscopy where the peak at 2111 cm^{-1} is indicative of the presence of an azide. Due to the presence of the secondary amine however, the acidic work up resulted in the formation of a salt, which was evident as the product was not found in the various organic washes but was recovered from the aqueous layer. The product was carried forward to the next reaction and an attempted coupling to **33** using HOBt and TBTU was performed. A complex mixture was obtained however, and **162** was not isolated. This approach was therefore abandoned.
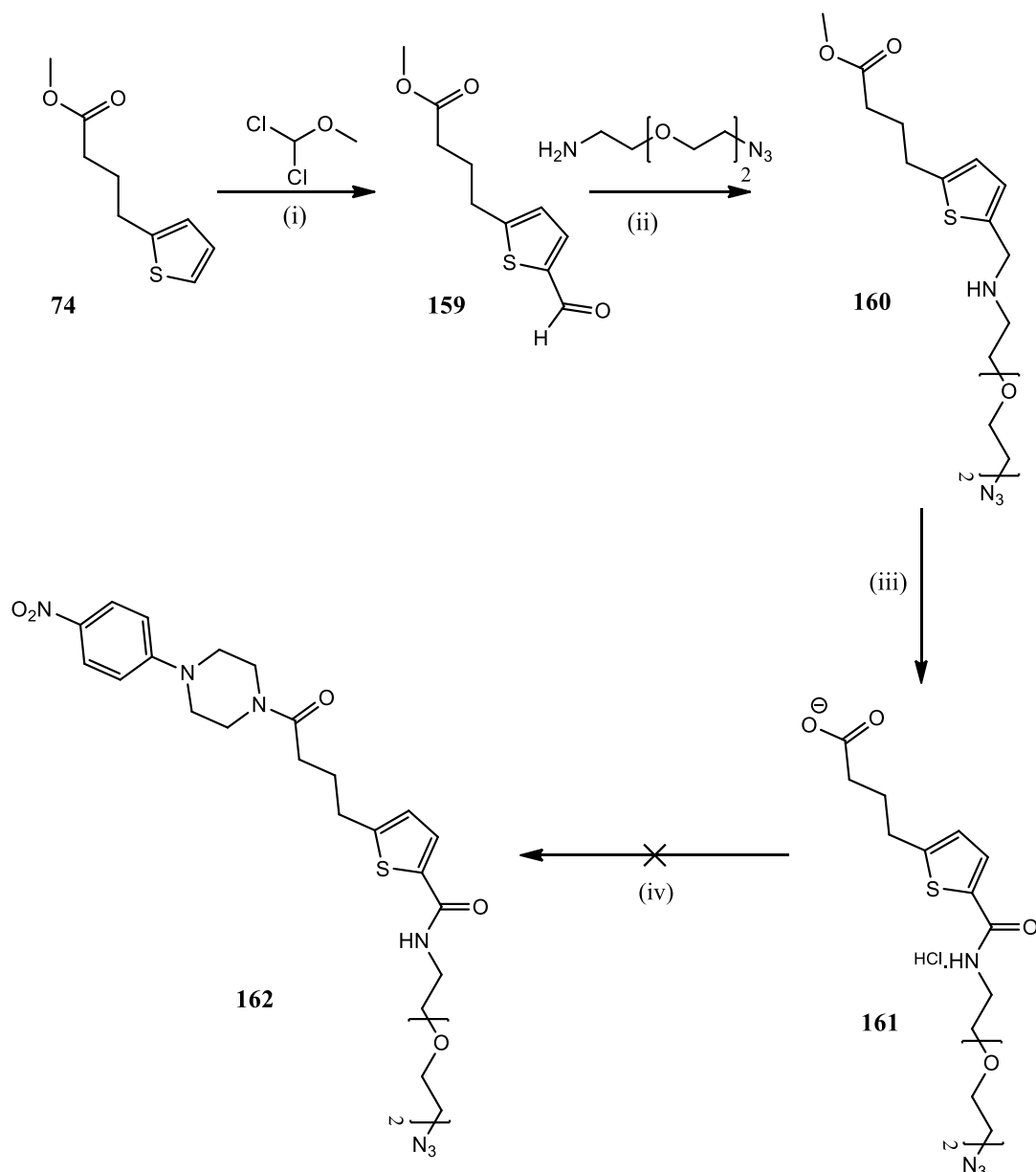
Scheme 7.11: Synthesis of **42**-PEG3 linker **162** (i) Tin(IV)chloride, DCM, N_2, rt, 1 hrs, 56% (ii) NaBH$_4$, MeOH, rt, 3 hrs, 58% (iii) KOH, EtOH, reflux, 2 hrs, quant. (iv) HOBt, TBTU, NEt$_3$, DMF, N_2, rt, overnight, product not isolated.

As it was hoped to verify the immobilization of the compounds to the bead using a coloured compound with a similar structure to **4** or **79**, the nitro derivative of **79** was synthesised. It was hoped that the nitro derivative of **79** would allow easy coupling to the PEG linker. The synthetic route for this approach is outlined in **Scheme 7.12**. 1-(4-Nitrophenyl)piperazine was coupled to mono methylazelate using HOBt and TBTU to give **163**. The ester was then hydrolysed to the acid using base catalysed ester hydrolysis. This gave **164** in a 79% yield. The Staudinger product, **164**, was then

attached *via* an amide bond to give **165**. The amide product was then transformed to the azide as before using the Staudinger reduction. This afforded the orange amino compound **166** (**Scheme 7.12**). This method did not require the use of a reducing agent and as a result the *para* nitro group remained intact. The synthesis of **166** was confirmed by IR spectroscopy firstly by the absence of the azide peak but also due to the presence of the N-H stretch at 3389 cm^{-1} and the N-H bend at 1631 cm^{-1}. The presence of the *para* nitro group was also evident form the IR spectrum due to the bands at 1597 cm^{-1} and 1321 cm^{-1}. ^{1}H NMR spectroscopy confirmed the presence of the phenyl group with the two doublets at 8.14 and 7.02 ppm, which are indicative of the protons *ortho* and *meta* to the piperazine ring.
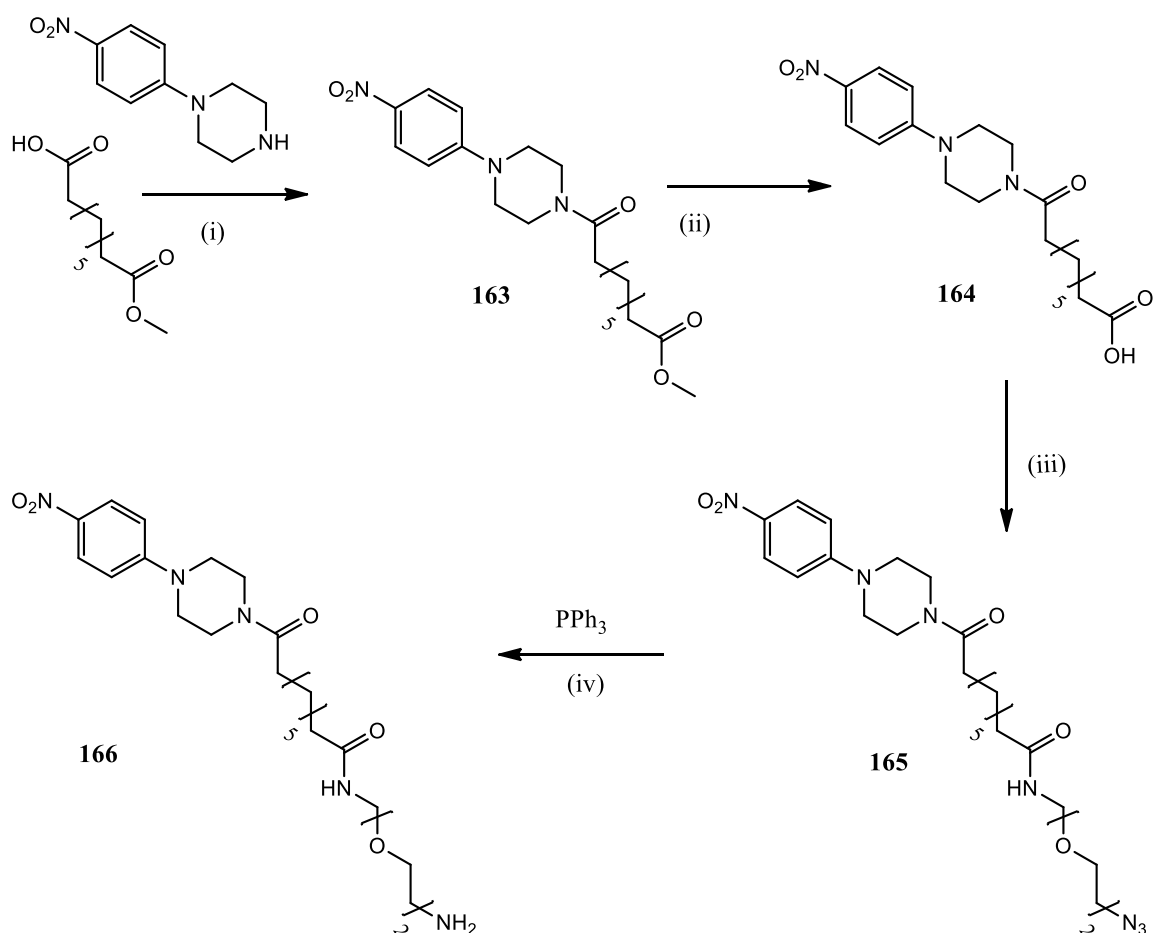
Scheme 7.12: Synthesis of **166** (i) HOBt, TBTU, NEt$_3$, DMF, rt, overnight, 81% (ii) KOH, EtOH, reflux, 4 hrs, 79% (iii) **154**, HOBt, TBTU, NEt$_3$, DMF, rt, overnight, 94% (iv) 1 M HCl, Et$_2$O, EtOAc, rt, overnight, 13%.

With a coloured PEG linked derivative now obtained, the next step was to attach the **166**-PEG3 construct to the sepharose bead as before. As with the previous examples, the

various organic and aqueous washes contained only small amounts of the ligand. **Table 7.2** shows the percentage of ligand immobilized onto the sepharose bead.

Compound	Starting amount (mg)	aqueous wash (mg)	MeOH wash (mg)	amount immobilized (mg)	% compound immobilized
166	20	2	4	14	70

Table 7.2: Percentage of compound **166** immobilized on the sepharose bead.

A notable observation when **166** was immobilized on the bead was the distinct orange colour of the bead. After several aqueous and organic washes, the orange colour remained. This indicated that **166** was immobilized on the sepharose bead (**Figure 7.9**). As a result we were satisfied that the protocol for the immobilization of active compounds was successful and that the **4** and **79** affinity columns were ready for use. The identification of the unknown protein target using the immobilized compounds and the procedure described by Kosaka *et al*. is currently on-going.[177]
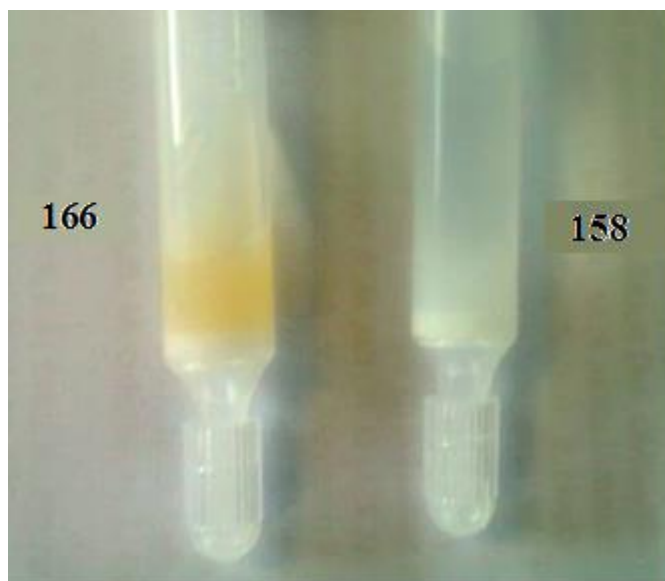
Figure 7.9. Colour comparison of compounds **158** and **166** immobilized onto the Sepharose beads.

7.2   Conclusion

The glucose uptake assay allowed for the identification of the functional groups required to evoke a biological response. The glucose uptake assay also allowed for the emergence of a secondary protein target as the glucose uptake assay activity was independent of RBP4. To work towards identifying this unknown target, the method described by Kosaka *et al*. was employed. This involved attaching the active compounds **4** and **79** to an affinity column where the subsequently bound proteins could be analysed using mass spectrometry.

To attach **4** and **79** to the sepharose bead, it was first necessary to attach a PEG linker to both compounds. Compound **4** was functionalised at the C2 position of the thiophene ring as the glucose uptake assay revealed that changes to the thiophene were tolerated. A formyl group was introduced (**147**) so that the amino PEG linker could be attached *via* a reductive amination. A Staudinger reduction was performed on a diazido PEG3 linker (**153**) generating the mono amino-product **154** which was attached to **147** *via* a reductive amination. This gave **155** in a 76% yield. A Staudinger reduction was again used to convert the remaining azide into the primary amine with **156** isolated in a 43% yield. A similar synthetic approach was applied when attaching the PEG3 linker to **79**, however as **79** contained a carboxylic acid the mono amino PEG linker **154** was attached *via* amide bond formation and was followed by a Staudinger reduction to give **158** in a 25% yield. Both compounds were covalently attached to the sepharose bead. The methodology for immobilising the ligand-PEG conjugates on the sepharose bead was verified by the attachment of the coloured derivative **166**. The use of the beads in the identification of the secondary protein target is currently on-going.

8. Use of cyclodextrin in the aqueous dissolution of compound 4.

8.1   Introduction

Modern methods for identifying biologically active compounds, such as high throughput screening and combinatorial chemistry, can be effective at uncovering pharmacologically active molecules.[66] However, these molecules can have poor drug-like properties such as poor water solubility, inadequate membrane permeability etc. These inadequacies can prevent an active molecule from reaching its target *in vivo* in which case methods that aid in the delivery of a drug molecule to its target are needed.

Drug delivery is defined as the administration of a pharmaceutical compound in humans or animals to achieve a therapeutic effect.[185] Many systems exist which can be employed to deliver a drug to the necessary target, ranging from chemical modifications (e.g. prodrugs, attachment of PEG linkers) to the encapsulation of drugs within a suitable vehicle (e.g. liposomes, cyclodextrins).[63] These systems work by improving certain lacklustre properties of a drug, such as premature metabolic degradation or poor water solubility, allowing the drug to reach its target and evoke a pharmacological response.[63,67]

8.1.1   Prodrugs

Prodrugs are derivatives of drug molecules that are enzymatically and/or chemically modified within the body resulting in the release of the active drug molecule, which can then cause the necessary biological effect.[66] They can be used to improve membrane permeability, water solubility and associated toxicity, amongst other properties.[63] For example, administering the steroid Oestrone as the lysine ester containing prodrug improves its water solubility. Hydrolysis of the prodrug then produces the active form of the drug while the metabolite is the non-toxic essential amino acid lysine (**Scheme 8.1**).[63]
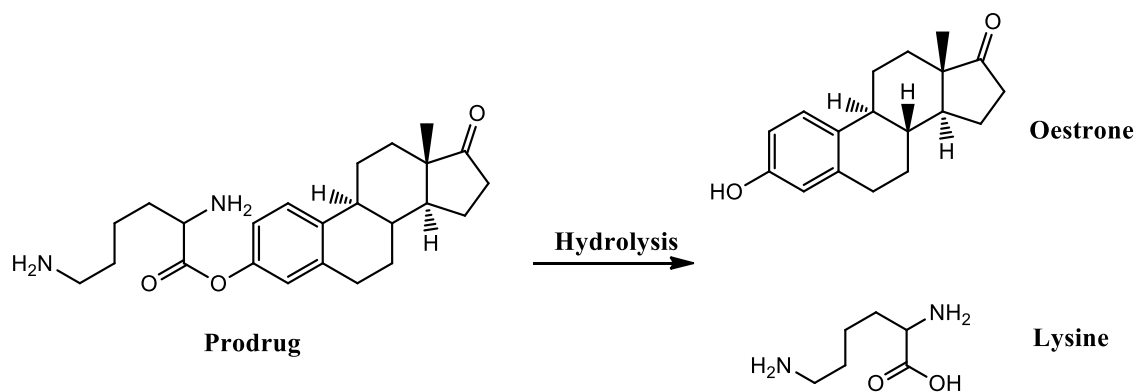
Scheme 8.1: Hydrolysis of the Oestrone prodrug to give Oestrone and lysine.[63]

An alternative drug delivery system which improves water solubility is that using cyclodextrins.

8.1.2   Cyclodextrins

Cyclodextrins (CD) improve the solubility, stability and bioavailability of drug molecules through their ability to form a non-covalent inclusion complex. This is simply the complex formed when the "guest" molecule (e.g. the drug) is present within the "host" molecule (e.g. CD).[67,186]

Cyclodextrins are chemically formed by glucopyranose molecules being bound together through α-(1-4) bonds. They are most commonly composed of 6 (α-CD), 7 (β-CD) or 8 (γ-CD) glucose units (**Figure 8.1**).[67]

A

B
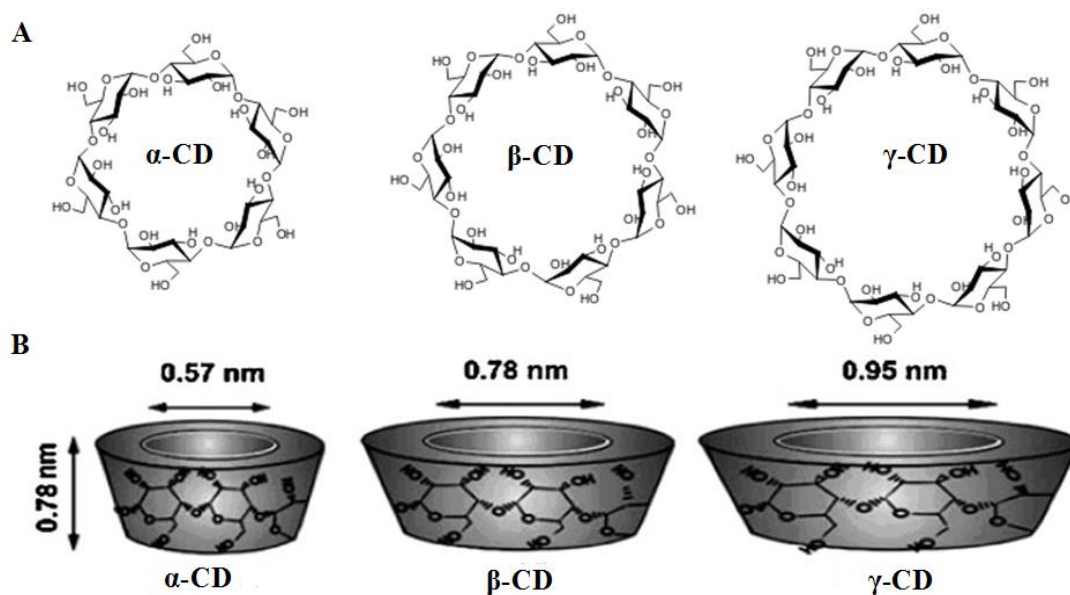
Figure 8.1. (A) Structure of α-, β-, and γ-CD (B) Approximate geometric dimensions of the three CD.[187]

Molecular polarity and the capability of the drug to fit within the hydrophobic cavity determines the binding observed within an inclusion complex.[67] β-CD is the CD of choice for many pharmaceutical applications due to its ready availability and the appropriate size of its cavity, allowing for the inclusion of the widest range of drugs.[186] However its low aqueous solubility and associated nephrotoxicity limits its use, particularly when drugs are delivered parenterally.[186] For this reason, modified CDs have been produced (**Table 8.1**).
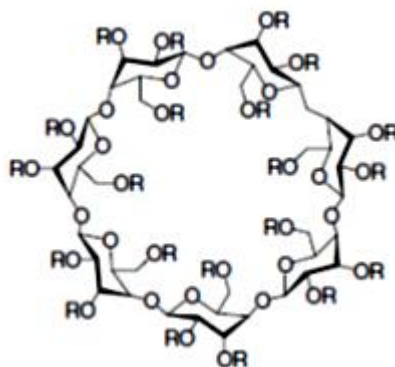
Cyclodextrin	R = H or
β-Cyclodextrin	-H
2-Hydroxypropyl-β-cyclodextrin	$-CH_2CHOHCH_3$
Sulfobutylether β-cyclodextrin sodium salt	$-(CH_2)_4SO_3^-Na^+$
Randomly methylated β-cyclodextrin (RAMEB)	$-CH_3$
Branched β-cyclodextrin	Glucosyl or maltosyl group

Table 8.1. Structures of modified CD.[188]

Hydroxylpropyl-β-cyclodextrin (HPBCD) is one such modified CD that is used for the encapsulation of drug molecules.[189] It has been used in parenteral, oral, transdermal, and ocular drug delivery systems due to its high water solubility and lack of toxicity *in vivo*.[189,190] For example, the antidiabetic drug glimepiride, which has poor aqueous solubility, was complexed with HPBCD (**Figure 8.2**).[31]
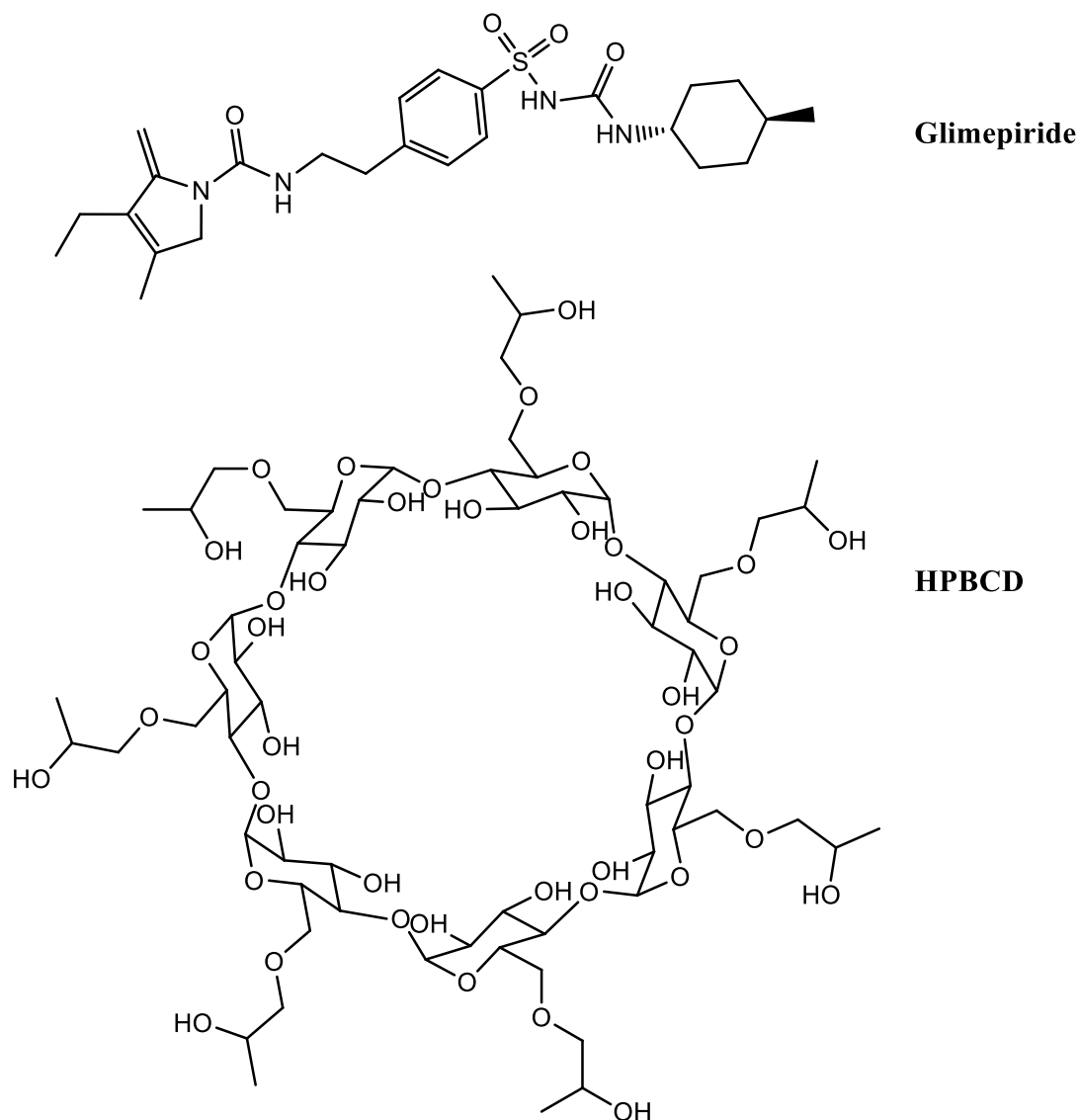
Figure 8.2. Structures of glimepiride and HPBCD.[32,191]

The addition of HPBCD to an aqueous mixture of glimepiride greatly improved its aqueous solubility due to the formation of an inclusion complex which allowed the drug to reach its biological target.

It is the hydrophobic cavity and the hydrophilic exterior that enables these cyclic oligosaccharides to accommodate a vast array of drugs allowing for an efficient delivery system.[67,192] The driving force behind the formation of an inclusion complex is the release of water molecules from the CD cavity. Electrostatic and hydrophobic interactions, van der Waals forces and H-bonding all contribute to the inclusion of a drug molecule within the CD cavity.[188] The delivery of a drug molecule, such as glimepiride, to the appropriate target can occur as these interactions are relatively weak

which makes it possible for the free drug molecule and uncomplexed cyclodextrin to be in equilibrium with the inclusion complex when in solution.[188]

8.1.2.1 Characterisation of an inclusion complex

Formation of an inclusion complex can result in a change in physical and chemical properties of the guest molecule. These changes can be monitored using a number of techniques such as UV-visible and NMR spectroscopy, to confirm complexation. These changes can then be used to evaluate certain characteristics of the complex, such as improvements to water solubility and the stoichiometry of the complex.

For example, a shift in the λ_{max} in the UV-visible spectrum of the guest molecule within the host molecule generally indicates the formation of an inclusion complex. This shift can then be used to determine the aqueous solubility and stoichiometry of the complex using the phase-solubility diagram method of Higuchi and Connors.[193]

8.1.2.1.1   Phase solubility method

The phase solubility method, proposed by Higuichi and Connors in 1972, is the most commonly used method for studying inclusion complexation.[192,193] This method probes the effect that a "host" molecule, e.g. CD, has on the solubility of the "guest" molecule, e.g. drug. It involves the addition of an excess of the "guest" molecule to solutions containing increasing concentrations of the "host" molecule, with analytical techniques such as UV visible and fluorescence spectroscopy used to analyse the solutions.[193] Results of the analysis gives information regarding the concentration of the "guest" molecule present in the phase solution. A phase solubility diagram is generated by plotting the molar concentration of the "host" molecule used, on the horizontal axis, against the total molar concentration of the "guest" molecule, dissolved in the aqueous phase due to the formation of the inclusion complex, on the vertical axis.[193] There are two main types of phase solubility diagrams, type A and type B, with subtypes found within both (**Figure 8.3**).

β-CD generally gives rise to B type diagrams, due to their poor water solubility, whereas A_L type curves are seen for HPBCD containing complexes due to the soluble nature of the complex.[192]
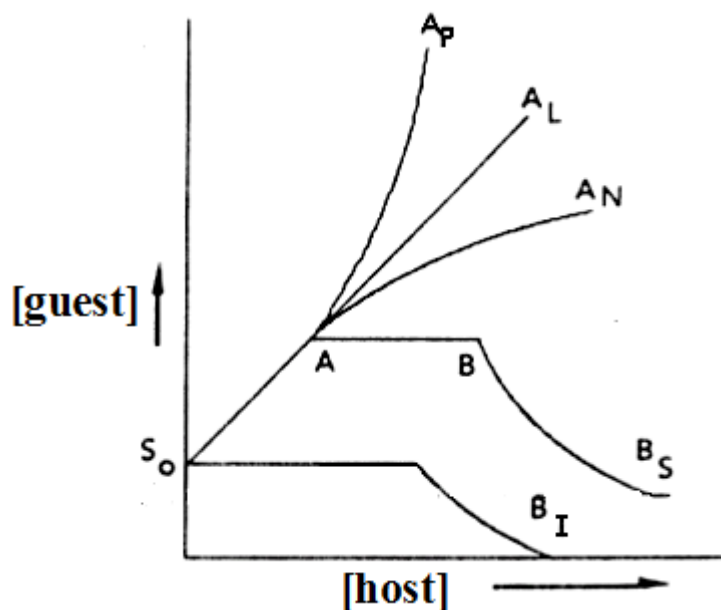
Figure 8.3. Types of phase solubility diagrams.[192]

8.1.2.1.2 Type A phase solubility diagrams

Type A phase solubility diagrams are commonly found when soluble inclusion complexes are formed.[192] Three subtypes exist with A_L type curves being associated with a linear increase in host solubility with increasing guest concentration.[192]

A_P type diagrams, which show positive deviation from linearity at higher concentrations, indicate the presence of higher order complexes such as 1:2 drug:CD type complexes.[192,194] Curves which negatively deviate from linearity are known as A_N type curves.[192] Felton reports that the meaning of these types of curves are uncertain but that one plausible explanation may be that at high concentrations of the host molecule, self-association between the molecules occurs, preventing the formation of inclusion complexes.[193,195]

8.1.2.1.3 Type B phase solubility diagrams

From **Figure 8.3**, the presence of B type curves is associated with the formation of insoluble complexes. There are two subtypes, with B_I type curves denoting the presence of insoluble complexes while B_S curves are associated with the formation of complexes with limited solubility.

B_S type curves first involve the formation of soluble complexes but at a certain point, A (**Figure 8.3**), the solubility limit of this complex is reached. This is the sum of the intrinsic solubility of the guest molecule and any guest molecule solubilized by the formation of a host guest complex. As more host molecule is added, the formation of additional complex occurs and precipitation of this complex ensues.[193] As long as solid and undissolved guest molecule is present however, dissolution and complexation can occur to keep the concentration of the guest molecule constant. This is evident from the plateau observed in the B_S type diagram (**Figure 8.3**). At point B, all of the guest molecule has been consumed by the host and has been removed from the system by precipitation of the insoluble complex (**Figure 8.3**).[193] This results in the observed decrease in guest molecule concentration.[195]

A recent publication by de Araujo *et al*. described the use of a phase solubility diagram to determine the effect that HPBCD had on the aqueous solubility of the compound pyrimethamine (PYR) (**Figure 8.4**).[189] The CD was found to linearly increase the aqueous solubility of PYR with increasing concentration of CD (**Figure 8.4**). From this, de Araujo was able to determine that the type of complex formed was an A_L type complex.[189]
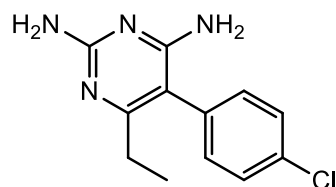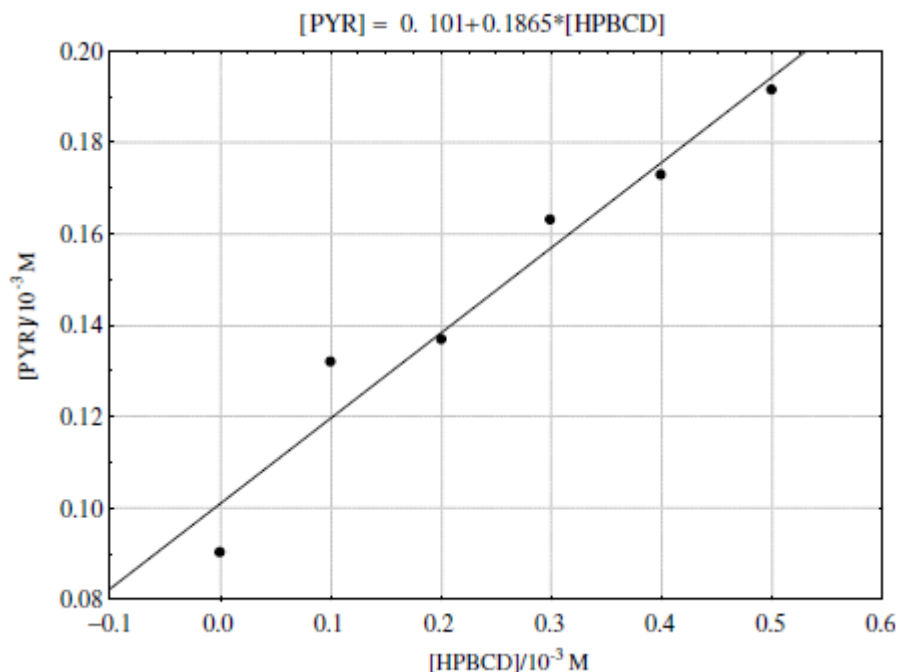
Figure 8.4. Structure of PYR and phase solubility diagram of an A_L type complex.[189]

8.1.2.1.4 Differential Scanning Calorimetry (DSC)

Calorimetry is a technique used for measuring the thermal properties of a substance. It is used to identify the relationship between temperature and specific properties of a material.[196] DSC is a common calorimetric technique used and measures the difference in the amount of heat needed to increase the temperature of a reference and sample as a function of temperature. The reference and sample are maintained at the same temperature, using a controlled temperature program, while the difference in the heat flow needed to keep both at the same temperature is measured as a function of temperature or time.[197] The change in the heat flow is attributed to the sample undergoing a physical transformation.[196] For example, when a sample undergoes a phase transition more or less heat will need to be applied to the sample to maintain both the sample and reference at the same temperature.[196]

DSC has a number of applications including the analysis of proteins, lipids and carbohydrates. The folding thermodynamics of nucleic acids can also be investigated using this thermoanalytical technique.[196] DSC can also be used to study and characterise "host-guest" interactions such as the inclusion of a molecule within the hydrophobic cavity of a suitable CD.[67] One such example is the inclusion of the anthelmintic drug, 6-chloro-5-(1-naphthyloxy)-2-(trifluoromethyl)-1*H*-benzimidazole (RCB20), within HPBCD. The below DSC curves highlight the differences in heat flow observed for RCB20 and its associated inclusion complex (**Figure 8.5**).[67]
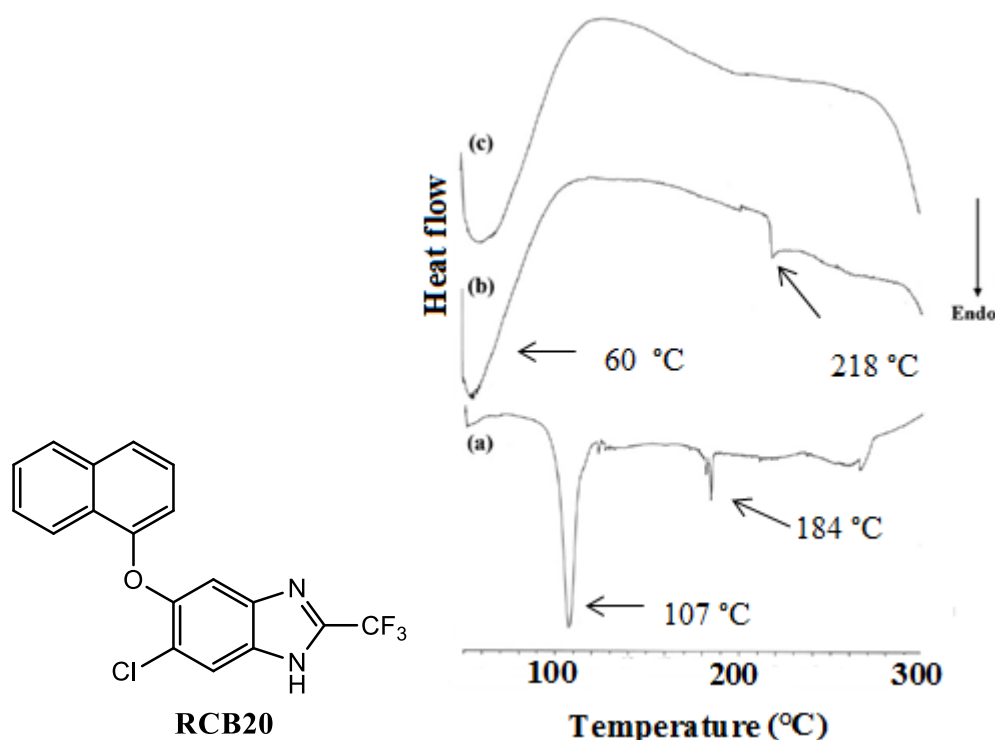
Figure 8.5. Structure of RCB20 and DSC curves for (a) RCB20 (b) HPBCD and (c) RCB20:HPBCD inclusion complex.[67]

From the above diagram, the DSC curve for RCB20 has two characteristic endothermic peaks at 107 °C and 184 °C which correspond to the melting and decomposition of the compound, respectively. The broad peak at 60 °C is due to the loss of water from the CD molecule while the sharp peak observed at 218 °C represents the decomposition of HPBCD. When the DSC curves for RCB20 and HPBCD are compared to that of the inclusion complex, it is evident that the endothermic peaks corresponding to the melting and decomposition of RCB20 are not present. This is a strong indication for the formation of an inclusion complex.

8.1.2.1.5 Scanning Electron Microscopy (SEM)

Primary electrons are generated from the extraction of electrons from a source and are driven by an electron potential through a column under vacuum.[198] These electrons can be manipulated into finely focused beams and scanned across a sample in a systematic fashion.[198] A number of useful and interesting interactions arise when a beam of primary electrons strike a sample surface.

Secondary electrons and backscattered electrons are the main signals used in SEM. The composition of a sample, as well as its surface topography, affect the emission of these signals which can be used to create an image.[198] This technique can be used to characterise the topography and morphology of CD inclusion complexes as many inclusion complexes are morphologically distinct from the parent guest and host molecules. This was the case as seen with the inclusion complex formed by Rojas-Aguirre *et al.*.[67] There was an obvious difference in the morphologies between the **(a)** "guest" molecule, **(b)** the "host" molecule (i.e. HPBCD), **(c)** the physical mixture (i.e. a mixture prepared by grinding the guest molecule and the host molecule together in the absence of water) and **(d)** the inclusion complex (**Figure 8.6**). As the morphology of the inclusion complex is distinct from that of the other three, it is supportive of a new, independent complex is formed.[67]
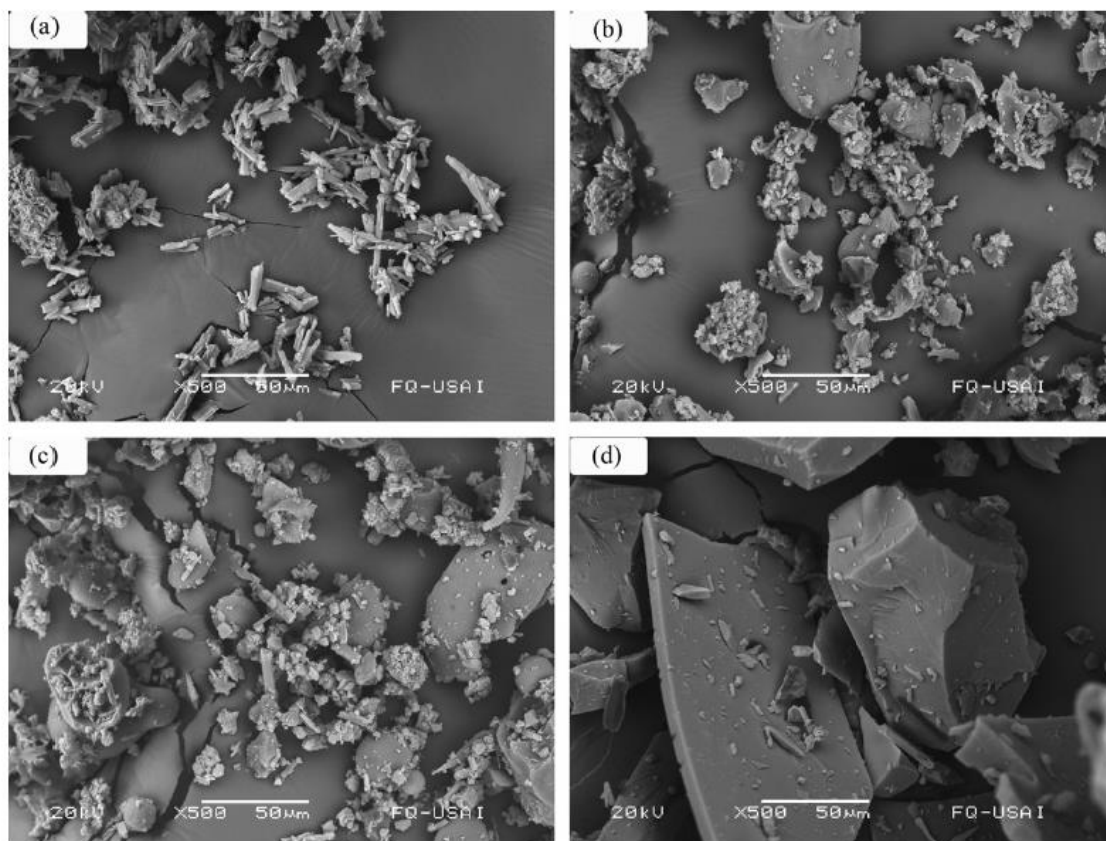
Figure 8.6. SEM analysis of an inclusion complexes (20 kv) at 500 magnifications **(a)** "guest" molecule, **(b)** "host" molecule i.e. HPBCD **(c)** Physical mixture **(d)** inclusion complex.[67]

8.2   Improving the aqueous solubility of compound 4 with the use of CDs

The role of compound **4** as a possible antidiabetic drug was evident from its ability to evoke a pharmacological response in the glucose uptake assay and in mice. Further animal experiments were considered involving **4**; however these required aqueous solutions of the compound. As **4** had previously proven to be highly insoluble in water it therefore would not have been possible to administer **4** as an aqueous solution. Aqueous solubility was not only desirable for the considered animal experiments but it is also an important ADME property for many drugs (i.e. logP). The calculated logP value for **4** is 4.79 and is very close to the upper limit of 5, ideal logP value for an orally administered drug, as was suggested by Lipinski.[63] The high logP value for **4** may explain its low aqueous solubility. As a result, a method for improving the aqueous solubility of **4** was sought.

The literature directed the investigation towards the use of CD as a way to improve aqueous solubility. This was a viable approach as numerous drugs, including antidiabetic drugs, were complexed with various CDs to improve several properties, such as aqueous solubility. A number of different CDs were available whose use may have improved the aqueous solubility of compound **4**.

α-CD is generally not used in the complexation of drug molecules due to the small size of its cavity, which has been found to be of insufficient size for many drugs.[192] While the size of the cavity of the α-CD deterred us from its use, it was the low aqueous solubility and associated nephrotoxicity, reported by Challa *et al*., which excluded β-CD from our choices of CD. The modified CD, hydroxylpropyl-β-CD (HPBCD) was therefore chosen due to its low toxicity, excellent water solubility and ability to complex a variety of drugs.[189,67]

The aim of this section of work was to prepare an aqueous 0.02 M solution of compound **4**. Our first attempt involved the use of 20 eq of HPBCD however; this did not result in the dissolution of **4**. The use of DMSO as a co-solvent was then considered and an aqueous solvent system containing 50% DMSO was used with 1, 2, 5, 10 or 12 eq of HPBCD. DMSO was chosen due to its low toxicity, but also experimental studies in the formation of inclusion complexes have suggested that stable inclusion complexes can be formed in the presence of DMSO.[199]

The 50% aqueous DMSO solution containing 12 eq of HPBCD was the only one that resulted in dissolution of the compound. The level of DMSO was considered too high and hence our next aim was to reduce the volume of DMSO required. An aqueous solvent system containing 10% DMSO and 12 eq of HPBCD was first prepared to which was added **4**. Unfortunately, precipitation of **4** occurred. Subsequently, the number of HPBCD equivalents was increased from 12 to 18. Initial results were promising however after one hour precipitation of a white solid occurred. The number of equivalents was then increased to 20. This resulted in the complete dissolution of **4** with a clear homogenous solution present after twenty four hours (**Entry 9**, **Table 8.2**).

We then further reduced the level of DMSO and an aqueous solution containing 5% DMSO with 20 eq of HPBCD was prepared which resulted in the complete dissolution of **4**. From **Figure 8.7**, it is clear that the improved aqueous solubility is due to the

presence of HPBCD. Compound **4** could not be dissolved in an aqueous solution containing 5% DMSO without the use of HPBCD (**Figure 8.7 (b)**).

The percentage of DMSO used was further decreased from 5% to 2%. This also gave rise to an aqueous solution of **4**; however; after 18 days the formation of a white precipitate occurred. The combination of 5% DMSO with twenty equivalents of HPBCD was considered optimal (**Entry 10, Table 8.2**).
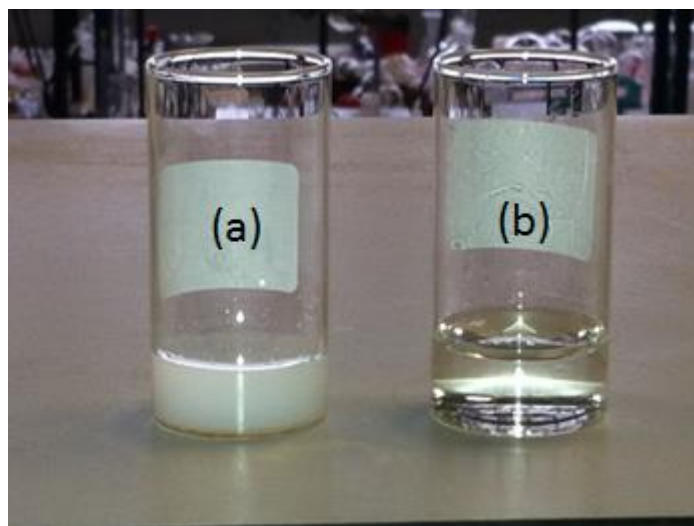
Figure 8.7. (a) Compound **4** in 5% DMSO/H$_2$O solution without HPBCD (b) Compound **4** in 5% DMSO/H$_2$O solution with HPBCD.

Entry	% DMSO	HPBCD (eq)	Solubility
1	0	20	Insoluble
2	50	1	Insoluble
3	50	2	Insoluble
4	50	5	Insoluble
5	50	10	Insoluble
6	50	12	Soluble
7	10	12	Insoluble
8	10	18	Insoluble
9	10	20	Soluble
10	**5**	**20**	**Soluble**
11	2	20	Insoluble*

Table 8.2: Conditions needed for the preparation of an aqueous 0.02 M solution of **4**.

*Initially appeared soluble but precipitate appeared after eighteen days.

We believe that the preparation of an aqueous solution of **4** was due, in part, to the formation of an inclusion complex. To characterise this inclusion complex, a number of analytical techniques were employed, namely a phase solubility diagram, NMR spectroscopy, DSC and SEM.

8.2.1   Phase Solubility Diagram

The previously described method by Higuichi and Connors, **section 8.1.2.1.1**, was used to elucidate the effect of HPBCD on the aqueous solubility of **4**. This is a widely accepted method for investigating the effects of CD on drug solubility, with an A_L type complex being the most common complex formed.[193]

To produce the phase-solubility diagram, a standard curve of **4** was required and this was generated using UV-visible spectroscopy. A series of solutions of compound **4** in MeOH were prepared and the UV absorption spectrum of each sample was obtained and the data analysed at 264 nm (λ_{max} of **4**). The absorbance values were then plotted against the varying concentrations of **4** (**Figure 5.8**).
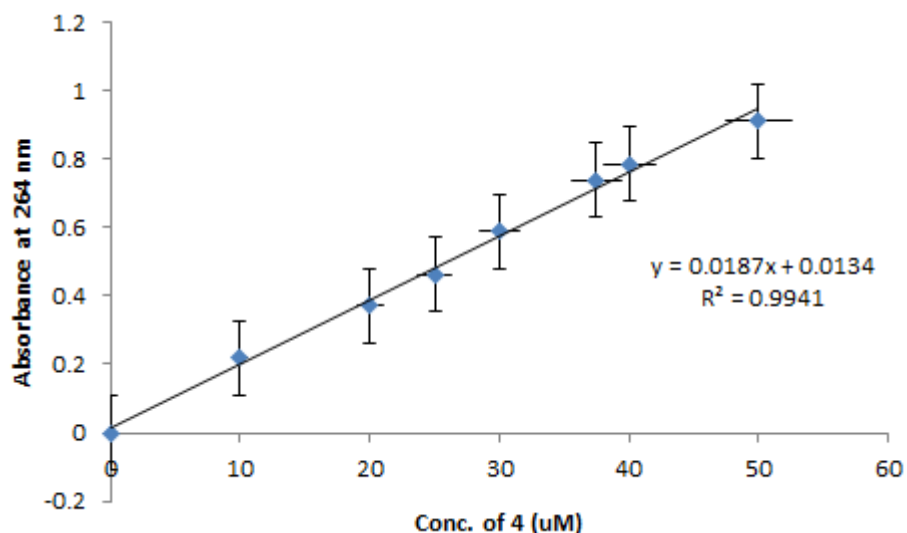
Figure 8.8. Standard curve of **4** generated in MeOH using UV-vis spectroscopy.

To produce the phase solubility diagram, a fivefold molar excess of **4** (i.e. 5.0 mM), relative to the highest concentration of HPBCD, was added to aqueous solutions containing increasing concentrations of HPBCD (0.2 mM, 0.4 mM, 0.6 mM, 0.8 mM, 1.0 mM). These mixtures were stirred for 72 hours at room temperature before analysis.[189]

After this time, the excess, uncomplexed, insoluble, **4** was removed by filtration and the different solutions were analysed using UV-visible spectroscopy. The below UV spectra (**Figure 8.9**) show an increase in the absorbance at 264 nm with increasing concentrations of HPBCD. This indicates an increase in the concentration of **4** in the aqueous solutions with increasing concentrations of HPBCD, which we believe is due to the formation of an inclusion complex.
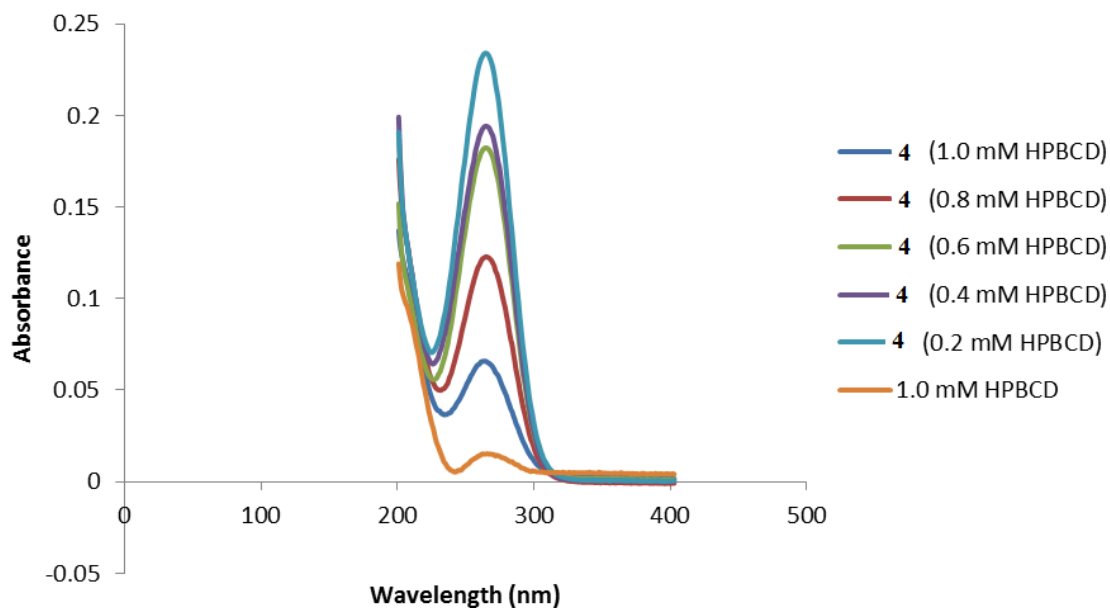
Figure 8.9. Absorbances of compound **4**, measured at 264 nm, in aqueous soulutions containing varying concentrations of HPBCD.

The above spectrum shows that 1.0 mM HPBCD exhibits only minimal absorption at 264 nm. As a result, the bands at 264 nm for the **4**:HPBCD complex would be expected to result significantly from the absorption of **4** within the inclusion complex. All measurements made at 264 nm for the **4**:HPBCD complex were corrected by subtracting the corresponding absorption resulting from HPBCD.

The standard curve was then used to calculate the concentration of **4** present in each aqueous solution. The calculated concentrations of **4** were plotted against the concentrations of HPBCD used and a phase solubility diagram was generated (**Figure 8.10**).
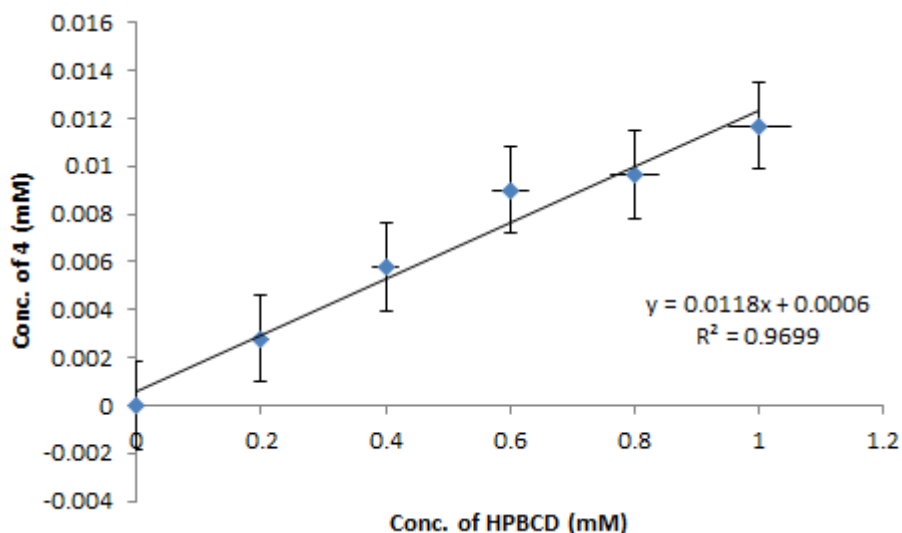
Figure 8.10. Phase solubility diagram. The conc. of **4** (x-axis) dissolved in aqueous solutions, due to the presence of HPBCD and calculated using the standard curve (**Figure 8.9**), are plotted against the various concentrations of HPBCD used in each solution (y-axis).

From the above diagram, it is clear that the solubility of **4** increases linearly with increasing concentrations of HPBCD. This is a feature of an A_L type complex, which indicates the presence of a water soluble complex. This is the most common complex observed for drug:CD interactions.[189] The slope, of value 0.012 in this case is less than one and can indicate the presence of a complex with a 1:1 stoichiometry.[193]

8.2.1.1 Calculation of the Stability Constant, K

The previously described weak molecular interactions, such as van der Waals forces, which are involved in the formation of the inclusion complex allow free drug molecules in solution to be in rapid equilibrium with drug molecules bound in the CD cavity (**Equation 8.1**).[188]

$$\textbf{D} \quad + \quad \textbf{CD} \quad \overset{\textbf{K}_{1:1}}{\rightleftharpoons} \quad \textbf{D/CD Complex}$$

Equation 8.1.

Equation 8.1 shows the observed equilibrium between unbound drug (D) and cyclodextrin (CD) and the inclusion complex (D/CD Complex), with $K_{1:1}$ the stability constant of an inclusion complex with a 1:1 stoichiometry.[188] The size of $K_{1:1}$ is an

indication of the strength of the interaction between drug and CD. The larger the $K_{1:1}$ value, the stronger the interaction between the drug and CD in the inclusion complex. A large $K_{1:1}$ value indicates the equilibrium lies in favour of the inclusion complex. Conversely, a small $K_{1:1}$ value indicates a weak interaction between drug and CD, with equilibrium lying in favour of the free drug.[190]

$K_{1:1}$ can be calculated according to **Equation 8.2**, where So is the intrinsic water solubility of the drug and the slope is the slope of the line generated from the phase-solubility diagram.[189]

$$K_{1:1} = \frac{Slope}{So(1 - Slope)}$$

Equation 8.2

The intrinsic water solubility was calculated by stirring **4** in water for seventy two hours. The excess **4** was removed and the UV absorption spectrum of the sample was obtained and the data analysed at 264 nm (λ_{max} of **4**). This gave an intrinsic water solubility of 0.32 μM. Using **Equation 8.2**, $K_{1:1}$ was calculated to be 34755 M^{-1}. Upadhye *et al.* reported a binding constant of 21137 M^{-1}, which indicated a strong bonding interaction between the drug molecule THC and a CD (**Figure 8.11**).[190] Upadhye also gave an example of a drug molecule which formed weak, unstable interactions within a CD molecule. In this case the molecule, THC-HS, a prodrug derivative of the previously mentioned THC, was found to have a $K_{1:1}$ value was 562.48 M^{-1}.[190] The large stability constant value obtained for **4** indicates a strong interaction between the molecule and HPBCD, with the equilibrium lying in favour of the inclusion complex.
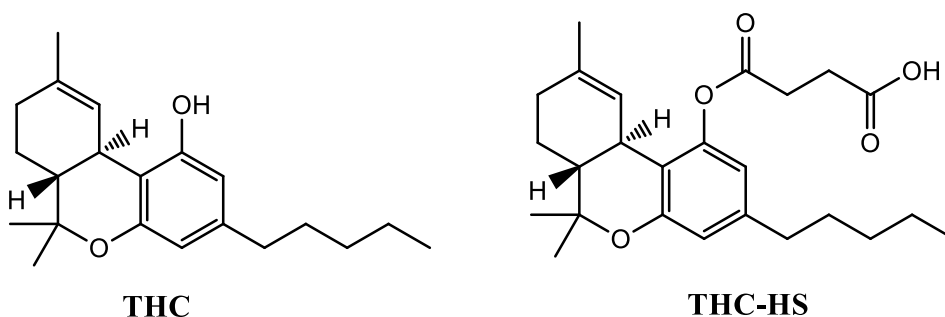
Figure 8.11. Structure of the drug THC and the ester derivative THC-HS.[190]

8.2.2   Non-inclusion complex

The formation of a complex with a 1:1 stoichiometry may appear somewhat contradictory to the previously prepared aqueous solutions of **4** that required twenty equivalents and not one equivalent of HPBCD. Rojas-Aguirre *et al*. explained that although a phase solubility diagram can indicate the presence of a complex with a 1:1 stoichiometry, the level of complexation can sometimes be low and excess CD is needed to fully dissolve the required concentration of drug.[67] In addition, the use of excess amounts of CD can achieve solubilisation of drug molecules by the formation of non-inclusion complexes.[200]

Gabelica *et al*. reported that CD can form both inclusion and non-inclusion complexes with certain molecules and that both complexes can exist simultaneously in aqueous solutions.[201] These non-inclusion complexes arise due to the formation of aggregates consisting of two or more CD molecules and drug/CD complexes. The water soluble aggregates can then function to further solubilise lipophilic drugs through the formation of a non-inclusion complex by creating a hydrophobic environment in which to accommodate the drug. Alternatively, Loftsson *et al*. suggested that solubilisation may also occur through the formation of a micelle like structure.[200]

The formation of these non-inclusion complexes may apply to the preparation of the 0.02 M **4** 5% aqueous DMSO solution. As was reported by Loftsson, these non-inclusion complexes occur when a high concentration of drug is present. Therefore, the preparation of a 0.02 M solution of **4** may have required 20 eq of HPBCD to allow the formation of, not only the 1:1 inclusion complex but also, the non-inclusion complex formed by the presence of a CD:inclusion complex aggregate.[200]

8.2.3   NMR analysis

^{1}H NMR analysis was used to investigate the binding mode of **4** within HPBCD. The encapsulation of **4**, either by one molecule of HPBCD or by the formed aggregates, can be seen by changes in the 1D ^{1}H NMR spectra of **4** for the inclusion complex.

Full characterisation of the **4**/HPBCD complex in D_2O was not possible, as **4** could not be solubilised in this solvent. Therefore, a 5% D_2O/CD_3OD solution was prepared in which both **4** and the complex were soluble. This gave the spectra below where the characteristic peaks of **4** were observed within the CD complex (**Figure 8.12 (b)**), blue

spectrum). A shift in the resonance of a number of peaks of **4** was observed and the difference in chemical shift is shown in (**Table 8.3**). This indicates that **4** is in a different environment when it is present in the CD inclusion or non-inclusion complexes. These small changes in chemical shifts are common, with Rojas-Aguirre *et al*. reporting changes in chemical shifts ranging from 0.001 ppm to 0.012 ppm for the previously mentioned RCB20 molecule.[67]

The information on the spatial proximity of **4** in the CD complexes was determined by means of two-dimensional rotating frame NOE spectroscopy (ROESY), which were performed by Dr. Paidraig McLoughlin. The 2D ROESY spectrum was also obtained in the 5% D_2O/CD_3OD solution with the contour plot revealing an interaction between H1, H2, H3, H4, H5 and H12 of **4** with the internal protons Ha and Hb of HPBCD, which were assigned by Rojas-Aguirre *et al*. (**Figure 8.13**).[67] This gives strong evidence towards the presence of **4** within the cavity of HPBCD, further supporting the formation of an inclusion complex.

(a)

(b)
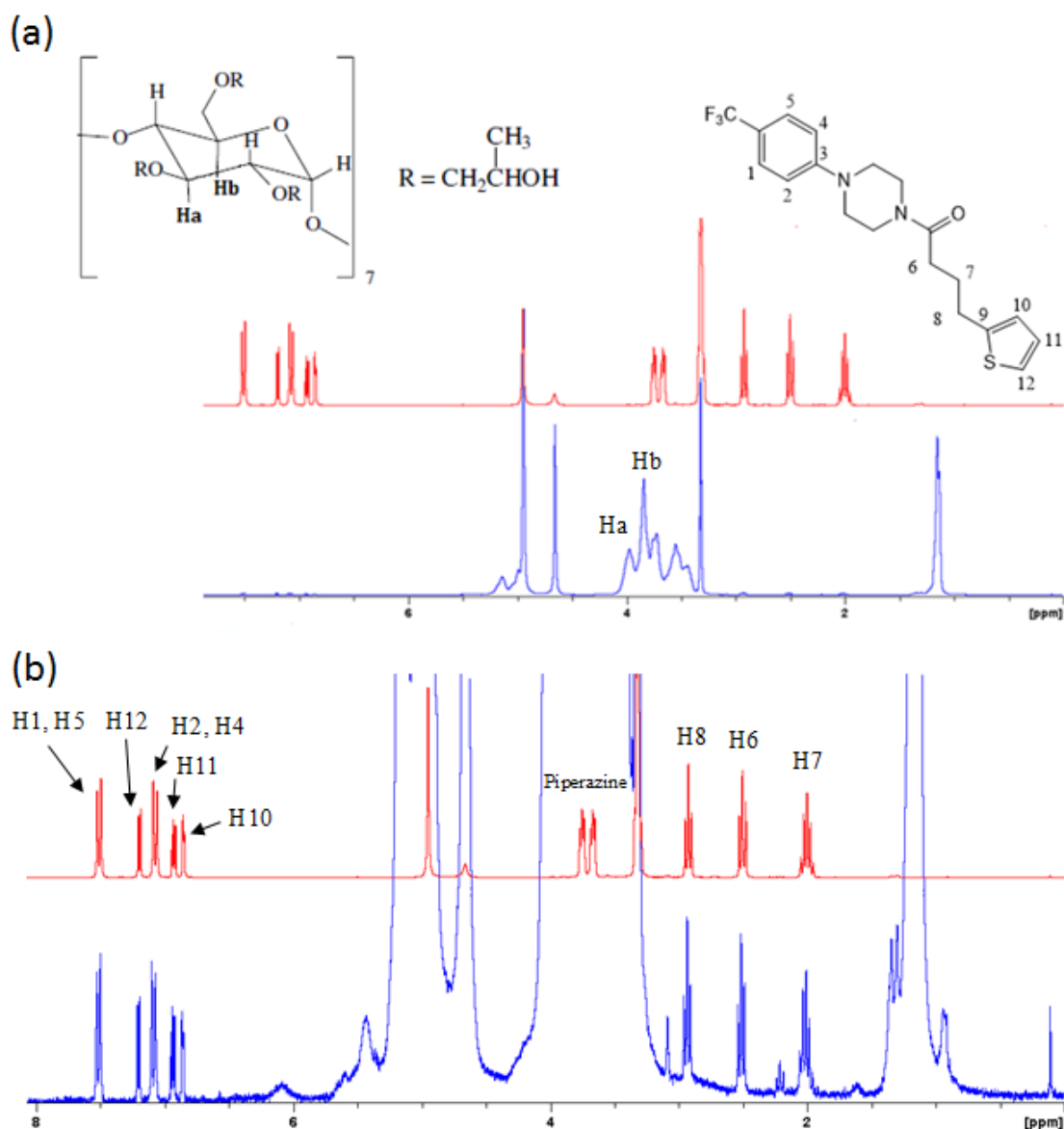
Figure 8.12. ^{1}H NMR spectra (300 MHz) in 5% D_2O/CD_3OD of (a) **4** (red) and the inclusion complex (blue) and (b) a magnified view of the spectrum.

Assignment (4)	δ* (Free 4)	δ* (Complex)	Δδ
H2, H4	7.0904	7.0784	0.0120
H6	2.5184	2.5078	0.0106
H8	2.9384	2.9289	0.0095
H10	6.8687	6.8621	0.0066
H11	6.9540	6.9465	0.0075

Table 5.2: Chemical shifts for free **4** and complexed **4**.*δ, ppm

(a)

(b)
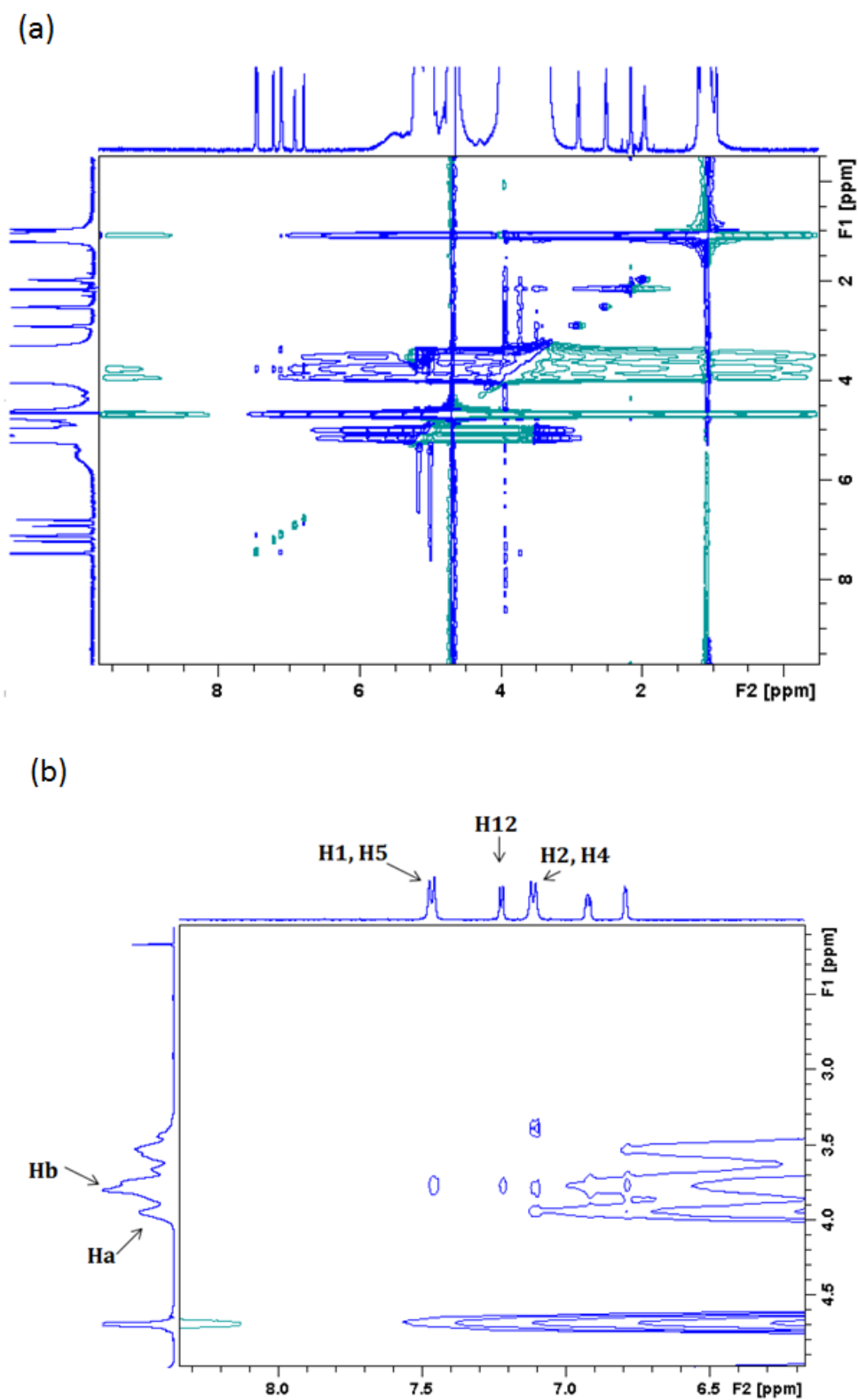
Figure 8.13. (a) ROESY spectrum of inclusion complex between **4** and HPBCD (b) ROESY spectrum expansion showing the crosspeaks between the aromatic signals of the inclusion complex between **4** and HPBCD protons.

8.2.4   Differential Scanning Calorimetry (DSC) analysis

The thermoanalytical technique, DSC, was used to determine the presence of the inclusion complex. The thermal behaviour of the inclusion complex was compared to that of **4**, HPBCD and a physical mixture of **4** and HPBCD. A physical mixture simply contained **4** and HPBCD in the same ratios as the inclusion complex and was prepared by grinding the two in the absence of solvent. An inclusion complex would not form under these conditions.

The DSC curve, **Figure 8.14 (a)**, for **4** shows a sharp endothermic peak at 94 °C, which is characteristic of the melting point of **4**. **Figure 8.14 (b)**, the curve for HPBCD, is in accordance with the literature and shows two broad endotherms ranging from 25-103 °C, due to the loss of water, and 280-340 °C, due to decomposition of the CD.[189,67] The physical mixture shows the characteristic peaks of both **4** and HPBCD, with the sharp peak at 94 °C due to the melting of **4** and the broad endotherm ranging from 25-103 °C showing the loss of water from the HPBCD cavity (**Figure 8.14 (c)**). This indicates the absence of any interaction between **4** and HPBCD.[67]

The inclusion complex, **Figure 8.14 (d)**, has a broad endotherm at 25-103 °C due to the loss of water. Work by Rojas-Aguirre has suggested that this is the loss of water molecules which are bound to the -OH groups on the exterior of the CD and not the loss of water from the cavity.[67] The sharp, endothermic peak observed at 94 °C, in the DSC curve of **4** and the physical mixture is notably absent from the DSC curve of the inclusion complex. This is a strong indication of the presence of a complex, whether it is an inclusion or non-inclusion complex, as the presence of **4** within either of these complexes would cause a change to its physicochemical properties.[200]
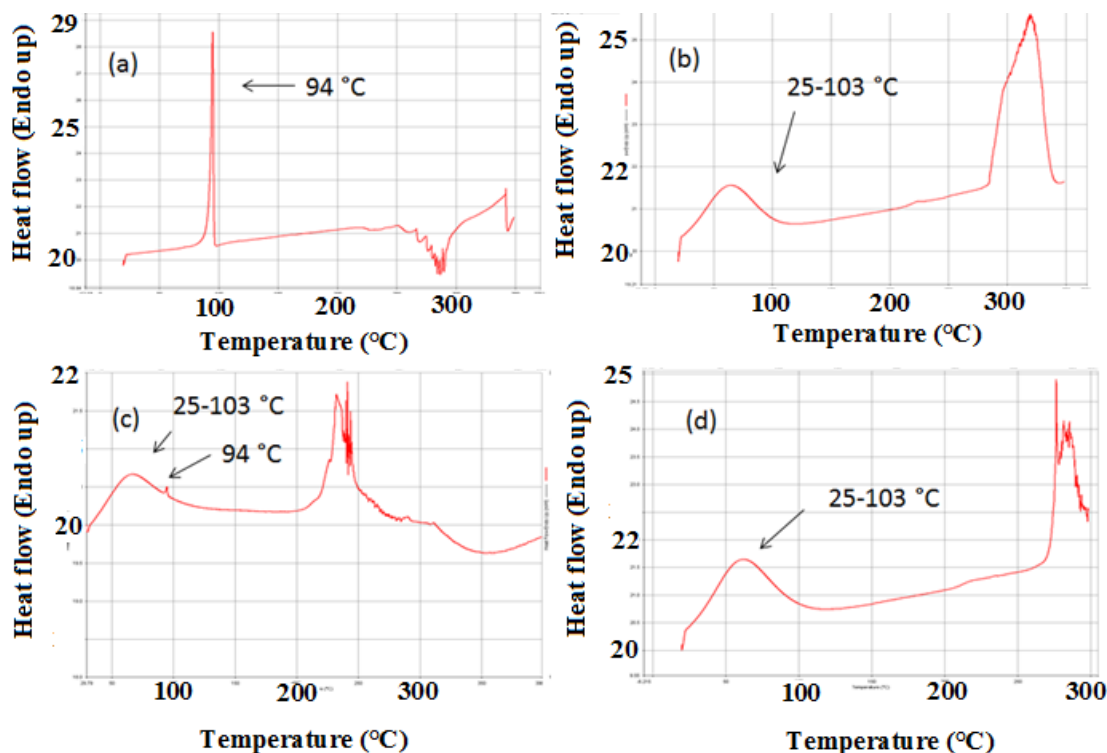
Figure 8.14. DSC curves: (a) **4** (b) HPBCD (c) Physical mixture (d) Inclusion complex.

8.2.5   Scanning Electron Microscopy (SEM)

SEM analysis was used to investigate and compare the shape and surface morphologies of HPBCD, **4**, the physical mixture and the inclusion complex. **Figure 8.15** shows the SEM images for HPBCD, **4**, the physical mixture and the inclusion complex at 500 magnifications. HPBCD and **4** show distinct morphologies, with **4** appearing to adopt a cluster like arrangement in the micrograph. The SEM image of the physical mixture (**Figure 8.15 (c)**) has a morphology comparable to that of both **4** and HPBCD. The characteristic clusters observed in the micrograph of **4** and the smooth morphology of HPBCD can be seen. This can be indicative of a lack of "host-guest" interactions.[67] The morphology of the inclusion complex is clearly different from that of the physical mixture and **4**. **Figure 8.15 (d)**, the inclusion complex, shows a smooth amorphous solid, without the cluster like structures observed in the SEM image of **4**. This change in morphology could be due to the formation of an inclusion complex (or the non-inclusion complex previously described). These changes in morphologies are similar to that observed by Rojas-Aguirre *et al*., described in **Figure 8.6**, **Section 8.1.2.1.5**.[67]
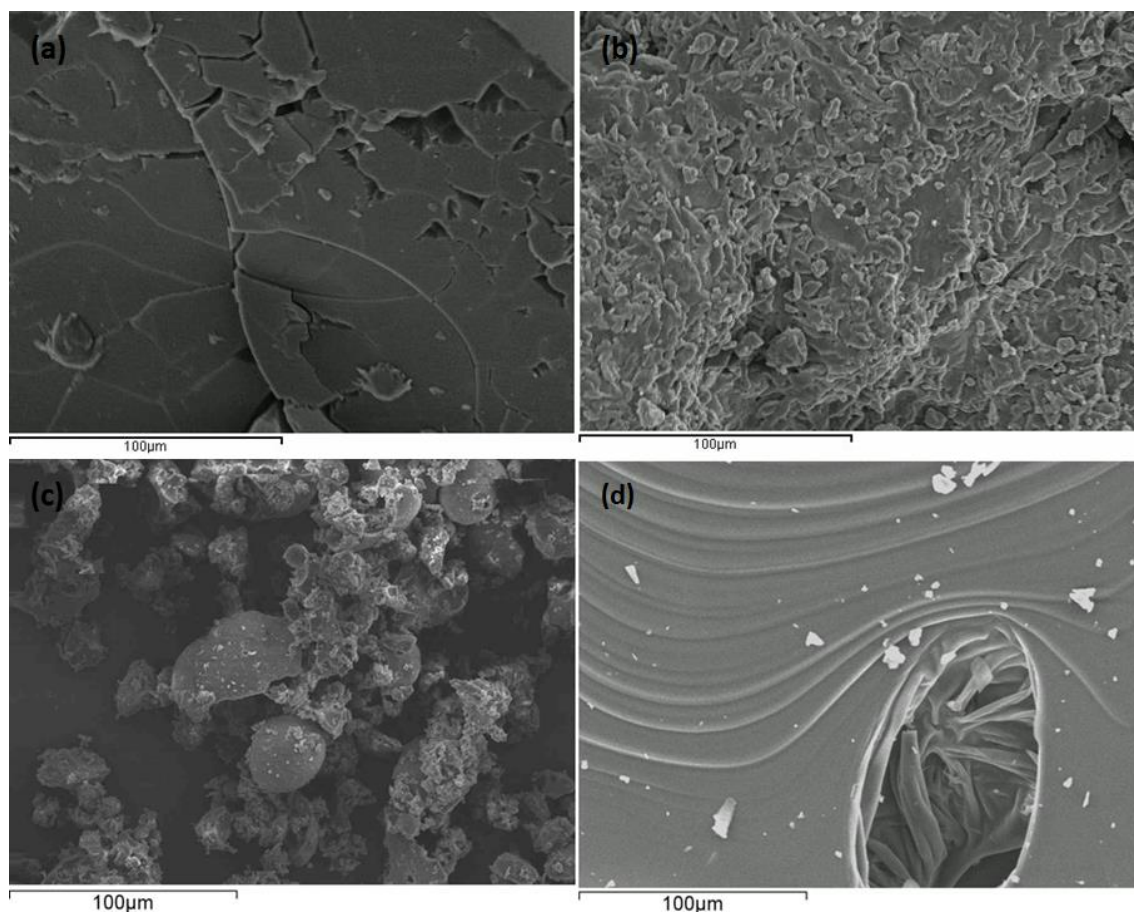
Figure 8.15. SEM images (20 kV) of (**a**) HPBCD (**b**) **4** (**c**) Physical mixture of **4** and HPBCD (**d**) Inclusion complex between **4** and HPBCD at 500 x magnification.

8.2.6   Glucose uptake assay

The activity of the **4**/HPBCD complex was investigated in the glucose uptake assay. This was to elucidate whether the complexation of **4** would hinder its ability to evoke a biological response. As the stability constant was large ($K_{1:1}$ = 34755 M^{-1}), it was possible that the concentration of free drug would be too low to evoke a response.

The assay was performed as before, using 10 μM of compound **4**. The results, shown in **Figure 8.16**, indicate that the binding of **4** in the HPBCD did not affect the compounds ability to stimulate glucose uptake. Although the stability constant was large, indicating the presence of strong interactions within the inclusion complex, it is still plausible for **4** to become disassociated from the CD and reach the target protein. Also, the $K_{1:1}$ value is only applicable for **4** within the inclusion complex and cannot be applied to describe the

interactions of **4** within the non-inclusion complex. It is therefore possible that **4** encapsulated by the solubilizing aggregates was able to act on the target protein.
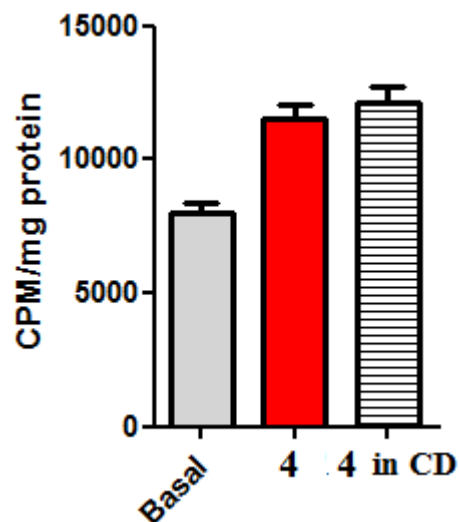
Figure 8.16. Glucose uptake assay results for **4**/HPBCD complex. 10 µM **4** used with 20 eq of HPBCD. C2C12 muscle cells incubated overnight at 37 ℃. Cells then exposed to ^{3}H deoxy-2-glucose for 10 mins and a scintillation count of the C2C12 muscle cells performed.

8.3   Conclusion

An efficient and convenient method for improving the aqueous solubility of **4** was identified with the use of the excipient HPBCD. The formation of **4**/HPBCD complexes, such as a 1:1 inclusion complex, was determined by means of a phase solubility diagram. The presence of non-inclusion complexes was also suggested as a means to account for the large excess of HPBCD needed to solubilise **4**.

These complexes were characterised using analytical techniques such as SEM and DSC, while NMR spectroscopy allowed for the interaction to be investigated at an atomic level. Encouragingly each method pointed to the same conclusion; compound **4** was present in an aqueous solution due to the formation of a CD complex.

9. Conclusion.

9.1   Conclusion

The initial aim of this project was to identify an RBP4-TTR inhibitor that also acted as an antidiabetic agent. Compounds **1**, **2** and **3** proved to be highly active in the SPR assay confirming their ability to inhibit the formation of the RBP4-TTR complex. Animal studies proved that these compounds were successful in controlling both glucose and insulin levels in diabetic mice. An additional important result was the reduced weight gain observed with the use of compound **1** in these mice. As many current antidiabetic drugs have the unwanted side effect of weight gain, a compound that can act as an insulin substitute while reducing weight gain would be highly beneficial to the diabetic patient.

Due to the encouraging results obtain from the SPR assay and the animal studies, an initial SAR study was performed on compound **1** which led to the design and synthesis of eight compounds, **4-11**, which were tested in a number of assays such as the fluorometric binding assay and the glucose uptake assay. The amide **4** proved to be more active than both compound **1** and the retinoid derivative Fen at inhibiting the formation of the RBP4-TTR complex in the SPR assay.

Amide bond formation was the key final step in the synthesis of compound **1** and the derivatives of this compound. The coupling reagents HOBt and TBTU were used in most cases with the amide product generally isolated in acceptable yields.

The synthesis of a number of arylpiperazines, required to investigate the importance of this functional group, involved the use of a number of different methods. Metal catalysed reactions were used in some cases but MW assisted S_NAr gave access to the same arylpiperazines in an improved yield and reduced reaction time. MW assisted synthesis was not useful in the synthesis of arylpiperazines which did not contain an electron withdrawing group (e.g. **35** and **36**, p-CH$_3$ and p-tBu respectively). The cyclocondensation of substituted anilines and bis(2-chloroethyl)amine.HCl was used to access these arylpiperazines. From the synthesis of arylpiperazines, it was clear that:

- MW synthesis was useful to access arylpiperazines containing electron withdrawing groups and improved yields and reduced reaction times

- the cyclocondensation approach was useful to access arylpiperazines that did not contain an electron withdrawing group

The synthesis of compounds **2** and **3** and the derivatives of these compounds involved the synthesis of a number of substituted pyrazoles. Substituted β-ketonitriles and hydrazines were used in the synthesis of the substituted pyrazoles required for the synthesis of the derivatives of compound **2**. β-Ketoesters and substituted hydrazines were used in the synthesis of the substituted pyrazoles necessary for the synthesis of the derivatives of compound **3**. MW irradiation again proved to be useful, with a novel method for the synthesis of the pyrazoles, compounds **91** and **96**, formed in good yields and short reaction times.

Compounds **1**, **2** and **3** and the derivatives of these compound were fully characterised using methods such as NMR spectroscopy, mass spectrometry, IR spectroscopy and in some cases CHN micro analysis.

A SAR study was subsequently performed on compound **4** to determine the key functional groups responsible for evoking such a biological response. A number of conclusions were drawn from this study:

- changes to the 1-(4-trifluoromethyl)phenyl group are not tolerated

- a piperazine ring is essential

- an amide carbonyl is required

- the thiophene ring is not necessary for activity

- the length of the molecule may play a vital role in ligand/protein interactions.

A loss or reduction of activity was the overall trend when changes were made to the trifluoromethyl phenyl group, as was seen with compounds **1**, **40**, **47**, or **67**. This is exemplified in the loss of activity observed for compound **1** compared to the activity observed for compound **10** when the Cl and N are removed from the aryl group. This may indicate that there is a very specific and sensitive binding occurring. Changes to the trifluoromethyl group, either changing its position on the aromatic ring or replacing it

with alternative functional groups, led to a loss of activity. This implies that the CF_3 group may act in a multi-purpose fashion:

- The steric bulk of this group may impact on the compounds conformation when in the protein active site resulting in an improved binding interaction.

- The lipophilicity of a molecule is affected by the presence of a CF_3. Lipophilicity is a key property for permeating cell membranes and hence a CF_3 may increase the amount of compound reaching the target protein.

- The electronic properties of the fluorine atoms can affect the electron density of the aromatic ring which in turn can affect the binding interaction. Changing the electron density of the aromatic ring may have reduced the biological activity as seen with **42** and **73** for example where a CF_3 group is replaced with a *p*-NO_2 and a *p*-NH_2 respectively.

Similarly, the role of the piperazine ring also proved important as no changes to this saturated heterocycle were tolerated. The piperazine carbonyl skeleton may serve to position the molecule in a suitable orientation for binding, while the aryl nitrogen may become involved in ionic interactions.

A loss of activity was observed when the carbonyl group was removed, implying that it may function as an important hydrogen bond acceptor. This was seen with the derivative **70**.

The role of the thiophene ring was found to be unimportant and it is suggested that it is the length of the molecule and not the presence of a terminal heterocycle that was important for activity as was seen with compounds **57**, **62** and **63**. Increasing the length of the molecule did not inhibit activity with compound **55** (an extra CH_2 in the alkyl chain) proving to be as active as **4** with **56** (two extra CH_2's in the alkyl chain) also demonstrating a high level of activity. Significantly, a drastic reduction in the length of the molecule did inhibit glucose uptake as was the case with compounds **58** and **67**. When the length of the molecule from the amide carbonyl was reduced to 7.710 Å, compound **59**, we did not observe glucose uptake. The exception to this however, is compound **61**, which remained active even though the length of the molecule from the amide carbonyl was reduced to 7.187 Å. This suggests the presence of a specific and sensitive binding interaction.

It was possible to optimise compound **4** and generate compounds with greater potency with the knowledge that it was the length of the molecule and not the presence of a terminal heterocycle that was critical for biological activity. The heterocycle was therefore replaced with different functional groups which led to the discovery of a number of compounds, such as **64** (terminal phenyl ring) and compound **81** (terminal ester), which proved to be more active than compounds **1** and **4**. The most prominent discovery was the identification of compound **79**, where the terminal carboxylic acid has the ability to operate as a hydrogen bond donor and acceptor or as a source of ionic interactions. This derivative proved to be the most active compound identified to date.

Compound **4** was as active as its predecessor, compound **1**, in an animal model. More importantly however were the results obtained with the use of compound **4** in an intervention study. Here we saw that the use of compound **4** restored both glucose and insulin sensitivity to normal levels

The information obtained from the SAR study allowed for the development of a pharmacophore model. The developed model best represents the key functional groups required for a molecule to act on the protein target and stimulate glucose uptake. The final pharmacophore model had a ROC score of 0.877.

The glucose uptake assay allowed for the identification of the functional groups required to evoke a biological response. It also allowed for the emergence of a secondary protein target as the glucose uptake activity was independent of RBP4. To work towards identifying this unknown target, the method described by Kosaka *et al*. was employed. This involved attaching the active compounds **4** and **79** to an affinity column where the subsequent bound proteins could be analysed using mass spectrometry. As compounds **4** and **79** are colourless, a coloured derivative, compound **166**, with structural similarities to compound **79**, was synthesised and attached to the sepharose bead. The resultant colour change of the bead indicated the successful attachment of compound **166**.

To attach **4** and **79** to the sepharose bead, it was first necessary to attach a PEG linker to both compounds. A hydrophilic linker was chosen as the bead conjugate was to be used in an aqueous environment. Compound **4** was functionalised at the C2 position of the thiophene ring as the glucose uptake assay revealed that changes to the thiophene ring

were tolerated. A formyl group was introduced (**147**) so that the amino PEG linker could be attached *via* a reductive amination. A Staudinger reduction was performed on a diazido PEG3 linker (**153**) generating the mono amino-product **154** which was attached to **147** *via* a reductive amination. This gave compound **155** in a 76% yield. A Staudinger reduction was again used to convert the remaining azide into the primary amine with compound **156** isolated in a 43% yield. A similar synthetic approach was applied when attaching the PEG3 linker to **79**, however as **79** contained a carboxylic acid, the mono amino PEG linker, compound **154**, was attached by forming an amide bond and was followed by a Staudinger reduction to give compound **158** in a 25% yield. Immobilising the ligand-PEG conjugate on the sepharose bead was verified by the attachment of the coloured derivative, compound **166**. The use of the beads in the identification of the secondary protein target is currently on-going.

Compound **4** has recently shown, by a colleague on our research team, to stimulate the activity of the enzyme AMPK. The activation of AMPK has been proposed as a possible mechanism of action for the antidiabetic drug metformin. Activation of this enzyme has been shown to stimulate glucose uptake and decrease hepatic gluconeogenesis.[38,39] Metformin is thought to activate AMPK through the inhibition of mitochondrial respiration by acting at Complex I. It is therefore possible that compound **4**, and other compounds active in the glucose uptake assay, are stimulating the uptake of glucose in muscles cells by acting on the mitochondrial enzyme Complex I. Further experiments are required to confirm this as the secondary protein target.

A SAR study was subsequently performed on these two compounds with the compound **2** derivative, compound **115**, proving to be highly active in the glucose uptake assay. A number of derivatives were synthesised and are awaiting biological testing.

The synthesis of these two structurally distinct compounds and their derivatives involved the synthesis of a number of substituted pyrazoles. Substituted β-ketonitriles and hydrazines were used in the synthesis of the substituted pyrazoles required for the synthesis of the compound **2** derivatives. β-Ketoesters and substituted hydrazines were used in the synthesis of the substituted pyrazoles necessary for the synthesis of the compound **3** derivatives. MW irradiation again proved to be useful, with a novel method for the synthesis of the pyrazoles, compounds **91** and **96**, formed in good yields and short reaction times.

Compound **4** proved to be highly insoluble in aqueous solutions. Further animal studies, which required aqueous solutions of compound **4**, were planned. As a result, a method for solubilising compound **4** in aqueous solutions was needed. The functionalised CD, HPBCD, was used and it was found that with twenty equivalents of the excipient, a 0.02 M 5% aqueous DMSO solution of compound **4** could be prepared. Compound **4** was solubilised due to the formation an inclusion complex and non-inclusion complexes. The stoichiometry of the inclusion complex was found to be 1:1, compound **4**:HPBCD. This was determined by means of a phase solubility diagram which demonstrated that the solubility of compound **4** increased linearly with increasing concentrations of HPBCD and indicated that the complex formed was an A_L type complex. The phase solubility diagram was also used to calculate the binding constant $K_{1:1}$ which was determined to be 34755 M^{-1}. This indicated that a strong interaction was formed between compound **4** and the CD. Other analytical techniques, such as DSC, SEM and NMR were all used in the analysis of the inclusion complex. Results from these all confirmed the presence of a novel complex.

In conclusion, this project has seen the identification, synthesis and testing of a number of novel and highly active compounds with the potential to act as antidiabetic agents.

9.2   Future work

This project has identified several compounds with the potential to act as antidiabetic agents. Future work will include the continuation of the SAR study of the active compounds and the biological evaluation of the compounds yet to be tested. This will allow the generation of even more accurate pharmacophore models and improved lead compounds. The optimization of compounds so as to improve their drug-likeness may also be necessary.

Confirming the identity of the secondary protein target is required. This may involve the use of the Kosaka method where active compounds have been immobilized on an affinity column. The affinity column is then used to bind and identify the secondary protein target. Subsequent assay work, including possible assay development, will be needed to confirm the identity of the secondary protein target.

10. Experimental

10.1 Instrumentation

Reagents and reactants were purchased from Aldrich or Alfa Aesar and used as received unless otherwise stated. DCM was distilled over CaH_2 and THF over Na wire and benzophenone. Anhydrous DMF was purchased from Sigma Aldrich

All NMR spectra were recorded on a Bruker Avance spectrometer at a probe temperature of 25 °C, unless otherwise stated, operating at 300 MHz for the ^1H nucleus and 75 MHz for the ^{13}C nucleus. Proton and carbon signals were assigned with the aid of 2D NMR experiments (COSY, HSQC) and DEPT experiments for novel compounds. 2D ROESY experiments were carried out in D_2O on a Bruker Advance 500 spectrometer at 500 MHz (Teagasc). High temperature NMR spectroscopy experiments were carried out by heating the probe. Spectra were recorded in $CDCl_3$ unless otherwise stated, with Me_4Si used as internal standard. Chemical shifts are given in ppm downfield form the internal standard and coupling constants are given in Hz. ^{13}C NMR spectra were recorded with complete proton decoupling.

Melting point analyses were carried out using a Stewart Scientific SMP11 melting point apparatus and are uncorrected.

High resolution mass spectra (HR-MS) were performed on an Agilent-L 1200 Series coupled to a 6210 Agilent Time-of-Flight (TOF) mass spectrometer equipped with an both a positive and negative electrospray source. Infrared spectra were obtained in the region 4000-400 cm^{-1} on a Nicolet Impact 400D spectrophotometer or using a Perkin Elmer 2000 FTIR spectrometer. SEM was performed using a Hitachi S-3200-N with a tungsten filament and the sample was coated in gold. Differential Scanning Calorimetry was carried out on a Perkin Elmer Pyris 6.0. Scintillation counts were obtained using a Wallac MicroBeta scintillation counter (Perkin Elmer).

Flash column chromatography was performed using silica gel 60 (Merck, 0.040-0.063 mm). Analytical thin layer chromatography was carried out on aluminium sheets pre-coated with Merck TLC Silica gel 60 F254. Developed sheets were visualised using a portable UVltec CV-006 lamp ($\lambda = 254, 365$ nm) or the appropriate stain.

† = Compounds synthesised that are awaiting biological evaluation.

10.2 General procedure for amide bond formation using HOBt and TBTU.

Carboxylic acid, HOBt, TBTU, anhydrous NEt$_3$ and anhydrous DMF were placed in an oven-dried Schlenk tube under a N$_2$ atmosphere. The resulting solution was stirred at rt for 15 mins. A second Schlenk tube was prepared containing amine and anhydrous DMF under a N$_2$ atmosphere. The resulting solution was transferred, *via* a cannula, to the first Schlenk tube containing the carboxylic acid. The solution was stirred under N$_2$ and the reaction progress monitored by TLC. The DMF was removed under reduced pressure and the resulting oil was acidified (pH = 3) using a 0.1 M aqueous HCl solution. The aqueous mixture was extracted with DCM (20 mL, followed by 4 x 10 mL). The organic combined layers were washed with a saturated aqueous solution of Na$_2$CO$_3$ (3 x 20 mL) and brine (3 x 20 mL) and dried over MgSO$_4$ and the residue was purified using flash chromatography.

10.3 Synthesis of 1-(4-(3-chloro-5-(trifluoromethyl)pyridin-2-yl)piperazin-1-yl)-3-(thiophen-2-ylthio)propan-1-one (RTB70) (1)
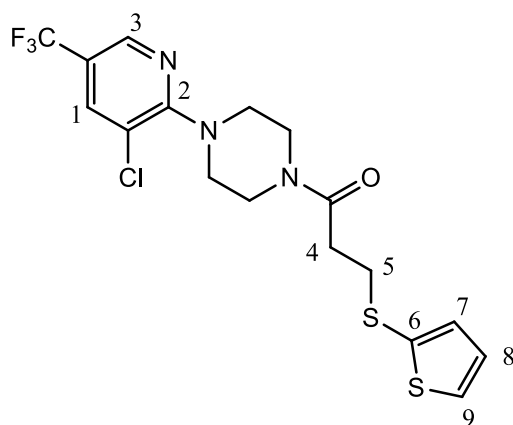
Prepare from 1-(3-chloro-5-(trifluoromethyl)pyridin-2-yl)piperazine (698 mg, 2.63 mmol) and compound **30** (450 mg, 2.39 mmol) using HOBt (698 mg, 2.63 mmol), TBTU (767 mg, 2.63 mmol), anhydrous NEt$_3$ (532 μL, 3.82 mmol) and anhydrous DMF (10 mL) and following the general procedure described in section **10.2**. The reaction mixture was stirred overnight at room temperature under a N$_2$ atmosphere. Purified using flash chromatography (3:2 EtOAc:*n*-hexane). The obtained product was dissolved in a minimal amount of DCM and Pet. Ether was added until precipitation began. The solution and the precipitate was stored at -20 °C overnight, and the resultant

crystals collected by vacuum filtration and washed with cold Pet. Ether (~ 20 mL) to give white needles, 2.1 g (71%).

¹H NMR: (300 MHz, CDCl₃) δ 8.41-8.40 (m, 1H, H3), 7.79-7.78 (m, 1H, H1), 7.35 (dd, J = 5.3 Hz, J = 1.2 Hz, 1H, H9), 7.45 (m, 1H, H7), 7.00-6.97 (m, 1H, H8), 3.78-7.75 (m, 2H*), 3.58-3.55 (m, 2H*), 3.50-3.46 (m, 4H*), 3.11 (t, J = 7.1 Hz, 2H, H5), 2.68 (t, J = 7.1 Hz, 2H, H4) *Piperazine. **¹³C NMR:** (75 MHz, CDCl₃) δ 170.1 (C=O), 160.1 (C2), 143.6 (q, J = 4.1 Hz, C3), 136.7 (q, J = 3.3 Hz, C1), 134.6 (C6, C9), 130.2 (C7), 128.3 (C8), 123.8 (q, J = 270.0 Hz, CF₃), 121.7 (CCl), 121.2 (q, J = 33.0 Hz, C-CF₃), 49.1 (C*), 45.7 (C*), 42.0 (C*), 34.8 (C5), 33.9 (C4) *Piperazine. **R$_f$:** 0.5 (3:2, EtOAc:n-hexane). **HR-MS:** calcd for C₁₇H₁₈ClF₃N₃OS₂ m/z: [M + H]⁺, 436.0526; found: 436.0531 [Diff (ppm) = 1.14]. **IR (KBr):** 2840 (C-H), 1636 (C=O), 1603 (C=C), 1452 (C=C), 1323 (C-F), 1248 (C-N), 706 (C-Cl) cm⁻¹. **m.p.:** 70-72 °C. **Anal. calcd** for C₁₇H₁₇ClF₃N₃OS₂; C, 46.84; H, 3.93; N, 9.64% found: C, 46.51; H, 3.84; N, 9.30%.

10.4 General procedure for the formation of a pyrimidinone ring using AcOH.

Substituted amino pyrazole was dissolved in AcOH and a substituted β-ketoester was added. The reaction mixture was heated at reflux. After cooling to rt, the AcOH was removed under reduced pressure. The resulting residue was triturated using EtOAc to give a white solid.

10.5 Synthesis of 5-(3,5-bis(trifluoromethyl)phenyl)-2-(*tert*-butyl)pyrazolo[1,5-a]pyrimidin-7(4H)-one (RTB69) (2)
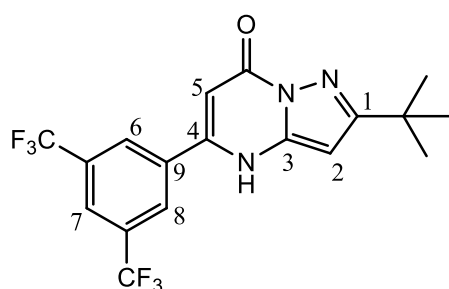
Prepared from 5-amino-3-(*tert*-butyl)-1H-pyrazole (124 mg, 0.89 mmol) and ethyl 3-(3,5-bis(trifluoromethyl)phenyl)-3-oxopropanoate (321 mg, 0.97 mmol) using HOAc (8 mL) and following the procedure described in section **10.4**. The reaction mixture was heated at reflux for 4 hrs and the residue triturated using EtOAc (2 mL) to give a white solid, 65 mg (18%).

^{1}H NMR: (300 MHz, d_6-DMSO) δ 12.59 (bs, 1H, NH), 8.52 (s, 2H, H6, H8), 8.34 (s, 1H, H7), 6.30 (s, 1H, H2), 6.14 (s, 1H, H5), 1.34 (s, 9H, (CH$_3$)$_3$). **^{13}C NMR:** (75 MHz, d_6-DMSO) δ 165.0 (C=O), 156.1 (C4), 146.2 (C3), 142.0 (C1), 134.9 (C9), 130.8 (q, J = 32.7 Hz), C-CF$_3$), 128.3 (C6, C8), 124.2 (C7), 123.2 (q, J = 269.8 Hz, CF$_3$), 95.4 (C2), 86.2 (C5), 2.4 (C(CH$_3$)$_3$), 29.9 ((CH$_3$)$_3$). **R$_f$:** 0.6 (1:9, MeOH:DCM). **HR-MS:** calcd for C$_{18}$H$_{16}$F$_6$N$_3$O m/z: [M + H]$^+$, 404.1192; found 404.1178 [Diff(ppm) = -3.46]. **IR (KBr):** 3390 (N-H), 2969 (C-H), 1667 (C=O), 1616 (C=C), 1577 (N-H), 1488 (C=C), 1280 (C-F), 1139 (C-N) cm^{-1} **m.p.:** Above 300 °C.

10.6 Synthesis of 4-(thiophen-3-yl)-1-(4-(4-(trifluoromethyl)phenyl)piperazin-1-yl)butan-1-one (RTB86) (3)
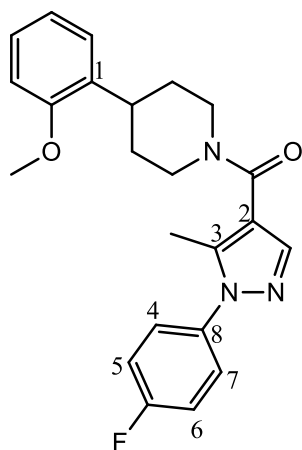
Compound **131** (54 mg, 0.24 mmol)**,** HOBt (333 mg, 0.27 mmol), TBTU (79 mg, 0.27 mmol), anhydrous NEt$_3$ (53 µL, 0.38 mmol) and anhydrous DMF (5 mL) were placed in an oven-dried Schlenk tube under a N$_2$ atmosphere. The resulting solution was stirred at rt for 15 mins. A second Schlenk tube, containing **137** (52 mg, 0.27 mmol) and anhydrous NEt$_3$ (36 µL, 0.26 mmol) in anhydrous DMF (2 mL) under a N$_2$ atmosphere, was stirred at rt. After 15 mins, the resulting solution was transferred, *via* a cannula, to the first Schlenk tube containing the carboxylic acid. The solution was stirred under N$_2$ and the reaction progress monitored by TLC. After 24 hrs, the DMF was removed under reduced pressure and the resulting oil was acidified (pH = 3) using a 0.1 M aqueous HCl solution. The aqueous mixture was extracted with DCM (20 mL, followed by 4 x 10 mL). The organic combined layers were washed with a saturated aqueous solution of Na$_2$CO$_3$ (3 x 20 mL) and brine (3 x 20 mL) and dried over MgSO$_4$ and the residue was

purified using flash chromatography (3:2 EtOAc:n-hexane) to give a white solid, 74 mg (77%).

^{1}H NMR: (300 MHz, CD$_3$CN, T = 60 °C) δ 7.67 (s, 1H, N=CH), 7.55-7.51 (m, 2H, H5, H6), 7.31-7.20 (m, 4H, H4, H7, Ar), 7.00-6.93 (m 2H, Ar), 4.57-4.36 (m, 2H*), 3.86 (s, 3H, OCH$_3$), 3.32-3.21 (m, 1H, Ar-CH), 3.11-3.03 (m, 2H*), 2.37 (s, 3H, CH$_3$), 1.89-1.85 (m, 2H*), 1.77-1.63 (m, 2H*).*Piperidine. **^{13}C NMR:** (75 MHz, CD$_3$CN, T = 60 °C) δ 164.0 (C=O), 162.3 (d, J = 245.7 Hz, C-F), 157.0 (C-OCH$_3$), 139.7 (C1), 138.6 (N=CH), 135.8 (d, J = 3.0 Hz, C8), 133.7 (C3), 127.3 (d, J = 8.8 Hz, C4, C7), 127.1 (Ar), 126.5 (Ar), 120.6 (Ar), 116.6 (C2), 115.8 (d, J = 22.9 Hz, C5, C6), 111.1 (Ar), 55.2 (OCH$_3$), 45.3 (C*), 35.7 (Ar-C), 31.9 (C*), 10.5 (CH$_3$).*Piperidine. **R$_f$:** 0.4 (3:2, EtOAc:n-hexane). **HR-MS:** calcd for C$_{23}$H$_{25}$FN$_3$O$_2$ m/z: [M + H]$^+$, 394.1925; found: 394.1944 [Diff(ppm) = 4.76]. **IR (KBr):** 2940 (CH), 1612 (C=O), 1392 (C-F), 1236 (C-N), 1220 (O-CH$_3$) cm^{-1}. **m.p.:** 140-141 °C.

10.7 Synthesis of 4-(thiophen-2-yl)-1-(4-(4-(trifluoromethyl)phenyl)piperazin-1-yl)butan-1-one (RTC1) (4)
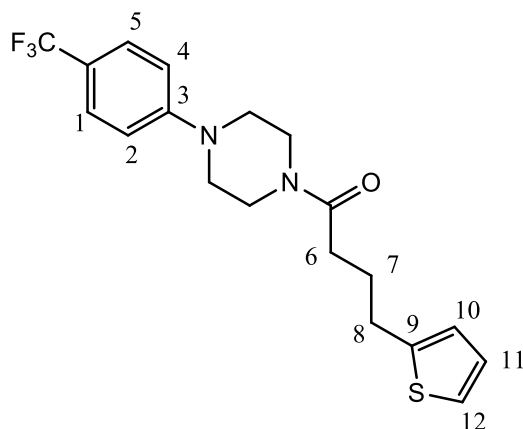
Prepared from compound **33** (100 mg, 0.43 mmol) and 4-(2-thienyl)butyric acid (50 µL, 0.34 mmol), using HOBt (58 mg, 0.43 mmol), TBTU (140 mg, 0.43 mmol), anhydrous NEt$_3$ (100 µL, 0.69 mmol) and anhydrous DMF (3 mL) and following the general procedure described in section **10.2**. The reaction mixture was stirred at rt overnight under a N$_2$ atmosphere. Purified using flash chromatography (3:2 EtOAc:n-hexane). The obtained product was dissolved in minimal DCM (~ 1 mL) and Pet. Ether was added until precipitation began. The solution was stored at -20 °C overnight, and the

resultant crystals collected by vacuum filtration and washed with cold Pet. Ether (~ 20 mL) to give white needles, 104 mg (80%).

^{1}H NMR: (300 MHz, CDCl$_3$) δ 7.49 (d, J = 8.7 Hz, 2H, H1, H5), 7.12 (dd, J = 5.1 Hz, 1.2 Hz, 1H, H12), 6.94-6.90 (m, 3H, H2, H4, H11), 6.82-6.80 (m, 1H, H10), 3.76 (m, 2H*), 3.56 (m, 2H*), 3.24 (m, 4H*), 2.91 (t, J = 7 Hz, 2H, H8), 2.38 (t, J = 7 Hz, 2H, H6), 2.11-2.0 (m, 2H, H7). *Piperazine. **^{13}C NMR:** (75 MHz, CDCl$_3$) δ 171.0 (C=O), 152.9 (C3), 144.3 (C9), 126.8 (C10), 126.5 (q, J = 3.6 Hz, C1, C5), 124.61 (q, J = 270.0 Hz, CF$_3$) 124.60 (C12), 123.2 (C11), 121.2 (q, J = 33.0 Hz, C-CF$_3$), 115.0 (C2, C4), 48.3 (C*), 48.1 (C*), 45.0 (C*), 41.1 (C*), 31.9 (C6), 29.2 (C8), 26.9 (C7). *Piperazine. **R$_f$:** 0.5 (3:2, EtOAc:n-hexane). **HR-MS:** calcd for C$_{19}$H$_{22}$F$_3$N$_2$OS m/z: [M + H]$^+$, 383.1399; found: 383.1402 [Diff(ppm) = 0.61]. **IR (KBr):** 2924 (C-H), 1653 (C=O), 1612 (C=C), 1438(C=C), 1331 (C-F), 1233 (C-N) cm^{-1}. **m.p.:** 90-94 °C. **Anal. calcd** for C$_{19}$H$_{22}$F$_3$N$_2$OS; C, 59.67; H, 5.54; N, 7.33% found: C, 59.71; H, 5.14; N, 7.17%.

10.8 Synthesis of 1-(thiophen-2-yl)-4-(4-(4-(trifluoromethyl)phenyl)piperazin-1-yl)butane-1,4-dione (RTC2) (5)
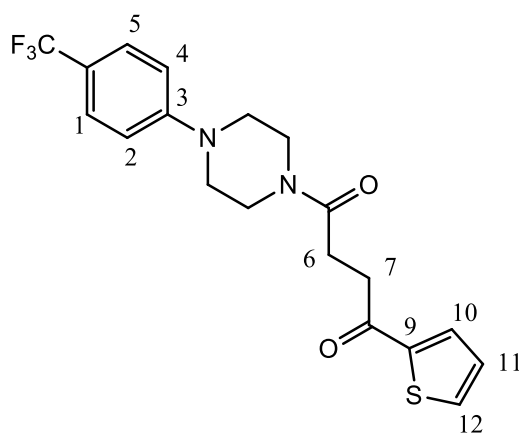
Prepared from compound **33** (100 mg, 0.43 mmol) and 4-oxo-4-(thiophen-2-yl)butanoic acid (63 mg, 0.34 mmol), using HOBt (58 mg, 0.43 mmol), TBTU (140 mg, 0.43 mmol), anhydrous NEt$_3$ (100 µL, 0.69 mmol) and anhydrous DMF (3 mL) and following the general procedure described in section **10.2**. The reaction mixture was stirred at rt overnight under an N$_2$ atmosphere. Purified using flash chromatography (3:2 EtOAc:n-hexane) to give an off white solid, 109 mg (81%).

¹H NMR: (300 MHz, CDCl$_3$) δ 7.81 (dd, J = 4.8 Hz, J = 1.0 Hz, 1H, H10), 7.63 (dd, J = 4.8 Hz, J = 1.0 Hz, 1H, H12), 7.50 (d, J = 8.7 Hz, 2H, H1, H5), 7.15-7.12 (m, 1H, H11), 6.92 (d, J = 8.7 Hz, 2H, H2, H4), 3.80-3.71 (m, 4H*), 3.54-3.31 (m, 4H*), 3.27-3.24 (m, 2H, H7), 2.82 (t, J = 6.6 Hz, 2H, H6).*Piperazine. **¹³C NMR:** (75 MHz, CDCl$_3$) 191.9 (C=O), 170.1 (N-C=O), 152.9 (C3), 143.8 (C9), 133.6 (C12), 128.1 (C11), 132.1 (C10), 126.5 (q, J = 3.7 Hz, C1, C5), 126.1 (q, J = 33.0 Hz, C-CF$_3$), 124.6 (q, J = 266.7 Hz, CF$_3$), 114.9 (C2, C4), 48.2 (C*), 48.0 (C*), 45.0 (C*), 41.3 (C*), 34.1 (C6), 27.0 (C7).*Piperazine. **R$_f$:** 0.5 (3:2, EtOAc:n-hexane). **HR-MS:** calcd for C$_{38}$H$_{38}$F$_6$N$_4$O$_4$S$_2$Na m/z: [2M + Na]$^+$, 815.2131; found: 815.2127 [Diff(ppm) = -0.51]. **IR (KBr):** 2954 (C-H), 1647 (C=O), 1612 (N-C=O), 1325 (C-F), 1230 (C-N) cm^{-1}. **m.p.:** 172-176 °C. **Anal. calcd** for C$_{19}$H$_{19}$F$_3$N$_2$O$_2$S; C, 57.56; H, 4.83; N, 7.07% found: C, 57.34; H, 4.62; N, 6.89%.

10.9 Synthesis of 1-(thiophen-2-yl)-4-(4-(5-(trifluoromethyl)pyridin-2-yl)piperazin-1-yl)butane-1,4-dione (RTC3) (6)
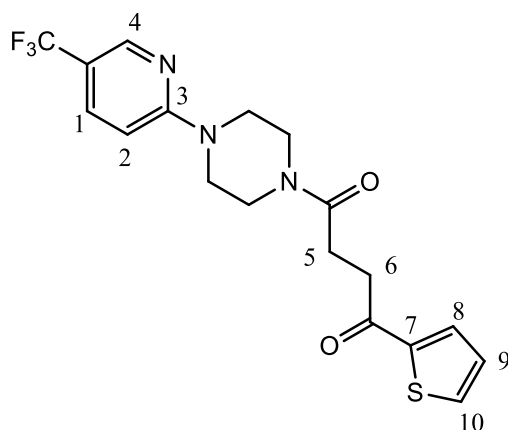
Prepared from 1-(5-(trifluoromethyl)pyridin-2-yl)piperazine (99 mg, 0.43 mmol) and 4-oxo-4-(thiophen-2-yl)butanoic acid (63 mg, 0.34 mmol), using HOBt (58 mg, 0.43 mmol), TBTU (140 mg, 0.43 mmol), anhydrous NEt$_3$ (100 μL, 0.69 mmol) and anhydrous DMF (3 mL) and following the general procedure described in section **10.2**. The reaction mixture was stirred overnight at room temperature under a N$_2$ atmosphere. Purified using flash chromatography (3:2 EtOAc:n-hexane) to give an off white solid, 85 mg, (63%).

¹H NMR: (300 MHz, CDCl$_3$) δ 8.41 (s, 1H, H4), 7.81-7.80 (m, 1H, H10), 7.68-7.63 (m, 2H, H1, H8), 7.15-7.12 (m, 1H, H9), 6.65 (d, J = 9.1 Hz, 1H, H2), 3.79-3.61 (m, 8H*),

3.34 (t, J = 6.9 Hz, 2H, H6), 2.82 (t, J = 6.9 Hz, 2H, H5). *Piperazine. **^{13}C NMR:** (75 MHz, CDCl$_3$) δ 191.9 (C=O), 170.3 (N-C=O), 160.0 (C3), 147.7 (q, J = 4.1 Hz, C4), 143.8 (C7), 134.7 (q, J = 3.3 Hz, C1), 133.5 (C8), 132.1 (C10), 128.1 (C9), 124.4 (q, J = 268.5 Hz, CF$_3$), 15.8 (q, J = 32.0 Hz, C-CF$_3$), 105.6 (C2), 44.9 (C*), 44.6 (C*), 44.2 (C*), 41.9 (C*), 34.1 (C6), 27.1 (C5). *Piperazine. **R$_f$:** 0.5 (3:2, EtOAc:n-hexane). **HR-MS:** calcd for C$_{36}$H$_{37}$F$_6$N$_6$O$_4$S$_2$ m/z: [2M + H]$^+$, 795.2216; found: 795.2223 [Diff (ppm) = 0.78]. **IR (KBr):** 1655 (C=O), 1638 (N-C=O), 1329 (C-F), 1102 (C-N) cm^{-1}. **m.p.:** 204-206 °C. **Anal. calcd** for C$_{18}$H$_{18}$F$_3$N$_3$O$_2$S$_1$: C, 54.40; H, 4.57; N, 10.58 found; C, 54.39; H, 4.27; N, 10.59.

10.10 Synthesis of 1-(4-(3-chloro-5-(trifluoromethyl)pyridin-2-yl)piperazin-1-yl)-4-(thiophen-2-yl)butane-1,4-dione (RTC4) (7)

Prepared from 1-(3-chloro-5-(trifluoromethyl)pyridin-2-yl)piperazine (114 mg, 0.43 mmol) and 4-oxo-4-(thiophen-2-yl)butanoic acid (63 mg, 0.34 mmol), using HOBt (58 mg, 0.43 mmol), TBTU (140 mg, 0.43 mmol), anhydrous NEt$_3$ (100 μL, 0.69 mmol) and anhydrous DMF (3 mL) and following the general procedure described in section **10.2**. The reaction mixture was stirred overnight at room temperature under a N$_2$ atmosphere. Purified using flash chromatography (3:2 EtOAc:n-hexane) to give an off white solid, 102 mg (70%).

^{1}H NMR: (300 MHz, CDCl$_3$) δ 8.41-8.40 (m, 1H, H3), 7.82-7.79 (m, 2H, H1, H7), 7.64 (dd, J = 4.0 Hz, J = 1.0 Hz, 1H, H9), 7.15-7.12 (m, 1H, H8), 3.80-3.72 (m, 4H*), 3.57-3.54 (m, 2H*), 3.50-3.47 (m, 2H*), 3.33 (t, J = 9.0 Hz, 2H, H5), 2.84 (t, J = 9.0 Hz, 2H, H4).*Piperazine. **^{13}C NMR:** (75 MHz, CDCl$_3$) 191.9 (C=O), 170.2 (N-C=O), 159.5 (C2), 143.9 (C6), 143.1 (q, J = 3.7 Hz, C3), 136.1 (q, J = 3.3 Hz, C1), 133.5 (C9),

132.1 (C7), 128.6 (q, J = 270.1 Hz, CF_3), 128.1 (C8), 121.1 (q, J = 33.2 Hz, C-CF$_3$), 121.0 (C-Cl), 48.5 (C*), 45.1 (C*), 41.5 (C*), 34.2 (C5), 27.1 (C4). *Piperazine. **R$_f$:** 0.5 (3:2, EtOAc:n-hexane). **HR-MS:** calcd for $C_{18}H_{18}F_3N_3O_2SCl$ m/z: [M + H]$^+$, 432.0755; found: 432.0765 [Diff(ppm) = 2.31]. **IR (KBr):** 2915 (C-H), 1647 (C=O), 1604 (N-C=O), 1416(C=C), 1319 (CF), 1231 (C-N), 844 (C-Cl) cm^{-1}. **m.p.:** 102-104 °C. **Anal. calcd** for $C_{18}H_{17}F_3N_3O_2SCl$; C, 50.06; H, 3.97; N, 9.73% found: C, 50.14; H, 3.77; N, 9.47%.

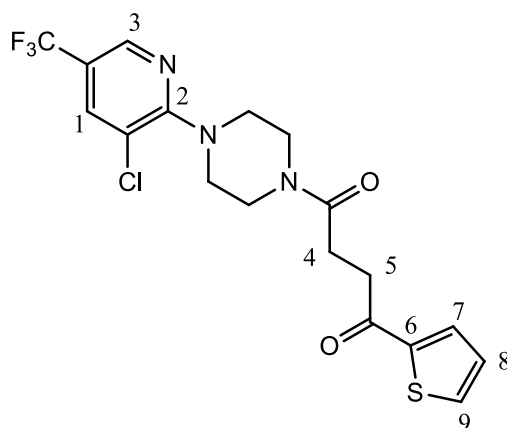## 10.11 Synthesis of 4-(thiophen-3-yl)-1-(4-(5-(trifluoromethyl)pyridin-2-yl)piperazin-1-yl)butan-1-one (RTC5) (8)

Prepared from 1-(5-(trifluoromethyl)pyridin-2-yl)piperazine (99 mg, 0.43 mmol) and 4-(2-thienyl)butyric acid (50 µL, 0.34 mmol) using HOBt (58 mg, 0.43 mmol), TBTU (140 mg, 0.43 mmol), anhydrous NEt$_3$ (100 µL, 0.69 mmol) and anhydrous DMF (3 mL) and following the general procedure described in section **10.2**. The reaction mixture was stirred overnight at room temperature under a N$_2$ atmosphere. Purified using flash chromatography (3:2 EtOAc:n-hexane) to give an off white solid, 104 mg (80%).

^{1}H NMR: (300 MHz, CDCl$_3$) δ 8.41-8.40 (m, 1H, H4), 7.66 (dd, J = 9.0 Hz, J = 2.0 Hz, 1H, H1), 7.13 (dd, J = 5.1 Hz, J = 1.2 Hz, 1H, H11), 6.94-6.91 (m, 1H, H10), 6.82-6.80 (m, 1H, H9), 6.64 (d, J = 8.7 Hz, 1H, H2), 3.75-3.69 (m, 4H*), 3.61-3.58 (m, 2H*), 3.54-3.51 (m, 2H*), 2.93 (t, J = 7.2 Hz, 2H, H7), 2.41 (t, J = 7.2, 2H, H5), 2.11-2.03 (m, 2H, H6).*Piperazine. **^{13}C NMR:** (75 MHz, CDCl$_3$) 171.2 (C=O), 160.4 (C3), 145.6 (q, J = 4.0 Hz, C4), 144.3 (C8), 134.6 (q, J = 4.0 Hz, C1), 126.8 (C10), 124.56 (C9), 124.52 (q, J = 268.5 Hz, CF$_3$), 123.2 (C11), 115.6 (q, J = 33.0 Hz, C-CF$_3$), 105.6 (C2), 44.9

(C*), 44.6 (C*), 44.3 (C*), 40.9 (C*), 31.9 (C7), 29.2 (C5), 26.9 (C6).*Piperazine. $\mathbf{R_f}$: 0.5 (3:2, EtOAc:n-hexane). **HR-MS:** calcd for $C_{18}H_{21}F_3N_3OS$ m/z: $[M + H]^+$, 384.1352; found: 384.1365 [Diff(ppm) = 3.38]. **IR (KBr):** 2953 (C-H), 1646 (C=O), 1611 (C=C), 1417 (C=C), 1325 (C-F), 1231 (C-N) cm^{-1}. **m.p.:** 107-109 °C. **Anal. calcd** for $C_{18}H_{20}F_3N_3OS$; C, 56.38; H, 5.26; N, 10.96% found: C, 56.64; H,4.95 ; N, 10.89%.

10.12 Synthesis of 1-(4-(3-chloro-5-(trifluoromethyl)pyridin-2-yl)piperazin-1-yl)-4-(thiophen-2-yl)butan-1-one (RTC6) (9)
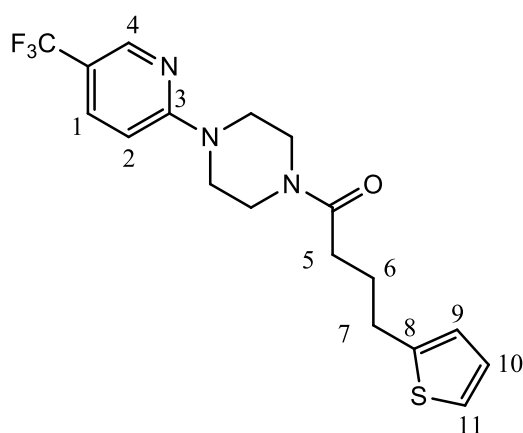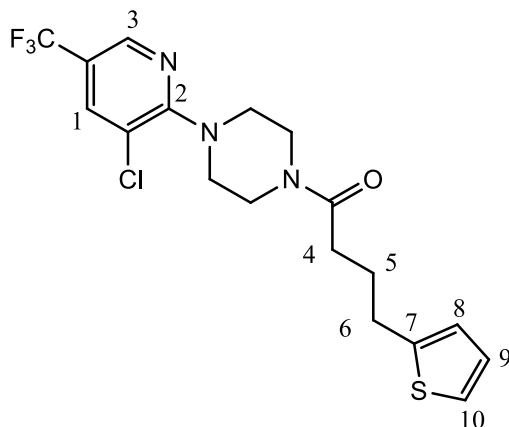

Prepared from 1-(3-chloro-5-(trifluoromethyl)pyridin-2-yl)piperazine (114 mg, 0.43 mol) and 4-(2-thienyl)butyric acid (50 μL, 0.34 mmol) using HOBt (58 mg, 0.43 mmol), TBTU (140 mg, 0.43 mmol), anhydrous NEt₃ (100 μL, 0.69 mmol) and anhydrous DMF (3 mL) and following the general procedure described in section **10.2**. The reaction mixture was stirred overnight at room temperature under a N_2 atmosphere. The reaction mixture was stirred at rt overnight. Purified using flash chromatography (3:2 EtOAc:n-hexane) to give a grey solid, 90 mg (64%).

¹H NMR: (300 MHz, CDCl₃) δ 8.40-8.39 (m, 1H, H3), 7.79 (d, J = 1.8 Hz, 1H, H1), 7.13 (dd, J = 5.1 Hz, J = 1.2 Hz, 1H, H10), 6.94-6.91 (m, 1H, H9), 6.82-6.80 (m, 1H, H8), 3.37-3.375 (m, 2H*), 3.58-3.55 (m, 2H*), 3.49-3.45 (m, 4H*), 2.93 (t, J = 7.2 Hz, 2H, H6), 2.41 (t, J = 7.2 H, 2H, H4), 2.11-2.01 (m, 2H, H5).*Piperazine. **¹³C NMR:** (75 MHz, CDCl₃) 171.2 (C=O), 159.5 (C2), 144.3 (C7), 143.1 (q, J = 3.7 Hz, C3), 136.1 (q, J = 3.7 Hz, C1), 126.8 (C9), 124.5 (C8), 123.23 (C10), 123.21 (q, J = 270.0 Hz, CF₃), 121.1 (C-Cl), 120.59 (q, J = 33.0 Hz, C-CF₃), 48.6 (C*), 45.2 (C*), 41.3 (C*), 32.0 (C4), 29.2 (C6), 26.9 (C5).*Piperazine. $\mathbf{R_f}$: 0.5 (3:2, EtOAc:n-hexane). **HR-MS:** calcd for $C_{18}H_{20}F_3N_3OSCl$ m/z: $[M + H]^+$, 418.0971; found 418.0962 [Diff(ppm) = 3.12]. **IR**

(KBr): 2913 (C-H), 1650 (C=O), 1604 (C=C), 1438 (C=C), 1319 (C-F), 1251 (C-N), 845 (C-Cl) cm^{-1}. **m.p.:** 52-54 °C. **Anal. calcd** for $C_{18}H_{19}F_3N_3OSCl$; C, 51.73; H, 4.58; N, 10.06% found; C, 52.17; H, 4.66 ; N, 9.89%.

10.13 Synthesis of 3-(thiophen-2-ylthio)-1-(4-(4-(trifluoromethyl)phenyl)piperazin-1-yl)propan-1-one (RTC7) (10)
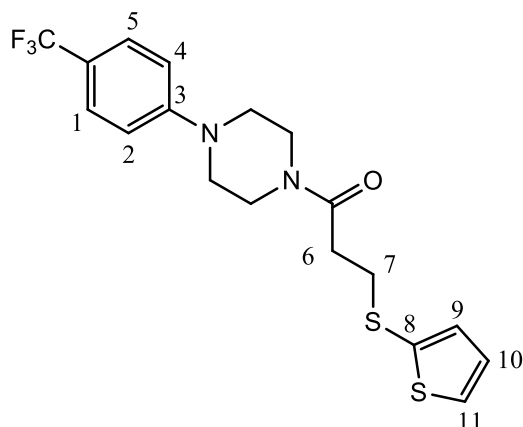
Prepared from 1-(4-trifluoromethyl phenyl)piperazine (50 mg, 0.22 mmol) and compound **30** (37 mg, 0.19 mmol) using HOBt (30 mg, 0.22 mmol), TBTU (70 mg, 0.22 mmol), anhydrous NEt$_3$ (44 µL, 0.32 mmol) and anhydrous DMF (2 mL) and following the general procedure described in section **10.2**. The reaction mixture was stirred overnight at room temperature under a N$_2$ atmosphere. Purified using flash chromatography (3:2 EtOAc:n-hexane) to give a brown solid, 47 mg (63%).

^{1}H NMR: (300 MHz, CDCl$_3$) δ 7.48 (d, J = 8.7 Hz, 2H, H1, H5), 7.34 (dd, J = 5.4 Hz, J = 1.2 Hz, 1H, H11), 7.13 (dd, J = 3.6 Hz, J = 1.2 Hz, 1H, H9), 6.99-6.96 (m, 1H, H10), 6.89 (d, J = 8.7 Hz, 2H, H2, H4), 3.77-3.74 (m, 2H*), 3.57-3.53 (m, 2H*), 3.27-3.22 (m, 2H*), 3.11 (t, J = 7.2 Hz, 2H, H7), 2.67 (t, J = 7.2 Hz, 2H, H6).*Piperazine. **^{13}C NMR:** (75 MHz, CDCl$_3$) δ 169.4 (C=O), 152.8 (C3), 133.97 (C9), 133.95 (C8), 129.5 (C11), 127.7 (C10), 126.5 (q, J = 3.3 Hz, C1, C5), 124.5 (q, J = 270.0 Hz, CF$_3$), 121.3 (q, J = 33.0 Hz, C-CF$_3$), 115.0 (C2, C4), 48.3 (C*), 48.0 (C*), 44.9 (C*), 41.2 (C*), 34.1 (C6), 33.2 (C7). *Piperazine. **R$_f$:** 0.5 (3:2, EtOAc:n-hexane). **HR-MS:** calcd for $C_{18}H_{20}F_3N_2OS_2$ m/z: $[M + H]^+$, 401.0964; found: 401.0969 [Diff (ppm) = 1.22]. **IR (KBr):** 2923 (C-H), 1643 (C=O), 1616 (C=C), 1465 (C=C), 1339 (C-F), 1231 (C-N) cm^{-1}. **m.p.:** 86-90 °C.

10.14 Synthesis of 1-(4-(2-chloro-4-(trifluoromethyl)phenyl)piperazin-1-yl)-4-(thiophen-2-yl)butan-1-one (RTC8) (11)
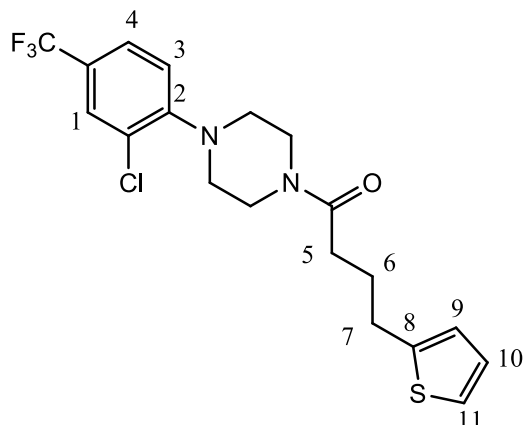
Prepared from compound **31** (90 mg, 0.34 mmol) and 4-(2-thienyl)butyric acid (46 µL, 0.32 mmol) using HOBt (47 mg, 0.34 mmol), TBTU (111 mg, 0.34 mmol), anhydrous NEt$_3$ (47 µL, 0.51 mmol) and anhydrous DMF (3 mL) and following the general procedure described in section **10.2**. The reaction mixture was stirred overnight at room temperature under a N$_2$ atmosphere. Purified using flash chromatography (3:2 EtOAc:Pet. Ether) to give an orange solid, 106 mg (80%).

^{1}H NMR: (300 MHz, CDCl$_3$) δ 7.63-7.62 (m, 1H, H1), 7.47 (dd, J = 8.7 Hz, J = 1.2 Hz, 1H, H4), 7.12 (dd, J = 5.1 Hz, J = 1.0 Hz, 1H, H11), 7.05 (d, J = 8.7 Hz, 1H, H3), 6.93-6.90 (m, 1H, H10), 6.81-6.80 (m, 1H, H9), 3.82-3.79 (m, 2H*), 3.61-3.57 (m, 2H*), 3.07-3.04 (m, 4H*), 2.93 (t, J = 7.2 Hz, 2H, H7), 2.41 (t, J = 7.2 Hz, 2H, H5), 2.10-2.01 (m, 2H, H6).*Piperazine. **^{13}C NMR:** (75 MHz, CDCl$_3$) δ 171.1 (C=O), 151.6 (C2), 144.3 (C8), 128.8 (C-Cl), 127.9 (q, J = 3.3 Hz, C1) 126.8 (C14), 125.9 (q, J = 33.0 Hz, C-CF$_3$), 124.8 (q, J = 3.5 Hz, C4), 124.5 (C13), 123.5 (q, J = 270.0 Hz, CF$_3$), 123.2 (C15), 120.3 (C3), 51.2 (C*), 50.7 (C*),45.5 (C*), 41.6 (C*), 32.0 (C5), 29.2 (C7), 27.0 (C6).*Piperazine. **HR-MS:** calcd for C$_{19}$H$_{21}$F$_3$N$_2$OSCl m/z: [M + H]$^+$, 417.101; found: 401.1017 [Diff (ppm) = 1.74]. **IR (KBr):** 2888 (C-H), 1633 (C=O), 1612 (C=C), 1436 (C=C), 1334 (C-F), 1231 (C-N), 700 (C-Cl) cm^{-1}. **R$_f$:** 0.7 (3:2, EtOAc:Pet. Ether). **m.p.:** 84-86 °C. **Anal. calcd** for C$_{19}$H$_{20}$F$_3$N$_2$OSCl; C, 54.74; H, 4.84; N, 6.72% found; C, 54.73; H, 4.60 ; N, 6.58%.

10.15 Synthesis of 3-(thiophen-2-ylthio)propanoic acid (RD23) (30)[115]
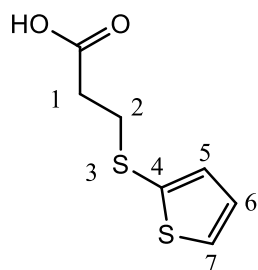
Thienyl-2-thiol (48 μl, 0.52 mmol), 3-bromopropanoic acid (80 mg, 0.52 mmol) and NaHCO₃ (130 mg, 1.56 mmol) were heated at reflux in EtOH (2 mL) and reaction progress monitored by TLC. After, 5 hrs the reaction mixture was allowed to cool to rt and the EtOH was removed under reduced pressure. The residue was dissolved in H₂O (2 mL) and washed with Et₂O (10 mL, followed by 3 x 10 mL). The aqueous layer was acidified to pH = 6 with 0.1 M aqueous HCl and extracted with Et₂O (10 mL, followed by 3 x 10 mL). The combined organic layers were concentrated under reduced pressure and the residue was purified using flash chromatography (1:9, MeOH:DCM) to give a clear oil, 83 mg (85%).

¹H NMR: (300 MHz, CDCl₃) δ 10.86 (br s, 1H, OH), 7.37 (dd, *J* = 5.1 Hz, *J* = 1.2 Hz, 1H, H7), 7.16 (dd, *J* = 2.4 Hz, *J* = 1.2 Hz, 1H, H6), 6.97-6.99 (m, 1H, H5), 2.97 (t, *J* = 7.2 Hz, 2H, H2), 2.64 (t, *J* = 7.2 Hz, 2H, H1). ¹H NMR data matches literature data.[115]
HR-MS: calcd for $C_7H_9O_2S_2$ m/z: [M + H]⁺, 189.0038; found: 189.0040 [Diff (ppm) = 1.05]. **Rf:** 0.3 (1:9, MeOH:DCM).

10.16 Synthesis of 1-(2-chloro-4-(trifluoromethyl)phenyl)piperazine (RD20) (31)
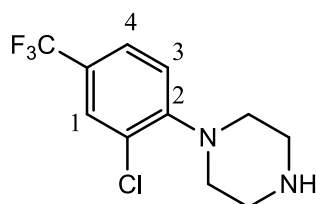
3-Chloro-4-fluorobenzotrifluoride (100 μL, 0.75 mmol) and piperazine (129 mg, 1.5 mmol) were dissolved in NMP (3 mL) and heated at 200 ° C for 30 mins in a microwave reactor. The reaction mixture was purified using flash chromatography (1:9, MeOH:DCM) to give a clear oil, 120 mg (61%).
¹H NMR: (300 MHz, CDCl₃) δ 7.61-7.60 (m, 1H, H1), 7.45 (dd, *J* = 8.4, *J* = 1.5 Hz, 1H, H4), 7.07 (d, *J* = 8.4 Hz, 1H, H3), 3.09 (bs, 8H*), 2.68 (bs, 1H, NH).*Piperazine.

^{1}H NMR data matches literature data.[84] **HR-MS:** calcd for $C_{11}H_{13}ClF_3N_2$ m/z: [M + H]$^+$, 264.06; found: 265.0711 [Diff (ppm) = -1.13]. **R$_f$:** 0.2 (1:9, MeOH:DCM).

10.17 Synthesis of 1-(4-(trifluoromethyl)phenyl)piperazine (RD269) (33)
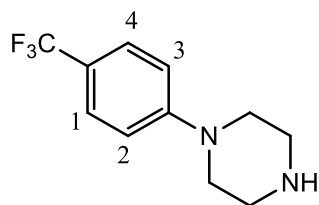
1-chloro-4-(trifluoromethyl)benzene (1.59 mL, 11.91 mmol) and piperazine (2.00 g, 23.82 mmol) were dissolved in NMP (5 mL) and heated at 200 ° C for 30 mins in a microwave reactor. The reaction mixture was purified using flash chromatography (1:9, MeOH:DCM) to give a white solid, 1.42 g (50%).

^{1}H NMR: (300 MHz, CDCl$_3$) δ 7.47 (d, J = 8.4 Hz, 2H, H1, H4), 6.91 (d, J = 8.4 Hz, 2H, H2, H3), 3.24-3.20 (m, 4H*), 3.03-3.00 (m, 2H*), 1.68 (bs, 1H, NH).*Piperazine. ^{1}H NMR data matches literature data.[205] **HR-MS:** calcd for $C_{11}H_{14}F_3N_2$ m/z: [M + H]$^+$, 231.1104; found: 231.1105 [Diff (ppm) = 0.69]. **R$_f$:** 0.2 (1:9, MeOH:DCM).

10.18 Synthesis of 1-(2-bromo-4-(trifluoromethyl)phenyl)piperazine (RD71) (34)
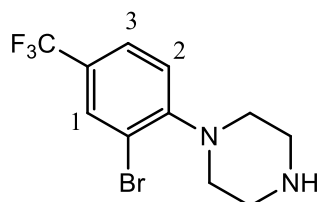
3-Bromo-4-chlorobenzotrifluoride (200 μL, 1.33 mmol) and piperazine (229 mg, 2.66 mmol) were dissolved in NMP (2 mL) and heated at 200 ° C for 30 mins in a microwave reactor. Compound **34** was used without further purification. Clear oil, 95 mg (23%, crude yield).

^{1}H NMR: (300 MHz, CDCl$_3$) δ 7.46 (d, J = 7.8 Hz, 1H, H3), 7.25-7.20 (m, 2H, H1, H2), 3.10 (m, 8H*), 2.95 (bs, 1H, NH).*Piperazine. **R$_f$:** 0.2 (1:9, MeOH:DCM).

10.19 Synthesis of 1-(p-tolyl)piperazine (RD115) (35)[85]
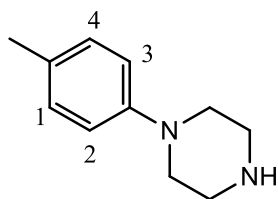
p-Toluidine (1.00 g, 9.34 mmol) and bis(2-chloroethyl)amine.HCl (1.66 g, 9.34 mmol) were dissolved in bis(2-methoxyethyl)ether (20 mL) and heated at reflux for 16 hrs after which the reaction mixture was allowed to cool to rt. Et$_2$O was added until the precipitation of a brown solid was complete. The precipitate was collected *via* vacuum filtration and washed with Et$_2$O (3 x 20 mL) to give the HCl salt of compound **35**, which was then dissolved in a 5% aqueous NaOH solution (10 mL) and stirred at rt for 4 hrs. The aqueous layer was extracted with DCM (10 mL, followed be 3 x 10 mL) and and the combined organic layers were dried over MgSO$_4$. The solvent was removed under reduced pressure and the residue was purified using flash chromatography to give a brown solid, 221 mg (13%).

¹H NMR: (300 MHz, CDCl$_3$) δ 7.07 (d, *J* = 8.4 Hz, 2H, H1, H5), 6.83 (d, *J* = 8.4 Hz, 2H, H2, H4), 3.14-3.13 (m, 4H*), 3.08-3.05 (m, 4H*), 2.26 (s, 3H, CH$_3$).*Piperazine. ¹H NMR data matches literature data.[85] **HR-MS:** calcd for C$_{11}$H$_{17}$N$_2$ m/z: [M + H]$^+$, 177.1385 found: 177.1394 [Diff (ppm) = 4.5]. **R$_f$:** 0.2 (1:9, MeOH:DCM).

10.20 Synthesis of 1-(4-(*tert*-butyl)phenyl)piperazine (RD268) (36)[85]
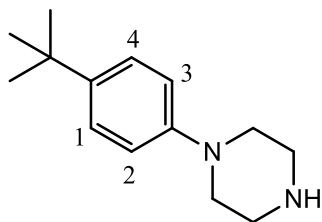
4-(*tert*-Butyl)aniline (500 μL, 3.1 mmol) and bis(2-chloroethyl)amine.HCl were dissolved in bis(2-methoxyethyl)ether (750 μL) and heated at reflux for 16 hrs after which the reaction mixture was allowed to cool to rt. Et$_2$O was added until the precipitation of a brown solid occurred. The precipitate was collected via vacuum filtration and washed with Et$_2$O (3 x 10 mL) to give the HCl salt of compound **36**. The HCl salt (470 mg, 1.84 mmol) was dissolved in 5% aqueous NaOH solution (10 mL) and stirred at rt for 4 hrs. The aqueous layer was extracted with DCM (10 mL, followed

be 3 x 10 mL) and dried over MgSO$_4$.The solvent was removed under reduced pressure to give a brown solid, 352 mg (87%), which was used without any further purification.

^{1}H NMR: (300 MHz, CDCl$_3$) δ 7.33 (d, J = 8.0 Hz, 2H, H1, H4), 6.91 (d, J = 8.0 Hz, 2H, H2, H3), 3.15-3.12 (m, 4H*), 3.05-3.02 (m, 4H*), 1.33 (s, 9H, (CH$_3$)$_3$).*Piperazine. ^{1}H NMR data matches literature data.[206] **HR-MS:** calcd for C$_{12}$H$_{18}$NO m/z: [M + H]$^+$, 192.1383; found: 192.1388 [Diff (ppm) = 2.60].**R$_f$:** 0.2 (1:9, MeOH:DCM).

10.21 Synthesis of piperazin-1-yl(4-(trifluoromethyl)phenyl)methanone (RD212) (37)
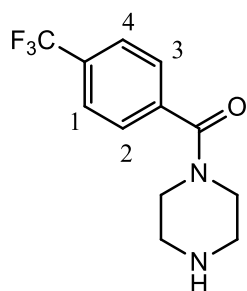
4-(Trifluoromethyl)benzoyl chloride (2.5 mL, 16.82 mmol) in DCM (15 mL) was added dropwise to a solution of piperazine (2.89g, 33.64 mmol) in DCM (15 mL) at 0 °C. The temperature of the reaction mixture was adjusted gradually to rt and stirred overnight at rt. The solvent was removed under reduced pressure and the residue was purified using flash chromatography (1:9; MeOH:DCM) to give an off white solid, 110 mg (3%). Bis-substituted product main species isolated.

^{1}H NMR: (300 MHz, CDCl$_3$, T = 45 °C) δ 7.62 (d, J = 8.7 Hz, 2H, H1, H4), 7.44 (d, J = 8.7 Hz, 2H, H2, H3), 3.49 (bs 4H*), 2.80 (bs, 4H*).*Piperazine. **R$_f$:** 0.2 (1:9, MeOH:DCM). **HR-MS:** calcd for C$_{12}$H$_{14}$F$_3$N$_2$O m/z: [M + H]$^+$, 259.1053; found: 259.1065 [Diff(ppm) = 4.60].

10.22 Synthesis of 1-(4-(trifluoromethyl)benzyl)piperazine (RD265) (38)[117]
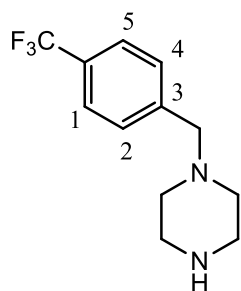
To a solution of 1-(bromomethyl)-4-(trifluoromethyl)benzene (500 mg, 0.21 mmol) in toluene (10 mL) was added piperazine (723 mg, 0.84 mmol) and the solution was heated at 85 °C. After 2 hrs the solution was cooled to rt, filtered and the filtrate was concentrated under reduced pressure. The residue was dissolved in 2 M aqueous HCl (10 mL) and the aqueous layer was washed with DCM (10 mL, followed by 2 x 10 mL). The pH of the aqueous layer was adjusted to pH = 14 with solid NaOH and extracted with DCM (10 mL, followed by 2 x 10 mL). The combined organic layers were dried over MgSO4 and concentrate under reduced pressure. The residue was purified using flash chromatography (1:9 MeOH:DCM) to give a clear oil, 293 mg (57%).

¹H NMR: (300 MHz, CD₃OD) δ 7.57 (d, *J* = 8.1 Hz, 2H, H1, H5), 7.48 (d, *J* = 8.1 Hz, 2H, H2, H4), 3.59 (s, 2H, ArCH₂), 2.85-2.82 (m, 4H*), 2.42 (bs, 4H*).*Piperazine.

R$_f$: 0.2 (1:9, MeOH:DCM). **HR-MS:** calcd for $C_{12}H_{16}F_3N_2$ m/z: $[M + H]^+$, 245.1260; found: 245.1260 [Diff(ppm) = 0.00].

10.23 Synthesis of 1-(4-(4-fluorophenyl)piperazin-1-yl)-4-(thiophen-2-yl)butan-1-one (RTC11) (40)
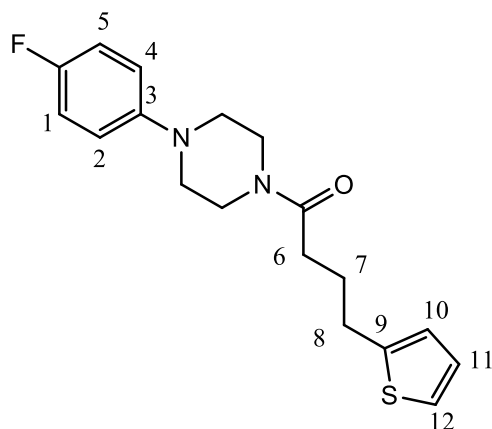
Prepared from 1-(4-fluorophenyl)piperazine (100 mg, 0.55 mmol) and 4-(2-thienyl)butyric acid (73 µL, 0.50 mmol) using HOBt (74 mg, 0.55 mmol), TBTU (177 mg, 0.55 mmol), anhydrous NEt₃ (123 µL, 0.80 mmol) and anhydrous DMF (5 mL) and following the general procedure described in section **10.2**. The reaction mixture was stirred overnight at room temperature under a N₂ atmosphere. Purified using flash chromatography (3:2 EtOAc:*n*-hexane) to give an off white solid, 119 mg (71%).

¹H NMR: (300 MHz, CDCl₃) δ 7.12-7.10 (m, 1H, H12), 6.99-6.80 (m, 5H, H1, H2, H4, H5, H11), 6.80-6.79 (m, 1H, H10), 3.78-3.74 (m, 2H*), 3.56-3.50 (m, 2H*), 3.05-3.02

(m, 4H*), 2.91 (t, J = 7.2 Hz, 2H, H8), 2.39 (t, J = 7.2 Hz, 2H, H6), 2.09-1.99 (m, 2H, H7).*Piperazine. ^{13}C NMR: (75 MHz, CDCl$_3$) 170.9 (C=O), 157.5 (d, J = 238.2 Hz, C-F), 147.6 (d, J = 2.2 Hz, C3), 144.1 (C9), 126.8 (C12), 124.5 (C10), 123.2 (C11), 118.6 (d, J = 7.3 Hz, C2, C4), 115.6 (d, J = 22.5 Hz, C1, C5), 50.7 (C*), 50.4 (C*), 45.4 (C*), 41.5 (C*), 32.0 (C6), 29.2 (C8), 27.0 (C7).*Piperazine. HR-MS: calcd for C$_{18}$H$_{22}$FN$_2$OS m/z: [M + H]$^+$, 333.1431; found 333.1431 [Diff (ppm) = 0.00]. IR (KBr): 2824 (C-H), 1651 (C=O), 1511 (C=C), 1437 (C=C) 1334 (C-F), 1203 (C-N) cm^{-1}. R$_f$: 0.6 (3:2, EtOAc:n-hexane). m.p.: 84-86 °C. Anal. calcd for C$_{18}$H$_{21}$FN$_2$OS; C, 54.74; H, 4.84; N, 6.72% found; C, 54.73; H, 4.60 ; N, 6.58%.

10.24 Synthesis of 4-(thiophen-2-yl)-1-(4-(2-(trifluoromethyl)phenyl)piperazin-1-yl)butan-1-one (RTC20) (41)
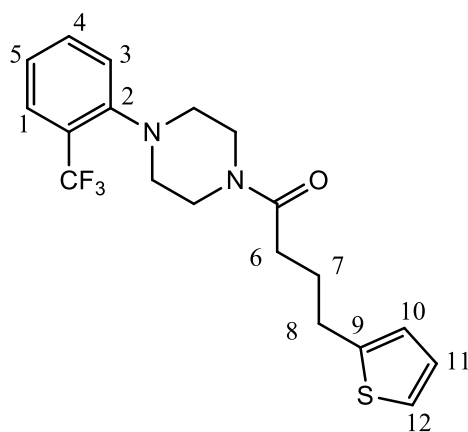
Prepared from 1-(2-(trifluoromethyl)phenyl)piperazine (83 µL, 0.43 mmol) and 4-(2-thienyl)butyric acid (57 µL, 0.39 mmol) using HOBt (58 mg, 0.43 mmol), TBTU (139 mg, 0.43 mmol), anhydrous anhydrous NEt$_3$ (60 µL, 0.62 mmol) and DMF (4 mL) and following the general procedure described in section 10.2. The reaction mixture was stirred overnight at room temperature under a N$_2$ atmosphere. Purified using flash chromatography (3:2 EtOAc:n-hexane) to give an light yellow oil, 74 mg (63%).

^{1}H NMR: (300 MHz, CDCl$_3$) δ 7.65-7.62 (m, 1H, H1), 7.55-7.50 (m, 1H, H4), 7.33-7.23 (m, 2H, H2, H3), 7.12 (dd, J = 5.1 Hz, J = 1.2 Hz, 1H, H12), 6.94 (m, 1H, H11), 6.82-6.81 (m, 1H, H10), 3.81-3.72 (m, 2H*), 3.55-3.52 (m, 2H*), 2.95-2.81 (m, 2H, H6, 4H*), 2.41 (t, J = 7.2 Hz, 2H, H8), 2.10-2.02 (m, 2H, H7).*Piperazine. ^{13}C NMR: (75 MHz, CDCl$_3$) δ 171.1 (C=O), 151.7 (C2), 144.4 (C9), 132.8 (C5), 127.4 (q, J = 28.3 Hz, C-CF$_3$), 127.2 (q, J = 3.3 Hz, C1), 126.8 (C11), 125.4 (C12), 124.5 (C10), 124.0 (C4),

123.9 (q, J = 271.1 Hz, CF$_3$), 123.1 (C3) 53.7 (C*), 53.0 (C*), 46.0 (C*), 42.0 (C*), 32.1 (C8), 29.3 (C6), 27.0 (C7).*Piperazine. **R$_f$:** 0.5 (3:2, EtOAc:*n*-hexane). **HR-MS:** calcd for C$_{19}$H$_{22}$F$_3$N$_2$OS m/z: [M + H]$^+$, 383.1399; found: 383.1412 [Diff (ppm) = 3.39]. **IR (neat):** 2919 (C-H), 1646 (C=O), 1587 (C=C), 1453 (C=C), 1315 (C-F), 1144 (C-N) cm^{-1}

## 10.25 Synthesis of 1-(4-(4-nitrophenyl)piperazin-1-yl)-4-(thiophen-2-yl)butan-1-one (RTC22) (42)
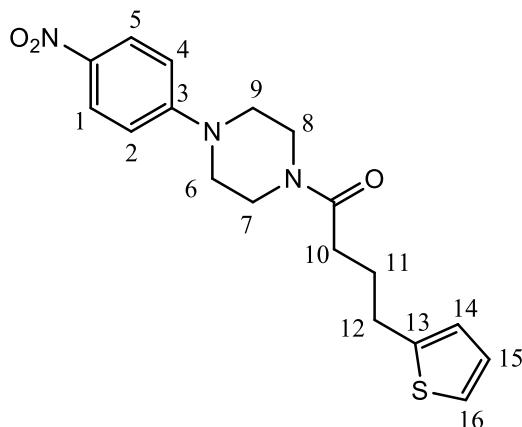
Prepared from 1-(4-nitrophenyl)piperazine (150 mg, 0.72 mmol) and 4-(2-thienyl)butyric acid (95 μL, 0.66 mmol) using HOBt (97 mg, 0.72 mmol), TBTU (232 mg, 0.72 mmol), anhydrous NEt$_3$ (146 μL, 1.05 mmol) and anhydrous DMF (6 mL) and following the general procedure described in section **10.2**. The reaction mixture was stirred overnight at room temperature under a N$_2$ atmosphere. Purified using flash chromatography (7:3 EtOAc:DCM) to give an orange solid, 178 mg (75%).

^{1}H NMR: (300 MHz, CDCl$_3$) δ 8.08 (d, J = 9.1 Hz, 2H, H1, H5), 7.11 (dd, J = 5.1 Hz, J = 1.2 Hz, 1H, H16), 6.93-6.90 (m, 2H, H15), 6.81-6.769 (m, 3H, H2, H4, H14), 3.81-3.77 (m, 2H*), 3.71-3.68 (m, 2H*), 3.46-3.41 (m, 4H*), 2.92 (t, J = 7.2 Hz, 2H, H12), 2.41 (t, J = 7.2 Hz, 2H, H10), 2.10-2.00 (m, 2H, H11).*Piperazine. **^{13}C NMR:** (75 MHz, CDCl$_3$) δ 171.2 (C=O), 154.3 (C3), 144.3 (C13), 138.6 (C-NO$_2$), 126.8 (C14), 125.9 (C1, C5), 124.5 (C15), 123.2 (C16), 112.7 (C2, C4), 46.7 (C*), 46.6 (C*), 44.5 (C*), 40.7 (C*).*Piperazine. **R$_f$:** 0.7 (7:3, EtOAc:DCM). **HR-MS:** calcd for C$_{18}$H$_{22}$N$_3$O$_3$S m/z: [M + H]$^+$, 360.1376; found: 360.1387 [Diff (ppm) = 3.05]. **IR (KBr):** 2856 (C-H), 1650 (C=O), 1600 (C=C), 1584 (NO), 1479 (C=C), 1324 (NO) cm^{-1}. **m.p.:** 120-121 °C.

10.26 Synthesis of 1-(4-(3,5-bis(trifluoromethyl)phenyl)piperazin-1-yl)-4-(thiophen-2-yl)butan-1-one (RTC26) (43)

Prepared from 1-(3,5-bis(trifluoromethyl)phenyl)piperazine (192 mg, 0.65 mmol) and 4-(2-thienyl)butyric acid (85 µL, 0.58 mmol) using HOBt (87 mg, 0.65 mmol), TBTU (207 mg, 0.65 mmol), anhydrous NEt_3 (129 µL, 0.92 mmol) and anhydrous DMF (5 mL) and following the general procedure described in section **10.2**. The reaction mixture was stirred overnight at room temperature under a N_2 atmosphere. Purified using flash chromatography (3:2 EtOAc:*n*-hexane) to give an off white solid, 103 mg (39%).

1H NMR: (300 MHz, CDCl$_3$) δ 7.33 (s, 1H, H1), 7.26 (s, 2H, H2), 7.13 (dd, J = 5.1 Hz, J = 1.2 Hz, H10), 6.96-6.91 (m, 1H, H9), 6.82-6.80 (m, 1H, H8), 3.82-3.79 (m, 2H*), 3.61-3.58 (m, 2H*), 3.29-3.25 (m, 4H*), 2.93 (t, J = 7.2 Hz, 2H, H6), 2.41 (t, J = 7.2 Hz, 2H, H4), 2.11-2.01 (m, 2H, H5).*Piperazine. **13C NMR:** (75 MHz, CDCl$_3$) δ 170.0 (C=O), 150.2 (C3), 143.2 (C7), 131.4 (q, J = 33.2 Hz, *C*-CF$_3$), 125.8 (C9), 123.5 (C8), 122.4 (q, J = 271.4 Hz, CF$_3$), 122.2 (C10), 114.1 (m, C2), 117.0 (m, C1), 47.3 (C*), 47.2 (C*), 43.8 (C*), 40.0 (C*), 30.8 (C6), 28.1 (C4), 25.8 (C5).*Piperazine. **R$_f$:** 0.5 (1:1, EtOAc:*n*-hexane). **HR-MS:** calcd for C$_{20}$H$_{21}$F$_6$N$_2$OS m/z: [M + H]$^+$, 451.1273; found: 451.1288 [Diff (ppm) = 3.25]. **IR (KBr):** 2950 (C-H), 1657 (C=O), 1621 (C=C), 1440 (C=C), 1315 (C-F), 1275 (C-N) cm^{-1}. **m.p.:** 46-49 °C. **Anal. calcd** for C$_{20}$H$_{20}$F$_6$N$_2$OS; C, 53.33; H, 4.48; N, 6.22% found: C, 53.41; H, 4.25; N, 6.27%.

10.27 Synthesis of 1-(4-methylpiperazin-1-yl)-4-(thiophen-2-yl)butan-1-one (RTC 32) (44)
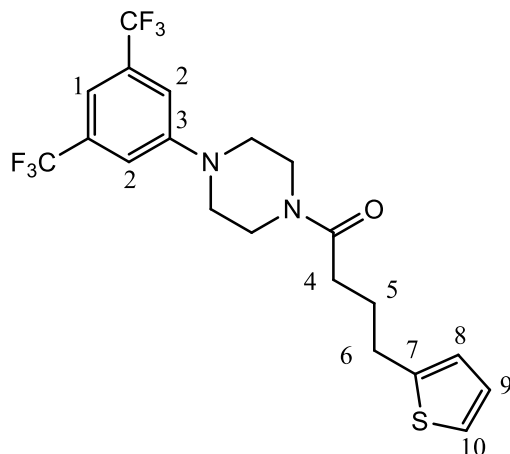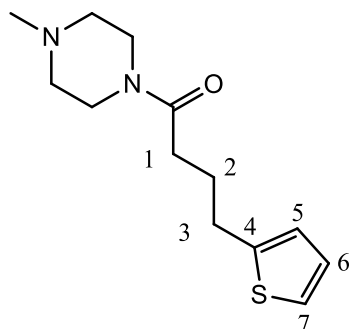

Prepared from 1-methylpiperazine (71 µL, 0.65 mmol) and 4-(2-thienyl)butyric acid (85 µL, 0.59 mmol) using HOBt (87 mg, 0.65 mmol), TBTU (207 mg, 0.65 mmol), anhydrous NEt$_3$ (90 µL, 0.94 mmol) and anhydrous DMF (4 mL) and following the general procedure described in section **10.2**. The reaction mixture was stirred overnight at room temperature under a N$_2$ atmosphere. Purified using flash chromatography (3:2, EtOAc:*n*-hexane) to give a yellow oil, 15 mg (10%).

¹H NMR: (300 MHz, CDCl$_3$) δ 7.12 (dd, J = 5.1 Hz, J = 1.2 Hz, 1H, H7), 6.93-6.90 (m, 1H, H6), 6.80-6.79 (m, 1H, H5), 3.64-3.61 (m, 2H*), 3.43-3.40 (m, 2H*), 2.90 (t, J = 7.2 Hz, 2H, H3), 2.38-2.33 (m, 4H*, 2H, H1), 2.29 (s, 3H, CH$_3$), 2.07-1.97 (m, 2H, H2).*Piperazine. **¹³C NMR:** (75 MHz, CDCl$_3$) δ 170.9 (C=O), 144.4 (C4), 126.7 (C6), 124.4 (C5), 123.1 (C7), 55.1 (C*), 54.7 (C*), 46.0 (CH$_3$), 45.3 (C*), 41.4 (C*), 32.0 (C1), 29.3 (C3), 27.0 (C2).*Piperazine. **R$_f$:** 0.5 (3:2, EtOAc:*n*-hexane). **HR-MS:** calcd for C$_{13}$H$_{21}$N$_2$OS m/z: [M + H]$^+$, 253.1369; found: 253.1375 [Diff (ppm) = 2.37]. **IR (neat):** 1630 (C=O), 1290 (C-N) cm^{-1}.

10.28 Synthesis of 1-(4-(6-chloro-5-(trifluoromethyl)pyridin-2-yl)piperazin-1-yl)-4-(thiophen-2-yl)butan-1-one (RTC44) (45)
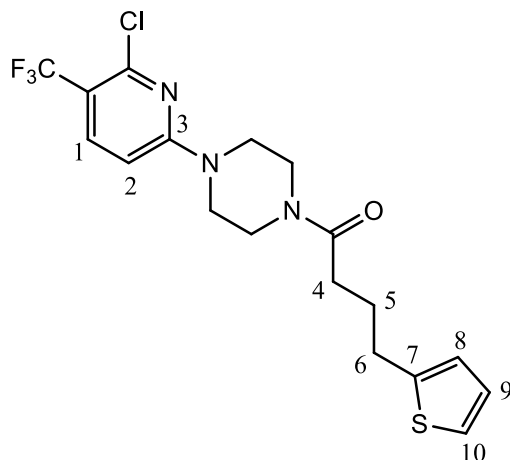
Prepared from 1-(6-chloro-5-(trifluoromethyl)pyridin-2-yl)piperazine (218 mg, 0.816 mmol) and 4-(2-thienyl)butyric acid (100 μL, 0.68 mmol) using HOBt (110 mg, 0.82 mmol), TBTU (262 mg, 0.82 mmol), anhydrous NEt$_3$ (152 μL, 1.08 mmol) and anhydrous DMF (5 mL) and following the general procedure described in section **10.2**. The reaction mixture was stirred overnight at room temperature under a N$_2$ atmosphere. Purified using flash chromatography (3:2 EtOAc:Pet. Ether) to give a beige solid, 192 mg (68%).

^{1}H NMR: (300 MHz, CDCl$_3$) δ 7.67 (d, J = 9.0 Hz, 1H, H1), 7.11 (dd, J = 5.1 Hz, J = 1.2 Hz, 1H, H10), 6.92-6.89 (m, 1H, H9), 6.80-6.79 (m, 1H, H8), 6.47 (d, J = 9.0 Hz, 1H, H2), 3.72-3.67 (m, 4H*), 3.59-3.57 (m, 2H*), 3.52-3.49 (m, 2H*), 2.91 (t, J = 8.1 Hz, 2H, H4), 2.39 (t, J = 7.2 Hz, 2H, H6), 2.09-1.99 (m, 2H, H5). *Piperazine. **^{13}C NMR:** (75 MHz, CDCl$_3$) δ 171.2 (C=O), 158.9 (C7), 147.5 (C-Cl), 144.2 (C7), 137.7 (q, J = 3.3 Hz, C1), 126.8 (C9), 124.5 (C8), 123.2 (q, J = 268.8 Hz, CF$_3$), 123.2 (C10), 112.7 (q, J = 33.0 Hz, C-CF$_3$), 103.2 (C2), 43.7 (C*), 43.4 (C*), 43.1 (C*), 39.7 (C*), 30.9 (C6), 28.1 (C4), 25.6 (C7). *Piperazine. **R$_f$:** 0.5 (3:2, EtOAc:n-hexane). **HR-MS:** calcd for C$_{18}$H$_{20}$ClF$_3$N$_3$OSCl m/z: [M + H]$^+$, 418.0962; found: 418.0953 [Diff (ppm) = -2.23]. **IR (KBr):** 2904 (C-H), 1678 (C=O), 1641 (C=C), 1416 (C=C), 1321 (C-F), 1120 (C-N), 698 (C-Cl) cm^{-1}. **m.p.:** 62-64 °C.

10.29 Synthesis of 1-(4-(2-bromo-4-(trifluoromethyl)phenyl)piperazin-1-yl)-4-(thiophen-2-yl)butan-1-one (RTC62) (46)
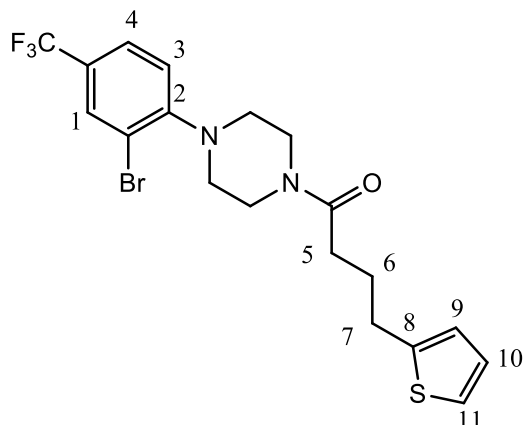
Prepared from compound **34** (95 mg, 0.30 mmol) and 4-(2-thienyl)butyric acid (41 μL, 0.28 mmol) using HOBt (41 mg, 0.30 mmol), TBTU (98 mg, 0.30 mmol), anhydrous NEt$_3$ (62 μL, 0.44 mmol) and anhydrous DMF (2 mL) and following the general procedure described in section **10.2**. The reaction mixture was stirred overnight at room temperature under a N$_2$ atmosphere. Purified using flash chromatography (1:1 EtOAc:Pet. Ether to give a clear oil, 60 mg (50%).

¹H NMR: (300 MHz, CDCl$_3$) δ 7.82 (s, 1H, H1), 7.53 (d, J = 8.7 Hz, 1H, H4), 7.12 (dd, J = 5.1 Hz, J = 1.2 Hz, 1H, H11), 7.05 (d, J = 8.7 Hz, 1H, H3), 6.94-6.91 (m, 1H, H10), 6.82-6.80 (m, 1H, H9), 3.83-3.80 (m, 2H*), 3.61-3.58 (m, 2H*), 3.06-3.03 (m, 4H*), 2.93 (t, J = 7.2 Hz, 2H, H7), 2.41 (t, J = 7.2 Hz, 2H, H5), 2.11-2.01 (m, 2H, H6). *Piperazine. **¹³C NMR:** (75 MHz, CDCl$_3$) 171.1 (C=O), 153.0 (C2), 144.3 (C8), 131. (q, J = 3.3 Hz, C1), 126.8 (C10), 126.3 (q, J = 33.0 Hz, C-CF$_3$), 125.5 (q, J = 3.3 Hz, C4), 124.5 (C9), 123.3 (q, J = 270.0 Hz, CF$_3$), 123.2 (C11), 120.8 (C3), 119.4 (C-Br), 51.6 (C*), 51.1 (C*), 45.6 (C*), 41.6 (C*), 32.0 (C7), 29.3 (C5), 27.0 (C6). *Piperazine. **R$_f$:** 0.8 (1:1 EtOAc:Pet. Ether). **HR-MS:** calcd for C$_{19}$H$_{20}$BrF$_3$N$_2$OSK m/z: [M + K]$^+$, 499.0063; found: 499.0079 [Diff (ppm) = 3.1]. **IR (neat):** 2914 (C-H), 1645 (C=O), 1605 (C=C), 1432 (C=C), 1324 (C-F), 1122 (C-N), 680 (C-Br) cm^{-1}.

10.30 Synthesis of 1-(4-phenylpiperazin-1-yl)-4-(thiophen-2-yl)butan-1-one (RTC162) (47)
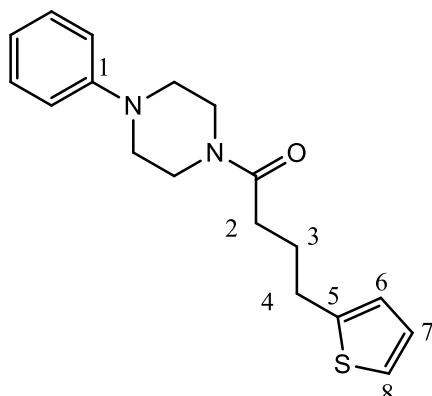
Prepared from 1-phenylpiperazine (100 µL, 0.64 mmol) and 4-(2-thienyl)butyric acid (84 µL, 0.58 mmol) using HOBt (86 mg, 0.64 mmol), TBTU (205 mg, 0.64 mmol), anhydrous NEt_3 (129 µL, 0.93 mmol) and anhydrous DMF (5 mL) and following the general procedure described in section **10.2**. The reaction mixture was stirred overnight at room temperature under a N_2 atmosphere. Purified using flash chromatography (3:2 EtOAc:*n*-hexane) to give a dark red oil, 109 mg (59%).

^{1}H NMR: (300 MHz, $CDCl_3$) δ 7.34-7.28 (m, 2H, Ar), 7.15 (dd, J = 5.1 Hz, J = 1.2 Hz, 1H, H8), 6.97-6.93 (m, 4H, Ar, H7), 6.85-6.84 (m, 1H, H6), 3.82-3.78 (m, 2H*), 3.58-3.55 (m, 2H*), 3.17-3.14 (m, 4H*), 2.96 (t, J = 7.2 Hz, 2H, H4), 2.43 (t, J = 7.2 Hz, 2H, H2), 2.14-2.04 (m, 2H, H3).*Piperazine. **^{13}C NMR:** (75 MHz, $CDCl_3$) δ 171.0 (C=O), 151.0 (C1), 144.5 (C5), 129.2 (Ar), 126.8 (C6), 124.5 (C8), 123.2 (C7), 120.5 (Ar), 116.6 (Ar), 49.7 (C*), 49.3 (C*), 45.4 (C*), 41.5 (C*), 32.0 (C6), 29.3 (C8), 27.0 (C7). **R_f:** 0.6 (3:2, EtOAc:*n*-hexane). **HR-MS:** calcd for $C_{18}H_{23}N_2OS$ m/z: $[M + H]^+$, 315.1526; found: 315.1527 [Diff (ppm) = 0.45]. **IR (KBr):** 2915 (C-H), 1669 (C=O), 1643 (C=C), 1439 (C=C), 1230 (C-N) cm^{-1}.

10.31 Synthesis of 4-(thiophen-2-yl)-1-(4-(p-tolyl)piperazin-1-yl)butan-1-one (RTC33) (48)†

Prepared from compound **35** (221 mg, 1.25 mmol) and 4-(2-thienyl)butyric acid (166 µL, 1.13 mmol) using HOBt (168 mg, 1.25 mmol), TBTU (401 mg, 1.25 mmol), anhydrous NEt_3 (253 µL, 1.82 mmol) and anhydrous DMF (5mL) and following the general procedure described in section **10.2**. The reaction mixture was stirred overnight at room temperature under a N_2 atmosphere. Purified using flash chromatography (1:1 EtOAc:*n*-hexane) to give an orange oil, 102 mg (24%).

^{1}H NMR: (300 MHz, CDCl$_3$) δ 7.16-7.11 (m, 3H, H1, H5, H12), 6.97-6.94 (m, 1H, H11), 6.88-6.83 (m, 3H, H2, H4, H10), 3.81-3.78 (m, 2H*), 3.59-3.55 (m, 2H*), 3.12-3.08 (m, 4H*), 2.95 (t, *J* = 7.2 Hz, 2H, H8), 2.43 (t, *J* = 7.2 Hz, 2H, H6), 2.31 (s, 3H, CH$_3$), 2.13-2.04 (m, 2H, H7).*Piperazine. **^{13}C NMR:** (75 MHz, CDCl$_3$) δ 170.9 (C=O), 148.8 (C3), 144.4 (C9), 130.1 (*C*-CH$_3$), 129.7 (C1, C5), 126.8 (C10), 124.5 (C12), 123.2 (C11), 117.0 (C2, C4), 50.3 (C*), 49.9 (C*), 45.5 (C*), 41.5 (C*), 32.0 (C6), 29.3 (C8), 27.0 (C7), 20.5 (CH$_3$).*Piperazine. **R$_f$:** 0.3 (1:1, EtOAc:*n*-hexane). **HR-MS:** calcd for C$_{19}$H$_{25}$N$_2$OS m/z: [M + H]$^+$, 329.1682; found: 329.1687 [Diff (ppm) = 1.56]. **IR (neat):** 2917 (C-H), 1642 (C=O), 1439 (C=C), 1232 (C-N) cm^{-1}.

10.32 Synthesis of 1-(4-(4-(*tert*-butyl)phenyl)piperazin-1-yl)-4-(thiophen-2-yl)butan-1-one (RTC72) (49)†
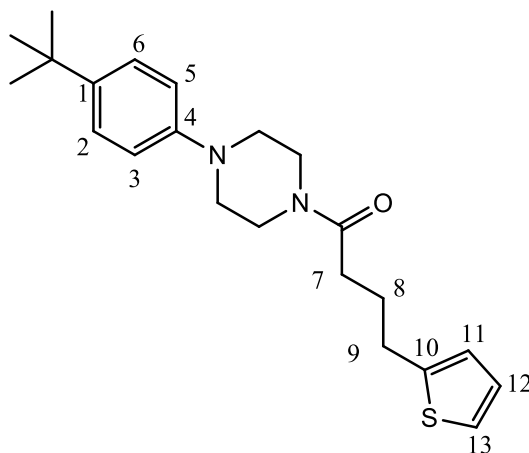
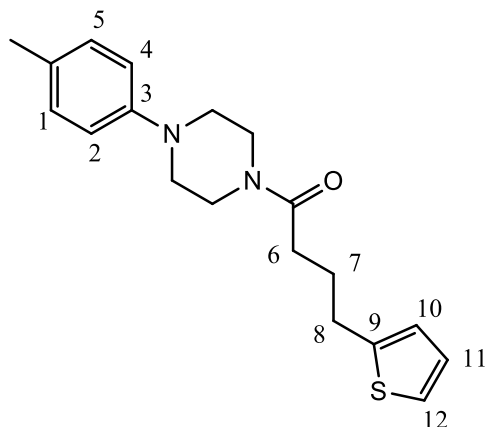

Prepared from compound **36** (200 mg, 0.92 mmol) and 4-(2-thienyl)butyric acid (121 µL, 0.83 mmol) using HOBt (123 mg, 0.92 mmol), TBTU (294 mg, 0.92 mmol), anhydrous NEt$_3$ (185 µL, 1.33 mmol) and anhydrous DMF (6 mL) and following the general procedure described in section **10.2**. The reaction mixture was stirred overnight at room temperature under a N$_2$ atmosphere. Purified using flash chromatography (3:2 EtOAc:*n*-hexane) to give a deep red oil, 292 mg (86%).

^{1}H NMR: (300 MHz, CDCl$_3$) δ 7.35 (d, *J* = 8.1 Hz, 2H, H3, H5), 7.16 (dd, *J* = 5.1 Hz, *J* = 1.2 Hz, H13), 6.97-6.95 (m, 1H, H12), 6.91 (d, *J* = 8.1 Hz, H2, H6), 6.86-6.84 (m, 1H, H11), 3.83-3.79 (m, 2H*), 3.60-3.57 (m, 2H*), 3.16-3.13 (m, 4H*), 2.96 (t, *J* = 7.2 Hz, 2H, H9), 2.45 (t, *J* = 7.2 Hz, 2H, H7), 2.14-2.03 (m, 2H, H8), 1.34 (s, 9H, (CH$_3$)$_3$). *Piperazine. **^{13}C NMR:** (75 MHz, CDCl$_3$) δ 171.1 (C=O), 148.5 (C4), 144.4 (C10), 143.4 (C1), 126.8 (C12), 126.4 (C5, C3), 124.5 (C11), 123.3 (C13), 116.0 (C6, C2), 50.0 (C*), 49.7 (C*), 45.5 (C*), 41.6 (C*), 34.0 (*C*(CH$_3$)$_3$), 32.0 (C7), 31.4 ((CH$_3$)$_3$), 29.3 (C9), 27.0 (C8). *Piperazine. **R$_f$:** 0.5 (3:2, EtOAc:Pet. Ether). **HR-MS:** calcd for C$_{22}$H$_{31}$F$_3$N$_2$OS m/z: [M + H]$^+$, 371.2152; found 371.2170 [Diff (ppm) = 4.84]. **IR (neat):** 2961 (C-H), 1643 (C=O), 1610 (C=C), 1450 (C=C), 1229 (C-N) cm^{-1}.

10.33 Synthesis of 4-(thiophen-2-yl)-1-(4-(4-(trifluoromethyl)benzoyl)piperazin-1-yl)butan-1-one (RTC86) (50)†
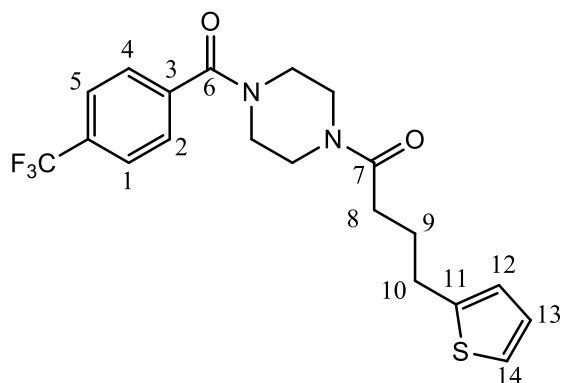
Prepared from compound **37** (50 mg, 0.19 mmol) and 4-(2-thienyl)butyric acid (34 µL, 0.17 mmol) using HOBt (27 mg, 0.19 mmol), TBTU (61 mg, 0.19 mmol), anhydrous NEt3 (38 µL, 0.28 mmol) and anhydrous DMF (3 mL) and following the general procedure described in section **10.2**. The reaction mixture was stirred overnight at room temperature under a N_2 atmosphere. Purified using flash chromatography (1:1 EtOAc:Pet. Ether) to give a clear oil, 36 mg (50%).

¹H NMR: (300 MHz, CDCl₃) δ 7.70 (d, *J* = 8.4 Hz, 2H, H1, H5), 7.52 (d, *J* = 8.4 Hz, 2H, H2, H4), 7.13-7.11 (m, 1H, H14), 6.93-6.90 (m, 1H, H13), 6.82-6.76 (m, 1H, H12), 3.74-3.39 (m, 8H*), 2.91 (t, *J* = 7.1 Hz, 2H, H10), 2.38 (bs, 2H, H8), 2.08-1.98 (m, 2H, H9).*Piperazine. **¹³C NMR:** (75 MHz, CDCl₃) δ 171.2 (C6), 169.1 (C7), 144.1 (C3), 138.6 (C11), 132.0 (q, *J* = 32.7 Hz, *C*-CF₃), 127.4 (C2, C4), 126.8 (C13), 125.7 (q, *J* = 3.3 Hz, C1, C5), 124.5 (C12), 123.6 (q, *J* = 270.0 Hz, CF₃), 123.3 (C14), 47.4 (C*), 45.1 (C*), 42.2 (C*), 41.6 (C*), 31.9 (C8), 29.1 (C10), 26.8 (C9).*Piperazine. **Rf:** 0.5 (1:1, EtOAc:Pet. Ether). **HR-MS:** calcd for $C_{20}H_{22}F_3N_2O_2S$ m/z: [M + H]⁺,411.1349; found: 411.1355 [Diff (ppm) = 1.52]. **IR (neat):** 2952 (C-H), 1650 (C=O), 1631 (C=C), 1433 (C=C), 1324 (C-F), 1161 (C-N) cm⁻¹.

10.34 Synthesis of 4-(thiophen-2-yl)-1-(4-(4-(trifluoromethyl)benzyl)piperazin-1-yl)butan-1-one (RTC95) (51)†
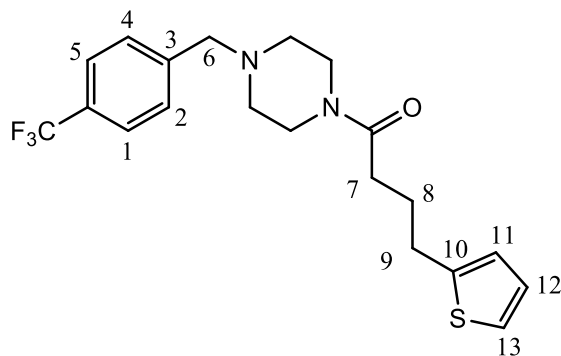
Prepared from compound **38** (293 mg, 1.19 mmol) and 4-(2-thienyl)butyric acid (158 μL, 1.08 mmol) using HOBt (162 mg, 1.19 mmol) TBTU (385 mg, 1.19 mmol), anhydrous NEt_3 (167 μL, 1.73 mmol) and anhydrous DMF (8 mL) and following the general procedure described in section **10.2**. The reaction mixture was stirred overnight at room temperature under a N_2 atmosphere. Purified using flash chromatography (1:1 EtOAc:Pet. Ether) to give an orange oil, 302 mg (73%).

^{1}H NMR: (300 MHz, $CDCl_3$) δ 7.57 (d, J = 8.1 Hz, 2H, H1, H5), 7.4 (d, J = 8.1 Hz, 2H, H2, H4), 7.09 (dd, J = 5.1 Hz, J = 1.0 Hz, 1H, H13), 6.79-6.78 (m, 1H, H12), 6.79-6.78 (m, 1H, H11), 3.64-3.61 (m, 2H*), 3.54 (s, 2H, H6), 3.42-3.38 (m, 2H*), 2.89 (t, J =7.9 Hz, 2H, H9), 2.42-2.37 (m, 4H*), 2.34 (t, J = 7.5 Hz, 2H, H7), 2.06-1.96 (m, 2H, H8).*Piperazine. **^{13}C NMR:** (75 MHz, $CDCl_3$) δ 171.0 (C=O), 144.4 (C3), 141.8 (C10), 129.4 (q, J = 31.0 Hz, C-CF_3), 129.2 (C11), 126.7 (C13), 125.2 (q, J = 3.3 Hz, C1, C5), 124.5 (C12), 124.2 (q, J = 270.0 Hz, CF_3), 123.1 (C2, C4), 62.1 (C6), 53.0 (C*), 52.7 (C*), 45.3 (C*), 41.4 (C*), 41.4 (C*), 32.0 (C7), 29.2 (C9), 27.0 (C8).*Piperazine. **R_f:** 0.5 (1:1, EtOAc:Pet. Ether). **HR-MS:** calcd for $C_{20}H_{24}F_3N_2OS$ m/z: [M + H]$^+$, 398.1587; found: 98.1604 [Diff (ppm) = 4.50]. **IR (neat):** 2940 (C-H), 1638 (C=O), 1616 (C=C), 1439 (C=C), 1326 (C-F), 1164 (C-N) cm^{-1}.

10.35 Synthesis of 1-(4-cyclohexylpiperazin-1-yl)-4-(thiophen-2-yl)butan-1-one (RTC13) (52)
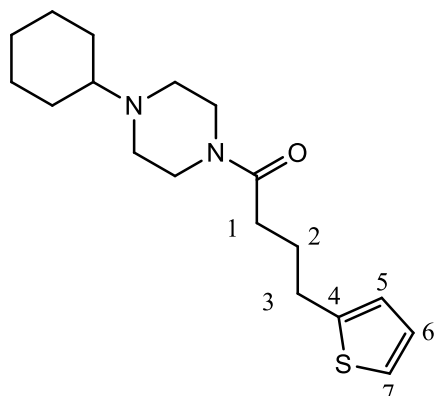
Prepared from 1-cyclohexylpiperazine (150 mg, 0.89 mmol) and 4-(2-thienyl)butyric acid (118 μL, 0.81 mmol) using HOBt (120 mg, 0.89 mmol), TBTU (285 mg, 0.89 mmol), anhydrous NEt_3 (180 μL, 1.29 mmol) and anhydrous DMF (6 mL) and following the general procedure described in section **10.2**. The reaction mixture was stirred overnight at room temperature under a N_2 atmosphere. Purified using flash chromatography (3:2 EtOAc:*n*-hexane) to give an orange solid, 76 mg (70%).

^{1}H NMR: (300 MHz, CDCl$_3$) δ 7.10 (d, *J* = 4.8 Hz, 1H, H7), 6.92-6.89 (m, 1H, H6), 6.79-6.78 (m, 1H, H5), 3.63-3.60 (m, 2H*), 3.42-3.39 (m, 2H*), 2.89 (t, *J* = 7.5 Hz, 2H, H3), 2.54-2.51 (m, 4H*), 2.37-2.26 (m, 3H, H1, N-CH), 2.06-1.98 (m, 2H, H2), 1.84-1.78 (m, 4H, Cy), 1.26-1.11 (m, 6H, Cy).*Piperazine. **^{13}C NMR:** (75 MHz, CDCl$_3$) δ 170.7 (C=O), 144.4 (C4), 126.7 (C6), 124.4 (C5), 123.1 (C7), 63.6 (N-CH), 49.2 (C*), 48.6 (C*), 45.8 (C*), 41.8 (C*), 32.0 (C3), 29.3 (C1), 28.7 (Cy), 27.0 (C2), 26.1 (Cy), 25.7 (Cy).*Piperazine. **R$_f$:** 0.5 (3:2, EtOAc:*n*-hexane). **HR-MS:** calcd for $C_{18}H_{29}N_2OS$ m/z: [M + H]$^+$, 321.1995; found: 321.005 [Diff (ppm) = 3.10]. **IR (KBr):** 2928 (C-H), 1634 (C=O), 1233 (C-N) cm^{-1} **m.p.:** 33-35 °C.

10.36 Synthesis of 4-(thiophen-2-yl)-*N'*-(4-(trifluoromethyl)phenyl)butane hydrazide (RTC21) (53)
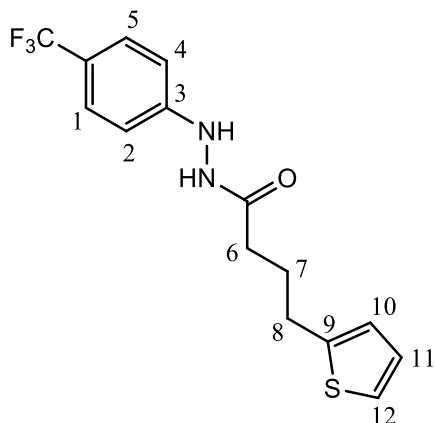
Prepared from (4-(trifluoromethyl)phenyl)hydrazine (195 mg, 1.11 mmol) and 4-(2-thienyl)butyric acid (149 µL, 1.03 mmol) using HOBt (149 mg, 1.11 mmol), TBTU (356 mg, 1.11 mmol), anhydrous NEt_3 (231 µL, 1.66 mmol) and anhydrous DMF (8 mL) and following the general procedure described in section **10.2**. The reaction mixture was stirred overnight at room temperature under a N_2 atmosphere. Purified using flash chromatography (elution gradient 1:1 EtOAc:*n*-hexane to 3:2 EtOAc:*n*-hexane) to give an off white solid, 235 mg (69%).

¹H NMR: (300 MHz, $CDCl_3$) δ 7.44 (d, *J* = 8.7 Hz, 2H, H1, H5), 7.36 (bs, 1H, Ar-NH), 7.15-7.14 (m, 1H, H12), 6.95-6.92 (m, 1H, H11), 6.83-6.78 (m, 3H, H2, H4, H10), 6.38 (bs, 1H, HN-C=O), 2.91 (t, *J* = 7.2 Hz, 2H, H8), 2.31 (t, *J* = 7.2 Hz, 2H, H6), 2.11-2.02 (m, 2H, H7). **¹³C NMR:** (75 MHz, $CDCl_3$) δ 172.7 (C=O), 150.7 (C3), 143.6 (C9), 128.7 (q, *J* = 288.4 Hz, CF_3), 126.9 (C11), 126.6 (q, *J* = 3.3 Hz, C1, C5), 124.7 (C10), 123.4 (C12), 123.0 (q, *J* = 34.2 Hz, *C*-CF_3), 112.7 (C2, C4), 32.9 (C8), 29.0 (C6), 26.9 (C7). **R_f:** 0.3 (1:1, EtOAc:*n*-hexane). **HR-MS:** calcd for $C_{15}H_{16}F_3N_2OS$ m/z: $[M + H]^+$, 330.0975; found: 330.096 [Diff (ppm) = 4.83]. **IR (KBr):** 3309 (N-H), 2963 (C-H), 1639 (C=O), 1614 (N-H), 1333 (C-F), 1104 (C-N) cm^{-1}. **m.p.:** 110-112 °C. **Anal. calcd** for $C_{15}H_{15}F_3N_2OS$; C, 54.87; H, 4.60; N, 8.53% found: C, 54.44; H, 4.39; N, 8.09%.

10.37 Synthesis of 4-(thiophen-2-yl)-1-(4-(4-(trifluoromethyl)phenyl)piperidin-1-yl)butan-1-one (RTC196) (54)
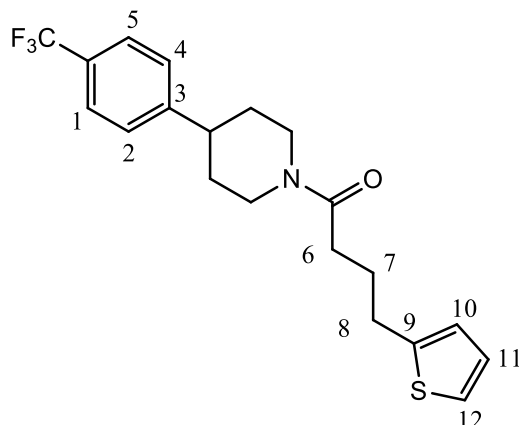
4-(2-Thienyl)butyric acid (50 µL, 0.34 mmol), HOBt (51 mg, 0.38 mmol), TBTU (122 mg, 0.38 mmol), anhydrous NEt_3 (55 µL, 0.54 mmol) and anhydrous DMF (2 mL) were placed in an oven-dried Schlenk tube under a N_2 atmosphere. The resulting solution was stirred at rt for 20 mins. A second Schlenk tube, containing 4-(4-(trifluoromethyl)phenyl)piperidine.HCl (100 mg ,0.38 mmol) and anhydrous NEt_3 (55 µL, 0.54 mmol) in anhydrous DMF (2 mL) was stirred for 15 mins under a N_2 atmosphere before transfer, *via* a cannula, to the first Schlenk tube containing the carboxylic acid. The solution was stirred under N_2 at rt. After 24 hrs, the DMF was removed under reduced pressure and the resulting oil was acidified (pH = 3) using a 0.1 M aqueous HCl solution. The aqueous mixture was extracted with DCM (20 mL, followed by 4 x 10 mL). The organic combined layers were washed with a saturated aqueous solution of Na_2CO_3 (3 x 20 mL) and brine (3 x 20 mL) and dried over $MgSO_4$ and the residue was purified using flash chromatography (3:2 EtOAc:*n*-hexane) to give an off white solid, 63 mg (48%).

^{1}H NMR: (300 MHz, CDCl$_3$) δ 7.56 (d, *J* = 8.7 Hz, 2H, H1, H5), 7.29 (d, *J* = 8.7 Hz, 2H, H2, H4), 7.12 (dd, *J* = 5.1 Hz, *J* = 1.2 Hz, 1H, H12), 6.93-6.90 (m, 1H, H11), 6.82-6.80 (m, 1H, H10), 4.84-4.80 (m ,1H, NCH), 3.94-3.90 (m, 1H, NCH), 3.14-3.06 (m, 1H, NCH), 3.14-3.05 (m, 1H, NCH), 2.93 (t, *J* = 7.2 Hz, 2H, H8), 2.84-2.74 (m, 1H, ArCH), 2.67-2.58 (m, 1H, NCH), 2.41 (t, *J* = 7.2 Hz, 2H, H6),2.10-2.00 (m, 2H, H7), 1.91-1.86 (m, 2H, CHC*H$_2$*), 1.68-1.51 (m, 2H, CHC*H$_2$*). **^{13}C NMR:** (75 MHz, CDCl$_3$) δ 170.8 (C=O), 149.1 (C3), 144.5 (C9), 128.8 (q, *J* = 32.2 Hz, *C*-CF$_3$), 127.1 (C2, C4),

126.7 (C11), 125.5 (q, J = 3.3 Hz, C1, C5), 124.4 (C10), 124.1 (q, J = 270.4 Hz, CF$_3$), 123.1(C12), 46.0 (NCH$_2$), 42.7 (ArCH), 42.1 (NCH$_2$), 33.6 (CHCH$_2$), 32.6 (CHCH$_2$), 32.2 (C6), 29.3 (C8), 27.1 (C7). **HR-MS:** calcd for C$_{20}$H$_{23}$F$_3$NOS m/z: [M + H]$^+$, 382.1447; found 382.1434 [Diff (ppm) = -3.39]. **IR (KBr):** 2947 (C-H), 1635 (C=O), 1619 (C=C), 1437 (C=C), 1336 (C-F), 1119 (C-N) cm^{-1}. **m.p.:** 48-49 °C.

10.38 Synthesis of 5-(thiophen-2-yl)-1-(4-(4-(trifluoromethyl)phenyl)piperazin-1-yl)pentan-1-one (RTC195) (55)
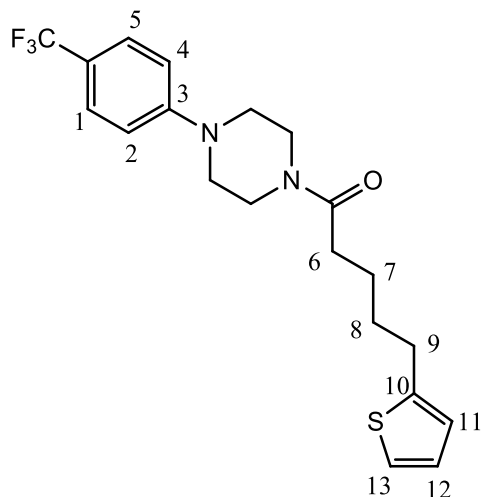
Prepared from compound **33** (100 mg, 0.43 mmol) and 5-(thiophen-2-yl)pentanoic acid (72 mg, 0.39 mmol) using HOBt (58 mg, 0.43 mmol), TBTU (138 mg, 0.43 mmol), anhydrous NEt$_3$ (86 µL, 0.62 mmol) and anhydrous DMF (4 mL) and following the general procedure described in section **10.2**. The reaction mixture was stirred overnight at room temperature under a N$_2$ atmosphere. Purified using flash chromatography (3:2 EtOAc:n-hexane) to give an orange solid, 41 mg (25%).

^{1}H NMR: (300 MHz, CDCl$_3$) δ 7.50 (d, J = 8.7 Hz, 2H, H1, H5), 7.09 (dd, J = 5.1 Hz, J = 1.2 Hz, 1H, H13), 6.92-6.88 (m, 3H, H2, H4, H12), 6.79-6.78 (m, 1H, H11), 3.79-3.75 (m, 2H*), 3.61-3.58 (m, 2H*), 3.26-3.22 (m, 4H*), 2.89-2.85 (m, 2H, H9), 2.41-2.63 (m, 2H, H6), 1.80-1.73 (m ,4H, H7, H8).*Piperazine. **^{13}C NMR:** (75 MHz, CDCl$_3$) δ 171.3 (C=O), 152.9 (C3), 144.9 (C10), 126.7 (C12), 126.4 (q, J = 3.3 Hz, C1, C5), 124.6 (q, J = 269.8 Hz, CF$_3$), 124.2 (C11), 122.9 (C13), 121.3 (q, J = 32.0 Hz, C-CF$_3$), 115.0 (C2, C4), 48.3 (C*), 48.1 (C*), 45.1 (C*), 41.1 (C*), 32.9 (C6), 31.4 (C8), 29.6 (C9), 24.6 (C7). *Piperazine. **R$_f$:** 0.6 (3:2, EtOAc:n-hexane). **HR-MS:** calcd for C$_{20}$H$_{24}$F$_3$N$_2$OS m/z: [M + H]$^+$, 397.1556; found: 397.1541 [Diff (ppm) = -3.75]. **IR**

(KBr): 2930 (C-H), 1637 (C=O), 1614 (C=C), 1439 (C=C), 1331 (C-F), 1230 (C-N) cm^{-1}. **m.p.:** 46-48 °C.

10.39 Synthesis of 5-(thiophen-2-yl)-1-(4-(4-(trifluoromethyl)phenyl)piperazin-1-yl) pentan-1-one (RTC537) (56)
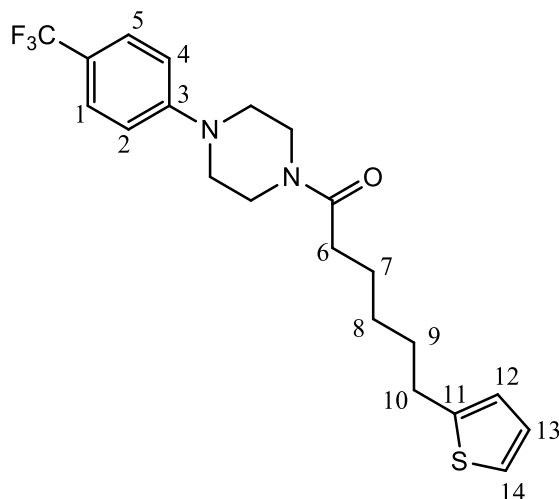
Prepared from compound **33** (100 mg, 0.43 mmol) and 5-(thiophen-2-yl)pentanoic acid (77 mg, 0.34 mmol) using HOBt (58 mg, 0.43 mmol), TBTU (138 mg, 0.43 mmol), anhydrous NEt$_3$ (87 μL, 0.63 mmol) and anhydrous DMF (4 mL) and following the general procedure described in section **10.2**. The reaction mixture was stirred overnight at room temperature under a N$_2$ atmosphere. Purified using flash chromatography (4:1 EtOAc:*n*-hexane) to give a brown solid, 120 mg (75%).

^{1}H NMR: (300 MHz, CDCl$_3$) δ 7.49 (d, *J* = 9.1 Hz, 2H, H1 H5), 7.08 (dd, *J* = 5.1 Hz, *J* = 1.2 Hz, 1H, H14), 6.92-6.88 (m, 3H, H2, H4, H13), 6.77-6.76 (m, 1H, H12), 3.78-3.75 (m, 2H*), 3.62-3.59 (m, 2H*), 3.27-3.22 (m, 4H*), 2.83 (t, *J* = 7.2 Hz, 2H, H10), 2.36 (t, *J* = 7.2 Hz, 2H, H6), 1.76-1.64 (m, 4H, H7, H9), 1.48-1.44 (m, 2H, H8).*Piperazine. **^{13}C NMR:** (75 MHz, CDCl$_3$) δ 171.5 (C=O), 152.9 (C3), 145.3 (C11), 126.7 (C13), 126.5 (q, *J* = 3.3 Hz, C1, C5), 124.1 (C12), 122.8 (C14), 124.6 (q, *J* = 270.0 Hz, CF$_3$), 121.7 (q, *J* = 32.0 Hz, *C*-CF$_3$), 114.9 (C2, C4), 48.3 (C*), 48.0 (C*), 45.1 (C*), 41.1 (C*), 33.0 (C6), 31.5 (C7), 29.7 (C10), 28.8 (C9), 24.9 (C8).*Piperazine. **R$_f$:** 0.5 (3:2, EtOAc:*n*-hexane). **HR-MS:** calcd for C$_{42}$H$_{50}$F$_6$N$_4$O$_2$S$_2$Na m/z: [2M + Na]$^+$, 843.3172; found: 843.3152 [Diff (ppm) = -2.27]. **IR (KBr):** 2926 (C-H), 1641 (C=O), 1613 (C=C), 1438 (C=C), 1332 (C-F), 1240 (C-N) cm^{-1}. **m.p.:** 50-52 °C.

### 10.40 Synthesis of 1-(4-(4-(trifluoromethyl)phenyl)piperazin-1-yl)octan-1-one (RTC533) (57)
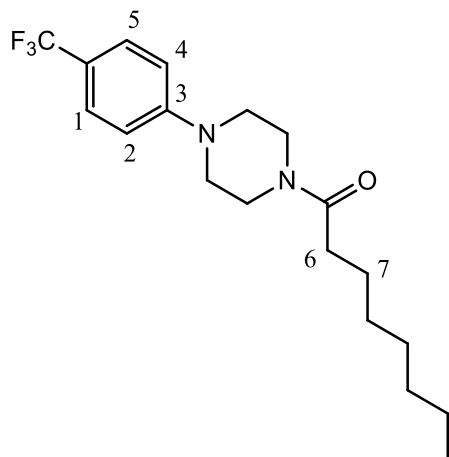
Prepared from compound **33** (100 mg, 0.43 mmol) and octanoic acid (62 µL, 0.39 mmol) using HOBt (58 mg, 0.43 mmol), TBTU (138 mg, 0.43 mmol), anhydrous NEt$_3$ (87 µL, 0.63 mmol) and anhydrous DMF (4 mL) and following the general procedure described in section **10.2**. The reaction mixture was stirred overnight at room temperature under a N$_2$ atmosphere. Purified using flash chromatography (3:2 EtOAc:*n*-hexane) to give a cloudy white oil, 88 mg (63%).

^{1}H NMR: (300 MHz, CDCl$_3$) δ 7.49 (d, *J* = 8.7 Hz, 2H, H1, H5), 6.92 (d, *J* = 8.7 Hz, 2H, H2, H4), 3.80-7.67 (m, 2H*), 3.57-3.62 (m, 2H*), 3.30-3.23 (m, 4H*), 2.36 (t, *J* = 7.2 Hz, 2H, H6), 1.70-1.60 (m, 2H, H7), 1.33-1.28 (m, 8H, CH$_2$ x 4), 0.88 (t, *J* = 6.0 Hz, 3H, CH$_3$).*Piperazine. **^{13}C NMR:** (75 MHz, CDCl$_3$) δ 171.8 (C=O), 152.9 (C3), 126.4 (q, *J* = 3.3 Hz, C1, C5), 124.6 (q, *J* = 269.5 Hz, CF$_3$), 121.2 (q, *J* = 32.7 Hz, *C*-CF$_3$), 114.9 (C2, C4), 48.3 (C*), 48.1 (C*), 45.1 (C*), 41.0 (C*), 33.2 (C6), 31.7 (CH$_2$), 29.4 (CH$_2$), 29.0 (CH$_2$), 25.3 (C7), 22.6 (CH$_2$), 14.0 (CH$_3$).*Piperazine. **R$_f$:** 0.7 (3:2, EtOAc:*n*-hexane). **HR-MS:** calcd for C$_{19}$H$_{28}$F$_3$N$_2$O m/z: [M + H]$^+$, 357.2148; found: 357.2136 [Diff (ppm) = -3.36]. **IR (neat):** 2927 (C-H), 1641 (C=O), 1616 (C=C), 1436 (C=C), 1331 (C-F), 1116 (C-N) cm^{-1}.

10.41 Synthesis of 1-(4-(4-(trifluoromethyl)phenyl)piperazin-1-yl)ethanone (RTC12) (58)
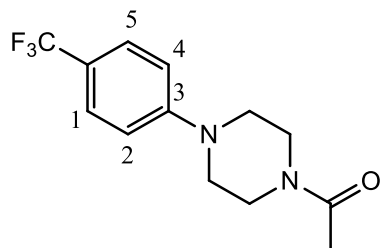
Prepared from compound **33** (150 mg, 0.65 mmol) and acetic acid (33 µL, 0.59 mmol) using HOBt (87 mg, 0.65 mmol), TBTU (208 mg, 0.65 mmol), anhydrous NEt$_3$ (131 µL, 0.94 mmol) and anhydrous DMF (3 mL) and following the general procedure described in section **10.2**. The reaction mixture was stirred overnight at room temperature under a N$_2$ atmosphere. Purified using flash chromatography (4:1 EtOAc:*n*-hexane) to give an off white solid, 91 mg (57%).

^{1}H NMR: (300 MHz, CDCl$_3$) δ 7.50 (d, *J* = 8.7 Hz, 2H, H1, H5), 6.92 (d, *J* = 8.7 Hz, 2H, H2, H4), 3.79-3.76 (m, 4H*), 3.65-3.61 (m, 2H*), 3.31-3.24 (m, 2H*), 2.14 (s, 3H, CH$_3$). *Piperazine. **^{13}C NMR:** (75 MHz, CDCl$_3$) δ 168.0 (C=O), 151.9 (C3), 125.5 (q, *J* = 3.3 Hz, C1, C5), 123.5 (q, *J* = 269.4 Hz, CF$_3$), 120.3 (q, *J* = 32.2 Hz, *C*-CF$_3$), 114.0 (C2, C4), 47.3 (C*), 47.0 (C*), 44.8 (C*), 40.0 (C*), 20.2 (C10).*Piperazine. **R$_f$:** 0.5 (4:1, EtOAc:*n*-hexane). **HR-MS:** calcd for C$_{13}$H$_{16}$F$_3$N$_2$O m/z: [M + H]$^+$, 273.1209; found: 273.1222 [Diff (ppm) = 4.80]. **IR (KBr):** 2847 (C-H), 1647 (C=O), 1615 (C=C), 1441 (C=C), 1336 (C-F), 1238 (C-N) cm^{-1}. **m.p.:** 76-80 °C. **Anal. calcd** for C$_{13}$H$_{15}$F$_3$N$_2$O; C, 57.34; H, 5.55; N, 10.29% found: C, 57.16; H, 5.40; N, 9.87%.

10.42 Synthesis of 3-(thiophen-2-yl)-1-(4-(4-(trifluoromethyl)phenyl)piperazin-1-yl)propan-1-one (RTC532) (59)
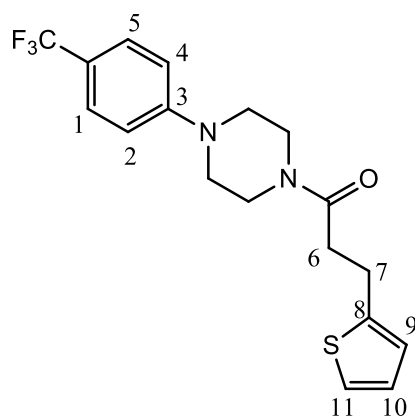
Prepared from compound **33** (81 mg, 0.35 mmol) and 3-(thiophen-2-yl)propanoic acid (50 mg, 0.32 mmol) using HOBt (47 mg, 0.35 mmol), TBTU (113 mg, 0.35 mmol), anhydrous NEt_3 (71 µL, 0.51 mmol) and anhydrous DMF (5 mL) and following the general procedure described in section **10.2**. The reaction mixture was stirred overnight at room temperature under a N_2 atmosphere. Purified using flash chromatography (3:2 EtOAc:*n*-hexane) to give an orange solid, 52 mg (44%).

^{1}H NMR: (300 MHz, $CDCl_3$) δ 7.49 (d, J = 8.7 Hz, 2H, H1, H5), 7.12 (dd, J = 5.1 Hz, J = 1.2 Hz, H11), 6.92-6.88 (m, 3H, H2, H4, H10), 6.85-6.83 (m, 1H, H9), 3.80-3.77 (m, 2H*), 3.59-3.56 (m, 2H*), 3.25-3.17 (m, 2H, H7, 4H*), 2.72 (t, J = 7.2 Hz, 2H, H6).*Piperazine. **^{13}C NMR:** (75 MHz, $CDCl_3$) δ 170.2 (C=O), 152.8 (C3), 143.6 (C8), 126.9 (C9), 126.5 (q, J = 3.3 Hz, C1, C5), 124.8 (C11), 124.5 (q, J = 269.7 Hz, CF_3), 123.5 (C10), 121.3 (q, J = 32.4 Hz, *C*-CF_3), 115.0 (C2, C4), 48.2 (C*), 48.0 (C*), 45.0 (C*), 41.2 (C*), 35.1 (C6), 25.5 (C7). **R_f:** 0.5 (3:2, EtOAc:*n*-hexane). **HR-MS:** calcd for $C_{18}H_{20}F_3N_2OS$ m/z: [M + H]$^+$, 369.1243; found: 369.1238 [Diff (ppm) = -1.25]. **IR (KBr):** 2826 (C-H), 1632 (C=O), 1615 (C=C), 1441(C=C), 1338 (C-F), 1229 (C-N) cm^{-1}. **m.p.:** 50-54 °C.

10.43 Synthesis of 1-(4-(4-(trifluoromethyl)phenyl)piperazin-1-yl)pentan-1-one (RTC194) (60)
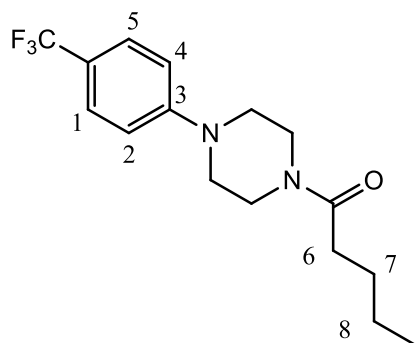
Prepared from compound **33** (246 mg, 1.07 mmol) and pentanoic acid (106 µL, 0.98 mmol) using HOBt (144 mg, 0.98 mmol), TBTU (343 mg, 0.98 mmol), anhydrous NEt_3 (216 µL, 1.56 mmol) and anhydrous DMF (6 mL) and following the general procedure described in section **10.2**. The reaction mixture was stirred overnight at room temperature under a N_2 atmosphere. Purified using flash chromatography (3:2 EtOAc:*n*-hexane) to give an off white solid, 178 mg (57%).

^{1}**H NMR:** (300 MHz, CDCl$_3$) δ 7.49 (d, J = 8.7 Hz, 2H, H1, H5), 6.92 (d, J = 8.7 Hz, 2H, H2, H4), 3.79-3.76 (m, 2H*), 3.66-3.62 (m, 2H*), 3.30-3.23 (m, 4H*), 2.37 (t, J = 7.2 Hz, 2H, H6), 1.69-1.59 (m, 2H, H7), 1.45-1.32 (m, 2H, H8), 0.94 (t, J = 7.5 Hz, 2H, CH$_3$).*Piperazine. ^{13}**C NMR:** (75 MHz, CDCl$_3$) δ 171.7 (C=O), 152.9 (C3), 126.4 (q, J = 3.3 Hz, C1, C5), 124.6 (q, J = 268.8 Hz, CF$_3$), 121.0 (q, J = 32.7 Hz, C-CF$_3$), 114.9 (C2, C4), 48.3 (C*), 48.0 (C*), 45.1 (C*), 41.0 (C*), 32.9 (C6), 27.4 (C7), 22.5 (C8), 13.8 (CH$_3$).*Piperazine. **R$_f$:** 0.6 (3:2, EtOAc:n-hexane). **HR-MS:** calcd for C$_{16}$H$_{22}$F$_3$N$_2$O m/z: [M + H]$^+$, 315.1679; found: 315.1688 [Diff (ppm) = 2.9]. **IR (KBr):** 2935 (C-H), 1650 (C=O), 1631 (C=C), 1450 (C=C), 1337 (C-F), 1228 (C-N) cm^{-1}. **m.p.:** 46-48 °C.

10.44 Synthesis of 2-(thiophen-2-yl)-1-(4-(4-(trifluoromethyl)phenyl)piperazin-1-yl)ethanone (RTC536) (61)
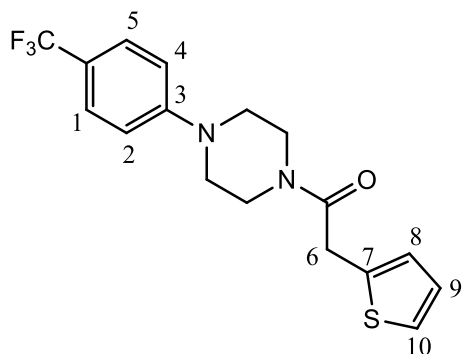
Prepared from compound **33** (100 mg, 0.43 mmol) and 2-(thiophen-2-yl)acetic acid (54 mg, 0.34 mmol) using HOBt (58 mg, 0.43 mmol), TBTU (138 mg, 0.43 mmol), anhydrous NEt$_3$ (87 µL, 0.63 mmol) and anhydrous DMF (4 mL) and following the general procedure described in section **10.2**. The reaction mixture was stirred overnight at room temperature under a N$_2$ atmosphere. Purified using flash chromatography (3:2 EtOAc:n-hexane) to give an orange solid, 27 mg (20%).

^{1}**H NMR:** (300 MHz, CDCl$_3$) δ 7.48 (d, J = 8.7 Hz, 2H, H1, H5), 7.20 (dd, J = 5.1 Hz, J = 1.2 Hz, 1H, H10), 6.97-6.87 (m, 4H, H2, H4, H8, H9), 3.95 (s, 2H, H6), 3.82-3.79 (m, 2H*), 3.69-3.65 (m, 2H*), 3.27-3.23 (m, 2H*), 3.18-3.15 (m, 2H*). *Piperazine. ^{13}**C NMR:** (75 MHz, CDCl$_3$) δ 168.5 (C=O), 152.8 (C3), 136.1 (C7), 126.9 (C8), 126.5 (q, J = 3.3 Hz, C1, C5), 126.1 (C9), 124.8 (C10), 124.5 (q, J = 268.4 Hz, CF$_3$), 121.4 (q, J = 32.7 Hz, C-CF$_3$), 115.0 (C2, C4), 48.2 (C*), 47.9 (C*), 45.8 (C*), 41.5 (C*), 35.2

(C6). *Piperazine. **R$_f$:** 0.5 (3:2, EtOAc:*n*-hexane). **HR-MS:** calcd for C$_{17}$H$_{18}$F$_3$N$_2$O$_2$S m/z: [M + H]$^+$, 355.1086; found: 355.1084 [Diff (ppm) = -0.56]. **IR (KBr):** 2910 (C-H), 1644 (C=O), 1616 (C=C), 1409 (C=C), 1337 (C-F), 1230 (C-N) cm^{-1}.

10.45 Synthesis of 3-(furan-2-yl)-1-(4-(4-(trifluoromethyl)phenyl)piperazin-1-yl)propan-1-one (RTC535) (62)

Prepared from compound **33** (100 mg, 0.43 mmol) and 3-(furan-2-yl)propanoic acid (54mg, 0.39 mmol) using HOBt (58 mg, 0.43 mmol), TBTU (138 mg, 0.43 mmol), anhydrous NEt$_3$ (87 μL, 0.63 mmol) and anhydrous DMF (4 mL) and following the general procedure described in section **10.2**. The reaction mixture was stirred overnight at room temperature under a N$_2$ atmosphere. Purified using flash chromatography (3:2 EtOAc:*n*-hexane) to give an orange solid, 43 mg (31%).

^{1}H NMR: (300 MHz, CDCl$_3$) δ 7.52 (d, *J* = 8.7 Hz, 2H, H1, H5), 7.31-7.30 (m, 1H, H11), 6.91 (d, *J* = 8.7 Hz, 2H, H2, H4), 6.29-6.27 (m, 1H, H10), 6.05-6.04 (m, 1H, H9), 3.80-3.79 (m, 2H*), 3.61-3.58 (m, 2H*), 3.26-3.21 (m, 4H*), 3.02 (t, *J* = 7.2 Hz, 2H, H7), 2.71 (t, *J* = 7.2 Hz, 2H, H6). *Piperazine. **^{13}C NMR:** (75 MHz, CDCl$_3$) δ 170.3 (C=O), 154.5 (C8), 152.8 (C3), 141.1 (C11), 126.5 (q, *J* = 3.3 Hz, C1, C5), 124.5 (q, *J* = 269.4 Hz, CF$_3$), 123.0 (q, *J* = 32.7 Hz, *C*-CF$_3$), 15.0 (C2, C4), 110.3 (C10), 105.5 (C9), 48.2 (C*), 48.0 (C*), 45.0 (C*), 41.2 (C*), 31.6 (C6), 23.8 (C7).*Piperaine. **R$_f$:** 0.6 (3:2, EtOAc:*n*-hexane). **HR-MS:** calcd for C$_{18}$H$_{20}$F$_3$N$_2$O$_2$ m/z: [M + H]$^+$, 353.1471; found: 353.1461 [Diff (ppm) = -2.83]. **IR (KBr):** 2921 (C-H), 1625 (C=O), 1616 (C=C), 1443 (C=C), 1334 (C-F), 1227 (C-N) cm^{-1}. **m.p.:** 77-81 °C.

10.46 4-(1H-Pyrazol-4-yl)-1-(4-(4-(trifluoromethyl)phenyl)piperazin-1-yl)butan-1-one (RTC193) (63)
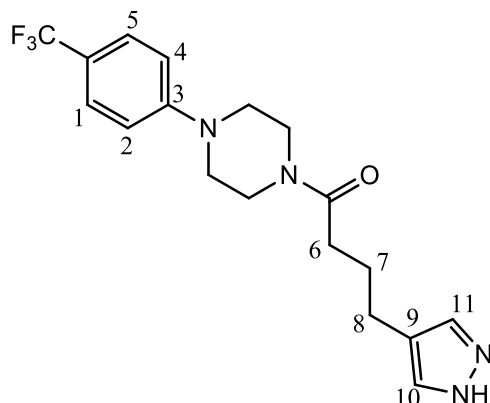
Prepared from compound **33** (100 mg, 0.71 mmol) and 4-(1H-pyrazol-4-yl)butanoic acid (100 mg, 0.65 mmol), using HOBt (96 mg, 0.71 mmol), TBTU (228 mg, 0.71 mmol), anhydrous NEt$_3$ (144 μL, 1.04 mmol) and anhydrous DMF (4 mL) and following the general procedure described in section **10.2**. The reaction mixture was stirred overnight at room temperature under a N$_2$ atmosphere. Purified using flash chromatography (3:2 EtOAc:*n*-hexane) to give an off white solid, 20 mg (10%).

^{1}H NMR: (300 MHz, CDCl$_3$) δ 7.52-7.47 (m, 2H, H1, H5, H10, H11)), 7.06 (d, *J* = 9.0 Hz, 2H, H2, H4), 3.76-3.62 (m, 4H*), 3.62-3.24 (m, 4H*), 2.60 (t, *J* = 7.5 Hz, 2H, H8), 2.48 (t, *J* = 7.5 Hz, 2H, H6), 1.97-1.85 (m, 2H, H7).*Piperazine. **R$_f$:** 0.5 (3:2, EtOAc:*n*-hexane). **HR-MS:** calcd for C$_{18}$H$_{22}$F$_3$N$_4$O m/z: [M + H]$^+$, 367.1740; found: 367.1750 [Diff (ppm) = 2.74].**IR (KBr):** 2954 (C-H), 1647 (N-*C*=*O*), 1612 (C=O), 1325 (C-*N*-C), 1230 (C-F) cm^{-1}.

10.47 Synthesis of 5-phenyl-1-(4-(4-(trifluoromethyl)phenyl)piperazin-1-yl)pentan-1-one (RTC16) (64)
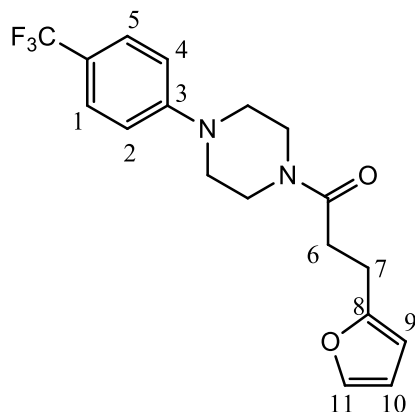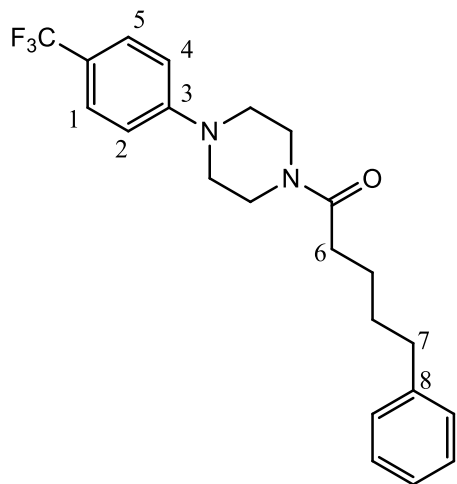

Prepared from compound **33** (150 mg, 0.65 mmol) and 5-phenylpentanoic acid (105 mg, 0.59 mmol) using HOBt (87 mg, 0.65 mmol), TBTU (208 mg, 0.65 mmol), anhydrous NEt$_3$ (131 µL, 0.94 mmol) and anhydrous DMF (5mL) and following the general procedure described in section **10.2**. The reaction mixture was stirred overnight at room temperature under a N$_2$ atmosphere. Purified using flash chromatography (4:1 EtOAc:*n*-hexane) to give an off white solid, 101mg (44%).

^{1}H NMR: (300 MHz, CDCl$_3$) δ 7.49 (d, *J* = 8.7 Hz, 2H, H1, H5), 7.28-7.24 (m, 2H, Ar), 7.18-7.16 (m, 3H, Ar), 6.98 (d, *J* = 8.7 Hz, 2H, H2, H4), 3.75-3.74 (m, 2H*), 3.57-3.55 (m, 2H*), 3.22-3.20 (m, 4H*), 2.67-2.63 (m, 2H, H7), 2.39-2.34 (m, 2H, H6), 1.7-1.68 (m, 4H, CH$_2$ x 2).*Piperazine. **^{13}C NMR:** (75 MHz, CDCl$_3$) δ 171.5 (C=O), 152.9 (C3), 142.1 (C8), 128.4 (Ar), 128.3 (Ar), 126.5 (q, *J* = 3.3 Hz, C1, C5), 125.8 (Ar), 124.7 (q, *J* = 271.1 Hz, CF$_3$), 121.2 (q, *J* = 33.0 Hz, *C*-CF$_3$), 114.9 (C2, C4), 48.35 (C*), 48.1 (C*), 45.1 (C*), 41.1 (C*), 35.7 (C7), 33.1 (C6), 31.10 (CH$_2$), 24.86 (CH$_2$).*Piperazine. **R$_f$:** 0.5 (4:1, EtOAc:*n*-hexane). **HR-MS:** calcd for C$_{22}$H$_{26}$F$_3$N$_2$O m/z: [M + H]$^+$, 391.1992; found: 391.1992 [Diff (ppm) = -5.0]. **IR (KBr):** 2857 (C-H), 1640 (C=O), 1612 (C=C), 1438(C=C), 1331 (C-F), 1201 (C-N) cm^{-1} **m.p.:** 72-76 °C. **Anal. calcd** for C$_{22}$H$_{25}$F$_3$N$_2$O; C, 67.67; H, 6.45; N, 7.18% found: C, 67.61; H, 6.51; N, 7.18%.

**10.48 Synthesis   of   thiophen-2-yl   (4-(4-(trifluoromethyl)phenyl)piperazin-1-yl)
         methanone (RTC93) (65)**
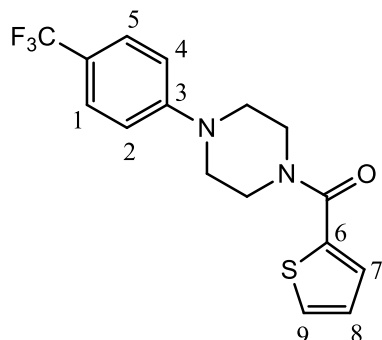
Prepared from compound **33** (154 mg, 0.66 mmol) and thiophene-2-carboxylic acid (77 mg, 0.61 mmol) using HOBt (90 mg, 0.66 mol), TBTU (214 mg, 0.66 mmol), anhydrous NEt_3 (150 μL, 0.97 mmol) and anhydrous DMF (6 mL) and following the general procedure described in section **10.2**. The reaction mixture was stirred overnight at room temperature under a N_2 atmosphere. Purified using flash chromatography (1:1 EtOAc:Pet. Ether) to give a green solid, 149 mg (73%).

^{1}H NMR: (300 MHz, CDCl$_3$) δ 7.51-7.46 (m, 3H, H1, H5, H7), 7.3 (dd, J = 3.2 Hz, J = 1.1 Hz, 1H, H9), 7.08-7.05 (m, 1H, H8), 6.92 (d, J = 8.7 Hz, 2H, H2, H4), 3.93-3.89 (m, 4H*), 3.35-3.31 (m, 4H*). *Piperazine. **^{13}C NMR:** (75 MHz, CDCl$_3$) δ 163.7 (C=O), 152.8 (C3), 136.6 (C6), 129.1 (C9), 129.0 (C7), 126.8 (C8), 126.5 (q, J = 3.3 Hz, C1, C5), 124.6 (q, J = 269.7 Hz, CF$_3$), 121.2 (q, J = 32.5 Hz, C-CF$_3$), 114.9 (C2, C4), 48.2 (C*). *Piperazine. **R$_f$:** 0.6 (1:1, EtOAc:Pet.Ether). **HR-MS:** calcd for $C_{16}H_{16}F_3N_2OS$ m/z: $[M + H]^+$, 342.0960; found: 342.0974 [Diff (ppm) = 4.07]. **IR (KBr):** 2836 (C-H), 1609 (C=O), 1523 (C=C), 1442 (C=C), 1338 (C-F), 1072 (C-N) cm^{-1}. **m.p.:** 126-130 °C. **Anal. calcd** for $C_{16}H_{15}F_3N_2OS$; C, 56.46; H, 4.44; N, 8.23% found: C, 56.72; H, 4.62; N, 8.42%.

10.49 Synthesis   of   4-hydroxy-4-(thiophen-2-yl)-1-(4-(4-(trifluoromethyl)phenyl)piperazin-1-yl)butan-1-one (RTC29) (66)
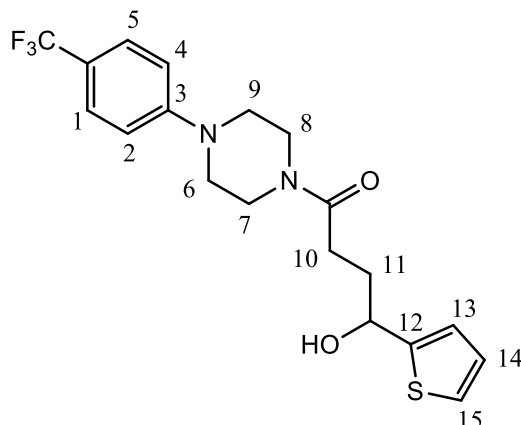
To a solution of compound **5** (350 mg, 0.88 mmol) in MeOH (3 mL) was added $NaBH_4$ (66 mg, 1.76 mmol) and the suspension was heated at 50 °C for 12 hrs. The reaction mixture was concentrated under reduced pressure and the resulting solid dissolved in EtOAc (15 mL). The organic layer was washed with H_2O (10 mL) and extracted with EtOAc (3 x 10 mL). The combined organic layers were dried over $MgSO_4$. The residue was purified using flash chromatography (elution gradient 1:1 MeOH:DCM to 1:9, MeOH:DCM) to give an off white solid, 350 mg (81%).

^{1}H NMR: (300 MHz, CDCl$_3$) δ 7.49 (d, *J* = 8.7 Hz, 2H, H1, H5), 7.23-7.21 (m, 1H, H15), 6.98-6.90 (m, 4H, H2, H4, H13, H14), 5.08-5.04 (m, 1H, C*H*OH), 3.80-3.77 (m, 2H*), 3.63-3.60 (m, 2H*), 3.23-3.18 (m, 4H*), 2.57-2.53 (m, 2H, H10), 2.30-2.15 (m, 2H, H11).*Piperazine. **^{13}C NMR:** (75 MHz, CDCl$_3$) δ 170.0 (C=O), 151.7 (C3), 147.8 (C12), 125.7 (C14), 125.5 (q, *J* = 3.7 Hz, C1, C5), 123.5 (q, *J* = 270.0 Hz, CF$_3$), 123.2 (C15), 122.2 (C13), 120.13 (q, *J* = 32.0 Hz, *C*-CF$_3$), 113.9 (C2, C4), 68.6 (CHOH), 47.2 (C*), 46.9 (C*), 44.1 (C*), 40.3 (C*), 32.9 (C11), 28.3 (C10). *Piperazine. **R$_f$:** 0.17 (1:1, EtOAc:*n*-hexane). **HR-MS:** calcd for C$_{19}$ H$_{22}$ F$_3$ N$_2$ O$_2$ S m/z: [M + H]$^+$, 399.1349; found 399.1339 [Diff(ppm) = -2.32]. **IR (KBr):** 3383, (OH), 2965 (C-H), 1635 (C=O), 1335 (C-N), 1100 (C-F) cm^{-1}. **m.p.:** 120-124 °C.

10.50 Synthesis of 1-methyl-4-(4-(trifluoromethyl)phenyl)piperazine (RTC31) (67)[202]
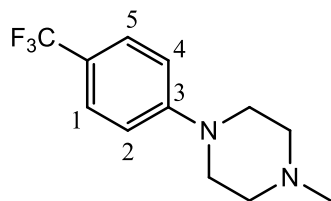
Compound **33** (283 mg, 1.22 mmol) was dissolved in absolute EtOH (5 mL) before formic acid (795 µL, 20.90 mmol) and formaldehyde (585 µL, 6.14 mmol) were consecutively added. The solution was heated at reflux for 3 hrs after which the EtOH was removed under reduced pressure and the residue dissolved in minimal H_2O. The aqueous solution was neutralised to pH ~ 13 using saturated aqueous $NaHCO_3$ and extracted with $CHCl_3$ (10 mL, followed by 3 x 10 mL). The organic layers were dried over $MgSO_4$ and concentrated *in vacuo*. The residue was purified using flash chromatograpy (1:1 EtOAc: Pet. Ether) to give an off white solid, 216 mg (72%).

¹H NMR: (300 MHz, $CDCl_3$) δ 7.46 (d, *J* = 9.0 Hz, 2H, H1, H5), 6.89 (d, *J* = 9.0 Hz, 2H, H2, H4), 3.27-3.24 (m, 4H*), 2.54-2.50 (m, 4H*), 2.32 (s, 3H, CH_3).*Piperazine. ¹H NMR data matches literature data.[203] **HR-MS:** calcd for $C_{12}H_{16}F_3N_2$ m/z: $[M + H]^+$, 245.1260; found: 245.1272 [Diff (ppm) = 4.89]

10.51 Synthesis of 4-(thiophen-2-yl)butan-1-ol (RD28) (68)[119]
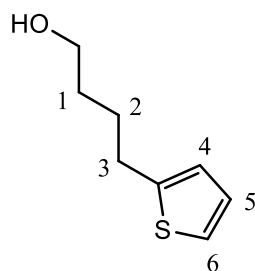
To a suspension of $LiAlH_4$ (130 mg, 3.43 mmol) in THF (2.5 mL) was added a solution of 4-(2-thienyl)butyric acid (500 µL, 3.43 mmol) in THF (2.5 mL). The suspension was stirred for 6 hrs at rt. The reaction mixture was quenched with MeOH (2 mL) and 10% aqueous NaOH (2 mL). The solution was neutralised with 10% aqueous HCl (2 mL) and the aqueous layer extracted with EtOAc (10 mL, followed by 3 x 10 mL). The

combined organic layers were dried over MgSO$_4$ and the residue purified using flash chromatography (DCM) to give a colourless oil, 481 mg (90%).

^{1}H NMR: (300 MHz, CDCl$_3$) δ 7.10 (dd, J = 5.1 Hz, J = 1.0 Hz, 1H, H6), 6.92-6.89 (m, 1H, H5) 6.79-6.77 (m, 1H, H4), 3.65 (t, J = 6.0 Hz, 2H, CH_2OH), 2.83 (t, J = 7.8 Hz, 2H, H3), 1.78-1.62 (m, 4H, H1, H2), 1.60 (bs, 1H, OH). ^{1}H NMR data matches literature data.[207] **HR-MS:** calcd for C$_8$H$_{13}$OS m/z: [M + H]$^+$, 157.0682; found: 157.0685 [Diff(ppm) = 1.99]. **R$_f$:** 0.25 (DCM).

10.52 Synthesis of 4-(thiophen-2-yl)butyl methanesulfonate (RD31) (69)
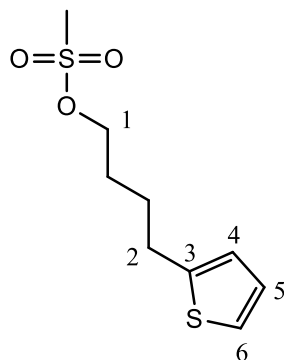
To a solution of compound **68** (135 mg, 0.86 mmol) and NEt$_3$ (142 μl, 1.01 mmol) in anhydrous DCM (3 mL) kept at 0 ºC, was added methanesulfonyl chloride (71 μl, 0.91 mmol). The reaction mixture was maintained at 0 °C for 1 hr, followed by warming to rt, where it was kept under vigorous stirring and a N$_2$ atmosphere for 3 hrs. The solvent was removed under reduced pressure and purified using flash chromatogrphy (3:2 EtOAc:Pet. Ether) to give a colourless oil, 152 mg (75%).

^{1}H NMR: (300 MHz, CDCl$_3$) δ 7.12 (dd, J = 5.1 Hz, J = 1.2 Hz, 1H, H6), 6.93-6.90 (m, 1H, H5) 6.80-6.78 (m, 1H, H4), 4.25-4.21 (m, 2H, H1), 2.98 (s, 3H, CH$_3$), 2.88-2.86 (m, 2H, H2), 1.83-1.78 (m, 4H, CH$_2$ x 2). **^{13}C NMR:** (75MHz, CDCl$_3$) δ 143.2 (C3), 125.8 (C5), 123.4 (C4), 122.2 (C6), 68.7 (C1), 36.3 (CH$_3$), 28.1 (C2), 27.4 (CH$_2$), 26.5 (CH$_2$). **HR-MS:** calcd for C$_9$H$_{14}$O$_3$S$_2$Na m/z: [M + Na]$^+$, 257.0277; found: 257.0273 [Diff(ppm) = **-**1.6]. **R$_f$:** 0.6 (3:2, EtOAc:n-hexane). **IR (neat):** 2924 (C-H), 1352 (S=O), 1173 (S=O) cm^{-1}.

10.53 Synthesis   of   1-(4-(thiophen-2-yl)butyl)-4-(4-(trifluoromethyl)phenyl)piperazine (RTC46) (70)
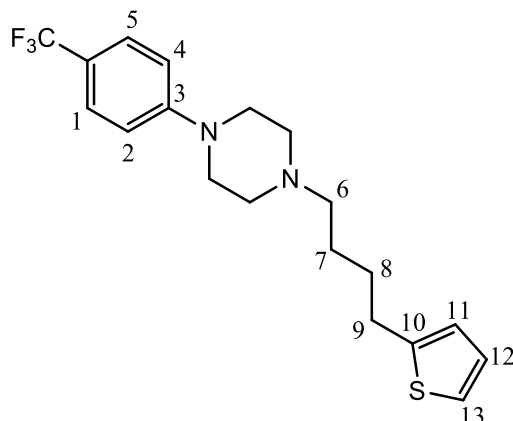
To a suspension of compound **69** (29 mg, 0.12 mmol) and Na_2CO_3 (26 mg, 0.24 mmol) in acetonitrile (5 mL), was added compound **33** (110 mg, 0.48 mmol). The mixture was heated at reflux for 24 hrs under vigorous agitation and a N_2 atmosphere. The solvent was removed under reduced pressure and the residue was purified using flash chromatography (3:2, EtOAc:*n*-hexane) to give a white solid, 40 mg (91%).

^{1}H NMR: (300 MHz, CDCl$_3$) δ 7.47 (d, *J* = 8.7 Hz, 2H, H1, H5), 7.12-7.10 (m, 1H, H13), 6.92-6.90 (m, 3H, H2, H4, H12), 6.79-6.78 (m, 1H, H11), 3.30-3.26 (m, 4H*), 2.86 (t, *J* = 7.2 Hz, 2H, H6), 2.60-2.56 (m, 4H*), 2.42 (t, *J* = 7.2 Hz, 2H, H9), 1.78-1.68 (m, 2H, H7), 1.65-1.60 (m, 2H, H8).*Piperazine. **^{13}C NMR:** (75MHz, CDCl$_3$) δ 153.3 (C3), 145.2 (C10), 126.7 (C12), 126.3 (q, *J* = 3.3 Hz, C1, C5), 124.7 (q, *J* = 269.4 Hz, CF$_3$), 124.1 (C11), 120.4 (q, *J* = 32.4 Hz, *C*-CF$_3$), 122.9 (C13), 114.4 (C2, C4), 58.2 (C9), 52.9 (C*), 47.9 (C*), 29.7 (C6), 29.6 (C7), 26.2 (C8).*Piperazine. **HR-MS:** calcd C$_{19}$H$_{24}$F$_3$N$_2$S m/z: [M + H]$^+$, 369.1067; found 369.1603 [Diff(ppm) = -1.1]. **IR (KBr):** 2932 (C-H), 1615 (C=C), 1469 (C=C), 1330 (C-F), 1292 (C-N) cm^{-1}. **m.p.:** 78-80 °C.

10.54 Synthesis of 1-(4-(4-aminophenyl)piperazin-1-yl)-4-(thiophen-2-yl)butan-1-one (RTC23) (73)
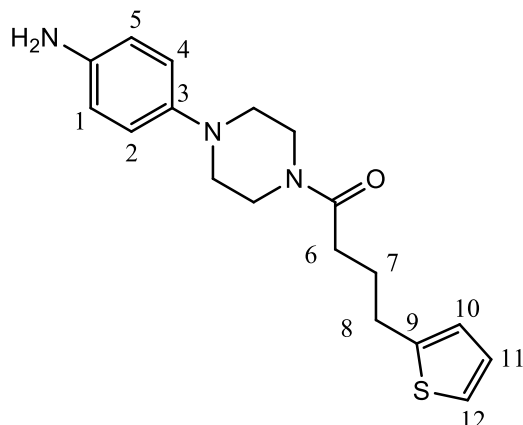
Compound **42** (143 mg, 0.39 mmol) was dissolved in MeOH (10 mL) in a round bottom flask and PtO_2 (20 mg, 0.08 mmol) was added. The resulting mixture was degassed and purged with H_2 (x3), stirred vigorously overnight at rt under an atmosphere of H_2 gas and monitored by TLC (7:1, EtOAc:DCM). The reaction mixture was passed through a bed of Celite and the filtrate was concentrated under reduced pressure. The residue was purified using flash chromatography (7:1, EtOAc:DCM) to give a brown oil, 75 mg (57%).

1H NMR: (300 MHz, $CDCl_3$) δ 7.11 (dd, *J* = 5.1 Hz, *J* = 1.2 Hz, 1H, H12), 6.92-6.90 (m, 1H, H11), 6.80-6.77 (m, 3H, H1, H5, H10), 6.94-6.20 (m, 2H, H2, H4), 3.76-3.72 (m, 2H*), 3.58-3.50 (m, 2H*, 2H, NH_2), 2.97-2.88 (m, 4H*, 2H, H6), 2.38 (t, *J* = 7.2 Hz, 2H, H8), 2.08-1.99 (m, 2H, H7).*Piperazine. **13C NMR:** (75 MHz, $CDCl_3$) δ 169.9 (C=O), 143.4 (C3), 142.8 (CNH_2), 139.9 (C9), 125.7 (C11), 123.4 (C10), 122.1 (C12), 118.2 (C1, C5), 115.4 (C2, C4), 50.5 (C*), 50.1 (C*), 44.6 (C*), 40.6 (C*), 31.0 (C8), 28.2 (C6), 26.0 (C7).*Piperazine. **Rf:** 0.5 (1:9, MeOH:DCM). **HR-MS:** calcd for $C_{18}H_{24}N_3OS$ m/z: $[M + H]^+$, 331.1664; found: 331.1669 [Diff (ppm) = 1.51]. **IR (KBr):** 3426 (N-H), 3343 (N-H), 2914 (C-H), 1635 (C=O), 1514 (N-H), 825 (N-H) cm^{-1}.

10.55 Synthesis of methyl 4-(thiophen-2-yl)butanoate (RTC19) (74)[204]
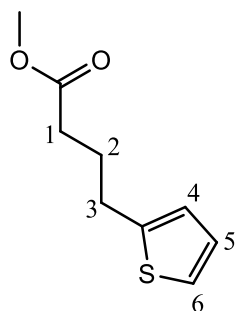
4-(2-Thienyl)butyric acid (1 mL, 6.86 mmol) was dissolved in MeOH (10 mL) and concentrated H_2SO_4 (1.15 mL, 21.95 mmol) was added was added dropwise. The reaction mixture was stirred overnight at rt. The MeOH was removed under reduced pressure and the residue dissolved in minimal H_2O. The pH was adjusted to ~7 using 2 M HCl and the aqueous layer was extracted with DCM (15 mL x 3). The combined organic layers were dried over $MgSO_4$ and the solvent removed under reduced pressure. The residue was purified using flash chromatography to give a clear oil, 1.03 g (81%)

^{1}H NMR: (300 MHz, CDCl$_3$) δ 7.09 (dd, J = 5.1 Hz, J = 1.2 Hz, 1H, H6), 6.90-6.78 (m, 1H, H5), 6.78-6.77 (m, 1H, H4), 2.85 (t, J = 7.0 Hz, H1), 3.65 (s, 3H, OCH$_3$), 2.35 (t, J = 7.0 Hz, H3), 2.04-1.94 (m, 2H, H2). ^{1}H NMR data matches literature data.[204] **R$_f$:** 0.7 (9:1, Pet. Ether:EtOAc). **HR-MS:** calcd for C$_9$H$_{13}$O$_2$S m/z: [M + H]$^+$, 207.0450; found: 207.0456 [Diff(ppm) = 2.90].

10.56 Synthesis of methyl 4-(5-bromothiophen-2-yl)butanoate (RD154) (75)
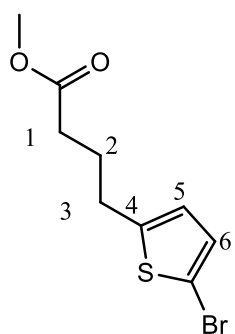
To a solution of compound **74** (310 mg, 1.82 mmol) in THF (5 mL) at 0 °C was added NBS (323 mg, 1.82 mmol) in small portions. The mixture was allowed to equilibrate to rt gradually after which the reaction mixture was stirred for 4 hrs. The solvent was

removed under reduced pressure and the residue was purified using flash chromatography (9:1, Pet.Ether:EtOAc) to give a light yellow oil, 361 mg (80%).

^{1}H NMR: (300 MHz, CDCl$_3$) δ 6.82 (d, J = 3.3 Hz, 1H, H6), 6.53 (d, J = 3.3 Hz, 1H, H5), 3.65 (s, 3H, OCH$_3$), 2.78 (t, J = 7.2 Hz, 2H, H1), 2.34 (t, J = 7.2 Hz, 2H, H3), 2.01-1.89 (m, 2H, H2). ^{1}H NMR data matches literature data.[208] **HR-MS:** calcd for C$_9$H$_{11}$BrO$_2$SNa m/z: [M + Na]$^+$, 287.9566; found: 287.9576 [Diff(ppm) = 3.75]. **R$_f$:** 0.8 (9:1, Pet. Ether:EtOAc).

10.57 Synthesis of 4-(5-bromothiophen-2-yl)butanoic acid (RD157) (76)
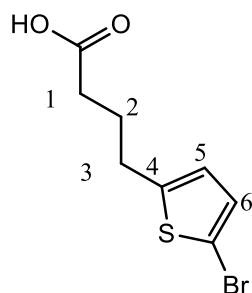
Compound **75** (457 mg, 1.74 mmol) was dissolved in EtOH (10 mL) and KOH (489 mg, 8.72 mmol) was added. The suspension was heated at reflux and reaction progress monitored by TLC (3:2 EtOAc:Pet. Ether). After 3 hrs the reaction mixture was allowed to cool to rt and EtOH was removed under reduce pressure. The residue was dissolved in H$_2$O (1 mL), the pH adjusted to pH = 6 with 2 M aqueous HCl and the aqueous layer extracted with DCM (20 mL, followed by 4 x 10 mL). The combined organic layers were washed with brine (3 x 20 mL), dried over MgSO$_4$ and evaporated under reduced pressure. The residue was purified using flash chromatography (1:9, MeOH:DCM) and the obtained product was dissolved in minimal DCM and Pet. Ether was added until precipitation began. The solution and precipitate were stored at -20 °C overnight, and the resultant solid collected by vacuum filtration and washed with cold Pet. Ether (20 mL) to give a beige solid, 151 mg (35%).

^{1}H NMR: (300 MHz, CDCl$_3$) δ 11.48 (bs, 1H, OH), 6.83 (d, J = 3.3 Hz, 1H, H6), 6.54 (d, J = 3.3 Hz, 1H, H5), 2.79 (t, J = 7.2 H, 2H, H1), 2.39 (t, J = 7.2 Hz, 2H, H3), 1.97-1.90 (m, 2H, H2). **^{13}C NMR:** (75 MHz, CDCl$_3$) 179.9 (C=O), 145.6 (C4), 129.6 (C6), 125.1 (C5), 109.3 (C-Br), 33.0 (C3), 29.3 (C1), 26.2 (C2). **R$_f$:** 0.6 (1:9, MeOH:DCM). **HR-MS:** calcd for C$_8$H$_{10}$BrO$_2$S m/z: [M + H]$^+$, 248.9579; found: 248.9579 [Diff(ppm) = 0]. **IR (KBr):** 2955 (C-H), 1708(C=O), 1211 (C-O), 797 (C-Br) cm^{-1}. **m.p.:** 50-54 °C.

10.58 Synthesis of 4-(5-bromothiophen-2-yl)-1-(4-(4-(trifluoromethyl)phenyl)piperazin-1-yl)butan-1-one (RTC30) (77)†
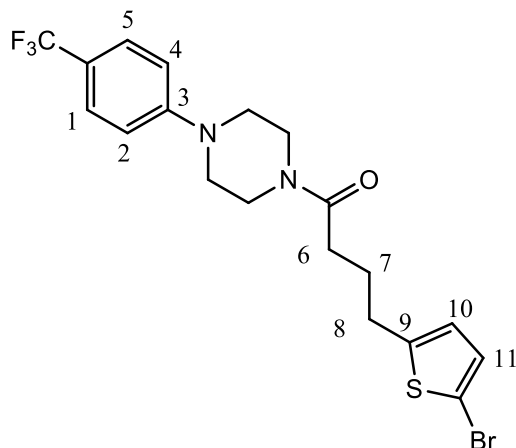
Compound **76** (149 mg, 0.66 mmol)**,** BOP (321 mg, 0.72 mmol), anhydrous NEt_3 (147 µL, 1.05 mmol) and anhydrous DCM (10 mL) were placed in an oven-dried three neck flask under a N_2 atmosphere. The resulting solution was stirred at rt for 15 mins. Compound **33** (167 mg, 0.72 mmol) was added and the reaction mixture stirred under a N_2 atmosphere and monitored by TLC. After 16 hrs, DCM was removed under reduced pressure and the resulting oil was acidified to pH = 3 using a 0.1 M aqueous HCl. The aqueous mixture was extracted with DCM (20 mL, followed by 4 x 10 mL) and the organic layer washed with a saturated aqueous solution of $NaHCO_3$ (3 x 20 mL) and brine (3 x 20 mL). The organic layer was dried over $MgSO_4$ and the solvent removed *in vacuo* and the residue was purified using flash chromatography (1:1 EtOAc:Pet. Ether) to give an light brown solid, 170 mg (55%).

¹H NMR: (300 MHz, $CDCl_3$) δ 7.48 (d, J = 8.7 Hz, 2H, H1, H5), 6.90 (d, J = 8.7 Hz, 2H, H2, H4), 6.84 (d, J = 3.3 Hz, 2H, H11), 6.56 (d, J = 3.3 Hz, 1H, H10), 3.85-3.72 (m, 2H*), 3.65-3.52 (m, 2H*), 3.31-3.19 (m, 4H*), 2.83 (t, J = 7.2 Hz, 2H, H8), 2.39 (t, J = 7.2 Hz, 2H, H6), 2.05-1.97 (m, 2H, H7).*Piperazine. **¹³C NMR:** (75 MHz, $CDCl_3$) 170.7 (C=O), 152.8 (C3), 146.2 (C9), 129.6 (C11), 126.5 (q, J = 3.3 Hz, C1, C5), 125.0 (C10), 124.6 (q, J = 269.7 Hz, CF_3), 121.1 (q, J = 32.7 Hz, *C*-CF_3), 114.9 (C2, C4), 109.0 (C-Br), 48.2 (C*), 48.0 (C*), 44.9 (C*), 41.1 (C*), 31.7 (C6), 29.6 (C8), 26.5 (C7). *Piperazine. **R_f:** 0.6 (1:1, EtOAc:Pet. Ether). **HR-MS:** calcd for $C_{19}H_{21}BrF_3N_2OS$ m/z: [M + H]⁺, 461.0505; found: 461.0489 [Diff (ppm) = -3.46]. **IR (KBr):** 2957 (C-

H), 1654 (C=O), 1616 (C=C), 149 (C=C), 1333 (C-F), 1114 (C-N), 652 (C-Br) cm^{-1}.

m.p.: 82-84 °C.

10.59 Synthesis of 1-(4-(4-(trifluoromethyl)phenyl)piperazin-1-yl)-4-(5-(4-(trifluoromethyl)phenyl) thiophen-2-yl)butan-1-one (RTC47) (78)†
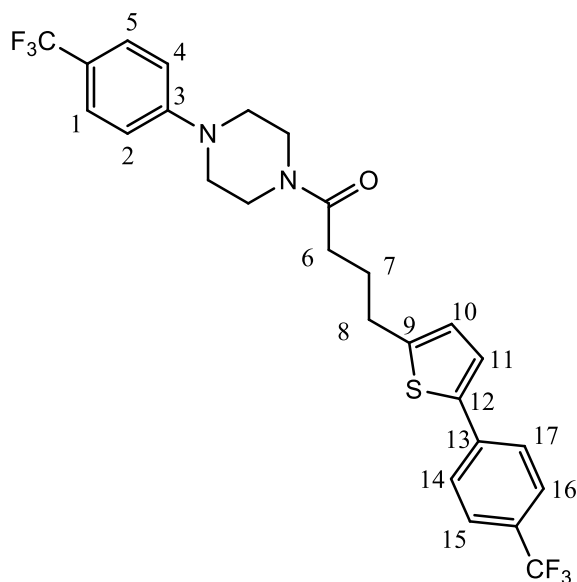
Trifluoromethylphenylboronic acid (15 mg, 0.07 mmol) and compound **77** (15 mg, 0.03 mmol) were dissolved in anhydrous THF (1 mL). Pd(PPh$_3$)$_4$ (10 mg, 0.0075 mmol) and 2 M aqueous Na$_2$CO$_3$ (535 µL) were added and the suspension was heated at reflux under a N$_2$ atmosphere and reaction progress monitored by TLC. After 6 hrs the solution was cooled and poured onto ice-cold H$_2$O and neutralised with 1 M aqueous HCl. The aqueous layer was extracted with EtOAc (10 mL, followed by 3 x 10 mL) and the combined organic layers were dried over MgSO$_4$. The solvent was removed under reduced pressure and the residue was purified using flash chromatography (1:1 EtOAc:Pet. Ether) to give an off white solid, 14 mg (82%).

^{1}H NMR: (300 MHz, CDCl$_3$) δ 7.62 (d, *J* = 8.7 Hz, 2H, H14, H17), 7.57 (d, *J* = 8.7 Hz, 2H, H15, H16), 7.48 (d, *J* = 8.7 Hz, 2H, H1, H5), 7.21 (d, *J* = 3.3 Hz, 1H, H11), 6.89 (d, *J* = 8.7 Hz, 2H, H2, H4), 6.81 (d, *J* = 3.3 Hz, 1H, H10), 3.80-3.76 (m, 2H*), 3.60-3.22 (m, 2H*), 3.26-3.22 (m, 4H*), 2.93 (t, *J* = 7.2 Hz, 2H, H8), 2.44 (t, *J* = 7.2 Hz, 2H, H6), 2.14-2.04 (m, 2H, H7).*Piperazine. **^{13}C NMR:** (75 MHz, CDCl$_3$) δ 169.8 (C=O), 151.8 (C3), 144.8 (C9), 139.2 (C13), 136.8 (C12), 127.7 (q, *J* = 33.1 Hz, *C*-CF$_3$), 125.4 (q, *J* = 3.3 Hz, C1, C5), 124.9 (C10), 124.8 (q, *J* = 3.3 Hz, C15, C16), 124.3 (C14, C17), 123.5

(q, J = 269.5 Hz, CF$_3$), 123.2 (C11), 123.1 (q, J = 270.1 Hz, CF$_3$), 120.2 (q, J = 32.5 Hz, C-CF$_3$), 113.9 (C2, C4), 47.2 (C*), 47.0 (C*), 40.1 (C*), 43.9 (C*), 30.8 (C6), 28.5 (C7), 25.6 (C8).*Piperazine. **R$_f$:** 0.7 (1:1, EtOAc:n-hexane). **HR-MS:** calcd for C$_{26}$H$_{25}$F$_6$N$_2$OS m/z: [M + H]$^+$, 527.1586; found 527.1599 [Diff(ppm) = 2.36]. **IR (KBr):** 2840 (C-H), 1652 (C=O), 1615 (C=C), 1443 (C=C), 1323 (C-F), 1110 (C-N) cm^{-1}. **m.p.:** 150-152 °C

10.60 Synthesis of 9-oxo-9-(4-(4-(trifluoromethyl)phenyl)piperazin-1-yl)nonanoic acid (RTC15) (79)
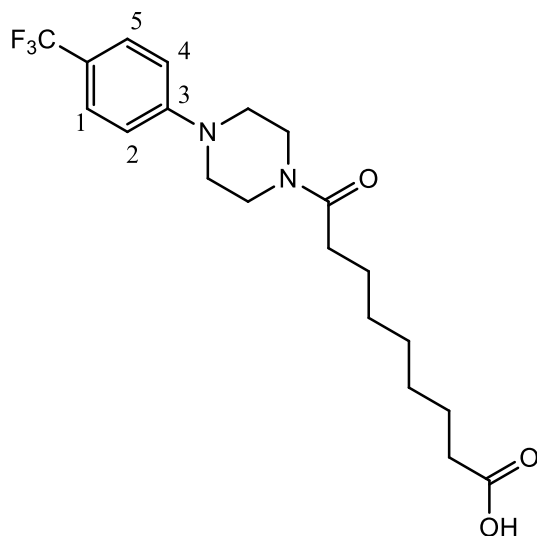
Compound **81** (131 mg, 0.31 mmol) and KOH (88 mg, 1.55 mmol) in EtOH (5 mL) were heated at reflux and reaction progress monitored by TLC (3:2 EtOAc: Pet. Ether). After 3 hrs the solution was allowed to cool to rt and EtOH was removed under reduce pressure. The residue was dissolved in H$_2$O (1 mL), the pH adjusted to pH = 6 with 2 M aqueous HCl and the aqueous layer extracted with DCM (20 mL, followed by 4 x 10 mL). The organic layers were washed with brine (3 x 20 mL), dried over MgSO$_4$ and evaporated under reduced pressure to give a white solid, 99 mg (80%).

¹H NMR: (300 MHz, CDCl$_3$) δ 10.30 (bs, 1H, OH), 7.50 (d, J = 8.7 Hz, 2H, H1, H5), 6.92 (d, J = 8.7 Hz, 2H, H2, H4), 3.78-3.77 (m, 2H*), 3.64-3.62 (m, 2H*), 3.31-3.24 (m, 4H*), 2.39-2.33 (m, 4H, (C=O)CH_2 x 2), 1.68-1.60 (m, 4H, (C=O)CH$_2$CH_2 x 2), 1.38-1.33 (m, 6H, CH$_2$ x 3).*Piperazine. **¹³C NMR:** (75 MHz, CDCl$_3$) δ 174.2 (COOH), 170.9 (C=O), 151.8 (C3), 125.4 (q, J = 3.7 Hz, C1, C5), 123.5 (q, J = 269.1 Hz, CF$_3$), 120.3 (q, J = 32.7 Hz, C-CF$_3$), 114.0 (C2, C4), 47.4 (C*), 47.1 (C*), 44.2 (C*), 40.1

(C*), 32.9 ((C=O)CH_2), 32.1 ((C=O)CH_2), 28.1 (CH_2), 27.9 (CH_2), 27.8 (CH_2), 24.1 ((C=O)CH_2CH_2), 23.6 ((C=O)CH_2CH_2).*Piperazine. **R_f:** 0.5 (1:19, MeOH:DCM) **HR-MS:** calcd for $C_{20}H_{28}F_3N_2O_3$ m/z: [M + H]$^+$, 401.2407; found: 401.2047 [Diff(ppm) = 0]. **IR (KBr):** 2935 (C-H), 1706 (C=O), 1617 (N-$C=O$), 1333 (C-F), 1204 (C-N) cm^{-1} **m.p.:** 90-92 °C **Anal. calcd** for $C_{20}H_{27}F_3N_2O_3$; C, 59.99; H, 6.80; N, 7.00% found; C, 60.40; H, 6.83; N, 6.85%.

10.61 Synthesis of methyl 9-oxo-9-(4-(4-(trifluoromethyl)phenyl)piperazin-1-yl)nonanoate (RTC56) (81)
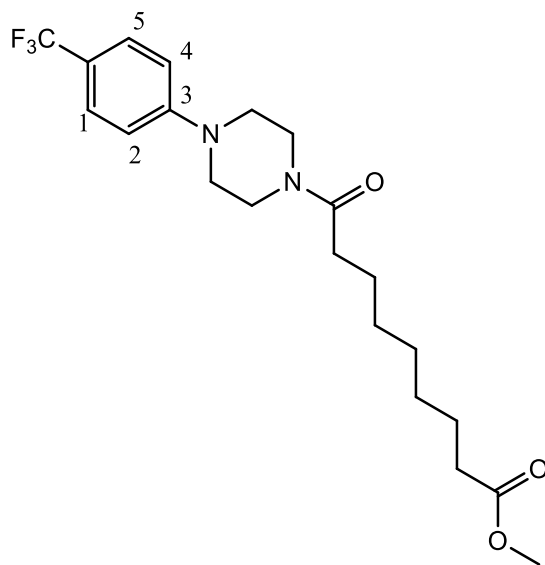
Methyl hydrogen azelate (479 mg, 2.30 mmol), BOP (1140 mg, 2.60 mmol), anhydrous NEt_3 (512 µL, 3.60 mmol) and anhydrous DCM (20 mL) were placed in an oven-dried three neck flask under a N_2 atmosphere. The resulting solution was stirred at rt for 15 mins. Compound **33** (600 mg, 2.60 mmol) was added and the reaction mixture stirred under a N_2 atmosphere and monitored by TLC. After 16 hrs, DCM was removed under reduced pressure and the resulting oil was acidified to pH = 3 using a 0.1 M aqueous HCl. The aqueous mixture was extracted with DCM (20 mL, followed by 4 x 10 mL) and the organic layer washed with a saturated aqueous solution of $NaHCO_3$ (3 x 20 mL) and brine (3 x 20 mL). The organic layer was dried over $MgSO_4$ and the solvent removed *in vacuo* and the residue was purified using flash chromatography (3:2, EtOAc:Pet.Ether) to give an off white solid, 952 mg (98%).

^{1}H NMR: (300 MHz, CDCl$_3$) δ 7.42 (d, *J* = 8.7 Hz, 2H, H1, H5), 6.86 (d, *J* = 8.7 Hz, 2H, H2, H4), 3.73-3.69 (m, 2H*), 3.63-3.53 (m, 2H*, 3H, OCH$_3$), 3.27-3.14 (m, 4H*),

2.33-2.21 (m, 4H, (C=O)CH$_2$ x 2), 1.65-1.48 (m, 4H, (C=O)CH$_2$CH_2 x 2), 1.35-1.21 (m, 6H, CH$_2$ x 3).*Piperazine. **^{13}C NMR:** (75 MHz, CDCl$_3$) 174.2 (*C*OOCH$_3$), 171.1 (N-C=O), 152.9 (C3), 126.4 (q, J = 3.3 Hz, C1, C5), 124.5 (q, J = 269.7 Hz, CF$_3$), 121.2 (q, J = 32.8 Hz, *C*-CF$_3$), 114.9 (C2, C4), 54.4 (OCH$_3$), 48.3 (C*), 48.0 (C*), 45.1 (C*), 41.0 (C*), 34.0 ((C=O)*C*H$_2$), 33.1 ((C=O)*C*H$_2$), 29.2 (CH$_2$), 29.0 (CH$_2$), 28.9 (CH$_2$), 25.1 ((C=O)CH$_2$*C*H$_2$), 24.8 ((C=O)CH$_2$*C*H$_2$). *Piperazine. **R$_f$:** 0.65 (3:2 EtOAc:Pet. Ether). **HR-MS:** calcd for C$_{21}$H$_{30}$F$_3$N$_2$O$_3$ m/z: [M + H]$^+$, 415.2203; found: 415.219 [Diff (ppm) = -3.14]. **IR:** 2954 (C-H), 1739 ((*C=O*)OCH$_3$), 1647 (N-*C=O*), 1613 (C=C), 1447 (C=C), 1334 (C-F), 1160 (C-N) cm^{-1}. **m.p.:** 81-85 °C.

10.62 Synthesis of (E)-3-(dimethylamino)acrylonitrile (RD302) (90)[211]
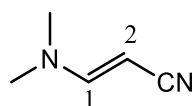
To a three-neck round bottom flask fitted with a reflux condenser and an addition funnel was added cyanoacetic acid (850 mg, 9.99 mmol) and anhydrous 1,4 dioxane (20 mL). The solution was heated at 80 °C and dimetylformamide dimethyl acetal (2 mL, 15.05 mmol) was added over 1 hr. The solution was heated at 80 °C for 1 hr after which the reaction was cooled to rt. The solvent was removed under reduce pressure. The product was extracted from the residue using DCM and purified using flash chromatography (DCM) to give a yellow oil, 837 mg (87%).

^{1}H NMR: (300 MHz, CDCl$_3$) δ 6.88 (d, J = 13.5 Hz, 1H, H1), 3.61 (d, J = 13.5 Hz, 1H, H2), 2.80 (bs, 6H, N(CH$_3$)$_2$). ^{1}H NMR data matches literature data.[211] **HR-MS:** calcd for C$_5$H$_9$N$_2$ m/z: [M + H]$^+$, 97.0760; found: 97.0763 [Diff (ppm) = 2.99]. **R$_f$:** 0.7 (DCM).

10.63 Synthesis of 1H-pyrazol-5-amine (RD305) (91)
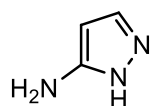
A solution of compound **92** (210 mg, 2.18 mmol) and hydrazine monohydrate (112 μL, 2.23 mmol) in MeOH (1 mL) was irradiated in a sealed microwave tube at 120 °C for 40 mins (100 W). MeOH was removed under reduced pressure and the residue was

triturated using Pet. Ether to give a brown solid. The product was used without further purification. Yellow oil, 164 mg (80%).

^{1}H NMR: (300 MHz, CD$_3$OD) δ 7.36 (d, J = 2.4 Hz, 1H, N=CH), 5.64 (d, J = 2.4 Hz, 1H, C=CH). Data matched literature data.[212] **HR-MS:** calcd for C$_3$H$_6$N$_3$ m/z: [M + H]$^+$, 84.0556; found: 84.0558 [Diff(ppm) = 2.45]. **R$_f$:** 0.2 (1:10:89, NEt$_3$:MeOH:DCM).

10.64 Synthesis of 3-phenyl-1H-pyrazol-5-amine (RD226) (93)[130]

A solution of benzoylnitrile (580 mg, 4.00 mmol) and hydrazine monohydrate (200 μL, 4.10 mmol) in MeOH (2 mL) was irradiated in a sealed microwave tube at 120 °C for 40 mins (100 W). MeOH was removed under reduced pressure and the residue was triturated using Pet. Ether to give a brown solid. The product was used without further purification. Brown solid, 480 mg (75%)

^{1}H NMR: (300 MHz, CD$_3$OD) δ 7.65-7.62 (m, 2H, Ar), 7.42-7.28 (m, 3H, Ar), 5.94 (s, 1H, C=CH). Data matched literature data.[213] **HR-MS:** calcd for C$_9$H$_{10}$N$_3$ m/z: [M + H]$^+$, 160.0869; found: 1660.0877 [Diff (ppm) = 5.00]. **m.p.:** 114-118 °C.

10.65 Synthesis of (1H-benzo[d][1,2,3]triazol-1-yl)(thiophen-2-yl)methanone (RD303) (94)
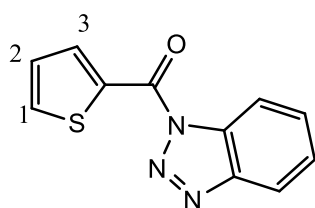
Thiophene-2-carboxylic acid (500 mg, 3.9 mmol) was dissolved in EtOAc (10 mL) and benzotriazole (464 mg, 3.9 mmol) and 4-dimethylaminopyridine (47 mg, 0.39 mmol) were added. The solution was placed in an ice bath at 0 °C and *N, N'*-dicyclohexylcarbodiimide (805 mg, 3.9 mmol) was added. The reaction temperature was adjusted to rt and the solution was stirred overnight. The white precipitate was removed *via* gravity filtration and was washed with EtOAc (3 x 10 mL). The filtrate

was concentrated under reduced pressure and the residue was purified using flash chromatography (DCM). The obtained product was dissolved in minimal DCM and Pet. Ether (~ 3 mL) was added until precipitation began. The solution was stored at -20 °C overnight, and the resultant crystals collected by vacuum filtration and washed with cold Pet. Ether (~ 20 mL) to give white needle, 890 mg (99%).

^{1}H NMR: (300 MHz, CDCl$_3$) δ 8.58 (dd, J = 3.9 Hz, J = 1.2 Hz, 1H, H1), 8.42-8.39 (m, 1H, Ar), 8.18-8.15 (m, 1H, Ar), 7.88 (dd, J = 4.9 Hz, J = 1.2 Hz, 1H, H3), 7.72-7.67 (m, 1H, Ar), 7.57-7.52 (m, 1H, Ar), 7.30-7.27 (m, 1H, H2). ^{1}H NMR data matches literature data.[144] **R$_f$:** 0.9 (DCM). **HR-MS:** calcd for C$_{11}$H$_8$N$_3$OS m/z: [M + H]$^+$, 230.0383; found: 230.0387 [Diff (ppm) = 1.77]. **m.p.:** 182-186 °C (DCM).

10.66 Synthesis of 3-oxo-3-(thiophen-2-yl)propanenitrile (RD320) (95)[144]
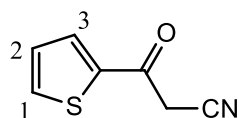
To a solution of acetonitrile (104 μL, 2 mmol) in anhydrous THF (10 mL) under an atmosphere of Ar at -78 °C, was slowly added *n*-BuLi (1.6 mL, 2.4mmol). The solution was stirred at -78 °C for 1 hr after which a solution of compound **94** (458 mg, 2 mmol) in THF (5 mL) was slowly added. The reaction mixture was stirred for 2 hrs at -78 °C. After this period, the reaction mixture was warmed to rt and poured in H$_2$O (10 mL). The aqueous solution was acidified to pH = 3 using aqueous 1 M HCl (2 mL) and extracted with EtOAc. The combined organic layers were dried over MgSO$_4$ and the solvent removed under reduced pressure. The residue was purified using flash chromatography (3:2, Pet. Ether: EtOAc) to give a yellow oil, 211 mg (70%).

^{1}H NMR: (300 MHz, CDCl$_3$) δ 7.81-7.78 (m, 2H, H1, H3), 7.22-7.19 (m, 1H, H2), 4.04 (s, 2H, CH$_2$). ^{1}H NMR data matches literature data.[144] **R$_f$:** 0.6 (3:2, Pet. ether: EtOAc). **HR-MS:** calcd for C$_7$H$_6$NOS m/z: [M + H]$^+$, 152.0165; found: 152.0161 [Diff(ppm) = -2.5].

10.67 Synthesis of 3-(thiophen-2-yl)-1H-pyrazol-5-amine (RD323) (96)[214]
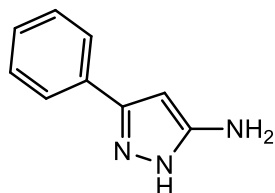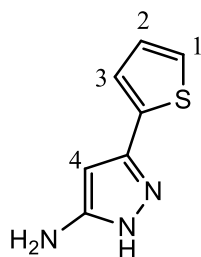

A solution of compound **95** (200 mg, 1.32 mmol) and hydrazine monohydrate (65, µL, 1.35 mmol) in MeOH (1 mL) was irradiated in a sealed microwave tube at 120 °C for 40 mins (100 W). MeOH was removed under reduced pressure and the residue was triturated using Pet. Ether. The product was used without further purification. Orange solid, 217 mg (55%)

¹H NMR: (300 MHz, CDCl₃) δ 7.09-7.07 (m, 2H, H1, H3), 6.86-6.83 (m, 1H, H2), 5.61 (s, 1H, H4). ¹H NMR data matches literature data.[214] **R_f:** 0.6 (3:2, Pet. ether: EtOAc). **HR-MS:** calcd for $C_7H_8N_3S$ m/z: $[M + H]^+$, 166.0433; found 166.0441 [Diff (ppm) = 4.35]. m.p.: 50-53 °C (EtOH).

10.68 Synthesis of 2-*iso*-propylpyrazolo[1,5-a]pyrimidin-7(4H)-one (RTC80) (98)†
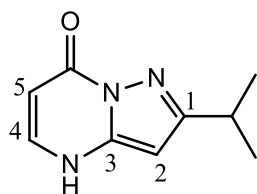
To a fine, stirred suspension of Na (575 mg, 0.25 x 10^{-2} g-atom) in toluene (10 mL) was added, in one portion, EtOAc (2.45 mL, 29.69 mmol). Ethyl formate (2.01 mL, 22.89 mmol) was added dropwise at 27 °C and the reaction mixture was stirred for 12 hrs at 27 °C. 3-*iso*-Propyl-1H-pyrazol-5-amine (1.56 g, 12.5 mmol) in EtOH (10 mL) was added and the reaction mixture was heated at reflux for 5 hrs. The solvent was removed under reduced pressure and the residue re-dissolved in minimal H_2O. The aqueous solution was acidified to pH = 2 using 6 M aqueous HCl (3 mL) which resulted in the precipitation of an orange/brown solid. The precipitate was recrystallized from EtOH to give an orange solid, 333 mg (15%).

¹H NMR: (300 MHz, d_6-DMSO) δ 12.32 (bs, 1H, NH), 7.80 (d, J = 7.5 Hz, 1H, H4), 6.02 (s, 1H, H2), 5.63 (d, J = 7.5 Hz, 1H, H5), 3.02-2.93 (m, 1H, C*H*(CH₃)₂), 1.24 (d, J

= 7.2 Hz, 6H, (CH$_3$)$_2$). **^{13}C NMR:** (75 MHz, d_6-DMSO) δ 161.5 (C=O), 156.4 (C3), 142.0 (C1), 138.9 (C4), 95.3 (C5), 85.9 (C2), 27.8 (CH(CH$_3$)$_2$), 22.7 ((CH$_3$)$_2$). **HR-MS:** calcd for C$_9$H$_{12}$N$_3$O m/z: [M + H]$^+$, 178.0975; found: 178.0978 [Diff(ppm) = 1.81]. **R$_f$:** 0.5 (1:9, MeOH:DCM). **IR (KBr):** 3165 (N-H), 1675 (C=O), 1632 (C=C), 1298 (C-N) cm^{-1}. **m.p.:** 288-290 °C (EtOH). **Anal. calcd** for C$_9$H$_{11}$N$_3$O; C, 61.00; H, 6.26; N, 23.72% found; C, 61.06; H, 6.29; N, 23.54%.

10.69 Synthesis of 2-(*tert*-butyl)pyrazolo[1,5-a]pyrimidin-7(4H)-one (RTC103) (101)[153]†
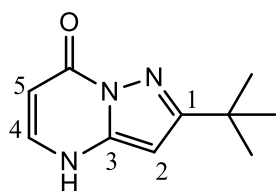
To a fine, stirred suspension of Na (575 mg, 0.25 x 10^{-2} g-atom) in toluene (10 mL) was added, in one portion, EtOAc (2.45 mL, 29.69 mmol). Ethyl formate (2.01 mL, 22.89 mmol) was added dropwise at 27 °C and the reaction mixture was stirred for 12 hrs at 27 °C. 5-Amino-3-(*tert*-butyl)-1H-pyrazole (1.74 g, 12.5 mmol) in EtOH (10 mL) was added and the reaction mixture was heated at reflux for 5 hrs. The solvent was removed under reduced pressure and the residue re-dissolved in minimal H$_2$O. The aqueous solution was acidified to pH = 2 using 6 M aqueous HCl (2 mL) which resulted in the precipitation of an orange/brown solid. The precipitate was recrystallized from EtOH to give a light brown solid, 318 mg (13%).

^{1}H NMR: (300 MHz, d_6-DMSO) δ 12.24 (bs, 1H, NH), 7.81-7.77 (m, 1H, H4), 6.05 (s, 1H, H2), 5.63-5.61 (d, J = 7.3 Hz, 1H, H5), 1.29 (s, 9H, (CH$_3$)$_3$). **^{13}C NMR:** (75 MHz, d_6-DMSO) δ 161.2 (C=O), 156.5 (C3), 141.9 (C1), 138.8 (C4), 95.2 (C5), 85.4 (C2), 32.3 (C(CH$_3$)$_3$), 30.03 ((CH$_3$)$_3$). **HR-MS:** calcd for C$_{10}$H$_{14}$N$_3$O m/z: [M + H]$^+$, 193.1160; found: 193.1167 [Diff (ppm) = 3.66]. **Rf:** 0.5 (1:9, MeOH:DCM). **IR (KBr):** 3155 (N-H), 3085 (C=CH), 2966 (C-H), 1673 (C=O), 1616 (C=C) 1595 (N-H), 142 (C=C), 1234 (C-N) cm^{-1}. **m.p.:** Above 300 °C.

10.70 Synthesis of ethyl 3-oxo-3-(4-(trifluoromethyl)phenyl)propanoate (RD74) (102)[154]
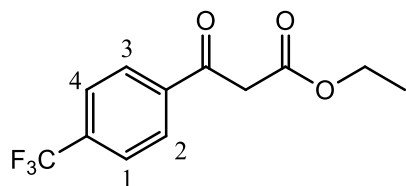
1-(4-(Trifluoromethyl)phenyl)ethanone (500 mg, 2.65 mmol), diethyl carbonate (3.84 mL, 31.90 mmol) and NaH (95 g, 3.98 mmol) were stirred at 80 °C for 1.5 hrs, after which H_2O (5 mL) was added. The aqueous mixture was neutralised with 1 M aqueous HCl and extracted with EtOAc (10 mL, followed by 3 x 10 mL). The combined organic layers were dried over $MgSO_4$ and concentrated under reduced pressure to give a colourless oil, 180 mg (crude yield). Compound **102** was used without further purification.

^{1}H NMR: (300 MHz, d_6-DMSO) δ 8.06 (d, J = 8.0 Hz, 2H, H1, H4), 7.75 (d, J = 8.0 Hz, 2H, H2, H3), 4.22 (q, J = 7.1 Hz, 2H, OCH_2), 4.01 (s, 2H, CH_2), 1.25 (t, J = 7.1 Hz, 3H, OCH_2CH_3). ^{1}H NMR data matches literature data.[154] **R_f:** 0.6 (9:1, Pet. Ether:EtOAc).

10.71 Synthesis of ethyl 3-oxo-3-(thiophen-2-yl)propanoateacid (RD256) (103)[155]
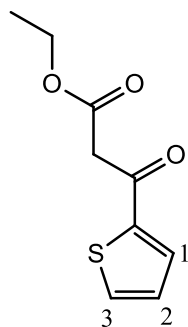
A solution of thiophene-2-carboxylic acid (370 mg, 2.88 mmol), 4-dimethylaminopyridine (708 mg, 5.77 mmol) and Meldrums acid (500 mg, 3.45 mmol) in anhydrous DCM (5 mL) was cooled to 0 °C. *N, N'*-Dicyclohexylcarbodiimide (655 mg, 3.16 mmol) was added and the reaction temperature was adjusted to rt. The reaction was stirred at rt for 2 hrs, after which the white precipitate was removed by gravity filtration. The filtrate was concentrated under reduced pressure and the residue was dissolved in absolute EtOH (16 mL). *p*-Toluene sulfonic acid monohydrate (1.30 g, 7.2

mmol) in EtOH (4 mL) was added and the solution was heated at reflux for 1 hr. The EtOH was removed under reduced pressure and the residue was dissolved in EtOAc and washed sequentially with H_2O, saturated aqueous $NaHCO_3$, and 1 M aqueous HCl and brine. The organic layer was dried over $MgSO_4$ and evaporated under reduced pressure. The residue was purified using flash chromatography (3:2, Pet.Ether:EtOAc) to give a yellow oil, 225 mg (39%).

¹H NMR: (300 MHz, CDCl₃) δ 7.66-7.65 (m, 1H, H3), 7.62-7.60 (m, 1H, H1), 7.07-7.04 (m, 1H, H2), 4.10 (q, $J = 7.5$ Hz, 2H, OCH₂), 3.83 (s, 2H, CH₂), 1.16 (t, $J = 7.5$ Hz, 3H, OCH₂CH₃). ¹H NMR data matches literature data.[155] **HR-MS:** calcd for $C_9H_{11}O_3S$ m/z: $[M + H]^+$, 199.0423; found 199.0418 [Diff(ppm) = -2.87]. **R$_f$:** 0.6 (2:3, Pet. Ether: EtOAc).

10.72 Synthesis of 2-(*tert*-butyl)-5-methylpyrazolo[1,5-a]pyrimidin-7(4H)-one (RTC101) (104)†
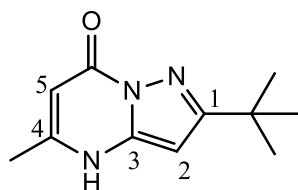
Prepared from 5-amino-3-(*tert*-butyl)-1H-pyrazole (400 mg, 2.87 mmol) and ethyl 3-oxobutanoate (330 µL, 2.61 mmol) using AcOH (10 mL) and following the procedure described in section **10.4**. The reaction mixture was heated at reflux for 4 hrs. Compound **104** was triturated from EtOAc (6 mL) to give an off white solid, 460 mg (78%).

¹H NMR: (300 MHz, d_6-DMSO) δ 12.07 (bs, 1H, NH), 5.95 (s, 1H, H2), 5.50 (s, 1H, H5), 2.26 (s, 3H, CH₃), 1.28 (s, 9H, (CH₃)₃). **¹³C NMR:** (75 MHz, d_6-DMSO) δ 164.2 (C=O), 156.2 (C4), 149.5 (C3), 141.8 (C1), 94.8 (C5), 84.7 (C2), 32.3 (*C*(CH₃)₃), 30.0 (C(*CH₃*)₃), 18.5 (CH₃). **R$_f$:** 0.6 (1:9, MeOH:DCM). **HR-MS:** calcd for $C_{11}H_{16}N_3O$ m/z: $[M + H]^+$, 206.1288; found: 206.1298 [Diff(ppm) = 4.69]. **IR (KBr):** 3158 (N-H), 1681 (C=O), 1613 (C=C), 1579 (N-H) cm^{-1}. **m.p.:** Above 300 °C. **Anal. calcd** for $C_{11}H_{15}N_3O$; C, 64.36; H, 7.37; N, 20.48% found; C, 64.21; H, 7.20; N, 19.96%.

10.73 Synthesis of 2-(*tert*-butyl)-5-ethylpyrazolo[1,5-a]pyrimidin-7(4H)-one (RTC54) (105)
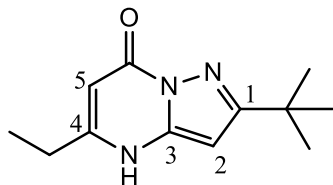
Prepared from 5-amino-3-(*tert*-butyl)-1H-pyrazole (100 mg, 0.71 mmol) and ethyl 3-oxopentanoate (93 µL, 0.64 mmol) using AcOH (15 mL) and following the procedure following the procedure described in section **10.4**. The reaction mixture was heated at reflux overnight. Compound **105** was triturated from EtOAc (4 mL) to give a white solid, 53 mg (33%)

^{1}H NMR: (300 MHz, d_6-DMSO) δ 5.96 (s, 1H, H2), 5.67 (s, 1H, H5), 3.45 (bs, 1H, NH), 2.58-2.56 (q, *J* = 7.2 Hz, 2H, CH$_2$), 1.28 (s, 9H, (CH$_3$)$_3$), 1.20 (t, *J* = 7.2 Hz, 3H, CH$_3$). **^{13}C NMR:** (75 MHz, d_6-DMSO) δ 164.3 (C=O), 156.5 (C4), 154.7 (C3), 141.9 (C1), 93.3 (C2), 84.8 (C5), 32.3 (*C*(CH$_3$)$_3$), 30.0 ((CH$_3$)$_3$), 25.5 (CH$_2$), 12.5 (CH$_3$). **R$_f$:** 0.6 (1:9, MeOH:DCM). **HR-MS:** calcd for C$_{12}$H$_{18}$N$_3$O m/z: [M + H]$^+$, 220.1444; found: 220.1453 [Diff (ppm) = 3.74]. **IR (KBr):** 3250 (N-H), 2963 (*C*=*C*H), 1678 (C=O), 1619 (C=C), 1484 (C=C), 1217 (C-N) cm^{-1} **m.p.:** Above 300 °C.

10.74 Synthesis of 2-(*tert*-butyl)-5-*iso*-propylpyrazolo [1,5-a] pyrimidin-7(4H)-one (RTC102) (106)
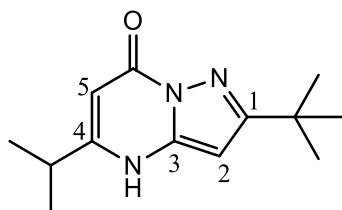
Prepared from 5-amino-3-(*tert*-butyl)-1H-pyrazole (400 mg, 2.87 mmol) and ethyl 4-methyl-3-oxopentanoate (421 µL, 2.61 mmol) using AcOH (10 mL) and following the procedure described in section **10.4**. The reaction mixture was heated at reflux for 4 hrs. Compound **106** was triturated from EtOAc (8 mL) to give a white solid, 72 mg (65%)

HR-MS: calcd for C$_{26}$H$_{38}$N$_6$O$_2$Na m/z: [2M + Na]$^+$; 489.2948; found: 489.2966 [Diff(ppm) = 3.68]. **R$_f$:** 0.6 (1:9, MeOH:DCM). **IR (KBr):** 3174 (N-H), 2963 (C-H),

1676 (C=O), 1630 (C=C), 1576 (N-H), 1238 (C-N) cm^{-1}. **m.p.:** Above 300 °C. **Anal. calcd** for $C_{13}H_{19}N_3O$; C, 66.92; H, 8.21; N, 18.01% found; C, 66.53; H, 8.13; N, 18.40%.

10.75 Synthesis of 2,5-di-*tert*-butylpyrazolo[1,5-a]pyrimidin-7(4H)-one (RTC55) (107)†
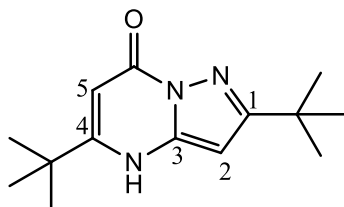
Prepared from 5-amino-3-(*tert*-butyl)-1H-pyrazole (100 mg, 0.71 mmol) and ethyl 4,4-dimethyl-3-oxopentanoate (116 μL, 0.65 mmol) using AcOH (10 mL) and following the procedure described in section **10.4**. The reaction mixture was heated at reflux overnight. Compound **107** was triturated from EtOAc (5 mL) to give a white solid, 42 mg (23%).

^{1}H NMR: (300 MHz, CD$_3$OD) δ 6.08 (s, 1H, H5), 5.74 (s, 1H, H2), 1.38 (s, 18H, (CH$_3$)$_3$ x 2).**^{13}C NMR:** (75 MHz, CD$_3$OD) δ 166.6 (C=O), 161.5 (C4), 158.5 (C1), 142.1 (C3), 91.4 (C5), 85.4 (C2), 34.8 (*C*(CH$_3$)$_3$), 32.3 (*C*(CH$_3$)$_3$), 29.2 ((CH$_3$)$_3$), 27.6 ((CH$_3$)$_3$). **R$_f$:** 0.6 (1:9, MeOH:DCM). **HR-MS:** calcd for $C_{14}H_{22}N_3O$ m/z: [M + H]$^+$, 248.1757; found: 248.1768 [Diff(ppm) = 4.45]. **IR (KBr):** 3090 (N-H), 2965 (C-H), 1670 (C=O), 1614 (C=C), 1570 (NH), 1481 (C=C), 1240 (C-N) cm^{-1}. **m.p.:** Above 300 °C.

10.76 Synthesis of 2-(*tert*-butyl)-5-phenylpyrazolo[1,5-a]pyrimidin-7(4H)-one (RTC81) (108)†
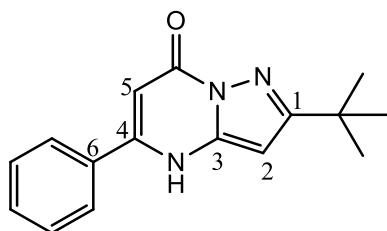
Prepared from 5-amino-3-(*tert*-butyl)-1H-pyrazole (400 mg, 2.87 mmol) and methyl 3-oxo-3-phenylpropanoate (448 μL, 2.61 mmol) using AcOH (10 mL) and following the

procedure described in section **10.4**. The reaction mixture was heated at reflux for 4 hrs. Compound **103** was triturated from EtOAc (5 mL) to give a white solid, 256 mg (40%).

^{1}H NMR: (300 MHz, d_6-DMSO) δ 12.35 (s, 1H, NH), 7.86-7.77 (m, 2H, Ar), 7.63-7.53 (m, 3H, Ar), 6.09 (s, 1H, H2), 6.00 (s, 1H, H5), 1.32 (s, 9H, (CH$_3$)$_3$). **^{13}C NMR:** (75 MHz, d_6-DMSO) δ 164.7 (C=O), 156.3 (C4), 149.3 (C3), 142.1 (C1), 132.4 (C6), 130.9 (Ar), 129.0 (Ar), 127.1 (Ar), 93.6 (C2), 86.0 (C5), 32.4 (C(CH$_3$)$_3$), 30.0 ((CH$_3$)$_3$) **HR-MS:** calcd for C$_{16}$H$_{17}$N$_3$ONa m/z: [M + Na]$^+$, 290.1264; found: 290.1278 [Diff(ppm) = 4.73]. **IR (KBr):** 3433 (N-H), 3127 (C-H), 1656 (C=O), 1611 (C=C), 1492 (C=C) cm^{-1}. **m.p.:** Above 300 °C. **Anal. calcd** for C$_{16}$H$_{17}$N$_3$O; C, 71.88; H, 6.41; N, 15.72% found: C, 71.71; H, 6.62; N, 15.79%.

10.77 Synthesis of 2-*iso*-propyl-5-methylpyrazolo[1,5-a]pyrimidin-7(4H)-one (RTC60) (109)†
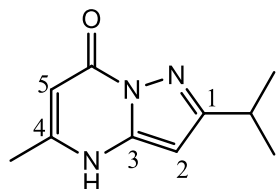
Prepared from 3-*iso*-propyl-1H-pyrazol-5-amine (241 mg, 1.92 mmol) and ethyl 3-oxobutanoate (222 µL, 1.75 mmol) using AcOH (10 mL) and following the procedure described in section **10.4**. The reaction mixture was heated at reflux for 4 hrs. Compound **109** was triturated from EtOAc (6 mL) to give a beige solid, 232 mg (69%).

^{1}H NMR: (300 MHz, d_6-DMSO) δ 12.13 (bs, 1H, NH), 5.62 (s, 1H, H2), 5.49 (s, 1H, H5), 3.02-2.88 (m, 1H, CH(CH$_3$)$_2$), 2.25 (s, 3H, CH$_3$), 1.23 (d, J = 6.9 Hz, (CH$_3$)$_2$). **^{13}C NMR:** (75 MHz, d_6-DMSO) δ 161.4 (C=O), 156.1 (C4), 149.5 (C3), 141.8 (C1), 94.8 (C5), 58.1 (C2), 27.8 (CH(CH$_3$)$_2$), 22.2 ((CH$_3$)$_2$), 18.4 (CH$_3$). **HR-MS:** calcd for C$_{10}$H$_{14}$N$_3$O m/z: [M + H]$^+$, 193.1160; found: 193.1167 [Diff(ppm) = 3.88]. **Rf:** 0.5 (1:9, MeOH:DCM). **IR (KBr):** 342 (N-H), 2963 (C-H), 1679 (C=O), 1626 (N-H), 1578 (C=C), 1409 (C=C), 1285 (C-N) cm^{-1}. **m.p.:** 262-265 °C.

10.78 Synthesis of 5-ethyl-2-*iso*-propylpyrazolo[1,5-a]pyrimidin-7(4H)-one (RTC87) (110)†
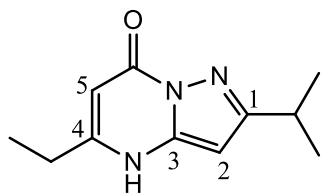
Prepared from 3-*iso*-propyl-1H-pyrazol-5-amine (100 mg, 0.79 mmol) and ethyl 3-oxopentanoate (125 μL, 0.87 mmol) using AcOH (10 mL) and following the procedure described in section **10.4**. The reaction mixture was heated at reflux for 5 hrs. Compound **110** was triturated from EtOAc (5mL) to give a brown solid, 100 mg (63%).

^{1}H NMR: (300 MHz, CD$_3$OD) δ 5.99 (s, 1H, H2), 5.62 (s, 1H, H5), 5.07 (bs, 1H, NH), 3.06-2.99 (m, 1H, CH(CH$_3$)$_2$), 2.63 (q, J = 7.2 Hz, 2H, CH$_2$), 1.32-1.27 (m, 9H, CH$_3$, (CH_3)$_2$). **^{13}C NMR:** (75 MHz, CD$_3$OD) δ 161.6 (C=O), 158.2 (C4), 156.0 (C3), 142.1 (C1), 93.0 (C5), 85.3 (C2), 28.3 (*C*H(CH$_3$)$_2$), 25.9 (CH$_2$), 21.5 ((CH$_3$)$_2$), 11.5 (CH$_3$). **HR-MS:** calcd for C$_{11}$H$_{16}$N$_3$O m/z: [M + H]$^+$, 206.1288; found: 206.1298 [Diff(ppm) = 4.90]. **Rf:** 0.5 (1:9 MeOH:DCM). **IR (KBr):** 3138 (N-H), 2965 (C-H), 1686 (C=O), 1630 (C=C), 1577 (NH), 1478 (C=C), 1293 (C-N) cm^{-1}. **m.p.:** 260-261 °C.

10.79 Synthesis of 2-*iso*-propyl-5-propylpyrazolo[1,5-a]pyrimidin-7(4H)-one (RTC63) (111)†

Prepared from 3-*iso*-propyl-1H-pyrazol-5-amine (219 mg, 1.75 mmol) and ethyl 3-oxohexanoate (255 μL, 1.59 mmol) using AcOH (10 mL) and following the procedure described in section **10.4**. The reaction mixture was heated at reflux for 4 hrs. Compound **111** was triturated from EtOAc (7 mL) to give a light brown solid, 253 mg (72%).

^{1}H NMR: (300 MHz, CD$_3$OD) δ 6.06 (s, 1H, H2), 5.70 (s 1H, H5), 5.00 (bs, 1H, NH), 3.11-2.97 (m, 1H, CH(CH$_3$)$_2$), 2.58 (t, J = 5.1 Hz, 2H, CH_2CH$_2$CH$_3$), 179-.67 (m, 2H, CH$_2$CH_2CH$_3$), 1.29 (d, J = 6.9 Hz, 6H, (CH$_3$)$_2$), 0.99 (t, J = 7.5, 3H, CH$_3$).**^{13}C NMR:**

(75 MHz, CD$_3$OD) δ 163.6 (C=O), 158.1 (C4), 154.6 (C3), 142.0 (C1), 93.9 (C5), 85.4 (C2), 34.5 (CH$_2$CH$_2$CH$_3$), 28.3 (CH(CH$_3$)$_2$), 21.5 (CH$_2$CH$_2$CH$_3$), (CH$_3$)$_2$), 12.4 (CH$_3$). **HR-MS:** calcd for C$_{12}$H$_{18}$N$_3$O m/z: [M + H]$^+$, 220.1444; found: 220.1455 [Diff (ppm) = 5.00]. **Rf:** 0.5 (1:9 MeOH:DCM). **IR (KBr):** 3246 (N-H), 2965 (C-H), 1672 (C=O), 1609 (C=C), 1477 (C=C), 1292 (C-N), 800 (N-H) cm^{-1}. **m.p.:** 258-260 °C. **Anal. calcd** for C$_{12}$H$_{17}$N$_3$O; C, 65.72; H, 7.81; N, 19.17% found; C, 66.08; H, 8.16; N, 19.44%.

10.80 Synthesis of 2,5-di-*iso*-propylpyrazolo[1,5-a]pyrimidin-7(4H)-one (RTC58) (112)†
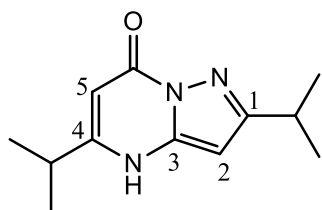
Prepared from 3-*iso*-propyl-1H-pyrazol-5-amine (312 mg, 2.49 mmol) and ethyl 4-methyl-3-oxopentanoate (365 µL, 2.27 mmol) using AcOH (10 mL) and following the procedure described in section **10.4**. The reaction mixture was heated at reflux for 4 hrs. Compound **112** was triturated from EtOAc (5 mL) to give a beige solid, 326 mg (66%).

^{1}H NMR: (300 MHz, d_6-DMSO) δ 11.97 (bs, 1H, NH), 5.94 (s, 1H, H2), 5.52 (s, 1H, H5), 3.03-2.89 (m, 1H, CH(CH$_3$)$_2$), 2.87-2.73 (m, 1H, CH(CH$_3$)$_2$), 1.24-1.22 (m, 12H, (CH$_3$)$_2$ x 2). **^{13}C NMR:** (75 MHz, d_6-DMSO) δ 161.5 (C=O), 158.5 (C4), 156.5 (C3), 141.9 (C1), 91.6 (C5), 85.4 (C2), 31.5 (CH(CH$_3$)$_2$), 27.9 (CH(CH$_3$)$_2$), 22.3 ((CH$_3$)$_2$), 21.0 ((CH$_3$)$_2$). **HR-MS:** calcd for C$_{12}$H$_{18}$N$_3$O m/z: [M + H]$^+$, 220.1444; found: 220.1446 [Diff (ppm) = 0.90]. **Rf:** 0.5 (1:9 MeOH:DCM) **IR (KBr):** 3142 (N-H), 2964 (C-H), 1674 (C=O), 1627 (C=C), 1480(C=C), 1291 (C-N) cm^{-1}. **m.p.:** Above 300 °C. **Anal. calcd** for C$_{12}$H$_{17}$N$_3$O; C, 65.72; H, 7.81; N, 19.17% found: C, 65.43; H, 7.98; N, 19.17%.

10.81 Synthesis of 5-(*tert*-butyl)-2-*iso*-propylpyrazolo[1,5-a]pyrimidin-7(4H)-one (RTC57) (113)†
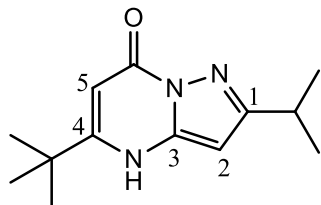
Prepared from 3-*iso*-propyl-1H-pyrazol-5-amine (164 mg, 1.31 mmol) and ethyl 4,4-dimethyl-3-oxopentanoate (213 μL, 1.19 mmol) using AcOH (10 mL) and following the procedure described in section **10.4**. The reaction mixture was heated at reflux for 4 hrs. Compound **113** was triturated from EtOAc (5 mL) to give a white solid, 36 mg (13%).

¹H NMR: (300 MHz, d_6-DMSO) δ 6.28 (s, 1H, H2), 6.05 (s, 1H, H5), 5.45 (bs, 1H, NH), 3.12-2.98 (m, 1H, CH(CH$_3$)$_2$), 1.35 (s, 9H, (CH$_3$)$_3$), 1.30 (d, J = 7.2 Hz, 6H, (CH$_3$)$_2$). **¹³C NMR:** (75 MHz, d_6-DMSO) δ 169.6 (C=O), 163.9 (C4), 161.5 (C3), 142.2 (C1), 91.4 (C5), 85.6 (C2), 34.8 (C(CH$_3$)$_3$), 28.3 (CH(CH$_3$)$_2$), 27.6 ((CH$_3$)$_3$), 21.5 ((CH$_3$)$_2$). **HR-MS:** calcd for C$_{13}$H$_{20}$N$_3$O m/z: [M + H]$^+$, 234.1600; found: 234.1061 [Diff (ppm) = -0.40]. **R$_f$:** 0.5 (1:9, MeOH:DCM). **IR (KBr):** 3240 (N-H), 2964 (C-H), 1681 (C=O), 1613 (C=C), 1482 (C=C), 1258 (C-N) cm^{-1}. **m.p.:** Above 300 °C.

10.82 Synthesis of 2-*iso*-propyl-5-phenylpyrazolo[1,5-a]pyrimidin-7(4H)-one (RTC61) (114)†
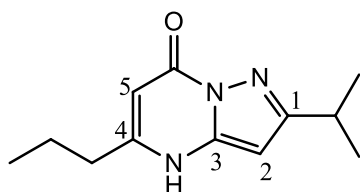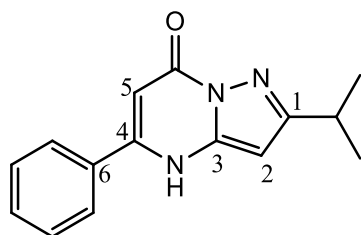

Prepared from 3-*iso*-propyl-1H-pyrazol-5-amine (164 mg, 1.32 mmol) and methyl 3-oxo-3-phenylpropanoate (208 μL, 1.19 mmol) using AcOH (10 mL) and following the procedure described in section **10.4**. The reaction mixture was heated at reflux overnight. Compound **114** was triturated from EtOAc (5 mL) to give a white solid, 84 mg (30%).

¹H NMR: (300 MHz, CD$_3$OD) δ 12.38 (bs, 1H, NH), 7.83-7.80 (m, 2H, Ar), 7.59-7.56 (m, 2H, Ar), 6.06 (s 1H, H2), 5.99 (s, 1H, H5), 3.06-2.97 (m, 1H, CH(CH$_3$)$_2$), 1.27 (d, J

= 6.9 Hz, 6H, (CH_3)$_2$). **^{13}C NMR:** (75 MHz, CD$_3$OD) δ 163.9 (C=O), 157.9 (C4), 151.0 (C3), 142.1 (C1), 132.4 (C6), 130.9 (Ar), 28.9 (Ar), 126.7 (Ar), 93.3 (C2), 86.4 (C5), 28.3 (*C*H(CH$_3$)$_2$), 21.5 ((CH$_3$)$_2$). **HR-MS:** calcd for C$_{15}$H$_{16}$N$_3$O m/z: [M + H]$^+$, 254.1288; found: 254.1298 [Diff (ppm) = 3.90]. **R$_f$:** 0.5 (1:9, MeOH:DCM). **IR (KBr):** 3239 (N-H), 2964 (C-H), 1662 (C=O), 1614 (C=C), 1490 (C=C), 1291 (C-N), 768 (N-H) cm^{-1}. **m.p.:** 248-251 °C.

10.83 Synthesis of 5-(3,5-bis(trifluoromethyl)phenyl)-2-*iso*-propylpyrazolo[1,5-a]pyrimidin-7(4H)-one (RTC53) (115)
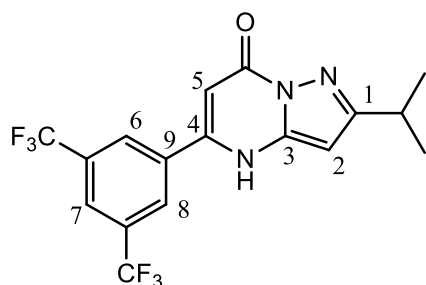
Prepared from 3-*iso*-propyl-1H-pyrazol-5-amine (70 mg, 0.55 mmol) and ethyl 3-(3,5-bis(trifluoromethyl)phenyl)-3-oxopropanoate (201 mg, 0.61 mmol) using AcOH (15 mL) and following the procedure outlined in section **10.4**. The reaction mixture was heated at reflux overnight. Compound **115** was triturated from EtOAc (3 mL) to give a beige solid, 60 mg (27%).

^{1}H NMR: (300 MHz, d_6-DMSO) δ 12.61 (bs, 1H, NH), 8.51 (s, 2H, H6, H8), 8.33 (s, 1H, H7), 3.07-2.98 (m, 1H, C*H*(CH$_3$)$_2$), 1.27 (d, J = 6.9 Hz, 6H, (CH$_3$)$_2$). **^{13}C NMR:** (75 MHz, d_6-DMSO) δ 162.2 (C=O), 156.0 (C4), 146.3 (C3), 142.1 (C1), 134.9 (C9), 130.8 (q, J = 33.0 Hz, *C*-CF$_3$), 128.7 (C6, C8), 124.3 (C7), 123.0 (q, J = 270.0 Hz, CF$_3$), 95.4 (C2), 86.7 (C5), 27.9 (*C*H(CH$_3$)$_2$), 22.2 ((CH$_3$)$_2$). **R$_f$:** 0.5 (1:9, MeOH:DCM). **HR-MS:** calcd for C$_{17}$H$_{14}$F$_6$N$_3$O m/z: [M + H]$^+$, 390.1036; found: 390.1051 [Diff(ppm) = 2.79]. **IR (KBr):** 3423 (N-H), 2972 (C-H), 1670 (C=O), 1617 (C=C), 1577 (N-H), 1481 (C=C), 1279 (C-F), 1139 (C-N) cm^{-1}. **m.p.:** Above 300 °C.

10.84 Synthesis of 5-(3,5-bis(trifluoromethyl)phenyl)-2-methylpyrazolo[1,5-a]pyrimidin-7(4H)-one (RTC83) (117)†
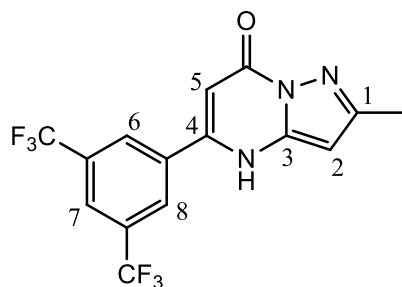
Prepared from 3-methyl-1H-pyrazol-5-amine (68 mg, 0.70 mmol) and ethyl 3-(3,5-bis(trifluoromethyl)phenyl)-3-oxopropanoate (208 mg, 0.64 mmol) using AcOH (10 mL) and following the procedure described in section **10.4**. The reaction mixture was heated at reflux for 4 hrs. Compound **117** was triturated from EtOAc (3 mL) to give an off white solid, 40 mg (49%).

^{1}H NMR: (300 MHz, d_6-DMSO) δ 8.53 (s, 2H, H6, H8) 8.32 (s, 1H, H7), 6.29 (s, 1H, H2), 6.08 (s, 1H, H5), 2.32 (s, 3H, CH$_3$). **^{13}C NMR:** (75 MHz, CD$_3$OD) δ 164.2 (C=O), 153.0 (C4), 148.8 (C3), 142.9 (C1), 135.5 (C9), 131.3 (q, J = 32.7 Hz, C-CF$_3$), 128.8 (C6, C8), 124.7 (C7), 123.6 (q, J = 272.2 Hz, CF$_3$), 96.0 (C2), 90.2 (C5), 14.5 (CH$_3$). **R$_f$:** 0.5 (1:9, MeOH:DCM). **HR-MS:** calcd for C$_{15}$H$_{10}$F$_6$N$_3$O m/z: [M + H]$^+$, 362.0723; found: 362.0738 [Diff(ppm) = 4.38]. **IR (KBr):** 3170 (N-H), 2986 (C-H), 1659 (C=O), 1601 (C=C), 1532 (N-H), 1431 (C=C), 1275 (C-N), 1138 (C-F) cm^{-1}. **m.p.:** Above 300 °C.

10.85 Synthesis of 5-(3,5-bis(trifluoromethyl)phenyl)-2-ethylpyrazolo[1,5-a]pyrimidin-7(4H)-one (RTC88) (118)†
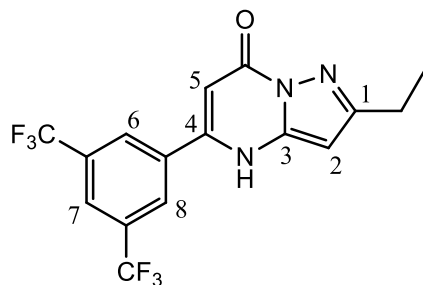
Prepared from 3-ethyl-1H-pyrazol-5-amine (81 μL, 0.73 mmol) and was 3,5-bis(trifluoromethyl)phenyl)-3-oxopropanoate (200 mg, 0.61 mmol) using AcOH (10 mL) and following the procedure described in section **10.4**. The reaction mixture was

heated at reflux for 4 hrs. Compound **118** was triturated using EtOAc (4 mL) to give a beige solid, 66 mg (42%).

^{1}H NMR: (300 MHz, d_6-DMSO) δ 12.64 (bs, 1H, NH), 8.51 (s, 2H, H6, H8), 8.33 (s, 1H, H7), 6.30 (s, 1H, H2), 6.12 (s, 1H, H5), 2.70 (q, J = 7.5 Hz, 2H, CH$_2$), 1.25 (t, J = 7.5 Hz, 3H, **^{13}C NMR:** (75 MHz, d_6-DMSO) δ 158.0 (C=O), 155.9 (C4), 146.3 (C3), 142.2 (C1), 135.0 (C9), 130.8 (q, J = 33.3 Hz, C-CF$_3$), 128.3 (C6, C8), 124.2 (C7), 123.0 (q, J = 270.0 Hz, CF$_3$), 95.3 (C2), 88.1 (C5), 21.5 (CH$_2$), 13.2 (CH$_3$). **R$_f$:** 0.5 (1:9, MeOH:DCM). **HR-MS:** calcd for C$_{16}$H$_{12}$F$_3$N$_3$O m/z: [M + H]$^+$, 376.0879; found: 376.0897 [Diff (ppm) = 4.79]. **IR (KBr):** 3174 (N-H), 2980 (C-H), 1666 (C=O), 1604 (C=C), 1524 (N-H), 1428 (C=C), 1277 (C-N), 1136 (C-F) cm^{-1}. **m.p.:** 244-248 °C

10.86 Synthesis of 5-(3,5-bis(trifluoromethyl)phenyl)-2-phenylpyrazolo[1,5-a] pyrimidin-7(4H)-one (RTC91) (119)†
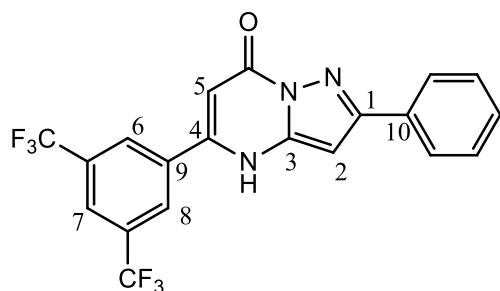
Prepared from compound **93** (88 mg, 0.55mmol) and ethyl 3-(3,5-bis(trifluoromethyl)phenyl)-3-oxopropanoate (164 mg, 0.50 mmol) using AcOH (10 mL) and following the procedure described in section **10.4**. The reaction mixture was heated at reflux for 4 hrs. Compound **119** was triturated from EtOAc (4 mL) and purified using flash chromatography (1:9 MeOH:DCM) to give an off white solid, 44 mg (21%)

^{1}H NMR: (300 MHz, d_6-DMSO) δ 12.89 (bs, 1H, NH), 8.56 (s, 2H, H6, H8), 8.37 (s, 1H, H7), 8.04-8.02 (m, 2H, Ar), 7.53-7.41 (m, 3H, Ar), 6.73 (s, 1H, H2), 6.41 (s, 1H, H5). **^{13}C NMR:** (75 MHz, d_6-DMSO) δ 156.0 (C=O), 153.5 (C4), 146.7 (C1), 143.0 (C3), 134.9 (C9), 132.1 (C10), 130.8 (q, J = 33.0 Hz, C-CF$_3$), 129.0 (Ar), 128.7 (Ar), 128.4 (C6, C8), 126.2 (Ar), 124.3 (C7), 123.0 (q, J = 270.0 Hz, CF$_3$), 95.7 (C2), 86.7 (C5). **HR-MS:** calcd for C$_{20}$H$_{12}$F6N$_3$O m/z: [M + H]$^+$, 424.0879; found: 424.0893 [Diff (ppm) = 3.25]. **R$_f$:** 0.4 (1:9, MeOH:DCM). **IR (KBr):** 3429 (N-H), 3132 (C=C), 1661 (C=O), 1527 (N-H), 1372 (C-F), 1278 (C-N), 808 (N-H) cm^{-1}. **m.p.:** Above 300 °C.

10.87 5-(3,5-bis(trifluoromethyl)phenyl)-2-(thiophen-2-yl)pyrazolo[1,5-a]pyrimidin-7(4H)-one (RTC97) (120)†
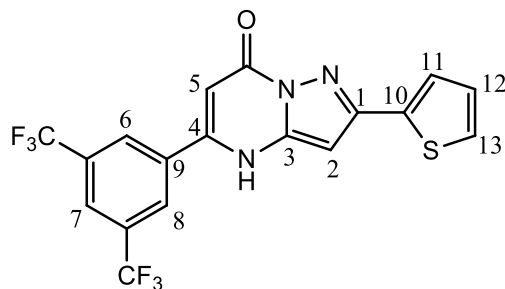
Prepared from compound **96** (120 mg, 0.72 mmol) and ethyl 3-(3,5-bis(trifluoromethyl)phenyl)-3-oxopropanoate (218 mg, 0.64 mmol) using AcOH (15 mL) and following the procedure described in section **10.4**. The reaction mixture was heated at reflux for 4 hrs. Compound **120** was precipitated using EtOAc (5 mL) to give a beige solid, 14 mg (30%).

^{1}H NMR: (300 MHz, d_6-DMSO) δ 12.86 (bs, 1H, NH), 8.55 (s, 2H, H6, H8), 8.35 (s, 1H, H7), 7.75-7.74 (m, 1H, H13), 7.65-7.62 (m, 1H, H11), 7.19-7.17 (m, 1H, H12), 6.63 (s, 1H, H2), 6.39 (s, 1H, H5). **^{13}C NMR:** (75 MHz, d_6-DMSO) 155.7 (C=O), 149.2 (C4), 146.7 (C1), 142.9 (C3), 135.2 (C10), 134.7 (C9), 130.8 (q, J = 32.0 Hz, C-CF$_3$), 128.5 (C6, C8), 127.8 (C12), 127.2 (C13), 127.0 (C11), 124.4 (C7), 123.0 (q, J = 271.1 Hz, CF$_3$), 95.9 (C2), 86.5 (C5). **R$_f$:** 0.5 (1:9, MeOH:DCM). **HR-MS:** calcd for C$_{18}$H$_{10}$F$_6$N$_3$OS m/z: [M + H]$^+$, 430.0443; found: 430.0431 [Diff (ppm) = -2.75]. **IR (KBr):** 3424 (N-H), 3139 (C=C), 1618 (C=O), 1573 (N-H), 1370 (C-F), 1281 (C-N), 822 (N-H) cm^{-1}. **m.p.:** Above 300 °C.

10.88 Synthesis of 2-*iso*-propyl-5-(4-(trifluoromethyl)phenyl)pyrazolo[1,5-a]pyrimidin-7(4H)-one (RTC59) (121)†
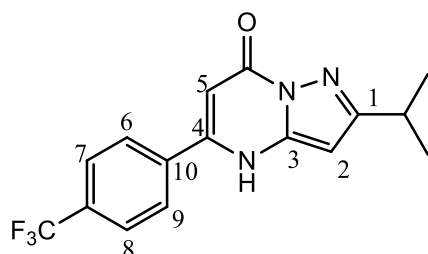
Prepared from compound **102** (164 mg, 0.63 mmol) and 3-*iso*-propyl-1H-pyrazol-5-amine (91 mg, 0.73 mmol) using AcOH (5 mL) and following the procedure described

in section **10.4**. The reaction mixture was heated at reflux for 4 hrs. Compound **121** was triturated from EtOAc (4.5 mL) to give a beige solid, 40 mg (17%)

^{1}H NMR: (300 MHz, d_6-DMSO) δ 8.04 (d, J = 8.3 Hz, 2H, H7, H8), 7.95 (d, J = 8.3 Hz, 2H, H6, H9), 6.09 (s, 2H, H2, H5), 3.05-2.98 (m, 1H, CH(CH$_3$)$_2$), 1.28 (d, J = 6.9 Hz, 6H, (CH$_3$)$_2$).**^{13}CNMR:** (75 MHz, CD$_3$OD) δ 164.2 (C=O), 157.1 (C4), 149.4 (C3), 142.3 (C1), 136.5 (C10), 132.4 (q, J = 32.7 Hz, C-CF$_3$), 127.7 (C6, C9), 125.7 (q, J = 3.6 Hz, C7, C8), 123.8 (q, J = 270.0 Hz, CF$_3$), 94.4 (C2), 86.5 (C5), 28.4 (CH(CH$_3$)$_2$), 21.4 ((CH$_3$)$_2$). **R$_f$:** 0.6 (1:9, MeOH:DCM). **HR-MS:** calcd for C$_{16}$H$_{15}$F$_3$N$_3$O m/z: [M + H]$^+$, 323.1192; found: 323.1205 [Diff (ppm) = 4.01]. **IR (KBr):** 3415 (N-H), 3972 (C-H), 1655 (C=O), 1613 (C=C), 1589 (N-H), 1432 (C=C), 1324 (C-F), 1165 (C-N) cm^{-1}. **m.p.:** Above 300 °C.

10.89 Synthesis   of   2-*iso*-propyl-5-(3-(trifluoromethyl)phenyl)pyrazolo[1,5-a]pyrimidin-7(4H)-one (RTC84) (122)†
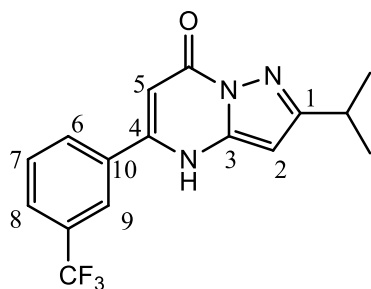
Prepared from 3-*iso*-propyl-1H-pyrazol-5-amine (132 mg, 1.05 mmol) and ethyl 3-oxo-3-(3-(trifluoromethyl)phenyl)propanoate (232 μL, 1.16 mmol) using AcOH (10 mL) and following the procedure described in section **10.4**. The reaction mixture was heated at reflux for 4 hrs. Compound **122** was triturated from EtOAc (4 mL) to give an off white solid, 101 mg (30%).

^{1}H NMR: (300 MHz, CD$_3$OD) δ 8.17 (s, 1H, H9), 8.14 (d, J = 8.1 Hz, 1H, H6), 7.93 (d, J = 7.5 Hz, 1H, H8), 7.82-7.77 (m, 1H, H7), 3.07-2.93(m, 1H, CH(CH$_3$)$_2$), 1.25 (d, J = 7.1 Hz, 6H, (CH$_3$)$_2$). **^{13}C NMR:** (75 MHz, CD$_3$OD) δ 162.1 (C=O), 156.1 (C4), 147.7 (C3), 142.1 (C1), 133.4 (C10), 131.4 (C6), 130.1 (C7), 129.6 (q, J = 32.6 Hz, C-CF$_3$), 127.3 (q, J = 3.7 Hz, C8), 123.80 (q, J = 270.0 Hz, CF$_3$), 123.84 (q, J = 3.7 Hz, C9), 94.4 (C2), 86.6 (C5), 27.9 (CH(CH$_3$)$_2$), 22.1 (CH$_3$)$_2$). **HR-MS:** calcd for C$_{16}$H$_{15}$F$_3$N$_3$O m/z: [M + H]$^+$, 322.1162; found: 322.1167 [Diff (ppm) = 1.6]. **IR (KBr):** 3183 (N-H),

2970 (C-H), 1671 (C=O), 1614 (C=C), 1593 (NH), 1437 (C=C), 1329 (C-F), 1249 (C-N), 803 (N-H) cm^{-1}. **m.p.:** Above 300 °C.

10.90 Synthesis of 5-(3,5-bis(trifluoromethyl)phenyl)-4-ethyl-2-*iso*-propylpyrazolo[1,5-a]pyrimidin-7(4H)-one (RTC64) (123)†
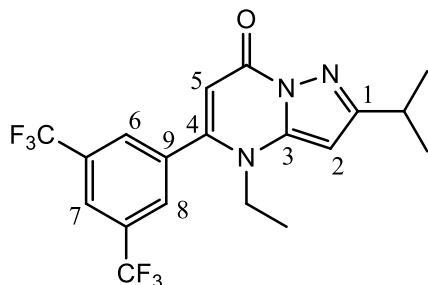
K$_2$CO$_3$ (105 mg, 0.75 mmol) was added to a solution of compound **115** (100 mg, 0.25 mmol) and iodoethane (31 μL, 0.37 mmol) dissolved in DMF (10 mL). The suspension was heated at reflux for 8 hrs after which the solvent was removed under reduced pressure. The residue was washed with 1 M aqueous HCl (10 mL) and the aqueous layer extracted with DCM (10 mL, followed by 3 x 10 mL). The combined organic layers were dried over MgSO$_4$ and the solvent removed under reduced pressure. The residue was purified using flash chromatography (4:1 EtOAc:Pet. Ether) to give a white solid, 20 mg (18%).

^{1}H NMR: (300 MHz, CD$_3$OD) δ 8.45 (s, 2H, H6, H8), 7.92 (s, 1H, H7), 6.49 (s, 1H, H2), 6.30 (s, 1H, H5), 4.89 (q, J = 7.5 Hz, 2H, CH$_2$), 3.09-2.96 (m, 1H, CH(CH$_3$)$_2$), 1.42 (d, J = 7.2 Hz, 6H, (CH$_3$)$_2$), 1.24 (t, J = 7.5 Hz, 3H, CH$_3$). **^{13}C NMR:** (75 MHz, CD$_3$OD) δ 159.6 (C=O), 158.2 (C4), 157.8 (C3), 153.6 (C1), 140.1 (C9), 131.9 (q, J = 33.0 Hz, C-CF$_3$), 127.2 (q, J = 3.3 Hz, C6, C8), 123.1 (q, J = 3.3 Hz, C7), 123.3 (q, J = 270.0 Hz, CF$_3$), 98.2 (C2), 96.5 (C5), 44.3 (CH$_2$), 25.4 (*C*H(CH$_3$)$_2$), 22.0 ((CH$_3$)$_2$), 14.7 (CH$_3$). **HR-MS:** calcd for C$_{19}$H$_{18}$F$_6$N$_3$O m/z: [M + H]$^+$, 418.1349; found: 418.1353[Diff(ppm) = 1.10]. **Rf:** 0.6 (4:1 EtOAc: Pet. Ether) **IR (KBr):** 2968 (C-H), 1697 (C=O), 1653 (C=C), 1482 (C=C), 1369 (C-F), 1278 (C-N) cm^{-1}. **m.p.:** 253-255 °C.

10.91 Synthesis of ethyl 2-((dimethylamino)methylene)-3-oxobutanoate (RD159) (124)[157]
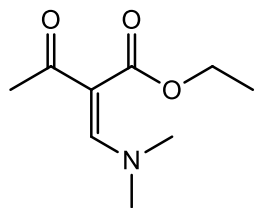
Ethyl acetoacetate (194 µL, 1.53 mmol) was stirred at rt and *N, N*-dimethyl formamide dimethyl acetal (256 µL, 1.92 mmol) was added dropwise over 10 mins and stirred at rt overnight. The reaction mixture was concentrated under reduced pressure and azeotroped with toluene (3 x 5 mL) to give compound **124** as a yellow oil which became orange on standing, 238 mg (83%).

^{1}H NMR: (300 MHz, CDCl$_3$) δ 7.66 (s, 1H, C=CH), 4.21 (q, *J* = 7.5 Hz, 2H, CH_2CH$_3$), 3.05 (bs, 6H, N(CH$_3$)$_2$), 2.28 (s, 3H, (C=O)CH$_3$), 1.31 (t, *J* = 7.5 Hz, 3H, CH$_2$CH_3). ^{1}H NMR data matches literature data.[218] **R$_f$:** 0.2 (4:1, EtOAc:*n*-hexane). **HR-MS:** calcd for C$_9$H$_{16}$NO$_3$ m/z: [M + H]$^+$, 186.1125; found: 186.1120 [Diff (ppm) = -2.69].

10.92 Synthesis of (Z)-ethyl 2-((dimethylamino)methylene)-3-oxopentanoate (RD347) (125)[219]
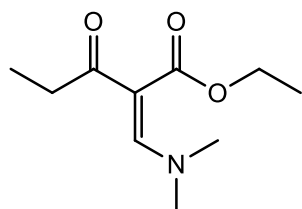
Ethyl 3-oxopentanoate (303 µL, 2.13 mmol) was stirred at rt and N, N-dimethyl formamide dimethyl acetal (500 µL, 3.76 mmol) was added dropwise over 10 mins and stirred at rt overnight. The reaction mixture was concentrated under reduced pressure and azeotroped with toluene (3 x 5 mL) to give compound **125** as a red oil, 410 mg (crude yield), which was used without further purification.

^{1}H NMR: (300 MHz, CDCl$_3$) δ 7.56 (s, 1H, C=CH), 4.13 (q, *J* = 7.14 Hz, 2H, OCH$_2$), 2.93 (bs, 6H, N(CH$_3$)$_2$), 2.63-2.55 (m, 2H, CH$_2$), 1.23 (t, *J* = 7.14. 3H, OCH$_2$CH_3), 1.01 (t, *J* = 7.38 Hz, 2H, CH$_2$CH_3). ^{1}H NMR data matches literature data.[219] **R$_f$:** 0.2 (4:1, EtOAc:*n*-hexane).

10.93 Synthesis of ethyl 1-(4-fluorophenyl)-5-methyl-1H-pyrazole-4-carboxylate (RD161) (126)[215]
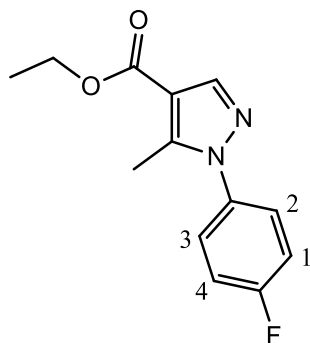
Compound **124** (542 mg, 2.90 mmol) was dissolved in EtOH (5 mL) in a 20 mL round bottom flask. In a second flask, (4-fluorophenyl)hydrazine.HCl (476 mg, 2.90 mmol) and NEt$_3$ (404 µL, 2.90 mmol) in EtOH (5 mL) were stirred for 10 mins at rt after which the solution was transferred to the round bottom containing compound **124**. The reaction mixture was heated at reflux and the reaction progress monitored by TLC. After 2 hrs the EtOH was removed under reduced pressure and the residue dissolved in a saturated aqueous NaHCO$_3$ solution (10 mL). The aqueous layer was extracted with EtOAc (10 mL, followed by 3 x 10 mL) and dried over MgSO$_4$. The combined organic layers were concentrated under reduced pressure and the residue was purified using flash chromatography (1:9, EtOAc:Pet. Ether) to give a beige solid, 647 mg (90%).

^{1}H NMR: (300 MHz, CDCl$_3$) δ 7.87 (s, 1H, N=CH), 7.32-7.25 (m, 2H, H2, H3), 7.08-7.00 (m, 2H, H1, H4), 4.18 (q, J = 7.2 Hz, 2H, C*H$_2$*CH$_3$), 2.41 (s, 3H, CH$_3$), 1.24 (t, J = 7.2 Hz, 3H, CH$_2$C*H$_3$*). ^{1}H NMR data matches literature data.[215] **Rf:** 0.5 (1:9, EtOAc:Pet. Ether). **HR-MS:** calcd for C$_{13}$H$_{14}$FN$_2$O$_2$ m/z: [M + H]$^+$, 250.1065; found: 250.1075 [Diff (ppm) = 4.13]. **m.p.:** 30-32 °C.

10.94 Synthesis of ethyl 5-methyl-1-phenyl-1H-pyrazole-4-carboxylate (RD1) (127)[222]
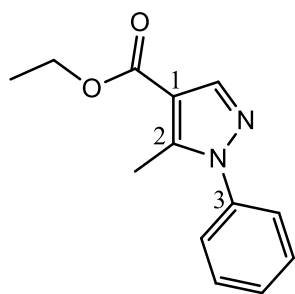
Compound **124** (596 mg, 3.22 mmol) was dissolved in EtOH (5 mL) in a 20 mL round bottom flask to which a solution of phenylhydrazine (317 µL, 3.22 mmol) in EtOH (5 mL) was added. The reaction mixture waa heated at reflux and the reaction progress monitored by TLC. After 4 hrs the EtOH was removed under reduced pressure and the residue dissolved in a saturated aqueous NaHCO$_3$ solution (10 mL). The aqueous layer was extracted with EtOAc (10 mL, followed by 3 x 10 mL) and dried over MgSO$_4$. The combined organic layers were concentrated under reduced pressure and the residue was purified using flash chromatography (9:1 EtOAc:n-hexane) to give a dark red solid, 720 mg (97%).

^{1}H NMR: (300 MHz, CDCl$_3$) δ 8.03 (s, 1H, N=CH), 7.53-7.40 (m, 5H, Ar), 4.33 (q, $J =$ 7.2 Hz, 2H, CH_2CH$_3$), 2.56 (s, 3H, CH$_3$), 1.37 (t, $J =$ 7.2 Hz, 3H, CH$_2$CH_3). ^{1}H NMR data matches literature data.[222] **^{13}C NMR:** (75 MHz, CDCl$_3$) δ 163.8 (C=O), 143.5 (C3), 141.8 (N=CH), 138.8 (C2), 129.2 (Ar), 128.6 (Ar), 125.5 (Ar), 112.9 (C1), 59.9 (*C*H$_2$CH$_3$), 14.4 (CH$_3$), 11.9 (CH$_2$*C*H$_3$). **R$_f$:** 0.8 (9:1 EtOAc:n-hexane). **HR-MS:** calcd for C$_{13}$H$_{15}$N$_2$O$_2$ m/z: [M + H]$^+$, 231.1128; found: 231.1134 [Diff(ppm) = 2.59]. **m.p.:** 160-161 °C.

10.95 Synthesis of ethyl 1-(4-chlorophenyl)-5-methyl-1H-pyrazole-4-carboxylate (RD2) (128)
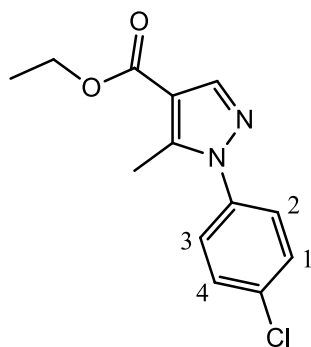
Compound **124** (677 mg, 3.66 mmol) was dissolved in EtOH (5 mL) in a 20 mL round bottom flask. In a second flask, (4-chlorophenyl)hydrazine.HCl (1.03 g, 3.66 mmol) using NEt$_3$ (561 µL, 4.02 mmol) in EtOH (5 mL) were stirred for 10 mins at rt after which the solution was transferred to the round bottom containing compound **124**. The reaction mixture was heated at reflux and the reaction progress monitored by TLC. After 2 hrs the EtOH was removed under reduced pressure and the residue dissolved in a saturated aqueous NaHCO$_3$ solution (10 mL). The aqueous layer was extracted with

EtOAc (10 mL, followed by 3 x 10 mL) and dried over MgSO$_4$. The combined organic layers were concentrated under reduced pressure. Compound **128** used without further purification. Red oil, 698 mg (72%, crude yield).

^{1}H NMR: (300 MHz, CDCl$_3$) δ 8.01 (s, 1H, N=CH), 7.45 (d, *J* = 8.7 Hz, 2H, H1, H4), 7.34 (d, *J* = 8.7 Hz, 2H, H2, H3), 4.31 (q, *J* = 7.1 Hz, 2H, C*H*$_2$CH$_3$), 2.54 (s, 3H, CH$_3$), 1.36 (t, *J* = 7.1 Hz, 3H, CH$_3$). **R$_f$:** 0.7 (9:1 EtOAc:*n*-hexane).

10.96 Synthesis of ethyl 1-(4-methoxyphenyl)-5-methyl-1H-pyrazole-4-carboxylate (RD3) (129)
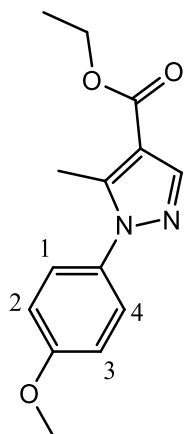
Compound **124** (544 mg, 2.9 mmol) was dissolved in EtOH (5 mL) in a 20 mL round bottom flask. In a second flask, (4-methoxyphenyl)hydrazine.HCl (513 mg, 2.9 mmol) using NEt$_3$ (404 μL, 2.9 mmol) and EtOH (10 mL) were stirred for 10 mins at rt after which the solution was transferred to the round bottom containing compound **124**. The reaction mixture was heated at reflux and the reaction progress monitored by TLC. After 2 hrs the EtOH was removed under reduced pressure and the residue dissolved in a saturated aqueous NaHCO$_3$ solution (10 mL). The aqueous layer was extracted with EtOAc (10 mL, followed by 3 x 10 mL) and dried over MgSO$_4$. The combined organic layers were concentrated under reduced pressure and compound **129** was used without further purification. Beige solid, 714 mg (crude yield).

^{1}H NMR: (300 MHz, CDCl$_3$) δ 7.99 (s, 1H, N=CH), 7.31 (d, *J* = 9.1 Hz, 2H, H2, H3), 6.97 (d, *J* = 9.1 Hz, 2H, H1, H4), 4.31 (q, *J* = 7.2 Hz, 2H, C*H*$_2$CH$_3$), 3.82 (s, 3H, OMe), 2.51 (s, 3H, CH$_3$), 1.36 (t, *J* = 7.2 Hz, 3H, CH$_2$C*H*$_3$). ^{1}H NMR data matches literature data.[138] **R$_f$:** 0.7 (9:1, EtOAc:Pet. Ether).

10.97 Synthesis of ethyl 5-ethyl-1-(4-fluorophenyl)-1H-pyrazole-4-carboxylate (RD348) (130)
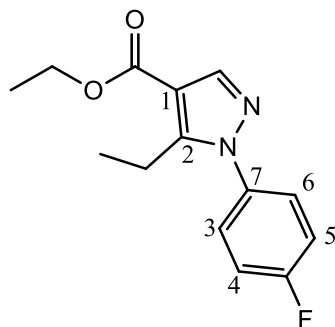
Compound **125** (426 mg, 2.13 mmol) was dissolved in EtOH (5 mL) in a 20 mL round bottom flask. In a second flask, (4-fluorophenyl)hydrazine.HCl (347 mg, 2.13 mmol) and NEt$_3$ (328 µL, 2.34 mmol) in EtOH (5 mL) were stirred for 10 mins at rt after which the solution was transferred to the round bottom containing compound **125**. The reaction mixture was heated at reflux and the reaction progress monitored by TLC. After 2 hrs the EtOH was removed under reduced pressure and the residue dissolved in a saturated aqueous NaHCO$_3$ solution (10 mL). The aqueous layer was extracted with EtOAc (10 mL, followed by 3 x 10 mL) and dried over MgSO$_4$. The combined organic layers were concentrated under reduced pressure and the residue was purified using flash chromatography (1:9, EtOAc:Pet. Ether) to give a yellow oil, 483 mg (90%).

¹H NMR: (300 MHz, CDCl$_3$) δ 7.88 (s, 1H, N=CH), 7.30-7.26 (m, 2H, H3, H6), 7.09-7.04 (m 2H, H4, H5), 4.20 (q, J = 7.1 Hz, 2H, OCH$_2$), 2.81 (q, J = 7.5 Hz, 2H, CH$_2$), 1.25 (t, J = 7.1 Hz, 3H, OCH$_2$CH_3), 1.04 (t, J = 7.5 Hz, 3H, CH$_2$CH_3). **¹³C NMR:** (75 MHz, CDCl$_3$) 162.7 (C=O), 161.4 (d, J = 247.4 Hz, C-F), 148.5 (C22), 141.0 (N=CH), 134.0 (d, J = 3.1 Hz, C7), 126.8 (d, J = 8.7 Hz, C3, C6), 115.2 (d, J = 22.1 Hz, C4, C5), 111.0 (C1), 58.9 (OCH$_2$), 17.5 (CH$_2$), 13.3 (OCH$_2$CH_3), 12.5 (CH$_2$CH_3). **R$_f$:** 0.5 (1:9, EtOAc:Pet. Ether). **HR-MS:** calcd for C$_{14}$H$_{16}$FN$_2$O$_2$ m/z: [M + H]$^+$, 265.1247; found: 265.1259 [Diff (ppm) = 4.43]. **IR (KBr):** 2981 (C-H), 1710 (C=O), 1605 (C=C), 1474 (C=C), 1264 (C-F), 1220 (C-N) cm^{-1}.

10.98 Synthesis of 1-(4-fluorophenyl)-5-methyl-1H-pyrazole-4-carboxylic acid (RD182) (131)[215]
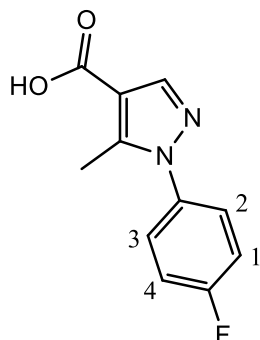
Compound **126** (424 mg, 1.71 mmol) and NaOH (341 mg, 8.55 mmol) in EtOH (10 mL) were heated at reflux and reaction progress monitored by TLC (3:2 EtOAc: Pet. Ether). After 5 hrs the solution was allowed to cool to rt and EtOH was removed under reduced pressure. The residue was dissolved in H_2O (3 mL), the pH adjusted to pH = 6 with 2 M aqueous HCl and the aqueous layer extracted with DCM (20 mL, followed by 4 x 10 mL). The organic layers were washed with brine (3 x 20 mL), dried over $MgSO_4$ and evaporated under reduced pressure. The residue was purified using flash chromatography (1:9, MeOH:DCM) to give a beige solid, 306 mg (81%).

¹H NMR: (300 MHz, CDCl₃) δ 8.10 (s, 1H, N=CH), 7.45-7.39 (m, 2H, H2, H3), 7.24-7.17 (m 2H, H1, H4), 2.57 (s, 3H, CH₃). ¹H NMR data matches literature data.[216] **Rf:** 0.4 (1:9, MeOH:DCM). **HR-MS:** calcd for $C_{11}H_{10}FN_2O_2$ m/z: [M + H]⁺, 221.0721; found: 221.0716 [Diff(ppm) = -2.26]. **m.p.:** 158-160 °C.

10.99 Synthesis of 5-methyl-1-phenyl-1H-pyrazole-4-carboxylic acid (RD4) (132)[215]
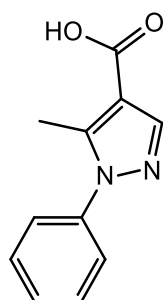
Compound **127** (494 mg, 2.15 mmol) and KOH (603 mg, 10.75 mmol) in EtOH (12 mL) were heated at reflux and reaction progress monitored by TLC (3:2 EtOAc: Pet. Ether). After 5 hrs the solution was allowed to cool to rt and EtOH was removed under reduced pressure. The residue was dissolved in H_2O (3 mL), the pH adjusted to pH = 6

with 2 M aqueous HCl and the aqueous layer extracted with DCM (20 mL, followed by 4 x 10 mL). The organic layers were washed with brine (3 x 20 mL), dried over MgSO$_4$ and evaporated under reduced pressure. The residue was purified using flash chromatography (1:9, MeOH:DCM) to give a light brown solid, 405 mg (93%).

^{1}H NMR: (300 MHz, CDCl$_3$) δ 12.04 (bs, 1H, OH), 8.13 (s, 1H, N=CH), 7.54-7.41 (m 5H, Ph), 2.58 (s 3H, CH$_3$). ^{1}H NMR data matches literature data.[216] **R$_f$:** 0.5 (1:9, MeOH:DCM). **HR-MS:** calcd for C$_{11}$H$_{11}$N$_2$O$_2$ m/z: [M + H]$^+$, 203.0815; found: 203.082 [Diff(ppm) = 2.55]. **m.p.:** 160-162 °C (DCM). Literature m.p.: 163-164 (Pet.Ether/Benzene).[223]

10.100 Synthesis of 1-(4-chlorophenyl)-5-methyl-1H-pyrazole-4-carboxylic acid (RD5) (133)[215]
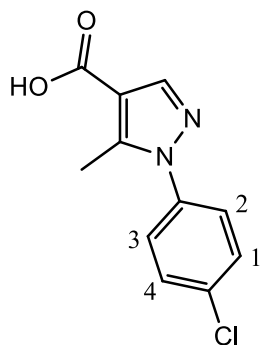
Compound **128** (703 mg, 2.66 mmol) and KOH (746 mg, 13.31 mmol) in EtOH (15 mL) were heated at reflux and reaction progress monitored by TLC (3:2 EtOAc: Pet. Ether). After 5 hrs the solution was allowed to cool to rt and EtOH was removed under reduced pressure. The residue was dissolved in H$_2$O (3 mL), the pH adjusted to pH = 6 with 2 M aqueous HCl and the aqueous layer extracted with DCM (20 mL, followed by 4 x 10 mL). The organic layers were washed with brine (3 x 20 mL), dried over MgSO$_4$ and evaporated under reduced pressure. The residue was purified using flash chromatography (1:9, MeOH:DCM) to give a brown solid, 365 mg (58 %).

^{1}H NMR: (300 MHz, d_6-DMSO) δ 12.53 (bs, 1H, OH), 7.98 (s, 1H, N=CH), 7.63 (d, J = 9.1 Hz, 2H, H1, H4), 7.58 (d, J = 9.1 Hz, 2H, H2, H3), 2.51 (s, 3H, CH$_3$). ^{1}H NMR data matches literature data.[221] **HR-MS:** calcd for C$_{11}$H$_9$ClN$_2$O$_2$K m/z: [M + K]$^+$, 274.9984; found 274.9972 [Diff(ppm) = -4.24]. **m.p.:** 182-184 °C. m.p. data matches literature data.[221]

10.101 Synthesis of 1-(4-methoxyphenyl)-5-methyl-1H-pyrazole-4-carboxylic acid (RD6) (134)[215]
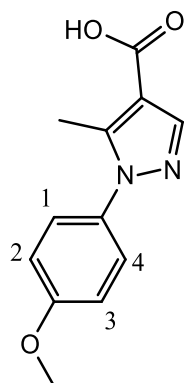
Compound **129** (714 mg, 2.7 mmol) and NaOH (486 mg, 12.15 mmol) in EtOH (10 mL) were heated at reflux and reaction progress monitored by TLC (3:2 EtOAc: Pet. Ether). After 5 hrs the solution was allowed to cool to rt and EtOH was removed under reduced pressure. The residue was dissolved in H_2O (3 mL), the pH adjusted to pH = 6 with 2 M aqueous HCl and the aqueous layer extracted with DCM (20 mL, followed by 4 x 10 mL). The organic layers were washed with brine (3 x 20 mL), dried over $MgSO_4$ and evaporated under reduced pressure. The residue was purified using flash chromatography (1:9, MeOH:DCM) to give a beige solid, 230 mg (33%).

¹H NMR: (300 MHz, $CDCl_3$) δ 8.07 (s, 1H, N=CH), 7.33 (d, J = 9.0 Hz, 2H, H2, H3), 7.00 (d, J = 9.0 Hz, 2H, H1, H4), 3.87 (s, 3H, OMe), 2.54 (s, 3H, CH_3). ¹H NMR data matches literature data.[220] **Rf:** 0.4 (1:9, MeOH:DCM). **HR-MS:** calcd for $C_{12}H_{13}N_2O_3$ m/z: $[M + H]^+$, 233.0921; found 233.0923 [Diff (ppm) = 1.15].

10.102 Synthesis of 5-ethyl-1-(4-fluorophenyl)-1H-pyrazole-4-carboxylic acid (RD349) (135)
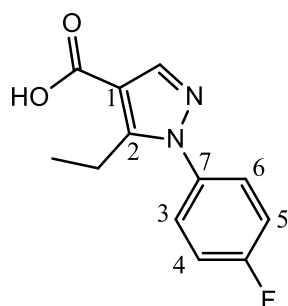
Compound **130** (335 mg, 1.27 mmol) and KOH (358 mg, 6.35 mmol) in EtOH (10 mL) were heated at reflux and reaction progress monitored by TLC (3:2 EtOAc: Pet. Ether).

After 5 hrs the solution was allowed to cool to rt and EtOH was removed under reduced pressure. The residue was dissolved in H_2O (3 mL), the pH adjusted to pH = 6 with 2 M aqueous HCl and the aqueous layer extracted with DCM (20 mL, followed by 4 x 10 mL). The organic layers were washed with brine (3 x 20 mL), dried over $MgSO_4$ and evaporated under reduced pressure. The residue was purified using flash chromatography (1:9, MeOH:DCM) to give an off white solid, 290 mg (96%).

^{1}H NMR: (300 MHz, CDCl$_3$) δ 12.08 (bs, 1H, OH), 8.10 (s, 1H, N=CH), 7.44-7.40 (m, 2H, H3, H6), 7.24-7.18 (m, 2H, H4, H5), 2.95 (q, J = 7.4 Hz, 2H, CH$_2$), 1.18 (t, J = 7.4 Hz, 3H, CH$_3$). **^{13}C NMR:** (75 MHz, CDCl$_3$) δ 168.9 (C=O), 162.3 (d, J = 248.1 Hz, C-F), 150.6 (C2), 142.8 (N=CH), 134.7 (d, J = 3.1 Hz, C7), 127.9 (d, J = 9.1 Hz, C3, C6), 116.3 (d, J = 23.2 Hz, C4, C5), 111.3 (C1), 18.6 (CH$_2$), 13.6 (CH$_3$). **R$_f$:** 0.5 (1:19, MeOH:DCM). **HR-MS:** calcd for C$_{12}$H$_{12}$FN$_2$O$_2$ m/z: [M + H]$^+$, 237.0932; found: 237.0942 [Diff (ppm) = 4.01]. **IR (KBr):** 3427 (OH), 1672 (C=O), 1477 (C=C), 1223 (C-F) cm^{-1}. **m.p.:** 140-143 °C.

10.103 Synthesis of 4-(2-methoxyphenyl)pyridine.HCl (RD215) (136)[159]
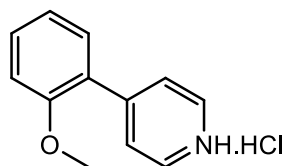
4-Bromopyridine.HCl (639 mg, 3.88 mmol) and (2-methoxyphenyl)boronic acid (500 mg, 3.39 mmol) were dissolved in toluene (20 mL). Pd(PPh$_3$)$_4$ (760 mg, 0.65 mmol) and Cs$_2$CO$_3$ (3.21 g, 10.17 mmol) were added and the suspension was heated at reflux overnight. The reaction was cooled to rt and passed through a bed of Celite. The filtrate was concentrated under reduced pressure to give compound **136** as a yellow oil, which was used without any further purification. 330 mg (crude yield).

^{1}H NMR: (300 MHz, D$_2$O) δ 8.76-8.46 (m, 2H, N=CH), 7.53-7.30 (m, 4H, Ar), 7.12-6.93 (m, 2H, Ar), 3.88 (s, 3H, OCH$_3$).

10.104 Synthesis of 4-(2-methoxyphenyl)piperidine (RD216) (137)[159]
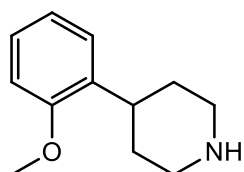
Compound **136** (330 mg, 1.48 mmol) was dissolved in MeOH (20 mL) and PtO_2 (168 mg, 0.74 mmol) was added. The flask was evacuated and purged with H_2 (x 3) and the reaction was stirred overnight at rt. The reaction mixture was filtered through a pad of Celite and washed with MeOH (15 mL, x 3). The filtrate was concentrated under reduced pressure and residue was dissolved in saturated aqueous $NaHCO_3$ (10 mL) and stirred for 2 hrs at rt. The aqueous layer was extracted with DCM (10 mL, x 3) and dried over $MgSO_4$. The combined organic layers were concentrated under reduced pressure and the residue was purified using flash chromatography (2:98, NEt_3:MeOH) to give a brown oil, 225 mg (18%).

^{1}H NMR: (300 MHz, $CDCl_3$) δ 7.20-7.18 (m, 2H, Ar), 6.95-6.84 (m, 2H, Ar), 4.81-4.23 (m, 1H, ArCH), 3.81 (s, 3H, OCH_3), 3.40-3.02 (m, 2H*), 2.95-2.71 (m 2H*), 1.81-1.67 (m, 4H*)*Piperidine. ^{1}H NMR data matches literature data.[217] **R_f:** 0.2 (2:98, NEt_3:MeOH). **HR-MS:** calcd for $C_{12}H_{18}NO$ m/z: $[M + H]^+$, 192.1383; found 192.1388 [Diff(ppm) = 2.6].

10.105 Synthesis of (5-methyl-1-phenyl-1H-pyrazol-4-yl(4-(4-(trifluoromethyl)phenyl)piperazin-1-yl) methanone (RTC206) (138)†
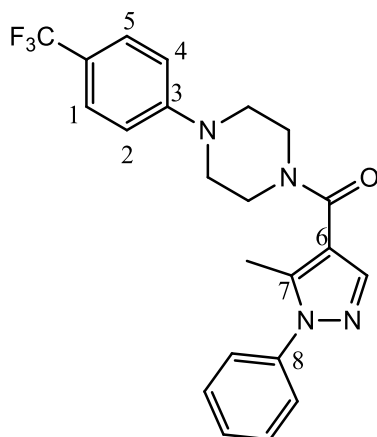
Prepared from compound **33** (270 mg, 1.17 mmol) and compound **132** (215 g, 1.06 mmol) using HOBt (158 mg, 1.17 mmol), TBTU (375 mg, 1.17 mmol), anhydrous NEt_3 (327 µL, 1.70 mmol) and anhydrous DMF (10 mL) and following the general procedure described in section **10.2**. The reaction mixture was stirred overnight at room temperature under a N_2 atmosphere. Purified using flash chromatography (3:2 EtOAc:Pet. Ether) to give an off white solid, 149 mg (36%).

¹H NMR: (300 MHz, CDCl₃) δ 7.68 (s, 1H, N=CH), 7.52-7.42 (m, 7H, H1, H5, Ar x 5), 6.95 (d, J = 8.7 Hz, 2H, H2, H4), 3.91 (m, 4H*), 3.36-3.32 (m, 4H*), 2.45 (s, 3H, CH₃).*Piperazine. **¹³C NMR:** (75 MHz, CDCl₃) δ 164.7 (C=O), 152.9 (C3), 141.2 (C7), 139.0 (C8), 138.8 (N=CH), 129.2 (Ar), 128.5 (Ar), 126.5 (q, J = 3.0 Hz, C1, C5), 125.3 (Ar), 124.6 (q, J = 269.5 Hz, CF₃), 121.3 (q, J = 33.1 Hz, C-CF₃), 115.1 (C6), 115.0 (C2, C4), 48.4 (C*), 11.7 (CH₃).*Piperazine. **Rf:** 0.4 (3:2 EtOAc:Pet. Ether). **HR-MS:** calcd for C₂₂H₂₂F₃N₄O m/z: [M + H]⁺, 416.1770; found: 416.1762 [Diff (ppm) = -1.95]. **IR(Br):** 2893 (C-H), 1626 (C=O), 1617 (C=C), 1426 (C=C), 1332 (C-F), 1232 (C-N) cm⁻¹. **m.p.:** 204-208 °C. **Anal. calcd** for C₂₂H₂₁F₃N₄O; C, 63.76; H, 5.11; N, 13.52% found: C, 63.53; H, 4.90; N, 13.20%.

10.106 Synthesis of (4-(3-chloro-5-(trifluoromethyl)pyridin-2-yl)piperazin-1-yl(1-(4-chlorophenyl)-5-methyl-1H-pyrazol-4-yl)methanone (RTC213) (139)†
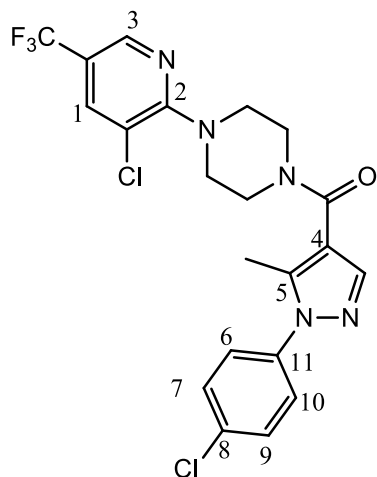
Prepared from 1-(3-chloro-5-(trifluoromethyl)pyridin-2-yl)piperazine (126 mg, 0.47 mmol) and compound **133** (102 mg, 0.43 mmol) using HOBt (64 mg, 0.47 mmol) TBTU (152mg, 0.47 mmol), NEt₃ (60 μL, 0.68 mmol) and DMF (6 mL) and following the general procedure described in section **10.2**. The reaction mixture was stirred at rt overnight under a N₂ atmosphere. Purified using flash chromatography (1:1 EtOAc:n-hexane) to give an off white solid, 95 mg (46%).

¹H NMR: (300 MHz, CDCl₃) δ 8.43-8.42 (m, 1H, H3), 7.82-7.81 (m, 1H, H1), 7.68 (s, 1H, N=CH), 7.48 (d, J = 9.2 Hz, 2H, H7, H9), 7.40 (d, J = 9.2 Hz, 2H, H6, H10), 3.91-3.86 (m, 4H*), 3.58-3.55 (m, 4H*), 2.46 (s, 3H, CH₃).*Piperazine. **¹³C NMR:** (75 MHz, CDCl₃) δ 164.6 (C=O), 159.5 (C2), 143.0 (q, J = 4.1 Hz, C3), 141.0 (C5), 139.1 (N=CH), 137.5 (C11), 136.1 (q, J = 3.3 Hz, C1), 134.3 (C8), 129.4 (C7, C9), 126.4 (C6,

C10), 123.1 (q, J = 270.0 Hz, CF$_3$), 121.2 (C-Cl), 120.6 (q, J = 33.0 Hz, C-CF$_3$), 115.6 (C4), 48.8 (C*), 11.7 (CH$_3$).*Piperazine. **R$_f$:** 0.3 (1:1 EtOAc:Pet. Ether). **HR-MS:** calcd for C$_{21}$H$_{19}$Cl$_2$F$_3$NO m/z: [M + H]$^+$, 484.0913; found: 484.0912 [Diff (ppm) = -0.25]. **IR (KBr):** 2863 (C-H), 1623 (C=O), 1604 (C=C), 1449 (C=C), 1314 (C-F), 1234 (C-N) cm^{-1}. **m.p.:** 122-124 °C. **Anal. calcd** for C$_{21}$H$_{18}$Cl$_2$F$_3$N$_5$O; C, 52.08; H, 3.75; N, 14.46% found: C, 51.76; H, 3.93; N, 14.56%.

10.107 Synthesis of (1-(4-methoxyphenyl)-5-methyl-1H-pyrazol-4-yl)(4-(2-methoxyphenyl)piperidin-1-yl)methanone (RTC218) (140)†
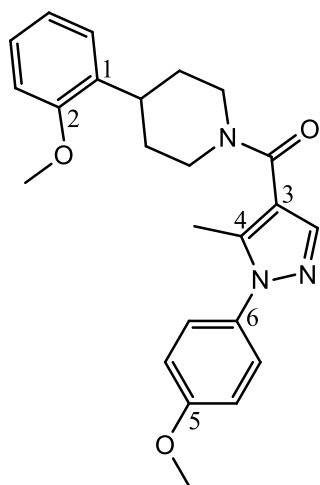
Compound **137** (50 mg, 0.21 mmol), BOP (70 mg, 0.15 mmol), anhydrous NEt$_3$ (30 µL, 0.21 mmol) and anhydrous DCM (6 mL) were placed in an oven-dried three neck flask under a N$_2$ atmosphere. The resulting solution was stirred at rt for 15 mins. In a second flask, compound **134** (28 mg, 0.12 mmol) and NEt$_3$ (30 µL, 0.21 mmol) in DCM (3 mL) were stirred under a N$_2$ atmosphere at rt for 15 mins after which the solution was transferred to the flask containing compound **137**. The reaction mixture stirred under a N$_2$ atmosphere and the reaction progress was monitored by TLC. After 12 hrs, DCM was removed under reduced pressure and the resulting oil was acidified to pH = 3 using a 0.1 M aqueous HCl. The aqueous mixture was extracted with DCM (20 mL, followed by 4 x 10 mL) and the organic layer washed with a saturated aqueous solution of NaHCO$_3$ (3 x 20 mL) and brine (3 x 20 mL). The organic layer was dried over MgSO$_4$ and the solvent removed *in vacuo* and the residue was purified using flash chromatography (3:2 EtOAc:Pet. Ether) to give an off white solid 68 mg (62%).

¹H NMR: (300 MHz, CD₃CN, T = 60 °C) δ 7.64 (s, 1H, N=CH), 7.43-7.38 (m, 2H, Ar), 7.24-7.19 (m, 2H, Ar), 7.10-7.06 (m, 2H, Ar), 7.00-6.92 (m, 2H, Ar), 4.46-4.42 (m, 2H*), 3.88 (s, 3H, OCH₃), 3.86 (s, 3H, OCH₃), 3.31-3.21 (m, 1H, Ar-CH), 3.10-3.02 (m, 2H*), 1.88-1.84 (m, 2H*), 1.76-1.62 (m, 2H*).*Piperidine. **¹³C NMR:** (75 MHz, CD₃CN, T = 60 °C) δ 164.3 (C=O), 159.6 (C5), 157.0 (C2), 139.6 (C1), 138.2 (N=CH), 133.7 (C6), 132.6 (C4), 127.2 (Ar), 126.7 (Ar), 126.5 (Ar), 120.7 (Ar), 116.1 (C3), 114.3 (Ar), 111.1 (Ar), 55.3 (OCH₃), 55.2 (OCH₃), 45.3 (C*), 35.8 (Ar-CH), 32.0 (C*), 10.6 (CH₃).*Piperidine. **R_f:** 0.7 (3:2 EtOAc:Pet.Ether). **HR-MS:** calcd for $C_{24}H_{28}N_3O_3$ m/z: [M + H]⁺, 406.2125; found: 406.2139 [Diff (ppm) = -3.4]. **IR (KBr):** 2935 (CH), 1614 (C=O), 1236 (C-N), 1219 (*O-C*H₃) cm⁻¹.**m.p.:** 176-178 °C.

10.108 Synthesis of (5-ethyl-1-(4-fluorophenyl)-1H-pyrazol-4-yl)(4-(2-methoxyphenyl)piperazin-1-yl)methanone (RTC217) (141)†
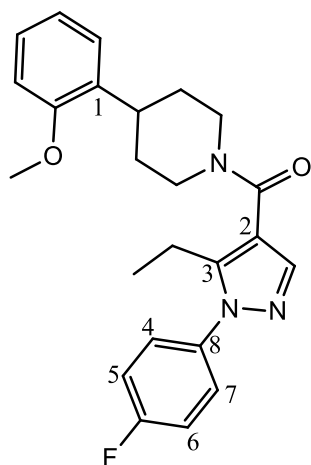
Compound **137** (50 mg, 0.21 mmol), BOP (70 mg, 0.15 mmol), anhydrous NEt₃ (30 μL, 0.21 mmol) and anhydrous DCM (6 mL) were placed in an oven-dried three neck flask under a N₂ atmosphere. The resulting solution was stirred at rt for 15 mins. Compound **135** (55 mg, 0.23 mmol) was added and the reaction mixture stirred under a N₂ atmosphere and the reaction progress was monitored by TLC. After 12 hrs, DCM was removed under reduced pressure and the resulting oil was acidified to pH = 3 using a 0.1 M aqueous HCl. The aqueous mixture was extracted with DCM (20 mL, followed by 4 x 10 mL) and the organic layer washed with a saturated aqueous solution of NaHCO₃ (3 x 20 mL) and brine (3 x 20 mL). The organic layer was dried over MgSO₄ and the solvent removed *in vacuo* and the residue was purified using flash chromatography (3:2 EtOAc:Pet. Ether) to give a colourless oil, 70 mg (67%).

^{1}H NMR: (300 MHz, CD$_3$CN, T = 60 °C) δ 7.64 (s, 1H, N=CH), 7.52-7.46 (m, 2H, H5, H6), 7.32-7.19 (m, 4H, Ar), 6.99-6.92 (m, 2H, H4, H7), 4.47-4.43 (m, 2H*), 3.85 (s, 3H, OCH$_3$), 3.31-3.21 (m, 1H, Ar-CH), 3.10-3.01 (m, 2H*), 2.81 (q, *J* = 7.5 Hz, 2H, C*H*$_2$CH$_3$), 1.90-1.80 (m, 2H*), 1.76-1.62 (m, 2H*), 1.08 (t, *J* = 7.5 Hz, 3H, CH$_2$C*H*$_3$)*Piperidine. ^{13}**C NMR:** (75 MHz, CD$_3$CN, T = 60 °C) δ 164.1 (C=O), 162.2 (d, *J* = 244.7 Hz, C-F), 157.0 (*C*-OCH$_3$), 145.4 (C1), 138.2 (N=CH), 135.9 (d, *J* = 3.0 Hz, C8), 133.6 (C3), 127.8 (d, *J* = 9.0 Hz, C4, C7), 127.1 (Ar), 126.5 (Ar), 120.6 (Ar), 115.8 (d, *J* = 22.9 Hz, C5, C6), 115.7 (C2), 111.0 (Ar), 55.1 (OCH$_3$), 45.2 (C*), 35.8 (Ar-C), 31.9 (C*), 17.9 (CH$_2$), 12.6 (CH$_3$).*Piperidine. **R$_f$:** 0.7 (3:2, EtOAc:Pet. Ether). **HR-MS:** calcd for C$_{24}$H$_{27}$FN$_3$O$_2$ m/z: [M + H]$^+$, 408.2082; found: 408.2088 [Diff (ppm) = 1.51]. **IR (KBr):** 2937 (CH), 1621 (C=O), 1373 (C-F), 1238 (C-N), 1218 (*O*-C*H*$_3$) cm^{-1}.

10.109 Synthesis of (1-(4-fluorophenyl)-5-methyl-1H-pyrazol-4-yl)(4-(2-methoxyphenyl)piperazin-1-yl)methanone (RTC220) (142)†
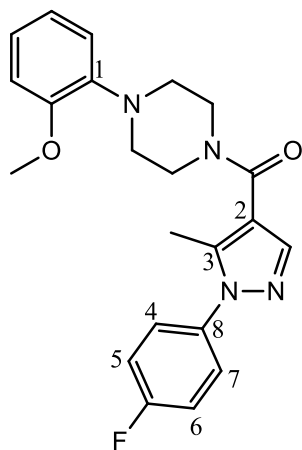
Compound **131** (200 mg, 0.90 mmol), BOP (401 mg, 0.90 mmol), anhydrous NEt$_3$ (200 μL, 1.44 mmol) and anhydrous DCM (20 mL) were placed in an oven-dried three neck flask under a N$_2$ atmosphere. The resulting solution was stirred at rt for 15 mins. 1-(2-Methoxyphenyl)piperazine (192 mg, 0.99 mmol) was added and the reaction mixture stirred under a N$_2$ atmosphere and the reaction progress was monitored by TLC. After 18 hrs, DCM was removed under reduced pressure and the resulting oil was acidified to pH = 3 using a 0.1 M aqueous HCl. The aqueous mixture was extracted with DCM (20 mL, followed by 4 x 10 mL) and the organic layer washed with a saturated aqueous solution of NaHCO$_3$ (3 x 20 mL) and brine (3 x 20 mL). The organic layer was dried

over MgSO$_4$ and the solvent removed *in vacuo* and the residue was purified using flash chromatography (3:2, EtOAc:Pet.Ether) to give a give a white solid, 70 mg (71%).

^{1}H NMR: (300 MHz, CD$_3$CN) δ 7.69 (s, 1H, N=CH), 7.54-7.49 (m, 2H, H5, H6), 7.31-7.25 (m, 2H, Ar), 7.05-6.90 (m, 4H, H4, H7, Ar), 3.86 (s, 3H, OCH$_3$), 3.86-3.77 (m, 4H*), 3.09-3.06 (m, 4H*), 2.37 (s, 3H, CH$_3$).*Piperazine. **^{13}C NMR:** (75 MHz, CD$_3$CN) δ 164.1 (C=O), 161.9 (d, *J* = 244.5 Hz, C-F), 152.6 (C1), 141.4 (C3), 139.9 (*C*-OCH$_3$), 138.7 (N=CH), 135.7 (d, *J* = 2.9 Hz, C8), 127.2 (d, *J* = 8.8 Hz, C4, C7), 122.9 (Ar), 121.0 (Ar), 118.5 (Ar), 116.1 (C2), 115.7 (*J* = 23.0 Hz, C5, C6), 112.4 (Ar), 55.1 (OCH$_3$), 50.6 (C*), 44.8 (C*), 10.6 (CH$_3$).*Piperazine. **Rf:** 0.4 (3:2, EtOAc:Pet. Ether) **HR-MS:** calcd for C$_{22}$H$_{24}$FN$_4$O$_2$ m/z: [M + H]$^+$, 397.1936; found: 397.1954 [Diff (ppm) = 4.5]. **IR (KBr):** 2758 (CH), 1629 (C=O), 1385 (C-F), 1236 (C-N), 1219 (*O*-CH$_3$) cm^{-1}.**m.p.:** 138-140 °C.

10.110 Synthesis of (1-(4-fluorophenyl)-5-methyl-1H-pyrazol-4-yl)(4-phenylpiperazin-1-yl)methanone (RTC200) (143)†
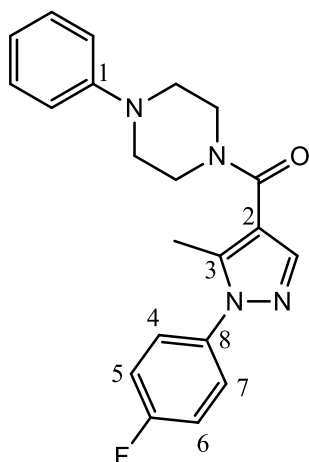
Prepared from 1-phenylpiperazine (65 mg, 0.42 mmol) and compound **131** (65 mg, 0.37 mmol) using HOBt (56 mg, 0.42 mmol), TBTU (133 mg, 0.42 mmol), anhydrous NEt$_3$ (84 µL, 0.60 mmol) and anhydrous DMF (5 mL) and following the general procedure described in section **10.2**. The reaction mixture was stirred overnight at room temperature under a N$_2$ atmosphere. Purified using flash chromatography (1:1 EtOAc:*n*-hexane) to give a beige solid, 112 mg (81%).

^{1}H NMR: (300 MHz, CDCl$_3$) δ 7.66 (s, 1H, N=CH), 7.43-7.38 (m, 2H, H4, H7), 7.31-7.26 (m, 2H, Ar), 7.20-7.15 (m, 2H, H5, H6), 6.96-6.88 (m, 3H, Ar), 3.89 (m, 4H*), 3.24-3.21 (m, 4H*), 2.42 (s, 3H, CH$_3$).*Piperazine. **^{13}C NMR:** (75 MHz, CDCl$_3$) δ

164.5 (C=O), 162.2 (d, J = 247.3 Hz, C-F), 150.9 (C1), 141.1 (C3), 138.9 (N=CH), 135.2 (d, J = 3.7 Hz, C8), 129.2 (Ar), 127.2 (d, J = 8.2 Hz, C4, C7), 120.5 (Ar), 116.6 (Ar), 116.2 (d, J = 23 Hz, C5, C6), 115.4 (C2), 49.8 (C*), 11.6 (CH_3).*Piperazine. **R_f:** 0.4 (3:2 EtOAc:Pet. Ether). **HR-MS:** calcd for $C_{21}H_{22}FN_4O$ m/z: $[M + H]^+$, 365.1772; found: 365.1771 [Diff (ppm) = -0.24]. **IR (KBr):** 2824 (C-H), 1601 (C=O), 1390 (C-F), 1222 (C-N) cm^{-1}. **m.p.:** 144-146 °C.

10.111 Synthesis of (1-(4-fluorophenyl)-5-methyl-1H-pyrazol-4-yl)(4-phenylpiperidin-1-yl)methanone (RTC216) (144)†
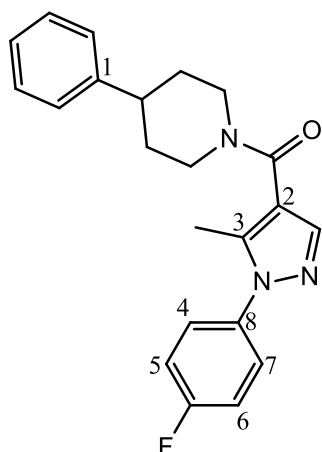
Compound **124** (100 mg, 0.45 mmol), BOP (221 mg, 0.49 mmol), anhydrous NEt_3 (101 μL, 0.72 mmol) and anhydrous DCM (10 mL) were placed in an oven-dried three neck flask under a N_2 atmosphere. The resulting solution was stirred at rt for 15 mins. 4-Phenylpiperidine (80 mg, 0.49 mmol) was added and the reaction mixture stirred under a N_2 atmosphere and the reaction progress was monitored by TLC. After 18 hrs, DCM was removed under reduced pressure and the resulting oil was acidified to pH = 3 using a 0.1 M aqueous HCl. The aqueous mixture was extracted with DCM (20 mL, followed by 4 x 10 mL) and the organic layer washed with a saturated aqueous solution of NaHCO_3 (3 x 20 mL) and brine (3 x 20 mL). The organic layer was dried over MgSO_4 and the solvent removed *in vacuo* and the residue was purified using flash chromatography (3:2, EtOAc:Pet.Ether) to give a white solid, 72 mg (60%).

^{1}H NMR: (300 MHz, d_6-DMSO, T = 60 °C) δ 7.75 (s, 1H, N=CH), 7.61-7.57 (m, 2H, H5, H6), 7.39-7.71 (m, 7H, Ar x 5, H4, H7), 4.36-4.42 (m, 2H*), 3.09-3.01 (m, 2H*), 2.88-2.80 (m, 1H, Ar-CH), 2.34 (s, 3H, CH_3), 1.89-1.84 (m, 2H*), 1.68-1.56 (m, 2H*).*Piperidine. **^{13}C NMR:** (75 MHz, d_6-DMSO, T = 60 °C) δ 163.5 (C=O), 161.4 (d,

J = 244.5 Hz, C-F), 145.5 (C1), 139.6 (C3), 138.7 (N=CH), 135.4 (d, J = 3.0 Hz, C8), 128.3 (Ar), 127.2 (d, J = 8.8 Hz, C4, C7), 126.6 (Ar), 126.1 (Ar), 116.1 (C2), 115.9 (d, J = 22.3 Hz, C5, C6), 45.9 (C*), 41.7 (Ar-CH), 33.1 (C*), 11.0 (CH$_3$). **R$_f$:** 0.3 (3:2 EtOAc: Pet. Ether).*Piperidine. **HR-MS:** calcd for C$_{22}$H$_{23}$FN$_3$O m/z: [M + H]$^+$, 365.1859; found: 365.1851 [Diff (ppm) = 2.21]. **IR (KBr):** 2938 (CH), 1614 (C=O), 1216 (C-N) cm^{-1}.**m.p.:** 158-159 °C.

10.112 Synthesis   of   N-(2-methoxyethyl)-9-oxo-9-(4-(4-(trifluoromethyl)phenyl)piperazin-1-yl)nonanamide (RTC18) (146)
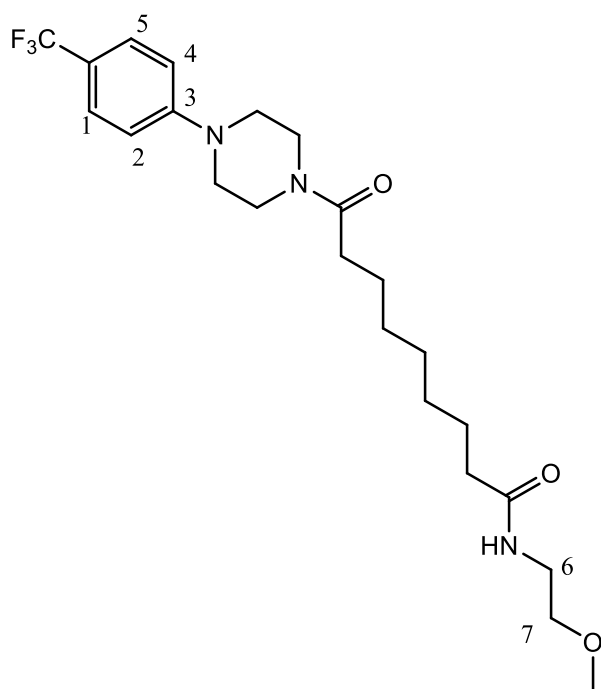
Prepared from compound **79** (137 mg, 0.34 mmol) and 2-methoxyethanamine (29 μL, 0.43 mmol) using HOBt (58 mg, 0.43 mmol), TBTU (140 mg, 0.43 mmol), anhydrous NEt$_3$ (100 μL, 0.69 mmol) and anhydrous DMF (2 mL) and following the general procedure described in section **10.2**. The reaction mixture was stirred overnight at room temperature under a N$_2$ atmosphere. Purified using flash chromatography (elution gradient 1:1 EtOAc:n-hexane to EtOAc:n-hexane 4:1) to give an white solid, 52 mg (34%).

^{1}H NMR: (300 MHz, CDCl$_3$) δ 7.50 (d, J = 8.4 Hz, 2H, H1, H5), 6.92 (d, J = 8.4 Hz, 2H, H2, H4), 5.81 (bs, 1H, NH), 3.79-3.76 (m, 2H*), 3.65-3.62 (m, 2H*), 3.49-3.41 (m, 4H, H6, H7), 3.62 (s, 3H, OCH$_3$), 3.32-3.22 (m, 4H*), 2.36 (t, J = 7.2 Hz, 2H, ((C=O)CH$_2$), 2.17 (t, J = 7.2 Hz, 2H, ((C=O)CH$_2$), 1.73-1.57 (m, 4H, CH$_2$), 1.41-1.299

(m, 6H, CH$_2$).*Piperazine. ^{13}**C NMR:** (75 MHz, CDCl$_3$) δ 173.0 (HN-(C=O)), 171.7 (N-C=O), 152.9 (C3), 126.5 (q, J = 3.3 Hz, C1, C5), 124.6 (q, J = 278.1 Hz, CF$_3$), 121.2 (q, J = 26.0 Hz, C-CF$_3$), 115.0 (C2, C4), 71.2 (C7), 58.7 (OCH$_3$), 48.4 (C*), 48.1 (C*), 45.1 (C*), 41.1 (C*), 39.0 (C6), 36.6 ((C=O)CH$_2$), 33.2 ((C=O)CH$_2$), 28.1 (CH$_2$), 27.9 (CH$_2$), 27.8 (CH$_2$), 24.1 (CH$_2$), 23.6 (CH$_2$). *Piperazine. **R$_f$:** 0.2 (4:1, EtOAc:n-hexane). **HR-MS:** calcd for C$_{23}$H$_{35}$F$_3$N$_3$O$_3$ m/z: [M + H]$^+$, 458.2625; found: 458.2631 [Diff (ppm) = 1.31]. **IR (KBr):** 2932 (C-H), 1676 (NH-C=O), 1636 (N-C=O), 1618 (C=C), 1442 (C=C), 1344 (C-F), 1208 (C-N) cm^{-1}. **m.p.:** 88-92 °C.

10.113 Synthesis of 5-(4-oxo-4-(4-(4-(trifluoromethyl)phenyl)piperazin-1-yl)butyl)thiophene-2-carbaldehyde (RTC82) (147)†
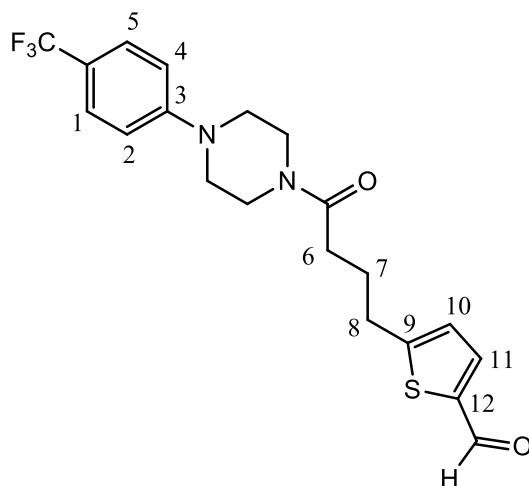
To a solution of dichloromethyl methyl ether (158 µL, 1.75 mmol) in anhydrous DCM (10 mL) at 0 °C was added tin(IV)chloride (1.76 mL, 15.00 mmol) under a N$_2$ atmosphere. After 5 mins, a solution of compound **4** (500 mg, 1.30 mmol) in anhydrous DCM (5 mL) was added dropwise over a period of 20 mins. The reaction mixture was stirred for 1 hr at rt, after which it was poured onto ice-water and stirred for 30 mins. The organic layer was removed and washed with H$_2$O (10 mL, followed by 2 x 10 mL), dried over MgSO$_4$ and concentrated *in vacuo*. The residue was purified using flash chromatography (3:2 EtOAc: Pet. Ether) to give a white solid, 332 mg, (62%).

^{1}**H NMR:** (300 MHz, CDCl$_3$) δ 9.82 (s, 1H, CHO), 7.62 (d, J = 3.3 Hz, 1H, H11), 7.50 (d, J = 8.7 Hz, 2H, H1, H5), 6.95-6.90 (m, 3H, H2, H4, H10), 3.80-3.77 (m, 2H*), 3.61-3.59 (m 2H*), 3.28-3.25 (m, 4H*), 2.98 (t, J = 7.2 Hz, 2H, H8), 2.42 (t, J = 7.2 Hz, 2H, H6), 2.15-2.04 (m, 2H, H7).*Piperazine. ^{13}**C NMR:** (75 MHz, CDCl$_3$) δ 181.1 (CHO),

169.4 (C=O), 155.1 (C3), 151.8 (C9), 140.9 (C12), 136.0 (C11), 125.5 (q, J = 3.0 Hz, C1, C5), 125.2 (C10), 123.5 (q, J = 269.2 Hz, CF$_3$), 120.4 (q, J = 32.7 Hz, C-CF$_3$), 114.0 (C2, C4), 47.3 (C*), 47.1 (C*), 44.0 (C*), 40.1 (C*), 30.7 (C6), 29.1 (C8), 25.1 (C7).*Piperazine. **R$_f$:** 0.3 (3:2, EtOAc:Pet. Ether). **HR-MS:** calcd for C$_{20}$H$_{22}$F$_3$N$_2$O$_2$S m/z: [M + H]$^+$, 411.1349; found: 411.1333 [Diff (ppm) = -3.75]. **IR (KBr):** 2907 (H(C=O)), 2833(CHO), 1661 (CHO), 1643 (C=O), 1615 (C=C), 1437 (C=C), 1333 (C-F), 1222 (C-N) cm^{-1}. **m.p.:** 98-100 °C.

10.114 Synthesis of 3,6,9,12,15-pentaoxaheptadecane-1,17-diyl-bis(4-methylbenzenesulfonate) (RD190) (148)[209]
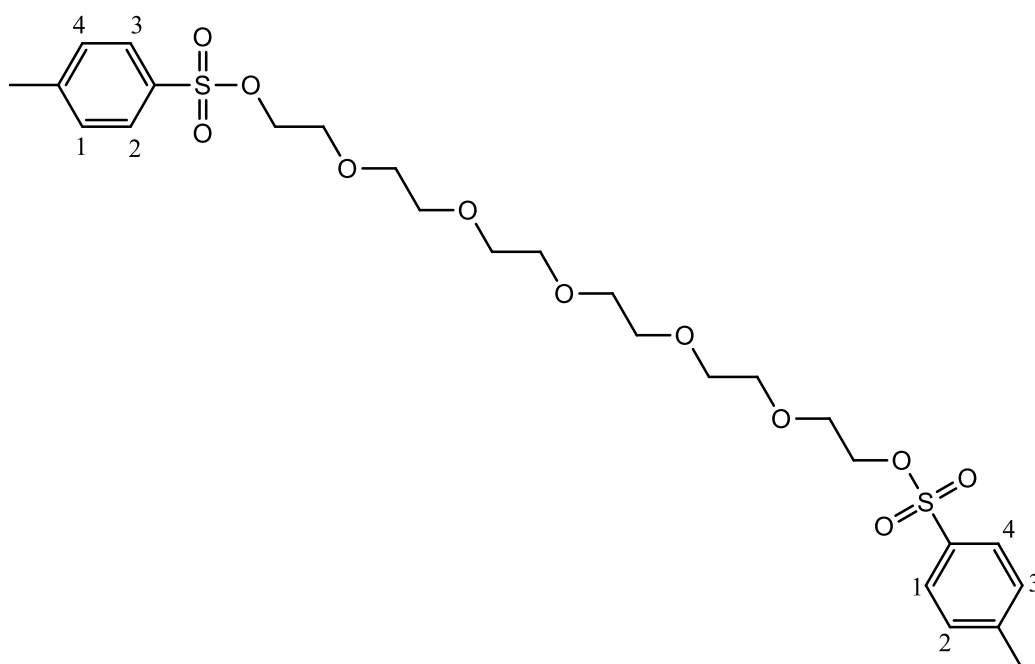
Hexaethylene glycol (1.23 g, 4.35 mmol) and DMAP (97 mg, 0.87 mmol) were dissolved in NEt$_3$ (1.22 mL, 9.58 mmol) and DCM (30 mL) and the solution cooled to 0 °C. Tosyl chloride (1.67 g, 9.58 mmol) was added and the reaction stirred at 0 °C for 15 mins. The reaction was allowed to warm to rt and was stirred for 24 hrs at rt and was monitored by TLC. The reaction mixture was diluted with DCM (50 mL) and washed with saturated aqueous NaHCO$_3$ (3 x 20 mL). The combined organic layer was dried over MgSO$_4$, filtered and the solvent removed under reduced pressure. The residue was purified using flash chromatography (3:2, EtOAc:Pet.Ether) to give a clear oil, 1.88 g (80%).

¹H NMR: (300 MHz, CDCl₃) δ 7.78 (d, *J* = 8.3 Hz, 4H, H2, H3), 7.34 (d, *J* = 8.3 Hz, 4H, H1, H4), 4.16-4.13 (m, 4H, OCH₂ x 2), 3.69-3.66 (m, 4H, OCH₂ x 2), 3.61 (bs, 8H, OCH₂ x 4), 3.57 (bs, 8H, OCH₂), 2.44 (s, 6H, CH₃ x 2). ¹H NMR data matches literature data.[209] **R_f:** 0.3 (3:2, EtOAc:Pet.Ether). **HR-MS:** calcd for $C_{26}H_{39}O_{11}S_2$ m/z: [M + H]⁺, 591.1928; found: 591.1928 [Diff(ppm) = 0.00].

10.115 Synthesis of 1,17-diazido-3,6,9,12,15-pentaoxaheptadecane (RD191) (149)[208]
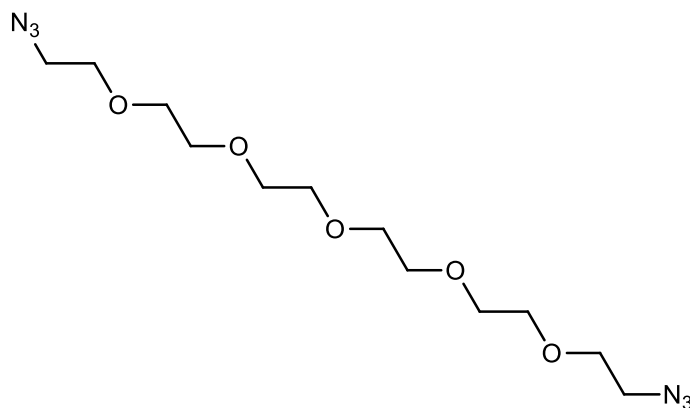
Sodium azide (0.56 g, 8.55 mmol) was added to a solution of compound **148** (2.3 g, 3.88 mmol) in acetonitrile (60 mL) and the mixture was heated at reflux. After 48 hrs, the white precipitate was removed by filtration and washed with Et₂O. The filtrate was concentrated under reduced pressure and the residue was purified using flash chromatography (3:2 EtOAc:Pet. Ether) to give a clear oil, 1.00 g (78%).

¹H NMR: (300 MHz, CDCl₃) δ 3.69-3.51 (m, 20H, OCH₂ x 10), 3.39 (t, *J* = 5.4 Hz, 4H, N₃CH₂ x 2). ¹H NMR data matches literature data.[209] **R_f:** 0.3 (3:2, EtOAc:Pet.Ether). **IR (neat):** 2106 (N=N=N), 1121 (C-O) cm⁻¹. **HR-MS:** calcd for $C_{12}H_{25}N_6O_5$ m/z: [M + H]⁺, 333.1881; found: 333.1879 [Diff(ppm) = -0.54].

10.116 Synthesis of 3,6,9,12,15-pentaoxaheptadecane-1,17-diamine (RD198) (150)[209]
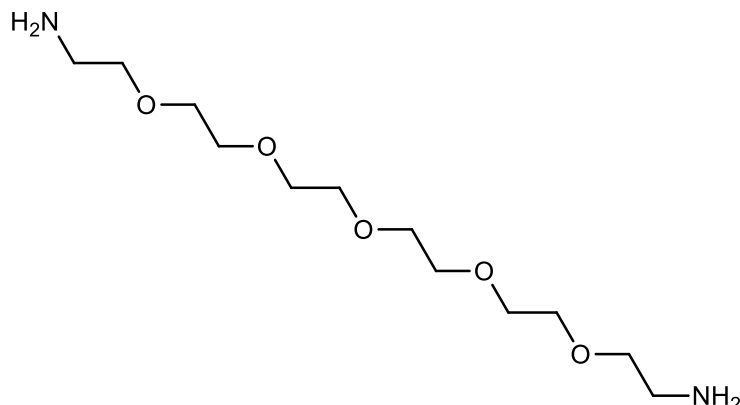
A solution of compound **149** (416 mg, 1.25 mmol) in MeOH (30 mL) was degassed three times and purged with H_2 gas (x 3). Platinum oxide (50 mg) was added and the mixture was stirred overnight under an atmosphere of H_2 gas. The platinum oxide was removed using a bed of Celite and the filtrate was reduced under reduced pressure to give an off white oil in a quantitative yield, which was used without any further purification.

1H NMR: (300 MHz, CDCl$_3$) δ 3.33-3.20 (m, 20H, OCH$_2$ x 10), 2.43-2.39 (m, 4H, NH$_2$CH$_2$ x 2). ^{1}H NMR data matches literature data.[209] **13CNMR:** (75 MHz, CDCl3) δ 70.3 (OCH$_2$), 70.2 (OCH$_2$), 70.2 (OCH$_2$), 70.08 (OCH$_2$), 70.04 (OCH$_2$), 69.9 (OCH$_2$), 48.9 (OCH$_2$). **R$_f$:** 0.1 (3:2, EtOAc:Pet.Ether). **HR-MS:** calcd for $C_{12}H_{28}N_2O_5K$ m/z: [M + K]$^+$, 319.163; found 319.1619 [Diff(ppm) = -3.44].

10.117 Synthesis of 4-(5-((propylamino)methyl)thiophen-2-yl)-1-(4-(4-(trifluoromethyl)phenyl)piperazin-1-yl)butan-1-one (RD222) (152)
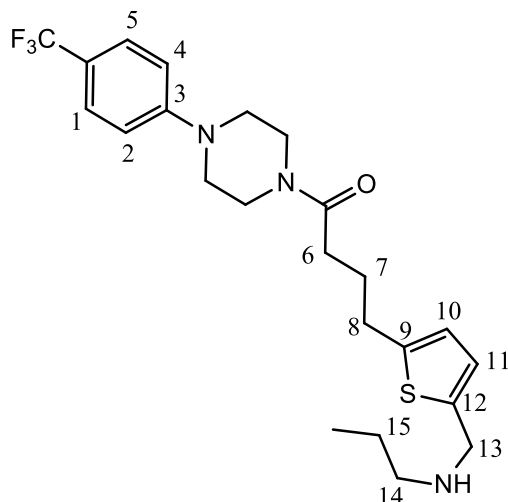
To a solution of compound **147** (50 mg, 0.13 mmol) in MeOH (4 mL), was added a solution of propan-1-amine (15 μL, 0.19 mmol) in MeOH (2 mL) and the resulting solution was stirred at rt. After 2 hrs, NaBH₄ (4 mg, 0.13 mmol) was added and the mixture stirred overnight at rt. MeOH was removed under reduced pressure and the residue was purified flash chromatography (1:9, MeOH:DCM) to give a colourless oil, 31 mg (56%).

¹H NMR: (300 MHz, CDCl₃) δ 7.50 (d, J = 8.7 Hz, 2H, H1, H5), 6.92 (d, J = 8.7 Hz, 2H, H2, H4), 6.77 (d, J = 3.3 Hz, 1H, H11), 6.62 (d, J = 3.3 Hz, 1H, H10), 3.94 (s, 2H, H13), 3.80-3.76 (m, 2H*), 3.60-3.57 (m, 2H*), 3.27-3.24 (m, 4H*), 2.87 (t, J = 7.2 Hz, 2H, H8), 2.64 (t, J = 7.2 Hz, 2H, H14), 2.52 (bs, 1H, NH), 2.41 (t, J = 7.2 Hz, 2H, H6), 2.07-1.98 (m, 2H, H7), 1.62-1.50 (m, 2H, H15), 0.92 (t, J = 7.2 Hz, 3H, CH₃).*Piperazine. **¹³C NMR:** (75 MHz, CDCl₃) δ 171.0 (C=O), 152.9 (C3), 143.8 (C9), 140.4 (C12), 126.5 (q, J = 3.7 Hz, C1, C5), 125.3 (C11), 124.5 (q, J = 268.0 Hz, CF₃), 124.1 (C10), 121.2 (q, J = 32.0 Hz, C-CF₃), 115.0 (C2, C4), 50.6 (C*), 48.3 (C*), 48.17 (C13), 48.11 (C*), 45.0 (C*), 41.1 (C6), 32.0 (C8), 29.5 (C7), 22.6 (C15), 11.7 (CH₃).*Piperazine. **R$_f$:** 0.4 (1:9, MeOH:DCM). **HR-MS:** calcd for C₂₃H₃₁F₃N₃OS m/z: [M + H]⁺, 454.2134; found: 454.2135 [Diff(ppm) = 0.20]. **IR (neat):** 3436 (N-H), 2928 (C-H), 1642 (C=O), 1616 (C=C), 1439 (C=C), 1331 (C-F), 1115(C-N) cm⁻¹.

10.118 Synthesis of 1,2-bis(2-azidoethoxy)ethane (RD208) (153)[209]
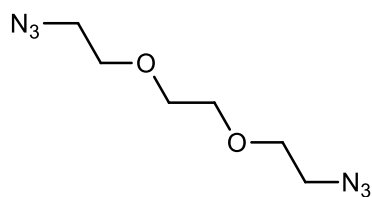
Prepared   from   (ethane-1,2-diylbis(oxy))bis(ethane-2,1-diyl)bis(4-methylbenzenesulfonate) (1 g, 2.18 mmol) using sodium azide (312 mg, 4.79 mmol) and CH_3CN (30 mL) and following the procedure described for the synthesis of compound **89**. The reaction mixture was heated at reflux for 48 hrs. Purified using flash chromatography (3:2 EtOAc:Pet. Ether) to give a yellow oil, 353 mg (80%).

^{1}H NMR: (300 MHz, $CDCl_3$) δ 3.58-3.55 (m, 8H, OCH_2 x 4), 3.28-3.25 (m, 4H, (N_3CH_2) x 2). ^{1}H NMR data matches literature data.[210] **R_f:** 0.7 (3:2, Pet. Ether:EtOAc). **HR-MS:** calcd for $C_6H_{12}N_6O_2Na$ m/z: [M + Na]$^+$, 223.0914; found: 223.0918 [Diff(ppm) = 1.70].

10.119 Synthesis of 2-(2-(2-azidoethoxy)ethoxy)ethanamine (RD225) (154)[209]
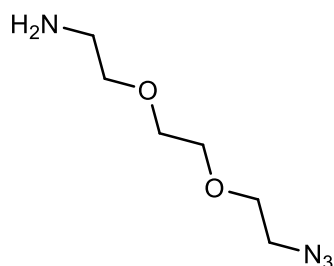
Et_2O (1.2 mL), 1 M aqueous HCl (3.52 mL) and EtOAc (1.2 mL) were added to compound **153** (353 mg, 1.76 mmol) in a round bottom flask and the resulting solution solution was cooled to 0 °C. Triphenylphosphine (461 mg, 1.76 mmol) was added, in four portions (4 x 115 mg), over 1 hr. The biphasic solution was warmed to rt and monitored by TLC. After 18 hrs, the aqueous layer was separated and washed with Et_2O (2 x 5 mL) to remove triphenyl phosphine oxide. The pH was adjusted to pH~13, with 2 M aqueous NaOH, before extraction with DCM (10 mL, followed by 3 x 10 mL). The combined organic layers were dried over $MgSO_4$ and concentrated under reduced pressure to give a light yellow oil, 305 mg (99%).

^{1}H NMR: (300 MHz, $CDCl_3$) δ 3.52-3.47(m, 2H, NH_2CH_2), 3.46-3.38 (m, 6H, OCH_2 x 3), 3.20-3.12 (m, 4H, OCH_2, N_3CH_2). ^{1}H NMR data matches literature data.[210]. **HR-**

MS: calcd for $C_6H_{13}N_4O_2$ m/z: $[M + H]^+$, 175.1190; found: 175.1191 [Diff (ppm) = 0.60]. **R$_f$:** 0.2 (MeOH)

10.120 Synthesis **of** **4-(5-(((2-(2-(2-azidoethoxy)ethoxy)ethyl)amino)methyl)thiophen-2-yl)-1-(4-(4-(trifluoromethyl)phenyl)piperazin-1-yl)butan-1-one (RD232) (155)**
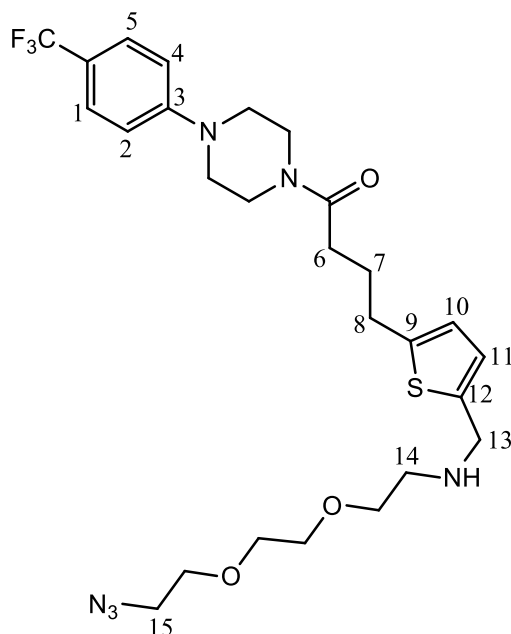
To a solution of compound **147** (50 mg, 0.13 mmol) in MeOH (4 mL), was added a solution of compound **154** (124 mg, 0.71 mmol) in MeOH (4 mL) and the resulting solution was stirred at rt. After 2 hrs, NaBH$_4$ (19 mg, 0.52 mmol) was added and the mixture stirred overnight at rt. MeOH was removed under reduced pressure and the residue was purified flash chromatography (1:24 MeOH:DCM) to give a yellow oil, 227 mg (76%).

^{1}H NMR: (300 MHz, CDCl$_3$) δ 7.49 (d, J = 8.7 Hz, 2H, H1, H5), 6.92 (d, J = 8.7 Hz, 2H, H2, H4), 6.74 (d, J = 3.3 Hz, 1H, H11), 6.62 (d, J = 3.3 Hz, 1H, H10), 3.94 (s, 2H, H13), 3.79-3.76 (m, 2H*), 3.67-3.56 (m, 2H*, 8H, OCH$_2$ x 4), 3.37 (t, J = 5.4 Hz, 2H, H14), 3.27-3.25 (m, 4H*), 2.88-2.82 (m, 4H, H8, H15), 2.67 (bs, 1H, NH), 2.41 (t, J = 7.2 Hz, 2H, H6), 2.07-1.97 (m, 2H, H7). *Piperazine. **^{13}C NMR:** (75 MHz, CDCl$_3$) δ 171.0 (C=O), 152.8 (C3), 143.6 (C9), 141.3 (C12), 126.4 (q, J = 3.2 Hz, C1, C5), 124.9 (C11), 124.6 (q, J = 268.5 Hz, CF$_3$), 124.0 (C10), 121.0 (q, J = 32.9 Hz, C-CF$_3$), 14.9 (C2, C4), 70.5 (OCH$_2$), 70.35 (OCH$_2$), 70.30 (OCH$_2$), 70.0 (OCH$_2$), 50.5 (C14), 48.4

(C13), 48.2 (C*, C15), 48.0 (C*), 45.0 (C*), 41.0 (C*), 32.0 (C6), 29.5 (C8), 26.8 (C7).*Piperazine. **R$_f$:** 0.3 (1:24, MeOH:DCM). **HR-MS:** calcd for $C_{26}H_{36}F_3N_6O_3S$ m/z: [M + H]$^+$, 569.2516; found: 569.2526 [Diff(ppm) = 1.8]. **IR (neat):** 3054 (N-H), 2924 (C-H), 2111 (N$_3$), 1643 (NH), 1617 (C=O), 1330 (C-F), 1265 (C-O), 1117 (C-N) cm^{-1}.

10.121 Synthesis of 4-(5-(((2-(2-(2-aminoethoxy)ethoxy)ethyl)amino)methyl)thiophen-2-yl)-1-(4-(4-(trifluoromethyl)phenyl)piperazin-1-yl)butan-1-one (RD240) (156)
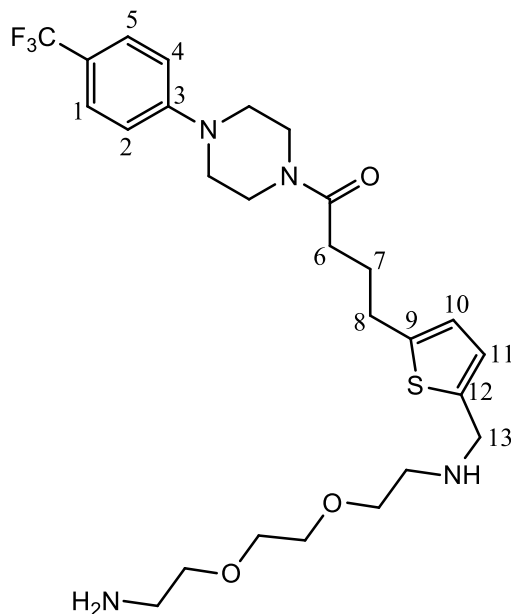
Et$_2$O (1 mL), 1 M aqueous HCl (3.03 mL) and EtOAc (2 mL) were added to compound **155** (167 mg, 0.29 mmol) in a round bottom flask and the resulting solution solution was cooled to 0 °C. PPh$_3$ (168 mg, 0.81 mmol) was added, in four portions (4 x 42 mg), over 1 hr. The biphasic solution was warmed to rt and monitored by TLC. After 18 hrs, the aqueous layer was separated and washed with Et$_2$O (2 x 5 mL) to remove triphenyl phosphine oxide. The pH was adjusted to pH~13, with 2 M aqueous NaOH, before extraction with DCM (10 mL, followed by 3 x 10 mL). The combined organic layers were dried over MgSO$_4$ and concentrated under reduced pressure. The residue was purified using flash chromatography (97:3, MeOH:NEt$_3$) to give a yellow oil, 70 mg (43%).

^{1}H NMR: (300 MHz, CDCl$_3$) δ 7.50 (d, J = 8.7 Hz, 2H, H1, H5), 6.92 (d, J = 8.7 Hz, 2H, H2, H4), 6.73 (d, J = 3.3 Hz, 1H, H11), 6.62 (d, J = 3.3 Hz, 1H, H10), 3.94 (s, 2H, H13), 3.79-3.76 (m, 2H*), 3.67-3.48 (m, 2H*, 8H, OCH$_2$ x 4), 3.29-3.22 (m, 4H*),

3.01-2.71 (m, 9H, H8, NH_2, NH, NCH_2 x 2), 2.41 (t, J = 7.2 Hz, 2H, H6), 2.07-1.96 (m, 2H, H7).*Piperazine. **^{13}C NMR:** (75 MHz, $CDCl_3$) δ 170.0 (C=O), 151.8 (C3), 142.5 (C9), 140.4 (C12), 125.4 (q, J = 3.0 Hz, C1, C5), 123.8 (C11), 123.5 (q, J = 268.7 Hz, CF_3), 123.0 (C10), 120.1 (q, J = 32.3 Hz, C-CF_3), 113.9 (C2, C4), 71.7 (C*), 69.3 (OCH_2), 69.2 (OCH_2), 69.1, (OCH_2), 47.2 (C13, C*), 47.0 (C14, C15, C*), 44.0 (OCH_2), 40.0 (C*), 31.0 (C6), 28.5 (C8), 25.7 (C7).*Piperazine. **R_f:** 0.3 (1:24, MeOH:DCM). **HR-MS:** calcd for $C_{26}H_{37}F_3N_4O_3SNa$ m/z: $[M + Na]^+$, 565.2431; found: 565.2445 [Diff(ppm) = 2.58]. **IR (neat):** 3420 (N-H), 2914 (C-H), 1640 (N-H), 1615 (C=O), 1331 (C-F), 1233 (C-O), 1112 (C-N) cm^{-1}.

10.122 Synthesis of (2-(2-(2-azidoethoxy)ethoxy)ethyl)-9-oxo-9-(4-(4-(trifluoromethyl)phenyl)piperazin-1-yl)nonanamide (RD295) (157)
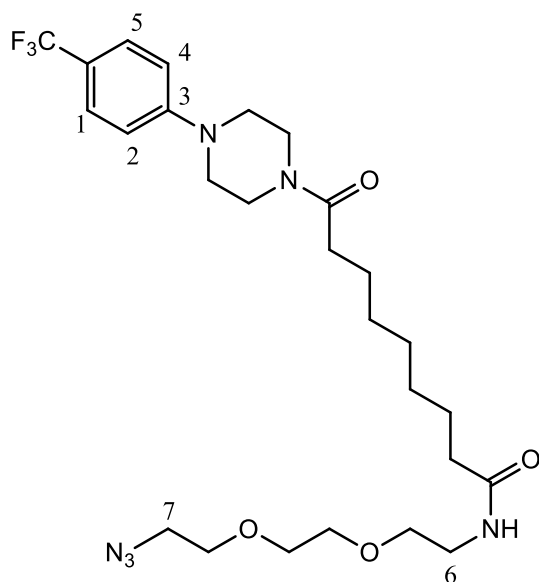
Prepared from compound **79** (60 mg, 0.15 mmol) and compound **154** (28 mg, 0.16 mmol) using HOBt (22 mg, 0.16 mmol), TBTU (52 mg, 0.16 mmol), anhydrous NEt_3 (33 µL, 0.24 mmol) and anhydrous DMF (4 mL) and following the general procedure described in section **10.2**. The reaction mixture was stirred overnight at room temperature under a N_2 atmosphere. Purified using flash chromatography (1:9, MeOH:DCM) to give a brown oil, 80 mg (96%).

^{1}H NMR: (300 MHz, $CDCl_3$) δ 7.50 (d, J = 8.7 Hz, 2H, H1, H5), 6.93 (d, J = 8.7 Hz, 2H, H2, H4), 6.16 (bs, 1H, NH), 3.79-3.76 (m, 2H*), 3.71-3.62 (m, 2H*, 6H, OCH_2 x 3), 3.57-3.54 (m, 2H, OCH_2), 3.47-3.44 (m, 2H, H6), 3.42-3.38 (m, 2H, H7), 3.31-3.24

(m, 4H*) , 2.36 (t, J = 7.5 Hz, 2H, (C=O)CH$_2$), 2.17 (t, J = 7.5 Hz, 2H, (C=O)CH$_2$), 1.64-1.60 (m, 4H, ((C=O)CH$_2$CH_2 x 2), 1.34-1.33 (m, 6H, CH$_2$ x 3).*Piperazine. **^{13}C NMR:** (75 MHz, CDCl$_3$) δ 173.2 (HN-C=O), 171.7 (N-C=O), 152.9 (C3), 126.4 (q, J = 3.3 Hz, C1, C5), 124.6 (q, J = 270.0 Hz, CF$_3$), 121.0 (q, J = 32.0 Hz, C-CF$_3$), 114.9 (C2, C4), 70.4 (OCH$_2$), 70.1 (OCH$_2$), 70.0 (OCH$_2$), 69.9 (OCH$_2$), 50.5 (C7), 48.3 (C*), 48.0 (C*), 45.1 (C*), 41.0 (C*), 39.0 (C6), 36.5 ((C=O)CH$_2$), 33.1 ((C=O)CH$_2$), 29.2 (CH$_2$), 29.08 (CH$_2$), 29.06 (CH$_2$), 25.6 ((C=O)CH$_2$$CH_2$), 25.1 ((C=O)CH$_2$$CH_2$).*Piperazine **R$_f$:** 0.5 (1:9, MeOH:DCM). **HR-MS:** calcd for C$_{26}$H$_{40}$F$_3$N$_6$O$_4$ m/z: [M + H]$^+$, 557.3058; found: 557.3046 [Diff (ppm) = -2.08]. **IR (neat):** 2928 (C-H), 2107 (N=N=N), 1645 (C=O), 1615 (C=O), 1331 (C-F), 1233 (C-N), 1114 (C-O) cm^{-1}.

10.123 Synthesis of N-(2-(2-(2-aminoethoxy)ethoxyethyl)-9-oxo-9-(4-(4-(trifluoromethyl)phenyl)piperazin-1-yl)nonanamide (RD298) (158)
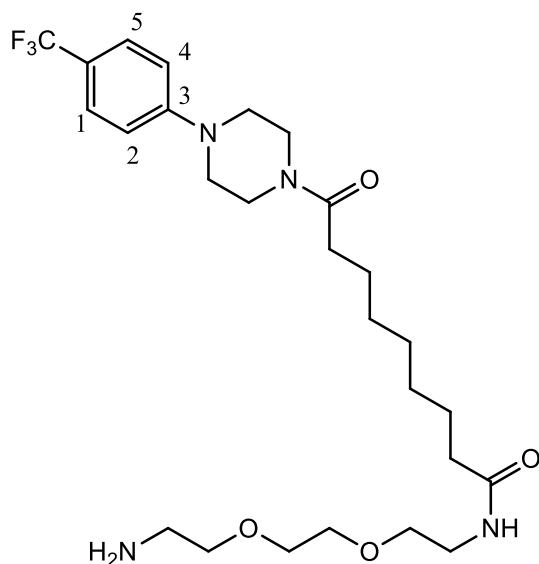
Et$_2$O (1000 µL), 1 M aqueous HCl (900 µL) and EtOAc (500 µL) were added to compound **157** (89 mg, 0.16 mmol) in a round bottom flask and the resulting solution solution was cooled to 0 °C. PPh$_3$ (48 mg, 0.18 mmol) was added, in four portions (4 x 12 mg), over 1 hr. The biphasic solution was warmed to rt and monitored by TLC. After 18 hrs, the aqueous layer was separated and washed with Et$_2$O (2 x 5 mL) to remove triphenyl phosphine oxide. The pH was adjusted to pH~13, with 2 M aqueous NaOH, before extraction with DCM (10 mL, followed by 3 x 10 mL). The combined organic layers were dried over MgSO$_4$ and concentrated under reduced pressure. The residue

was purified using flash chromatography (89:10:1, DCM:MeOH:NEt$_3$) to give a clear oil, 21 mg (25%).

^{1}H NMR: (300 MHz, CDCl$_3$) δ 7.50 (d, J = 8.7 Hz, 2H, H1, H5), 6.93 (d, J = 8.7 Hz, 2H, H2, H4), 6.36 (bs, 1H, (C=O)NH), 3.79-3.76 (m, 2H*), 3.65-3.63 (m, 6H, OCH$_2$ x 3), 3.58-3.54 (m, 2H*, 2H, OCH$_2$), 3.47-3.42 (m, 2H, NCH$_2$), 3.30-3.24 (m, 4H*), 2.92 (bs, 2H, NH$_2$), 2.36 (t, J = 8.4 Hz, 2H, (C=O)CH$_2$), 2.20-1.93 (m, 4H, (C=O)CH$_2$, NCH$_2$), 1.64-1.63 (m, 4H, (C=O)CH$_2$CH_2 x 2), 1.34-1.33 (m, 6H, CH$_2$ x 3).*Piperazine.
^{13}C NMR: (75 MHz, CDCl$_3$) δ 173.2 (HN-C=O), 171.7 (N-C=O), 152.9 (C3), 126.4 (q, J = 3.3Hz, C1, C5), 124.6 (q, J = 270.0 Hz, CF$_3$), 121.0 (q, J = 32.5 Hz, C-CF$_3$), 114.9 (C2, C4), 69.2 (OCH$_2$), 69.0 (OCH$_2$), 68.9 (OCH$_2$), 47.3 (C*), 47.0 (C*), 44.1 (C*), 40.0 (C*), 38.0 (OCH$_2$), 35.5 (NCH$_2$), 32.1 (NCH$_2$), 29.2 (CH$_2$), 29.08 (CH$_2$), 29.06 (CH$_2$), 25.6 (C=O)CH$_2$CH$_2$), 25.1 (C=O)CH$_2$CH_2).*Piperazine. **R$_f$:** 0.5 (1:9, MeOH:DCM). **HR-MS:** calcd for C$_{26}$H$_{40}$F$_3$N$_6$O$_4$ m/z: [M + H]$^+$, 557.3058; found: 557.3046 [Diff(ppm) = -2.08]. **IR (neat):** 3373 (N-H), 2930 (C-H), 1643 (N-H), 1639 (HN-C=O), 1616 (N-C=O), 1331 (C-F), 1233 (C-O), 1114 (C-N) cm^{-1}.

10.124 Synthesis of 4-(5-formylthiophen-2-yl)butanoic acid (RD283) (159)
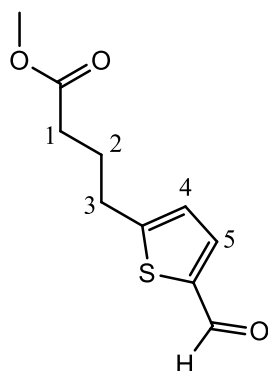
To a solution of dichloromethyl methyl ether (212 µL, 2.34 mmol) in anhydrous DCM (5 mL) at 0 °C was added tin(IV)chloride (610 µL, 2.07 mmol) under a N$_2$ atmosphere. After 5 mins, a solution of compound **74** (320 mg, 1.73 mmol) in DCM (4 mL) was added dropwise over a period of 20 mins. The reaction mixture was stirred for 1 hr at rt, after which it was poured onto ice-water and stirred for 30 mins. The organic layer was removed and washed with H$_2$O (10 mL followed by 2 x 10 mL), dried over MgSO$_4$ and concentrate *in vacuo* to give compound **99** as a clear oil, 193 mg (52%, crude yield).

¹H NMR: (300 MHz, CDCl₃) δ 9.82 (s, 1H, CHO), 7.63 (d, J = 3 Hz, H5), 6.94 (d, J = 3 Hz, H4), 3.68 (s, 3H, CH₃), 2.94 (t, J = 7.5 Hz, 2H, H3), 2.39 (t, J = 7.5 Hz, 2H, H1), 2.09-1.99 (m, 2H, H2). **R$_f$:** 0.6 (9:1, Pet.Ether:EtOAc).

10.125 Synthesis of methyl 4-(5-((((2-(2-azidoethoxy)ethyl)amino)methyl)thiophen-2-yl)butanoate (RD290) (160)
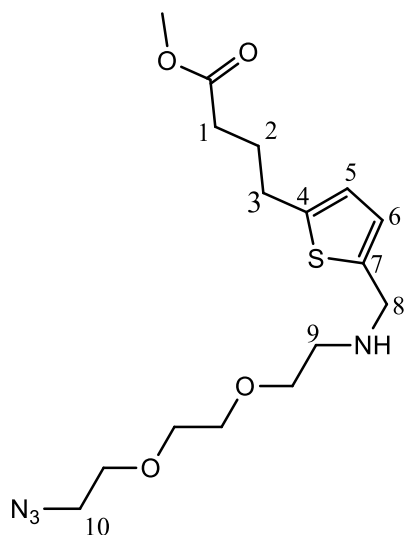
To a solution of compound **159** (100 mg, 0.43 mmol) in MeOH (4 mL), was added a solution of compound **154** (114 mg, 0.64 mmol) in MeOH (2 mL) and the resulting solution was stirred at rt. After 2 hrs, NaBH₄ (16 mg, 0.43 mmol) was added and the mixture stirred overnight at rt. MeOH was removed under reduced pressure and the residue was purified using flash chromatography (1:9, MeOH:DCM) to give an range oil, 94 mg (58%).

¹H NMR: (300 MHz, CDCl₃) δ 6.72 (d, J = 3.3 Hz, 1H, H6), 6.60 (d, J = 3.3 Hz, 1H, H5), 3.92 (s, 2H, H8), 3.68-3.59 (m, 11H, CH₃, OCH₂ x 4), 3.39-3.35 (m, 2H, H9), 2.84-2.78 (m, 4H, H3, H10), 2.39 (t, J = 7.3 Hz, 2H, H1), 2.02-1.92 (m, 2H, H2). **¹³C NMR:** (75 MHz, CDCl₃) δ 171.8 (C=O), 141.3 (C4), 139.7 (C7), 122.9 (C6), 122.1 (C5), 68.6 (OCH₂), 68.5 (OCH₂), 68.4 (OCH₂), 68.1 (OCH₂), 49.6 (CH₃), 48.7 (C9), 46.6 (C8), 46.4 (C10), 31.2 (C1), 27.5 (C3), 24.7 (C2). **R$_f$:** 0.5 (1:9, MeOH:DCM). **HR-MS:** calcd for C₁₆H₂₇N₄O₄S m/z: [M + H]⁺, 374.1756; found: 374.1771 [Diff(ppm) = 4.02]. **IR (neat):** 3325 (N-H), 2867 (C-H), 2109 (N=N=N), 1736 (C=O), 1123 (C-O), 804 (N-H) cm⁻¹.

10.126 Synthesis **of** **4-(5-(((2-(2-(2-azidoethoxy)ethoxy)ethyl)amino)methyl)thiophen-2-yl)butanoic acid (RD296)** **(161)**
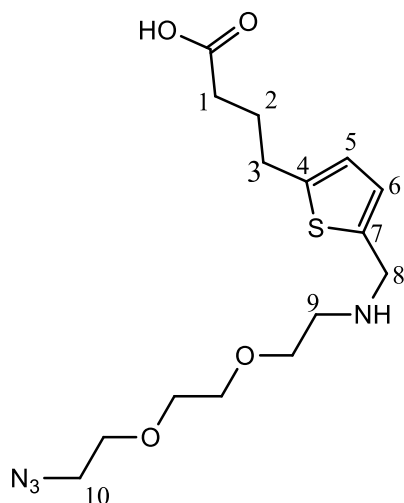
Compound **160** (94 mg, 0.25 mmol) and KOH (71 mg, 1.26 mmol) in EtOH (5 mL) were heated at reflux and reaction progress monitored by TLC (3:2 EtOAc: Pet. Ether). After 3 hrs the solution was allowed to cool to rt and EtOH was removed under reduce pressure. The residue was dissolved in H_2O (1.5 mL), the pH adjusted to pH = 6 with 2 M aqueous HCl and the aqueous layer extracted with DCM (20 mL, followed by 4 x 10 mL). The organic layers were washed with brine (3 x 20 mL), dried over $MgSO_4$ and evaporated under reduced pressure to give an orange solid, 90 mg, (98%).

^{1}H NMR: (300 MHz, D_2O) δ 7.08-7.07 (m, 1H, H6), 6.86-6.85 (m, 1H, H5), 4.31 (s, 2H, H8), 3.80-3.73 (m, 8H, OCH_2 x 4), 3.54-3.51 (m, 2H, H9), 3.17-3.15 (m, 2H, H10), 2.88-2.83 (m, 2H, H3), 2.27-2.22 (m, 2H, H1), 1.97-1.87 (m, 2H, H2). **^{13}C NMR:** (75 MHz, D_2O) δ 183.0 (C=O), 148.7 (C4), 131.1 (C7), 129.7 (C6), 125.3 (C5), 69.7 (OCH_2), 69.4 (OCH_2), 65.8 (OCH_2), 50.3 (C9), 45.9 (C10), 45.4 (C8), 37.0 (C1), 29.3 (C3), 28.0 (C2). **HR-MS:** calcd for $C_{15}H_{25}N_4O_4S$ m/z: [M + H]$^+$, 357.1591; found 357.1587 [Diff(ppm) = -1.17]. **IR (KBr):** 2922 (C-H), 2110 (N=N=N), 1625 (C=O), 1119 (C-O) cm^{-1}.

10.127 Synthesis of methyl 9-(4-(4-nitrophenyl)piperazin-1-yl)-9-oxononanoate (RTC98) (163)†
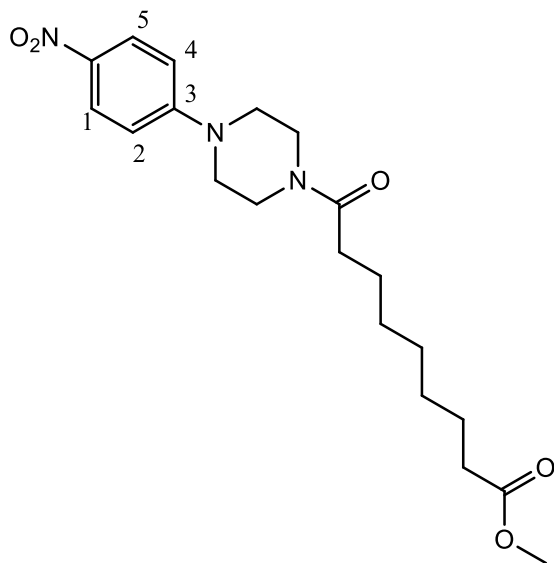
Prepared from 1-(4-nitrophenyl)piperazine (500 mg, 2.40 mmol) and 9-methoxy-9-oxononanoic acid (424 μL, 2.18 mmol) using HOBt (325 mg, 2.40 mmol), TBTU (775 mg, 2.40 mmol), anhydrous NEt$_3$ (489 μL, 3.49 mmol) and anhydrous DMF (10 mL) and following the general procedure described in section **10.2**. The reaction mixture was stirred overnight at room temperature under a N$_2$ atmosphere. Purified using flash chromatography (1:9 MeOH:DCM) to give an orange solid, 682 mg (80%).

^{1}H NMR: (300 MHz, CDCl$_3$) δ 8.01 (d, J = 9.1 Hz, 2H, H1, H5), 6.75 (d, J = 9.1 Hz, 2H, H2, H4), 3.75-3.71 (m, 2H*), 3.64-3.61 (m, 2H*), 3.58 (s, 3H, OCH$_3$), 3.45-3.36 (m, 4H*), 2.30 (t, J = 7.2 Hz, 2H, (C=O)CH$_2$), 2.23 (t, J = 7.2 Hz, 2H, (C=O)CH$_2$), 1.60-1.52 (m, 4H, (C=O)CH$_2$C*H*$_2$ x 2), 1.28-1.26 (m, 6H, CH$_2$ x 3).*Piperazine. **^{13}C NMR:** (75 MHz, CDCl$_3$) δ 174.2 (*C*OOCH$_3$), 171.9 (C=O), 154.4 (C3), 139.0 (C-NO$_2$), 125.8 (C1, C5), 112.7 (C2, C4), 51.4 (OCH$_3$), 46.8 (C*) 46.7 (C*), 44.6 (C*), 40.7 (C*), 33.9 ((C=O)*C*H$_2$), 33.1 ((C=O)*C*H$_2$), 29.1 (CH$_2$), 28.9 (CH$_2$), 28.8 (CH$_2$), 24.7 ((C=O)CH$_2$*C*H$_2$), 25.0 ((C=O)CH$_2$*C*H$_2$).*Piperazine. **R$_f$:** 0.7 (1:9, MeOH:DCM). **HR-MS:** calcd for C$_{20}$H$_{30}$N$_3$O$_5$ m/z: [M + H]$^+$, 392.2180; found: 39.2198 [Diff (ppm) = 4.60]. **IR (KBr):** 2911 (C-H), 1736 ((*C=O*)OCH$_3$), 1649 (C=O), 1587 (NO), 1320 (NO) cm^{-1}. **m.p.:** 97-100 °C.

10.128 Synthesis of 9-(4-(4-nitrophenyl)piperazin-1-yl)-9-oxononanoic acid (RTC99) (164)†
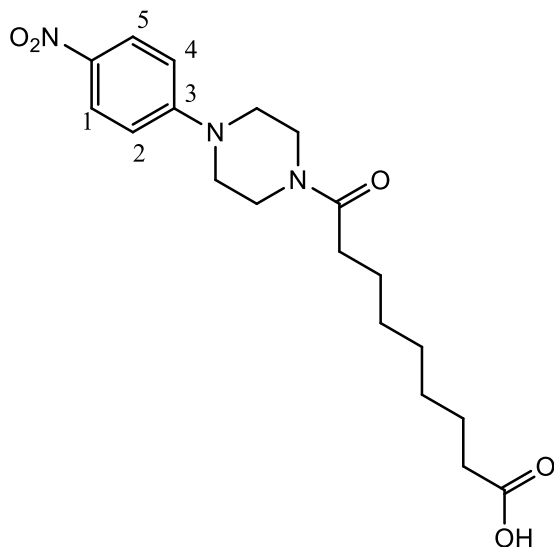
Compound **163** (300 mg, 0.76 mmol) and KOH (172 mg, 3.06 mmol) in EtOH (5 mL) were heated at reflux and reaction progress monitored by TLC (3:2 EtOAc: Pet. Ether). After 5 hrs the solution was allowed to cool to rt and EtOH was removed under reduced pressure. The residue was dissolved in H_2O (1.5 mL), the pH adjusted to pH = 6 with 2 M aqueous HCl and the aqueous layer extracted with DCM (20 mL, followed by 4 x 10 mL). The organic layers were washed with brine (3 x 20 mL), dried over $MgSO_4$ and evaporated under reduced pressure. The residue was purified using flash chromatography (1:9, MeOH:DCM) to give an orange solid, 230 mg (79%).

¹H NMR: (300 MHz, CDCl₃) δ 8.14 (d, *J* = 9.1 Hz, 2H, H1, H5), 6.82 (d, *J* = 9.1 Hz, 2H, H2, H4), 3.82-3.79 (m, 2H*) 3.69-3.66 (m, 2H*), 3.49-3.42 (m, 4H*), 2.40-2.31 (m, 4H, (C=O)C*H₂* x 2), 1.65-1.60 (m, 4H, (C=O)CH₂C*H₂* x 2), 1.45-1.25 (m, 6H, CH₂ x 3).Piperazine.**¹³C NMR:** (75 MHz, CDCl₃) δ 179.0 (C=O), 172.2 (N-C=O), 154.3 (C3), 138.8 (C-NO₂), 125.9 (C1, C5), 112.8 (C2, C4), 46.8 (C*) 46.7 (C*), 44.7 (C*), 40.8 (C*), 34.1 ((C=O)C*H₂*), 33.1 ((C=O)C*H₂*), 29.1 (CH₂), 28.9 (CH₂), 28.8 (CH₂), 25.0 ((C=O)CH₂C*H₂*), 24.6 ((C=O)CH₂C*H₂*).Piperazine. **R_f:** 0.7 (1:9, MeOH:DCM). **HR-MS:** calcd for $C_{19}H_{28}N_3O_5$ m/z: [M + H]⁺, 378.2023; found: 378.2040 [Diff(ppm) = 4.50]. **IR (KBr):** 3430 (OH), 2920 (C-H), 1776 (C=O), 1598 (N-C=O), 1598 (NO), 1320 (NO) cm⁻¹. **m.p.:** 98-100 °C.

10.129 Synthesis   of   N-(2-(2-(2-azidoethoxy)ethoxy)ethyl)-9-(4-(4-nitrophenyl)piperazin-1-yl)-9-oxononanamide (RD333) (165)
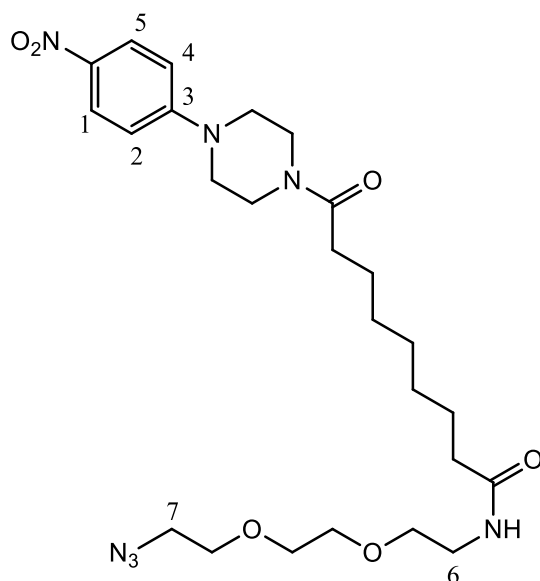
Prepared from compound **164** (112 mg, 0.29 mmol) and compound **154** (57 mg, 0.33 mmol) using HOBt (44 mg, 0.29 mmol), TBTU (105 mg, 0.29 mmol), anhydrous NEt_3 (157 µL, 0.47 mmol) and anhydrous DMF (4 mL) and following the general procedure described in section **10.2**. The reaction mixture was stirred overnight at room temperature under a N_2 atmosphere. Purified using flash chromatography (1:9, MeOH:DCM) to give an orange oil, 150 mg (94%).

^{1}H NMR: (300 MHz, $CDCl_3$) δ 8.13 (d, J = 9.3 Hz, 2H, H1, H5), 6.83 (d, J = 9.3 Hz, 2H, H2, H4), 3.82-3.78 (m, 2H*), 3.71-3.62 (m, 2H*, 6H, OCH_2 x 3), 3.57-3.54 (m, 2H, OCH_2) 3.50-3.38 (m, 4H*, 4H, H6, H7), 2.36 (t, J = 7.3 Hz, 2H, $(C=O)CH_2$), 2.16 (t, J = 7.3 Hz, 2H, $(C=O)CH_2$), 1.67-1.60 (m, 4H, $(C=O)CH_2CH_2$ x 2), 1.35-1.33 (m, 6H, CH_2 x 3).*Piperazine. **^{13}C NMR:** (75 MHz, $CDCl_3$) δ 173.1 (HN-C=O), 171.8 (N-C=O), 154.4 (C3), 138.8 (C-NO_2), 125.9 (C1, C5), 112.8 (C2, C4), 70.4 (OCH_2), 70.1 (OCH_2), 70.0 (OCH_2), 69.9 (OCH_2), 50.5 (C7), 46.9 (C*), 46.8 (C*), 44.7 (C*), 40.7 (C*), 39.0 (C6) 36.5 ($(C=O)CH_2$), 33.1 ($(C=O)CH_2$), 29.1 (CH_2), 29.06 (CH_2), 29.04 (CH_2), 25.5 ($(C=O)CH_2CH_2$), 25.0 ($(C=O)CH_2CH_2$).*Piperazine. **R_f:** 0.6 (1:9, MeOH:DCM). **HR-MS:** calcd for $C_{25}H_{40}N_7O_6$ m/z: $[M + H]^+$, 534.3035; found: 534.3046 [Diff(ppm) = 2.17]. **IR (neat):** 2928 (C-H), 2106 ($N=N^+=N^-$), 1643 (C=O), 1597 (NO), 1322 (NO) cm^{-1}.

10.130 Synthesis of N-(2-(2-(2-aminoethoxy)ethoxy)ethyl)-9-(4-(4-nitrophenyl)piperazin-1-yl)-9-oxononanamide (RD341) (166)
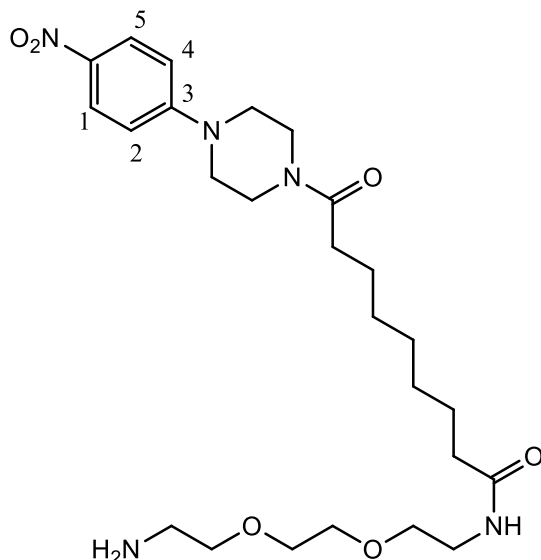
Et$_2$O (2 mL), 1 M aqueous HCl (2 mL) and EtOAc (2 mL) were added to compound **165** (204 mg, 0.38 mmol) in a round bottom flask and the resulting solution solution was cooled to 0 °C. PPh$_3$ (112 mg, 0.38 mmol) was added, in four portions (4 x 38 mg), over 1 hr. The biphasic solution was warmed to rt and monitored by TLC. After 18 hrs, the aqueous layer was separated and washed with Et$_2$O (2 x 5 mL) to remove triphenyl phosphine oxide. The pH was adjusted to pH~13, with 2 M aqueous NaOH, before extraction with DCM (10 mL, followed by 3 x 10 mL). The combined organic layers were dried over MgSO$_4$ and concentrated under reduced pressure. The residue was purified using flash chromatography (1:9, MeOH:DCM) to give an orange oil, 26 mg (13%).

^{1}H NMR: (300 MHz, CD$_3$OD) δ 8.14 (d, J = 9.4 Hz, 2H, H1, H5), 7.02 (d, J = 9.4 Hz, 2H, H2, H4), 3.75-3.48 (m, 8H*, 8H, OCH$_2$ x 4), 3.39-3.35 (m, 2H, NCH$_2$), 3.10-2.93 (m, 2H, NCH$_2$), 2.46 (t, J = 7.2 Hz, 2H, (C=O)CH$_2$), 2.21 (t, J = 7.2 Hz, 2H, (C=O)CH$_2$), 1.63-1.62 (m, 4H,(C=O)CH$_2$CH_2 x 2), 1.47-1.33 (m, 6H, CH$_2$ x 3). **^{13}C NMR:** (75 MHz, CD$_3$OD) δ 175.0 (HN-C=O), 172.9 (N-C=O), 154.7 (C3), 138.2 (C-NO$_2$), 125.3 (C1, C5), 112.5 (C2, C4), 69.8 (OCH$_2$), 69.2 (OCH$_2$), 69.1 (OCH$_2$), 46.5 (C*), 46.1 (C*), 44.6 (C*), 40.8(C*), 39.9 (C*), 38.7 (OCH$_2$), 35.6 (C6), 32.5 (C7), 28.87 (CH$_2$), 28.80 (CH$_2$), 28.7 (CH$_2$), 25.5 ((C=O)CH$_2$CH_2), 24.9 ((C=O)CH$_2$CH_2). **R$_f$:** 0.6 (1:10:89, NEt$_3$:MeOH:DCM). **HR-MS:** calcd for C$_{25}$H$_{42}$N$_5$O$_6$ m/z: [M + H]$^+$,

509.316; found: 509.3184 [Diff(ppm) = 4.77]. **IR (neat):** 3389 (N-H), 2923 (C-H), 1645 (HN-*C=O*), 1638 (N-*C=O*), 1631 (N-H), 1597 (NO), 1321 (NO), 1237 (C-N) cm^{-1}

10.131 Fluorometric binding assay

The binding of compounds to His-RBP4 was monitored by titration of the intrinsic fluorescence emission of the protein in the presence of increasing concentrations of compounds (0, 0.2, 0.4, 0.6, 1.0, 1.5, 2.0, 5.0, 10.0, 15.0 μM). The quenching of protein fluorescence due to the transfer of energy to the ligand was evaluated using excitation and emission wavelengths of 280 and 350 nm, respectively, in a Cary Eclipse fluorescence spectrophotometer (Varian). Purified His-RBP4 expressed with the *P. pastoris* system was diluted to a concentration of 1 μM in PBS buffer, and small increments of compound solutions in ethanol were added. The system was mixed and allowed to equilibrate for 5 mins before the fluorescence emission of the compound His-RBP complex was recorded. The final concentration of ethanol never exceeded 2%. A solution of *N*-acetyl-L-tryptophanamide was used as a blank.

10.132 Glucose Uptake Assay

C2C12 muscle cells were incubated with 10 μM of compound at 37 °C for ~12 hrs. Following treatment, the media was removed and the cells were washed in KRB (x 3) and ^{3}H deoxy-2-glucose (1μCi/mL; specific activity 8mCi/mmol) added for 10 mins at 37 °C. The cells were washed in ice-cold KRB (x 3) and solubilized in 0.1% SDS for 30 mins. The cells were harvested and 500μl (~250 μg protein) added to 2 mL scintillation fluid (Ultima Gold, Perkin Elmer, UK). Counts were read, per minute, using a Wallac MicroBeta scintillation counter (Perkin Elmer) and results are expressed as counts per minute per mg protein (CPM/ mg).

10.133 Immobilisation of compounds onto sepharose bead

10.133.1   General procedure for the immobilisation of compounds onto sepharose bead

The cyanogen activated sepharose beads were transferred to a column where they were soaked and swelled in 1 mM aqueous HCl. The beads were then washed with 0.1 M aqueous NaHCO$_3$ containing NaCl (x 3). The compound to be immobilised was dissolved in DMF and added to a 0.1 M NaHCO$_3$ solution containing and NaCl

solution. The solution was then mixed with the sepharose beads and gently agitated in a water bath at 25 °C for 20 hrs. A 0.2 M aqueous glycine solution (5 mL) containing NaHCO$_3$ (43 mg, 0.5 mmol) was added and the bead solution was stirred for a further 2 hrs to deactivate the remaining active groups. The bead solution was then washed with distilled H$_2$O followed by washing with 0.15 M NaCl (5 mL), 1M NaCl (5 mL) and 0.15 M NaCl (5 mL). This wash cycle was repeated five times and the aqueous washes were extracted with DCM (10 mL x 3) and the combined organic layers were dried over MgSO$_4$. The organic layers were concentrated under reduced pressure and analysed using ^{1}H NMR spectroscopy. The beads were washed with MeOH (5 mL x 3) and the organic layers were concentrated under reduced pressure. The residue was analysed using ^{1}H NMR spectroscopy. The beads were then stored in a 1 M NaCl solution at 2-8 °C.

10.133.2 Immobilisation of compound 156 onto sepharose bead

The cyanogen activated sepharose beads (100 mg) were swelled in 1mM HCl (10 mL) for 30 mins and washed with 0.1 M aqueous NaHCO$_3$ containing NaCl (146 mg, 0.05 mol) (5 mL) x 3). Compound **156** (23 mg, 0.04 mmol) was dissolved in DMF (400 µL) and added to a 0.1 M NaHCO$_3$ solution containing and NaCl (146 mg, 0.05 mol) (1 mL). The solution was then mixed with the sepharose beads and gently agitated in a water bath at 25 °C for 20 hrs. The series of washes describe in section **10.133.1** were then performed. Analysis revealed that 18 mg (78%) of compound **156** was immobilised on the sepharose bead.

10.133.3 Immobilisation of compound 158 onto sepharose bead

The cyanogen activated sepharose beads (100 mg) were swelled in 1mM HCl (10 mL) for 30 mins and washed with 0.1 M aqueous NaHCO$_3$ containing NaCl (146 mg, 0.05 mol) (5 mL) x 3). Compound **158** (20 mg, 0.04 mmol) was dissolved in DMF (400 µL) and added to a 0.1 M NaHCO$_3$ solution containing and NaCl (146 mg, 0.05 mol) (1 mL). The solution was then mixed with the sepharose beads and gently agitated in a water bath at 25 °C for 20 hrs. The series of washes describe in section **10.133.1** were then performed. Analysis revealed that 16 mg (80%) of compound **158** was immobilised on the sepharose bead.

10.133.4   Immobilisation of compound 166 onto sepharose bead

The cyanogen activated sepharose beads (100 mg) were swelled in 1mM HCl (10 mL) for 30 mins and washed with 0.1 M aqueous $NaHCO_3$ containing NaCl (146 mg, 0.05 mol) (5 mL) x 3). Compound **166** (20 mg, 0.04 mmol) was dissolved in DMF (400 µL) and added to a 0.1 M $NaHCO_3$ solution containing and NaCl (146 mg, 0.05 mol) (1 mL). The solution was then mixed with the sepharose beads and gently agitated in a water bath at 25 °C for 20 hrs. The series of washes describe in section **10.133.1** were then performed. Analysis revealed that 14 mg (70%) of compound **166** was immobilised on the sepharose bead.

10.134 Cyclodextrin studies

10.134.1   Preparation of compound 4 and HPBCD inclusion complex

The inclusion complex was prepared by dissolving compound **4** (1 eq) and HPBCD (20 eq) in a DMSO-water solution (5:95). The solvent was removed under reduced pressure to give the solid inclusion complex as a white crystalline solid.

10.134.2   Preparation of compound 4 and HPBCD physical mixture

The physical mixture was prepared by thoroughly grinding compound **4** (1 eq) and HPBCD (20 eq) in a mortar and pestle for 5 mins.

10.134.3   Standard curve

A series of solutions of compound **4** (10, 20, 25, 30, 37.5, 40 and 50 µM) in MeOH were prepared and the UV absorption spectrum of each sample was obtained and the data analysed at 264 (λ_{max} of compound **4**). The absorbance values were then plotted against the varying concentrations of compound **4**. This experiment was performed three times using new solutions of compound **4**.

10.134.4   Phase-solubility diagram[193]

Compound **4** (47 mg, 0.125 mmol) was added to aqueous 25 mL HPBCD solutions of increasing concentrations (0.2, 0.4, 0.6, 0.8, and 1.0 mM) (fivefold molar excess of compound **4** used, relative to the highest conc. of HPBCD i.e. 5.0 mM compound **4** solution required). The mixtures were stirred for 72 hrs at rt after which each solution was centrifuged and filtered through a 0.45 µm Millipore filter. The absorbance value of

each solution was determined using UV spectroscopy at 264 (λ_{max} of compound **4**). The final concentration was then determined using the standard curve. This experiment was repeated three times using new compound **4** and HPBCD solutions. New data ws recorded each time.

10.134.5   Differential Scanning Calorimetry

Work pans containing approximately 2 mg of samples were heated from 20 to 400 °C, at a constant rate of 10 °C/min, under a N_2 atmosphere. The instrument used was a Perkin Elmer Pyris 6.0 apparatus and the result were recorded and analysed by means of Pyris Data Analysis software.

10.134.6   Scanning Electron Microscopy

SEM was used to examine the morphologies of the samples. SEM analysis was carried out using a Hitachi S-3200-N instrument. In all cases samples were mounted on aluminium stubs with carbon tabs. Prior to imaging, the samples were gold sputtered using an Agar automatic sputter coater B7341. An accelerating voltage of 20 kV was used in all cases.

10.134.7   NMR spectroscopy

^{1}H NMR spectra were acquired on a Bruker Advance 300 spectrometer at 300 MHz; the samples were referenced relative to the residual peak of CD_3OD at δ ppm. 2D ROESY spectra were acquired in D_2O on a Bruker Advance 500 spectrometer at 500 MHz.

11. Bibliography

1. Knip, M.; Veijola, R.; Virtanen, S. M.; Hyöty, H.; Vaarala, O.; Åkerblom, H. K., *Diabetes* **2005**, *54* (2), 125-136.

2. Daneman, D., *The Lancet* **2006**, *367* (9513), 847-858.

3. http://www.idf.org/diabetesatlas/5e/the-global-burden, accessed (11/10/13)

4. Baptist, G., *Diabetes, Metabolic Syndrome and Obesity: Targets and Therapy* **2013**, *6*, 1-9.

5. Richards, S.; Larson, C. J.; Koltun, E. S.; Hanel, A.; Chan, V.; Nachtigall, J.; Harrison, A.; Aay, N.; Du, H.; Arcalas, A.; Galan, A.; Zhang, J.; Zhang, W.; Won, K.-A.; Tam, D.; Qian, F.; Wang, T.; Finn, P.; Ogilvie, K.; Rosen, J.; Aoyama, R.; Plonowski, A.; Cancilla, B.; Bentzien, F.; Yakes, M.; Mohan, R.; Lamb, P.; Nuss, J.; Kearney, P., *Journal of Medicinal Chemistry* **2012**, *55* (9), 4322-4335.

6. Bräuer, S.; Almstetter, M.; Antuch, W.; Behnke, D.; Taube, R.; Furer, P.; Hess, S., *Journal of Combinatorial Chemistry* **2005**, *7* (2), 218-226.

7. Skyler, J. S., *Journal of Medicinal Chemistry* **2004**, *47* (17), 4113-4117.

8. Mikami, S.; Kitamura, S.; Negoro, N.; Sasaki, S.; Suzuki, M.; Tsujihata, Y.; Miyazaki, T.; Ito, R.; Suzuki, N.; Miyazaki, J.; Santou, T.; Kanzaki, N.; Funami, M.; Tanaka, T.; Yasuma, T.; Momose, Y., *Journal of Medicinal Chemistry* **2012**, *55* (8), 3756-3776.

9. Negoro, N.; Sasaki, S.; Mikami, S.; Ito, M.; Tsujihata, Y.; Ito, R.; Suzuki, M.; Takeuchi, K.; Suzuki, N.; Miyazaki, J.; Santou, T.; Odani, T.; Kanzaki, N.; Funami, M.; Morohashi, A.; Nonaka, M.; Matsunaga, S.; Yasuma, T.; Momose, Y., *Journal of Medicinal Chemistry* **2012**, *55* (8), 3960-3974.

10. Fowler, M. J., *Clinical Diabetes* **2008**, *26* (2), 77-82.

11. Standl, E.; Schnell, O.; Balletshofer, B.; Schleicher, E.; Muhr, D.; Ziegler, A. G.; Haslbeck, M., *Diabetologia* **1997**, *40* (2), 125-126.

12. Gelberman, R. H.; Hergenroeder, P. T.; Hargens, A. R.; Lundborg, G. N.; Akeson, W. H., *The Journal of Bone & Joint Surgery* **1981**, *63* (3), 380-383.

13. Semenkovich, C. F., *The Journal of Clinical Investigation* **2006**, *116* (7), 1813-1822.

14. Campbell, N. A., Reece, J. B., *Biology,* 7th ed, Pearson Education, **2005**.

15. Renard, C.; Van Obberghen, E., *Diabetes & Metabolism* **2006**, *32* (1), 15-29.

16. Caballero, A. E., *Obesity Research* **2003**, *11* (11), 1278-1289.

17.   Goldberg, I. J., *Journal of Clinical Endocrinology & Metabolism* **2001**, *86* (3), 965-971.

18.   Taskinen, M. R., *Diabetologia* **2003**, *46* (6), 733-749.

19.   Gadi, R.; Samaha, F., *Current Diabetes Reports* **2007**, *7* (3), 228-234.

20.   Jonas, D.; Van Scoyoc, E.; Gerrald, K., Wines; R., A., H.; Runge, T.; Triplette, M.
       http://derp.ohsu.edu/about/

21.   Wherrett, D. K.; Bundy, B.; Becker, D. J.; DiMeglio, L. A.; Gitelman, S. E.; Goland,
       R.; Gottlieb, P. A.; Greenbaum, C. J.; Herold, K. C.; Marks, J. B.; Monzavi, R.; Moran,
       A.; Orban, T.; Palmer, J. P.; Raskin, P.; Rodriguez, H.; Schatz, D.; Wilson, D. M.;
       Krischer, J. P.; Skyler, J. S., *The Lancet 378* (9788), 319-327.

22.   Ross, S. A.; Gulve, E. A.; Wang, M., *Chemical Reviews* **2004**, *104* (3), 1255-1282.

23.   DeFronzo, R. A., *Diabetes* **2009**, *58* (4), 773-795.

24.   Lombardi, A.; Ulianich, L.; Treglia, A. S.; Nigro, C.; Parrillo, L.; Lofrumento, D. D.;
       Nicolardi, G.; Garbi, C.; Beguinot, F.; Miele, C.; Jeso, B., *Diabetologia* **2012**, *55* (1),
       141-153.

25.   Holcombe, J. H.; Kim, D. D.; Stonehouse, A. H.; Kendall, D. M., *Drug Development
       Research* **2006**, *67* (7), 545-552.

26.   Harrigan, R. A.; Nathan, M. S.; Beattie, P., *Annals of Emergency Medicine* **2001**, *38*
       (1), 68-78.

27.   Chan, H. W. E.; Ashan, B.; Jayasekera, P.; Collier, A.; Ghosh, S., *Diabetes &
       Metabolic Syndrome: Clinical Research & Reviews* **2012**, *6* (4), 224-228.

28.   Virally, M.; Blicklé, J. F.; Girard, J.; Halimi, S.; Simon, D.; Guillausseau, P. J.,
       Diabetes & Metabolism **2007**, *33* (4), 231-244.

29.   Kamp, F.; Kizilbash, N.; Corkey, B. E.; Berggren, P.-O.; Hamilton, J. A., *Diabetes*
       2003, *52* (10), 2526-2531.

30.   Tian, Y. A.; Johnson, G.; Ashcroft, S. J., *Diabetes* **1998**, *47* (11), 1722-1726.

31.   Ammar, H. O.; Salama, H. A.; Ghorab, M.; Mahmoud, A. A., *International Journal of
       Pharmaceutics* **2006**, *309* (1–2), 129-138.

32.   Bergström, C. A. S.; Wassvik, C. M.; Johansson, K.; Hubatsch, I., *Journal of Medicinal
       Chemistry* **2007**, *50* (23), 5858-5862.

33.   Adrogué, H. J.; Madias, N. E., *New England Journal of Medicine* **2000**, *342* (21), 1581-
       1589.

34. Gribble, F. M.; Tucker, S. J.; Seino, S.; Ashcroft, F. M., *Diabetes* **1998**, *47* (9), 1412-1418.

35. Hansen, A. M. K.; Hansen, J. B.; Carr, R. D.; Ashcroft, F. M.; Wahl, P., *British Journal of Pharmacology* **2005**, *144* (4), 551-557.

36. Scheen, A. J.; Paquot, N., *Diabetes & Metabolism* **2013**, *39* (3), 179-190.

37. Ouyang, J.; Parakhia, R. A.; Ochs, R. S., *Journal of Biological Chemistry* **2011**, *286* (1), 1-11.

38. Oh, S.; Kim, S. J.; Hwang, J. H.; Lee, H. Y.; Ryu, M. J.; Park, J.; Kim, S. J.; Jo, Y. S.; Kim, Y. K.; Lee, C.-H.; Kweon, K. R.; Shong, M.; Park, S. B., *Journal of Medicinal Chemistry* **2010**, *53* (20), 7405-7413.

39. Larsen, S.; Rabøl, R.; Hansen, C. N.; Madsbad, S.; Helge, J. W.; Dela, F., *Diabetologia* **2012**, *55* (2), 443-449.

40. Huttunen, K. M.; Mannila, A.; Laine, K.; Kemppainen, E.; Leppänen, J.; Vepsäläinen, J.; Järvinen, T.; Rautio, J., *Journal of Medicinal Chemistry* **2009**, *52* (14), 4142-4148.

41. Donnelly, P. S.; Liddell, J. R.; Lim, S.; Paterson, B. M.; Cater, M. A.; Savva, M. S.; Mot, A. I.; James, J. L.; Trounce, I. A.; White, A. R.; Crouch, P. J., *Proceedings of the National Academy of Sciences* **2012**, *109* (1), 47-52.

42. Sazanov, L. A., *Biochemistry* **2007**, *46* (9), 2275-2288.

43. Chittiboyina, A. G.; Venkatraman, M. S.; Mizuno, C. S.; Desai, P. V.; Patny, A.; Benson, S. C.; Ho, C. I.; Kurtz, T. W.; Pershadsingh, H. A.; Avery, M. A., *Journal of Medicinal Chemistry* **2006**, *49* (14), 4072-4084.

44. Pirat, C.; Farce, A.; Lebègue, N.; Renault, N.; Furman, C.; Millet, R.; Yous, S.; Speca, S.; Berthelot, P.; Desreumaux, P.; Chavatte, P., *Journal of Medicinal Chemistry* **2012**, *55* (9), 4027-4061.

45. Murphy, G. J.; Holder, J. C., *Trends in Pharmacological Sciences* **2000**, *21* (12), 469-474.

46. Reddy, K. A.; Lohray, B. B.; Bhushan, V.; Reddy, A. S.; Mamidi, N. V. S. R.; Reddy, P. P.; Saibaba, V.; Reddy, N. J.; Suryaprakash, A.; Misra, P.; Vikramadithyan, R. K.; Rajagopalan, R., *Journal of Medicinal Chemistry* **1999**, *42* (17), 3265-3278.

47. Ferreira, S. B.; Sodero, A. C. R.; Cardoso, M. F. C.; Lima, E. S.; Kaiser, C. R.; Silva, F. P.; Ferreira, V. F., *Journal of Medicinal Chemistry* **2010**, *53* (6), 2364-2375.

48. Hanefeld, M.; Cagatay, M.; Petrowitsch, T.; Neuser, D.; Petzinna, D.; Rupp, M., *European Heart Journal* **2004**, *25* (1), 10-16.

49. Shimpukade, B.; Hudson, B. D.; Hovgaard, C. K.; Milligan, G.; Ulven, T., *Journal of Medicinal Chemistry* **2012**, *55* (9), 4511-4515.

50. Greene, R. J.; Tu, H.; Gibbs, J. P.; Slatter, J. G., *Xenobiotica* **2011**, *41* (11), 945-957.

51. Monami, M.; Iacomelli, I.; Marchionni, N.; Mannucci, E., *Nutrition, Metabolism and Cardiovascular Diseases* **2010**, *20* (4), 224-235.

52. Potashman, M. H.; Duggan, M. E., *Journal of Medicinal Chemistry* **2009**, *52* (5), 1231-1246.

53. Ohtake, Y.; Sato, T.; Kobayashi, T.; Nishimoto, M.; Taka, N.; Takano, K.; Yamamoto, K.; Ohmori, M.; Yamaguchi, M.; Takami, K.; Yeu, S.-Y.; Ahn, K.-H.; Matsuoka, H.; Morikawa, K.; Suzuki, M.; Hagita, H.; Ozawa, K.; Yamaguchi, K.; Kato, M.; Ikeda, S., *Journal of Medicinal Chemistry* **2012**, *55* (17), 7828-7840.

54. Jurczak, M. J.; Lee, H.-Y.; Birkenfeld, A. L.; Jornayvaz, F. R.; Frederick, D. W.; Pongratz, R. L.; Zhao, X.; Moeckel, G. W.; Samuel, V. T.; Whaley, J. M.; Shulman, G. I.; Kibbey, R. G., *Diabetes* **2011**, *60* (3), 890-898.

55. Mascitti, V.; Thuma, B. A.; Smith, A. C.; Robinson, R. P.; Brandt, T.; Kalgutkar, A. S.; Maurer, T. S.; Samas, B.; Sharma, R., *MedChemComm* **2013**, *4* (1), 101-111.

56. Preitner, F.; Mody, N.; Graham, T. E.; Peroni, O. D.; Kahn, B. B., *American Journal of Physiology - Endocrinology and Metabolism* **2009**, *297* (6), 1420-1429.

57. Campos-Sandoval, J. A.; Redondo, C.; Kinsella, G. K.; Pal, A.; Jones, G.; Eyre, G. S.; Hirst, S. C.; Findlay, J. B. C., *Journal of Medicinal Chemistry* **2011**, *54* (13), 4378-4387.

58. Yang, Q.; Graham, T. E.; Mody, N.; Preitner, F.; Peroni, O. D.; Zabolotny, J. M.; Kotani; Quadro, L.; Kahn, B. B., *Nature* **2005**, *436* (7049), 356-362.

59. Flower, D. R.; North, A. C. T.; Sansom, C. E., *Biochimica et Biophysica Acta- Protein Structure and Molecular Enzymology* **2000**, *1482* (1–2), 9-24.

60. Zanotti, G.; Folli, C.; Cendron, L.; Alfieri, B.; Nishida, S. K.; Gliubich, F.; Pasquato, N.; Negro, A.; Berni, R., *FEBS Journal* **2008**, *275* (23), 5841-5854.

61. Findlay, J. B. C.; Sivaprasadarao, A.; Sundaram, M.; Van Aalten, D. M. F., *Biochemical Journal* **2002**, *362* (2), 265-271.

62.   Coward, P.; Conn, M.; Tang, J.; Xiong, F.; Menjares, A.; Reagan, J. D., *Analytical Biochemistry* **2009**, *384* (2), 312-320.

63.   Patrick, G. L., *An Introduction to Medicinal Chemistry,* 4th ed, Oxford University Press Inc., **2009**.

64.   Patrick, G. L., *An Introduction to Medicinal Chemistry,* 2nd ed, Oxford University Press Inc., **2001**.

65.   Veber, D. F.; Johnson, S. R.; Cheng, H.-Y.; Smith, B. R.; Ward, K. W.; Kopple, K. D., *Journal of Medicinal Chemistry* **2002**, *45* (12), 2615-2623.

66.   Rautio, J.; Kumpulainen, H.; Heimbach, T.; Oliyai, R.; Oh, D.; Järvinen, T.; Savolainen, J., *Nature Reviews Drug Discovery* **2008**, *7* (3), 255-270.

67.   Rojas-Aguirre, Y.; Yépez-Mulia, L.; Castillo, I.; López-Vallejo, F.; Soria-Arteche, O.; Hernández-Campos, A.; Castillo, R.; Hernández-Luis, F., *Bioorganic and Medicinal Chemistry* **2011**, *19* (2), 789-797.

68.   Pattnaik, P., *Applied Biochemistry and Biotechnology* **2005**, *126* (2), 79-92.

69.   Stephens, J.; Kinsella, G.; Martin, D.; Devine, R.; Velasco-Torrijos, T.; Findlay, J. B. C. WO2013060860A1, **2013**.

70.   Tovey, M. G., *Detection and quantification of antibodies to biopharmaceuticals: practical and applied considerations,* 1st ed, Hoboken, N.J. : Wiley, **2011**.

71.   Motani, A.; Wang, Z.; Conn, M.; Siegler, K.; Zhang, Y.; Liu, Q.; Johnstone, S.; Xu, H.; Thibault, S.; Wang, Y.; Fan, P.; Connors, R.; Le, H.; Xu, G.; Walker, N.; Shan, B.; Coward, P., *Journal of Biological Chemistry* **2009**, *284* (12), 7673-7680.

72.   Dobri, N.; Qin, Q.; Kong, J.; Yamamoto, K.; Liu, Z.; Moiseyev, G.; Ma, J.-x.; Allikmets, R.; Sparrow, J. R.; Petrukhin, K., *Investigative Ophthalmology & Visual Science* **2013**, *54* (1), 85-95.

73.   Ford, E. S.; Williamson, D. F.; Liu, S., *American Journal of Epidemiology* **1997**, *146* (3), 214-222.

74.   Kim, Y. L.; Kim, T. K.; Cheong, E. S.; Shin, D. G.; Choi, G. S.; Jung, J.; Han, K.-A.; Min, K. W., *Diabetes Metab J* **2012**, *36* (6), 415-421.

75.   Jang, D.-J.; van den Berg, R.; El-Sayed, M. A., *FEBS Letters* **1990**, *261* (2), 279-282.

76.   Cline, G. W.; Petersen, K. F.; Krssak, M.; Shen, J.; Hundal, R. S.; Trajanoski, Z.; Inzucchi, S.; Dresner, A.; Rothman, D. L.; Shulman, G. I., *New England Journal of Medicine* **1999**, *341* (4), 240-246.

77.   Ferré, P.; Leturque, A.; Burnol, A. F.; Penicaud, L.; Girard, J., *The Biochemical journal* **1985**, *228* (1), 103-110.

78.   De Savi, C.; Waterson, D.; Pape, A.; Lamont, S.; Hadley, E.; Mills, M.; Page, K. M.; Bowyer, J.; Maciewicz, R. A., *Bioorganic and Medicinal Chemistry Letters* **2013**, *23* (16), 4705-4712.

79.   Sıdır, Y. G.; Sıdır, İ., *Journal of Molecular Structure* **2013**, *1045* (0), 131-138.

80.   Short, F. W.; Elslager, E. F., *Journal of Medicinal and Pharmaceutical Chemistry* **1962**, *5* (3), 642-646.

81.   Hayat, F.; Cho, S.; Rhim, H.; Indu Viswanath, A. N.; Pae, A. N.; Lee, J. Y.; Choo, D. J.; Choo, H.-Y. P., *Bioorganic and Medicinal Chemistry* **2013**, *21* (17), 5573-5582.

82.   Liu, K. G.; Robichaud, A. J., *Tetrahedron Letters* **2005**, *46* (46), 7921-7922.

83.   Scholz, U. US2005/250791, **2005**.

84.   Pinard, E.; Alanine, A.; Alberati, D.; Bender, M.; Borroni, E.; Bourdeaux, P.; Brom, V.; Burner, S.; Fischer, H.; Hainzl, D.; Halm, R.; Hauser, N.; Jolidon, S.; Lengyel, J.; Marty, H.-P.; Meyer, T.; Moreau, J.-L.; Mory, R.; Narquizian, R.; Nettekoven, M.; Norcross, R. D.; Puellmann, B.; Schmid, P.; Schmitt, S.; Stalder, H.; Wermuth, R.; Wettstein, J. G.; Zimmerli, D., *Journal of Medicinal Chemistry* **2010**, *53* (12), 4603-4614.

85.   Anastasiadis, C.; Hogarth, G.; Wilton-Ely, J. D. E. T., *Inorganica Chimica Acta* **2010**, *363* (13), 3222-3228.

86.   Hassan, J.; Sévignon, M.; Gozzi, C.; Schulz, E.; Lemaire, M., *Chemical Reviews* **2002**, *102* (5), 1359-1470.

87.   Nelson, T. D.; Crouch, R. D., *Cu, Ni, and Pd Mediated Homocoupling Reactions in Biaryl Syntheses: The Ullmann Reaction,* 1st ed, John Wiley & Sons, Inc., **2004**.

88.   Ma, D.; Xia, C., *Organic Letters* **2001**, *3* (16), 2583-2586.

89.   Xi, M.; Bent, B. E., *Journal of the American Chemical Society* **1993**, *115* (16), 7426-7433.

90. Nadri, S.; Azadi, E.; Ataei, A.; Joshaghani, M.; Rafiee, E., *Journal of Organometallic Chemistry* **2011**, *696* (18), 2966-2970.

91. Goodbrand, H. B.; Hu, N.-X., *The Journal of Organic Chemistry* **1998**, *64* (2), 670-674.

92. Hoffmann-la Roche, A. G. F.; Chen, L.; Feng, L.; Huang, M.; Liu, Y.; Wu, G.; Wu, J. Z.; Zhou, M. WO2011/128251, **2011**.

93. Sperotto, E.; van Klink, G. P. M.; van Koten, G.; de Vries, J. G., *Dalton Transactions* **2010**, *39* (43), 10338-10351.

94. Urgaonkar, S.; Verkade, J. G., *The Journal of Organic Chemistry* **2004**, *69* (26), 9135-9142.

95. Paul, F.; Patt, J.; Hartwig, J. F., *Journal of the American Chemical Society* **1994**, *116* (13), 5969-5970.

96. Guram, A. S.; Buchwald, S. L., *Journal of the American Chemical Society* **1994**, *116* (17), 7901-7902.

97. Guram, A. S.; Rennels, R. A.; Buchwald, S. L., *Angewandte Chemie International Edition in English* **1995**, *34* (12), 1348-1350.

98. Louie, J.; Hartwig, J. F., *Tetrahedron Letters* **1995**, *36* (21), 3609-3612.

99. Silverman, L. S.; Caldwell, J. P.; Greenlee, W. J.; Kiselgof, E.; Matasi, J. J.; Tulshian, D. B.; Arik, L.; Foster, C.; Bertorelli, R.; Monopoli, A.; Ongini, E., *Bioorganic and Medicinal Chemistry Letters* **2007**, *17* (6), 1659-1662.

100. Clayden, J.; Greeves, N.; Warren, S.; Wothers, P., *Organic Chemistry,* 1st ed, Oxford University Press Inc., **2001**.

101. Gianotti, M.; Tehan, B. G.; Seri, C.; Lovell, P. J. WO2008/152089, **2008**.

102. Kappe, C. O., *Microwaves in organic and medicinal chemistry,* 2nd ed, Weinheim : Wiley-VCH., **2005**.

103. Stuerga, D., Delmotte, M., Perreux, L., Loupy, A., *Microwaves in Organic synthesis,* 1st ed, WILEY-VCH GmbH& Co. KGaA., **2002**.

104. Hayes, B., *Microwave Synthesis: Chemistry at the Speed of Light,* 1st ed, CEM publishing, **2002**.

105. Meng, X.; Cai, Z.; Xiao, S.; Zhou, W., *Journal of Fluorine Chemistry* **2013**, *146* (0), 70-75.

106. Akkani, A.; Paterlini, G.; Gleason, W. B.; Ojala, W. H.; Abul-Hajj, Y. J., *Journal of Medicinal Chemistry* **1997**, *40* (20), 3263-3270.

107. Neves, M. A. C.; Dinis, T. C. P.; Colombo, G.; Sá e Melo, M. L., *Journal of Medicinal Chemistry* **2008**, *52* (1), 143-150.

108. van Meeuwen, J. A.; Nijmeijer, S.; Mutarapat, T.; Ruchirawat, S.; de Jong, P. C.; Piersma, A. H.; van den Berg, M., *Toxicology and Applied Pharmacology* **2008**, *228* (3), 269-276.

109. Stauffer, F.; Furet, P.; Floersheimer, A.; Lang, M., *Bioorganic and Medicinal Chemistry Letters* **2012**, *22* (5), 1860-1863.

110. Kim, B. T.; Min, Y.; Heo, J. N.; Lee, H.; Chang, S. Y.; Park, N. K.; Song, S. W.; Oh, J. J. WO2008/153325, **2008**.

111. Milkiewicz, K. L.; Lu, T.; Player, M. R.; Parks, D. J.; Pan, W.; Markotan, T. P.; Thieu, T. V. WO2006/47415, **2006**.

112. Juvale, K.; Wiese, M., *Bioorganic and Medicinal Chemistry Letters* **2012**, *22* (21), 6766-6769.

113. Valeur, E.; Bradley, M., *Chemical Society Reviews* **2009**, *38* (2), 606-631.

114. Sheehan, J. C.; Hess, G. P., *Journal of the American Chemical Society* **1955**, *77* (4), 1067-1068.

115. Cauquil-Caubère, I.; Kamenka, J.-M., *European Journal of Medicinal Chemistry* **1998**, *33* (11), 867-877.

116. Hammam, A. E.-F. G.; Youssif, N. M., *Journal of Chemical & Engineering Data* **1982**, *27* (2), 207-208.

117. Capuano, B.; Crosby, I. T.; Lloyd, E. J.; Taylor, D. A., *Australian Journal of Chemistry* **2002**, *55* (9), 565-576.

118. Ishihara, Y.; Terauchi, J.; Suzuki, N.; Takekawa, S.; Aso, K. US2003/158177, **2003**.

119. Acheson, R. M.; Cooper, M. W., *Journal of the Chemical Society, Perkin Transactions : Organic and Bio-Organic Chemistry (1972-1999)* **1980**, 1185-1193.

120. Romeiro, L. A. S.; da Silva Ferreira, M.; da Silva, L. L.; Castro, H. C.; Miranda, A. L. P.; Silva, C. L. M.; Noël, F.; Nascimento, J. B.; Araújo, C. V.; Tibiriçá, E.; Barreiro, E. J.; Fraga, C. A. M., *European Journal of Medicinal Chemistry* **2011**, *46* (7), 3000-3012.

121. Waldo, J. P.; Mehta, S.; Larock, R. C., *The Journal of Organic Chemistry* **2008**, *73* (17), 6666-6670.

122. Sugimoto, N.; Osakabe, M., *Pest Management Science* **2013**.

123. Fustero, S.; Román, R.; Sanz-Cervera, J. F.; Simón-Fuentes, A.; Cuñat, A. C.; Villanova, S.; Murguía, M., *The Journal of Organic Chemistry* **2008**, *73* (9), 3523-3529.

124. Penning, T. D.; Talley, J. J.; Bertenshaw, S. R.; Carter, J. S.; Collins, P. W.; Docter, S.; Graneto, M. J.; Lee, L. F.; Malecha, J. W.; Miyashiro, J. M.; Rogers, R. S.; Rogier, D. J.; Yu, S. S.; Anderson, G. D.; Burton, E. G.; Cogburn, J. N.; Gregory, S. A.; Koboldt, C. M.; Perkins, W. E.; Seibert, K.; Veenhuizen, A. W.; Zhang, Y. Y.; Isakson, P. C., *Journal of Medicinal Chemistry* **1997**, *40* (9), 1347-1365.

125. Terrett, N. K.; Bell, A. S.; Brown, D.; Ellis, P., *Bioorganic and Medicinal Chemistry Letters* **1996**, *6* (15), 1819-1824.

126. Heller, S. T.; Natarajan, S. R., *Organic Letters* **2006**, *8* (13), 2675-2678.

127. Lee, B.; Lee, K. H.; Cho, J.; Nam, W.; Hur, N. H., *Organic Letters* **2011**, *13* (24), 6386-6389.

128. Lee, B.; Kang, P.; Lee, K. H.; Cho, J.; Nam, W.; Lee, W. K.; Hur, N. H., *Tetrahedron Letters* **2013**, *54* (11), 1384-1388.

129. Hanzlowsky, A.; Jelenčič, B.; Rečnik, S.; Svete, J.; Golobič, A.; Stanovnik, B., *Journal of Heterocyclic Chemistry* **2003**, *40* (3), 487-498.

130. Bagley, M. C.; Davis, T.; Dix, M. C.; Widdowson, C. S.; Kipling, D., *Organic & Biomolecular Chemistry* **2006**, *4* (22), 4158-4164.

131. Hanamoto, T.; Hakoshima, Y.; Egashira, M., *Tetrahedron Letters* **2004**, *45* (41), 7573-7576.

132. Aggarwal, V. K.; de Vicente, J.; Bonnert, R. V., *The Journal of Organic Chemistry* **2003**, *68* (13), 5381-5383.

133. Martín, R.; Rodríguez Rivero, M.; Buchwald, S. L., *Angewandte Chemie International Edition* **2006**, *45* (42), 7079-7082.

134. Anderson, K. W.; Tundel, R. E.; Ikawa, T.; Altman, R. A.; Buchwald, S. L., *Angewandte Chemie International Edition* **2006**, *45* (39), 6523-6527.

135.   Antilla, J. C.; Baskin, J. M.; Barder, T. E.; Buchwald, S. L., *The Journal of Organic Chemistry* **2004**, *69* (17), 5578-5587.

136.   Zhu, L.; Guo, P.; Li, G.; Lan, J.; Xie, R.; You, J., *The Journal of Organic Chemistry* **2007**, *72* (22), 8535-8538.

137.   Olivera, R.; SanMartin, R.; Domínguez, E., *The Journal of Organic Chemistry* **2000**, *65* (21), 7010-7019.

138.   Alinezhad, H.; Tajbakhsh, M.; Zare, M., *Journal of Fluorine Chemistry* **2011**, *132* (11), 995-1000.

139.   Pellegrino, G.; Leonetti, F.; Carotti, A.; Nicolotti, O.; Pisani, L.; Stefanachi, A.; Catto, M., *Tetrahedron Letters* **2010**, *51* (13), 1702-1705.

140.   Longhi, K.; Moreira, D. N.; Marzari, M. R. B.; Floss, V. M.; Bonacorso, H. G.; Zanatta, N.; Martins, M. A. P., *Tetrahedron Letters* **2010**, *51* (24), 3193-3196.

141.   Cuny, G. D.; Laha, J. K.; Xing, X.; Yu, P. B.; Lai, C. S.; Deng, D. Y.; Bloch, K. D.; Liu, J.-F.; Sachidanandan, C.; Peterson, R. T., *Bioorganic and Medicinal Chemistry Letters* **2008**, *18* (15), 4388-4392.

142.   Xiao Jia, Y.; Guan Hong, X.; Xu, S.; Yan, P.; Xing, J.; Ke, J.; Fei, L., *Molecules* **2010**, *15* (6), 4261-4266.

143.   El-Araby, M. E.; Bernacki, R. J.; Makara, G. M.; Pera, P. J.; Anderson, W. K., *Bioorganic and Medicinal Chemistry* **2004**, *12* (11), 2867-2879.

144.   Katritzky, A. R.; Huang, T.-B.; Voronkov, M. V.; Steel, P. J., *The Journal of Organic Chemistry* **2000**, *65* (23), 8069-8073.

145.   Nenaidenko, V.; Golubinskii, I.; Lenkova, O.; Shastin, A.; Balenkova, E., *Russian Journal of Organic Chemistry* **2004**, *40* (10), 1518-1520.

146.   Lu, Y.; Miet, C.; Kunesch, N.; Poisson, J. E., *Tetrahedron: Asymmetry* **1993**, *4* (5), 893-902.

147.   Edvinsson, S.; Johansson, S.; Larsson, A., *Tetrahedron Letters* **2012**, *53* (50), 6819-6821.

148.   Sato, M.; Yoneda, N.; Katagiri, N.; Watanabe, H.; Kaneko, C., *Synthesis* **1986**, *1986* (8), 672-674.

149.   Dollé, F.; Hinnen, F.; Valette, H.; Fuseau, C.; Duval, R.; Péglion, J.-L.; Crouzel, C., *Bioorganic and Medicinal Chemistry* **1997**, *5* (4), 749-764.

150.   Gopalsamy, A.; Shi, M., *Organic Letters* **2003**, *5* (21), 3907-3909.

151.   Shaikh, A. C.; Chen, C., *Bioorganic and Medicinal Chemistry Letters* **2010**, *20* (12), 3664-3668.

152.   Piasecki, Shawn K.; Taylor, Clint A.; Detelich, Joshua F.; Liu, J.; Zheng, J.; Komsoukaniants, A.; Siegel, Dionicio R.; Keatinge-Clay, Adrian T., *Chemistry & biology* **2011**, *18* (10), 1331-1340.

153.   Senga, K.; Novinson, T.; Wilson, H. R.; Robins, R. K., *Journal of Medicinal Chemistry* **1981**, *24* (5), 610-613.

154.   Pidathala, C.; Amewu, R.; Pacorel, B.; Nixon, G. L.; Gibbons, P.; Hong, W. D.; Leung, S. C.; Berry, N. G.; Sharma, R.; Stocks, P. A.; Srivastava, A.; Shone, A. E.; Charoensutthivarakul, S.; Taylor, L.; Berger, O.; Mbekeani, A.; Hill, A.; Fisher, N. E.; Warman, A. J.; Biagini, G. A.; Ward, S. A.; O'Neill, P. M., *Journal of Medicinal Chemistry* **2012**, *55* (5), 1831-1843.

155.   Nagarathnam, D.; Hatoum-Mokdad, H.; Pluempe, H.; Boyer, S.; Dumas, J. US2004/2507, **2004**.

156.   Charton, M., *Journal of the American Chemical Society* **1975**, *97* (6), 1552-1556.

157.   Bach, P.; Bostroem, J.; Brickmann, K.; Cheng, L.; Giordanetto, F.; Groneberg, R.; Harvey, D. M.; O'Sullivan, M. F.; Zetterberg, F. WO2006/73361, **2006**.

158.   Fernanda, A. R.; Pablo, M.; Pamela, S. V.; Helio, G. B.; Nilo, Z.; Marcos, A. P. M., *ChemInform* **2008**, *39* (44).

159.   Zhang, L.; Brodney, M. A.; Candler, J.; Doran, A. C.; Duplantier, A. J.; Efremov, I. V.; Evrard, E.; Kraus, K.; Ganong, A. H.; Haas, J. A.; Hanks, A. N.; Jenza, K.; Lazzaro, J. T.; Maklad, N.; McCarthy, S. A.; Qian, W.; Rogers, B. N.; Rottas, M. D.; Schmidt, C. J.; Siuciak, J. A.; Tingley, F. D.; Zhang, A. Q., *Journal of Medicinal Chemistry* **2011**, *54* (6), 1724-1739.

160.   Neuwoehner, J.; Fenner, K.; Escher, B. I., *Environmental Science & Technology* **2009**, *43* (17), 6830-6837.

161.   Purser, S.; Moore, P. R.; Swallow, S.; Gouverneur, V., *Chemical Society Reviews* **2008**, *37* (2), 320-330.

162.   Waring, M., J., *Expert Opinion on Drug Discovery* **2010**, *5* (3), 235-248.

163.   Xing, L.; Glen, R. C., *Journal of Chemical Information and Computer Sciences* **2002**, *42* (4), 796-805.

164.   Martinez, C. R.; Iverson, B. L., *Chemical Science* **2012**, *3* (7), 2191-2201.

165.   Lacivita, E.; Leopoldo, M.; Giorgio, P. D.; Berardi, F.; Perrone, R., *Bioorganic & Medicinal Chemistry* **2009**, *17* (3), 1339-1344.

166.   Zhou, P.; Tian, F.; Lv, F.; Shang, Z., *Proteins: Structure, Function, and Bioinformatics* **2009**, *76* (1), 151-163.

167.   Li, J. J., *Heterocyclic Chemistry in Drug Discovery,* 1st ed, Wiley, John & Sons, Inc., **2013**.

168.   Sutton, J. M.; Clark, D. E.; Dunsdon, S. J.; Fenton, G.; Fillmore, A.; Harris, N. V.; Higgs, C.; Hurley, C. A.; Krintel, S. L.; MacKenzie, R. E.; Duttaroy, A.; Gangl, E.; Maniara, W.; Sedrani, R.; Namoto, K.; Ostermann, N.; Gerhartz, B.; Sirockin, F.; Trappe, J.; Hassiepen, U.; Baeschlin, D. K., *Bioorganic and Medicinal Chemistry Letters* **2012**, *22* (3), 1464-1468.

169.   King, F. D., *Medicinal Chemistry Principle and Practice.,* 2nd ed, The Royal Society of Chemistry., **2002**.

170.   Yang, S.-Y., *Drug Discovery Today* **2010**, *15* (11–12), 444-450.

171.   Kaufman, L.; Rousseeuw, P. J., *Finding Groups in Data: An Introduction to Cluster Analysis,* 1st ed, John Wiley & Sons, **2009**.

172.   Ogihara, N.; Clement, O. http://accelrys.com/resource-center/case-studies/archive/studies/catalyst_odorants.pdf.

173.   Schwab, C. H., *Drug Discovery Today: Technologies* **2010**, *7* (4), 245-253.

174.   Cook, N. R., *Circulation* **2007**, *115* (7), 928-935.

175.   (a) Metz, C. E.; Herman, B. A.; Shen, J.-H., *Statistics in Medicine* **1998**, *17* (9), 1033-1053; (b) Wan, S.; Zhang, B., *Statistics in Medicine* **2007**, *26* (12), 2565-2586.

176.   Miller, J. J.; Sigman, M. S., *Angewandte Chemie International Edition* **2008**, *47* (4), 771-774.

177.   Kosaka, T.; Okuyama, R.; Sun, W.; Ogata, T.; Harada, J.; Araki, K.; Izumi, M.; Yoshida, T.; Okuno, A.; Fujiwara, T.; Ohsumi, J.; Ichikawa, K., *Analytical Chemistry* **2005**, *77* (7), 2050-2055.

178.   Dou, D.; Tiew, K.-C.; He, G.; Mandadapu, S. R.; Aravapalli, S.; Alliston, K. R.; Kim, Y.; Chang, K.-O.; Groutas, W. C., *Bioorganic and Medicinal Chemistry* **2011**, *19* (20), 5975-5983.

179. Jung, M. E.; Ouk, S.; Yoo, D.; Sawyers, C. L.; Chen, C.; Tran, C.; Wongvipat, J., *Journal of Medicinal Chemistry* **2010**, *53* (7), 2779-2796.

180. Damásio, A. R. d. L.; Pessela, B. C.; Mateo, C.; Segato, F.; Prade, R. A.; Guisan, J. M.; de Lourdes Teixeira de Moraes Polizeli, M., *Journal of Molecular Catalysis B: Enzymatic* **2012**, *77* (0), 39-45.

181. Romero, O.; Guisán, J. M.; Illanes, A.; Wilson, L., *Journal of Molecular Catalysis B: Enzymatic* **2012**, *74* (3–4), 224-229.

182. Rajčanová, M.; Tichá, M.; Kučerová, Z., *Journal of Separation Science* **2012**, *35* (15), 1899-1905.

183. Katagiri, F.; Ishikawa, M.; Yamada, Y.; Hozumi, K.; Kikkawa, Y.; Nomizu, M., *Archives of Biochemistry and Biophysics* **2012**, *521* (1–2), 32-42.

184. McMahon, A.; Han, S.; Walker, I., *Journal of Virological Methods* **2010**, *169* (2), 253-258.

185. Tiwari, G.; Tiwari, R.; Sriwastawa, B.; Bhati, L.; Pandey, S.; Pandey, P.; Bannerjee, S. K., *International Journal of Pharmaceutical Investigation* **2012**, *2* (1), 2-11.

186. Sri, K. V.; Kondaiah, A.; Ratna, J. V.; Annapurna, A., *Drug Development & Industrial Pharmacy* **2007**, *33* (3), 245-253.

187. Srinivasan, K.; Stalin, T.; Sivakumar, K., *Spectrochimica Acta Part A: Molecular and Biomolecular Spectroscopy* **2012**, *94* (0), 89-100.

188. Loftsson, T.; Brewster, M. E.; Másson, M., *American Journal of Drug Delivery* **2004**, *2* (4), 261-275.

189. de Araújo, M. V. G.; Vieira, E. K. B.; Lázaro, G. S.; de Souza Conegero, L.; Ferreira, O. P.; Almeida, L. s. E.; Barreto, L. S.; da Costa Jr, N. B.; Gimenez, I. F., *Bioorganic and Medicinal Chemistry* **2007**, *15* (17), 5752-5759.

190. Upadhye, S.; Kulkarni, S.; Majumdar, S.; Avery, M.; Gul, W.; ElSohly, M.; Repka, M., *AAPS PharmSciTech* **2010**, *11* (2), 509-517.

191. Wang, X.; Brusseau, M. L., *Environmental Science & Technology* **1993**, *27* (13), 2821-2825.

192. Challa, R.; Ahuja, A.; Ali, J.; Khar, R. K., *AAPS PharmSciTech* **2005**, *6* (2), 329-357.

193. Higuichi, T.; Connors, K., *Advances in Analytical Chemistry and Instrumentation* **1965**, 117-210.

194. Worthington, M. S.; Glass, B. D.; Penkler, L. J., *Journal of inclusion phenomena and molecular recognition in chemistry* **1996**, *25* (1-3), 153-156.

195. Felton, L., *Remington: Essentials of Pharmaceutics,* 1st ed, Pharmaceutical press, 2013, **2013**.

196. Gill, P.; Moghadam, T. T.; Ranjbar, B., *Journal of biomolecular techniques : JBT* **2010**, *21* (4), 167-193.

197. Höhne, G.; Hemminger, W. F.; Flammersheim, H.-J., *Differential Scanning Calorimetry,* 2nd ed, Springer, **2003**.

198. Stokes, D., *Principles and Practice of Variable Pressure: Environmental Scanning Electron Microscopy (VP-ESEM),* 3rd ed, Wiley, **2009**.

199. Song, L. X., Li, B. L., Jiang, R., *Chinese Chemical Letters* **1997**, *8* (7), 1.

200. Loftsson, T.; Másson, M.; Brewster, M. E., *Journal of Pharmaceutical Sciences* **2004**, *93* (5), 1091-1099.

201. Gabelica, V.; Galic, N.; De Pauw, E., *Journal of the American Society for Mass Spectrometry* **2002**, *13* (8), 946-953.

202. Manetti, D.; Bartolini, A.; Borea, P. A.; Bellucci, C.; Dei, S.; Ghelardini, C.; Gualtieri, F.; Novella Romanelli, M.; Scapecchi, S.; Teodori, E.; Varani, K., *Bioorganic and Medicinal Chemistry* **1999**, *7* (3), 457-465.

203. Brenner, E.; Schneider, R.; Fort, Y., *Tetrahedron* **1999**, *55* (44), 12829-12842.

204. Baloglu, E.; Ghosh, S.; Lobera, M.; Schmidt, D. WO2011/88187, **2011**.

205. Brenner, E.; Schneider, R.; Fort, Y., *Tetrahedron* **2002**, *58* (34), 6913-6924.

206. Nam, G.; Pae, A. N.; Choi, K. I.; Choo, H.; Devegowda, V. N.; Seo, S. H. US2011/319619, **2011**.

207. Graham, S. L. US4665090, **1987**.

208. Afzali, A.; Breen, A.; Kagan, T. L.; Renee, C. US2002/72618, **2002**.

209. LaFrate, A. L.; Carlson, K. E.; Katzenellenbogen, J. A., *Bioorganic and Medicinal Chemistry* **2009**, *17* (10), 3528-3535.

210. Friscourt, F.; Fahrni, C. J.; Boons, G.-J., *Journal of the American Chemical Society* **2012**, *134* (45), 18809-18815.

211. Vorbrueggen, H., *Synlett* **2008**, (11), 1603-1617.

212. Klebe; Habraken, *Synthesis* **1973**, 294-295.

213. Lassagne, F.; Snegaroff, K.; Mongin, F.; Roisnel, T.; Nassar, E., *Heterocyclic Communications* **2011**, *17* (3-4), 139-145.

214. Bruni, F.; Costanzo, A.; Selleri, S.; Guerrini, G.; Fantozzi, R.; Pirisino, R.; Brunelleschi, S., *Journal of Pharmaceutical Sciences* **1993**, *82* (5), 480-486.

215. Ushio, H.; Ishibuchi, S.; Naito, Y.; Sugiyama, N.; Kawaguchi, T.; Chiba, K.; Ohtsuki, M.; Naka, Y. EP1176140, **2002**.

216. Menozzi, G.; Mosti, L.; Schenone, P., *Journal of Heterocyclic Chemistry* **1987**, *24* (6), 1669-1675.

217. Kaisha, M. S. US6355642, **2002**.

218. Sumino, Y.; Okamoto, K.; Masui, M.; Akiyama, T. US2012/22251, **2012**.

219. Antonsson, T.; Bylund, R. G., F.; Brickmann, K.; Bach, P.; Johansson, J.; Zetterber, F. US2008/176827, **2008**.

220. Hamanaka, E. S.; Webster, R. T.; Mularski, C. J.; Ruggeri, R. B.; Guzman-Perez, A. US6492401, **2002**.

221. Dreger, A.; Cisneros Camuña, R.; Münster, N.; Rokob, T. A.; Pápai, I.; Schmidt, A., *European Journal of Organic Chemistry* **2010**, *2010* (22), 4296-4305.

222. Suzuki, K.; Yamaguchi, T.; Tamura, A.; Nishizawa, T.; Yamaguchi, M. EP2308838, **2011**.

223. Volodina, M. A., *J. Gen. Chem. USSR (Engl. Transl.)* **1964**, *34*, 469-475.

Poster presentations

2011

- Synthesis and analysis of potential Type-II Diabetes Mellitus therapeutics; 20th conference of the Groupement des Pharmacochimistes de l'Arc Atlantique (GP2A), Cork.

2010

- Combatting Type-II Diabetes: Synthesis of novel compounds as potential inhibitors of the retinol mediated insulin resistant pathway; High Performance Computing at the Chemistry/Biology Interface, Galway.

- Design and synthesis of novel compounds as potential therapeutics for Type-II Diabetes Mellitus; Centre for Synthesis & Chemical Biology Symposium, Dublin.